A. G. GREBENIKOV

METHODOLOGY OF INTEGRATED DESIGNING AND MODELLING OF AIRCRAFT ASSEMBLY STRUCTURES

2010

MINISTRY OF EDUCATION AND SCIENCE OF UKRAINE
NATIONAL AEROSPACE UNIVERSITY BY N. E. ZHUKOVSKIY
”KHARKOV AVIATION INSTITUTE”

A. G. GREBENIKOV

METHODOLOGY OF INTEGRATED DESIGNING AND MODELLING OF AIRCRAFT ASSEMBLY STRUCTURES

Training guide

Kharkov 2010

УДК 629.735:33
Grebenikov A. G. Methodology of integrated designing and modelling of aircraft assembly structures: training guide / A. G. Grebenikov. – Kharkov: National Aerospace University "Kharkov Aviation Institute", 2010. – 425 pages.

ISBN 978-966-218-4

In this training guide the following issues were considered: the concept, principles and methods of integrated designing and three-dimensional computer modelling of aircraft assembly structures, creation of aircraft master-geometry, space distribution, analytical standards of units and components using CAD/CAM/CAE/PLM systems, methods of integrated designing and achievement of designated service life of bolted and riveted joints of aircraft assembly structures, fatigue cracks growth delay methods using installation of fasteners with elastoplastic radial interference and tightening. In addition, this training guide considers the following problems: the methods of identifying the influence of structurally-technological parameters and loading level on the value of local specific energy of deformation, contact pressures, projection of rivet set heads after riveting, the value of compliance and workload of extreme rows of multirow bolted and riveted joints using CAD/CAE ANSYS system, which allow to forecast the service life of airframe.

This training guide is intended for scientists and engineers of aircraft industry, and also for postgraduates, lecturers and students of higher education institutions.

Розглянуто концепцію, принципи та методи інтегрованого проектування і тривимірного комп'ютерного моделювання збірних літакових конструкцій, створення мастер-геометрії літака, розподілення простору, аналітичних еталонів вузлів і деталей за допомогою систем CAD/CAM/CAE/PLM, методи інтегрованого проектування та досягнення регламентованої довговічності болтових і заклепкових з'єднань збірних літакових конструкцій, методи затримки росту втомних тріщин установленням кріпильних елементів з пружнопластичним радіальним натягом і затягуванням. Розроблено методику визначення впливу конструктивно-технологічних параметрів і рівня навантаження на величину локальної питомої енергії деформування, контактних тисків, виступання закладних головок заклепок після клепання, величину піддатливості та ступінь завантаження крайніх рядів багаторядних болтових з'єднань за допомогою системи CAD/CAE ANSYS, що дозволяє прогнозувати ресурс планера літака.

Для наукових та інженерно-технічних працівників авіаційної промисловості, а також для аспірантів, викладачів і студентів вищих навчальних закладів.

Illustrations 404. Tables 29. Bibliography: 477 articles.

Reviewers: I.V. Malkov, D.S., Prof. Eastern-Ukrainian National University named after Vladimir Dal' **V.A. Trofimov,** D.S. Antonov Aeronautical Scientific/Technical Complex of The Ministry of industrial policy of Ukraine

Approved at the meeting of Academic Board of National Aerospace University Kharkov Aviation Institute on 20.01.2010 (record of proceedings №10) as teaching aids

ISBN 978-966-662-218-4

CONTENTS

σ_{ult} – material ultimate tensile strength

σ_{frac} – fracture strength

σ_{btar} – bearing stress

$\delta holecrumpl$ – hole crumpling

$\delta_{b.\,bear}$ – bolt bearing

$\delta_{b.bend}$ – bolt bending

$\delta_{b\,shift}$ – bolt shift

σ_{shear} – shearing stress

σ^{gr} – nominal stresses in "gross" section of structural member

σ_0^{gr} – nominal stresses in "gross" section of structural member reduced to zero-to compression/tension stress cycle

σ_a – amplitude stresses of fatigue/loading cycle

σ_{max} – maximum fatigue/loading cycle stresses

$\sigma_{\grave{a}\,fr}$ – amplitude value of cyclic nominal tensile strength in structural members in fretting corrosion zone

$\sigma_{m\,fr}$ – mean value of cyclic nominal tensile stresses in structural members in fretting corrosion zone

σ_c – contact stresses in fretting corrosion zone

$\sigma_{eqv\,max}$ – maximum equivalent stresses

$\sigma_{x\,max}$ – maximum tensile stresses

$\sigma_{cont\,max}$ – maximum value of contact pressures between surfaces

D_{srh} – snap rivet head diameter

R_σ – asymmetry ratio of fatigue/loading cycle

P_{max} – maximum cyclic load

P_t – bolt tightening force

Q_d – lateral force in design section

M_{bend} – sectional bending moment

E_{bear} – bearing stress module

d_b – bolt body diameter

$M_{nut\ torq}$ – bolt nut tightening torque

θ – contact pressure concentration factor between contact surfaces

W – total specific strain energy

W_{elast} – specific strain energy elastic component

W_{plast} – specific strain energy plastic component

ϑ	–	hole ovality
f_{fric}	–	friction coefficient between contact surfaces
l	–	fatigue crack length
N	–	fatigue/loading cycle durability
N_{res}	–	residual durability
N_{bcd}	–	number of fatigue/loading cycles prior to crack detection
N_{wc}	–	number of fatigue/loading cycles prior to failure of structure with crack
CAD	–	Computer Aided Design
CAM	–	Computer Aided Manufacturing
CAE	–	Computer Aided Engineering

INTRODUCTION

Aircraft industry takes one of the leading places among priority directions of industry development in Ukraine. To produce new competitive products it is necessary to carry out new researches and to develop design methods more perfect as compared with competitors. In this case assigned aircraft service life (about 80000...90000 flight hours) under minimum fuel mass consumption is one of the main factors of its competitiveness while the problem of its achievement is determined by the main methodology of integrated design and construction of the aircraft thin-walled assembly structures. Their development is an advanced research. Many national and foreign scientists took part in developing the design methods of the aircraft assembly structures. Among Ukrainian scientists the most well-known works have been prepared by: O.K. Antonov, G.A. Krivov, V.A. Titov, V.I. Ryabkov, Ya.S. Karpov, D.S. Kiva, V.N. Korol, V.A. Trofimov, E.A. Shakhatuni, S.N. Konyukhov, I.V. Pavlov, E.T. Vasilevsky, V.I. Matusevich, E.A. Bolshakov, O.P. Cheranovsky, L.A. Malashenko, A.I. Ryzhenko, V.G. Sukhorebry, A.G. Lebedinsky, L.P. Semenov, V.S. Shekhovtsov, G.G. Ongirsky, V.A. Matvienko, S.G. Kushnarenko, Yu.A. Boborykin, A.I. Babushkin, V.V. Knigin, I.V. Malkov, V.T. Troshenko, A.I. Radchenko, P.A. Fomichev, V.E. Gaidachuk, E.A. Djura and many others.

However, in developing these methods the advanced, science intensive, computer-aided integrated systems CAD/CAM/CAE found application but not in full scope. Their introduction in design practice required the development of ew methodology in designing, modelling, engineering analysis and preproduction of aircraft thin-walled assembly structures.

Lack of skills in achievement of the specified durability characteristics of the aircraft structural members using CAD/CAM/CAE systems is an obstacle to integration of calculated experimental design methods and methods in computer-aided modeling of the structural members making it impossible to perform perfect integrated design of aircraft assembly structures providing their service life.

In connection with everything mentioned above, the methodology of development of aircraft structure integrated design and computer-aided modeling is very urgent while the developing methods in achievement of the specified service life characteristics of the assembly structures and their joints under mass minimization is of great practical importance in solving the problem to provide flight safety under conditions of aircraft long-term operation.

The goal of this text-book is to provide the specified service life of aircraft assembly structures by development of integrated design and modeling methods using the computer systems.

The following scientific and practical problems sufficiently significant for designing the aircraft assembly structures have been solved to achieve the assigned goal:

– concept and scientific backgrounds of integrated design methodology and achievement of specified service life of aircraft thin-walled assembly structures have been developed;

– method of integrated design and achievement of specified service life of aircraft assembly structure shear bolted joint has been created;

– new design and technological solutions for aircraft assembly structure shear bolted joints of assigned service life have been obtained using the method of integrated design and achievement of specified service life;

– method of integrated design and achievement of specified service life of aircraft thin-walled structure shear-riveted joints has been created;

– new design and technological solutions for aircraft thin-walled structure shear-riveted joints have been obtained using the method of integrated design and achievement of specified service life;

– new design and technological methods and techniques in fatigue crack growth delay have been developed to extend service life of thin-walled assembly structures;

– developed design methods and structural-technological solutions have been implemented into theory and practice of aircraft assembly structure creation using integrated CAD/CAM/CAE systems.

In solving assigned problems the following methods have found wide application: mathematical methods in analysis of design concepts, methods of automated design and three-dimensional computer-aided modelling of aircraft thin-walled assembly structures using advanced computer-aided integrated systems (CAD/CAM/CAE); strength analysis methods of aircraft structural members; experiment-calculated methods in determination of the design-engineering parameters effect on the fatigue resistance characteristics of the thin-walled structures and models of their joints. Determination of the local deflected mode characteristics in assembly structural members has been performed by the finite-element method realized in CAD/CAM/CAE system. Energy approach has been realized to predict service life of the joints with the elastoplastic interference of the fasteners. The probabilistic-statistic method of analysis has been used in processing of the fatigue test results.

Adequacy of the estimated models has been tested under fatigue tests of the standard test-piece models and assembly units of the thin-walled structures. The authenticity of the integrated design methodology has been checked under computer-aided modelling of AN-140 airplane units. The methods in achievement of the specified service life have been confirmed by the numerical and physical analyses of the fatigue resistance characteristics of the aircraft assembly structure bolted and riveted joints.

This text book offers, for the first time, the method in forming the geometry of the aircraft assembly structures using CAD/CAM/CAE systems. On the basis

of the unified computer paradigm of the aircraft outer surface, a new concept and principles of aircraft assembly structure integrated design have been offered.

The process of the specified durability of the aircraft assembly structures has been integrally connected for the first time with the main phases of the aircraft life cycle – design, manufacturing, operation:

– for the design analysis phase the new estimating-experimental models of shear-bolted and riveted joints fatigue resistance enabling to predict service life of assembly structures in the areas of probable fatigue failure have been offered with the allowance made for the concentration of the specific strain energy, contact pressures and fretting corrosion as well as new means in unloading the shear joint extreme rows by applying straps, unloading holes and glue;

– for the aircraft structure manufacturing phase the influence of the local radial interference on the deflected mode characteristics and cyclic life time of the shear bolted and riveted joints has been specified; the up-to-date design of bolts and rivets realizing local radial interference to provide assigned fatigue service life, pressurization and the unit outer surface quality without milling the manufactured rivet heads after riveting has been developed; the method has been offered to reduce the adverse effect of technological abnormality and fretting-corrosion on the joint service life by applying the polymeric fillers;

– for the operation phase the new design-manufacturing methods and procedures in fatigue crack growth delay have been developed by installation of the additional fasteners with axial and radial interferences at their highest points.

The following provisions are made for practical implementation of the integrated design concept, the principles, procedures and techniques in achievement of the assigned service life characteristics of the aircraft thin-walled assembly structures and for development of the mathematical reference models of the aircraft jointed structures on the basis of the article unified database:

– implementation of the analytical standards of the aircraft thin-walled assembly structures using CAD/CAM/CAE integrated system without application of the traditional loft floor method (full size layouts of aircraft structural components) and saving design labour by 25...30 as compared with the traditional automated design labour intensity;

– development of the new advanced rivets and bolts as well as methods and techniques of their installation with radial interference;

– prediction of the fatigue characteristics of the thin-walled assembly structures at design stage and selection of the joint structural parameters to achieve the assigned service life on the basis of obtained deflected mode characteristics as well as the fatigue resistance of the standard joint models;

– 90...95 % labor intensity reduction in milling the manufactured countersunk rivet heads due to the use of the rivets with the cylindrical compensator firstly developed under the guidance of the author and realization of

the developed installation procedures under specified characteristics of the riveted joint serviceability;

– fatigue durability increase of standard joints in 2...7 times by using the developed design-technological variants of the countersunk bolted joints with the local radial interference and anti-fretting coating;

– 8...10 times durability increase of thin-walled assembly structures with the fatigue cracks corresponding to the service life extension in 1.5...2 times due to implementation of the fatigue crack growth delay procedures introduced by the author of the textbook;

– obtaining the optimal parameters of the aircraft structure joints with the assigned characteristics with the minimum joint mass. The developed methods of the integrated design have been realized during design and manufacture of AN-74, AN-22, AN-124, AN-225, IL-96, TU-334, AN-140, AN-148 aircraft bolted and riveted joints and in repair of thin-walled structures for all aircraft operated in CIS states as well as during service life tests of the aircraft.

The author of this text book highly appreciates the contribution to preparation and issue of this textbook made by the specialists and experts of the CAD/CAM/CAE scientific and research center of KhAI, ANTONOV ASTC, TsAGI, KhAI aircraft and helicopter design department, AST limited liability company “KNK”.

Section 1
DESCRIPTION OF PROBLEM IN DESIGNING OF AIRCRAFT ASSEMBLY STRUCTURES WITH ASSIGNED SERVICE LIFE

1.1. Analysis of methods in designing of aircraft assembly structures

To design means to create and to make something new. Designing often results in creation of an item providing profit earning. Engineering designing is a continuous process when scientific and technological information is used for creation of a new system, new device or a fabrication process being of public benefit.

Design skill is a science and an art at the same time. Designing as a science can be mastered by systematic knowledge acquisition, innovation activity, accumulation of experience and solution of problems. As an art designing requires hard work from those who wants to become proficient in it. Provision is made in designing for the use of analysis and synthesis in designing process. The science and the art, the analysis and synthesis are integral being developed simultaneously [191, 457]. In the process of designing technical publications are the subject of development to provide industrial manufacturing of a new compatible airplane meeting desired requirements and its reliable operation under specified conditions. The purpose of engineering design lies in development and creation of new objects, processes or systems nonexistent in the past. Though this purpose can be achieved using known principles or elements as the base, an imaginative search for a new, original means is always required to combine these elements and processes which would result in attaining new qualitative or quantitative results [6, 194, 195, 225, 300, 301].

Two principles can be used in design: evolutionary modifications and creation of something brand new. In the first case, the article is modified over some definite time by the introduction of minor improvements. As this takes place, it is not risky to make some significant mistake.

Breakthrough in scientific and engineering discoveries, the total time history of public development brought to the fore the problem of creating the articles which are based on the new technical approach. This way of designing presents a considerable challenge. Practically, in correspondence to the dialectics of design, evolutionary changes and appearance of something new are simultaneously in progress, that is to say, a designer creates something new and provides evolutionary changes at one time (at the same time – ed). To realize such approach in designing of aircraft, some definite stage of aviation development was found to be essential in accumulation of experience and facts, generalization of these data to the system of knowledge – that is to say, to the science in designing of a new type of equipment, facilities and machinery [51, 194, 268].

This time history is characterized by the development of the methodology in designing of aircraft. Methodology of designing implies a combination of principles, techniques and procedures as well as a body of mathematics used for solving the project and design problems [194, 327]. Let us consider the way of development of the design methods by the example of problem solution in selection of the design parameters, which specify a configuration and dimension of an aircraft. First of all, it should be noted that all design methods are combined by a single principle of successive approximation (iteration method). This principle describes a general approach (irrespective of the design method) to solve the design problems. It has a sense in solving the complex of the design problems successively by the use of the clarifying and progressing approximations (iterations) complementing each other [322, 327].

The basis for the designing of the first airplanes is a copying method (similitude method) that leans mainly upon the analogous laws. Lacking sufficient experience to design and without knowledge of the aerodynamic flight laws, the designers created the airplanes copying configuration of the birds and night bats…

A lot of designs of heavier-than-air aircraft have been developed [24].

In the 20-s of the XX century when a considerable experience and knowledge in development and construction of the first aircraft and gliders were accumulated and when acrial locomotion sciences (mainly, breakthrough of aerodynamic development) allowed to establish the main links between the aircraft configuration and dimension and its performance, the copying method was replaced by what is known as a statistical technique (method). Some scientific approaches already lie at the heart of this method that has its origin in estimation of the previous experience and establishment of the empirical trial-and-error regularities demonstrating the normal design laws. According to this method, the parameters of a new aircraft are determined on the basis of extrapolation of the statistically processed data of the previously created aircraft with the similar purpose (prototype airplane). This method is based on the assumption that some parameters and performance of the definite type aircraft are a subject of continuous and smooth change with the passage of time. But extrapolation of parameters and performance due to a great time required for creation of the up-to-date aircraft (six – ten years) under conditions of the scientific and technological revolution may result in essential and fundamental errors. Disadvantage of this method lies in the fact that it does not make any allowance for the change of physical links between the aircraft parameters and performance and consequently determine the way of changing these prototypes. Clearly, the application of this method is justified only in the use of the trial-and-error (evolutionary) principle of designing. When a radically new aircraft is under designing, the possibilities of such method are limited. But the experience of aircraft industry testifies that just few projects can be accepted as brand new and even under their development a

considerable number of technical concepts are taken on the basis of the past experience. For this reason, the statistical method just as before is partially or totally used by designers and it has been transformed in the so-called method of design from prototype.

Subsequent development of methods for calculation of aerodynamic and weight characteristics, stability and controllability, aircraft efficiency values forms the actual basis for the development of the analytical methods in determination of its main design parameters.

These methods lean upon the simultaneous solution of a set of equations that incorporate the most important links between the parameters and the characteristics of the aircraft as well as different types of limitations. As a result of such decision, the search for the acceptable project version is in progress (from the standpoint of satisfying the equation of the aircraft existence) [23, 33, 36, 40, 44, 76, 259, 294, 300, 301].

Application of the analytical methods offers strong possibility for the conduction of the parametric researches in determination of influence produced by the change of the design parameters and limitations on the aircraft technical and operating characteristics. Hence, one step on the road to the solution of problems in searching of the most feasible (optimal) aircraft parameters, which meet criteria selected in estimation of the design advantages.

This stimulated the development of what is known as methods of optimal design of the aircraft. The first investigations in presenting the methods of optimal design made its appearance in the late 1930 s. Practical realization of the optimal design methods for a long time became more complicated because of just computation problems, especially, in solving the multiparametric problems.

Application of the sequential optimization of certain parameters has met with only limited success. The essential prerequisites for the subsequent development of the aircraft design theory appeared around 1960. The most essential are as follows:

– development of the general theory of the complicated technical systems (system engineering);

– development of the applied aeronautical researches that reveal the sense of the phenomenon specifying the laws of aircraft and its systems configuration, layout and arrangement.

– substantial progress toward mathematics, primarily, theory of optimization and numerical methods;

– the appearance and development of the electronic computer systems.

An analytical method in determination of the turboprop transport airplane parameters at the conceptual design stage when an aircraft take-off weight is taken as a criterion of optimality and the desired technical and airworthiness requirements as limitations is illustrated in Fig. 1.1 having been developed and detailed in the papers [300, 301].

Purpose:
find such vector of aircraft parameters ($x=x_1, x_2,...x_n$), that specifies its structure, configuration and size (aircraft layout, engine installation arrangement *PP*, S, R_0, t_0, C_y, K, S_{vp}, $\bar{S}_{tp}$, D_f, λ_f, λ_w, χ_w, $\bar{c}_w$, b_0, η), to meet philosophy requirements in creation of a new aircraft, technical assignment for designing [*Y*] and achievement of criterion function extremium (γ).

Fundamental relationship of aircraft physical realizability (aircraft existence equation)

$$1.\sum \bar{m}_i = 1; \quad 2.\ n_y mg = Y; \quad 3.\ P - X - m\frac{dV}{dT} = 0; \quad 4.\ \bar{x}_T - \bar{x}_F = -m_z^{C_y}; \quad 5.\sum m_i z_i = 0.$$

Aircraft parameters *X* and its characteristics *Y* are limited by a set of constrains

$$\left.\begin{aligned} x_i^n \le x_i \le x_i^e, i = 1,2,...,m \\ y_j^n \le y_j(x) \le y_j^e, j = 1,2,...,n \end{aligned}\right\}.$$

Optimization problem is solved for the specified constraints: $min\gamma\ (x)$, $x \in x_{add}$.
Aircraft parameters and characteristics are interrelated by the relationship equation $Y=f(x)$:

$$t_{0cruise} = \frac{1{,}429 \cdot 10^{-5} \rho_H V_{cruise}^3 \left(F_{1cruise} + F_{2cruise} p\right)}{\xi_V \xi_H \xi_{\partial p} \eta_{e.cruise} p};$$

$$V_{cruise} = 11{,}4473 \sqrt{\frac{\xi_{cruise} t_0 p \eta_{e.cruise}}{\rho_{Hcruise} C_{x0}}};$$

$$t_{0p} = \frac{0{,}04}{\xi_{take\,off} \eta_{e.neg}} \sqrt{\frac{p}{C_{yneg}}} \left[\frac{0{,}832\,p}{L_p C_{yneg}} + \frac{1}{3}\left(\frac{1}{K_{neg}} + 2f\right)\right];$$

$$L_{run} = \frac{0{,}832\,p}{C_{yneg}\left[24{,}75 \eta_{e.take\,off} \xi_{take\,off} t_0 \sqrt{\frac{C_{yneg}}{p}} - \frac{1}{3}\left(\frac{1}{K_{neg}} + 2f\right)\right]};$$

$$t_{0runway} = \frac{n_{dv}}{\xi_{take\,off}(n_{dv} - 1)} \frac{0{,}03 L_{runway} C_{yneg} + 0{,}57\,p}{L_{runway} C_{yneg} - 2{,}04\,p};$$

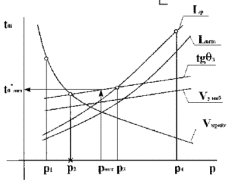

$$L = 1020 \frac{KM}{c_e} ln \frac{m_0}{m_к};$$

$$t_{0\theta} = \frac{0{,}04 n_{dv}}{\xi_{take\,off} \eta_{e.dv} (n - 1)} \sqrt{\frac{p}{C_{yneg}}} \left(\frac{1}{K_{neg}} + tg\theta_3\right);$$

$$p_{slat}^{V_{land}} = \frac{V_{land}^2 C_{yland}}{183\left(1 - 0{,}8 \bar{m}_{mcp}\right)};$$

$$t_{0V_y} = \frac{0{,}01}{\xi_{take\,off} \eta_{e.neg}} \left[7{,}02 \sqrt[4]{A^3 p^2 \left(F_{1climb} + F_{2climb} p\right)} + V_y\right];$$

$$K = C_{yneg} / C_{xneg};$$

$$p_{slat}^{n_y} = \frac{57{,}3 C_y^{\alpha} VW}{16}.$$

Aircraft take off weight is taken for criterion of optimality:

$$m_0 = \frac{m_{eqv} + m_{eqp} + m_{com}}{1 - \left(\bar{m}_k(p) + \bar{m}_{pp}(p) + \bar{m}_m(p)\right)};$$

$$\bar{m}_к = 0{,}5\left(A - Bp + \frac{c}{1 - De^{-0{,}001p}}\right);$$

$$\bar{m}_{pp} = R_{dv} t_{0max}(p);$$

$$\bar{m}_{m.cruise} = 0{,}00602 \frac{C_e I_{cons} \sqrt{A C_{x0cruise}}}{\eta_{e.cruise}};$$

$$m_{eq} = 95 n_{pass}\left(5 \cdot 10^{-5} L + 0{,}66\right).$$

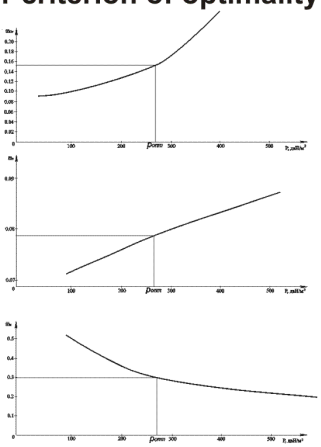

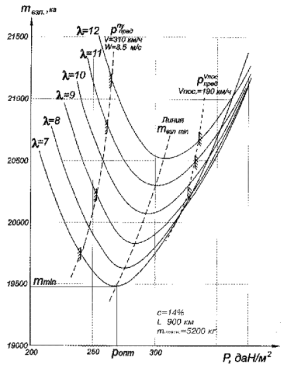

Selection of aircraft geometrical parameters:

$$S = \frac{m_{0\,min} g}{10 p_{opt}}; \quad \ell = \sqrt{\lambda_{opt} S}; \quad b_к = \frac{2S}{\ell(\eta + 1)}; \quad b_0 = \eta b_к; \quad L_f = \lambda_f D_f; \quad S_{tp} = \bar{S}_{tp} S; \quad S_{vp} = \bar{S}_{vp} S.$$

Fig. 1.1. Analytical method in determination of transport airplane parameters at conceptual design stage

Following accumulation of experience in solving the different optimization problems of some aircraft components, wider use of the electronic computers to solve these problems, the number of the parameters involved in the process of simultaneous optimization was progressively increased. Criteria for estimation of the design solutions were sophisticated in the direction of taking into account a multipurpose nature of the aircraft use and the time history of requirements to the airplane while in operation [37-39, 52, 54, 77-79, 80, 86, 89].

Besides, the general design theory of large systems has been under development around which the theory and practice of aircraft designing acquire gradually a logical completion providing the true scientific approach to the prediction of the future aircraft parameters and characteristics. The ideas of the system design have been intuitionally used in designing of aircraft before. They were embodied in separation of the design process into stages and division of an aircraft into sub-systems and units. System design leans upon a well defined, all-round approach involving complicated relation and interaction between the system components with optimization method as a constituent part included.

They differ from a widely accepted optimization procedures of some facilities and characteristics of the systems by the application of the system, all-round (generalized), in particular, optimization criteria, the use of the mathematical model describing significant system properties as a whole, a body of mathematics, wide use of electronic computers [238, 271, 273, 281, 305, 320, 323-325, 417].

The second half of the XX century is characterized by the radical changes in the field of the human being labour activity. Just as the industrial revolution has been related to the change-over from a manual labour to the mechanized one, so the scientific and technical revolution is associated with the switch to the automated production. Wider promotion of the automated production processes on the basis of the electronic computer facilities, microelectronics and robotics is an important line of the scientific revolution.

Significant results have been achieved in solving such complicated and integrated problem as the automation of the design and research works. In the second half of the XX-th century the computer-aided design systems (CAD) were created, developed and found wide application in the scientific-research centres and design offices. Their appearance became possible due to the development of the design theoretical backgrounds, progress in the field of the calculus mathematics, programming and computer engineering [1, 2, 4, 8-10, 17, 60, 194, 351, 419, 428, 470, 472, 473].

As far as this moment is concerned, the automatic computer-aided design systems allowed to implement widely the following most essential computer design capabilities:

– fast and efficient performance of a great number of mathematical operations;

– storage and transmission of a great scope of information;

– visualizing of the design results (both final and intermediary) by the use of the computer graphics techniques;

– communication between a designer and a computer in dialog mode to provide continuity of the design constructive process;

– comfortable and efficient transmission of the design results directly to production (for fabrication of the design object).

In such systems, in addition to the remarkable capability to automate calculations, the computer turns into consolidation means to achieve a common objective of the professionals in the different fields of designing. This integration basing on the generalization of the methodological, information provision, hardware and collective dialogue of the computer users allows to remove obstacles of narrow specialization of the engineers who take part in the development of the up-to-date complicated systems with the aviation ones included.

According to the publications [51, 53, 273, 353], the application of the automatic computer-aided design systems at the end of the XX-th century allowed to cut the design time and aircraft development by two-three times and preproduction period by three-five times.

In this case, the development costs are reduced by 50-80%. But in this case, just as in the event of the application of the analytical design methods and procedures, the general designing resulted in development of: an aircraft outline drawing (Fig. 1.2), theoretical drawings of aircraft units and components (Fig. 1.3), exploded view diagram and etc, performed by using the methods of the descriptive geometry.

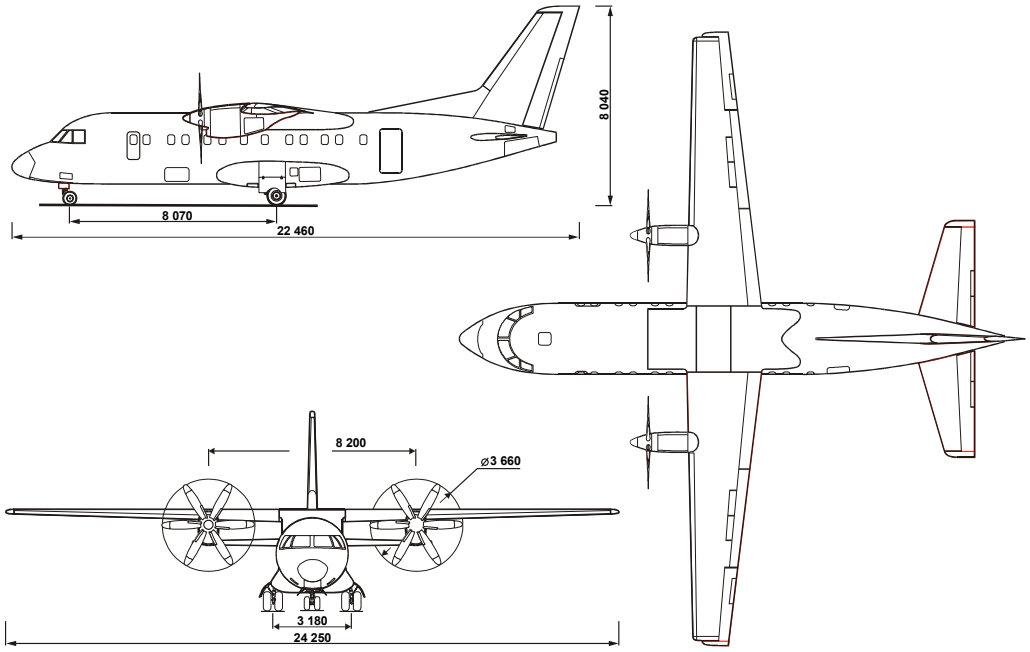

Fig. 1.2. Outline drawing fragment

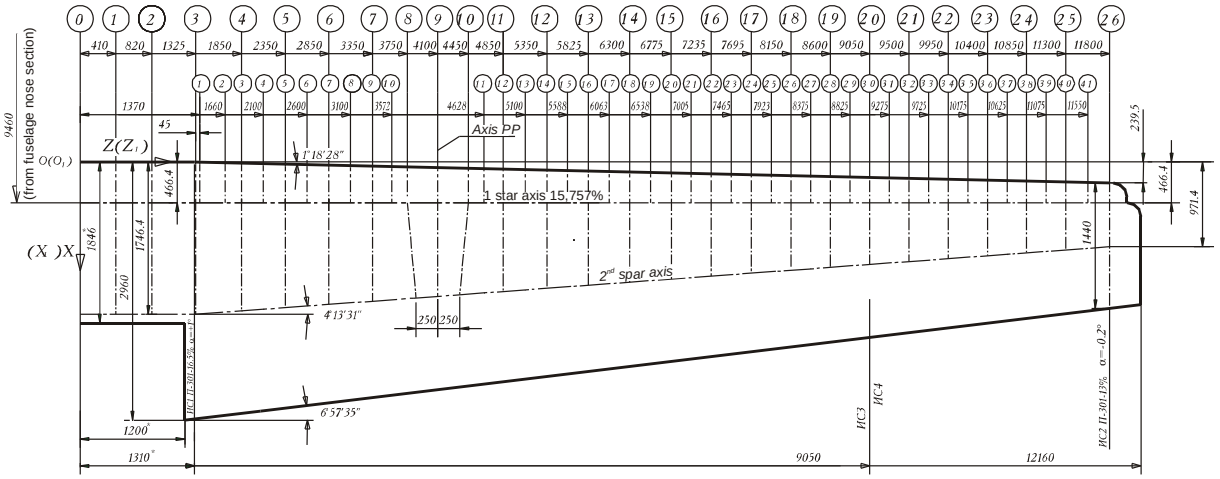

Fig. 1.3. Wing theoretical drawing fragment

So, the application of the automatic computer-aided design systems allowed at that moment in time to provide an improvement of the articles and items designed, shortening of the design cycle, that is, increase of labour productivity and appeared to be an essential factor in speeding-up of the scientific and technical progress but did not completely provide integration of the article/item design process and process engineering as wall as an engineering analysis [190, 211, 258, 261, 331, 351 460, 461, 465].

The more complicated designer's tools are used, the higher designer's qualification must be.

The automatic computer-aided design ACAD systems made new, advanced demands to the qualification and training of the aircraft indusrty mechanical engineers both in the fields of acquiring methods of automated designing (that allows to set correctly, to describe formally and to solve research and design problems) and exploring the possibilities and peculiarities in operation of the advanced design engineering tools and softwares. But at the same time, ACAD system was grounded on two-dimensional model in designing aircraft assembly structures and made any allowances for the design philosophy of the new types of the assembly structure joints and the advanced fasteners, their new attachment techniques, assembly procedures, preloading effect to the characteristics of the local deflected mode (mode of deformation) and fatigue resistance, peculiarities of their contact interaction, capabilities of the fatigue crack growth delay methods. It didn't allow designing assembly structures and their attaching parts providing optimal relationship of the weight (mass), life, aerodynamic and aesthetic characteristics of the aircraft structures. The aviation technical publications were developed using the descriptive geometry methods and presented for the aircraft production on the paper carriers. Integration of the design was performed using the design lofts that did not always allow to identify faults caused by the imperfection of the design methods and underlying design documents [211].

The development of the information technologies made it possible to solve some problems in design of the aircraft assembly structures. An aircraft exploded view drawing that involves a great number of assembly structures is illustrated in Fig. 1.4. But because of the multifactor current task and as a result, the necessity of different specialists involvement (strength engineers, designers, process engineers, operators), the integration of their efforts to solve the problem in creation of the aircraft assembly structures was not succeeded.

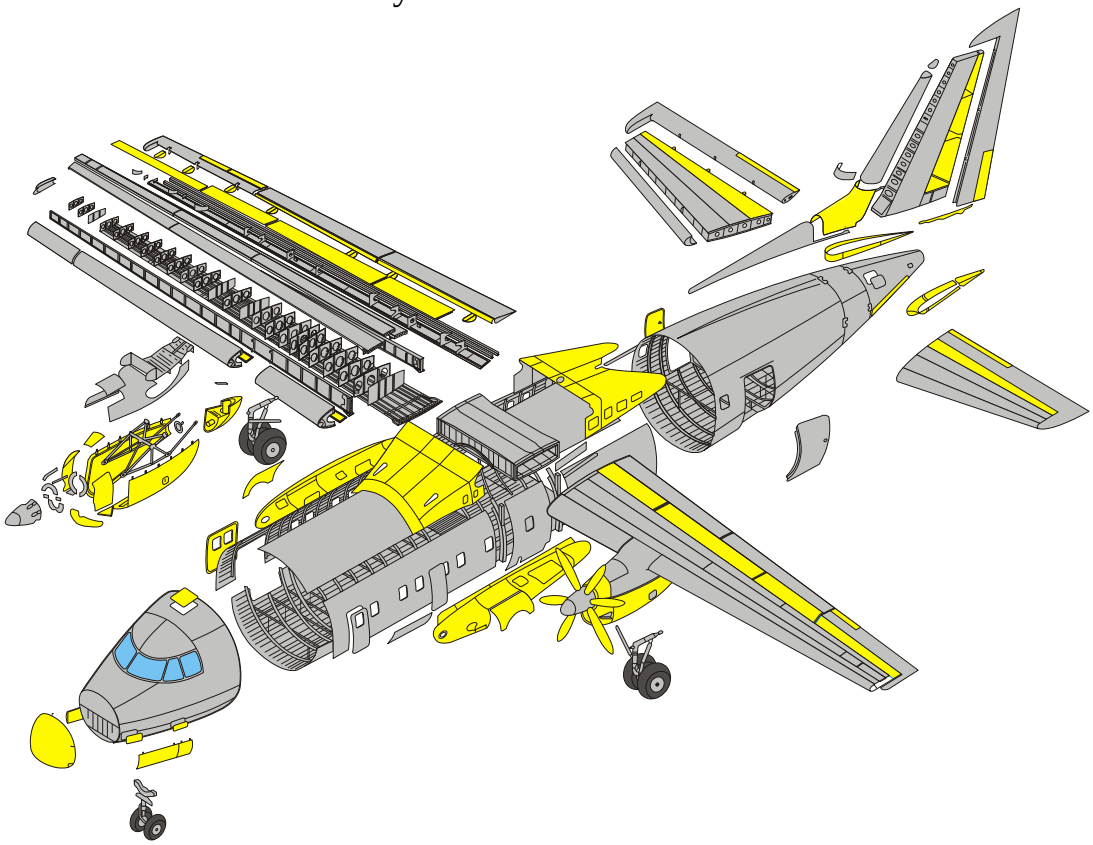

Fig. 1.4. Aircraft exploded view drawing

Everything mentioned-above resulted in need for creation of a new design methodology that must involve the new methods and procedures of aircraft structure designing, preproduction, test and operation.

The new method must be an integrated method of the aircraft assembly structures designing and modelling with the aid of the CAD/CAM/CAE/PLM computer integrated system basing on the development of the three-dimensional analytical master copy of aircraft surface, its components, assembly units, new structural components, fasteners, computer-aided methods of analysis of the three-dimensional local deflected mode in joint member, new procedures in setting the fasteners with the elastoplastic radial interference followed by the experimental computing method in determination of the fatigue life characteristics of the standard joint models. This will make possible to design the assembly structure joints with the specified static strength, fatigue life, air-tightness and

external surface quality characteristics under minimal expenditure of mass.

The integrated design and computer-aided engineering method is today the most advanced one for involving the elements of the earlier developed methods and computer-aided integrated design technologies using CAD/CAM/CAE/PLM systems. The realization of the integrated technologies in the design process was launched under

Design methods are schematically presented in Table 1.1.

Table 1.1

Aircraft assembly structures design methods

<table>
<tr><td colspan="3">Principle of successive approximations (iteration)</td></tr>
<tr><td colspan="2">Indirect methods</td><td>Direct methods</td></tr>
<tr><td>Form-copying method</td><td>Statistical method</td><td>Analytical methods</td></tr>
<tr><td colspan="3">Optimal design methods</td></tr>
<tr><td colspan="3">Computer-aided design</td></tr>
<tr><td colspan="3">Engineering methods</td></tr>
</table>

Development of AN-140, AN-74TK-300, AN-148 aircraft. But the design techniques of the aeronautical engineering object require further scientific and practical development.

1.2. Analysis of design techniques with account taken for fatigue of shear bolted joints of aircraft assembly structures with assigned service life

It is known that the service life of the aircraft structures is determined by the service life of its structural components to be significantly dependent on the working life of the bolted joints (Fig. 1.5) being the sources of the fatigue crack initiation caused by both constructive stress concentration and the development of the fretting corrosion (Fig. 1.6). Standard fatigue failure analysis and wing joints working life data obtained as a result of tests conducted in TsAGI (ЦАГИ) are illustrated in Fig. 1.7. It has been established that the working life of the crosswise joints is within the limits of the plate with a hole. It has been also established, that installation of bolts in the holes of the joint parts with axial and radial interference is one of the best efficient means to enhance the fatigue life of the shear bolted joints [26-32, 34, 42, 47, 48, 50, 56, 62, 63, 66, 81, 85, 122, 123, 149, 180-182, 184, 197, 216, 220, 257, 280, 420, 426, 440, 441, 468]. But, the theoretical justification of this phenomenon has not been presented.

The accumulated information showing influence of the joint working life enhancement procedures by change of the design-technological parameters under

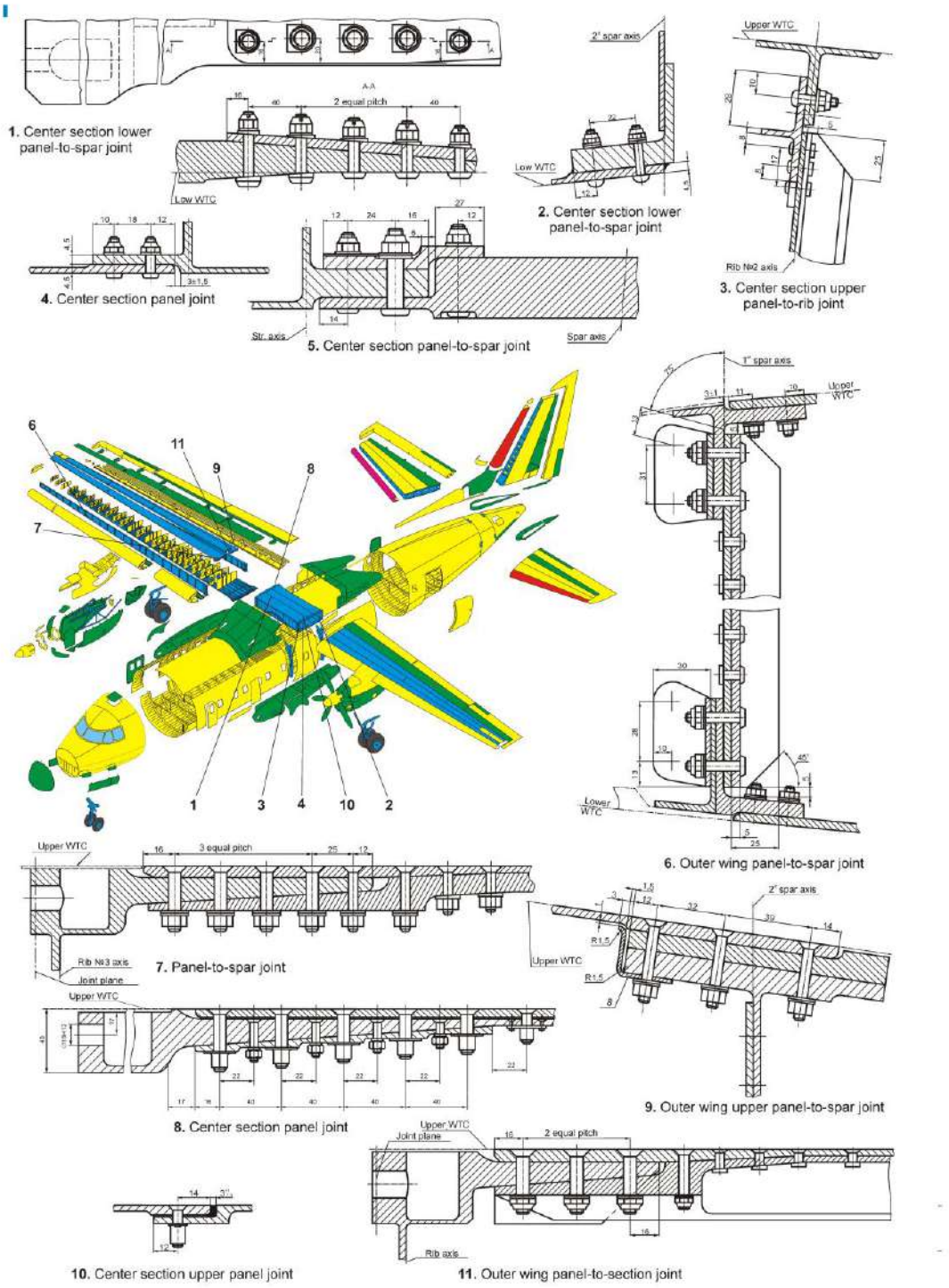

Fig. 1.5. Aircraft airframe. Aircraft assembly structures. Typical bolted joints

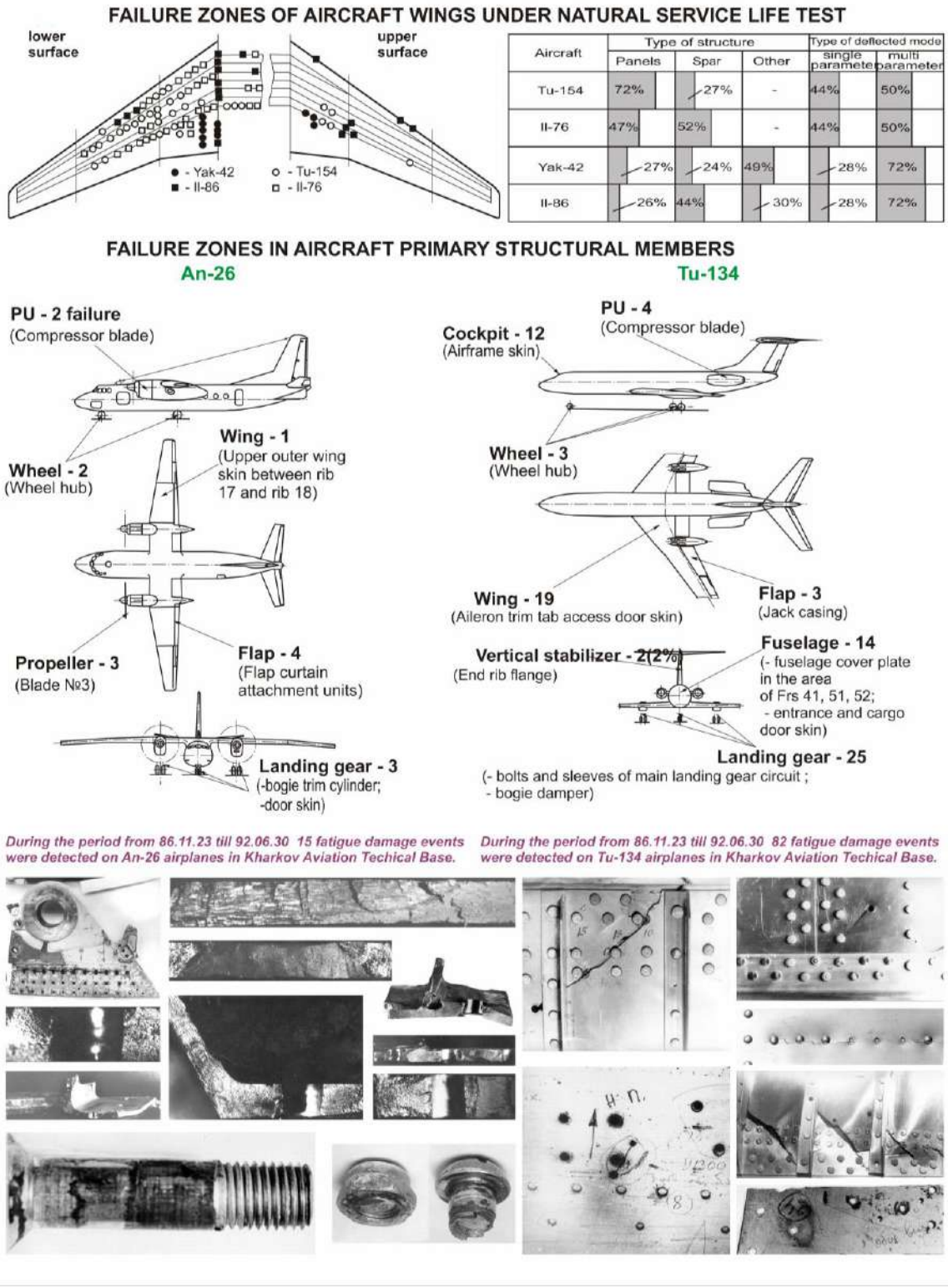

Fig. 1.6. Aircraft primary structure under operation and service life test. Fatigue failure zones and patterns

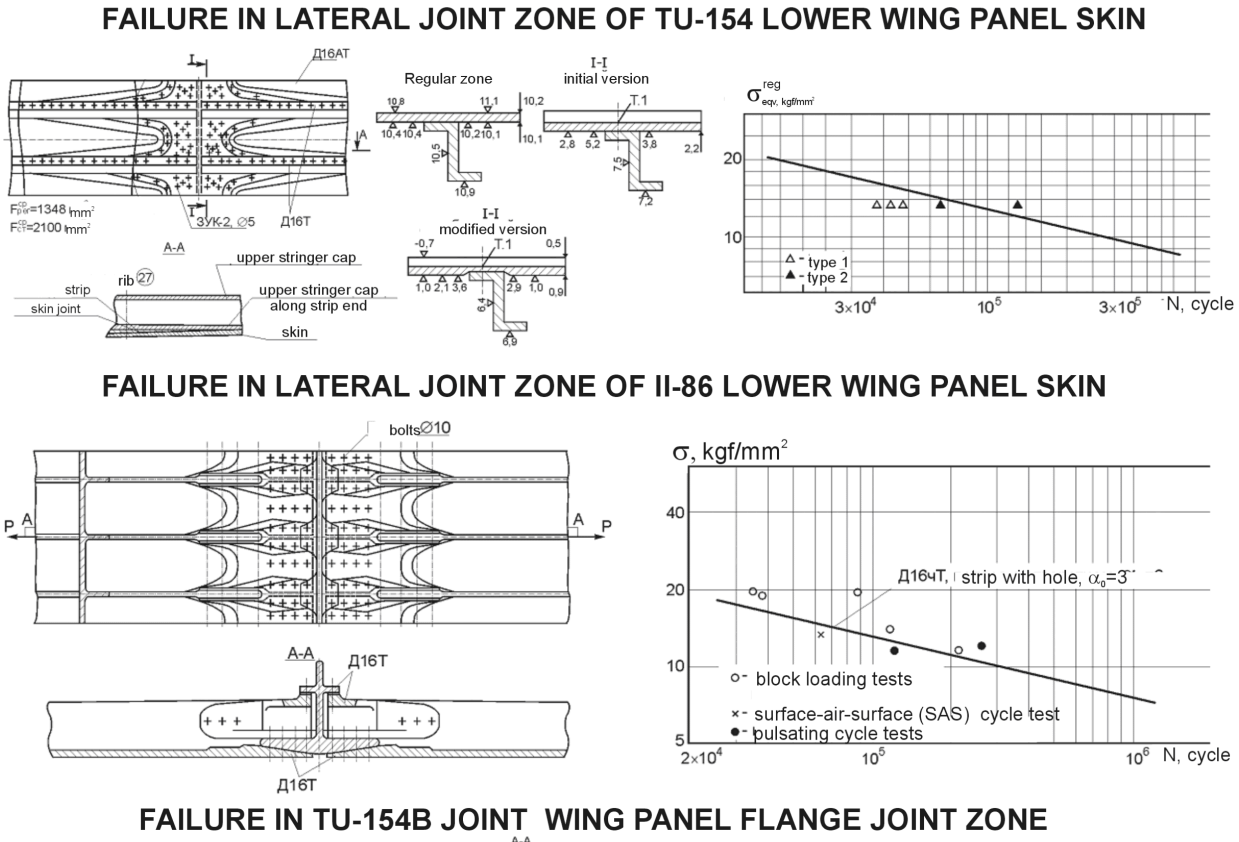

Fig. 1.7. Typical fatigue failures and service life analysis
(by reference to TsAGI materials) wing joints

their implementation carries a statistical nature that favors the development of the new service life calculating methods with the account taken for the design technological peculiarities in making the bolted joints and structural irregularities [104, 108, 111, 113, 117, 120, 124, 129, 131, 133, 144, 154, 156, 345-348].

The design methods of the shear bolted joints of the aircraft structure with the allowance made for the fatigue can be conventionally divided into three groups:

1) design methods used to provide a static capacity of the joints in calculation with reference to the directive stresses;

2) methods where the theoretical and efficient coefficients of the stress concentration are used.

3) methods based on determination of the actual stress and deformation values in the most loaded stress point.

Three fundamental principles must be adhered in creation of the structure to provide its safety with reference to the strength conditions: damage admissibility, destruction safety (damage) and safe life (service life). In this case, the estimation of the strength characteristics, parts design and quality of manufacture must provide and certify that the catastrophic failure because of the fatigue, corrosion or inadvertent damage will not occur within the total service life of an aircraft [345, 346].

Therefore, the assignment of the tolerable stresses under design of aircraft structures to obtain optimal characteristics of the structure mass, its strength and life time alongside with the correct selection of the design and material to be made of is one of the most essential problems [64]:

– under compression $\sigma_{tol} \le \sigma_{crit}$;

– under tension $\sigma_{tol} = K_1 \sigma_{ult}$; $K_1 = 0{,}93$,

Where σ_{ult} – material ultimate tensile strength; K_1 – stress concentration sensitivity coefficient of material, out of which the structure is made.

The representative load spectrum in operation must be determined for every structural component to specify the tolerable stresses of the regular zone on the assumption of the fatigue life support. This spectrum is based on the type flights involving all flight conditions (towing, taxiing to take off position, engine ground test, running, climbing, cruising flight, descending, landing approach, landing run and taxiing in for parking with an allowance for their duration and combination of other parameters specifying every condition listed-above). The type flight is translated according to the known dependence to the equivalent fatigue cycle with reference to the damageability. Zero-to-tension stress cycle is taken for the prime structure of the aircraft airframe (with the stress ratio equal to zero). Generally, the recalculation of the fatigue cycles is performed basing on the equal fatigue life determined by the Oding's formula:

$$\sigma_0 = \sqrt{2 \cdot \sigma_{à} \cdot \sigma_{max}},$$

where σ_0 – zero – to – tension stress cycle, σ_a, σ_{max}– amplitude and maximal fatigue stress cycle.

The calculation of the structural component fatigue life is performed according to the fatigue cycle determined in the first approximation by tolerable stresses on the basis of the static strength conditions. If calculation results meet the required values of the life parameters specified in aircraft performance, revision of the tolerable stresses with regard to the fatigue life conditions is not conducted. If calculation results do not meet the performance requirements with reference to the life, the tolerable stresses come down to provide achievement of the required life characteristics.

It is necessary to use the power dependence of the endurance curve to determine the level reduction rate of the tolerable stresses:

$$N(\sigma_0)^m = const,$$

where N – fatigue life at the level of zero-to-tension stress cycle σ_0; m – exponent of power.

As it is known, an exponent of power is empirically determined for the structural components with the holes fabricated from different materials. For the components from the exponents from the aluminium alloys of type Д16Т, В95, this exponent is close to 4. Hence, a degree of reduction in tolerable stress level in the second approximation for the components made of aluminium alloys can be determined in correspondence with the following formula:

$$K = \sqrt[4]{T_{des} / \grave{O}_{1\text{-}st\ approx.}},$$

where K – tolerable stress reduction coefficient; T_{des} – desired service life; $\grave{O}_{1\text{-}st\ approx.}$ – service life determined in the first approximation.

Then, the level of the tolerable stresses for the 2[d] approximation is as following:

$$[\sigma_0]_2 = [\sigma_0] / K.$$

Reasoning from the given level of the tolerable stresses in the second approximation, the components of the regular structural zone are subjected to reinforcement followed by recalculation of stresses in the typical flight to determine the service life in the second approximation.

In designing and development of the irregular structural zones, their life must be equal to the life of the regular zone or exceed it.

The first design method group of the shear bolted joints of the irregular zones with the provision made for the static strength of the structural components. In shear bolted joints the load P causes the fracture stress σ_{fract}, bearing stress σ_{bear}, shear stress $\tau_{sh.b}$ in the part joints as well as the bolt shear stress in the

fasteners. Tightening forces and breaking loads result in origination of the tensile breaking stresses σ_{fract}. The value of these stresses depends on a value of load materials used and joint geometrical parameter.

The second group of the design methods is based, with an allowance for fatigue, on the equivalence hypothesis of the local maximum stress force at the stress raiser contour under elastic deformation and stress in a test-piece free from the stress raiser. An endurance curve of a smooth test piece or a specimen with the stress raiser known is assumed to be a basic endurance curve. The application of the theoretical stress concentration factor provides low accuracy in estimation of the fatigue life of the full scale structures to be feasible at the predesign stage. Empirical correction coefficients reflecting design, structural and assembly procedure features [126, 220, 234, 402, 409, 456] are entered to conform calculation and experimental data. In this case, the principle of the superposition of the solutions with the separation of loads applied to the sheet and accepted by the fastener [186] is used in the joints for the calculation of the stress concentration factors:

$$\sigma_{loc} = \alpha\beta\left(K_1 \frac{\Delta P}{dS}\theta_\sigma + K_2 \frac{P}{WS} \right),$$

where K_1 – stress concentration factor with respect to the reference misshape caused by the force P; K_2 – stress concentration factor in regular cross-section caused by a force flowing about a force point; d – hole diameter; S – – sheet thickness; α – coefficient accounting a hole manufacturing technique, surface roughness and cold work hardening residual stresses; β – hole occupation ratio considering interference between the fastener and the hole; θ_σ – coefficient accounting local stress increase caused by the fastener deformation.

The values of the required stress concentration factors have been determined under solving the problem in elastic problem formulation. In aircraft structure joints an elastoplastic deformation is originated in the part joints under installation of the fasteners that requires application of the finite element method for the analysis of the local deflected mode (mode of deformation) implemented in the advanced certified CAD/CAE systems. The method of forces, design procedures and experimental techniques are used to determine with the use of the Swift formula [84, 446].

This method of compliance determination requires considerable experiment costs while the analytical expressions specify the experiments under joint elastic loading with any allowance made for the installation of the hardware parts. The estimation of the force distribution with reference to joints coupling is performed by application of the schematization of the jointed members using the rods or a method of finite elements (FEA). Though an accuracy of service life estimation with the use of the second group methods is upgraded, the determination of the number of cycles prior to failure of the full– scale joints would prefer to perform on

the basis of the statistical material using this method just as the foundation for the identification of the critical areas of the elements and components and for design but not for the estimation of the joints service life.

The third group of the design methods is based on the equivalence hypothesis of the deflected mode in the most loaded point of the raiser (concentrator) and a smooth test-piece for the fixed amount of the cycles prior to crack formation. The estimation is based on the actual values (with plasticity taken into account) of the stresses and deformations with the allowance made for their change under cyclic change of loads [59, 409, 438, 439, 450].

The fatigue curve of the smooth test-piece and the cyclic diagrams of the elastoplastic deformation are used for estimation.

The analysis of the design methods of the assembly structures with the fatigue taken into account (Fig 1.8) demonstrates that further development of the forecast methods of the design and processing factor influences on the endurance of the bolted joints is required to provide their service life.

At the present time, design methods using service life estimation of the aircraft structural components, deformation and energy criteria as the base and assuming occurrence of the material limiting stage determined by deformation critical value (its total or inelastic component) or irreversible dissipated energy are under development. For example, in study (450) a value of dissipated energy per cycle determined by the amplitude of the stresses and residual deformations in the stress concentration zone is considered to be the main parameter specifying the moment of the crack origination:

$$N = \frac{1}{W_{rd}^{\alpha} R_m},$$

where $R_m = R\left(1 - r\left(\sigma_m / \sigma_{ult}\right)\right)$.

The authors confirmed reliability of the proposed method in estimation of the connection fatigue endurance performed according to slide assembly under low-cycle loading.

The service life of the aircraft structural components is also dependent on the accumulated residual plastic or elastic deformation:

$$\left(\Delta\varepsilon_{plast}\right) N^{\underset{\alpha=0.6}{\alpha}} = const; \qquad \left(\Delta\varepsilon_{elast}\right) N^{\underset{\beta=0.12}{\beta}} = const.$$

The experimental-calculated dependence [25] developed by the author is used to account for the fretting corrosion influence on the service life of the connection a long the joint face (Fig. 1.9).

$$\sigma_{afr} = 2.344\left(\sigma_{â} - \sigma_{mfr}\right)^{0,63} \cdot \left[0,64 + 43,3\left(lg\, N\right)^{-2,1}\right] - \\ - 4.068\left(lg\, N\right)^{0,918 K_{coat}} \sigma_c^{0,32} K_{ò}\, K_{fc}, \qquad (1.1)$$

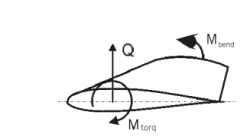

Determination of design loads, typical flight loads and their equivalent zero cycle

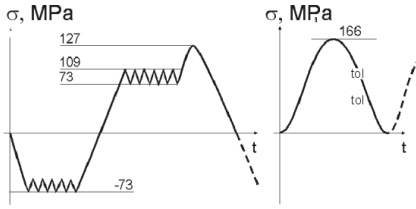

Typical flight and equivalent zero cycle

$$\sigma_{0eqv} = \begin{cases} \sqrt{2\sigma_a\sigma_{max}} & \sigma_m \geq 0; \\ \sqrt{2}(\sigma_a + 0{,}2\sigma_m), & \sigma_m \leq 0 \text{ and } \sigma_{max} \geq 0; \\ 0 & \sigma_{max} < 0. \end{cases}$$

$$\sigma_{0eqv} = \sqrt[4]{\sum_{i=1}^{k} n_i \cdot \sigma_{0i}^4}.$$

Determination of the geometrical parameters provided that structural static strength is reached:

undercompression $\sigma_{tol} \leq \sigma_{crit}$,

under tension $\sigma_{tol} = K_1\sigma_{ult}$, $K_1 = 0{,}93$.

Determination of the regular zone life at the sketch design stage from the equation of the plate endurance curve with a hole:

$$N = \frac{C}{\sigma_{0eqv}^m} \geq N_{given}.$$

Correction of the tolerable stresses lever (2[d]approximation):

$$K_2 = \sqrt[4]{\frac{N_{des}}{N_{1\,apprx}}}; \quad [\sigma_{calc\ 1}]_2 = [\sigma_{calc\ 1}]/K_2.$$

Correction of the regular zone geometrical parameters at the 2[d] approximation stage.

Determination of the geometrical parameters of the aircraft assembly structure joints:

$$P = \frac{\delta \cdot t}{m \cdot n}\sqrt{\sigma^2 + \tau^2} \leq P_{fract} = K_i\sigma_B F_i;$$

$$P_{bear} = \delta d \sigma_{bear\ fract\ loc} \leq P_{fract};$$

$$P_{sh\ loc} = 2H\delta\tau_{sh\ fract\ loc} \leq P_{fract};\ P_{sh} \leq \frac{\pi d^2}{4}\tau_{sh\ fract\ bolt} \cdot n_{bolt}\,\xi \cdot m.$$

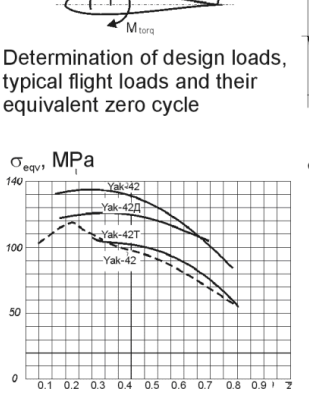

Equivalent stresses on the wing lower surface spanwise for different aircraft

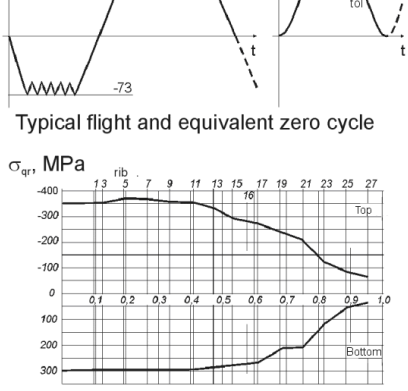

Distribution of the design gross stresses on the lower and upper panels of Yak-42 aircraft wing

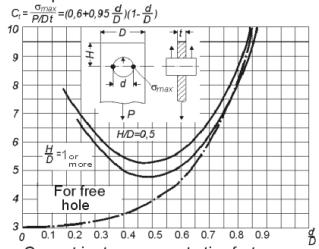

Geometric stress concentration factors for loaded eyes related to the eye gross cross-section

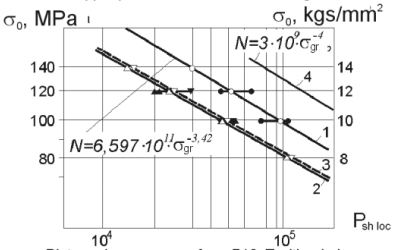

Plate endurance curve from Д16чТ with a hole:
1 - plate as-received condition with a parallel hole;
2 - plate as-received condition with a countersink hole;
3 - plate anodized in HX with a countersink hole;
4 - Il-86 aircraft wing lower panel longitudinal connection;

Determination of the typical joints life according to the techniques known:

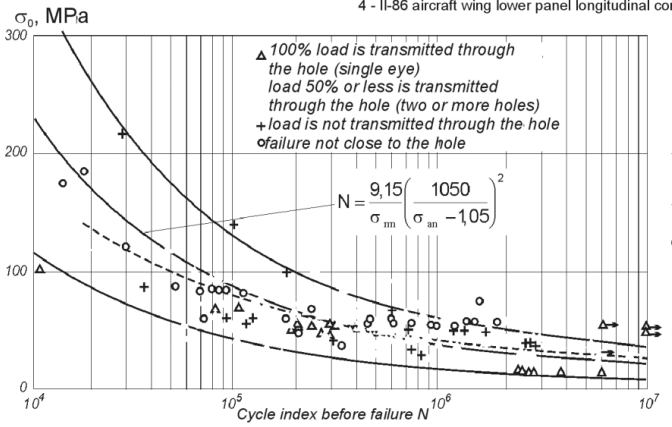

Experimental service life of typical aircraft joints made from aluminum alloys

$$\lg N_{pr} = \left[\frac{\sigma_{apr}}{101{,}505(\sigma_{ult} - \sigma_{mpr})^{0{,}63}} - 0{,}01478\right]^{-0{,}47619}, \quad R_f = \frac{C}{\varepsilon_{eqv}^m},$$

$$K_a = \frac{\sigma_a}{\sigma_{an}} = K_s + [0{,}0394K_t(25{,}4 + d)\beta - K_s]\frac{(\lg N)^4}{1000 + (\lg N)^4},$$

$$K_t = 0{,}6 + 0{,}95\frac{D}{d}, \quad K_{eff} = g(K_t - K_s) + K_s,$$

$$K_A = K_\sigma R + K_a(1 - R), \quad C_{T\Pi} = [2 + (1 - \tfrac{d}{D})^3]/(1 - \tfrac{d}{D}),$$

$$\sigma_{afr} = 2{,}344(\sigma_{ult} - \sigma_{mfr})^{0{,}63}\left[0{,}64 + 43{,}3(\lg N)^{-2{,}1}\right] -$$

$$-4{,}068(\lg N)^{0{,}918K_n}\sigma_c^{0{,}32}K_m,$$

$$\sigma_0^*(N) = k_{bear}(N)\sigma_{bear} + k_{loc}\sigma_{loc} + k_{bnd}(N)\sigma_{bnd},$$

$$N = \frac{1}{W_{rd}^{\alpha} R_m}, \quad \text{where} \quad R_m = R\left(1 - r\frac{\sigma_m}{\sigma_{ult}}\right),$$

$$(\Delta\varepsilon_{plast})N^{\alpha} = \underset{\alpha=0{,}6}{\text{const}}, \qquad (\Delta\varepsilon_{elast})N^{\beta} = \underset{\beta=0{,}12}{\text{const}},$$

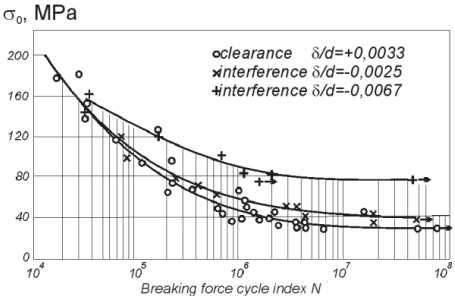

Interference influence on the service life of the eyes from aluminum alloys

$$N_c \geq N_{reg},$$

$$T_i = \frac{N_{bcd}}{\eta} + \frac{N_{wc}}{\eta^T} \geq T_{given},$$

$$\eta = \eta_1 \cdot \eta_2 \cdot \eta_3 \cdot \eta_4 \cdot \eta_5 \geq 6; \quad \eta_T \geq 2.$$

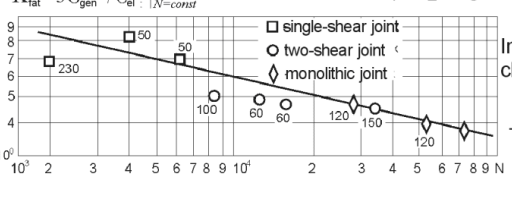

Fatigue ratio-to-service life dependence on the joint type

Influence of loading condition change on the service life:

$$\frac{N'}{N''} = \frac{\sigma''_{mn}}{\sigma'_{mn}}\left(\frac{\sigma''_{an} - 1{,}05}{\sigma'_{an} - 1{,}05}\right)^2.$$

Fig. 1.8. Analysis of design methods of assembly structures with fatigue taken into account

a) CONTACT PRESSURE INFLUENCE ON THE PLATE LIFE

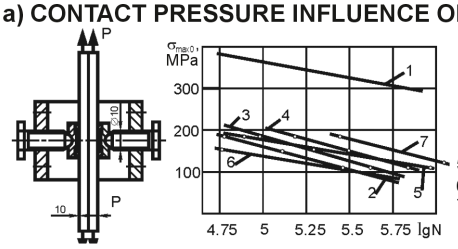

1 - smooth plate, Д16АТmaterial
2 - clad plate, σ_c = 91 MPa, washer material 30ХГСА;
3 - clad plane, σ_c = 45,5 MPa;
4 - clad+anodized σ_c = 91 MPa;
5 - clad+anodized+ФЛ-86, σ_c = 91 MPa;
6 - plate with free hole;
7 - plate with a hole filled with a pin fit with interference 1%

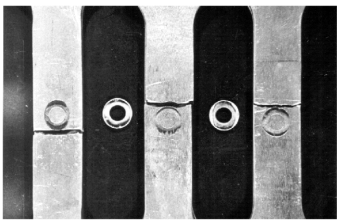

b) MICRODISPLACEMENT INFLUENCE ON FLAT PLATE LIFE

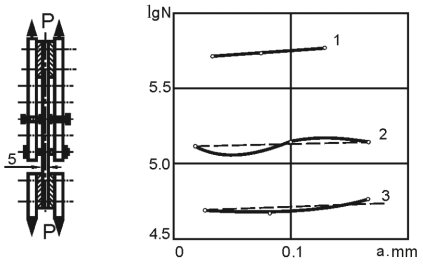

1 - σ_{max0} = 113,8 MPa;
2 - σ_{max0} = 151,8 MPa;
3 - σ_{max0} = 227,6 MPa

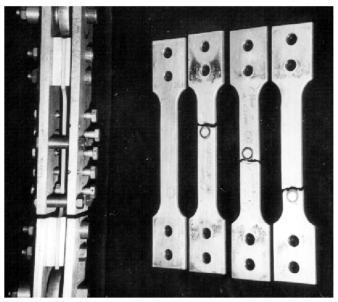

c) AXIAL AND RADIAL INTERFERENCE INFLUENCE ON THE SERVICE LIFE OF THE PLATE WITH A HOLE

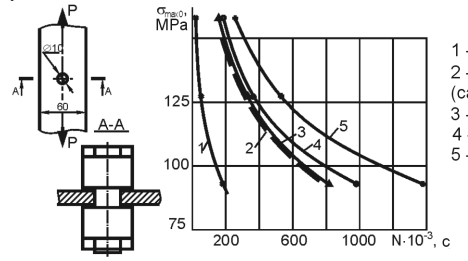

1 - without tightening and interference (A);
2 - with tightening free of interference (calculation);
3 - with tightening free of interference (B);
4 - with tightening and interference (C);
5 - with tightening with interference (D)

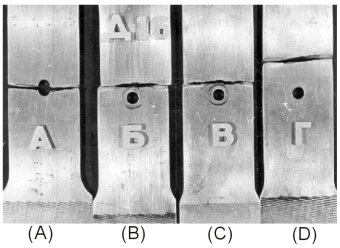

d) CONTACT AREA AND TIGHTENING INFLUENCE ON THE SERVICE LIFE OF THE TWO SHEAR CONNECTION

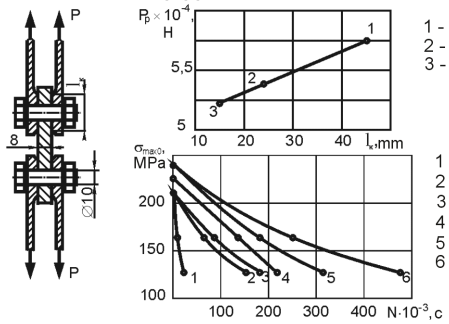

1 - l_c = 44 mm;
2 - l_c = 24 mm;
3 - l_c = 14 mm

1 - smooth sample M_t = 0 Nm;
2 - reduced contact area - l_c = 14 mm, M_t = 20 Nm;
3 - reduced contact area - l_c = 14 mm, M_t = 30 Nm;
4 - reduced contact area - l_c = 24 mm, M_t = 20 Nm;
5 - smooth sample M_t = 20 Nm;
6 - smooth sample M_t = 20 Nm;

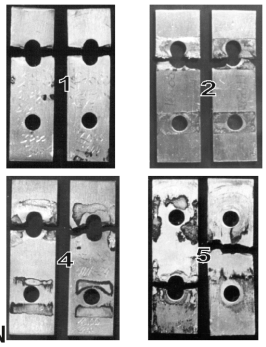

e) COATINGS INFLUENCE ON THE SERVICE LIFE OF THE SINGLE SHEAR CONNECTION

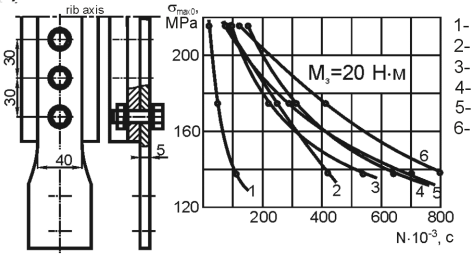

1- clad without tightening
2- with tightening, clad layer removed;
3- with tightening, anodized;
4- with tightening, clad;
5- with tightening, anodized+ФЛ-086;
6- with tightening, anodized+ФЛ-086+ЗП-3

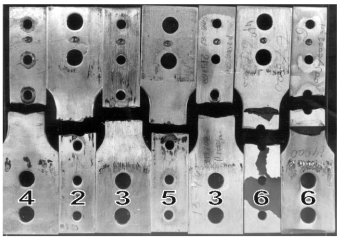

$$\sigma_{afr} = 2.344(\sigma_{ult} - \sigma_{mfr})^{0,63}[0.64 + 43.3(\lg N)^{-2,1}] - 4.068(\lg N)^{0,918K_{coat}}\sigma_c^{0,32}K_m K_{fc}$$

Fig. 1.9. Contact pressure, microdisplacement, design-processing factors influence on the service life of structural components of the assembly structure bolted joints under fretting-corrosion conditions

where σ_{afr} and σ_{mfr} – respectively, amplitude and mean value of cyclic nominal tension stresses in the structural components in the fretting corrosion zone, MPa; σ_{ult} – aluminium alloy ultimate stress limit, MPa; σ_c – contact stress in fretting corrosion zone; K_{coat} – coefficient accounting coating influence on reduction of the amplitude stress values under assigned service life;

K_{coat} = 1 – for clad plate parts, $\hat{E}_{coat}$ = 0.86 – for anodized parts; K_{coat} = 0.89 – for anodized parts and those coated with ФЛ-086 primer; K_m – under contact squared shape; K_m = 1 – under contact squared shape; K_{coat} = 1.36 – under plate-to-washer contact; K_{fc} – coefficient accounting the bolt fit character; under analysis of the joint service life fit with interference and tightening be equal to 0.9… 0.95.

The quality of the structural irregularities is determined by the fatigue ratio used under assigned service life. Should an endurance curve can be easily obtained using the expression $\sigma_{el} = 3\sigma_{spec} / \hat{E}_f$.

Numerous experimental data processing has shown that single – shear joints of the wing panels have $\hat{E}_f$ = 4..5.5, and two-shear joints – 3.5..4, operational single shear connection piece joints have a fatigue quality of 5… 8 and two shear ones have 3… 5.

In estimation of the design quality it is assumed that if $\hat{E}_f < 3$, the structure is considered to be good, if $\hat{E}_f = 3…4$, the structure is satisfactory but if $\hat{E}_f > 4$, the structure is unsatisfactory requiring improvement [376].

The basic endurance curve of the plate with a hole (Д16чТ material) are of the form

$$N = 3 \cdot 10^9 \sigma^{-4},$$

where $\sigma = \sigma^{gr}_{max.0}$ daN/mm^2.

They give approximate service life value because no provision is made for the structural changes of the hole shape and their processing technique.

The problem of the method development in estimation of the life time of the high endurance joints performed with the axial and radial interference involving both the statistic material and the new methods of the local deflected mode engineering analysis in the stress concentrator zones with the account for the history of the assembly structure loading remains urgent at the present time.

The use of the CAD/CAM/CAE computer system will enable to combine the design theory of the aircraft assembly structure joints with the methods of the engineering analysis and three-dimensional computerized modelling.

1.3. ANALYSIS OF THE DESIGN METHODS OF THE AIRCRAFT ASSEMBLY STRUCTURE RIVETED JOINTS WITH THE ASSIGNED SERVICE LIFE

The riveted joints of the thin-walled structures made from aluminium alloys are the most accepted joints used in the aircraft industry.

The typical riveted joints of the aircraft airframe structural components are illustrated in Fig. 1.10. They are performed by the use of the countersunk rivets and rivets with the convex manufactured head. At the draft design stage the parameters of the riveted joints are selected to provide their static capacity under the action of the specified failure loads [283, 299, 332, 352, 354, 421-424, 427, 431, 471].

The joint rivets work in shear, compression and tearing off the heads in some cases (Fig. 1.11) the load acting on one plane of the rivet shear in case of absence of stability loss in jointed structural components is determined by the expression:

$$P = \frac{\delta \cdot t}{m \cdot n} \sqrt{\sigma^2 + \tau^2}\ , \qquad (1.2)$$

where δ – thickness of the component joint; σ and τ – design normal and tangential stress in the joint component; t – pitch of rivets in the row; m – number of rivet shear planes; n – number of rivet rows in the joint.

The stress obtained for a single plane of the rivet shear is compared with the rivet ultimate load.

In the event when the riveted joint is intended for shear force transfer, the expression (1.2) is represented by

$$P = \frac{q \cdot t}{m \cdot n},$$

where q – linear shearing force

To obtain geometrical characteristics of the loaded shear riveted joints, it is necessary to perform computations for shear and bearing stress of the sheets of the rivets and the sheet edges.

The shear breaking stress of the rivets inserted in the structure can be calculated by the following formula

$$\tau_{str} = \tau_{rvt},$$

where τ_{str} – shear breaking stress of the rivets inserted in the structure; τ_{rvt} – shear breaking stress of the rivet material; K – coefficient specifying the joint and the structure strength.

K values depending on the rivet material are given below:

rivet material	–	Д16	Д17	Д18	В65
K	–	1.15	1.14	1.09	1.11

Value

$$\tau_{str} = \frac{4Đ_k}{nm\pi d^2},$$

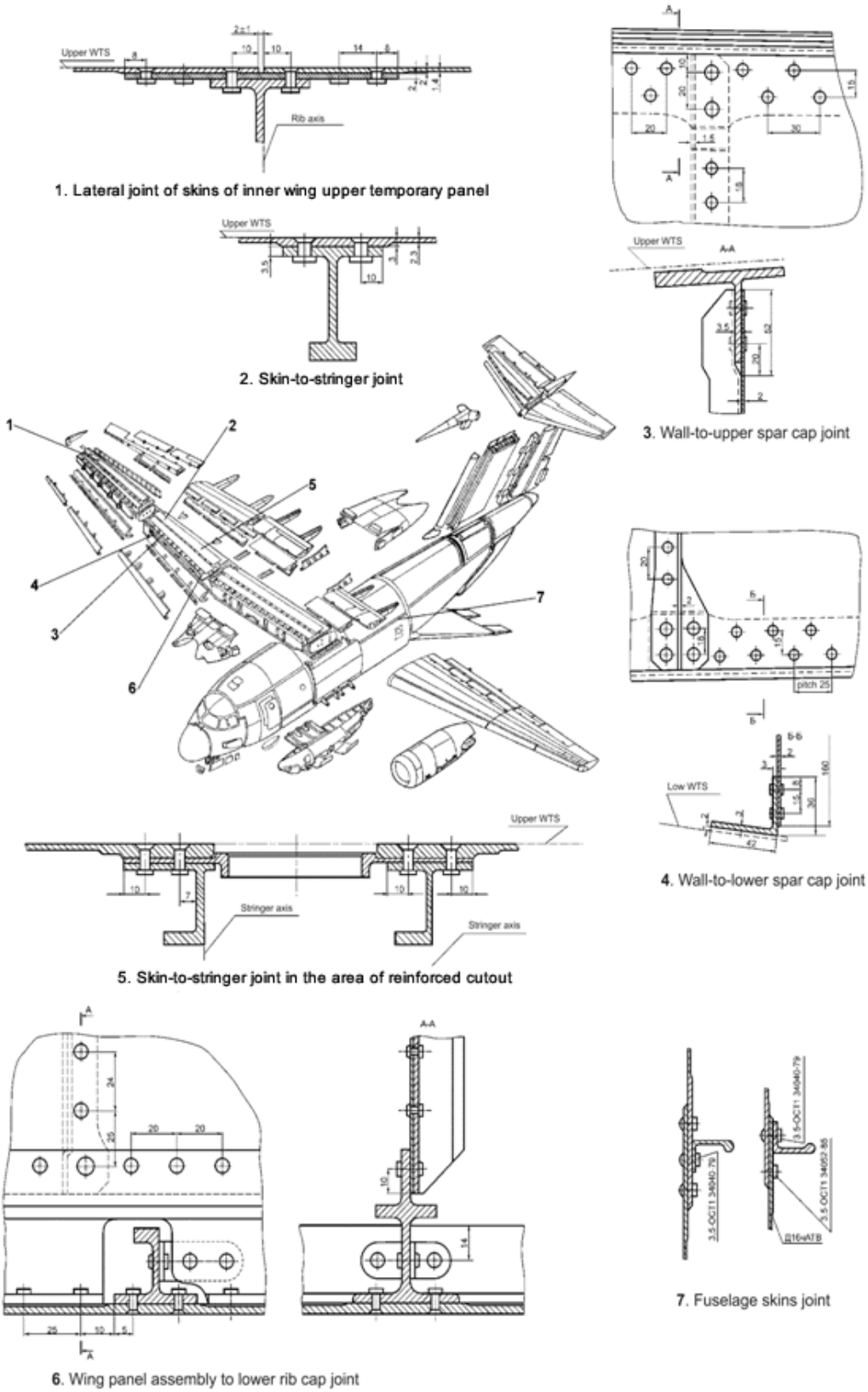

Fig. 1.10. Aircraft airframe structural components typical riveted joints

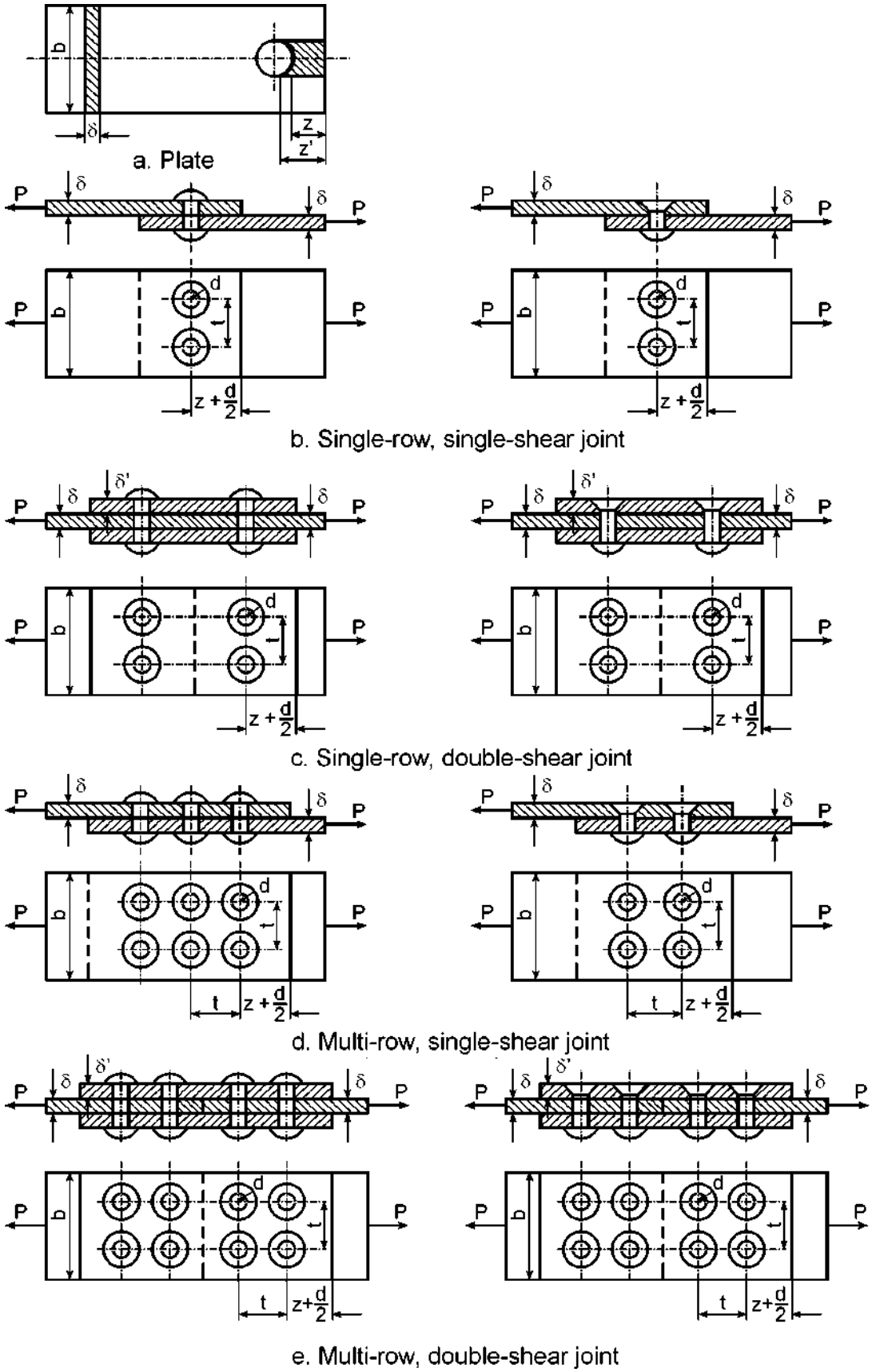

Fig. 1.11. Typical riveted joints. Models. Static strength determination

where P_k – a force acting upon the riveted joint; d – rivets diameter; n – number of rivets; m – number of rivet shear plates.

The analysis of the test results performed by the TsAGI [283] points to the fact that the type of the riveted joints and the riveting pattern have little influence on the value of the rivet shear stresses. The investigation results have also demonstrated that the diameter of the rivets produces little influence on the value of the shear breaking stresses.

Following the investigation results, the working (design) stresses of the rivets shear in joint are taken as equal to:

rivet material	–	Д16,	В65,	Д1,	Д18;
τ_{str}, MPa	–	275,	276,	240,	200.

Using accepted shear working stresses as the base, the relationship between the shear breaking force and the rivet diameter can be found to be expressed by the following parabolic law:

$$P = 0{,}785 m \tau_{str} d^2,$$

where m – number of the rivet shear planes,

Graphic representation of these relationships are illustrated in Fig. 1.12. Points are used to indicate experimentally obtained shear stresses. The relationship between the stresses and the shear deformations are shown in Fig. 1.13.

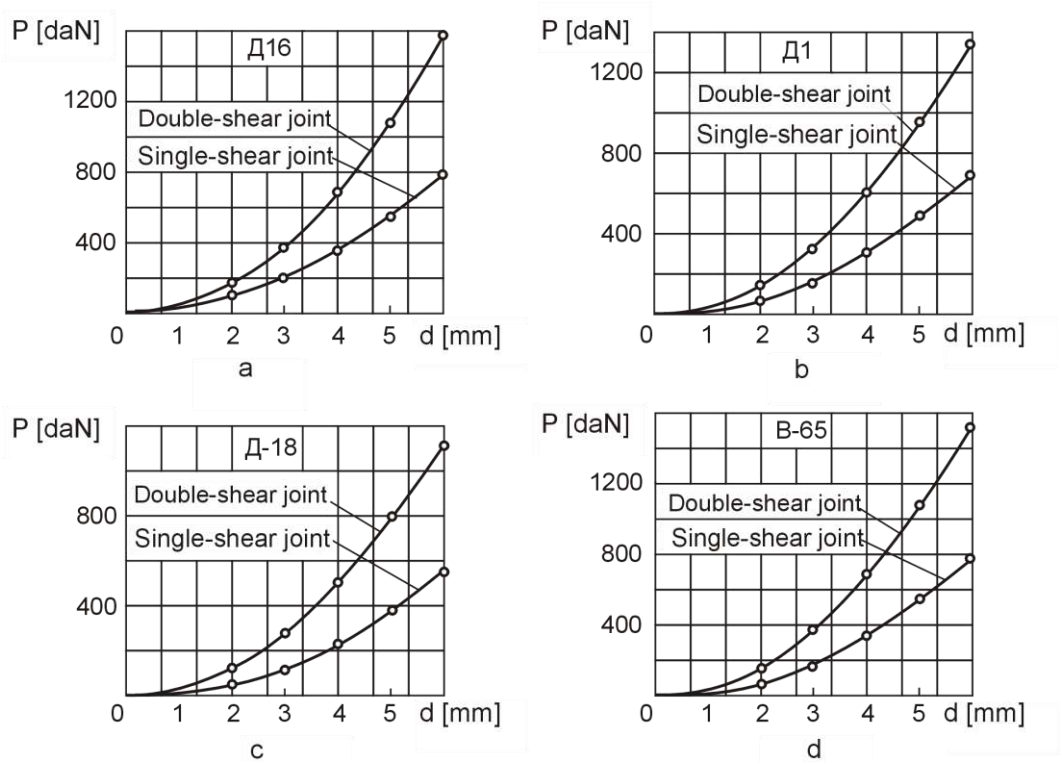

Fig. 1.12. Relationship between shear breaking forces and rivets diameter:
a – rivet material Д16; b – rivet material Д18;
c – rivet material Д1; d – rivet material В-65

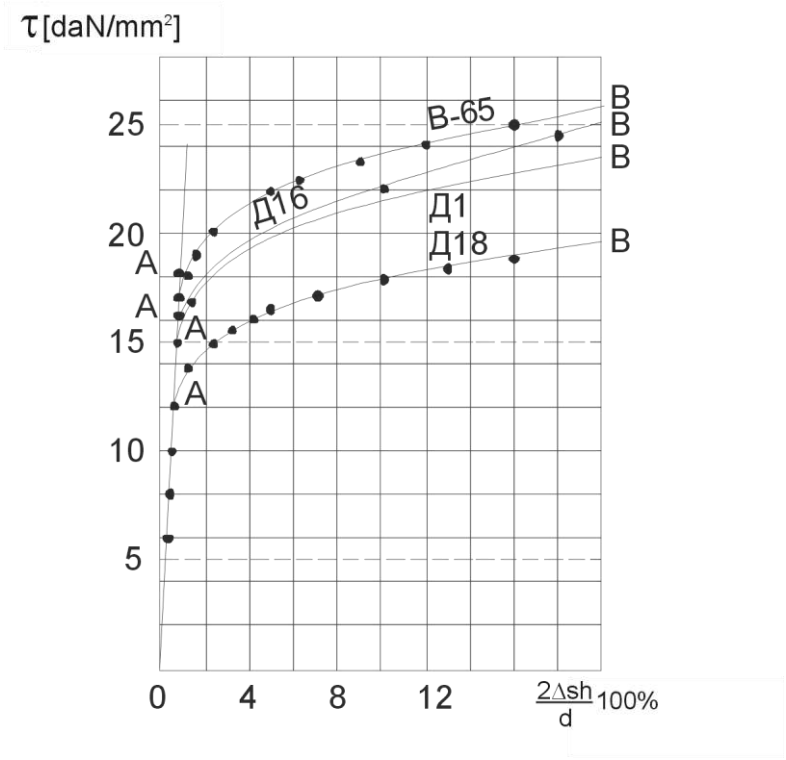

Fig. 1.13. Relationship diagram between rivet shear stresses and deformations

Determination of the working bearing stresses of the riveted sheets involves significant difficulties. They are caused by the absence of data indicating to what extreme bearing deformation value the riveted joint can be loaded to avoid occurence of the high material fluidity capable to result in deterioration of the riveted joint serviceability.

The relationship between the deformations and the bearing stresses [238] has been experimentally found in TsAGI to determine the working bearing stresses.

From the experimental investigations it follows that, firstly, there is a direct proportionality to some extent between the stresses and bearing deformations that can be represented by the following equation:

$$\sigma_{bear} = P/d \cdot \delta = E_{bear}(\Delta d/d), \tag{1.3}$$

whence it follows that

$$\Delta d = P/(E_{bear}\delta), \tag{1.4}$$

where P – rivet load, daN; δ – thickness of riveted sheet bearing relative deformation; E_{bear} – coefficient of proportionality under sheet bearing failure and bearing deformations for the sheets of different thickness are insignificantly distinct from each other.

Because of this, the generalized graphs of the bearing stresses depending on deformations can be recommended for practical use (Fig. 1.14).

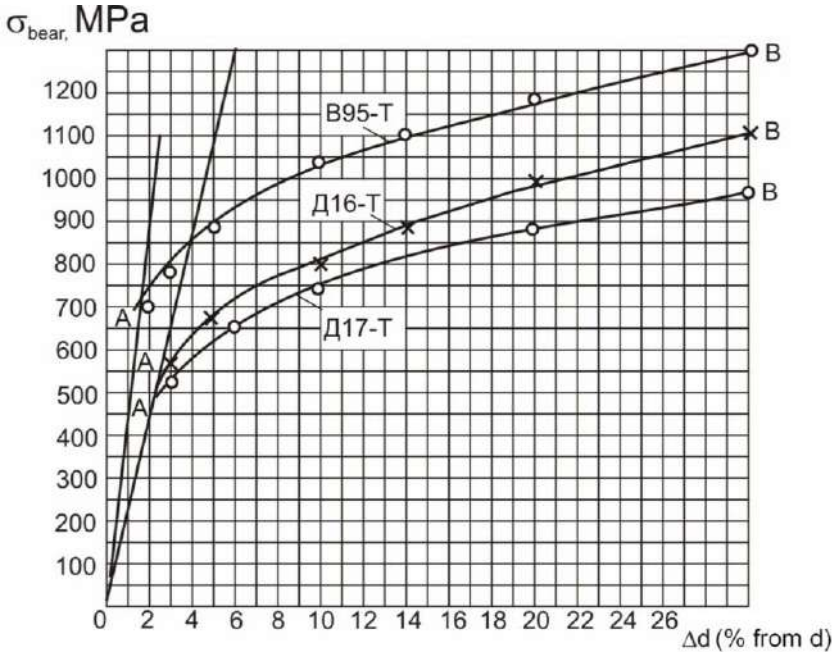

Fig. 1.14. Dependencies between stresses and bearing deformations

Generalized design graphs as a result of the test it has been found that the bearing stresses and regularity of curves both for the countersunk and common riveted joints do not differ from each other. As seen from the graphs, the direct proportionality holds true for the sheets made of Д16Т up to 480… 500 MPa, for the sheets made from Д17Т up to 440… 450 MPa and for the sheets made from B95T up to 640… 650 MPa. Straight line slope of the given curves exhibits a value of the bearing ratio to be equal to 22100 MPa for the sheets made from Д16Т and Д17Т and 42500 MPa for the sheets made from B95T.

In contrast to civil engineering constructions the aircraft strength analysis is performed according to the failure stresses; in this case, it is essential that the permanent deformations of tension or compression under limiting operational stress should not be more than 0.2% from the component original length.

If ultimate load is taken for the calculated load in analysis of compression, the load much less than the ultimate one is forced to accept for the calculated load in bearing analysis of the riveted joints because so high residual deformations are originated just under this load that they may be realistically considered to be breaking deformations.

The stress rate equal to the proportionality limit multiplied by a load factor equal to 1.5 for the aircraft structural components can be naturally taken for the bearing failure stress within the limits of the operational loads to avoid residual deformations. As shown by the experiment, the conventional failure stress equal to 1.5 $\sigma_{(bear)fr}$ corresponds to the relative bearing failure $(\Delta d/d)\cdot 100\%=6\%$ irrespective of the rivets diameter.

In this case, calculated bearing stresses turn out to be equal to:

Sheet material – Д16Т, Д17Т, В95Т;
σ_{bear}, MPa – 700, 650, 925,

The following is taken for the calculated stress of the sheet shear in joint with a distance of z ≤ 2d, (z – distance from the edge of the rivet first row holes to the edge of the riveted sheets).

Sheet material – Д16Т, Д17Т, В95Т;
τ_{sh}, Mpa 248, 210, 283,

With z > 2d τ_{sh} is decreased and a sheet must be a subject of the bearing analysis.

The graphs of dependence between the shear bearing stresses and a distance to the edge Z are illustrated in Fig. 1.15.

In selection of the reasonable shear and bearing riveted joint it is necessary to give condition of strength balance for sheet bearing failure and shear of rivets:

$$n\delta d\sigma_{bear} = nm\frac{\pi d^2}{4}\tau_{str}, \qquad (1.5)$$

where n – number of rivets; m – number of rivet shear planes.

Therefore, the rivet diameter under given sheet thickness would be determined in the following way:

for a single shear riveted joint

$$d = \frac{4\delta}{\pi}\frac{\sigma_{bear}}{\tau_{str}},$$

for two-shear riveted joint

$$d = \frac{2\delta}{\pi}\frac{\sigma_{bear}}{\tau_{str}}.$$

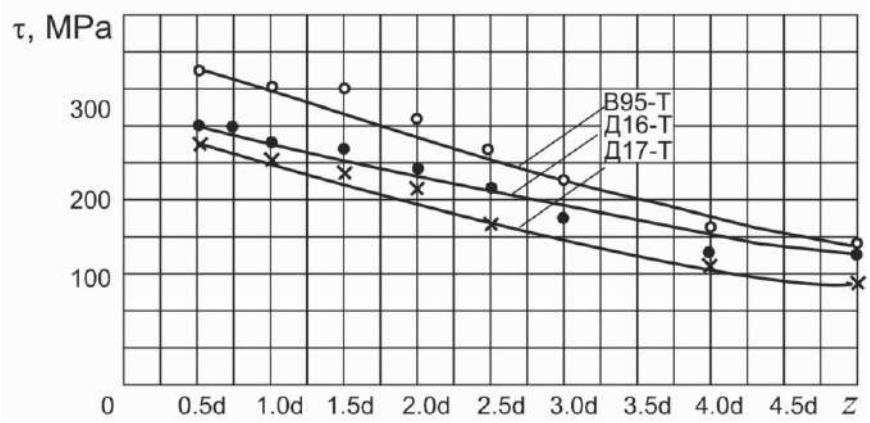

Fig. 1.15. Dependence between shearing stress and distance from the hole edges of the rivet first row to the sheet edge

The rivet diameters are determined for different sheet thickness by substituting the calculated values for σ_{bear} and $\tau_{ê}$ required to provide the uniform strength of the riveted joint. In the case that the calculated sheet thickness

does not meet the standard, the closest large thickness is advisable to take according to OCT to provide reliability of the joint work.

In addition, the strength of the riveted joints depends on the distance Z – i.e. the distance between the hole edges of the first rivet row and the edges of the riveted sheets.

Therefore, using the uniform strength conditions of the riveted joint, we may define the relationship between the bearing stresses and the stresses of the sheets shear on the one hand as well as the stresses of the rivets shear on the other hand. Then the distance between the edge of the riveted sheets and the holes edges of the first rivet row will be:

For a single-shear joint

$$\left.\begin{aligned} z = \frac{2\sigma_{bear} - \tau_{sh}}{4\tau_{sh}} d = \frac{d}{4}\left(2\frac{\sigma_{bear}}{\tau_{sh}} - 1\right), \\ z = \frac{1}{4} d\left(1{,}57\frac{d}{\delta}\frac{\tau_{str}}{\tau_{sh}} - 1\right), \end{aligned}\right\}$$

for two-shear joint

$$z = \frac{1}{4} d\left(\frac{\pi d}{\delta}\frac{\tau_{str}}{\tau_{sh}} - 1\right).$$

The distance t between two parallel joints (pitch of riveted joint) can be found in the following way:

for a single-shear joint

$$d\delta\sigma_{bear} = (t-d)\delta\,\sigma_{fract} = \frac{\pi d^2}{4}\tau_{str},$$

whence it follows that

$$\left.\begin{aligned} t = \frac{\sigma_{bear} + \sigma_{fract}}{\sigma_{fract}} d, \\ \text{or} \\ t = d\left(0{,}785\frac{d}{\delta}\frac{\tau_{str}}{\sigma_{fract}} + 1\right), \end{aligned}\right\} \qquad (1.6)$$

where σ_{fract} – sheet fracture stress with allowance made for the stress concentration around the rivet holes;

for two-shear joint

$$t = d\left(1{,}57\frac{d}{\delta}\frac{\tau_{str}}{\sigma_{fract}} + 1\right); \qquad (1.7)$$

for the sheets made of Д16Т and Д17Т material while $\sigma_{fract} = 0{,}85\sigma_b$, for the sheets made from B95 material $\sigma_{fract} = 0{,}98\sigma_b$.

Substituting their values for σ_{bear} and σ_b we may get the following for the sheet made from the material Д16Т, Д17Т, В95.

Д16Т – t =2,85 d ; Д17Т – t =2,82 d ; В95Т – t =2,85 d .

In calculation practice, the pitch of the riveted joint is assumed to be no less than $t = 3d$.

The force acting on the riveted joint is unevenly distributed between the rivets, In the multiple riveted joint, the end rivets are slightly overloaded as compared with the load based on the assumption of the even force distribution along the rivets. The overloading of the end rivets is increased as the quality of rows increases.

The graph of force distribution along the rivets is illustrated in Fig. 1.16.

1) Forces in rivets Ni [%P];

2) Theoretical

3) Number of rivets.

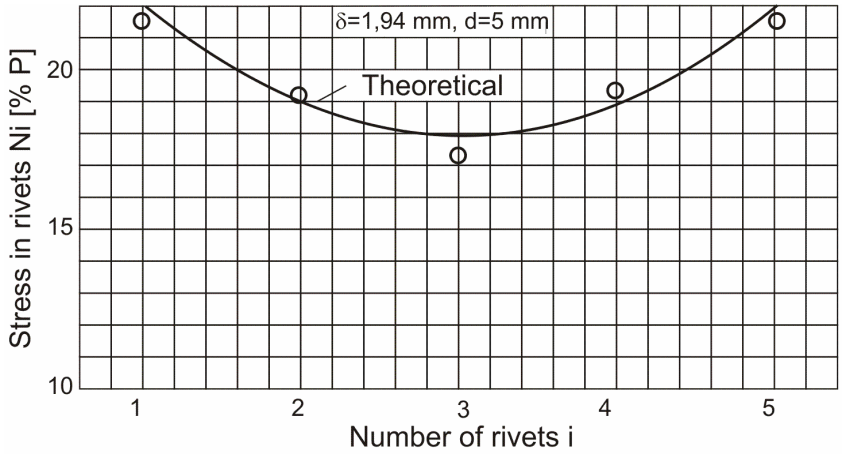

Fig. 1.16. Distribution of forces along the rivets in five-row, single-shear, riveted joint. Sheet material – Д16Т, Rivet material – Д16

In designing of the riveted joints, it is well to bear in mind that, wherever possible, we should select the less length of the pitch and the less number of rivets in the longitudinal row to obtain more even distribution of forces along the rivets. It is not feasible to place more than six or seven rivets in a row.

When working with the thin skins, proper allowance must be made for actual distribution of forces between the rows of the riveted joint to be differed from the calculated or designed one. The reason is that the thin skins have a tendency to corrugation and shrinkage that occurs after riveting process and result in more uneven distribution of forces. An accurate calculation, in this case, is probable by the use of the FEM (finite-element method) accounting for the influence of the residual stresses and deformations that occur after the riveting process on the behavior of the force distribution between the rows of the riveted joint. In connection with the increase of the up-to-date airplane speeds, the large local

aerodynamic forces are acting on the wing and tail unit in flight making efforts to separate the skin from the frame and thus, forcing the rivets to operate, on the one hand, for the extension and shear of a head rod, and, on the other hand, for tearing through the skin under the rivet head. The strength of the riveted joint carrying the separation stresses depends mainly on the following factors:

1) thickness and material grade of the riveted elements of the riveted joints, 2) type of the riveted joint (regular or countersunk), 3) type and material of the rivets used and 4) nature of acting load (symmetrical or asymmetrical).

The riveted joint failure under the action of the tearing load is most often caused either by tearing through the sheet under the rivet heads or by the rivet shear stresses, or less common as a result of the shank failure or the rivet head tearing. The last two kinds of failures show evidence just in joints riveted by the round head rivets. To some extent, the breaking shearing stresses of the rivet heads depend on the thickness of the riveted joint elements. The breaking shearing force is increased following the increase of the riveted element thickness under the same diameter of the rivets. The reason is that the rivet shank is deformed and attains a tapered shape (Fig. 1.17) in making of a snap rivet head. The reference diagrams allowing to determine the diameter of the rivets by shearing and damaging conditions (Fig. 1.18) are used to determine a tolerable force taken by the rivets from the material B95 in joining sheets from material Д16T.

The methods developed to determine parameters of the riveted joints reasoning from the provision of the static strength are used at the aircraft manufacturing companies at the predesigning phase and at the creation stage of the space distribution model. After determination of the joint parameters reasoning from the provision of the static strength, the joint life time is subject to estimation under variable loads to be equivalent to the loads of the standard flight.

The methods of the riveted joints fatigue strength analysis of the assembly structures can be combined in three groups:

1) statistical methods;

2) methods using the geometric stress concentration factors;

3) methods using stress and deformation actual values in the most loaded point of the concentrator.

The first group of methods based on the use of the statistical data of the results preceding the tests of the structural members or assemblies (for example, wing) allows to avoid crude errors but complicates the efficiency estimation of the new design concept, implementation of the advanced technological process and new materials. It is associated with the fact that the statistical data are obtained by the tests of the aircraft structural members of the previous generation, less perfect, as a rule, and corresponds to the specified materials and joint assembly practices. Despite disadvantages, the method finds application for analysis of the lower boundary of the failure cycle index in practice of the national and foreign aircraft industry. The second group is based on the equivalence hypothesis of the local

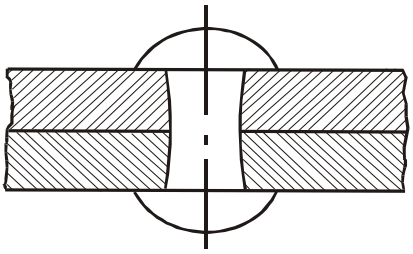

Fig. 1.17. Rivet expansion nature

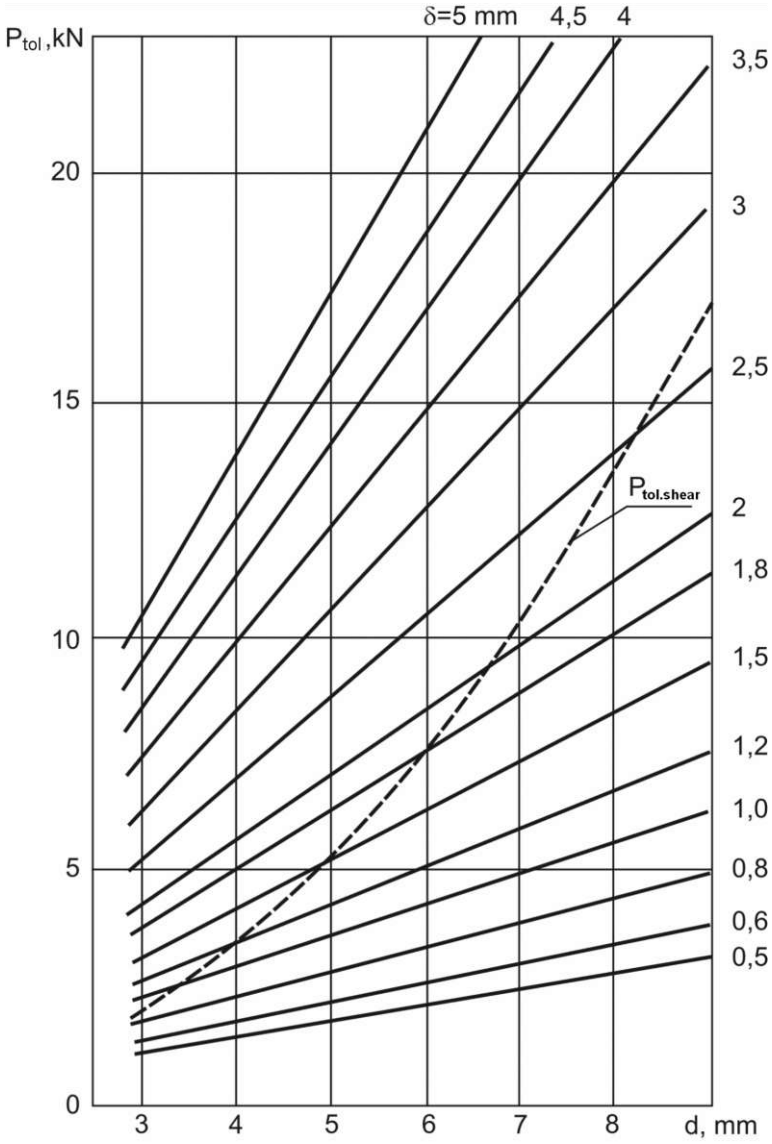

Fig. 1.18. Tolerable forces taken by the rivet from material B65 in joining sheets from the material Д16Т with respect to damage and shear at a single plane determined reasoning from the provision of the static strength

maximum stress action on the concentrator contour under elastic deformation and stresses in the test-piece without the concentrator. The test – piece fatigue curve with a specified concentrator is a calculated curve. The use of the theoretical stress concentration factor provides low accuracy of life time calculation. The empirical correction factors reflecting design features and peculiarities of the joining procedure [192, 280, 329] are introduced to coordinate analysis and experimental data. In doing so, the principle of superposition of solutions with separation of loads going around the sheet and taken by the fasteners [409, 456] is used for analysis of the stress concentration factor. Although, accuracy of analysis is increased, in this case, the estimation of the number of cycles prior to failure of

actual joints is preferred to do on the basis of the statistical data using this method just as the guide for revealing the critical points of the components and just for construction but not for analysis of the joint life time. The third group of methods is based on the equivalence hypothesis of the deflected mode at the most loaded point of the smooth test-piece concentrator for a fixed number of cycles before crack formation. The analysis is based on the actual values (with the account of plasticity) of the stresses and deformations with the allowance made for the cycles change of loads. The fatigue curve of the smooth test-piece and cyclic diagrams of the elastoplastic deformation are used for analysis. Although, the methods of the third group are assumed to be the most accurate the complexity of the analysis procedure for the actual loading conditions substantially delays their development. The use of the base endurance curve bearing information on the fatigue properties of the join element materials is common to all. The possibility exists for the enhancement of calculation accuracy provided that the curve carrying information on the fatigue properties of the joint element components and technique features is taken as a design curve [69, 71, 75, 146, 148, 185, 199, 213, 409]. For this purpose, the effective stress concentration factors considering the actual material properties and peculiarities of the joints assembly techniques must be used instead of the theoretical ones. Then, the expression for the local stresses on the loaded hole outline in the joint $\sigma_{loc.j}$ can be represented with the use of the superposition principle in the following way

$$\sigma_{loc.j} = k_{bear}^{eff}\sigma_{bear} + k_{l}^{eff}\sigma_{l.s}, \qquad (1.8)$$

where $\sigma_{bear}, \sigma_{l.s}$ – nominal stresses due to the force taken by the rivet of the row analyzed and a force passing along the sheet in respect to the rest rows of rivets, respectively; k_{bear}^{eff}, k_{l}^{eff} – the effective stress concentration factors for a single-row joint (total load is taken by the rivet) and for the joint with the rivet unloaded for shear, respectively.

Procedure of riveted joint life prediction with reference to the local mode of deformation [371, 403, 437, 450] has been also developed involving [91]:

1. General analysis of the deflected mode of the structural area in the jointing zone, determination of stresses by the fastener.

2. Analysis of the local deflected mode, determination of the maximum and minimum elastic reduced stresses on the periphery of the filled and loaded holes.

3. Determination of the elastic-plastic deflected mode on the hole periphery with the use of Neyber's dependence and formation of the local stress cycles and deformation in compliance with the loading program.

4. Calculation of the stress gradients.

5. Analysis of service life.

The use of the energy criterion in service life analysis by the geometric concentrator according to the local deflected mode gives the best conformance to

the experimental data. That's why, the same criterion is assumed to be used in the analysis of the service life. The main parameter characterizing the moment of the crack initiation is a value of the dissipated energy during the loading cycle:

$$W_r = K_s \sigma_a \varepsilon_{ar}, \tag{1.9}$$

where K_s – shape factor of the hysteresis loop; σ_a – stress amplitude at a point of maximum stress concentrations; ε_{ar} – amplitude of residual deformation in the stress concentrator.

At the first half cycle the material is deformated in correspondence to the monotone deformation curve:

$$\varepsilon_t = \frac{\sigma_{\max}}{E} + \left(\frac{\sigma_{\max}}{K_c} \right)^{1/m_o}, \tag{1.10}$$

where $\sigma_{\max}$, ε_t – maximum local stress and its associated deformations.

Local elastic-plastic stresses at a point of maximum concentration are determined according to the Neyber's formula:

$$\sigma_{max} \varepsilon_t = \frac{\left(\sigma_{red}^{max}\right)^2}{E}, \tag{1.11}$$

where σ_{red}^{max} – maximum local elastic reduced stress determined basing on the finite element method (FEA).

Determined due to joint solution of the equations (1.10) and (1.11), the values of $\sigma_{\max}$, ε_t are assumed to be the reversing point coordinates of the stresses and deformations in analysis of the local cycle parameters.

Further deformation will pass in compliance with the cyclic deformation pattern. It is assumed that in transition from the monotone deformation pattern to the cyclic one, the transient processes are ignored. Neyber's equation under the cyclic regular loading for the filled and loaded holes takes the form

$$\sigma_a \varepsilon_{at} = \frac{\left(0{,}5\left(\sigma_{red}^{max} - \sigma_{red}^{min}\right)\right)^2}{E},$$

where $\sigma_{red}^{max}, \sigma_{red}^{min}$ – maximum and minimum reduced local stresses in the loading cycle.

The amplitude of the total deformation ε_{at} is determined with regard to the cyclic material deformation pattern under asymmetric loading:

$$\varepsilon_{at} = \frac{\sigma_a}{E} + \left(\frac{\sigma_a}{K_m} \right)^{1/m}; \; K_m = K\left(1 - \left(\frac{\sigma_m}{\sigma_{ult}} \right)^{\upsilon}\right),$$

where σ_{ult} – ultimate strength stress; K, m, ν – parameters of the cyclic material deformation pattern obtained according to the test results of the smooth test-pieces.

Mean cycle stress

$$\sigma_m = \sigma_{\max} - \sigma_a .$$

The amplitude of the residual deformation at the point of the maximum concentration on the contour of the filled and loaded holes will be

$$\varepsilon_{ar} = \varepsilon_{at} + \frac{0{,}5\left(\sigma_{red}^{max} - \sigma_{red}^{min}\right)}{E} .$$

An energy value dissipated during the loading cycles is calculated according to the formula (1.9). A value of the dissipated energy at a distanced can be found as

$$W_{rd} = W_r - G_{W_r} d; \;\; G_{W_r} = dW_r / dz ,$$

where G_{W_r} – gradient of dissipated energy.

Number of cycles prior to formation of the microcracks in the stress concentrator under regular loading is determined in correspondence to the energy criterion of the fatigue failure:

$$R_m W_{rd}^{\alpha} N = 1 ,$$

where

$$R_m = R\left(1 - r\frac{\sigma_m}{\sigma_b}\right),$$

where R, r, α – parameters of the material failure energy criterion obtained according to the test results of the smooth test-pieces.

The fact that the fatigue curve of the smooth test-piece taken as a base without regard to the nature of the contact interaction of the joint elements under formation and loading with the low loads included is the disadvantage of this method.

Going into analysis of the riveted joint-structure (Fig.1.19), we can say that the development of their structures and manufacturing techniques is also directed toward the service life increase using the large diametral interference and increasing the axial tightening of the pack; as this takes place, the problem, in most cases, is solved in filling the enlarged hole with interference for the heads of the countersunk rivets.

Under ordinary riveting with the use of the countersunk rivets, the diametral interference is achieved, as a rule, just close to the closing, barrel shape head to decrease rapidly without reaching the jointing plane of the parts. The countersunk rivets are used in aircraft structures for the relatively thin skins (1-1.5 mm). In this case the countersunk rivet head hole occupies almost the total thickness and the shin practically has any interference. This is one of the main reasons because the

fatigue failures begin from the skin of the riveted joints. Under self-sealing riveting, the inner joint sealing is required that drastically exaggerates and extends the assembly cycle resulting in the significant increase of the structure weight.

The leading aircraft manufacturing companies develop the design and manufacturing techniques of the riveted joints with the extended interference created by both the shank and the countersunk head in the skin.

Noteworthy are NASA rivets used in the USA for more than 18 years. The main peculiarity of this rivet (Ref. Countersunk snap rivet head illustrated in Fig. 1.19) lies in the fact that the countersunk tapered head is closed to be a snap rivet head in this case. Excess of the closed countersunk head material going beyond the skin is subject to milling to result in improvement of the lift-drag ratio. The riveting technique with the use of the countersunk snap rivet head can be used just in case if the depth of the hole cylindrical portion in the loaded skin after countersinking is less at 25% of the skin thickness. In case of countersinking at greater depth, the skin will be intensively corrugated during riveting resulting in loss of tightness.

The special compensating rivets in staggered form on the snap rivet head (see Fig. 1.19) have been developed to increase endurance, decrease loosening and provide tightness of the fuselage riveted joints without internal joint sealing.

The purpose of the compensator is to improve the filling of countersinking under closing the projection, thereby to increase both the joints endurance and tightness. In closing of such rivets the compensator projections often remain incompletely closed increasing the roughness of the outer surface. On the other hand, there are a lot of cases when the holes are not filled sufficiently full due to the small compensator volume. In the USA they rejected to use these rivets in manufacture and they are used just under repair. In development of the “Tristar” aircraft by the Lockheed company, the firm has developed the L-10052 rivet for the same purpose (Lockheed company standard) [423, 424] and used it widely in the fuselage structure of this aircraft (see Fig. 1.19). Due to the skin thickness increase, riveting by shanks has been under development for several years in the USA. In this case, both heads were simultaneously close (see Fig. 1.19). When so, sufficient radial interference is achieved by both heads, that is, in the skin and the frame part simultaneously.

In our country the countersinking riveted joints are performed in the airframe structure of An-aircraft family using the rivets with the crown compensator in compliance with the industry Standard OCT1 34052-85. Peculiarity of such riveted joints is that the required projection of the snap rivet heads according to the outer surface condition can be realized by means of the mechanical finishing (milling) because the volume of the manufactured rivet part (compensator volume) projected before riveting is significantly higher than the value needed for

feeling the clearances in the area of the countersunk hole and for creation of the radial interference in the joint according to the rivet height. In the process of

	Standard	With compensator	Lockheed Company	Countersunk rivet head	Shank	Ring release	Combined clamped rivet
	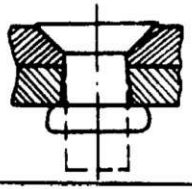	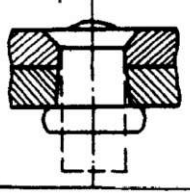	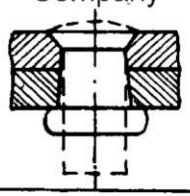	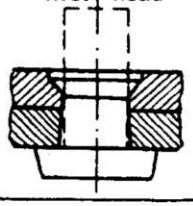	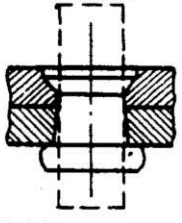	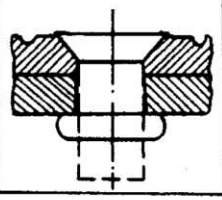	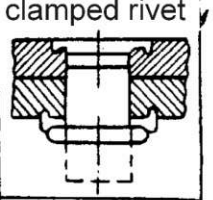
Endurance (k=0,3)	100%	500%	700%	800%	1000%	1000%	10 000%
Sealing characteristics	In-seam sealing	In-seam sealing	———	———	———	In-seam sealing	———
A - making holes B - riveting C - refinement	Drilling (D)A_5 Single (S) Not required (NR)	D, A_5 S+group (G) reguired (R)	D, A_5 S+G R	D, A_4 S+G R	D, A_4 S+G R	D, A_5 S NR	D+reaming (A_3) S NR
Applicability (pack)	from 1,5+1,5 till 10+10 everywhere	from 1,2+1,2 till 2,0+2,0 repair version	from 1,2+1,2 till 4,0+4,0 everywhere	from 1,8+1,8 till 4,0+4,0 everywhere	from 2,0+2,0 till 15+15 everywhere	from 1,5+1,5 till 10+10 special application	> 4,0+4,0 special application
Interference nature with refere-nce to pack height 							
Failure nature	On skin	On skin	On airframe	On skin	On skin	———	———

Fig. 1.19. Influence of riveted joints design and manufacturing techniques on flight endurance

finishing the anti-corrosive protective coating is removed from the manufactured rivet head and there is the probability of the skin and its damage on the areas neighbouring to the manufactured rivet head due to the contraction of the latter as well as due to the use of the manually – operated mechanical tools for finishing. The results in measuring the values of the 3 mm – diameter manufactured rivet heads projected over the skin surface have shown that the projection height of the manufactured rivet heads between riveting and milling actually lies from 0.3 mm to 0.71 mm. while after milling it is from 0.03 mm to 0.27 mm. In this case, just 44% rivets have a projection height of up to 0.1 mm. At the same time, a skin tightening value in the areas of attachment to the frames reaches 0.42 mm. The tightening up to 0.05 mm is available in the installation area of 50 % rivets while the tightening from 0.051 to 0.1 mm is in the installation area of 24% rivets. So, the development of the new rivet types, installation procedure, strategy of their integrated design and modelling, methods of endurance forecasting using the computer-aided systems remains an actual problem.

1.4. ANALYSIS OF CRACK GROWTH DELAY METHODS IN AIRCRAFT THIN-WALLED ASSEMBLEDY STRUCTURES

The structures of the aircraft airframes designed in compliance with the safe damage philosophy or operated according to the operational status must have sufficient survivability and service life if fatigue cracks of subcritical length [87, 337] are available in their components. The service life of the aircraft assembly structures can be determined by the expression

$$T = \frac{N_{bcd}}{\eta} + \frac{N_{wc}}{\eta},$$

where N_{bcd} – life before initiation of crack, N_{wc} – life from the moment of crack formation to the failure of structure, η – reliability coefficient.

The life of the structure previously designed in compliance with the safe service life philosophy and still operated, information value of their fatigue tests can be significantly increased by application of integrated methods in delay of the fatigue crack growth, restoration of strength and tightness.

The fatigue crack growth at its head is delayed because of decrease in:

– stress intensity;

– stress concentration;

– value or amplitude of cycle stress and deformations.

The stress intensity decrease at the crack apex is achieved by the load transfer to the repair strips and structural members located nearby without change in natural sharpness of the crack apex [87, 377, 404, 412]. The stress concentration in the crack area is decreased by making a hole at its apex, a system of holes, sawcuts.

An amplitude decrease of the local tensile stresses is achieved by creation of the residual stresses at the crack apex to be obtained by applying to the structure a single crack opening overloads or by the local severe plastic deformation [55, 233, 311, 338, 343]. For the development and proof of the actual (compatible with the aircraft production and operation requirements) manufacturing techniques in delay of the fatigue crack growth [369, 377-379, 392, 393].

It is necessary to determine:

– initiation area, kinetics and character of the fatigue crack development in the thin-walled structures of the aircraft airframes under operation and life test conditions;

– influence of the fatigue crack and techniques in growth prevention on deflected mode of the aircraft thin-walled structural components;

– technical efficiency of the fatigue crack growth prevention techniques under laboratory and operation conditions.

The following design-manufacturing irregularities are the zones of the probable fatigue crack initiation: part joints, holes and cutouts, radius thickness transition, “oil can” in thin-walled components and etc. (Fig. 1.20.) [43, 173, 188, 205, 212, 214, 219, 223, 226, 228, 267, 282, 287, 292, 313, 344, 435, 443, 448, 452 – 454, 458, 459].

In repair of the thin-walled structures of the aircraft airframes the small cracks are subject to drilling at their tips using the drill d=2…3 mm [337]. When patching the structural component having the crack, the crack apexes are also subject to drilling.

To select the parameters of the holes performed in the crack apexes, the character of the fatigue crack development is subject to study using the structural test-pieces made of the following aluminium alloys Д16А-Т л.2,5, Д16А-Т л.1, Д16А-Т л.5, В95п.ч. АТ1СВ л.2, В95п.ч. АТ1СВ л.5.

Kinetic analysis of the fatigue crack growth has shown that the cracks 1…2 mm long can be visually deflected. With 80…100 mm in length the probability of their detection is approximating to 100% [349, 435]. It must be noted that the range of their stable growth corresponds to the specified lengths of the fatigue cracks [229].

The analysis of the fatigue crack development character using the structural test-pieces made of the aluminium alloys Д16АТл.5.0 demonstrates that the fatigue crack in the spar webs, panel skins and the sheets are developed in the direction perpendicular to the action of the main tensile stresses σ_1 (see Fig. 1.20).

The deviation from this direction does not exceed 1…1.5 σ under half-length of the crack l<20 σ and can be explained by the nature of the microprocesses at the crack apexes, specifically, by the crack branching or change of the failure type – from separated to the shear one. At the beginning of its development the plane of the fatigue crack is perpendicular to the middle surface

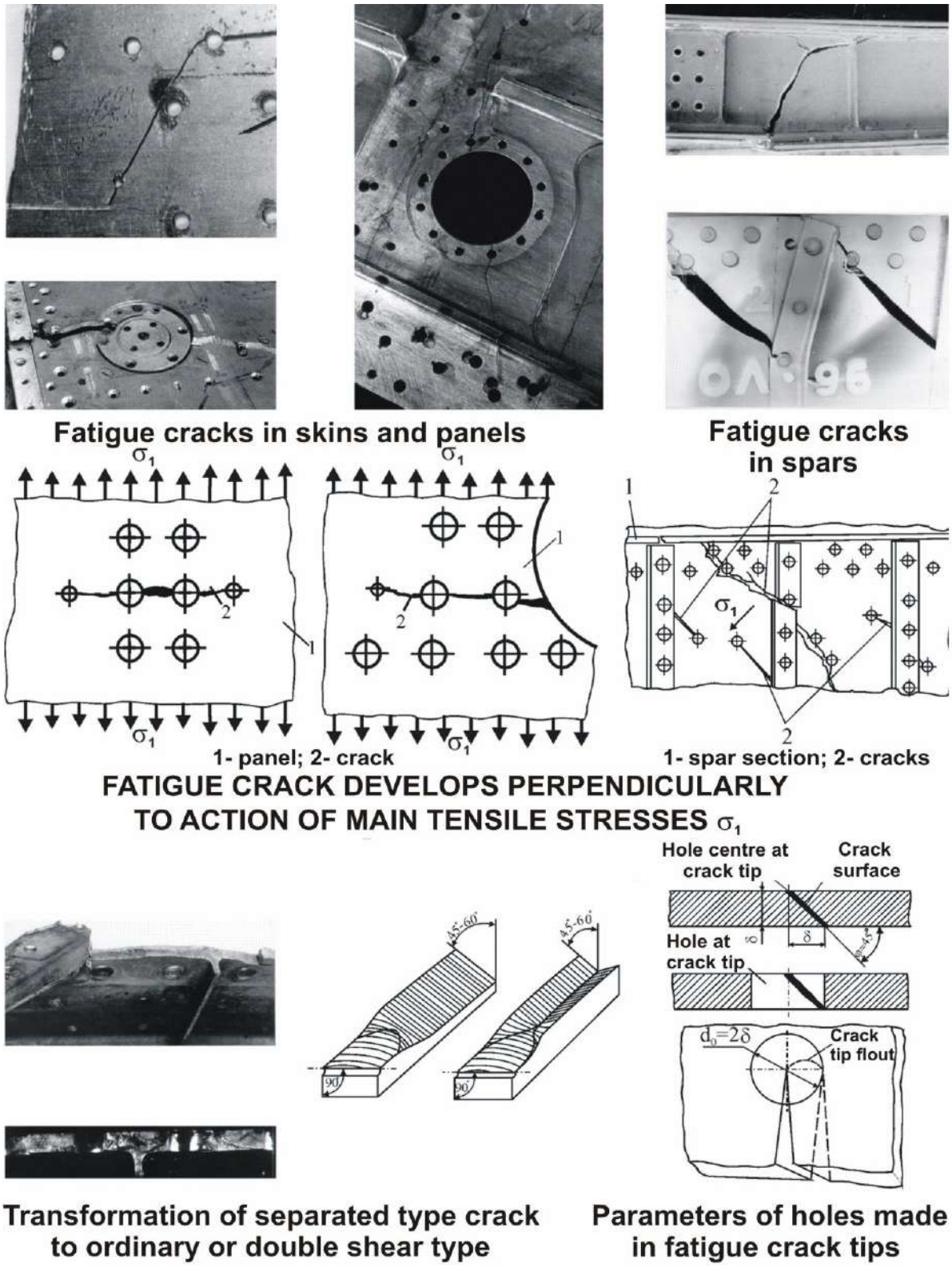

Fig. 1.20. Nature of fatigue crack development in thin-walled structures of aircraft airframe under operation and life test conditions

of the plate followed by its turning to this surface at an angle of φ=45°…60°(See Fig. 1.20.). The crack of the separation type is changed into an ordinary type and (or) double shift. Transition from ordinary to double shift in the sheets $\sigma = 2...2.5$ mm thick is observed at the fatigue crack lengths 2·l=80…120 mm and in the sheets 5 mm thick at the length of 2·l=20…50 mm under operational level of cycle stresses. In this case, the front of the fatigue crack apex in the areas of its stable growth in the aircraft thin-walled structures has a convex (elliptic or oval) shape.

Change of failure type in the thin-walled structures is explained by the increase of the plasticity zone and, as a result, the transition from the plane-strain condition to the plane stress state at the crack apexes under its length increase.

The experimental investigations show that the irregularities in the thin-walled structures significantly change the direction of the fatigue crack development: holes, stiffeners, directional property (anisotropy) of the sheet article, redistribution of the stress fields as a result of crack development.

In crack approaching the hole (or the part edge), the bridge between the front of the crack apex and the hole wall is normally failed according to the separation type or by the cleavage (shear) in compliance with a shear type.

Basing on the identified character of the fatigue crack development and the type of the thin-walled structure fatigue failure, it is feasible to perform the hole at the crack apex with a diameter to be equal to the double thickness σ of the sheet article crack or more than that (see Fig. 1.20). The diameter can be decreased with the arrangement of the hole center at a distance from the crack apex toward the direction of its growth [432].

The hole contour with a center at the crack apex must cover for sure the total front of its tip. Due to the fact the plane of the fatigue crack developed according to shear type is about φ=45° with the middle surface of the sheet article, the nominal diameter of the hole at the crack apex should be selected on condition that $d_0 \geq 2\delta$.

Formation of the hole with such diameter is not always probable and feasible due to the design-manufacturing limitations, for instance, at great thickness of the sheet articles. Besides, the necessity often arises to make a hole with its center shifted relatively to the initial direction of the fatigue crack growth.

The holes made at the crack apexes delay the crack growth but do not stop it. An increase of the residual life under such technique of crack delay 30 mm long at an operational load level is 1.5…2 time as compared with the residual skin life with a hole without drilling its ends. To provide assigned service life with availability of crack, it is necessary to develop the new techniques in delay of their growth at the stage of operation.

1.5. DEFINITION OF THE RESEARCH TARGET AND GOALS

The analysis of the previous researches in the field of the design methods of the aircraft assembled structures with the restricted service life and presented in sections 1.1-1.4 allows to define the purpose of this research and to determine the problems to be solved.

The purpose of this research is to provide the assigned service life of the aircraft assembled structures at all stages of the aircraft life cycle by developing methods of their integrated design using computer-aided systems.

To achieve assigned task, it is necessary to solve a family of methodological and scientific-technical problems:

– development of the philosophy and scientific grounds of the integrated design methodology and achievement of the assigned service life of the aircraft assembled thin-walled structures;

– development of the integrated design method and achievement of the assigned service life of the aircraft assembled structure shear bolted joints;

– obtaining with use of integrated design method and achievement of the assigned service life for the new design-manufacturing solutions for the shear bolted joints of the aircraft assembled structures with the assigned service life;

– development of the integrated design method and achievement of the assigned service life for the shear riveted joints of the aircraft assembled thin-walled assembled structures;

– obtaining with use of integrated design method and achievement of the assigned service life for the new design-manufacturing solutions for the shear riveted joints of the aircraft assembly thin-walled structures;

– development of the new design-manufacturing techniques and methods of the fatigue crack growth delay for the extension of the thin-walled assembly structures service life;

– implementation of the developed design methods and design-manufacturing solutions in theory and practice of the aircraft assembly structure creation using CAD/CAM/CAE integrated systems.

Section 2
INTEGRATED DESIGN FRAMEWORK AND SCIENTIFIC METHODOLOGY PRINCIPLES. ACHIEVEMENTS IN ASSIGNED SERVICE LIFE OF AIRCRAFT ASSEMBLY STRUCTURES USING CAD/CAM/CAE SYSTEMS

2.1. INTEGRATED DESIGN FRAMEWORK AND PRINCIPLES OF AIRCRAFT ASSEMBLY STRUCTURES

At present, no single aircraft manufacturing company can remain competitive if it is not capable to provide high quality of the manufactured aircraft models, their quick modification or family change. But presence of a great number of the basic model modified versions (AN-74, AN-74TK-100, AN-74TK-200, AN-74TK-300, ATR.42 and ATR.72, A310, A319, A320, A321 and etc) on the recent market is considered to be normal. It is too difficult to provide high work progress keeping high quality of the final product ant its high product mix without application of the CAD/CAM/CAE computer-aided integrated system enabling to integrate design, engineering analysis and aircraft pre-production processes [46, 51, 57, 61, 190, 235, 237, 265, 291, 335, 291, 35, 350, 426].

The process of aircraft equipment and its modified versions development is followed by the development of its design methods. The stage of the statistic, analytical, optimal, automated and system design methods have been already completed. The method of the optimal design on the basis of the integral quality criterion of the modern aircraft selected to meet the Customer's (Buyer's) requirements to the aircraft and Airworthiness Regulations lies in the basis of the aircraft design methodology [194-196, 266, 290, 300, 301, 322, 327, 416, 436].

At present, transportation costs and provision of flight safety are assumed to be an admitted quality criteria in quality estimation of the civil aircraft. The designers designing the aircraft and airframe achieve conceptually assigned qualitative indices of the quality criterion by:

– decreasing the structural mass as a main factor resulting in decrease of the direct operating costs due to the probability of the payload increase;

– increasing the structure service life and endurance to provide reliability and flight safety as factors reducing expenses for depreciation, maintenance and overhauls.

The requirement for creation and operation of the reliable fail-safe design structure of minimum mass with the assigned life is the main criteria lying in foundation of the modern methods of aircraft structure design. In this case, the possibility of damage detection before achieving the tolerable critical sizes and reserve of sufficient residual strength of the structure must be guaranteed. It is obvious that creation of the fail-safe structure envisaged by the strength standards

and Airworthiness Regulations and designing to meet assigned life under minimum mass are associated with the economic problems.

The program of the aircraft industry development in Ukraine covers creation of the new regional passenger and transport aircraft with a wide range of their functional capabilities differing in:

– up-to-date technical and operational level of development being higher than the development level in the twentieth century to be reached on the basis of the new concepts, scientific-research solutions and innovations in the field of aerodynamics, designing, construction, strength, weight advantages, power unit, aircraft systems, equipment, materials, manufacturing techniques and its pre-fabrication process, operability, reliability and safety.

– correspondence to the modern Airworthiness requirements and Aviation regulation meeting FAR (JAR) requirements, quality standards and next-generation ecological standards;

– high level of the production and operational unification and succession with modern aircraft;

– economic efficiency as a result of similar aircraft low price as compared with the competitor, under comparable operational data, assigned design service life of 80000 flight hours (40000 flights), service life (30 years) and total assigned engine life of 30000 hours (1500 cycles);

– use of on-condition maintenance strategy;

– application of integrated design technologies, preproduction, engineering analysis, tests, certification, information support of aviation complex life cycles using CAD/CAM/CAE/PLM and ERP systems.

Development of the integrated systems to provide high quality, long life, reliability and life time, certification of aircraft and equipment, scientific and production development makes background for modification of the next aircraft family with the use of the computer-aided design, manufacturing, engineering systems for the preproduction process, serial production, flight tests on the basis of the continuous information support of the aircraft life cycle (CALS-technology) to be an important goal of aircraft production under present market condition [3, 16, 57, 61, 95, 183, 193, 235, 250, 251].

Information technologies together with the progressive aircraft design and manufacturing procedures under availability of a unified information field allow to increase significantly the labor intensity, quality of the manufacturing as well as production of the new, up-to-date aircraft meeting the Buyer’s demands.

Integration of the design, production and operation database into a unified database is required to organize a unique information field.

The idea in creation of a unique information field and its integration into every level of the aircraft maintenance within the life cycles also favours compliance with the main goal of the Ukrainian aviation that is to provide safety transportation under minimum costs for transportation of cargo ton-kilometer or

one passenger-kilometer, reduction in value of the aircraft life cycle.

To meet the problems of the aircraft maintenance within the life cycles, the unique data base must contain data with respect to the aircraft under development by the Manufacturing companies and the service centers followed by description of the current organization, design and manufacturing processes. At present, the methods and ideas in aircraft maintenance within the life cycle and integrated information technologies based on these methods find wide application in all aircraft manufacturing companies throughout the world.

Development of information technologies allows intensifying the development processes of the technical, design and manufacturing documentation, preproduction, production control and aircraft maintenance and what is the most important, to realize information support of the aircraft life cycle in compliance with the diagram presented in Fig. 2.1.

The infotainment data are collected and regulated in a unique data base distributed among organizations with an access open for all maintenance members within the life cycle.

In development of a new aircraft and during design and engineering preproduction, the integrated information system describes the aircraft structure, its structural members and components included: parts, units, assembly units, vendor items, materials by using the CAD/CAM/CAE/PLM integrated systems.

Application of the integrated information technologies to the aircraft designing process allows to reduce cost for development, production and maintenance within aircraft life cycle and increase labour intensity and human labour engineering by 30% that finally result in improvement of product quality and competitive ability better engineering activity.

The information technology of aircraft integrated designing assumes application of a parametric analytical structure standard developed in CAD/CAM system presented in calculation of: aerodynamic and strength; service life and operability; aircraft mass and its centering; structural dynamics and its operational safety as well as under preproduction, quality, operation and overhaul control [5, 93, 106, 107, 137-139, 276].

The method of integrated design covers designing and computer-aided parametric three-dimensional modeling of aircraft structure both integrally and partially. The aircraft involves many parts, assemblies, units and components joined by different types of detachable and undetachable joints. The mass, service life, aerodynamic and industrial design characteristics of aircraft depend upon the quality of their design and fabrication. The previously used methods in designing of aircraft assembly structures were based on two-dimension models and their loft coordination that made impossible to take all design and manufacturing peculiar features into account and that resulted in the necessity of the development of the integrated design method. The new concept of aircraft assembly structure integrated design is illustrated in Fig. 2.2.

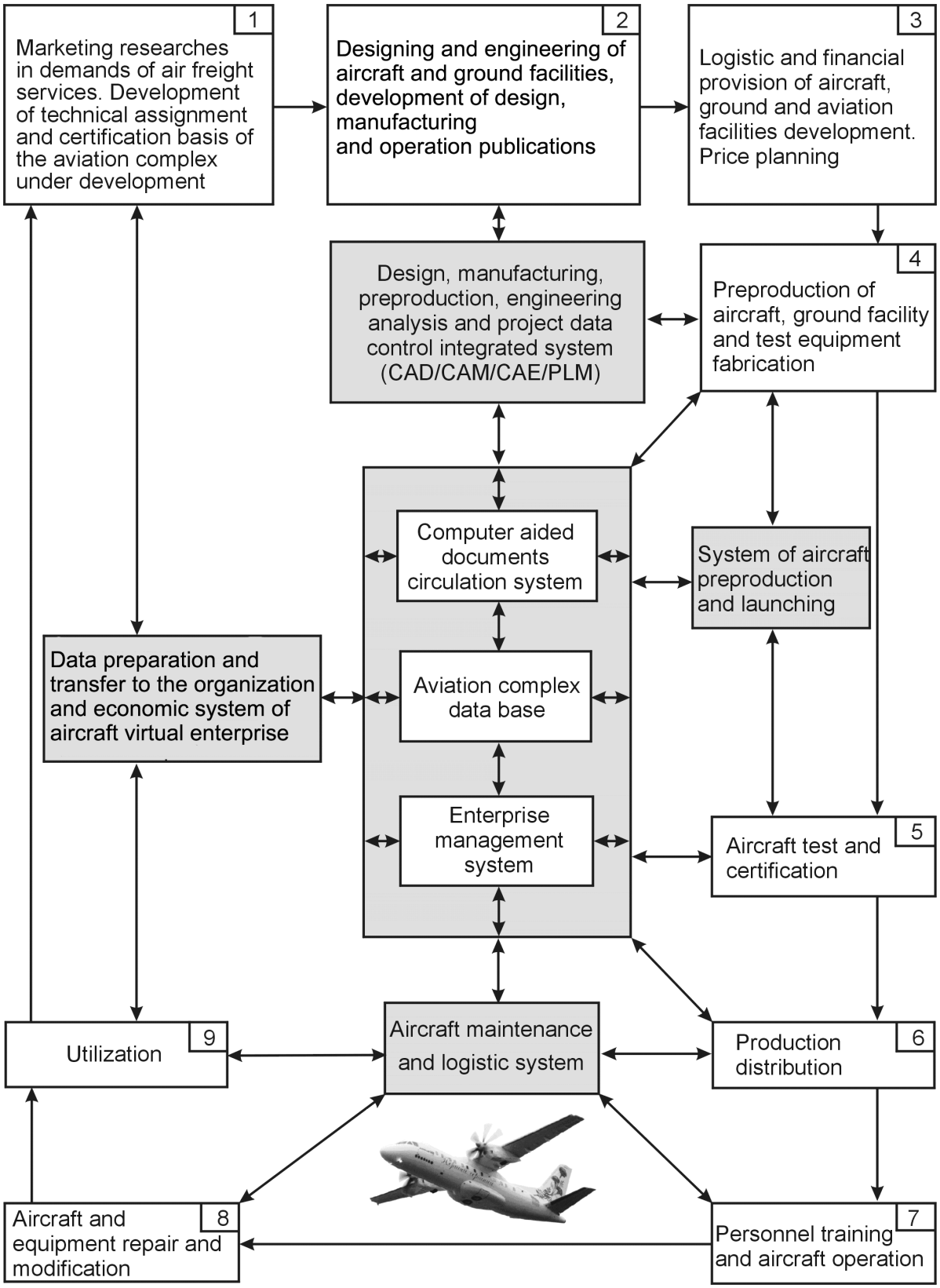

Fig. 2.1. Aircraft life cycle components and its information support

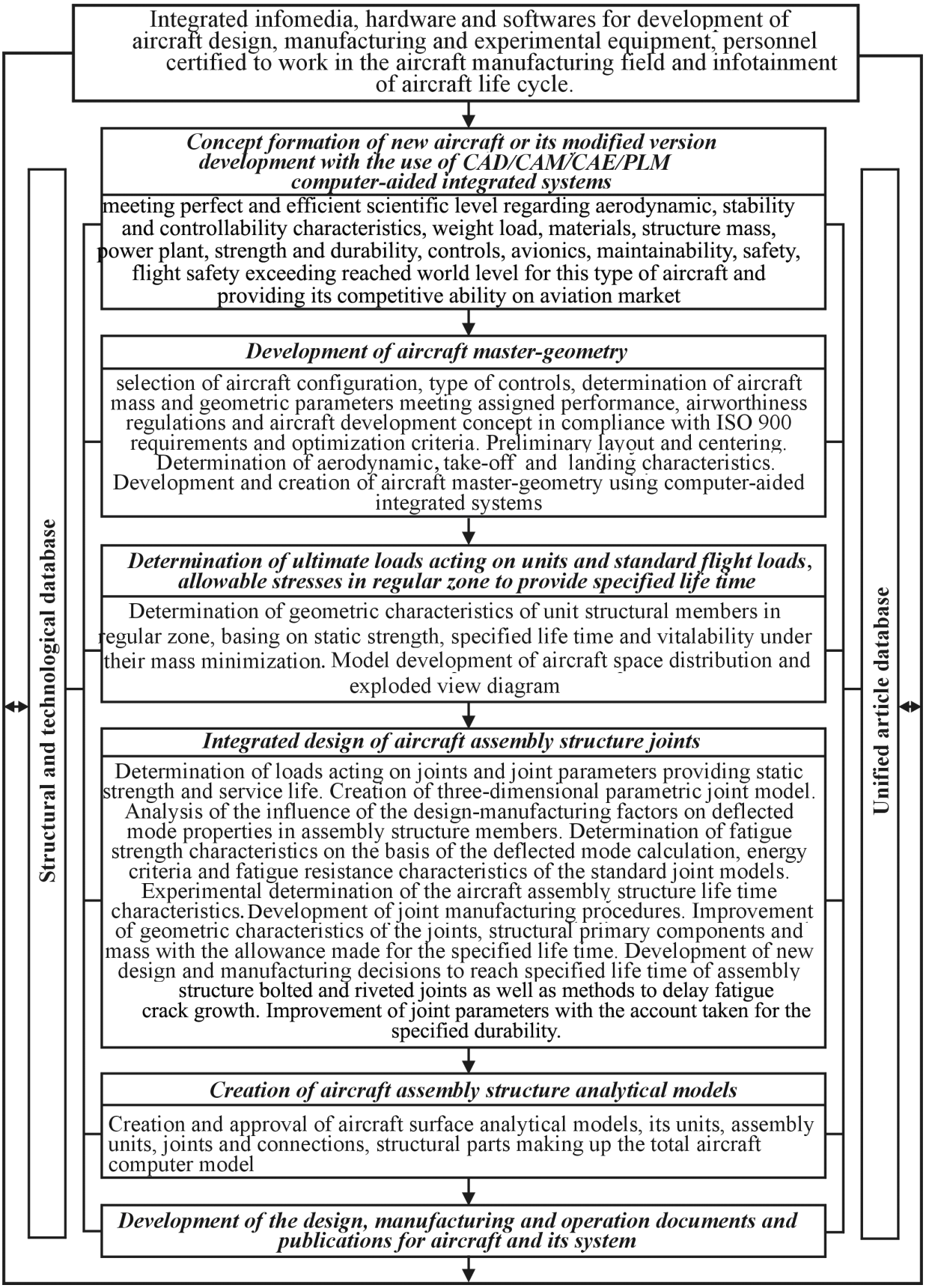

Fig. 2.2. New Concept of Aircraft Assembly Structure Integrated Design

Developed concept of the aircraft assembly structure integrated design is used as a methodological basis for the development of the airframe primary structural member joints with the assigned static strength, life time, tightness and quality of external surface under minimum joint weight (mass).

The integrated design of the aircraft assembly structures can be subdivided into stages with the association between them presented in Fig. 2.2.

1. Creation of integrated information media, hardwares and softwares for the development of the aircraft design, manufacturing and experimental capabilities, high-skilled and executive team.

2. Concept formation of new aircraft or its modified version development with the use of the CAD/CAM/CAE/PLM computer-aided integrated systems.

3. Development of aircraft master-geometry in CAD/CAM/CAE/PLM system.

4. Determination of ultimate loads acting on aircraft units and standard flight loads, allowable stresses in regular zone to provide specified life time.

5. Integrated design of aircraft assembly structure joints

6. Creation of aircraft assembly structure analytical models.

7. Development of the design, manufacturing, operation documents and technical publications.

All works in integrated design of the aircraft assembly structures are performed using a unique data base of the aircraft under design with the use of the design and manufacturing data base. On the basis of the concept proposed by the author, the integrated design principles of the aircraft assembly structures have been developed:

1. Principle in creation of the aircraft assembly structure analytical models.

Three-dimensional computer models of the master-geometry, space distribution, analytical models of the aircraft assembly structural members are created by the methods of the analytical geometry using CAD/CAM/CAE/PLM integrated system in the unified information media of the aircraft life cycle maintenance.

2. Creation principle of aircraft configuration master-geometry

Parameters of new aircraft configuration of minimum mass and specified life time must meet the specified advanced performance requirements, Airworthiness Regulations, new aircraft development concept to be determined by the following relation:

$$\text{PR, AR} \rightarrow \text{aircraft configuration} \rightarrow$$

$$\rightarrow m_0 = \frac{m_{crew} + m_{cnt.eq} + m_{pld}}{1 - \left[\bar{m}_{constr}(p, n_p, N_{reg}, \lambda, MG) + \bar{m}_{pu}(p, t_0, \gamma_{eng}, R, N_{eng}) + \bar{m}_T(p, C_T, k, L) \right]} \rightarrow$$

$$\rightarrow m_{0\min} \rightarrow p_{opt} \rightarrow t_{opt} \rightarrow P_0 \rightarrow S_i \rightarrow \text{profiles} \rightarrow (l_i, \lambda_i, \chi_i, \bar{c}_i, \eta_i, D_f, L_{vt}, L_{ht}) \rightarrow$$

$$\rightarrow (\bar{x}_T - \bar{x}_F) \rightarrow \text{analytical model of the aircraft surface.}$$

3. Principle in designing of aircraft assembly structure regular zones.

Design parameters and implementation practices of the aircraft structure regular zones must provide taking of ultimate destructive loads, regulating life under load equal to the standard flight loads in operation environment, desired gain of the fatigue quality (K_f), desired quality of the external surface, tightness level and must meet the following inequalities:

$$P_{fract} \geq P_{calc}(CP_{r.z..}, \sigma_{tr.z..}(N_{reg.r.z..})); \; N_{reg} \leq N_{calc.r.z.}(CP_{r.z.}, \sigma_{0eqv}, \sigma_c, TR);$$

$$\Delta_3 < 0 \qquad P = Đ_{op}; \; \Delta h \leq 0{,}05mm; \; \hat{E}_f \leq 3.$$

4. Principle in designing of aircraft assembly structure irregular zones.

Design parameters and implementation practices of the aircraft structure irregular zones must provide taking of ultimate loads in irregular zone under static loading, regulating life, external surface quality static loading, regulating life, external surface quality and tightness equal to characteristics of the regular zone or exceeding them and must meet the following inequalities:

$$P_{fract} \geq P_{calc}(CP_{ir.z.}, \sigma_{tir.ð.ç.}(N_{reg.ir.z.})); \; \Delta h_{ir.z.} \leq \Delta h_{r.z.}; \; \Delta_{Çir.z} < \Delta_{Çðç};$$

$$N_{reg} \leq min(N_{calc.ir.z.}(CP_{ir.z..}, (\sigma_{0eqv} \cdot \varepsilon_{eqv}), \sigma_c, TR); \; N_{exp}(CP_{ir.z.}, \sigma_0, \sigma_c, TR)).$$

5. Principle in maintenance and reaching vitality of aircraft assembly structures with the fatigue crack.

Design parameters of the safe destructed aircraft assembly structures must provide capability to monitor critical points, detection of the fatigue crack and application of the advanced growth delay techniques, recovery of the carrying capacity and tightness of damaged structure and must meet the following inequalities:

$$(N_{res.FCDRM} / N_{res.str}) > 1; \; \Delta_{Ç,FCDRM} < 0.$$

Development of the scientifically grounded methods of integrated design is required to realize these principles.

2.2. METHODS IN CREATION OF THE MASTER-GEOMETRY, SPACE DISTRIBUTION MODELS AND AIRCRAFT ASSEMBLY STRUCTURE STANDARDS

Limited design capabilities when using descriptive geometry, high labour intensity caused by the need to make lofts and loft flooring of parts, units and components as well as the total aircraft can be removed with the use of the analytical geometry.

Development of the computer-aided facilities and computerized assistants of computerized assistants of an engineer such as CADDS-5, CATIA, EUCLID, UNIGRAPHICS gave a chance. As an example, the structure of CAD/CAM/CAE/PLM UNIGRAPHICS computer-aided integrated system is illustrated in Fig. 2.3. Integrated design of the aircraft assembly structures [3, 19, 45, 51, 189, 273] can be performed using these systems.

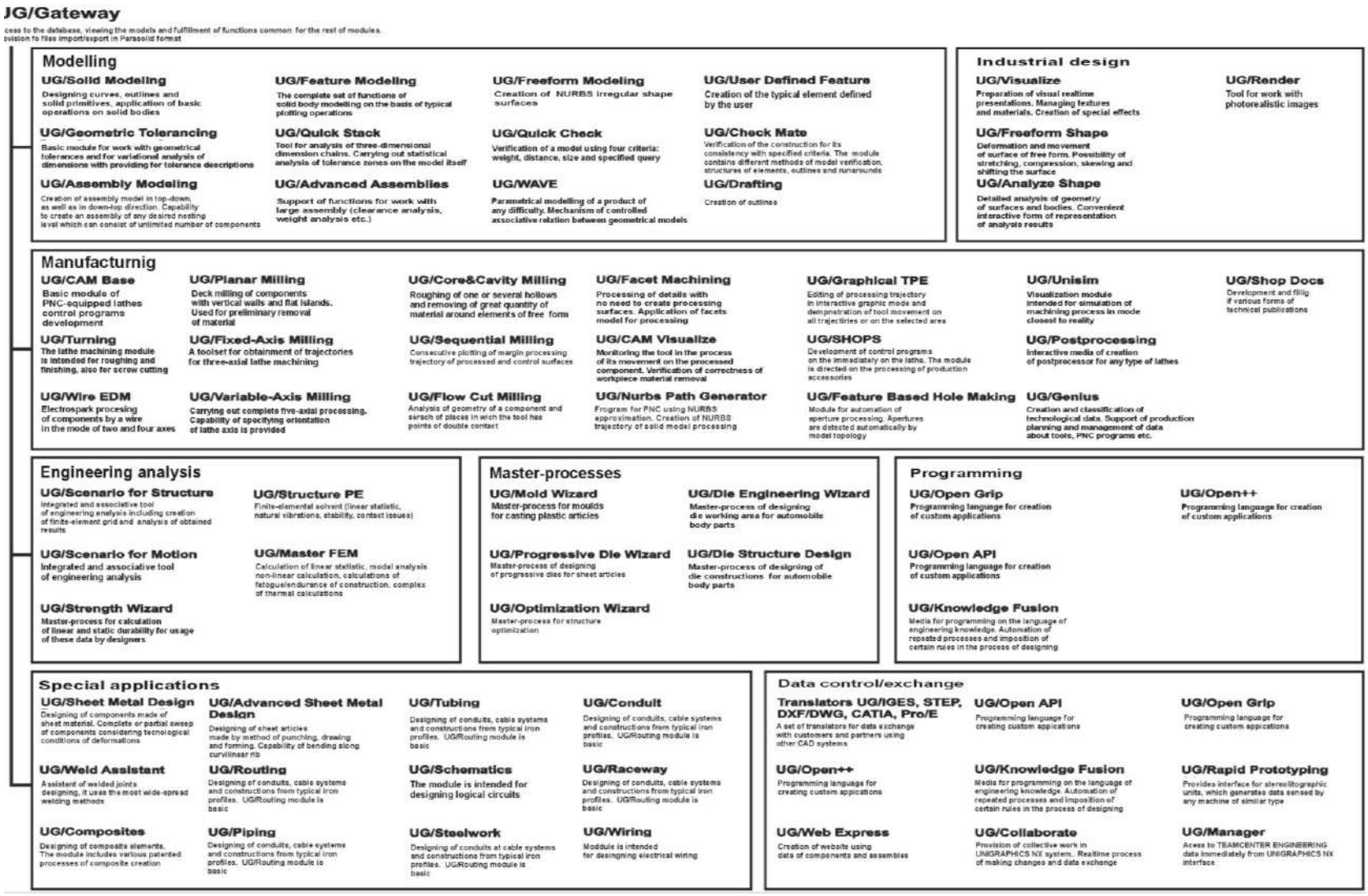

Fig. 2.3. Composition and structure of modules of CAD/CAM/CAE/PLM UNIGRAPHICS computer integrated systems

But application of such systems significantly changes both traditional form of the design and technical publications and the design process of parts and units making it more evident and obvious. Frankly speaking, the use of the computer-aided design and technical publications produces new problems associated with the easy entry of revisions in computer-aided models and low reliability of the long information storage by the use of the computer data carriers.

Part geometry model in computer form (hereinafter referred to as an analytical standard) assumes to be basis, the primary structural members under computer-aided design of the new aircraft. It involves reference coordinates of all part surface points in the given coordinate system representing the basis of the computer-aided aircraft geometry design. At present, a computer-aided design is assumed to be a system of the design, calculated and technological models as well as data for certification, quality control, maintenance when in use, utilization, etc, aircraft life cycle control [3, 211].

Aircraft computer-aided design involves the following models [272]:

– Model №1. Aircraft master-geometry (or aircraft surface model determining all points lying on the aircraft surface);

– Model №2. Aircraft space distribution model;

– Model №3. Joint and connection models with reference to the design-production joints;

– Model №4. Geometry model of the total aircraft (analytical standards of all parts, units, components and the total aircraft), that is, the model of the total computer-aided estimation of an aircraft.

Let’s discuss creation process of every above-listed aircraft models.

Model №1. Aircraft master-geometry.

Creation process of model №1 can be divided into the following stages:

1) development of the aircraft mathematical model;
2) development of component theoretical drawings;
3) creation of the components surface models and their integration in the model of aircraft surface.
4) creation of primary structure (drawing traces of basic surface of design structural members within the scope of the theoretical drawing and design-structural diagram).

Creation method of aircraft master-geometry using computer-aided integrated systems is illustrated in Fig. 2.4. while realization of this method in creation of aircraft master-geometry (surface models) developed by the use of the CAD/CAM UNIGRAPHICS systems is presented in Fig 2.5.

Model №2. Aircraft space distribution model. The Model №2 creation process can be subdivided into the following stages:

1) Development of the design-manufacturing exploded-view;
2) panelling
3) creation of design loads carrying structure

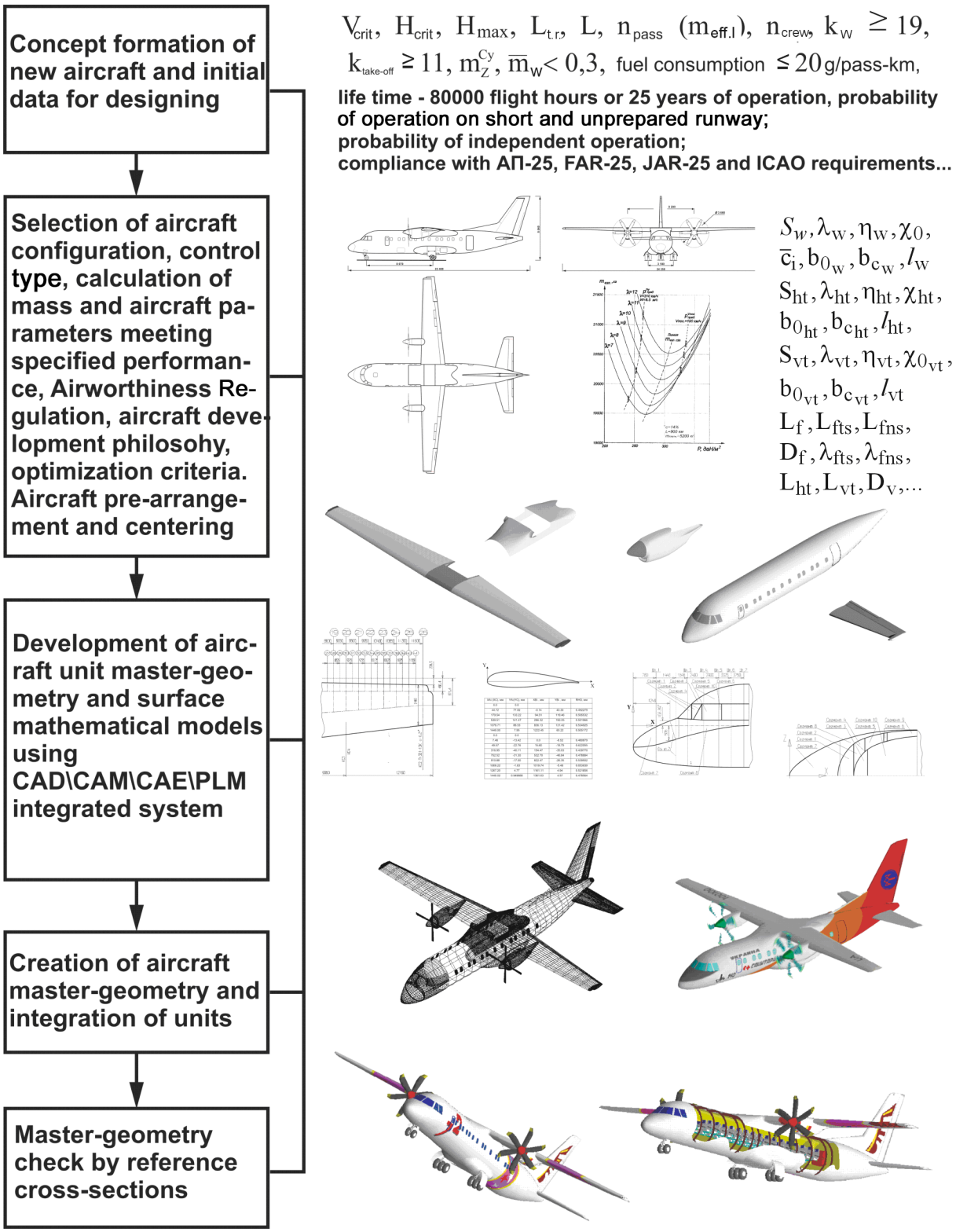

Fig. 2.4. Aircraft master-geometry creative method by the use of computer-aided integrated systems

a

b

c

Fig. 2.5. Aircraft master-geometry (surface models) created by using CAD/CAM/CAE UNIGRAPHICS:
A – AN-140; b – AN-74TK-300; c – AN-148

4) creation of structural members

5) arrangement of equipment, instruments, vendor items and etc.

6) system layout;

7) cockpit layout;

8) passenger cabin (cargo compartment) layout;

9) attachment of units and systems;

10) creation of aircraft design tree;

A fragment of fuselage compartment space distribution model created by the use of CAD/CAM/CAE UNIGRAPHICS systems is illustrated in Fig. 2.6.

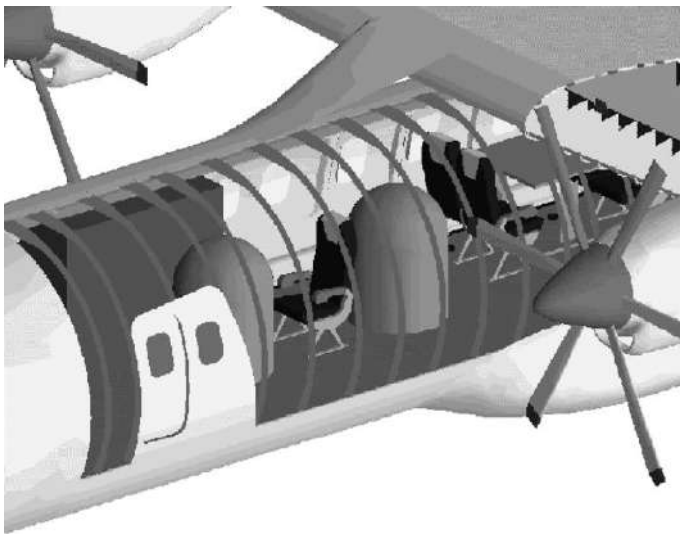

Fig. 2.6. Fragment of space distribution model

Model №3 Joint and connection models with reference to the design-production joints.

Model №3. Development involves the following stages:

1. Complete determination of joints and connections design.
2. Purpose of associated tolerance system for the joint elements.

Element of attachment fitting is illustrated in Fig. 2.7.

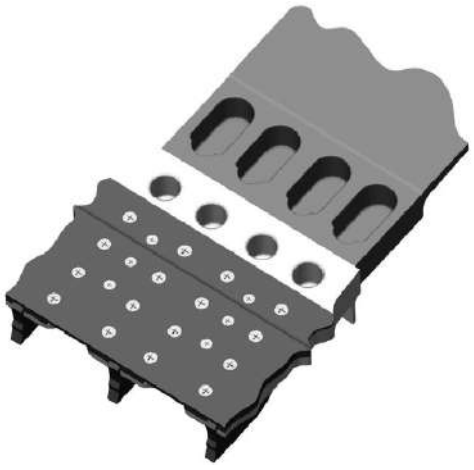

Fig. 2.7. Element of attachment fitting

Model №4. Geometrical model of the total aircraft.

Development of model №4 involves the following stages:

1. Zone modeling:

– dimensionally accurate structural components with all links and connections;

– systems with structural attachment elements;

– outlines of units and instruments with accurate attachment element reference as well as structural member test for mutual penetration and clearances, assemblability.

2. Sectionalized modelling:

– analytical standards of all structural members;

– drawing data base;

– attributive information accumulation.

3. Unit-by-unit modelling:
– systems going through the units without manufacturing division into parts;
– collection and monitoring of the total design information.

Fragment of model №4 of the aircraft fuselage is shown in Fig. 2.8.

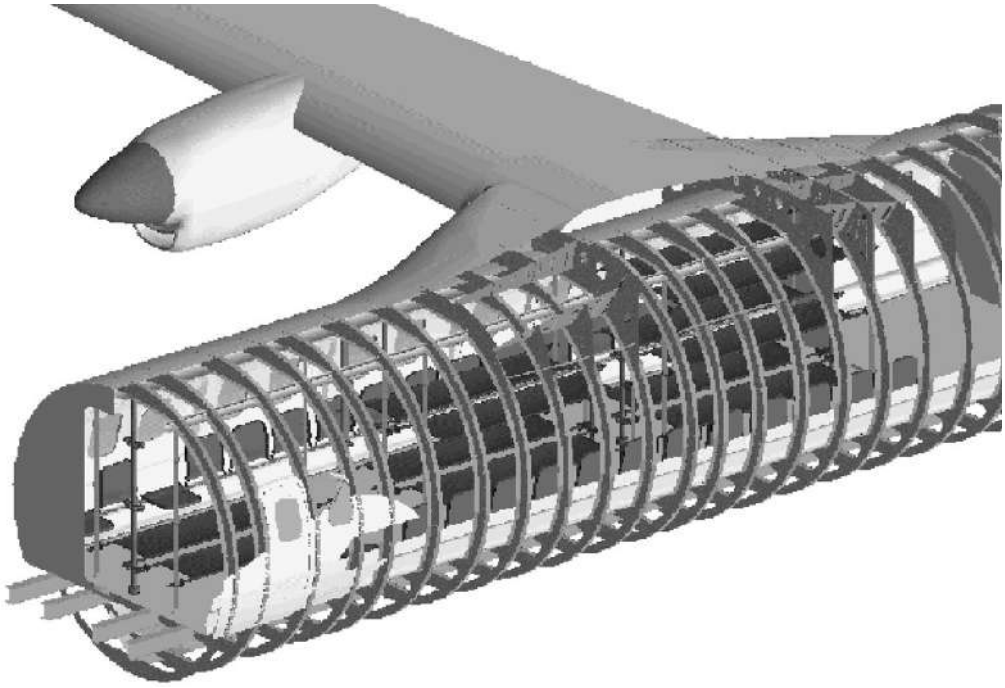

Fig. 2.8. Fragment of model №4

Integrated designed and modelling methods of aircraft units by the use of the computer-aided integrated systems are given below: wing (Fig. 2.9.), fuselage (Fig. 2.10), horizontal stabilizer (Fig. 2.11).

As an example, let's discuss the method in creation of the analytical standards of the aircraft assembly structures when designing the horizontal stabilizer as a unit of an aircraft airframe by the use of the CAD/CAM/CAE UNIGRAPHICS system.

Initial data for the horizontal stabilizer design are developed at a stage of aircraft draft design. Tail unit design must provide acquisition of the desired stability characteristics and aircraft controllability under all probable flight condition as well as sufficiently efficient controls to return the aircraft to normal level flight after inadvertent exceeding critical angles of attack and aircraft unvoluntary spin. The purpose of stabilizer design involves determination of its relative parameters and geometric sizes, selection of optimal configuration, selection of structural-loading pattern, determination of effective loads, analysis of stabilizer mass and stabilizer influence on the aircraft centering. Using present procedures [327] and created softwares, we can determine the following parameters: area, aspect ratio, taper, sweep, trailing edge strip and root section, characteristics of control surface. In addition at the stage of draft design it is

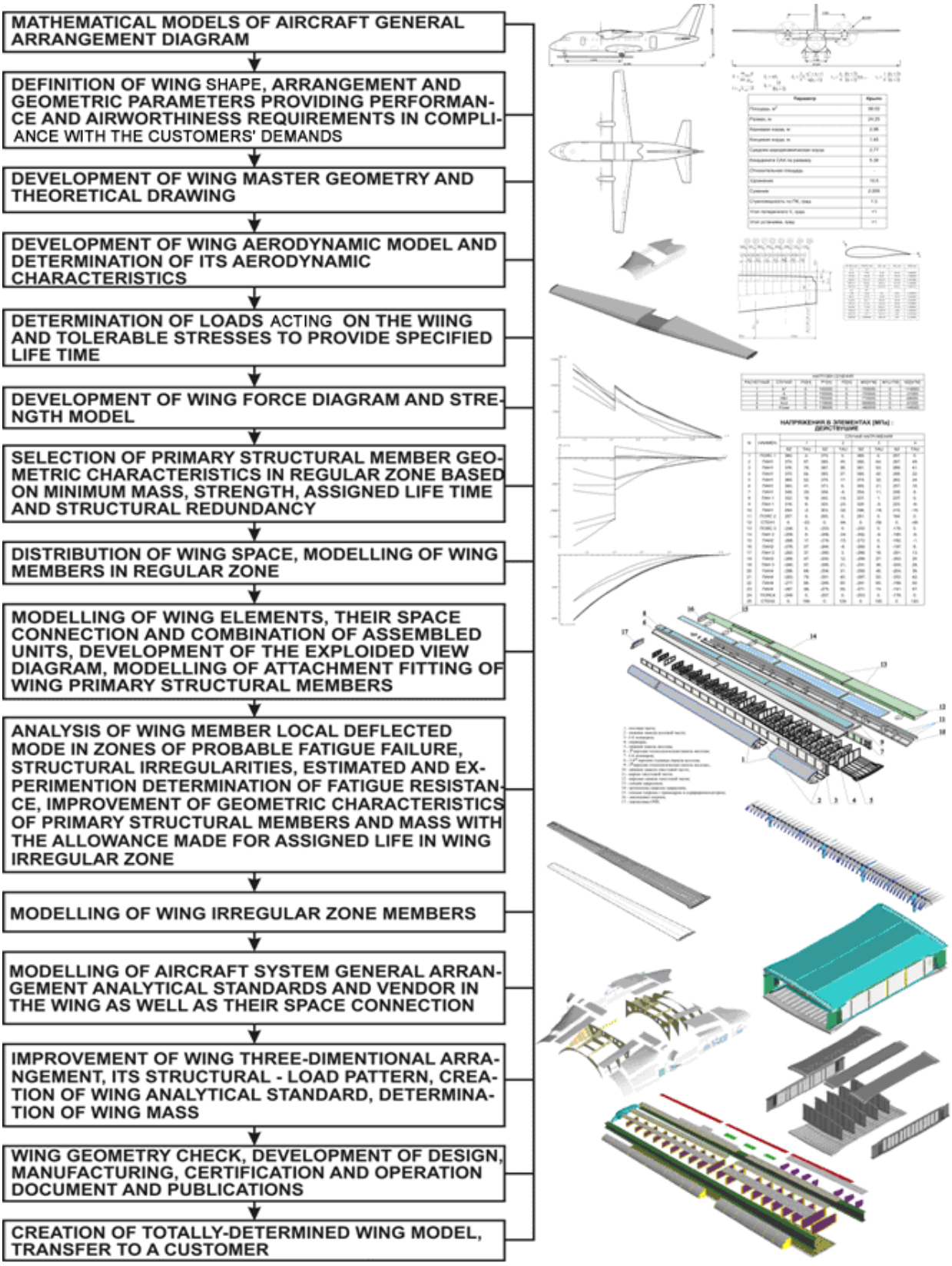

Fig. 2.9. Integrated design and computer-aided modelling method using CAD/CAM/CAE system

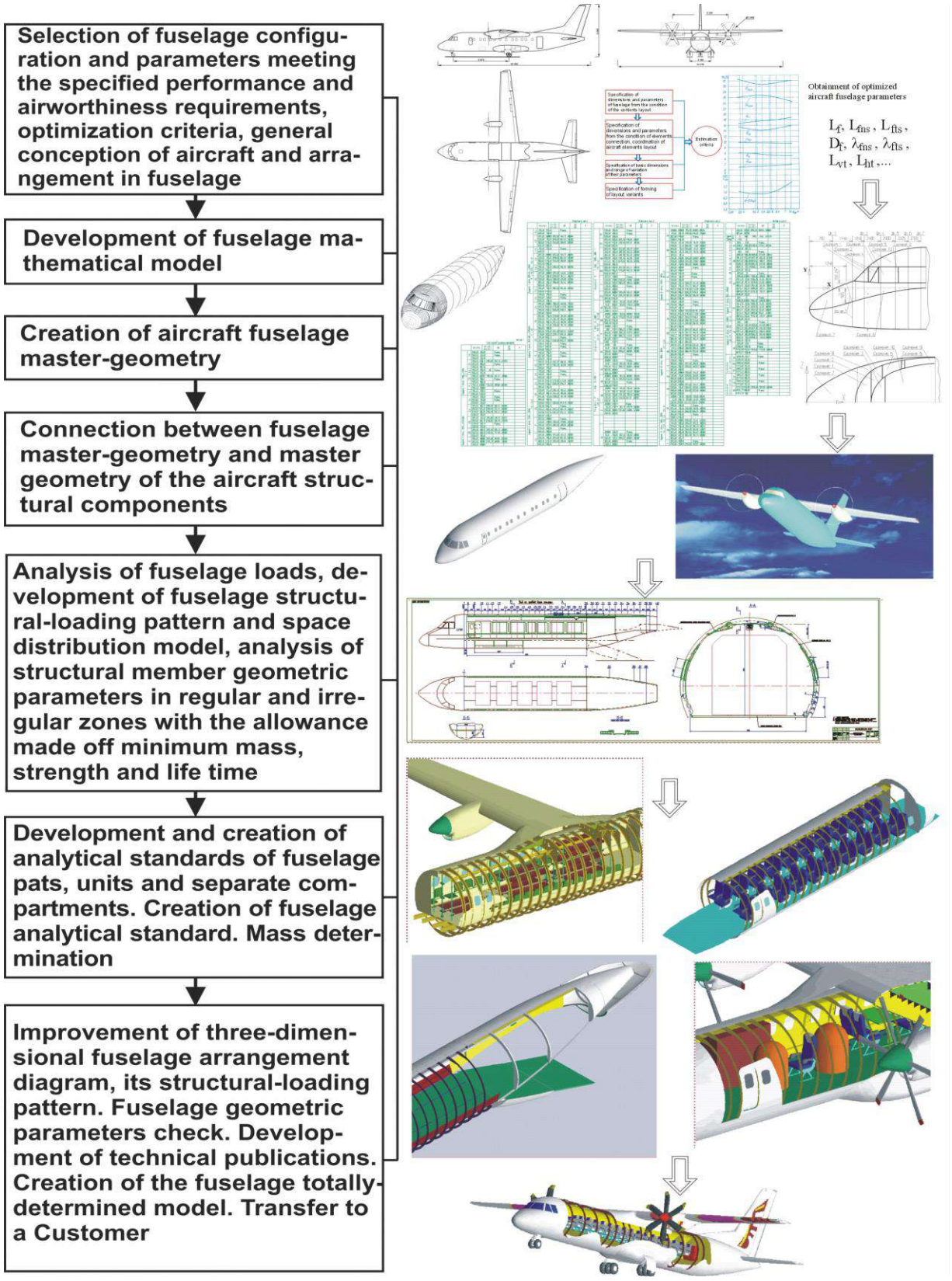

Fig. 2.10. Fuselage integrated design and computer-aided modelling method using CAD/CAM/CAE system

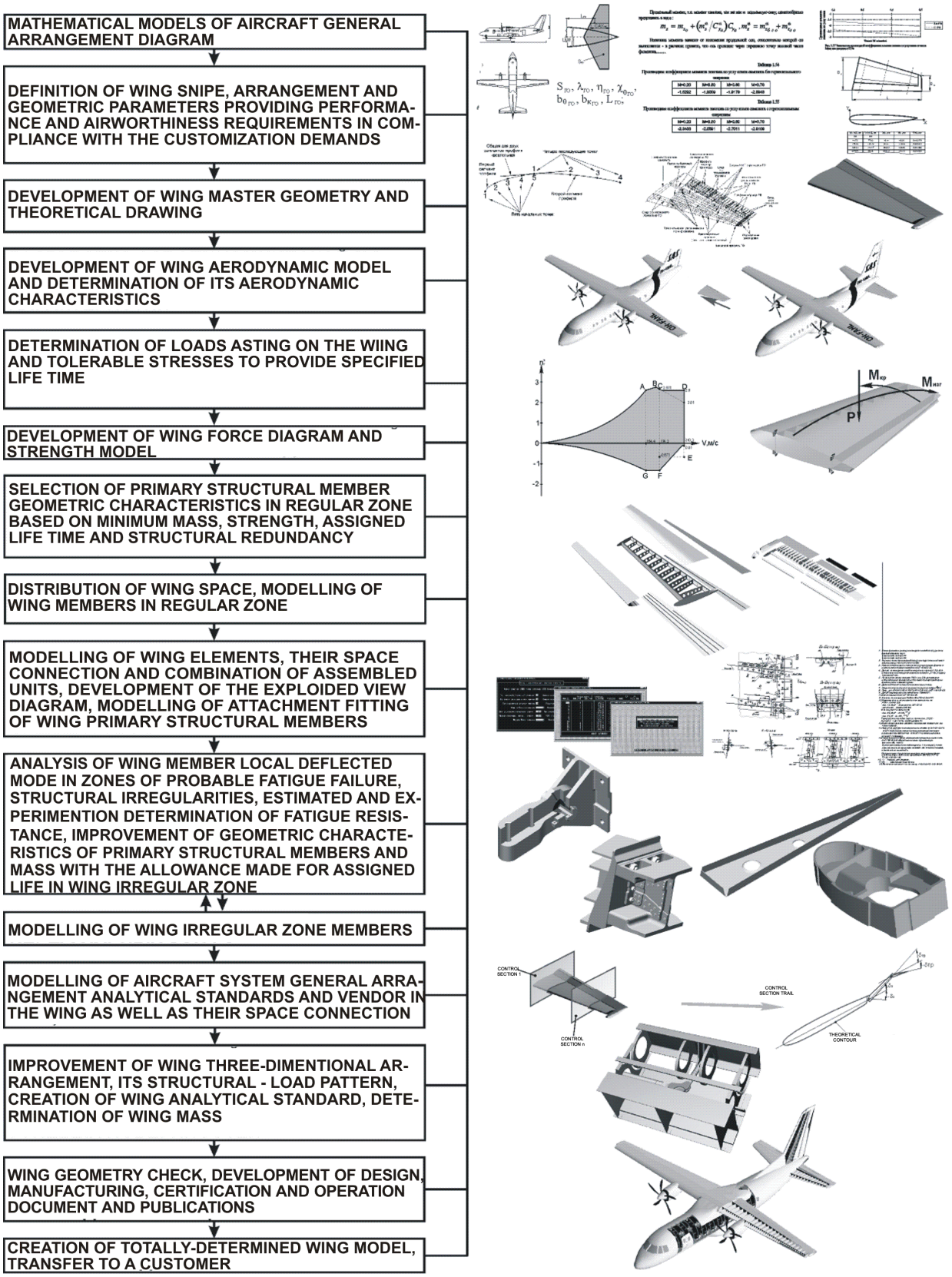

Fig. 2.11. Horizontal stabilizer integrated design and computer-aided modelling method using CAD/CAM/CAE system

necessary to specify conditions of units-to-units attachment. The point coordinates of stabilizer-to-fuselage, stabilizer-to-elevator attachment (in the cause of further designing, their position can be changed but it will result in chain change in associated units) will become such conditions for the horizontal stabilizer.

Using CAD/CAM/CAE UNIGRAPHICS system, the horizontal stabilizer geometric model can be constructed in the following way:

- a combination of curves are created to describe theoretical outlines of the horizontal stabilizer as well as position of structural – loading pattern members;
- theoretical outline surface model is performed in respect to existing combination of curves;
- three-dimensional models of primary structural member, skins and attachment fitting are created;
- connection of primary structural members, skins and attachment fittings are performed and accuracy characteristics of their relative position are analyzed.

The curves of the second order are widely used in aviation to describe flat outlines because they have curvature of like signs, that is, they don't have points of inflection to be vitally important condition for construction of airfoils. Equation giving general description of such curves has the following form.

$$Ax^2+Bxy+Cy^2+Dx+Ey+F=0.$$

To determine coefficients of this equation it is necessary to solve a set of five equations with five unknowns. Five conditions are sufficiently enough to solve this problem, for instance, curve passing through five points. The mathematical apparatus integrated in UNIGRAPHICS system allows to construct a curve of the second order in compliance with the following procedures:

– by five points;
– by four point and tangent direction in single extreme point;
– by three points and two directions of the tangent at extreme points;
– by engineering triangle method;
– by two points, two directions of tangents at extreme points and discriminant;
– by method of specifying coefficients of the second order curve equation.

In relation to the fact that airfoils are most commonly selected in the form of the theoretical tables of the common point coordinates, the following technique (Fig. 2.12) has been accepted in construction: the first airfoil segment is constructed through five taken start points. The next segments are constructed through four points (with the first one to be aligned with the last point of the previous curve) and the tangent direction is specified as a tangent to the previous curve (to specify tangent to the curve in creation of the second order curves using UNIGRAPHICS system, it is just enough to specify those curves to which tangent is constructed in the area of its end point). Such technique allows to get a set of curves smoothly

joined by tangent. Using an object information function, in what follows the system produces capabilities to describe constructed curves in the form of the engineering triangle solution (accuracy of common points coordinates and discriminant presentation reaches fourteenth decimal digit). After construction of all airfoil segments, it is necessary to approximate all segments, involved in unified airfoil, in single curve to facilitate subsequent construction of the model.

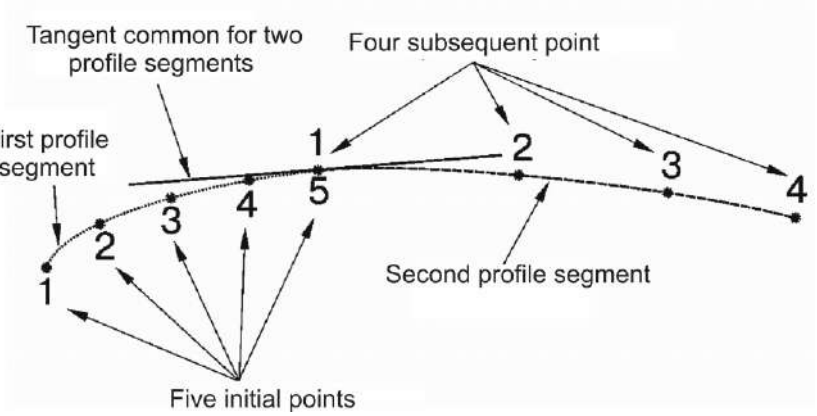

Fig. 2.12. Accepted pattern in construction of the second order curves

After construction of a single airfoil by the similar manner, let's construct all the rest airfoils of specified sectional view and make a combination of curves required for construction of surface model (traces of front and rear spars, frames of elevator, trim tab, geared trim tab and etc.) (Fig. 2.13).

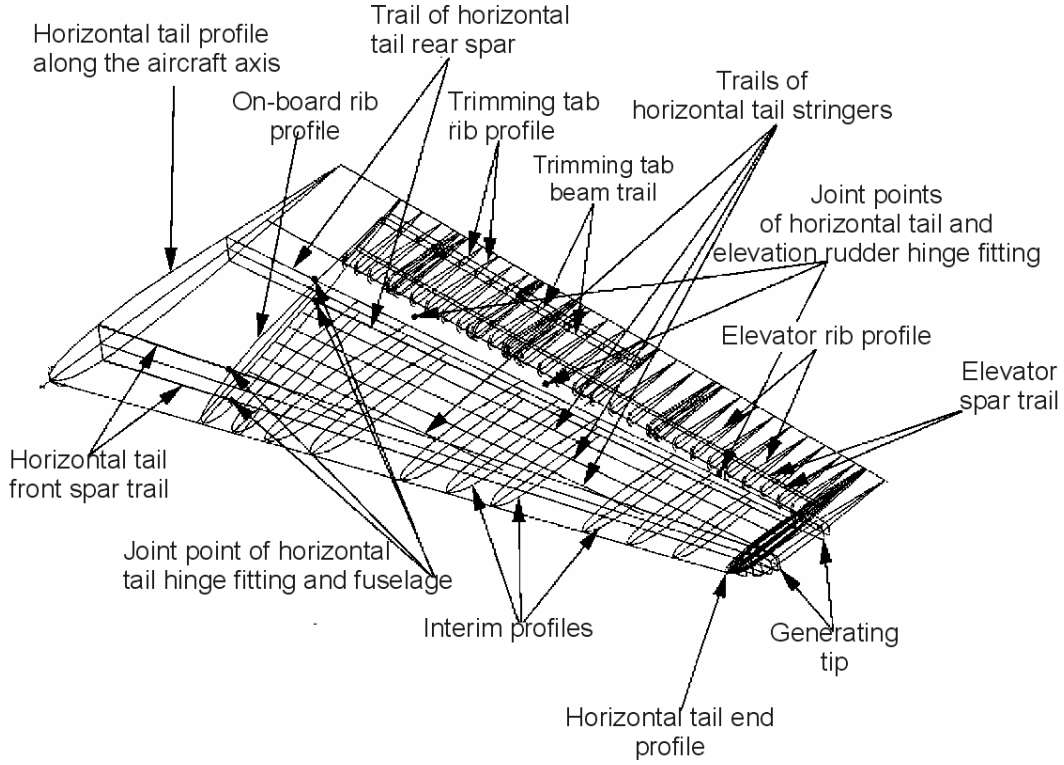

Fig. 2.13. Combination of curves required for construction of horizontal stabilizer model

Formation of curves combination is performed by the plane-parallel transfer of the constructed sectional view from the working plane to its point of reference (determined by geometric construction of the leading edge and trace line of the specified section).

Above-mentioned constructions are subsequently used for the development of the horizontal theoretical and assembly drawings. So, we have got a possibility to use one and the same geometric constructions for creation of both a unit surface model (computer standard) and drawing documentation excluding the probability of error when transferring sizes from the drawings to the model and from the model to the drawing. In addition, these constructions can be actually used in development of the operation and repair documents.

The next step is creation of the surface model of the tail unit theoretical outlines.

Surface construction module in UNIGRAPHICS system is used to make this model. This system module provides sufficiently great number of different techniques (totally fourteen main ones) in construction of surfaces but the use of the linear surface is most feasible for theoretical models as well as a trim tab and geared trim tab. The sense of surface construction of this type lies in selection of two boundary curves with the surface to be constructed according to the linear generating lines (Fig. 2.14). So, the surface is a result of line movement between two curves followed by their equivalent breaking into equal unlimited great number of segments. The stabilizer tip is the most complicated element for construction, so let's discuss its creation process more fully. For the aircraft under design, it is simultaneously used as an elevator horn balance.

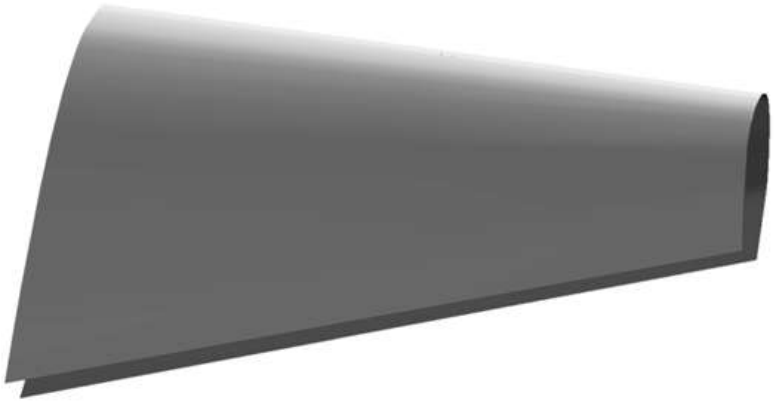

Fig. 2.14. Theoretical outline of stabilizer surface model

The use of the bisurface method as a construction technique for tip formation is assumed to be the most feasible. The sense of the method lies in generator movement by several generating curves (Fig. 2.15). In this case, the number of generators may vary (but not less than two) with the first one degenerating to the point.

1) generating curves; 2) curve generators.

The shape of the generators is determined with respect to aerodynamic reasons (induced drag reduction) while the arcs of the trailing edge (upper and lower) and the shape of the stabilizer tip are the generating curves in plan view. Take care that the percentage lines on the main stabilizer surface would be tangent to the start and end points. So, the surface is a result of variable curve generator movement by generating curves with biquadratic approximation of its modification (Fig. 2.16).

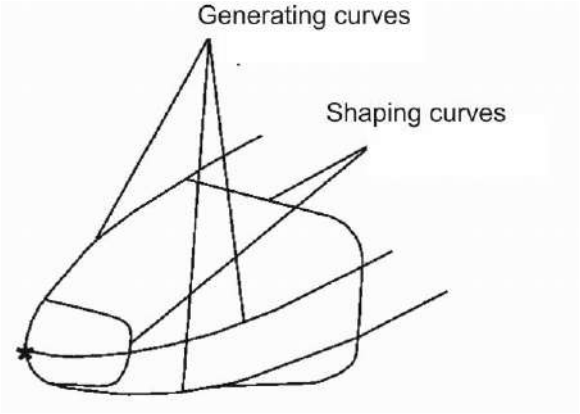

Fig. 2.15. Curve selection diagram for construction of bisurface

The next step during the further work is stabilizer theoretical line surface model division. With this aim view, decision is made to divide stabilizer skin into several segments (leading edge, interspar component parts trailing edge and etc.) in compliance with the proposed general arrangement diagram, assembly procedure and selected structural-loading diagram. Design analysis is performed for the structural-loading diagram. After completion the main geometric sizes of the structural members are determined. Analysis is made using either CAEmodule of UNIGRAFICS system or other application softwares, for example, RIT MOK. Thickness is given to the specified skin members in correspondence to the analysis performed. So, a set of stabilizer skins is a result of fulfilling this step in compliance with the theoretical outline and geometric parameters of the primary structural members.

Fig. 2.16. Horizontal Stabilizer Tip

In what follows, it is necessary to start making just a load-carrying set of stabilizer (elevator). It is constructed using solids modelling module of UNIGRAPHICS system. Different construction methods (given in sufficiently enough amount) are used for construction of different component types.

Procedure of section contour drawing along the generating line is the most feasible for the spar caps. Procedure of “squeezing-out” the specified geometry from the plane is the most suitable for rib formation. Revolution of curve generator around the axis is good for creation of fasteners models and elements of

the link type. Several different techniques followed by elements integration in the unified solid body are used for forming parts of complicated shape. Stabilizer-to-fuselage hinge fitting is the most complicated member in the construction. It is associated with the following reasons:

– multiparts (example given below involves ninety five parts);

– complicated exterior forms;

– necessity for connecting a great number of components.

Hinge fitting model is created as an assembly involving definite number of parts. In this case, all parts are formed in separate files resulting in significant decrease of the computer loading at this stage of work and, therefore, accelerating the model creation process. The solid modelling module of UNIGRAPHICS system and all techniques mentioned above are also used to create parts. This module has a through parameterization (both part sizes and graphic primitives as a basis for construction play a role of parameters) subsequently allowing geometry of parts and assemblies involved.

The unit structure is assembled by the method of attaching the files involved in assembly of parts to the main file. Parts positioning is performed according to the working coordinate systems followed by the check of the part mating. Overall view of the analytical standard of the stabilizer front hinge fitting is illustrated in Fig. 2.17.

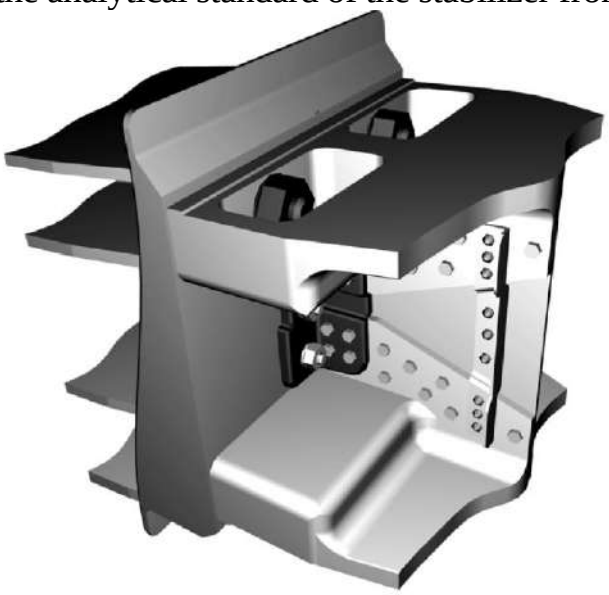

Fig. 2.17. Analytical standard of tail unit front hinge fitting

Having formed geometry of the primary structural members, we may start to "assemble" the horizontal stabilizer. This operation is performed using a special option of UNIGRAPHICS system that monitor member positioning to the point strictly defined by a designer in compliance with the strictly specified spatial orientation (INFO option produces data on mutual special position of parts displayed both in digital format and graphical form). Creation of analytical standards of elevator hinge fittings is the last step in making models of stabilizer and elevator. Taking into account that conditions of unit attachment have been still specified at the stage of draft design but the geometry of the primary structural members have been determined at the subsequent stages, we may start to create analytical standards of the attachment fittings.

They are also constructed in the solid modeling mode with the use of the same principles that were described above when discussing formation problems of the primary structural members and stabilizer attachment fitting. Obtained

analytical standard of the attachment fitting (Fig. 2.18.) passes just the same stages of analysis as the main structure of stabilizer and elevator.

Creation of stabilizer and elevator assembly and their exploided view diagrams is the final step (Fig. 2.19 and 2.20). It is used for formation of the aircraft complete assembly-arrangement model. All constructions done are parametric and, therefore, it would not be difficult to enter revisions into geometry of the members (when entering revisions in geometry, it is necessary to repeat the stages of the strength analysis).

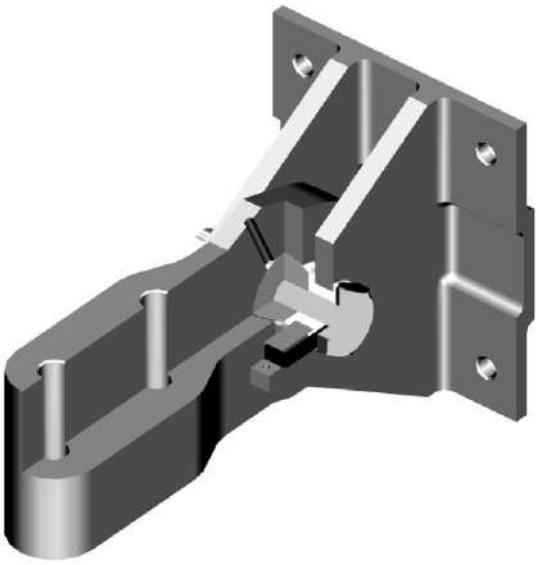

Fig. 2.18. Analytical standard of elevator attachment fitting

The geometry of the obtained members is the primary information source for the CAM module of the UNIGRAPHICS system. The programs for the numerically controlled machine tools are prepared in this module as well as design of other manufacturing procedures.

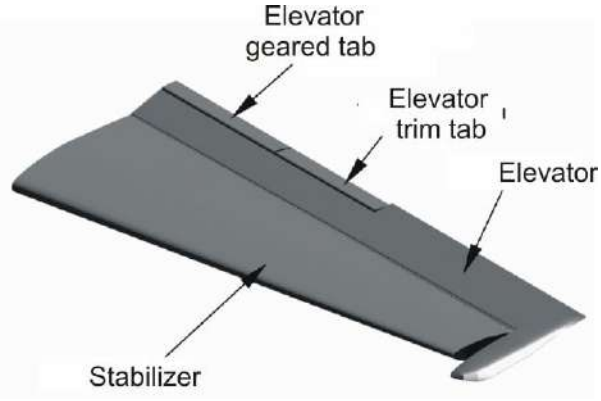

Fig. 2.19. Stabilizer and elevator assembly model

In this case, the geometry complexity and accuracy requirements do not put serious obstacles (with the experimental point in view, the author prepared programs for NC machines with a geometry track accuracy at an order less than the tool deformation value. Total problem processing time by the machine increased at a value not exceeding25…27%), in addition to the programs, the module allows to organize design of stamping, cutting, casting procedures and etc. in automatic mode. Designed parts are subdivided into groups in compliance with the type of the expected processing (milling, turning, casting, stamping and etc.), and their manufacturing procedure is subject to analysis.

Besides, obtained models are used for formation of the fixtures and equipment and for development of the design and production publications. This process is significantly simplified in computer systems. It is connected with the fact that presentation of the three-dimensional model in three main projections is automatically provided but construction of geometric sections is a process of construction of model body intersectional curves and secant plane (also automated). Thus, in creation of the drawing publications, the creation errors are

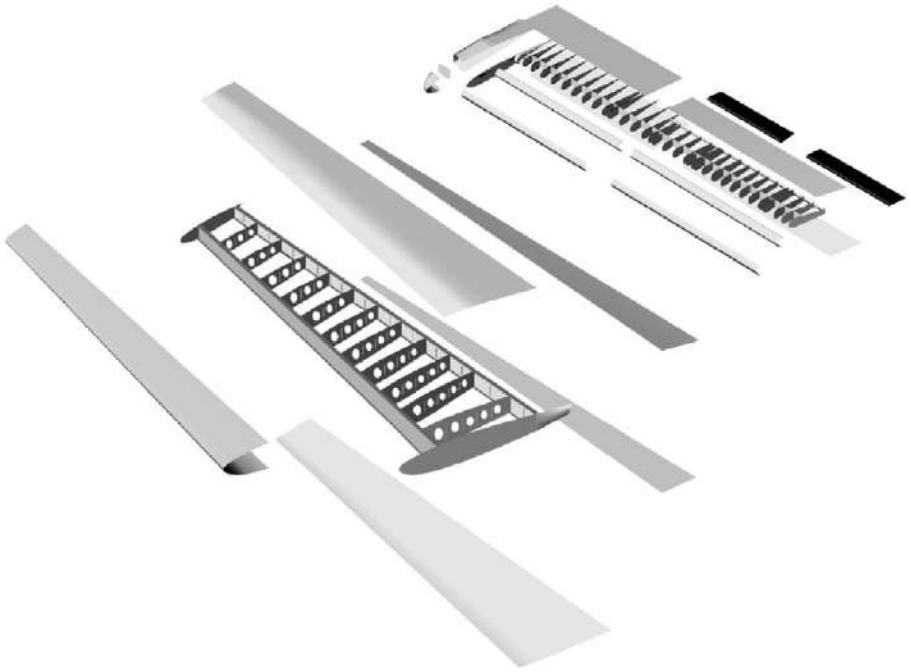

Fig. 2.20. Stabilizer and elevator exploded view diagram

practically excluded because all constructions are performed using a single original source (modals of parts units and etc.) The process of the obtained unit "disassemble" into components must be performed to create the operation and repair publications. The process is significantly simplified by the fact that the process of the specification and required design publications development is conducted simultaneously with the formation of the models. The units divided into groups are arranged on the margin of the explanatory drawings in compliance with the requirements for issuance of the repair and operation publications while textual part is created on the basis of the available design publications.

So, the application of the CAD/CAM/CAE systems allows to design aircraft airframe units more efficiently due to the following advantages:

– created modules are information primary sources for the other modules and systems used or external software;

– all constructions performed can be further used for creation of the design, manufacturing, operation and repair documentation;

– processes of unit structural and manufacturing development can be practically performed simultaneously;

– work with a total set of publications is simplified with the use of the information management;

– significantly high accuracy values of the designed units;

– manufacturing problems are revealed at early stages of the unit design in contrast to the manufacturing process and can be quickly removed;

– it becomes possible to design uniform-strength structures with continuous

revision of the geometric parameters;

– significant labor intensity reduction in designing and manufacturing of the unit parts and components.

Presented procedure in creation of aircraft structural standards is typical for the creation of the wing, fuselage and vertical stabilizer analytical standards. Some peculiar features of its implementation are given by the author in scientific digests and tutorials [13,46, 109, 112, 127, 150-152, 170, 172, 237, 240-244, 278, 285, 286, 326, 333, 429, 462].

2.3. Analysis of structurally-manufacturing parameters influences on the volume characteristics of the models deflected modes of aircraft assembly structure regular zone members by using of the CAD/CAM/CAE ANSYS systems

An aircraft airframe structure has a great number of stress concentrators and structural irregularities in the form of the holes for the installation of the attaching parts and fasteners. [141, 142, 147].

In the process of operation and service life tests of the modern aircraft structures it has been found that fatigue failure of the primary structural members occurs both in the zone of stress concentration and in the intensive zone of fretting-corrosion development. [35, 41, 73, 98, 214, 221, 253, 312, 413, 443, 456, 466].

The service life of an aircraft airframe must correspond to the service life of assembly structure regular zones. Life time of irregular zones must be higher or equal the life time of the regular zones. The holes filled with fasteners are the typical concentrators of the assembly structure regular zones. The service life of the structural members with such concentrators is determined by the characteristics of the local deflected mode initiated in the process of the variable loads application to the members [96].

Let’s discuss the effect of the structural and process variables on the deflected mode characteristics of the models of the assembly structure regular zone members.

2.3.1. Effect of load application level and fit type on the change of the plate deflected mode with a parallel hole bolt-fitted with interference and tightening

For prediction of life time and its change under specified level of load application, it is necessary to analyze the local deflected mode and also, to decrease amplitude of the local stresses and deformations in the installation zone of the fasteners.

The principle of superposition [456] was used to analyze the deflected mode in the joint members with the use of the elastic models. In doing so, overestimated values of stresses have been obtained, resulted in error in determination of the joint member life time. The elastoplastic deformation has been initiated in the installation of bolt with radial and axial interference. The application of a calculated software support complex of the finite element method with ANSYS (474) to be one of them, allows to take into account and to analyze the local deflected mode with an allowance made for elastoplastic behavior of material. As has been noted in the work [437], plasticity is a non-conservative process with the dissipation of energy depending on the model load application history. Therefore, in discussing this phenomenon a sequence of modelling process in installation of fasteners and the application of loads becomes a significant problem.

A stretchable plate with a hole filled with a bolt has been selected as an object of inquiry. In this case, different variants of bolt installation have been under discussion; with a radial interference of 1%; with an axial tightening of $P_з$ = 12072, 17140 and 24000 N; radial interference and axial tightening (Fig. 2.21).

1) Bolt 8-16 Кд ОСТ 1 31103-80
2) Nut 8– Кд Industry Standard ОСТ 1 33026-80
3) Washer 2-8-16 Ц ОСТ 1 34506-80

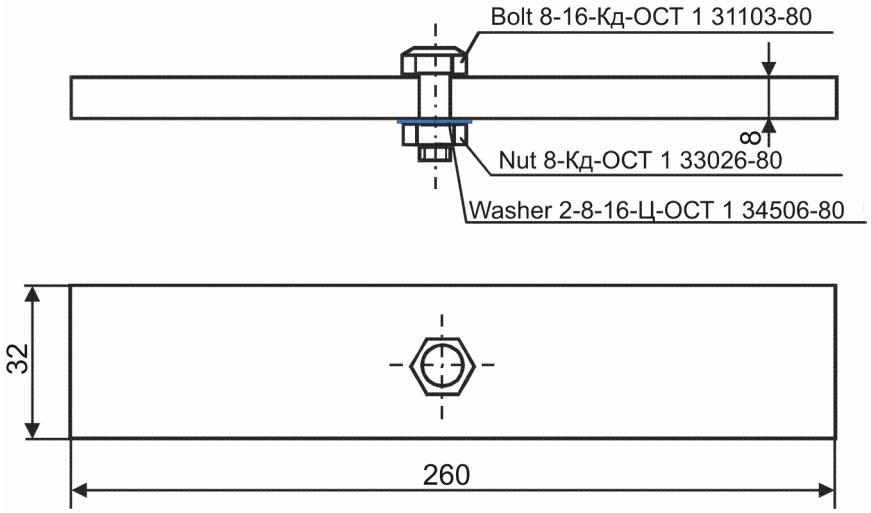

Fig. 2.21. Plate geometric model with a hole filled with bolt

In determination of the local deflected mode, the plate with a hole filled with fastener has three types of nonlinearity:

1. Geometric.
2. Physical – nonlinear dependence between stress and deformations. The plate material is Д16АТ aluminium alloy with an elastic modulus of E=70000 MPa and Poisson's ratio of v=o.3 [11, 12]. A polylinear elastoplastic model has been used for the plate material with an allowance made for the kinematic strengthening. Bolt material is 30ХГСА steel with

an elastic modulus of E = 210000 MPa and Poisson's ration of v=0.3. A model of linear elasticity being a numerical implementation of the Hooke's law has been used for the bolt.

3. Contact – change of contact surfaces condition in the process of deformation.

With an allowance made for the geometric symmetry and nature of the plate load application, let's discuss ¼ of the plate with the corresponding boundary conditions (Fig. 2.22).

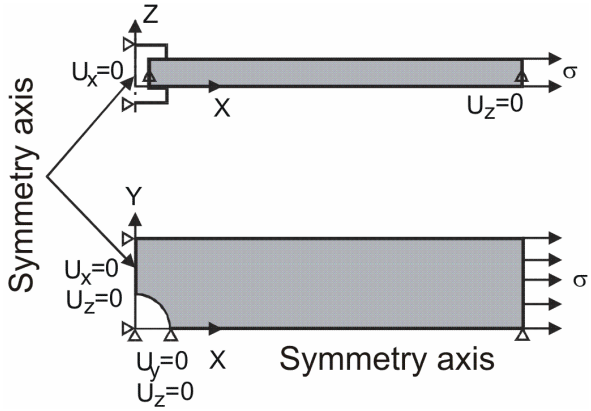

Fig. 2.22. Plate calculated pattern with a hole filled with bolt

Symmetry conditions have been specified by lines of symmetry (plane 2x and 2y). To limit the displacement along Z axis, the limitations have been specified according to the Z components of the displacement vector for the medial units located at the plate line of symmetry.

Analysis of the local deflected mode has been performed by the use of the ANSYS engineering analysis system.

The finite element model (Fig. 2.23) consists of twenty-three dimensional elements SOLID 95 as well as contact members of the second order TARGE 170 and CONTA 174.

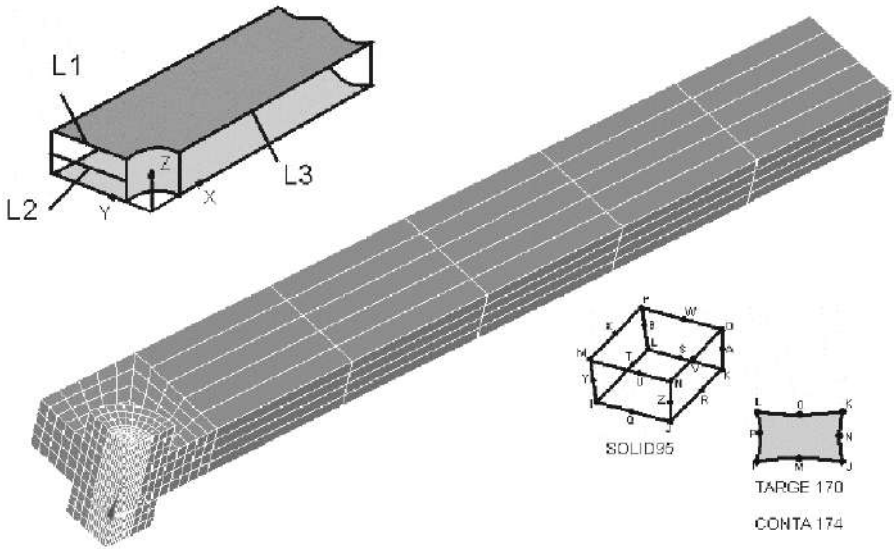

Fig. 2.23. Plate finite-element model with a hole filled with bolt

The plate with a free hole and a hole filled with the bolt has been subject to analysis of the local mode of deformation. The nature of the equivalent stress distribution in plate with a hole filled with by bolt under stresses in gross section of σ^{gr} = 100 MPa is illustrated in Fig. 2.24, 2.25.

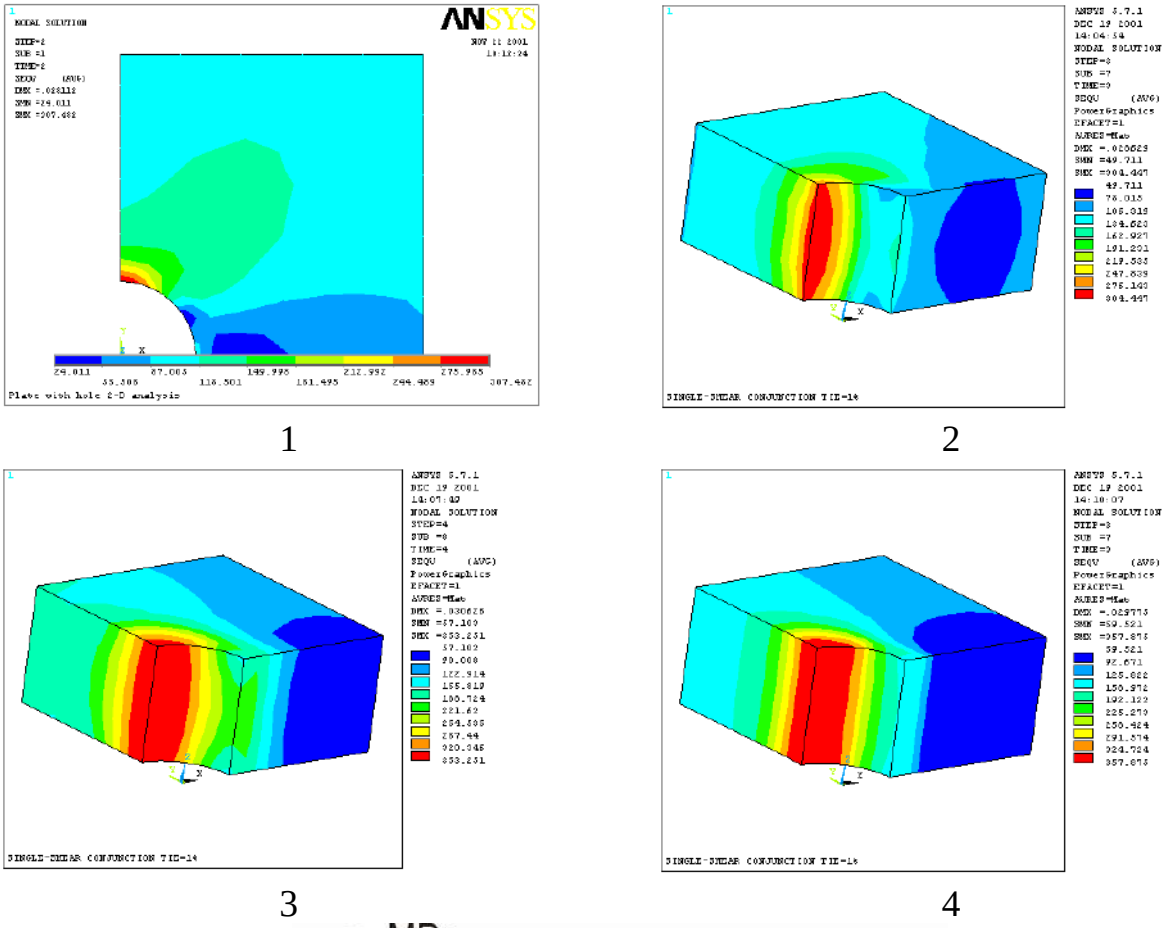

Fig. 2.24. Distribution of equivalent stresses in plate with the hole filled with bolt: 1 – free hole (without tightening and interference); 2 – with tightening P_t = 17140 N without interference; 3 – with radial interference 1% d_b and axial tightening P_t = 17140 N; 4 – with radial interference 1%d_b

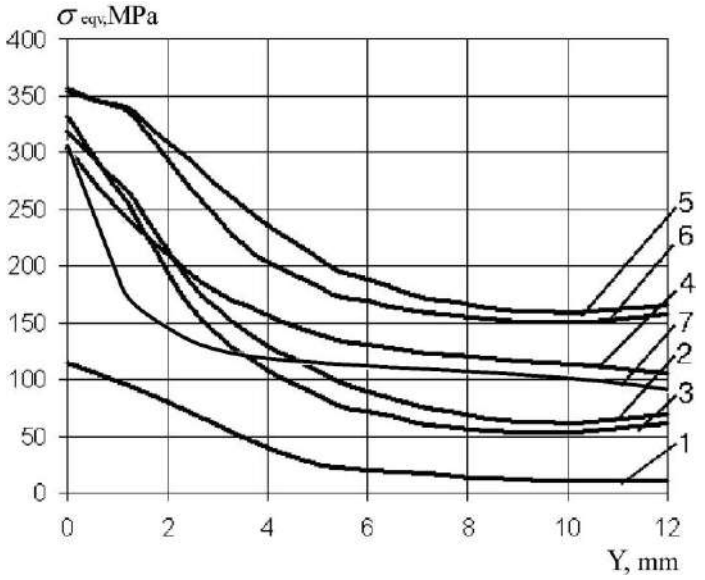

Fig. 2.25. Distribution of equivalent stresses in plate with a hole filled with bolt: 1 – with tightening of P_t = 17140 N (σ^{gr} = 0 MPa); 2 – with radial interference of 1% d_b and tightening of P_t =17140 N (P_t = 0 MPa); 3 – with radial interference of 1% d_b (P_t = 0 MPa); 4 – with tightening of P_t = 17140 N (σ^{gr} = 100 MPa); 5 – with radial interference of 1% d_b and tightening of P_t = 17140 N (σ^{gr} = 100 MPa); 6 – with radial interference of 1% d_b (σ^{gr} = 100 MPa); 7 – plate with a hole (σ^{gr} = 100 MPa)

The effect of the load application level in the local deflected mode in the plate has been investigated as well as the amplitude and mean values of the local equivalent stresses and deformations have been a subject to analysis. The results of analysis are illustrated in Fig. 2.26 – 2.29 where: 1 – without tightening and interference; 2 – with radial interference of 1% d_b; 3 – with tightening P_t = 17140 N; 4 – with radial interference of 1% d_b and axial tightening of P_t = 17140N (the principle of superposition).

It has been found as following:

1. Bolt installation in the plate hole with a radial interference with 1% d_b results in decrease of the local stresses amplitude within the range of the operating loads under analysis in 9-14 times and in the increase of mean stresses in 1.7-1.8 times in comparison with a plate with a hole not filled with the fastener and that, in turn, causes an increase of predicted life time 45 – 100 times.

2. Within an operating range (σ^{gr} = 90…150 MPa) an amplitude value of local stresses for the models using the principle of superposition exceeds the corresponding value for the model 4 without using the principle of superposition 1.3-3 times.

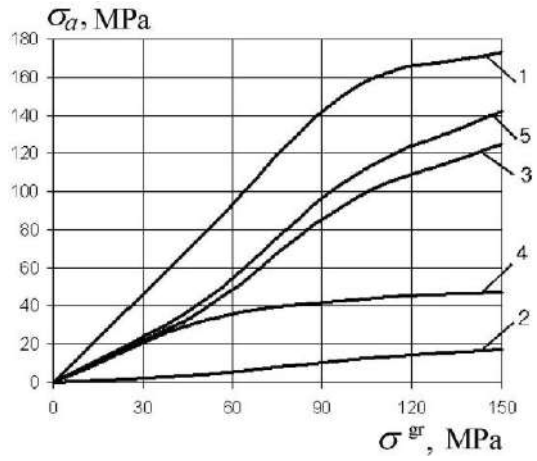

Fig. 2.26. Effect of load application level σ^{gr} on the amplitude value of local stresses in plate with hole filled with bolt

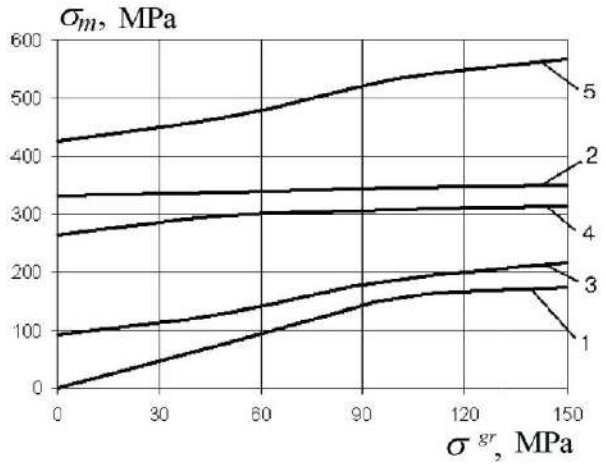

Fig. 2.27. Effect of load application level σ^{gr} on local stresses mean value in plate with hole filled with bolt

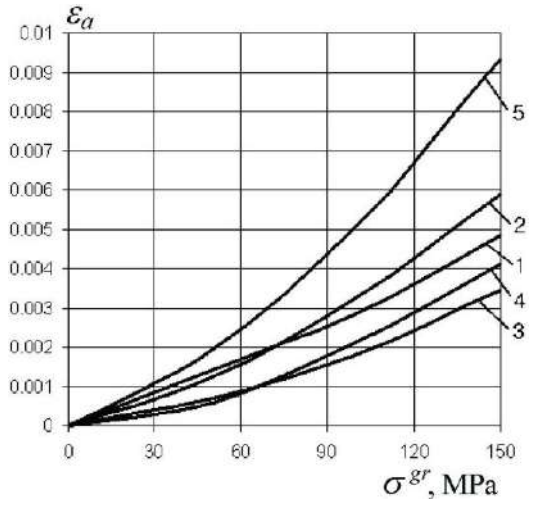

Fig. 2.28. Effect of load application level σ^{gr} on the amplitude value of local deformations in plate with hole filled with bolt

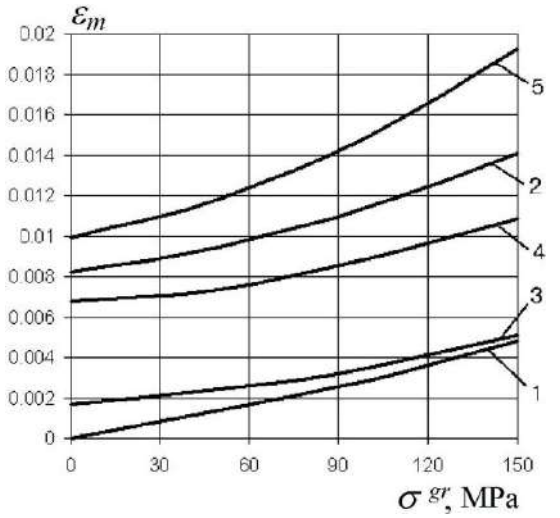

Fig. 2.29. Effect of load application level σ^{gr} on local deformations mean value in plate with hole filled with bolt

3. A value of mean local stresses for the model using the principle of superposition exceeds a respective value, for the model 4 that doesn't use the principle of superposition 1.75-1.8 times.

4. The amplitude value of the local deformations for the model using the principle of superposition exceeds a respective value in 2.3 – 3.25 times for the model 4 that doesn't use the principle of superposition.

5. The value of mean local deformations for the model using the principle of superposition exceeds a respective value for the model 4 that doesn't use a

principle of superposition 1.6-1.8 times.

The local deflected mode in a plate with a hole filled with bolt has been also analyzed according to the values of maximum tangential (shearing) stresses.

The influence of the tightening force on the amplitude and mean local stresses within an operating range of the loads corresponding to the stresses in the plate gross section from 0 to 150 MPa has been subject to analysis.

The analysis result is illustrated by the graphs (Fig. 2.30 – 2.34).

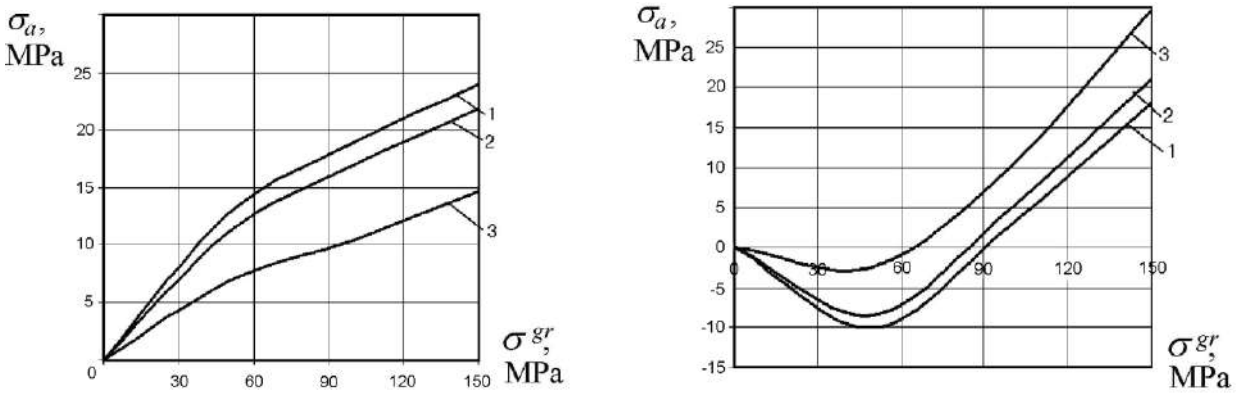

а в

Fig. 2.30. Effect of load application level σ^{gr} on the amplitude value of local equivalent stresses in plate with hole filled with bolt

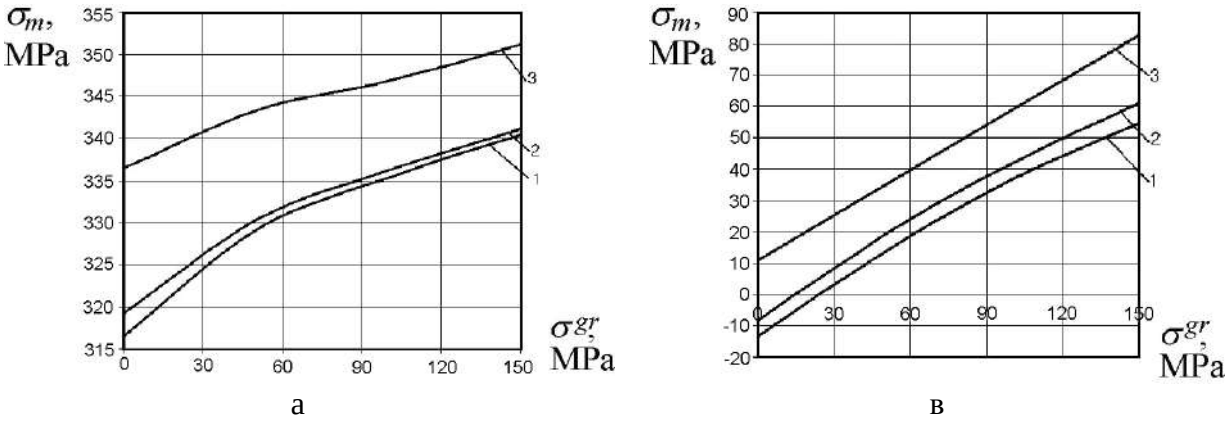

а в

Fig. 2.31. Effect of load application level σ^{gr} on the mean value of local equivalent stresses in plate with hole filled with bolt

The nature of the hole filling with bolt is identified with the digits: 1 – with radial interference of $1\%d_b$ and bolt tightening force of P_t = 12072 N; 2 – with radial interference of $1\%d_b$ and bolt tightening force of P_t = 17140 N; 3 – with radial interference of $1\%d_b$ and bolt tightening force of P_t = 24000 N; while by the letters respectively:

a – allocation along the line L2; b – allocation along the line L3.

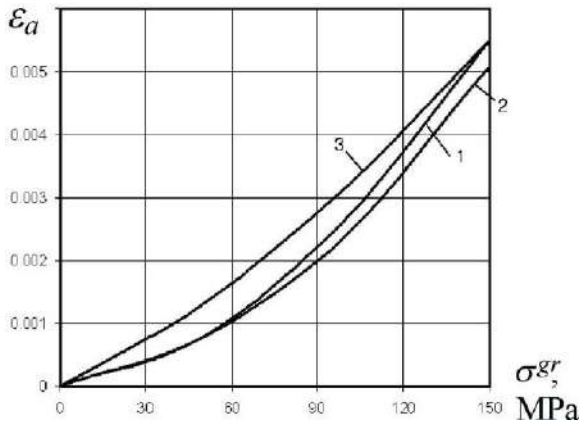

Fig. 2.32. Effect of load application level on the amplitude of equivalent deformations in plate with hole filled with bolt (allocation along line L2)

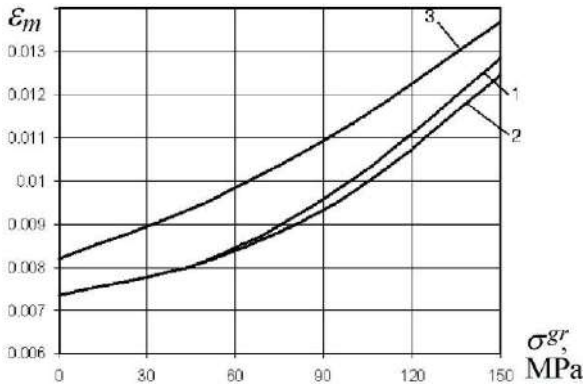

Fig. 2.33. Effect of load application level on value of mean equivalent deformations in plate with hole filled with bolts (allocation along line L2)

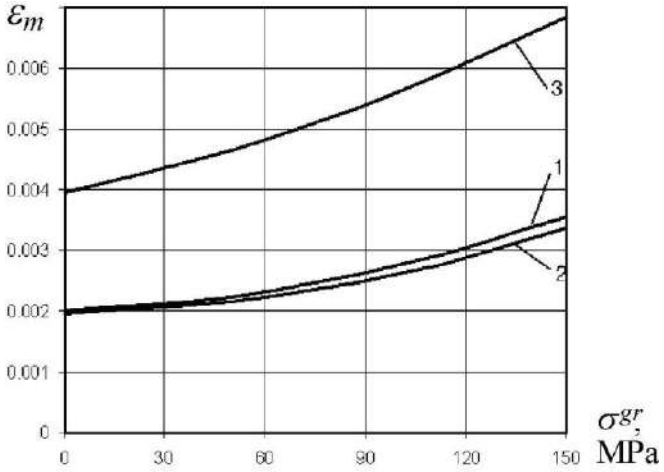

Fig. 2.34. Effect of the load application level on value of mean deformations in plate with hole filled with bolt (allocation along line L2)

After analyzing the results obtained, we may come to the following conclusions:

1. Increase in axial tightening within the range under study from P_t = 12072 N to P_t = 24000 N results in stresses amplitude decrease by 10 – 80% within the range of stresses σ^{gr} = 80…150 MPa.

2. Axial tightening increase causes increase of mean stresses by 3 – 10% within the range of stresses σ^{gr} = 80…150 MPa.

3. Axial tightening increase causes decrease of deformation amplitude by 2 – 11 % within the range of stresses σ^{gr} = 50…150 MPa.

4. Tightening increase results in decrease of mean deformations by 2.3 – 9.8 % within the range of stresses σ^{gr} = 50…150 MPa.

As mentioned above, fretting-corrosion originated in case of

microdisplacement between the surfaces of contacting parts is due to the fatigue failure. There is an uneven contact distribution in the contact zone (Fig. 2.35).

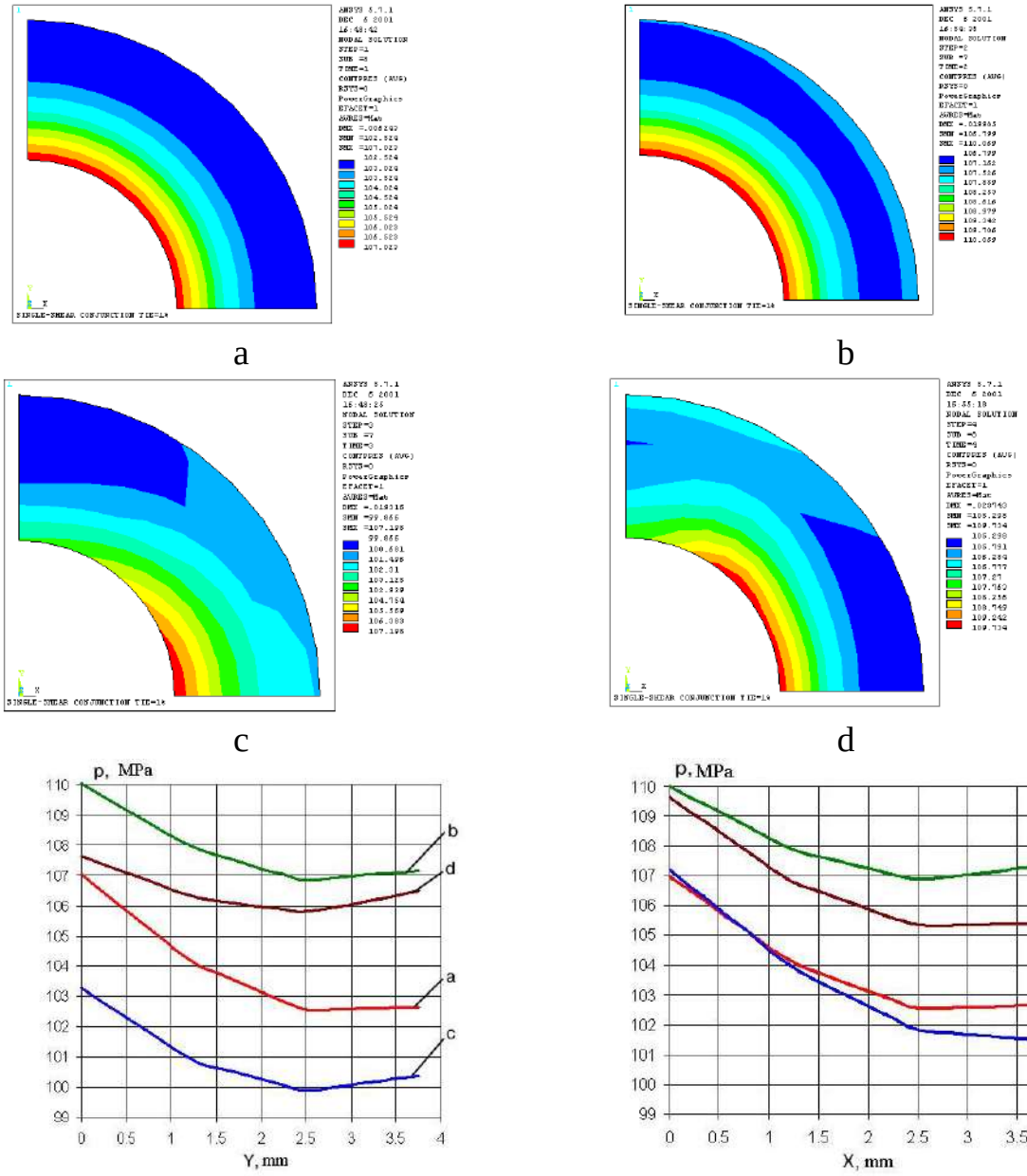

Crosswise direction Lengthwise direction

Fig. 2.35. Contact pressure distribution field under the bolt head in plate with hole filled with bolt: a – with an axial tightening of P_t = 17140 N; b – with radial interference of 1% d_b and axial tightening force of P_t = 17140 N; c – combined stresses of P_t = 17140 N and tensile stresses σ^{gr} = 100 MPa; d – combined action of a radial interference 1% d_b, axial tightening of P_t = 17140 N and tensile stresses of σ^{gr} = 100 MPa

Analyzing the results it must be noted that the application of the external tensile load results in redistribution of the contact pressures. In this case, their mean value is decreased by 2.8 – 4% in comparison with the contact pressures in unloaded joint. It can be seen from the Fig. 2.34 that maximum value of the contact pressures is acting by the hole contour, and it takes place under application of the tensile stresses the maximum offsets to the point lying on the holes longitudinal axis making, ipso facto, this direction is potentially hazardous.

An amplitude change of local stresses along the lines L3 in the load range under study exceeds the respective value along the line L2 1.3 times providing the reasons to draw conclusion: an area under the bolt head along the direction L3 is a probable zone of the fatigue failure in plate with the hole filled with bolt installed with the radial interference and axial tightening under the acting conditions of the variable tensile stresses and fretting-corrosion development.

2.3.2. Local deflected mode analysis of plate with cylinder – conic hole filled with bolt with countersunk head

A plate model with a cylinder-conic hole filled with a countersunk bolt is a basic model for predicting their endurance for the countersunk shear joints. Different cases of bolt installation have been examined in the process of modeling: without interference and tightening; with radial interference of 1% d_b; with axial tightening of P_t = 10 kN; with radial interference of 1% d_b and axial tightening of P_t = 10 kN.

The model is a plate made of Д16АТл5 sheet having dimension of 200x48x5 with a cylinder-conic hole of Ø 8mm and a countersink angle of 90° and a plate of 32×48×5 also fabricated of Д16АТл5 connected with steel bolt 8-22-Кд-ОСТ 1-3 1191-80.

Part geometry is illustrated in Fig. 2.36. In case of bolt installation with interference, the difference between the diameter of the bolt and the hole is 0.08 mm.

Bolt material is steel 30ХГСА, modulus of elasticity is E = 210000 MPa, Poisson's ratio is 0.3. Linear-elastic behavior of the bolt material described by the Hooke's law has been taken for the analysis.

Plate material is an aluminium alloy Д16Т, modulus of elasticity is E = 70000 MPa, Poisson's ratio is 0.3. A multilinear model with the kinematic strengthening law has been selected to describe a behavior of the plate material. The joint members when loaded with the tensile strain have been used for the analysis of the local deflected mode using the engineering analysis system ANSYS for the following variants:

1) Plate with a cylinder –conic hole;

2) Plate with a cylinder-conic hole and a plate connected with bolt installed in the hole with a radial interference and axial tightening;

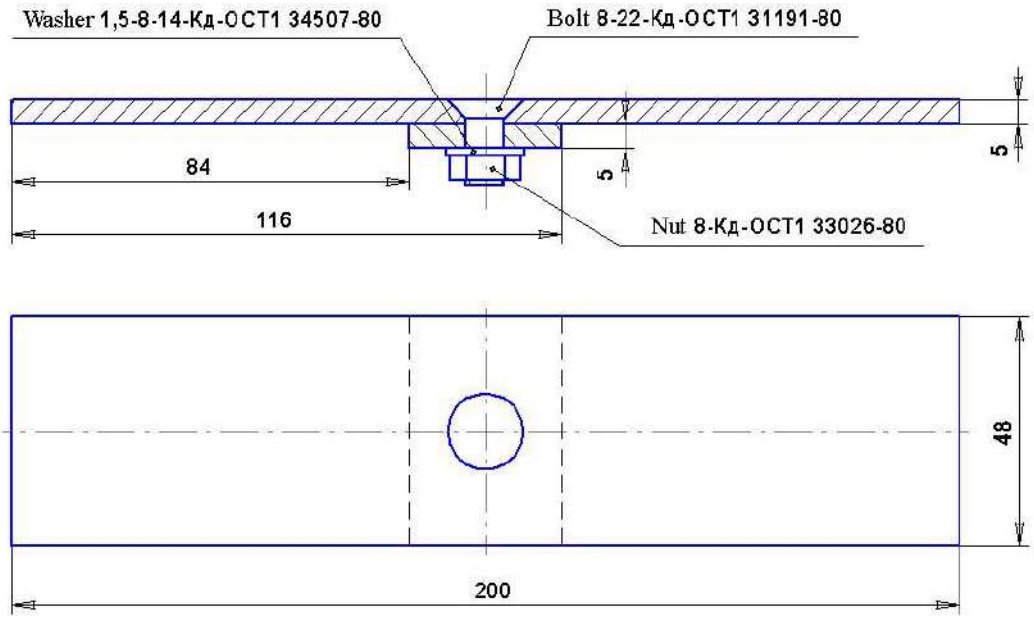

Fig. 2.36. Geometry model of plate with cylinder-conic hole filled with countersunk bolt

3) Plate with a cylinder-conic hole and a plate connected with bolt installed in the hole with a radial interference of 1% d_b;

4) Plate with a cylinder-conic hole and a plate connected with bolt installed in the hole with an axial tightening of P_t = 10 kN;

5) Plate with a cylinder-conic hole and a plate connected with bolt installed in the hole with a radial interference of 1% d_b and axial tightening of P_t = 10 kN.

1/4 model with the respective boundary conditions has been examined with an allowance made for the geometric symmetry and the nature of an external load application (Fig. 2.37).

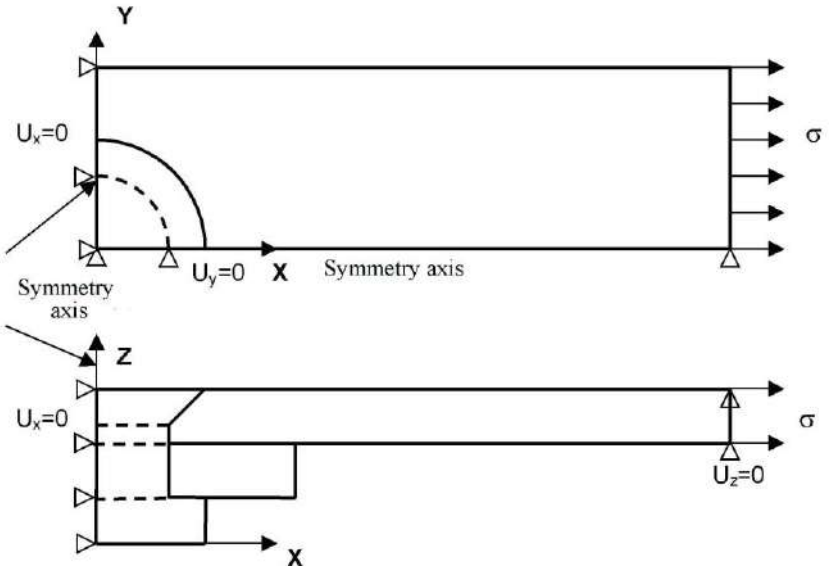

Fig. 2.37. Loading of the diagram of plate model with cylinder-conic hole, plate and bolt

The symmetry conditions have been specified by the symmetry axis (plains ZX and ZY). Limitations have been specified by Z-displacement vector component for all units located on the end of the surface at the application point of the external tensile load to limit displacement of the model along Z-axis.

The finite-element model (Fig. 2.38, 2.39) consists of volumetric eight-unit elements SOLID 45 as well as of contact elements CONA 173 and tightening elements PRETS 179 presented in ANSYS system [474].

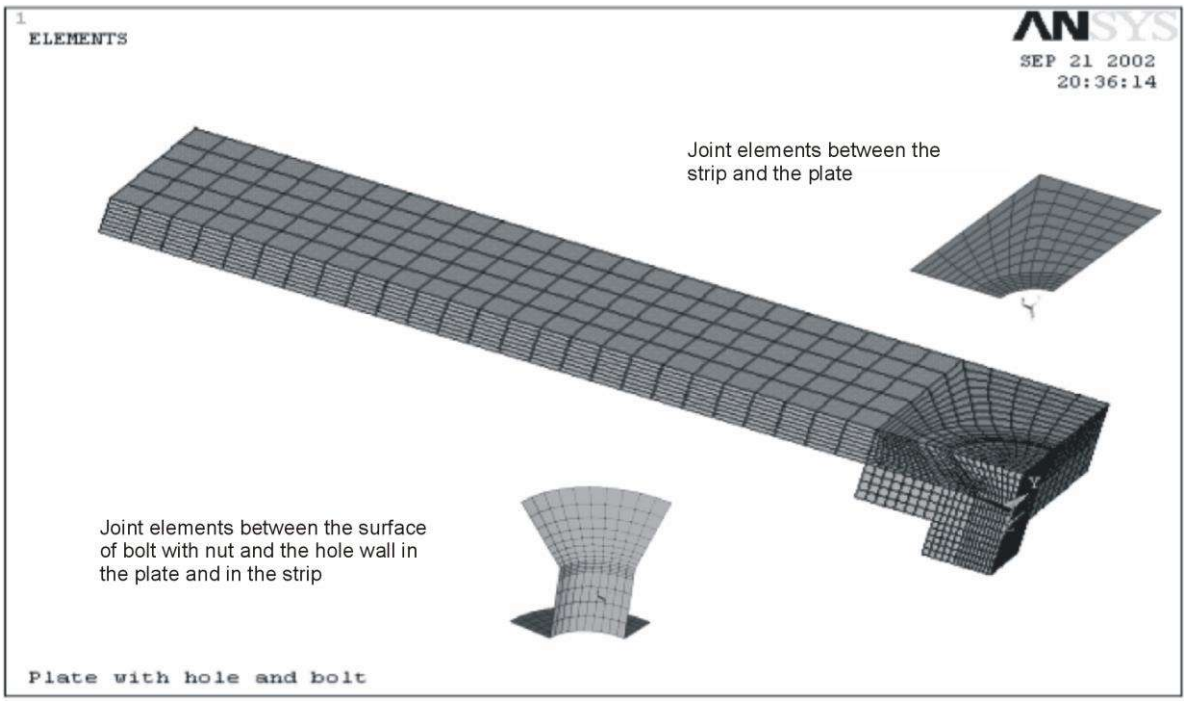

Fig. 2.38. Plate finite-element model with cylinder-conic hole filled with bolt

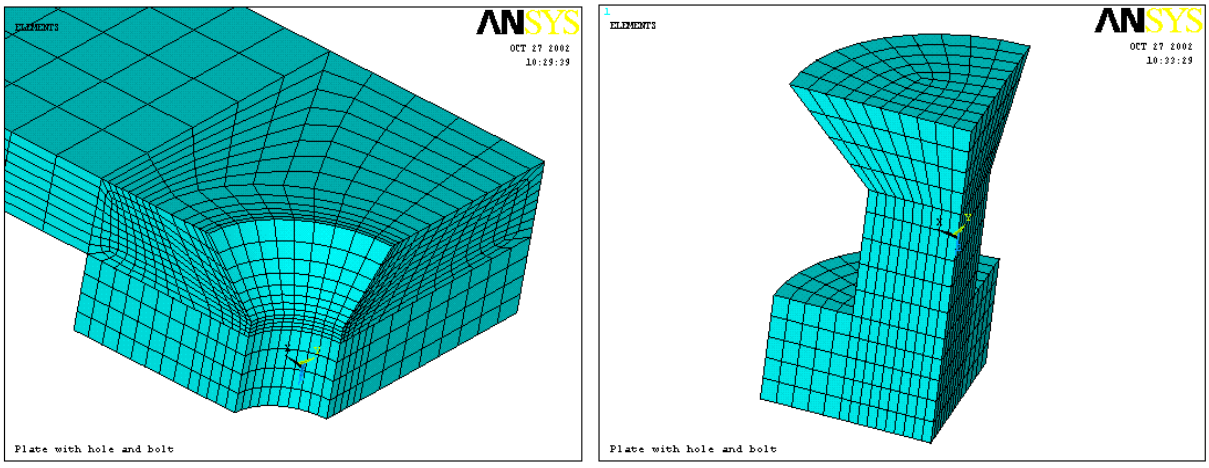

a b

Fig. 2.39. Plate finite-element model with cylinder-conic hole filled with bolt: a – plate and piece; b – nut bolt

The radial interference has been simulated by realizing an effect of the "initial penetration" of the bolt body in the hole wall under contact algorithm. In the modeling of contact interaction a "surface-to-surface" contact model has been selected and an elastic coulomb friction model with a friction coefficient of 0.15 has been used. Axial bolt tightening and pre-stressed state in joint members initiated as a result of axial tightening application has been simulated by application of the special tightening element PRETS 179. Preliminarily meshed bolt has been "dissected" into two parts and the special tightening elements PRETS 179 have been generated by insertion of the finite elements junction lying in the dissected section.

The following options have been taken for analysis involving: allowance for the effect of great deformations, complete method of Newton-Raphson solution without adaptive descent, PCG solver type with an accuracy of 1E-5 as a result of the finite –element problem solution, a local deflected mode in plate, piece and bolt due to the action of the radial interference, axial tightening and their combined action has been analyzed under conditions of the plate uniaxial tension. Distribution field of the equivalent stresses σ_{eqv} in joint members under the load application level of σ^{gr} =100 MPa and different variants of bolt installation are illustrated in Fig. 2.40.

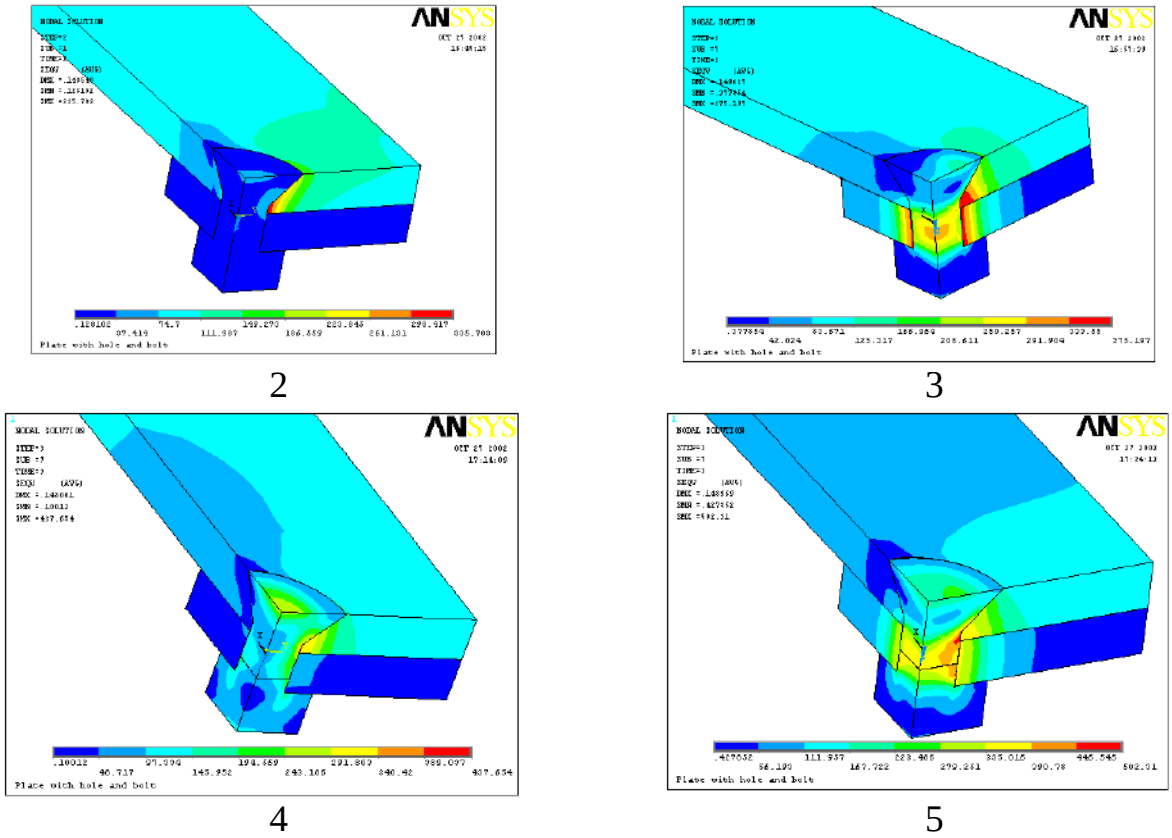

Fig. 2.40. Distribution field of equivalent stresses σ_{eqv} in joint members under the load application level of σ^{gr} = 100 and different variants of the bolt installation

The local deflected mode in the plate with a cylinder-conic hole filled with bolt and unfilled one has been also estimated in correspondence to the maximal normal values of tensile stresses and deformations (Fig. 2.41, 2.42). Radial interference and axial tightening effect on the local deflected mode of plate has been analyzed.

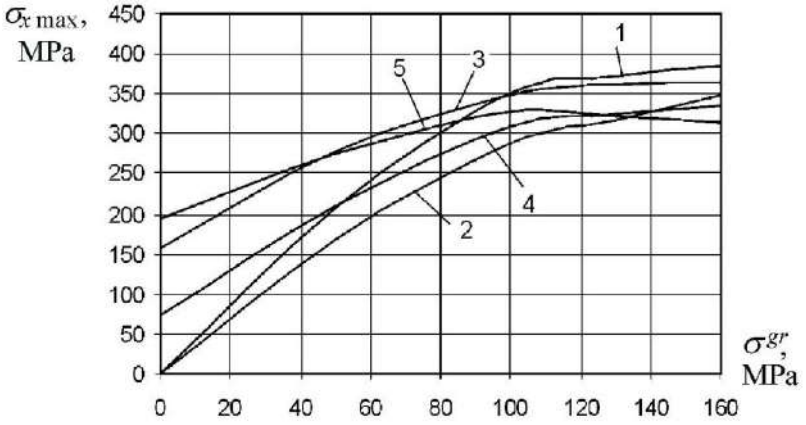

Fig. 2.41. Load application level effect (σ^{gr}) on value of maximal tensile stresses $\sigma_{x\,max}$ in plate with the cylinder-conic hole

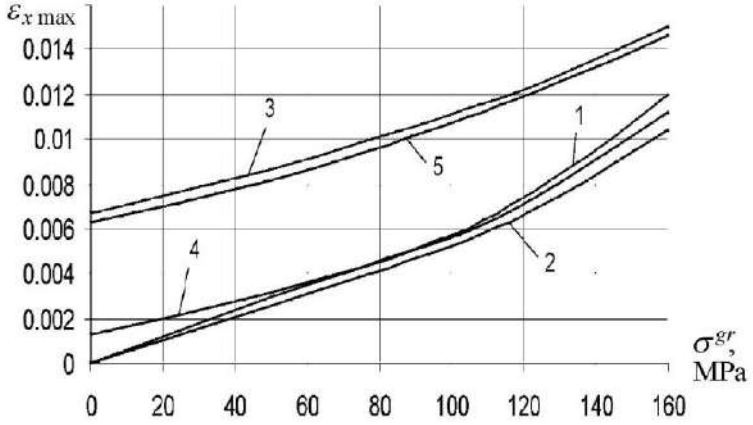

Fig. 2.42. Load application level effect (σ^{gr})on value of tensile deformations $\varepsilon_{x\,max}$ in plate with the cylinder-conic hole

It should be noted that maximal tensile stresses $\sigma_{x\,max}$ are acting at the different points of the plate under different variants of bolt installation and application of the external load.

Following bolt installation with a radial interference of 1% d_b in the plate hole and increase of external load application level of σ^{gr}=100 MPa, the zone, where maximal values of tensile stresses are initiated, moves smoothly from the cylinder portion of the plate hole to the conic one in the crosswise direction from the hole axis. With an increase of the external load application level

σ^{gr}=0…160 MPa, this zone is insignificantly displaced in crosswise direction down the plate. In bolt installation with a radial interference of 1% d_b and axial tightening of P_t =10 kN, not displaced and is arranged in the lower field of the plate hole cylinder portion.

But in increase of the external load application level σ^{gr} >110 MPa, there is a marked drop of the tensile stress maximal values from 327 MPa (at σ^{gr}=100 MPa) to 315 MPa (at σ^{gr} =160 MPa).

The zone of maximal tensile deformations under bolt installation with an axial tightening of P_t =10 kN is localized in the plate hole cylinder portion and is not displaced within the total range of σ^{gr} =0…160 MPa. With a radial interference of 1% d_b , the zone of initiation of maximal tensile deformations is located in the plate hole cylinder portion to be displaced in the direction of Z axis following growth of σ^{gr} in case of bolt installation with a radial interference of 1% d_b and axial tightening of P_t=10 kN, the zone of maximal tensile deformations is located in the lower field of the plate hole cylinder portion and is not displaced in change of the external load application level σ^{gr} .

The positive effect due to the application of the radial interference 1% d_b as well as its use in combination with an axial tightening of P_t =10 kN lies in the fact that the initial tensile stresses are initiated in the hole zone (stress concentrator) and totalizing with the stresses caused by the external load action they reduce the degree of irregularity and amplitude of stresses within the total range of σ^{gr} in comparison with a plate having a hole.

In case of bolt installation with a radial interference the maximal tensile deformations (see Fig. 2.42) exceed in 2.13. times the maximal tensile deformations corresponding to the bolt installation without radial and axial interferences under identical level of load application σ^{gr} =100 MPa.

The addition of the axial tightening to the radial interference increases the maximal values of the mean deformations in 1.02…1.07 times. The difference becomes less in increase of the external load level.

The influence of the bolt installation character and external load application level (σ^{gr}) on the distribution field of the equivalent stresses $\sigma_{eqv\ \max}$ in plate (Fig. 2.43) and maximal values of equivalent stresses in plate (Fig. 2.44.) has been demonstrated. Comparing values $\sigma_{eqv\ \max}$ by the variants of the bolt installation, it should be noted that maximal values of the equivalent stresses in plate within the total range of change of the external load application σ^{gr} correspond to these values under the variant of the bolt installation with a radial interference of 1% d_b (curve 3). Joint application of the radial interference 1%d_b and axial tightening of P_t = 0 kN results in a slightly lesser values of $\sigma_{eqv\ \max}$.

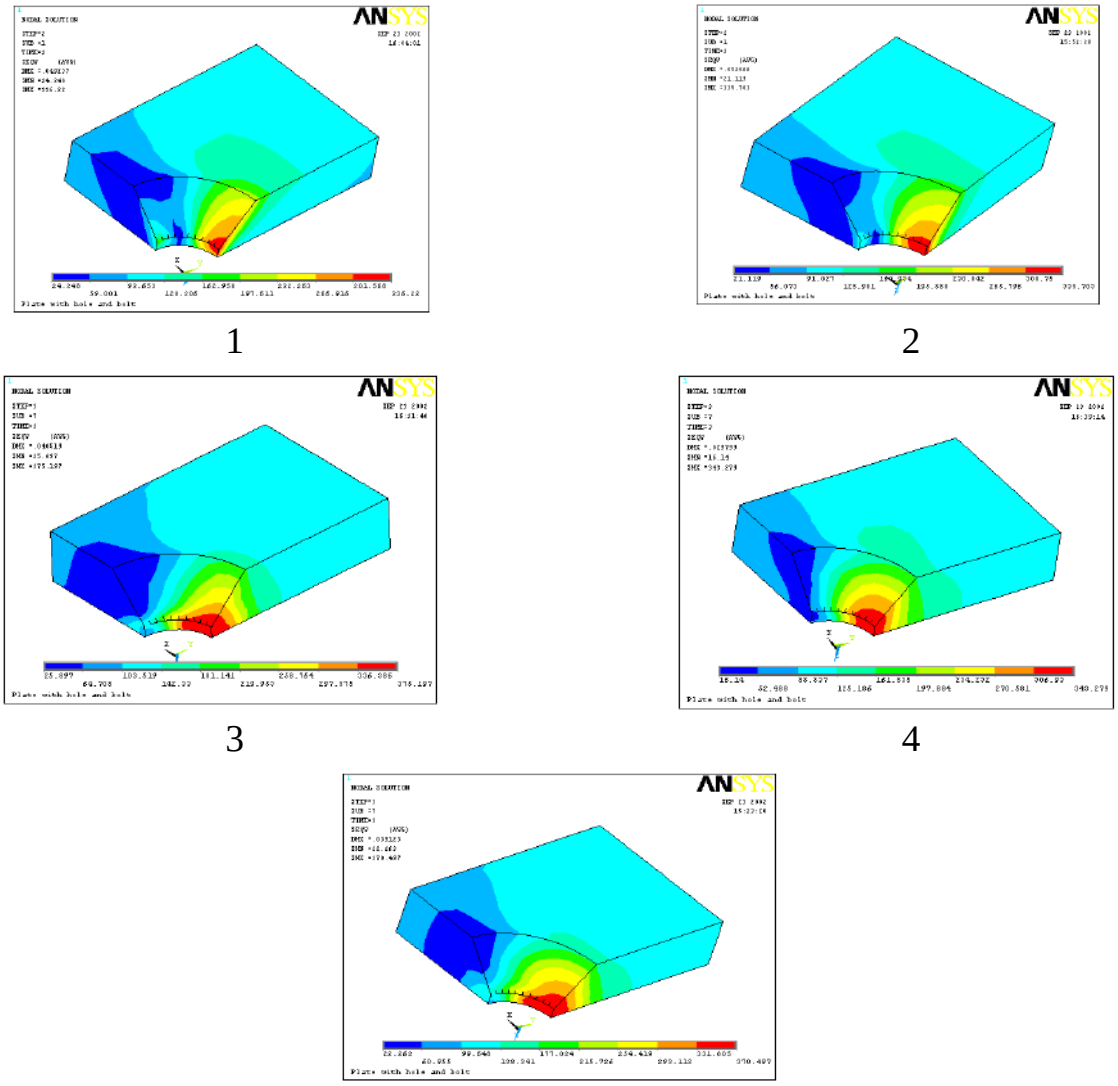

Fig. 2.43. Distribution field of equivalent stresses σ_{eqv} in plate under load application level of σ^{gr} = 100 MPa and different variants of bolt installation

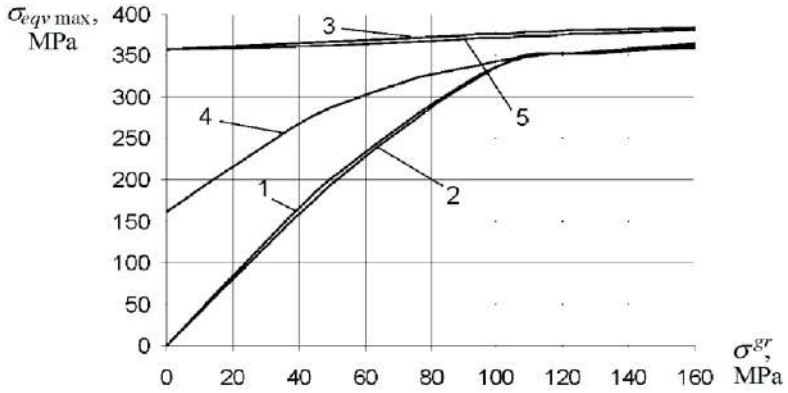

Fig. 2.44. Influence of the external load application level and bolt installation character on value of maximal equivalent stresses of $\sigma_{eqv\,\max}$ in plate

We can estimate stress distribution degree of irregularities by calculating values of the concentration factors of the local tensile stresses $K_\sigma = \sigma_{max} / \sigma^{gr}$ and deformations $K_\varepsilon = \varepsilon_{max} / \varepsilon^{gr}$ under different variants of bolt installation and external load application level (Fig. 2.45. a,b).

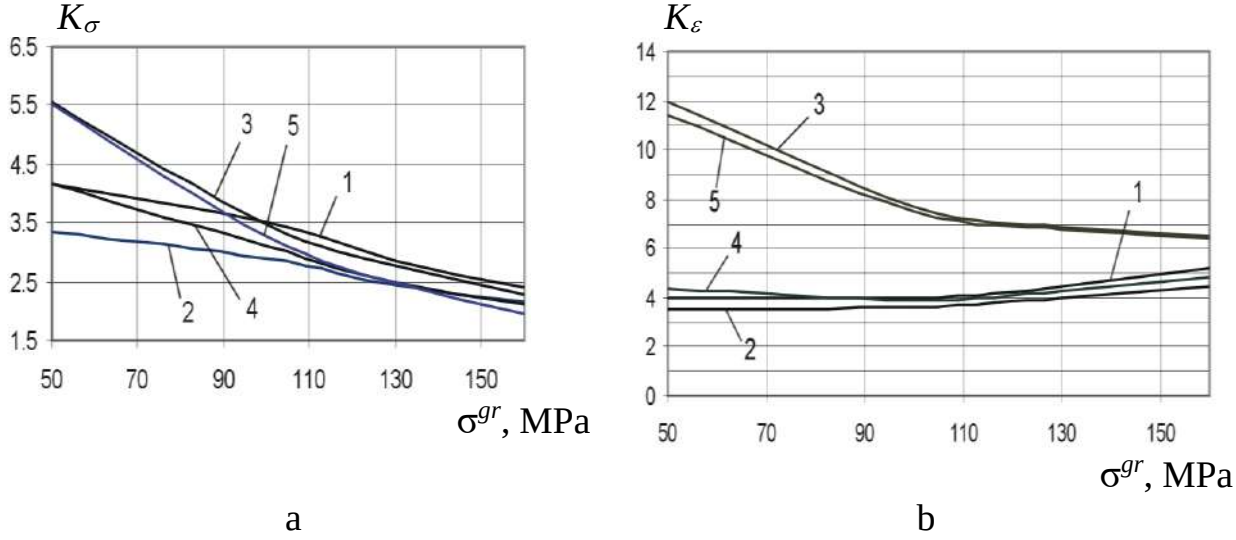

a b

Fig. 2.45. Effect of load application level σ^{gr} on concentration factor value of tensile stresses (a) and deformation (b)

It is evident from the graph (Fig. 2.45, a) that radial interference application of 1% d_b 1% d_b alone does not reduce stress concentration factor in the plate with an unfilled hole at σ^{gr} < 100 MPa. In this case, the stress concentration factor under the bolt installation with a radial interference will increase in 1.05…1.65 times in comparison with stress concentration factor under bolt installation without radial interference and axial tightening and will take maximal values in comparison with the other variants of the bolt installation at σ^{gr} < 100 MPa. But, radial interference in combination with the axial tightening at σ^{gr} >135 MPa gives the lowest stress factor of concentration (up to 1.1 times at σ^{gr} =160 MPa in comparison with the bolt installation without radial and axial interferences).

Analysis of the deformation factor of concentration has shown that application of the radial interference 1% d_b increases K_ε in 1.44…3.35 times. This difference has decreased following growth of the external load application level. Joint application of the radial interference 1% d_b and axial tightening P_t =10 kN also gives relatively high deformation factor of concentration though, to some extent, less than under interference of 1% d_b. At σ^{gr} > 110 MPa this difference becomes insignificant. So far as the stress concentration and deformation factors do not allow to estimate definitely the positive effect resulting in application of the radial interference 1% d_b and axial tightening P_t =10 kN, the maximum values of

amplitude and mean local stresses and deformations in plate have been selected as additional criteria. Results in estimation of the amplitude and mean values of local stresses and deformations are presented in Fig. 2.46.

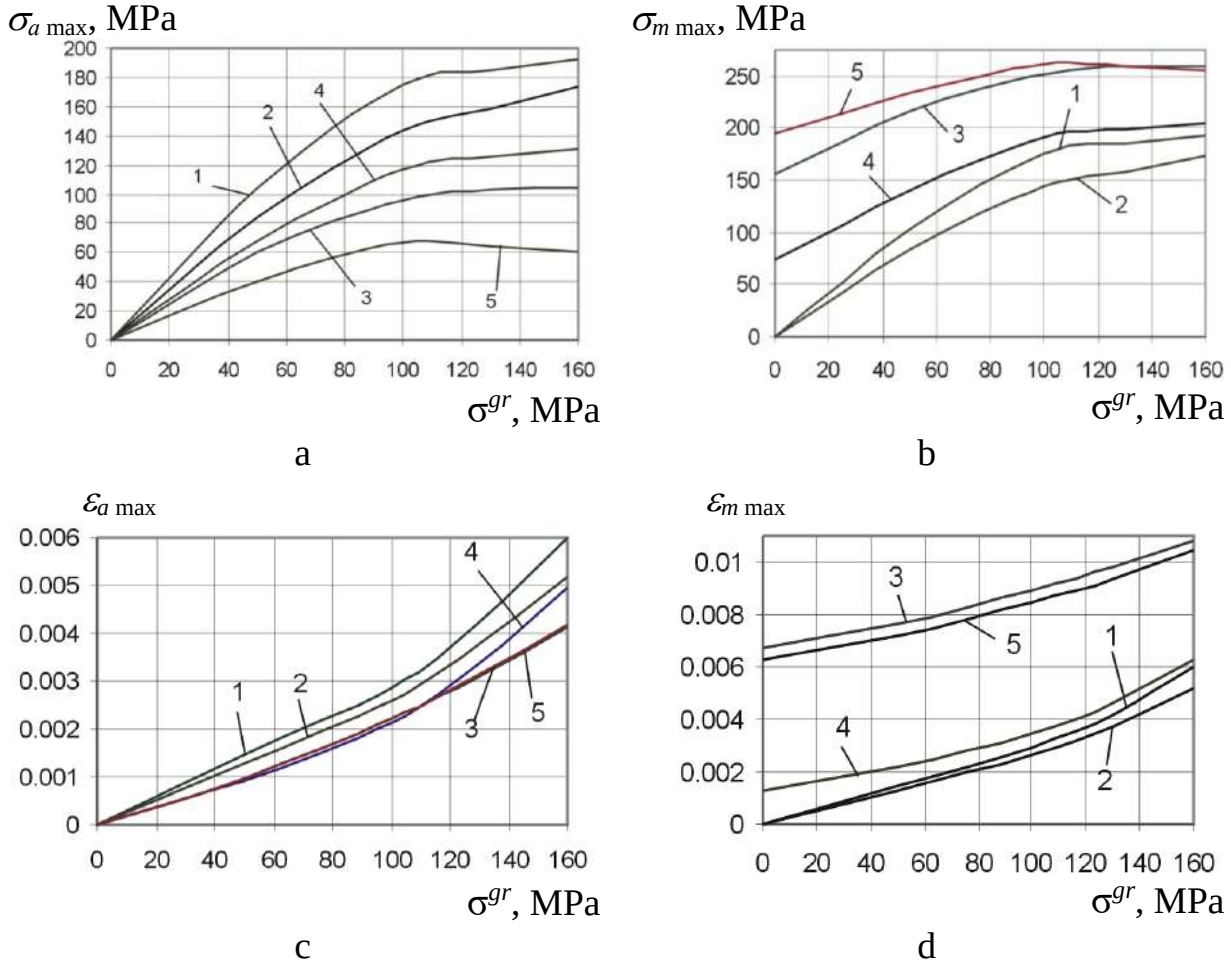

Fig. 2.46. Load application level effects on (σ^{gr}): a – amplitude of maximal local stresses in plate with a countersunk hole filled with countersunk bolt; b – mean maximal local stresses in plate with a countersunk hole filled with countersunk bolt; c – amplitude of maximal local deformations in plate with a countersunk hole filled with a countersunk hole filled with a countersunk bolt; d – mean maximal local deformations in plate with a countersunk hole filled with countersunk bolt

It has been found that application of the radial interference reduces maximal amplitude local stresses much more efficiently than axial tightening. Joint application of the radial interference with an axial tightening reduces amplitude of local stresses in 2.17 times at σ^{gr} = 100 MPa in comparison with the bolt installation without axial and radial interferences. The maximum amplitude local deformations after application of the radial interference are also decreased (1.17 times in comparison with the case of bolt installation without radial and axial interferences). The peculiar feature is that the axial tightening of the bolt in

combination with radial interference doesn't produce practically any effect on the distribution pattern of the maximum amplitude local stresses in the plate after the radial interference at the different level of external load application σ^{gr}.

The maximal mean stresses under an external load application level of $\sigma^{gr} < 130$ MPa correspond to the variant of the bolt installation with a radial interference and axial tightening (1.82 times greater in comparison with the variant without axial and radial interferences at an external load application level of $\sigma^{gr} = 100$ MPa).

At a level of $\sigma^{gr} > 130$ MPa, the maximum one corresponds to the variant with a radial interference.

The maximum mean deformations are significantly increased after application of the radial interference (3.41 times in comparison with a variant without radial and axial interferences at an external load application level of σ^{gr} =100 MPa). The application of a radial interference of 1% d_b with an axial tightening of P_t = 10 kN in decreases maximum mean deformations 1.05 times at external load application level of σ^{gr} = 100 MPa. The local analysis of the contact pressures between the surfaces of the structural joint members is one of the significant criteria to predict and analyze the failure of the structural joint members by the countersunk bolt. The distribution field of the contact pressures between the shank surfaces of a bolt, nut, plate and piece is illustrated in Fig. 2.47 – 2.50.

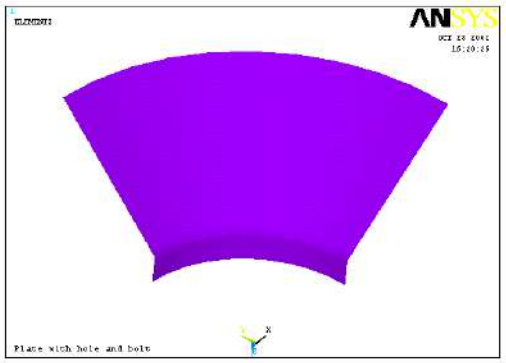

2

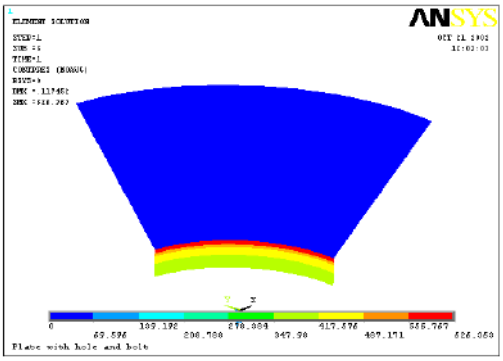

3

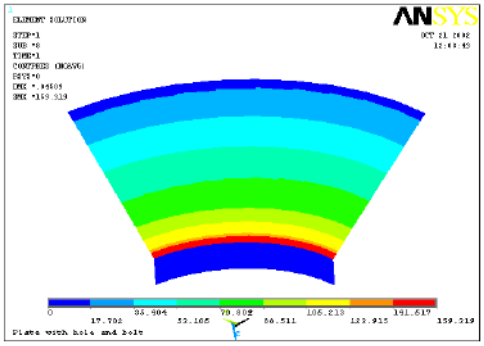

4

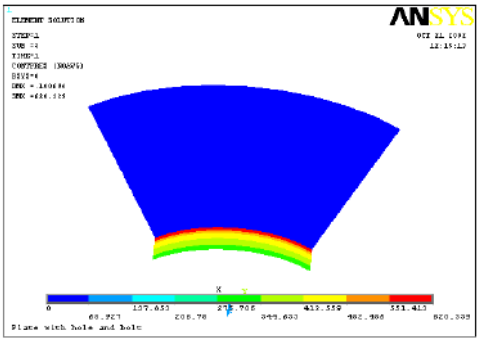

5

Fig. 2.47. Distribution field of contact pressures along cylinder-conic surface in contact zone of bolt shank with hole wall at an external load application level of σ^{gr} = 0 MPa and different variants of bolt installation

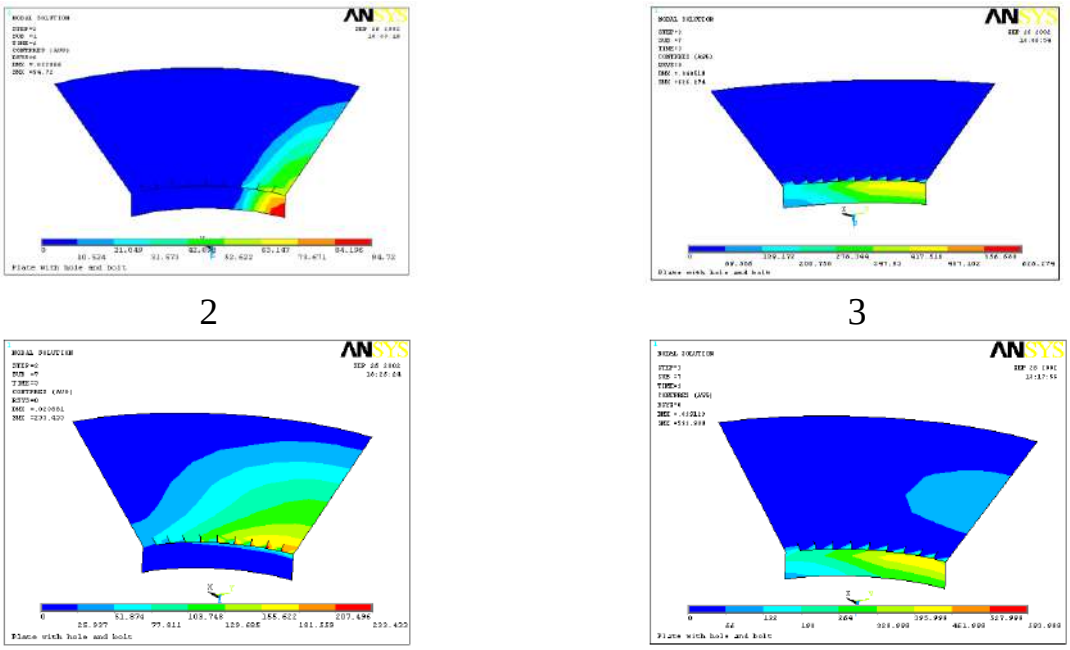

Fig. 2.48. Distribution field of contact pressures along cylinder-conic surface in contact zone of bolt shank with a hole wall at an external load application level of σ^{gr} = 100 MPa and different variants of bolt installation

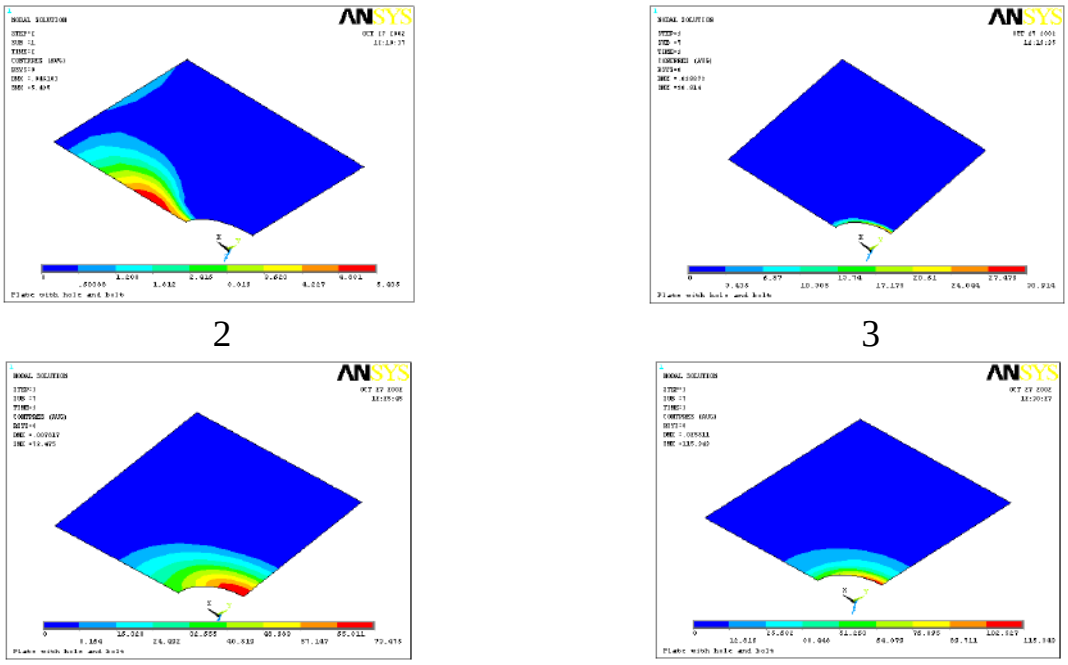

Fig. 2.49. Distribution field of contact pressures along the plate-to-piece contacting surface at an external load application level of σ^{gr} = 100 MPa and different variants of bolt installation

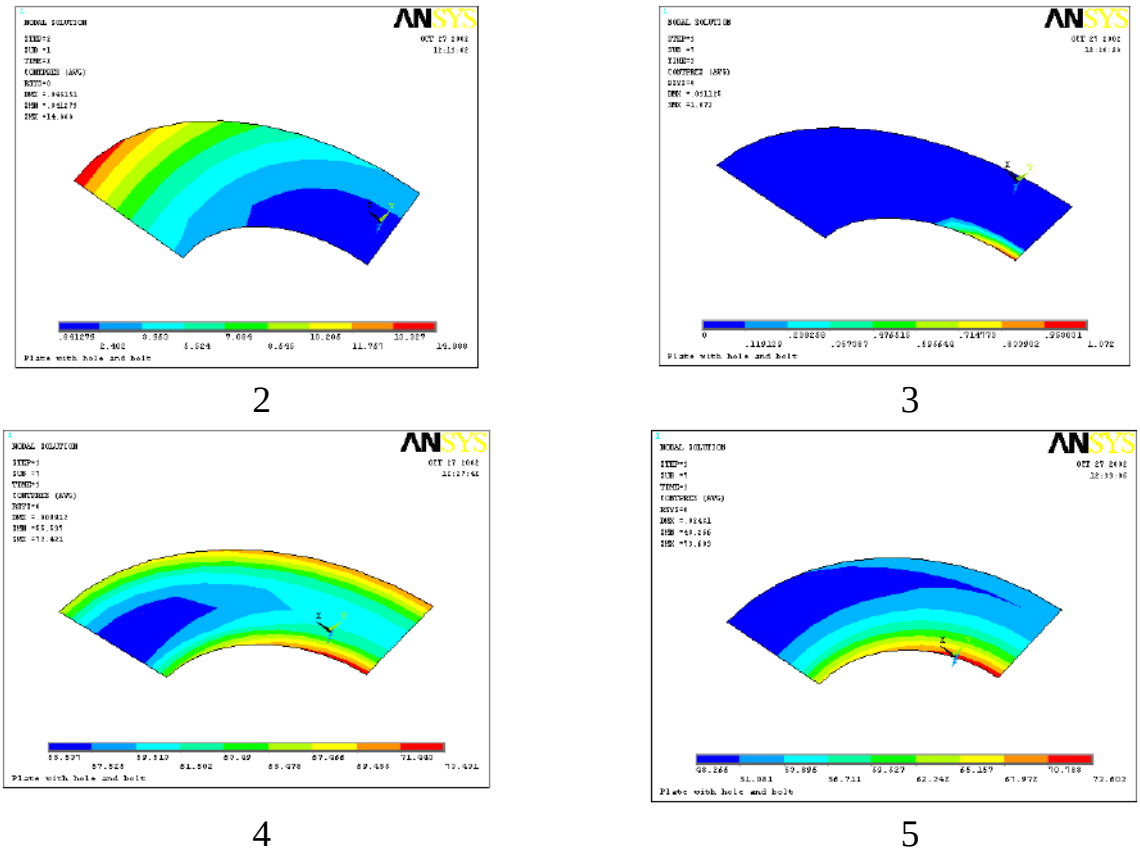

Fig. 2.50. Distribution field of contact pressures along nut-to-piece contacting surface at an external load application level of σ^{gr} = 100 MPa and different variants of bolt installation

Analyzing the distribution filed of contact pressures between a bolt shank and a hole wall in the plate (See fig. 2.47, 2.48), it can be noted that the highest contact pressures in a plate with a cylinder-conic hole are initiated in the following zones:

- For variants 2, 3 and 5 – in crosswise direction in the hole cylinder portion;
- For variant 4 – in crosswise direction in the hole conic portion.

The contact pressure distribution between the plate and the piece as well as between the bolt nut and the piece has been also analyzed. The distribution field of a contact pressures along plate – to – piece and nut shank– to – piece contacting surfaces at an external load application level of load application level of σ^{gr} = 100 MPa and different variants of bolt installation is illustrated in Fig. 2.48, 2.50.

With allowance made for everything mentioned above, the following paths for representation of the contact pressures and clearance values have been selected: L1,L2,….L7 (Fig. 2.51).

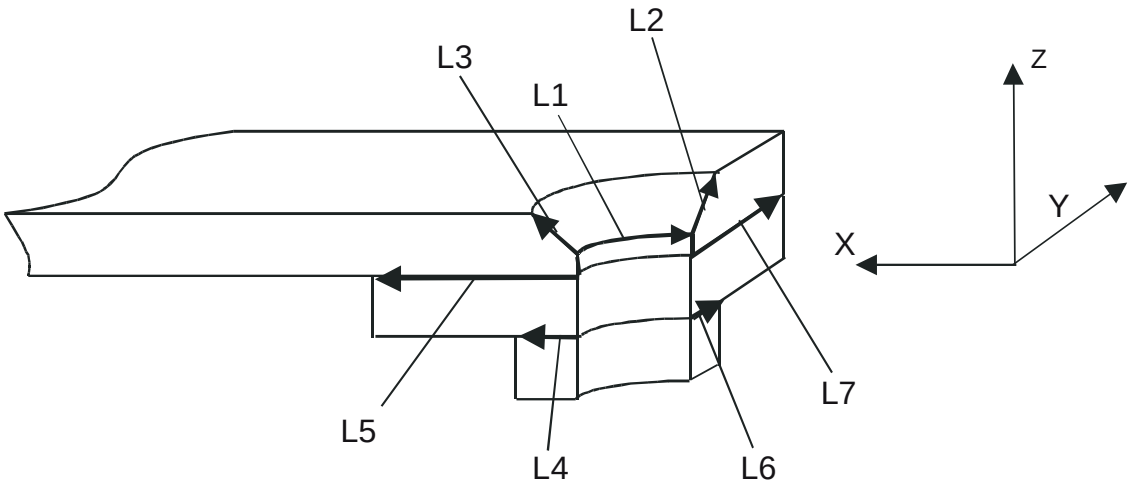

Fig. 2.51. Arrangement of L1, L2…L7 paths for representation of contact pressures and clearances between joint member surfaces

At a zero level of the plate external load application the contact pressures along the L1 path are practically at the same level. Following growth of σ^{gr}, irregularity of contact pressure distribution at L1 (Fig. 2.52) path becomes apparent; closer to the end of the path count, the contact pressures are increased, while to the beginning one, they are practically decreased to zero to the highest level of the external load application. Such model behavior can be explained by its deformation in the hole zone; in crosswise direction the plate is compressed and in lengthwise direction it is expanded. Finally, the contact pressures in the lengthwise direction drop to zero and the clearance origination between the hole wall and the bolt shank becomes possible.

Analyzing the graphs in Fig. 2.53, 2.54, it should be noted that application of the radial interference results in the peak increase of contact pressure values along the path L2 in the plate hole cylinder portion.

The graphs (Fig. 2.55 – 2.59) showing load application level and bolt installation pattern effect on distribution of clearances Δ on the way of their most possible origination L3 specify a distribution pattern of clearances and contact pressures between the plate hole wall and the bolt shank.

The application of the radial interference 1%d_b results in the initiation of the clearance within the range of 2…3x10^{-2}mm in the plate hole conic portion on the path L3. After the joint application of the radial interference with the axial tightening, the clearance on the path L3 is practically absent both along the cylinder and conic portion of the hole (excluding intermediate length level of an external load application (σ^{gr} = 0 MPa).

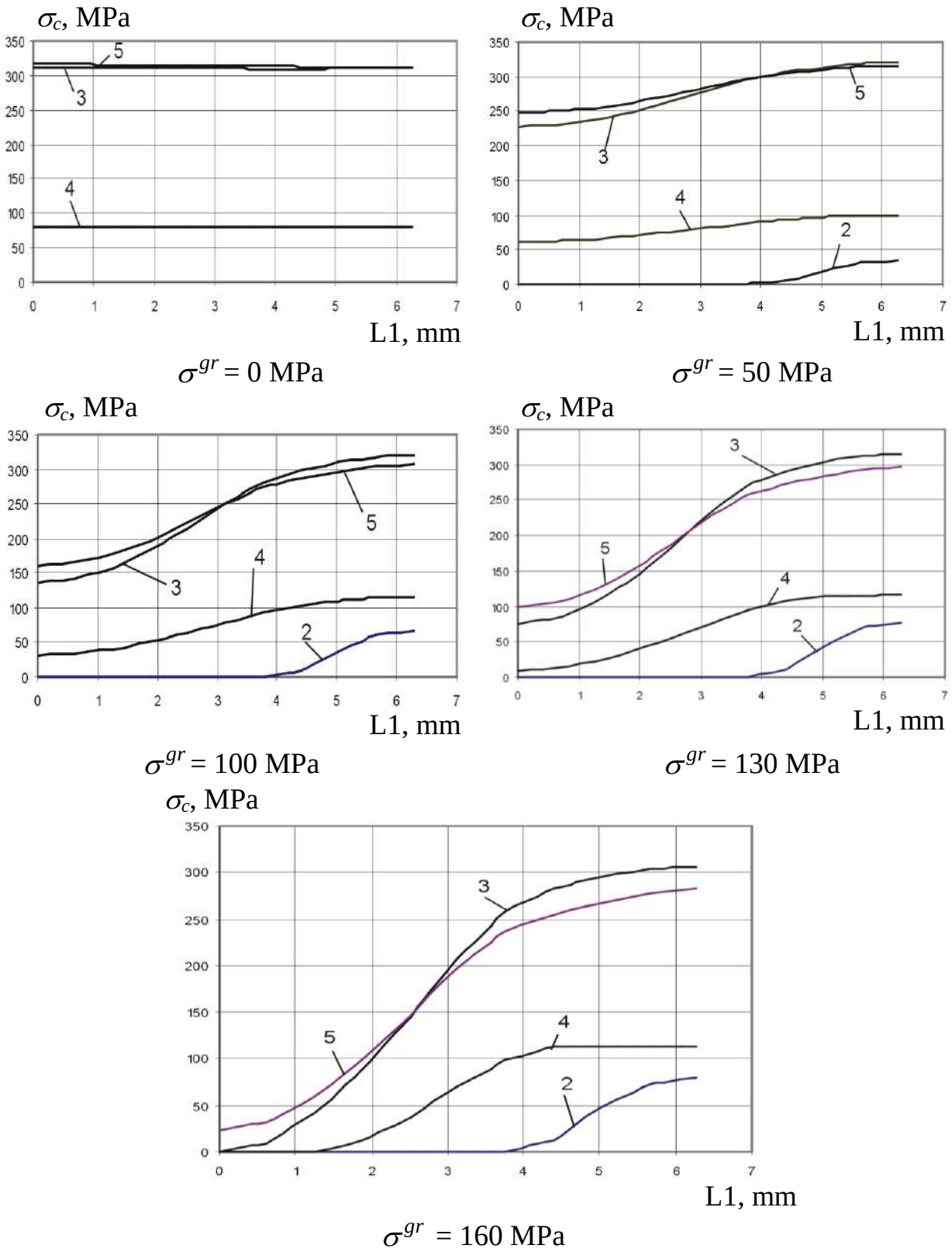

Fig. 2.52. Effect of load application level σ^{gr} on distribution pattern of contact pressures σ_c on the path L1

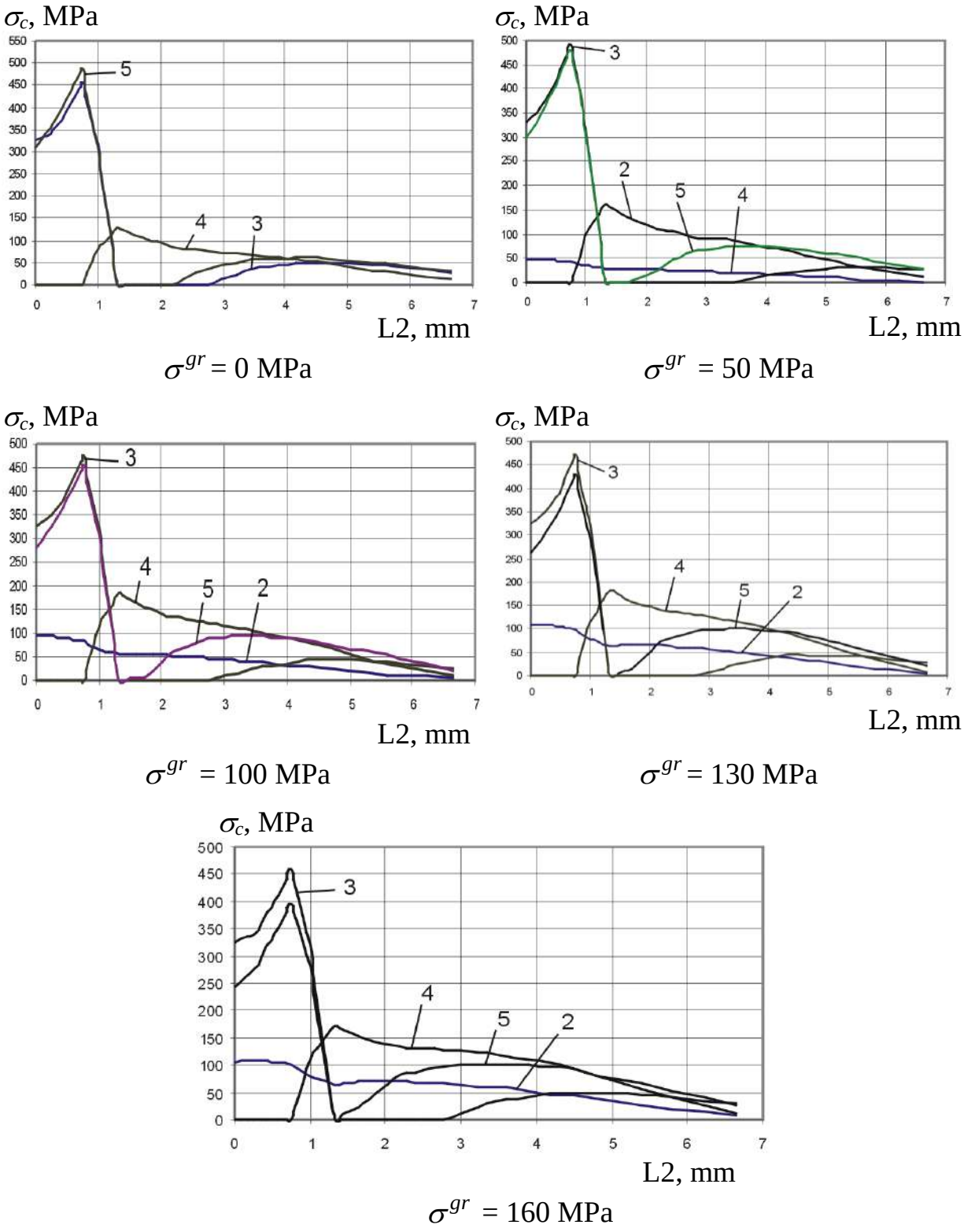

Fig. 2.53. Effect of load application level σ^{gr} on distribution pattern of contact pressures σ_c on the path L2

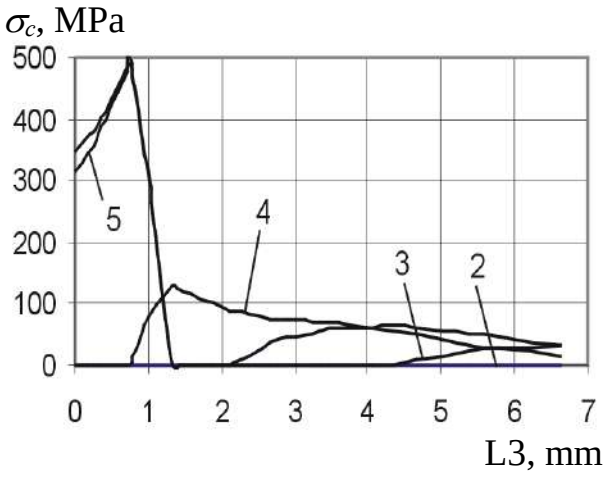

σ^{gr} = 0 MPa

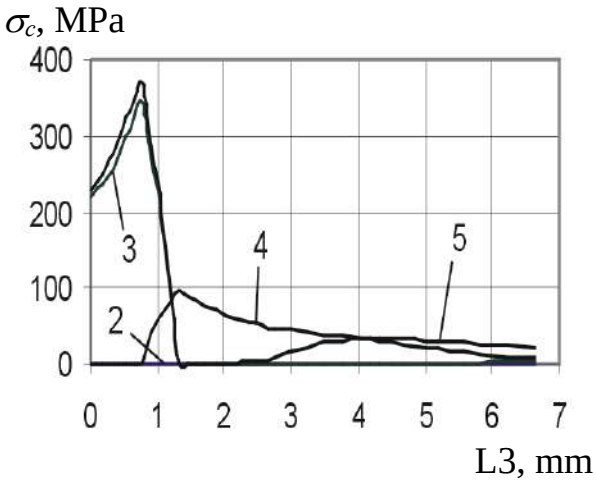

σ^{gr} = 50 MPa

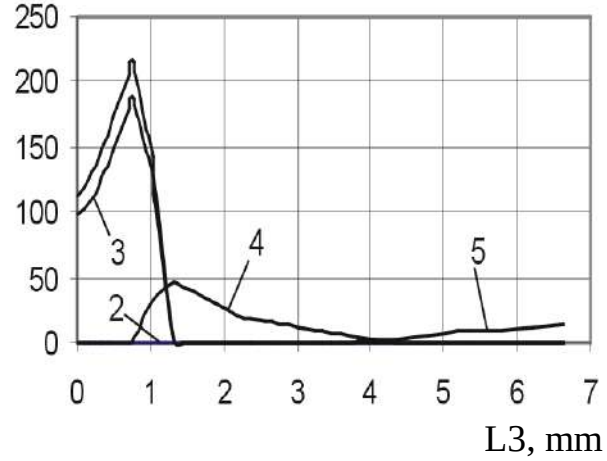

σ^{gr} = 100 MPa

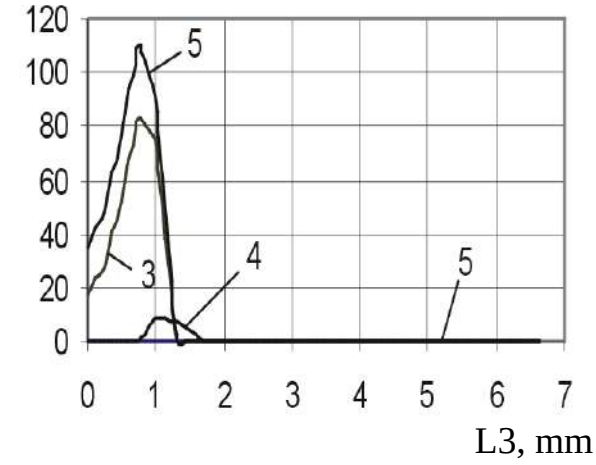

σ^{gr} = 130 MPa

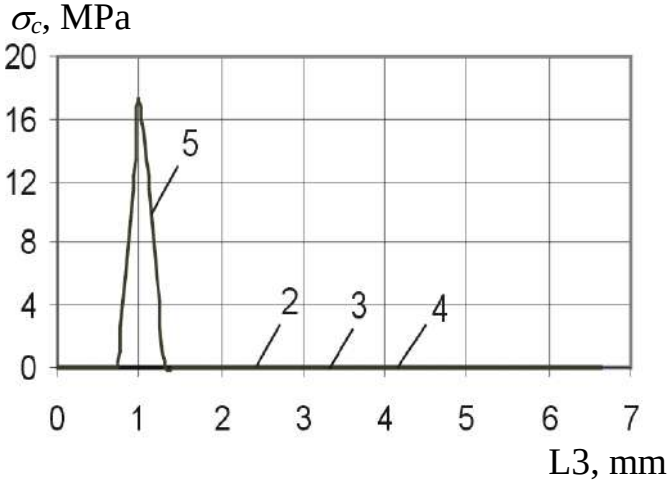

σ^{gr} = 160 MPa

Fig. 2.54. Effect of load application level σ^{gr} on distribution pattern of contact pressures σ_c on the path L3

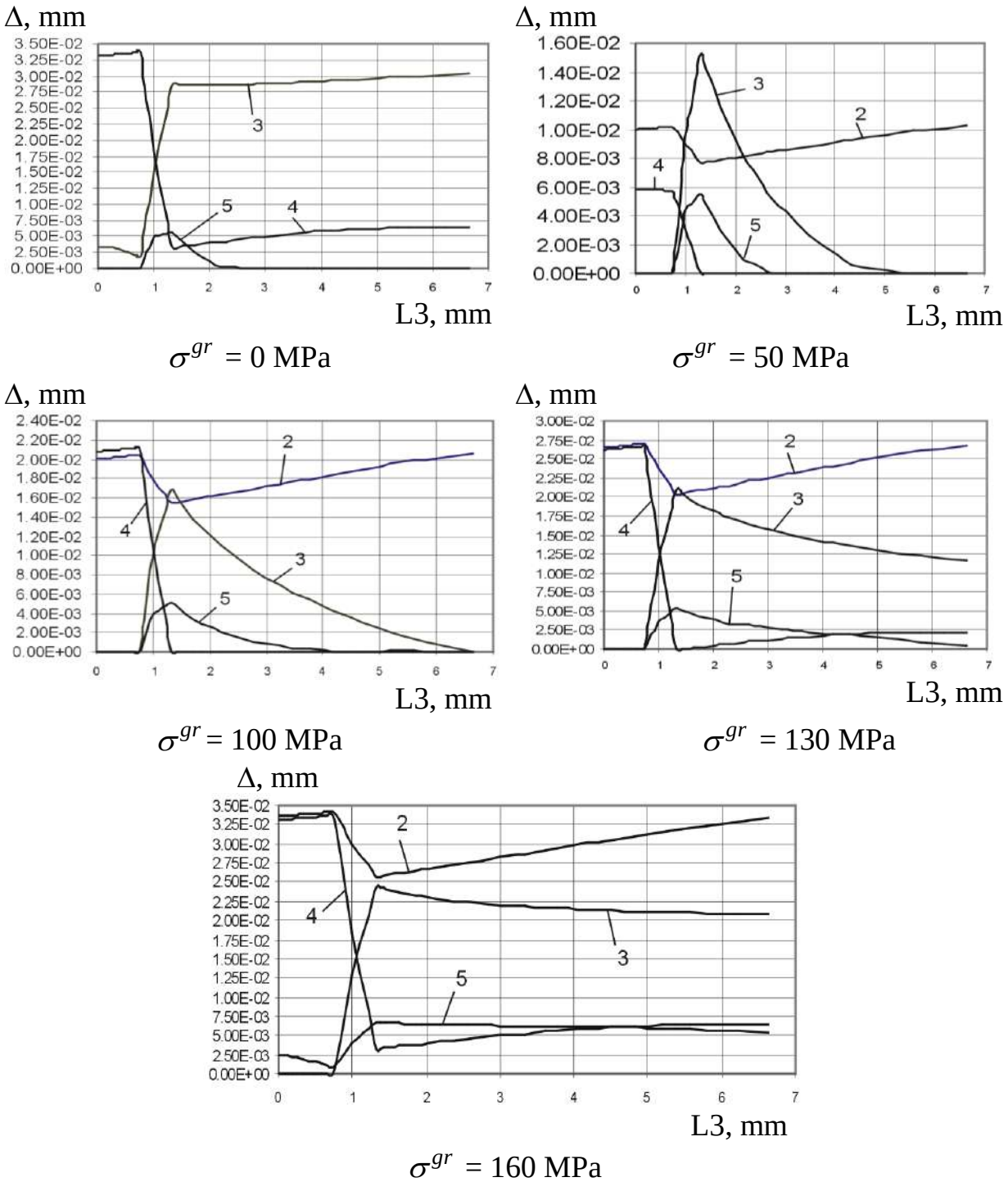

Fig. 2.55. Load application level effect σ^{gr} on distribution pattern of clearances Δ between the bolt shank and the wall

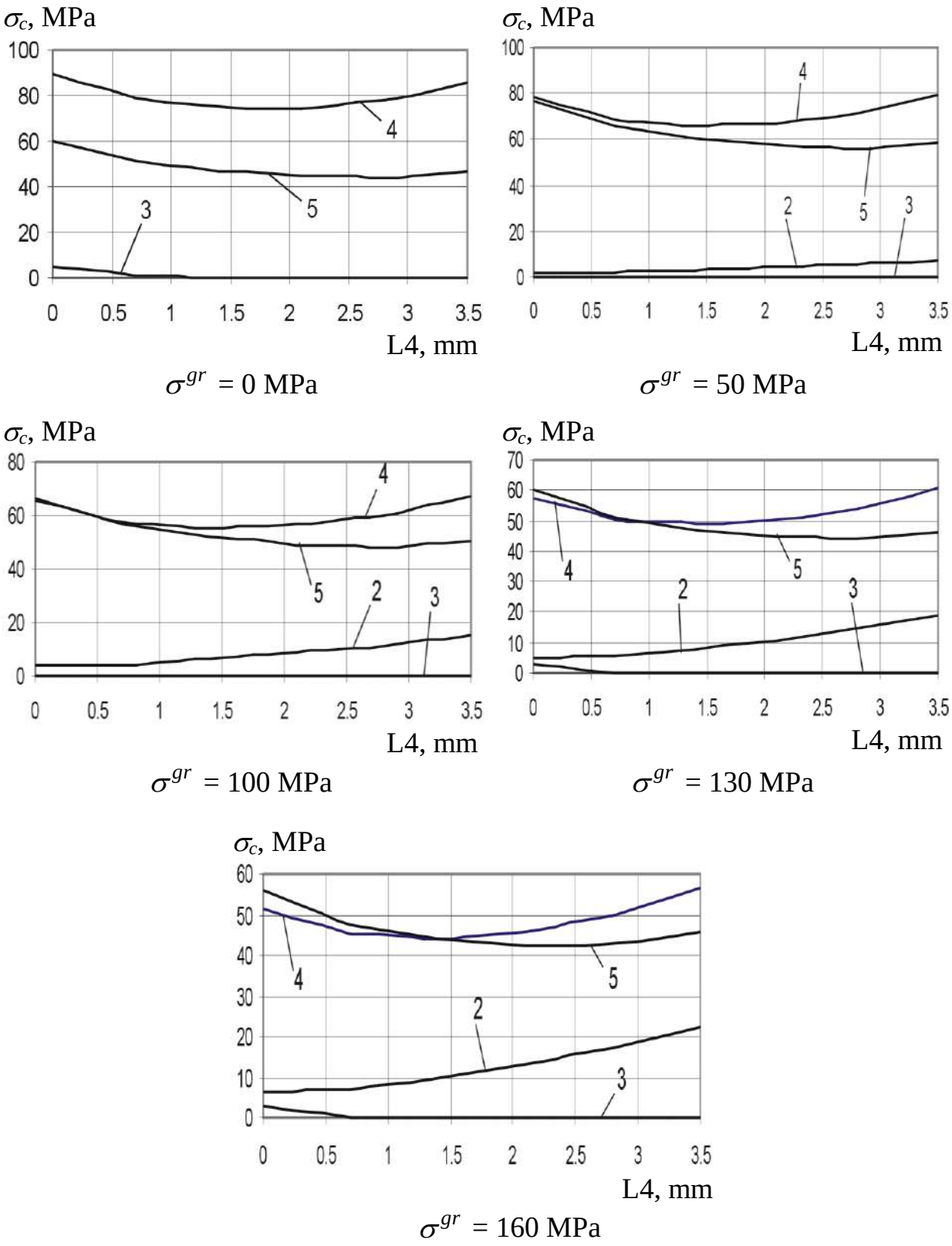

Fig. 2.56. Load application level effect σ^{gr} on distribution pattern of contact pressures σ_c on the path L4

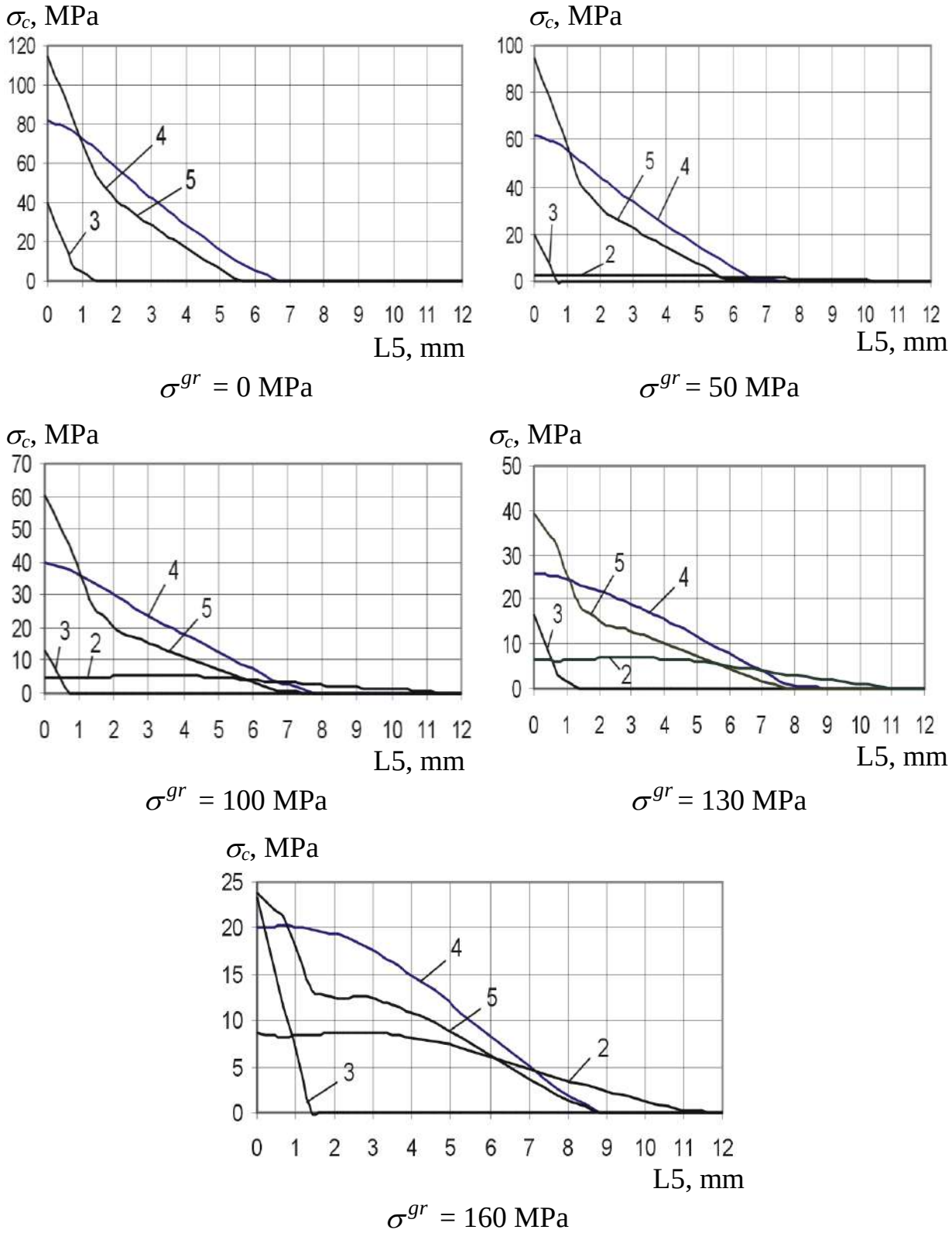

Fig. 2.57. Load application level effect σ^{gr} on distribution pattern of contact pressures σ_c on the path L5

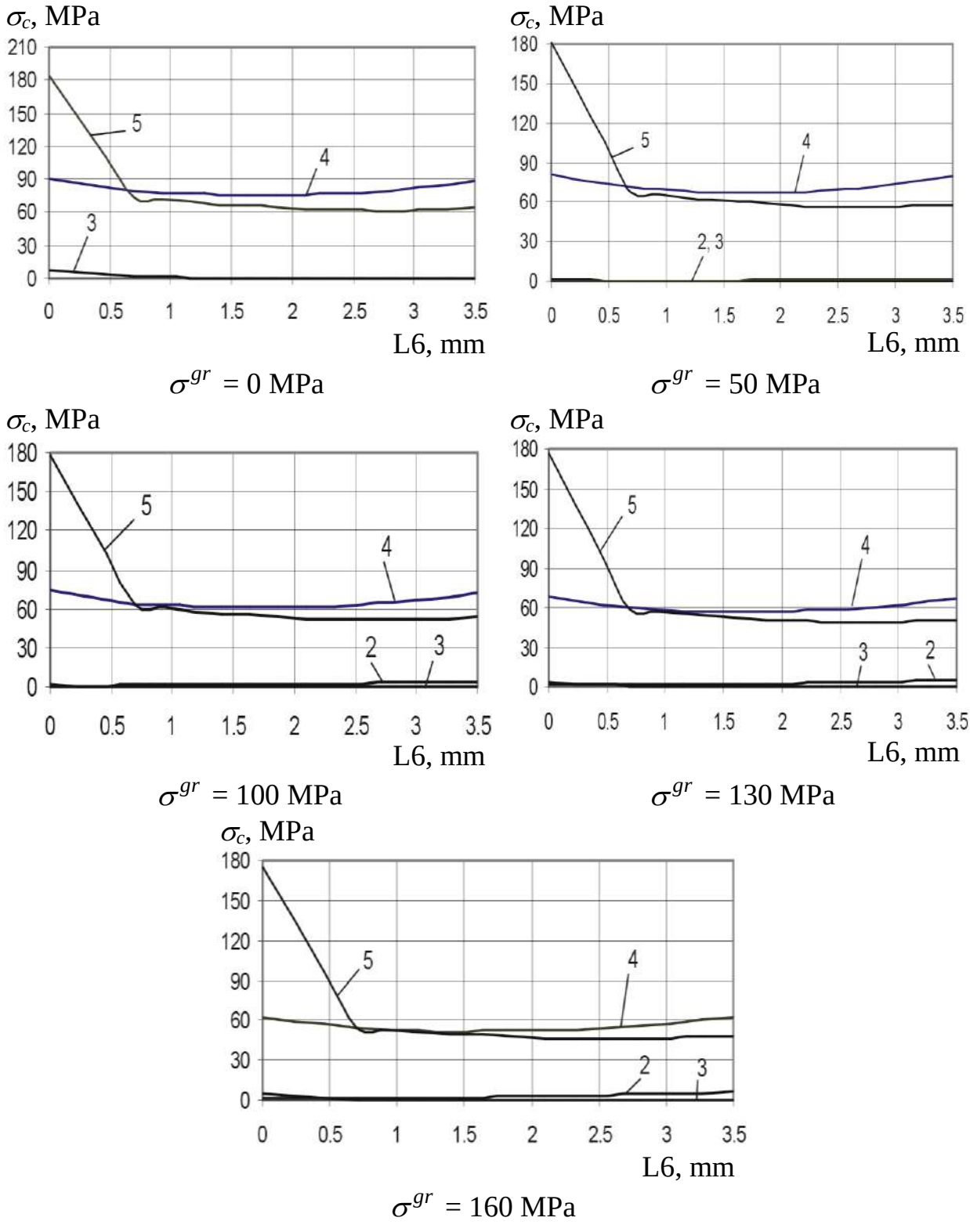

Fig. 2.58. Load application level effect σ^{gr} on distribution pattern of contact pressures σ_c on the path L6

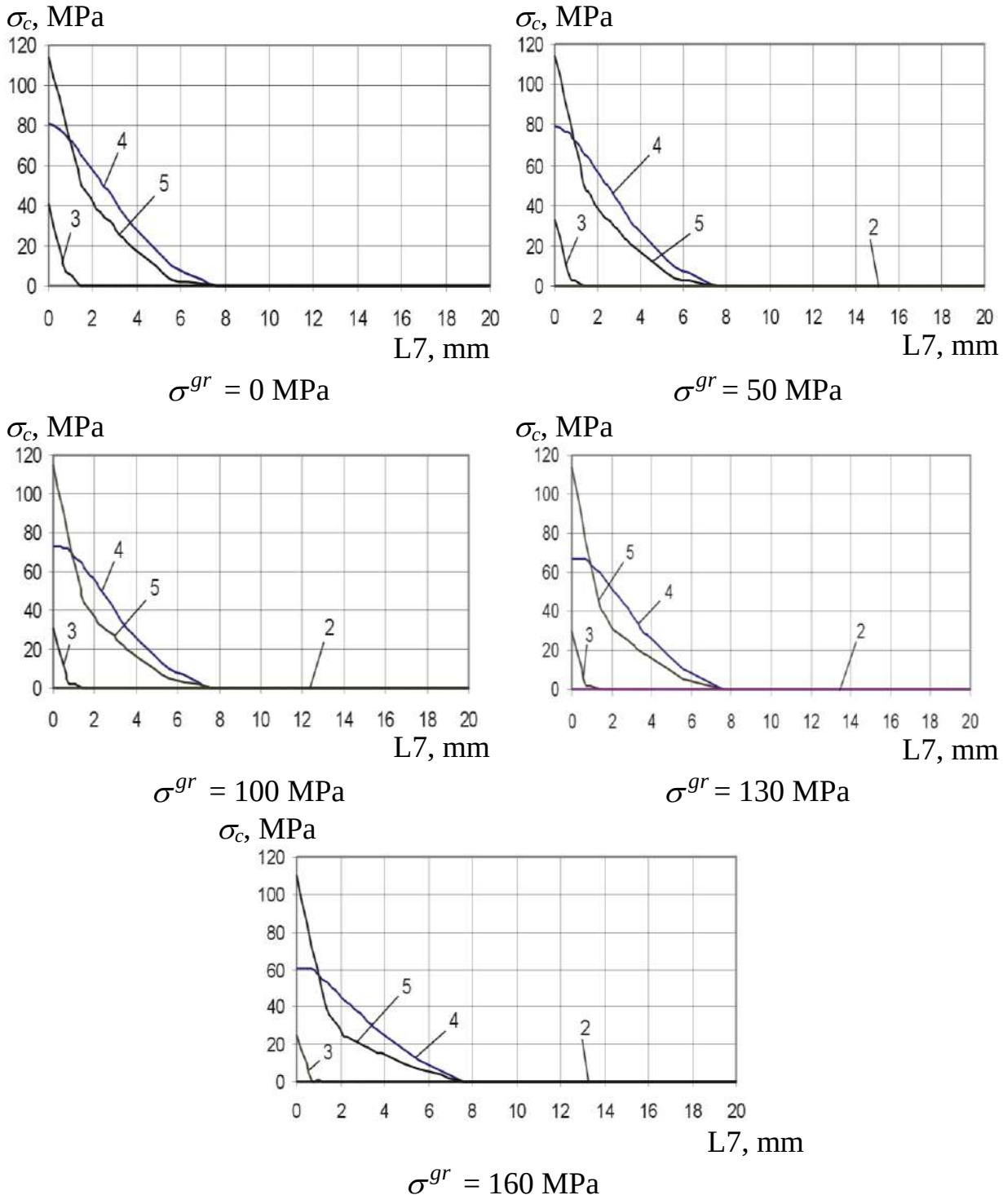

Fig. 2.59. Load application level effect σ^{gr} on distribution pattern of contact pressures σ_C on the path L7

The application of the external tensile load σ^{gr} results in the initiation of the clearance zone between the hole wall and the bolt shank to be expanded following growth of σ^{gr} and covers the total plate hole conic portion at a local application level of σ^{gr} = 130 MPa. It should be noted that the clearance in combination with

a bolt installed without radial and axial interferences is practically initiated just after application of the external load. The clearance is initiated in combination with an axial tightening at σ^{gr} equal 135..140 MPa. In case of bolt installation with a radial interference of 1% d_b, the clearance between a hole wall and a bolt shank is initiated at an extreme load application level of σ^{gr} = 160 MPa.

Following the results of the analyses we may come to the following conclusions:

1. Bolt installation into the hole with an interference of 1% d_b results in the increase of the stress concentration factor in a plate with unfilled hole at σ^{gr} =50 MPa, in the increase of the load application level up to 100 MPa, the stress concentration factors for the variants 1 and 3 become equal; at the operating level of the external load application (σ^{gr} = 100…160 MPa). The stress concentration factor in the plate with a hole filled with fastener with a radial interference of 1% d_b becomes less (1…1.05 times) in comparison with the stress concentration factor in the plate. The application of tightening P_t =10 kN decreases the stress concentration factor in the plate in 1…14 times in comparison with the stress concentration factor in the plate with unfilled hole.

2. Bolt installation in the hole with an interference of the maximum local stresses 1.82…1.84 times in comparison with the unfilled hole variant at an operating level of the external load application σ^{gr}. The tightening at P_t =10 kN decreases the amplitude of the maximum local stresses 1.46…1.49 times at the operating level of the external load application. The joint application of the radial interference of 1% d_b and axial tightening P_t =10 kN decreases an amplitude of the maximum local stresses in 2.58…3.19 times.

3. The interference of 1% d_b decreases the amplitude of maximum local amplitude deformations 1.28…1.44 times in comparison with the amplitude of maximum local amplitude deformations in the plate with unfilled hole. The tightening at P_t =10 kN decreases the amplitude of the maximum local deformations 1.21….1.34 times. The joint action from a radial interference of 1% d_b and axial tightening of P_t =10 kN allows to decrease the amplitude of maximum local deformations in the plate 1.27…1.43 times.

4. In comparison with the maximal values of contact pressures for the different variants of the bolt installation, it has been found that the application of a radial interference of 1% d_b results in the increase of the maximum contact pressures within the total range in the change of the external load application level (6.61 times at σ^{gr} = 100 MPa) in comparison with the variant without radial and axial interferences. The joint application of the radial interference with an axial tightening slightly reduces the contact pressures (1.01…1..1 times) with this difference increased following the increase of the external load application level.

But the distinguishing feature is that for the variants of the bolt installation with the radial interference (either just radial interference of 1% d_b or a radial interference of 1% d_b +axial tightening of P_t =10 kN), the maximum contact pressures begin to reduce following level increase of the external load application. For the variants with the axial tightening and without axial tightening and radial interference, the maximum contact pressures are also increased following growth of the external load application σ^{gr} . Analyzing the effect of the load application level (σ^{gr}) on the value of the maximum contact stresses, it should be noted that the application of the radial interference of 1% d_b significantly increases danger in the initiation and development of the fretting-corrosion on the joint faces.

5. The provision of tightness in use characterized by the occurrence of the clearances in the joint is one of the requirements for the efficient use of the modern aircraft structural components. As a result of the clearance analysis it has been found that the application of a radial interference of 1% d_b prevents initiation of the clearance between the bolt shank and the hole wall in the plate hole cylinder portion. The joint application of a radial interference of 1% d_b and axial tightening of P_t =10 kN allows to decrease the clearance value in the plate hole conic portion in the lengthwise direction in 4…6.1 times in comparison with a variant of the bolt installation without radial and axial interferences at a maximum level of an external load application with σ^{gr} = 160 MPa.

2.3.3. Analysis of general and local deflected mode characteristics in plates with unloaded hole filled with rivet according to OCT 34055-92 (АНУ 0309)

The geometric parameters of the rivet under study, a shear joint and a test-piece with the filled unloaded hole are illustrated in Fig. 2.60, 2.61.

A seat shape and size for the manufactured rivet head correspond to the geometry of a countersunk head.

The rivet material is the aluminium alloy B65 with a modulus of elasticity E = 71000 MPa and a Poisson's ratio of μ = 0.3. A multilinear model with the isotropic strengthening law to describe the behavior of the rivet material [11,12].

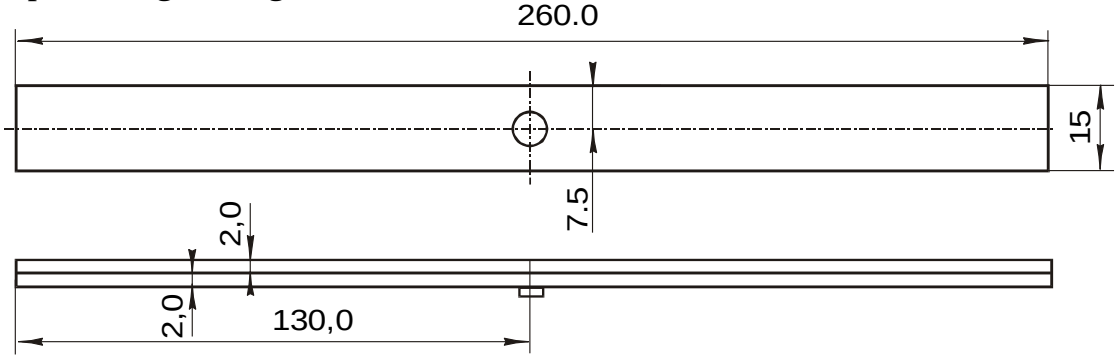

Fig. 2.60. Test-piece with the filled rivet unloaded hole

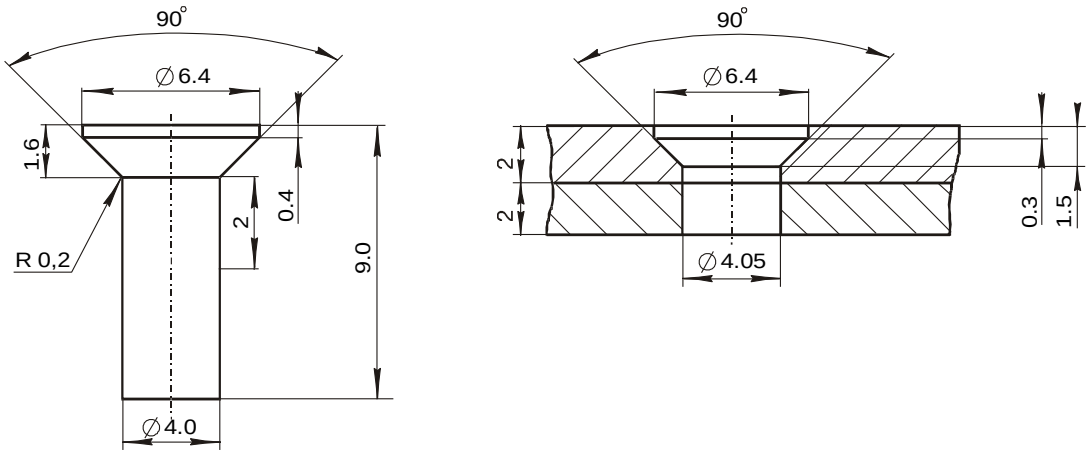

Fig. 2.61. Geometric parameters of rivet under studying АНУ 0309 (at the left) and countersunk hole for the rivet according to АНУ 0309 (at the right)

The material of the plate with the rivet installed is an aluminium alloy Д16Тл2 with a modulus of elasticity E = 72000 MPa and a Poisson's ration μ = 0.3. A multilinear model with a kinematic strengthening law [11] has been taken for analysis. In creation of the finite-element model an allowance has been made for friction in the contact algorithm by specifying a friction coefficient ν = 0.02 between the rivet and the plates and ν = 0,15 – between the plates, stamp and rivet. The snap rivet head has been upset to a height of $0.4d_t$, in this case, the diameter of the snap rivet $D_{srh} = 1.69d_r = 5.91$ mm corresponding to the requirements as specified in ТИ 36-21-86.

With the symmetry of the test-piece and external load application pattern taken into account, 1/4 model under the corresponding attachment conditions has been used in analysis. Zero movement at Z-component has been specified to limit model displacement along Z axis for all units located on the plate face surface at the point of the external load application. The limitations by the X and Y vector components of the movement have been specified by the model symmetry plane (Fig. 2.62).

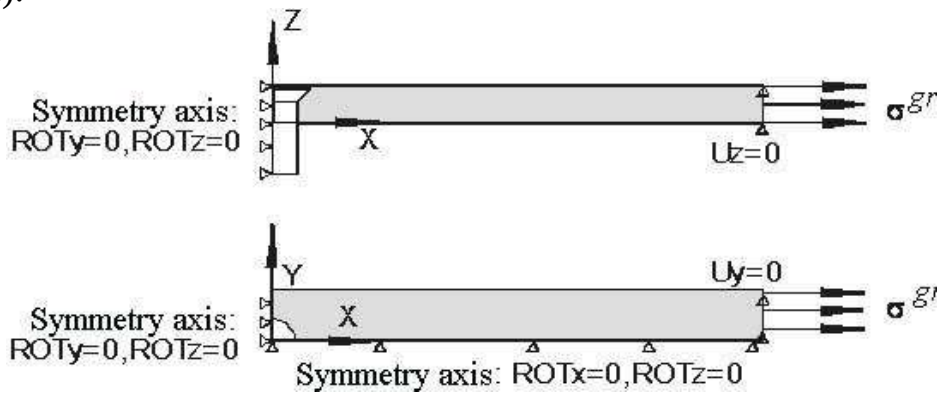

Fig. 2.62. Loading diagram of riveted joint not loaded for shear

The finite-element model (Fig. 2.63) consists of the three-dimensional eight component elements SOLID 45, contact elements of the second order TARGE170 and CONTA173 presented in ANSYS system [474].

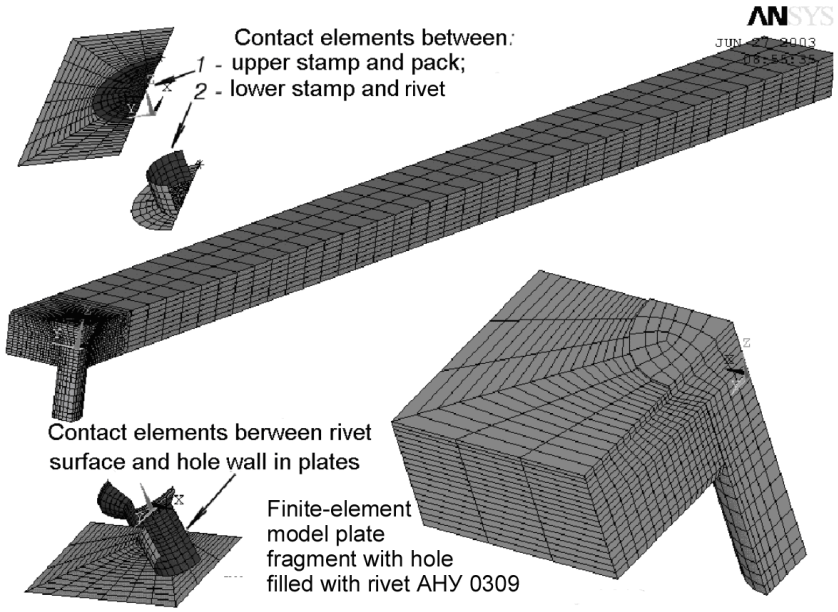

Fig. 2.63. Rivet joint finite-element model

The rivet deformation behavior and distribution pattern of the equivalent stresses in the plate hole are illustrated in Fig. 2.64.

Maximum equivalent stresses $\sigma_{eqv\,\max}$ and maximum tensile stresses $\sigma_{x\,\max}$ in plate have been determined in the course of the local deflected mode analysis. The distribution pattern of these stresses in plate fragment as viewed from the side of the manufactured rivet head is illustrated in Fig. 2.64, 2.65. The plate is shown as viewed from the side of the snap rivet head because the highest stresses are observed there.

1. Axis of symmetry

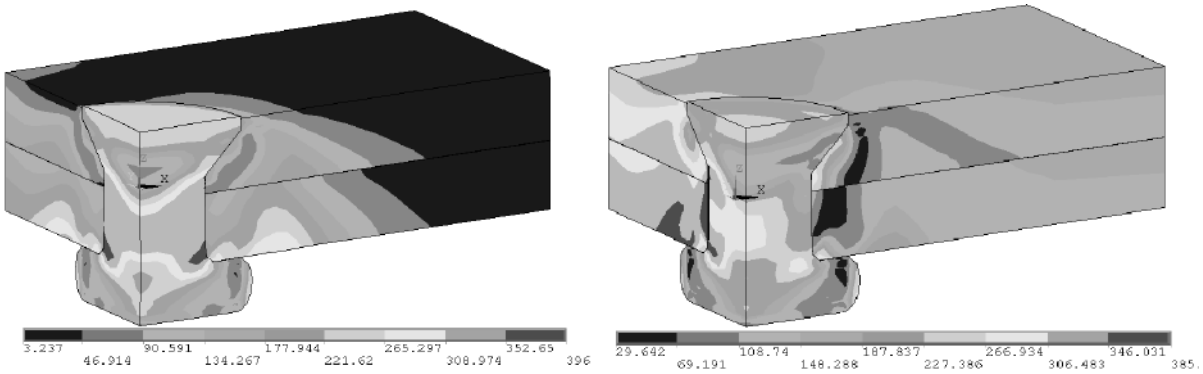

σ^{gr} = 0 MPa σ^{gr} = 150 MPa

Fig. 2.64. Distribution pattern of equivalent stresses σ_{eqv} in the plate hole filled with upset rivet AHY 0309 for the different variants of the load application σ^{gr}

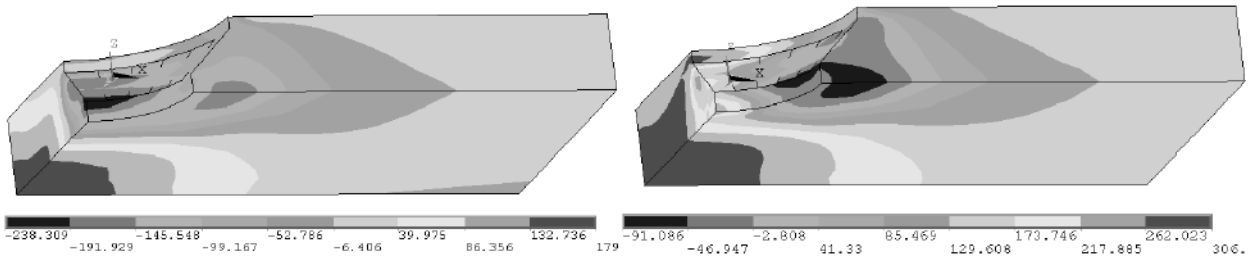

σ^{gr} = 0 MPa σ^{gr} = 150 MPa

Fig. 2.65. Distribution pattern of plate stresses σ_x for different variants of load application σ^{gr}

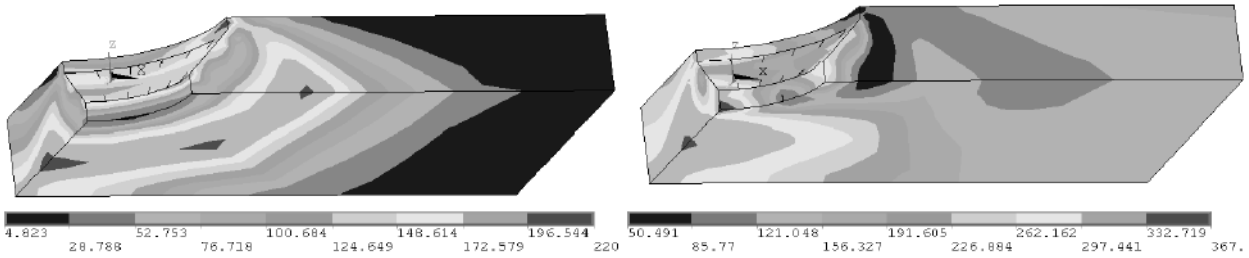

σ^{gr} = 0 MPa σ^{gr} = 150 MPa

Fig. 2.66. Distribution pattern of plate stresses σ_{eqv} for different variants of load application σ^{gr}

Dependencies of $\sigma_{\max}$, $\sigma_{a\,\max}$, $\sigma_{m\,\max}$, $\sigma_{0\,\max}$, as well as $\varepsilon_{\max}$, $\varepsilon_{a\,\max}$, $\varepsilon_{m\,\max}$ and $\varepsilon_{0\,\max}$ for equivalent and axial stresses from an external load application level σ^{gr} are illustrated in Fig. 2.66 – 2.70. Zero-to-tension stresses have been determined according to Oding formula for the asymmetric application cycle.

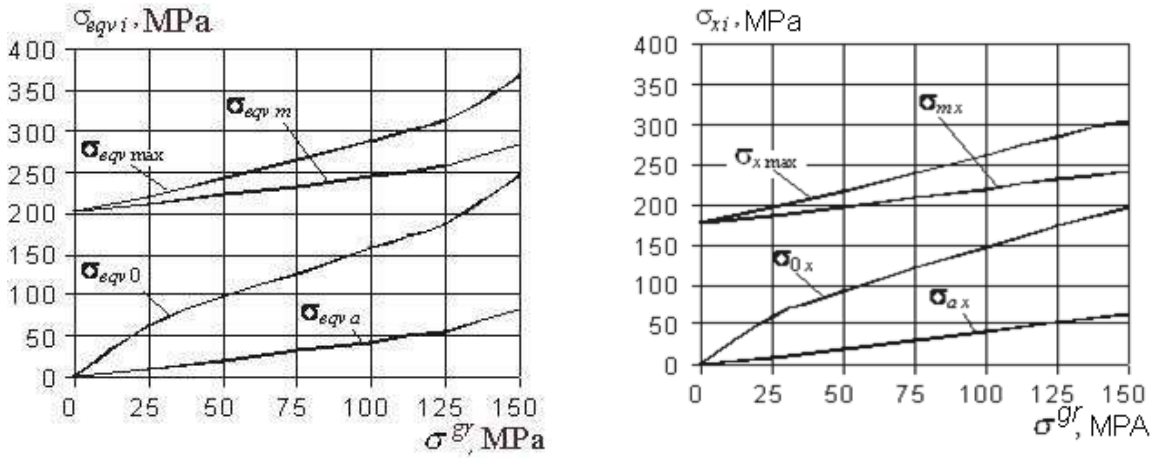

Fig. 2.67. Dependencies of $\sigma_{\max}$, σ_a, σ_m and σ_0 on external load application level σ^{gr}

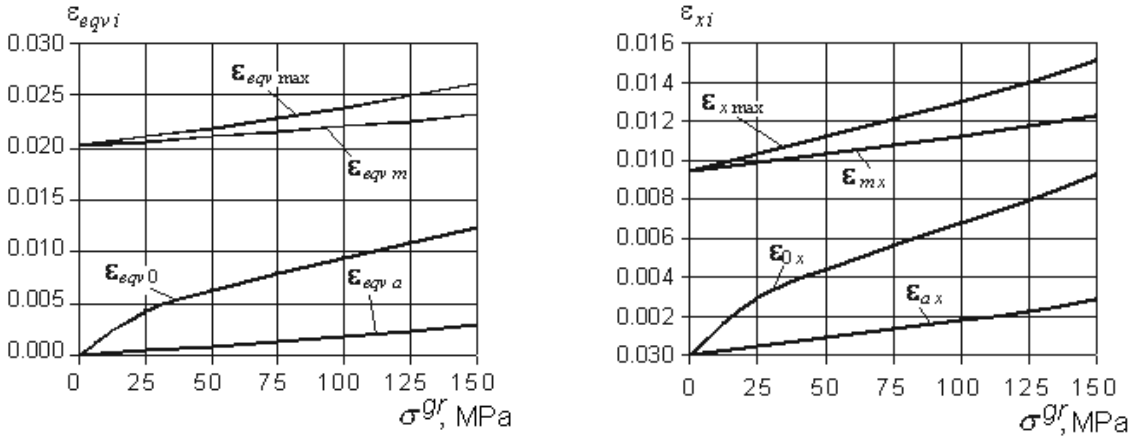

Fig. 2.68. Dependencies of $\varepsilon_{\max}$, ε_a, ε_m and ε_0 on external load application level σ^{gr}

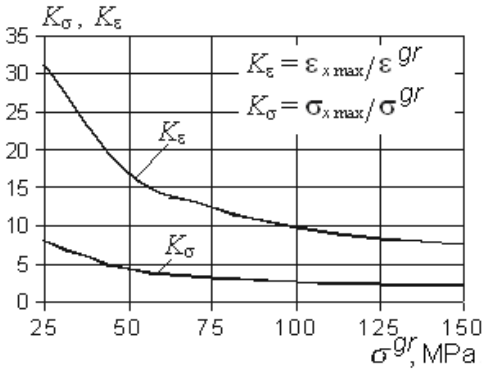

Fig. 2.69. Load application level effect σ^{gr} on change of tensile stress concentration factor σ_x and tensile deformations ε_x

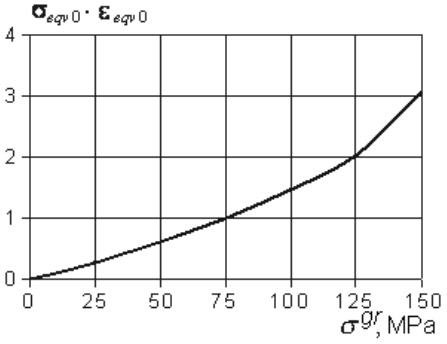

Fig. 2.70. Load application level effect σ^{gr} on product of $\sigma_{eqv0} \cdot \varepsilon_{eqv0}$

It should be noted that amplitude values of the equivalent and axial stresses do not exceed 83 MPa. This is associated with the great residual stresses in the plate after riveting process.

A distribution field of contact pressures between the rivet and a packet is illustrated in Fig. 2.71. Its irregularity along the paths L1 and L2 depending on the load application level is evident (Fig. 2.72).

It has been found that the distribution of contact pressures between the rivet and the packet is extremely irregular. The greatest contact pressures are initiated in the area of the snap rivet head. In this area their value reaches 365 MPa. The greatest contact pressures in the plate are observed in the hole conic portion under the countersunk rivet head. The digital values of contact pressures in this area lie within the range of 100...150 MPa. The contact pressures are decreased to zero value in the area of cylinder compensator and in the conic-to-cylinder transient zone when reaching σ^{gr} σ^{gr} = 150 MPa. Since these zones are local and revealed just under a load application level corresponding to σ^{gr} = 150 MPa, it may be

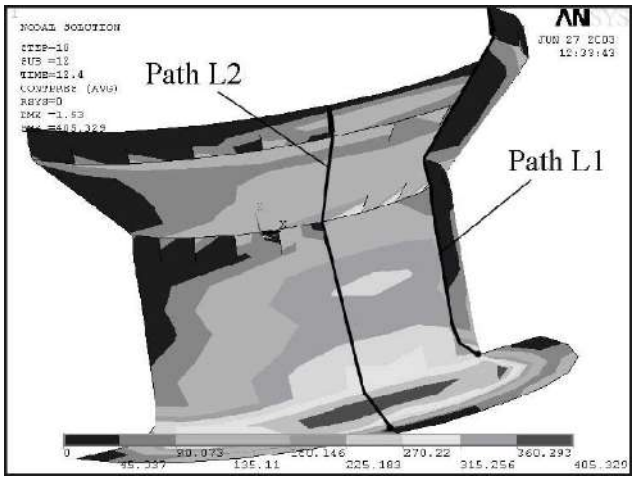

Fig. 2.71. Distribution field of contact pressures between rivet and packet.

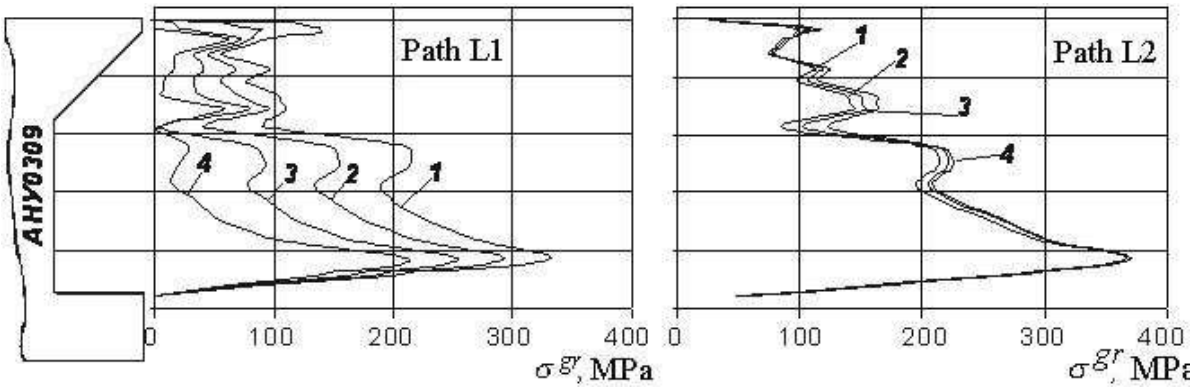

Fig. 2.72. Effect of external load application level on distribution of contact pressures between rivet shank and packet on the path L1:
1 – σ^{gr} = 0 MPa, 2 – σ^{gr} = 50 MPa, 3 – σ^{gr} = 100 MPa, 4 – σ^{gr} = 150 MPa

stated that the joint is proof within the total range of the loads under study. Interference distribution pattern throughout the packet thickness after riveting process is illustrated in Fig. 2.73.

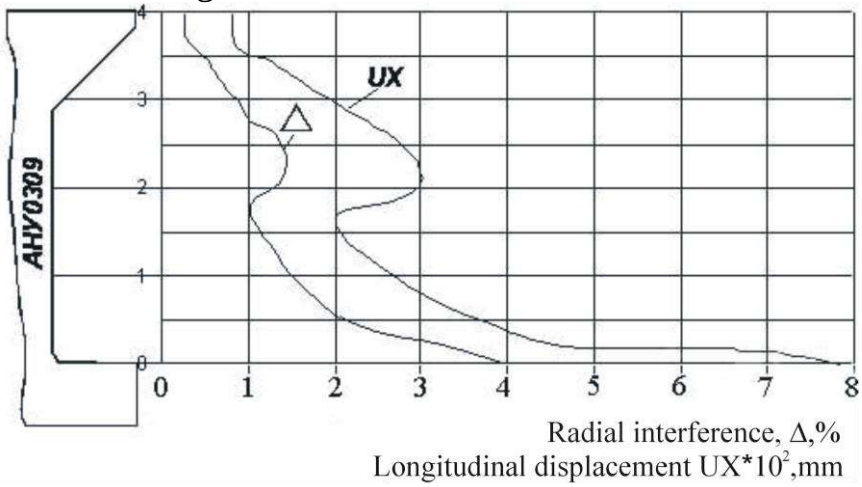

Fig. 2.73. Distribution pattern of radial interference throughout packet thickness

The interference value under snap rivet head reaches 3.51%, In the middle of the packet its values lie within the range from 1 to 2%d_r. The least value of the radial interference is observed at cylinder compensator and in this area its value doesn't exceed 0.25%d_c.

The application of the rivets АНУ 0314 with their installation in the Д16Тл2 plate holes has been subject to analysis to compare the efficiency in the height decrease of the countersunk rivet snap head. Maximum equivalent stresses $\sigma_{eqv\,\max}$ and maximum tensile stresses $\sigma_{x\,\max}$ in plate have been determined in the course of the local deflected mode analysis. Distribution pattern of these stresses in plate fragment as viewed from the side of the manufactured rivet head is illustrated in Fig. 2.74, 2.75. The plate is shown as viewed from the side of the snap rivet head because the greatest stresses are observed there.

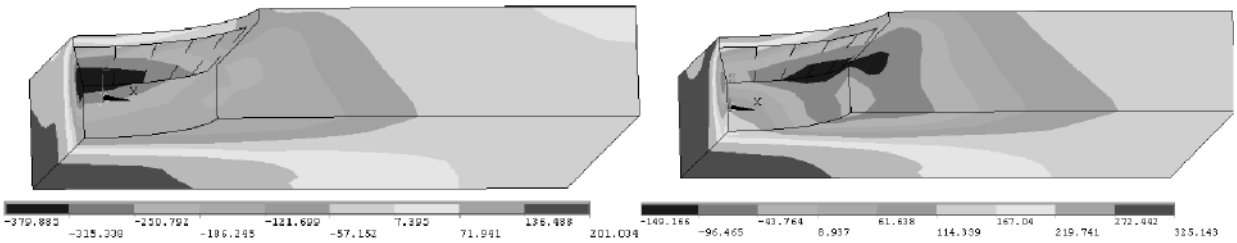

σ^{gr} = 0 MPa σ^{gr} = 150 MPa

Fig. 2.74. Plate stress distribution pattern σ_x for the different variants of the load application σ^{gr} (АНУ 0314)

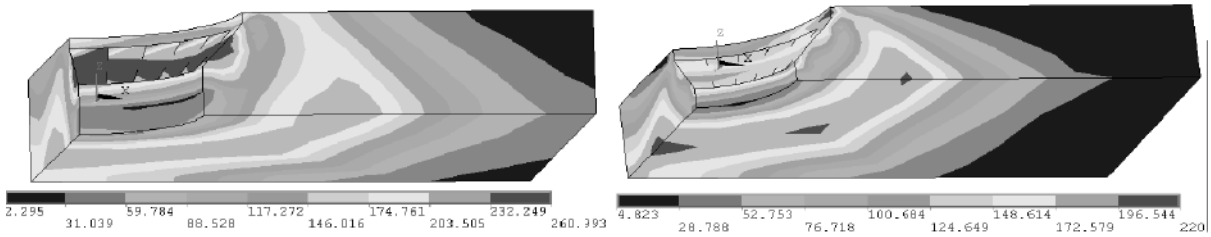

σ^{gr} = 0 MPa σ^{gr} = 150 MPa

Fig. 2.75. Plate equivalent stress distribution pattern σ_{eqv} for the different variants of load application σ^{gr} (АНУ 0314)

In application of the rivet АНУ 0314 with the reduced countersunk head, the maximum residual equivalent stresses are observed in the conic area after the riveting process. Digitally, these stresses have been increased at 15% averagely and practically covered the total area of the cylinder compensator. The greatest residual stresses $\sigma_{x\,\max}$ in plate for both variants of the rivets are initiated in the cylinder-to-conic portion of the transient area. They are considered as the compression stresses. But in case of АНУ 0314 rivet application, the stresses $\sigma_{x\,\max}$ cover the major size of the plate and exceed the similar stresses, initiating after installation of the rivet АНУ 0309, averagely at 38%.

The dependencies of $\sigma_{\max}$, $\sigma_{a\,\max}$, $\sigma_{m\,\max}$, $\sigma_{0\,\max}$ as well as $\varepsilon_{\max}$, $\varepsilon_{a\,\max}$, $\varepsilon_{m\,\max}$ and $\varepsilon_{0\,\max}$ for equivalent and axial stresses on an external load application σ^{gr} are illustrated in Fig. 2.76, 2.77. The characteristics of the plate hole deflected mode filled with АНУ 0309 rivet are illustrated in the figures by the solid line while АНУ 0314 rivet with dotted line.

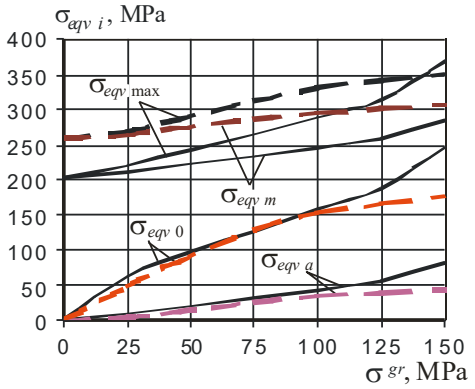

Fig. 2.76. The dependencies $\sigma_{\max}$, σ_a, σ_{m} and σ_0 on the level of external load application $\sigma^{gr\,r}$

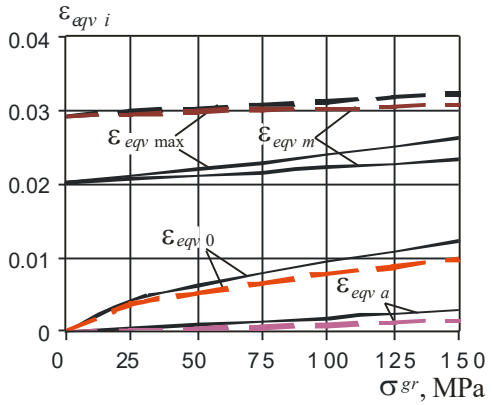

Fig. 2.77. The dependencies $\varepsilon_{\max}$, ε_{a}, ε_m and ε_0 on the level of external load application σ^{gr}

Despite the fact that maximum plate stresses and deformations in case of АНУ 0314 rivet installation is 25…33% more than in case of АНУ 0309 rivet installation. The amplitude and zeroed stresses and deformations have digital values in average less by 3…6%. The analysis of the energy criterion $\sigma_{eqv0} \cdot \varepsilon_{eqv0}$ (Fig. 2.78.), as the most fully reflecting efficiency of the joint operability has shown that the most efficient rivet is АНУ 0314. For this rivet the digital values curve of this criterion within the total range of the operating loads lies below the curve describing behavior of the plate energy criterion with the rivet АНУ 0309. So, for the tensile loads corresponding to the stresses σ^{gr} = 100 MPa, the difference between the specific works of deformations is equal to 0.3, and at σ^{gr} = 100 MPa – 1.34, that must favor higher life time of the joints performed with the application of the rivets АНУ 0314.

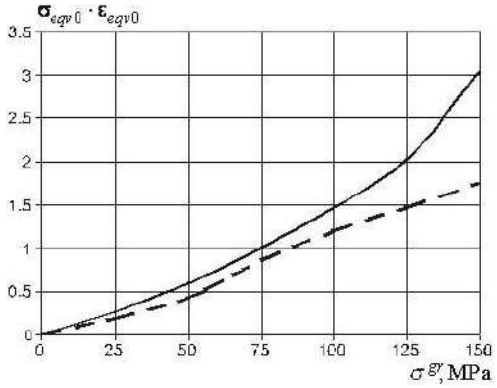

Fig. 2.78. Load application level effect σ^{gr} on product of $\sigma_{eqv0} \cdot \varepsilon_{eqv0}$

2.4. STANDARD MEMBER FATIGUE RESISTANCE CHARACTERISTICS OF AIRCRAFT ASSEMBLY STRUCTURE REGULAR ZONES

2.4.1. Experimental investigation of the life time of plates with hole

The special test pieces of the flat plates from Д16АТл5 material have been manufactured to analyse the fatigue resistance characteristics: plates with a cylinder hole; "HX" anodized plates with the countersinking holes. Countersinking was performed under 90 deg to 4 mm in depth. The plates had the following characteristics: width – 50mm; thickness – 5 mm, hole diameter – 8mm (Fig. 2.79). The fatigue tests have been conducted using the ЦДМ-10Пу – a hydraulic pulsator with maximum cyclic loads $P_{\max}$ equal 40, 30 and 25 kN (σ_{p0}^{gr}= 158,119 and 99 MPa), stress ratio R_σ =0.1 and a frequency of 13 Hz. Six (6) test pieces have been subjected to test at every level of the cyclic loads. The fatigue failure of plates with hole occurred at section along the hole axis.

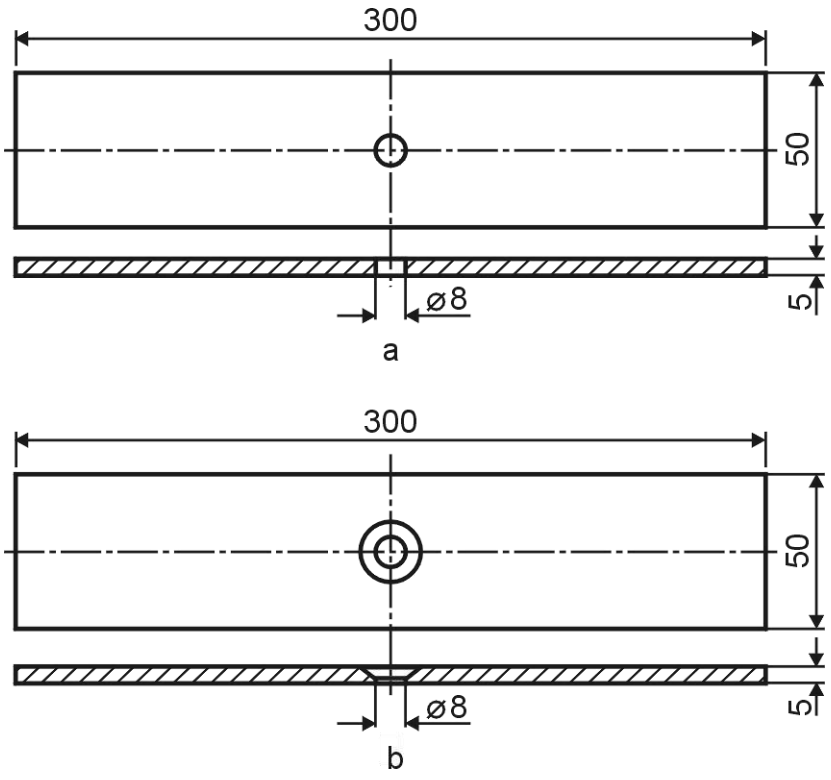

Fig. 2.79. Manufacturing version of plate test pieces with hole: a – plate with cylindrical hole; b – plate with countersunk hole

Fatigue test results are shown in Fig. 2.80. Curve points have been calculated according to N mean values at every level of load application. Interval of values dispersion for every type of test-pieces has been also illustrated.

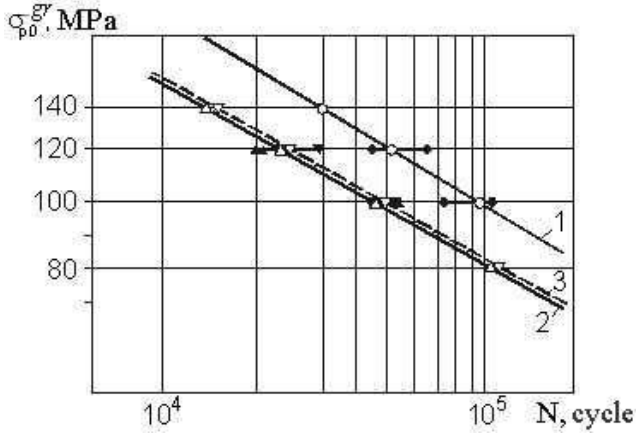

Fig. 2.80. Fatigue curves of plates with hole:
1 – Plate with cylindrical hole;
2 – Plate with countersunk hole;
3 – "HX" anodized plate with countersunk hole

The expressions for fatigue curves have been obtained according to the fatigue test results:

– Plates with cylindrical hole (Fig. 2.79, curve 1):

$$N \cdot \sigma^{3.42484} = 6.59712 \cdot 10^{11} \text{ or } \sigma = 2.82534 \cdot 10^3 N^{-0.291985};$$

– Plates with countersunk hole (plates as-received condition, Fig. 2.78, curve 2):

$$N \cdot \sigma^{3.64667} = 8.68077 \cdot 10^{11} \text{ or } \sigma = 1.87854 \cdot 10^3 N^{-0.474222};$$

– Plates with countersunk hole (anodized plates, Fig. 2.79, curve 3):

$$N \cdot \sigma^{3.58377} = 6.97894 \cdot 10^{11} \text{ or } \sigma = 2.01763 \cdot 10^3 N^{-0.279036}.$$

The following has been found according to the test results:

1) Endurance of plate with cylindrical hole is 2 times higher in comparison with the endurance of plate with countersunk hole at the countersinking depth of 80% from the plate thickness;
2) Endurance of plate with countersunk hole when anodized is increased approximately by 7 %.

2.4.2. Experimental investigation of the lifetime of plates with holes filled with bolts

The lifetime of plate with hole filled with hexagon-headed bolt in the installation of bolts by sliding fit

Experimental investigation of the plate endurance with a hole filled with unloaded hexagon-headed bolt installed by sliding fit has been performed using ЦДМ-10Пу testing machine. A cyclic tensile load has been applied at a frequency of 800 cycles per minute with a stress ratio equal to 0.1. Maximum load Pmax was 50, 40 and 30 kN, corresponding to σ_{p0}^{gr} = 158.1; 126.5; 94.9 MPa.

Five test-pieces have been subjected to test at every level of load application to obtain the endurance characteristics of plates with cylindrical hole filled by hexagon-headed bolt installed by sliding fit without tightening ($M_{nut\ torq}$ = 0 N*m).

Fatigue failure of the test pieces at every level of load application occurred at section along the hole axis.

Five test-pieces have been subjected to test at every level of load application to obtain endurance characteristics of plates with the cylindrical hole filled by hexagon-headed bolt installed by sliding fit with tightening ($M_{nut\ torq}$ = 30 N*m).

The fatigue failure of test pieces at load application levels of P_{max} = 40 kN and 30 kN corresponding to σ_{p0}^{gr} =126.5; 94.9 MPa occurred in the zone of intensive fretting-corrosion on the outer contact boundary of the washer and the plate surface at P_{max} = 50 kN (σ_{p0}^{gr}=158.1 MPa) – at section along the axis hole.

Endurance of strip with cylindrical hole filled with bolt without tightening and without interference is presented by curve 1 (Fig. 2.81). Endurance of strip with hole filled with bolt with tightening but without interference is presented by curve 2. Curve points have been calculated according to N mean values at every level of load application. Intervals of N values dispersion have been also shown in graph.

The experiment-calculated dependencies have been obtained according to the fatigue test results to determine a number of N cycles before plate failure with a cylindrical hole filled with a hexagon-headed bolt without tightening ($M_{nut\ torq}$ = 0 N*m) and interference (2.1) and the hexagon-headed bolt with tightening ($M_{nut\ torq}$ = 30 N*m) without interference (2.2):

$$N \cdot \sigma^{4.27519} = 4.92978 \cdot 10^{13} \quad \text{or} \quad \sigma = 1.59537 \cdot 10^{3} \cdot N^{-0.233908}; \qquad (2.1)$$

$$N \cdot \sigma^{3.04806} = 7.91196 \cdot 10^{11} \quad \text{or} \quad \sigma = 8.00872 \cdot 10^{3} \cdot N^{-0.328078}. \qquad (2.2)$$

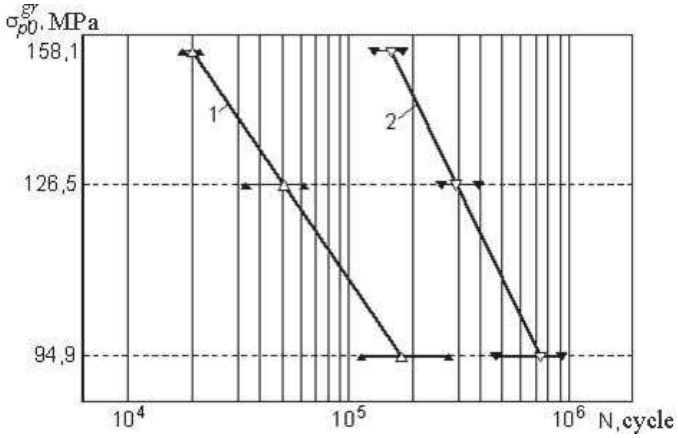

Fig. 2.81. Fatigue curves of strip with hole filled with hexagon-headed bolt with the use of sliding fit:
1 – $M_{nut.torq}$ = 0 Nm; 2 – $M_{nut.torq}$ = 30 Nm

The analysis of the test results shows that the tightening of the nuts to $M_{nut\ torq}$ = 30 N x m under bolt sliding fit has increased life time 4.3 times at

P_{max} = 30 kN, 6.1 times at P_{max} = 40 kN and 8 times at P_{max} = 50 kN.

Life time of the strip with hole filled with hexagon-headed bolt with tightening and interference

The bolts installed with interference were fabricated by reprocessing the 3003A-10-46 bolts by the use of the turning machine. Reprocessing involved the chamfering of the bolt lead-in at the angle of 10°(deg.) and rounding the conic section transition to the cylindrical one with a radius of R = 2 mm.

Press fitting of bolts installed with interference was performed using a hydraulic press without lubrication. The 3401A-1-10-20 washers were installed under the bolt heads and nuts. The steel linear bushings 12 mm in height with outer diameter of 20 mm and inner diameter of 10 mm are installed in the strip between the washer and the nut (bolt head) in an effort to distribute contact pressure from nut tightening more evenly. Nuts were tightened with the torque wrench corresponding to a moment of $M_{nut\ torq}$ = 30 Н·м. Such tightening produces contact pressures under the washer equal 91 MPa. Fatigue life of the strip with the filled unloaded hole under installation of the hexagon-headed bolts with the interference equal 1.5% d_b has been experimentally determined using ЦДМ-10Пу machine. Variable tensile load has been applied at a frequency of 800 cycles per minute with the stress ratio equal to 0.1. Maximum load P_{max} = 50.40 and 30 kN corresponding to σ_{p0}^{gr} =158.1 Pa; 126.5; 94.9 MPa.

Three test pieces for every level of load application have been subjected to test to obtain strength characteristics of the plate with cylindrical hole filled with the hexagon-headed bolt installed with interference without tightening ($M_{nut\ torq}$ = 0 N x m). Fatigue failure of the test pieces at the levels of the load application P_{max} = 50 and 40 kN (σ_{p0}^{gr} =158.1 MPa, 126.5 MPa) occurred in the zones of the chip nicks originated in processing the test pieces and with a single test piece failed along transitional radius. Under the load P_{max} = 30 kN the test pieces have been loaded up to 1.4 million cycles thereafter to be removed from test unfailed. Three test pieces for every level of application have been subjected to test to obtain strength characteristics of the plate with cylindrical hole filled with hexagon-headed bolt installed with the interference and tightening ($M_{nut\ torq}$ = 30 N x m).

Fatigue failure of the test pieces at every level of the load application occurred in the zone of the intensive fretting-corrosion at the outer boundary of the contact between the washer and plate surface.

Endurance of the strip with a cylindrical hole filled with bolt with interference without tightening is presented by the curve 3 (Fig. 2.82). Endurance of the strip hole filled with bolt with interference and tightening is presented by the curve 4. The curve points have been calculated according to the N mean values at every level of load application. The intervals of N values dispersion are also illustrated in the graph.

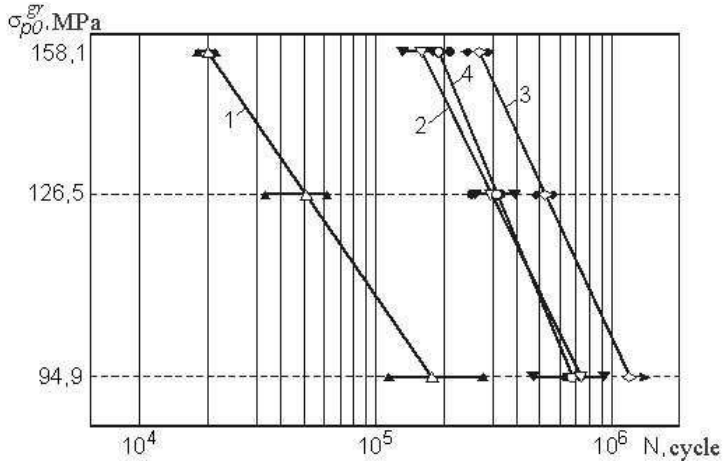

Fig. 2.82. Fatigue curves on the strip with holes filled with bolt:
1 – without tightening and interference; 2 – with tightening without interference;
3 – without tightening with interference; 4 – with tightening and interference

The experiment-calculated dependencies have been obtained according to the fatigue test result to determine a number of N cycles prior to failure of the plate with a cylindrical hole filled by a hexagon-headed bolt with interference without tightening ($M_{nut\ torq}$ = 0 N·m) (2.3) and a hexagon-headed bolt with interference and tightening ($M_{nut\ torq}$ = 30 N·m) (2.4):

$$N \cdot \sigma^{2.86761} = 5.59214 \cdot 10^{11} \quad \text{or} \quad \sigma = 1.24925 \cdot 10^4 \cdot N^{-0.348723}; \qquad (2.3)$$

$$N \cdot \sigma^{2.56359} = 8.02379 \cdot 10^{10} \quad \text{or} \quad \sigma = 1.79292 \cdot 10^4 \cdot N^{-0.390078}. \qquad (2.4)$$

In bolts fit with interference equal to 1.5% d_b, and tightening, the strip endurance has not practically changed in comparison with the strip endurance where the bolt has been installed just with tightening (See Fig. 2.81, curve 4). The reason is that the fatigue cracks, in this case, are originated at the strip-to-washer contact boundary (Fig. 2.83) at every level of load application, that is, the strip endurance is characterized by the fretting-corrosion intensity rather than geometric stress concentration in the section along the hole axis.

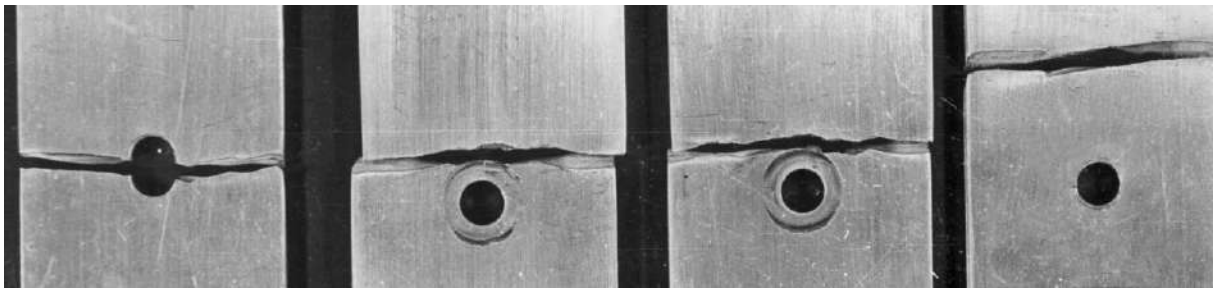

a b c d

Fig. 2.83. Failure zones of plate with holes filled by hexagon-headed bolt: a – without interference and tightening; b – with tightening; c – with interference and tightening; d – with interference

In case of bolt installation with interference of 1.5% d_b without tightening under a load of P_{max} = 40 and 50 kN, the fatigue cracks were originated at the dents and nicks obtained when manufacturing the test-pieces and probable in the process of the actual structural component manufacture as a result of the mechanical damage inflicted with chips and tools. Thus, the initial mechanical damages of the Д16АТ material clad layer that may be initiated in processing and assembly result in decrease of the joint member strength provided with the elastoplastic interference of the bolts. It is obvious that the test-piece life time with interference without tightening is the highest because, in this case, there are no contact pressures fretting corrosion under the washers.

Analysis of plate fatigue resistance characteristics with hole filled with countersunk unloaded bolts

Special test-pieces of the flat plates (Fig. 2.84) have been manufactured to analyse the plate fatigue resistance characteristics with hole filled with the countersunk unloaded bolts.

The plates and straps for the test-pieces were fabricated from Д16АТл5 sheet "НХ" anodized by milling around the contour.

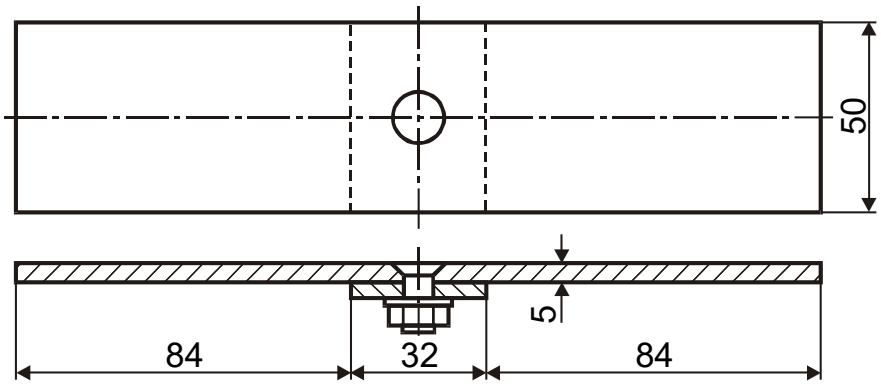

Fig. 2.84. Manufacturing version of plate test-pieces with filled unloaded hole

The 5015A steel bolts with a radial interference of 0.8-1.2% d_b (where d_b – bolt body diameter) have been installed in the cylinder – conic holes. The nuts have been tightened with the torque wrench: first – torque moment $M_{nut\ torq}$ =25 N·m followed by unloading to $M_{nut\ torq}$ =0 N·m and final tightening to $M_{nut\ torq}$ =20 N·m.

The fatigue tests have been conducted using the ЦДМ-10Пу hydraulic pulsator with maximal cyclic loads P_{max} equal 30 and 25 kN (σ^{gr}_{p0}=119 and 99 MPa), cycle ratio of R_σ=0.1 and a frequency of 13 Hz. 8 test pieces have been tested at a level of loads P_{max}=30 kN and 4 test-pieces at P_{max}=25 kN.

The plate fatigue failure with the countersunk hole filled with the countersunk bolt with the radial interference and tightening mainly occurred in

the plate as a result of the intensive fretting-corrosion development along the contact surface between the plate and the strap.

Fatigue test results are illustrated in Fig. 2.85. The curve points have been calculated according to N-mean values at every level of load application. Value dispersion intervals for every type of the test pieces are also shown in the graph.

Fatigue test results of the plate test pieces with the cylinder-conic hole filled with the countersunk unloaded bolt with the radial and axial interference failed along the plate in the zone of the joint faces due to the action of the fretting-corrosion are presented in Fig. 2.86, curve 2.

The summarized expression for the fatigue curve of the plate with holes filled with unloaded bolts installed with the radial and axial interference in case of the plate failure in the strap installation zone due to the action of the fretting corrosion takes the form:

$$N_{fr} \cdot \sigma^{3.42313} = 5.14378 \cdot 10^{12} \quad \text{or} \quad \sigma = 5.16829 \cdot 10^{3} N^{-0.29213} .$$

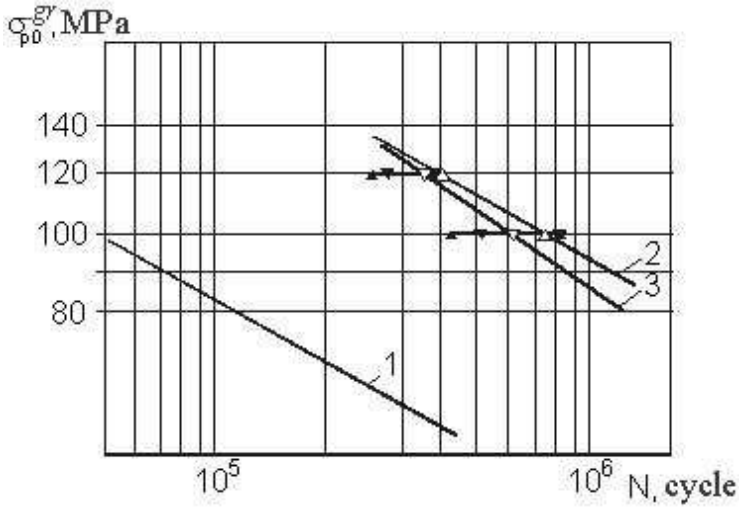

Fig. 2.85. Fatigue curves of plates with cylinder-conic holes filled with 5015 A unloaded steel bolts:

1 – anodized test-pieces with cylinder-conic hole;

2 – test-pieces with bolts interference and tightening failed along the plate in zone of joint faces due to action of fretting corrosion;

3 – test-pieces with bolts interference and tightening failed in strap installation zone due to action of fretting corrosion and failed in section along hole axis

The summarized expression for the fatigue curve of the plate with holes filled with unloaded bolts installed with the radial and axial interference in case of the plate failure in the strap installation zone due to the action of the fretting corrosion takes the form (see Fig. 2.85, curve 3).

$$N \cdot \sigma^{3.07512} = 8.66973 \cdot 10^{11} \text{ or } \sigma = 7.62293 \cdot 10^{3} N^{-0.32519}.$$

In compliance with the results of the analysis, it has been found that an allowance must be made both for the action of the cycle tensile stresses and intensive action of the fretting-corrosion to predict the endurance of the plates with the cylinder-conic holes. Application of the radial interference Δ-(1±0.2)% d_b and a calibrated tightening in correspondence to $M_{nut\ torq}$ = 20 N·m provides endurance increase of plate with cylinder-conic hole in 10…12 times and displays failure zone from section along the hole axis to the fretting-corrosion zone between the plate and the strap.

2.4.3. Fatigue resistance of plates with holes and standard riveted joints

Test results analysis of the test-pieces of the wing one-to-one size panels made from Д16ХТ alloy and their joints shows that their endurance is comparable with the endurance of the strip with a hole made from the same material.

Under operating conditions the fatigue failure of the structural components joined by the use of the rivets is initiated both in the normal stress concentration zone and intensive fretting corrosion development.

Therefore, the analysis of the fatigue resistance characteristics of the structural components with a free hole and a hole filled with the advanced rivets must be performed to predict the endurance of aircraft airframe riveted joints. It is determined by the expressions [192]:

$$\sigma^{*}_{red}(N) = k_{bear}(N) \cdot \sigma_{bear} + \sigma_{tens} + k_{bend}(N) \cdot \sigma_{bend} \qquad (2.5)$$

or

$$\sigma^{*}_{red.fr}(N) = k_{bear.fr}(N) \cdot \sigma_{bear} + \sigma_{tens} + k_{bend}(N) \cdot \sigma_{bend}, \qquad (2.6)$$

depending on failure zone: (2.5) – along the hole axis, (2.6) – in fretting corrosion zone.

Endurance of plates with free unloaded hole

A strip from Д16АТл2 material 30 mm wide with a hole (Fig. 2.86) has been used to provide fatigue tests. The hole was drilled by means of a drill 4.05 mm in diameter. The holes have been chamfered 120×0.1-0.2 mm. The tests have been conducted using УПМ-200 machine at a frequency of 40 Hz and cycle ratio of R_σ=0.1 at three levels of load application corresponding to $\sigma^{gr}_{ð0}$=221.4; 189.7 and 158.1 MPa (where $\sigma^{gr}_{ð0}$ is a value of maximum equivalent zero-to-tension stress cycle).

The test pieces have been tested up to the failure in one among tested zones, then, up to the failure in other calculated zone. Six (6) test pieces have been subject to test at every level of load application.

The fatigue test results are illustrated in Fig. 2.86.

Failure of every test piece occurred over plate in section along hole axis.

Expression for the fatigue curve of the plate made of Д16АТл2 alloy with a free hole has the following form:

$$N \cdot \sigma^{3.658109} = 6.758 \cdot 10^{12} \quad \text{or} \quad \sigma = 3.21534 \cdot 10^{3} \cdot N^{-0.273365}$$

Life time of plate with a hole filled with rivet

Special test-pieces (Fig. 2.86, pos. 2) have been manufactured to investigate the fatigue resistance characteristics of the skin with a hole filled with a rivet according to Industry Standard ОСТ1 34052-85 loaded to carry the shear stresses.

The skin and the strip have been manufactured by milling along the contour of Д16АТл2 sheet "НХ" anodized in correspondence to the series procedure. The plates have been chamfered 45°×0.1-0.2 mm along the perimeter 4-9 ОСТ л 34052-85 rivet holes have been drilled by means of a drill 4.05 mm in diameter. The holes have been chamfered 120°×0.1-0.2 mm along the perimeter. Countersinking was performed to a depth of 1.55±0.55 mm. The rivets were unriveted using КП-204М press. Snap rivet heads 1.9-2.0 mm in depth have been formed in the process of riveting.

Fatigue tests of the test-pieces have been performed using УПМ-2000 fatigue test machine at a frequency of 40 Hz and a cycle ratio of $R_\sigma = 0.1$ at three levels of load application corresponding to $\sigma_{\partial 0}^{gr} = 221$; 189.7 and 158.1 MPa with 15…35 test-pieces at every level. The test-pieces having two tested zones have been installed in the machine grip and loaded till the moment of joint failure in one of the tested zone to analyse the fatigue resistance characteristics.

Fatigue test results of the skin test-pieces with a hole filled with a countersunk rivet until failure of the test-pieces in one among two tested zones are illustrated in Fig. 2.85 (pos. 2). The analysis of the test results shows that the test-pieces worked until failure at $\sigma_{\partial\hat{i}}^{\acute{a}\partial} = 158.1$ MPa 464900, 496200, 587500 and 662300 loading cycles have been failed due to the fatigue cracks developed along the skin as a result of the fretting-corrosion effect in the strap zone. The rest test-pieces have been failed along the skin in section along the axis of the rivets.

The expression of the plate fatigue curve of Д16АТл2 sheet with the rivet ОСТ1 34052-85 has the following form

$$N \cdot \sigma^{4.833427} = 1.7947987 \cdot 10^{16} \quad \text{or} \quad \sigma = 2.3058676 \cdot 10^{3} \cdot N^{-0.2068925}.$$

The special test-pieces (see Fig. 2.86, pos. 3) have been manufactured to analyse the fatigue resistance characteristics of the skin with a hole filled by the rivet 4-9 ОСТ1 34040-79 unloaded for shear of rivet. The skin and the strip (Fig. 2.86) have been manufactured by milling along the contour of Д16АТл2 "НХ" anodized sheet. The plate has been chamfered 45°×0.1-0.2 mm along the perimeter.

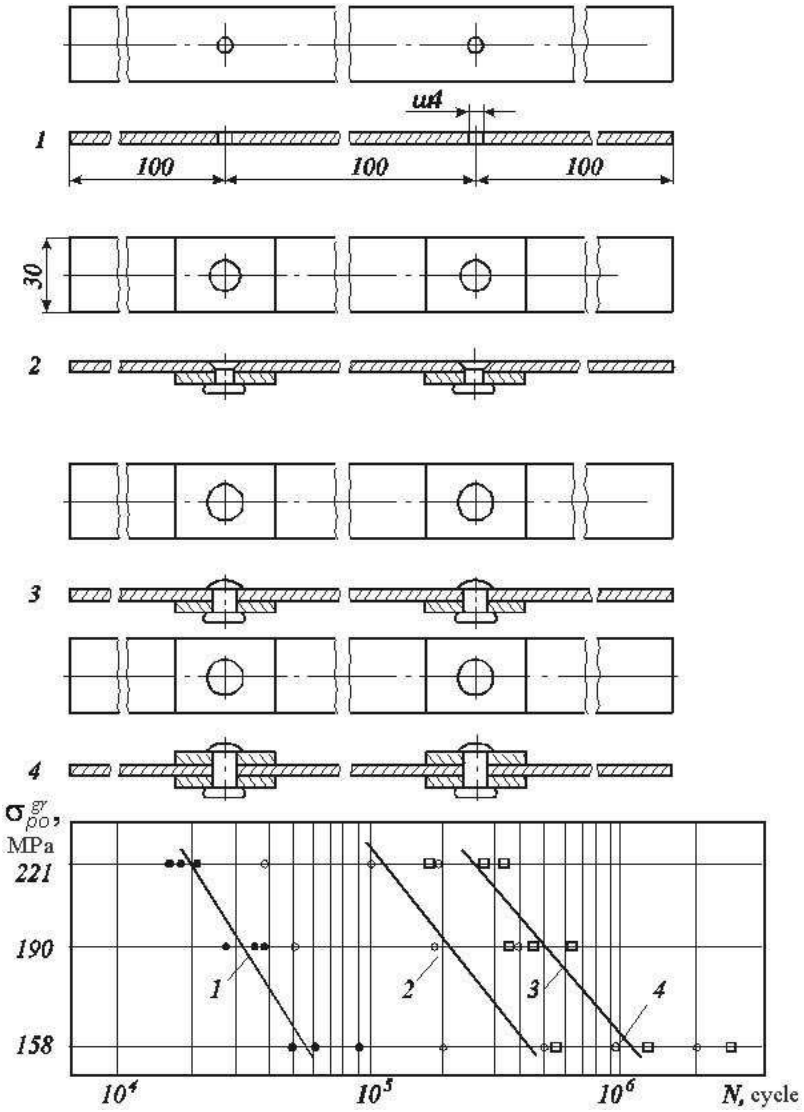

Fig. 2.86. Test-pieces for fatigue tests and their fatigue test results: 1 – free unloaded hole; 2 – hole filled with rivet OCT1 34052-85; 3,4 – hole filled with rivet OCT1 34040-79

OCT1 34040-79 rivet holes 4 mm in diameter have been drilled by means of the drill 4.05 mm in diameter.

The holes have been chamfered 120°×0.1-0.2 mm along perimeter. The rivets have been unriveted using КП-204М press. Snap rivet heads 1.9-2.0 mm in height have been formed in the process of riveting.

The test-pieces have been subject to fatigue tests using УРМ-2000 machines at a frequency of 40 Hz and a cycle ratio of $R_\sigma = 0.1$ at three levels of load application with 21…25 test pieces for every level. The test-pieces having two tested zones have been installed in the machine grips and loaded until the moment of joint failure in one of the tested zones to analyse the fatigue resistance characteristics.

The fatigue test results of the skin test-pieces are illustrated in Fig. 2.85 (pos. 3).

An expression of the strip fatigue curve with hole filled by rivet OCT1 34040-79 has the following form:

$$N \cdot \sigma^{4.415393} = 5.853562 \cdot 10^{15} \quad \text{or} \quad \sigma = 3.72402 \cdot 10^{3} \cdot N^{-0.2264804}.$$

In failure beyond the strip zone, the expression of the plate fatigue curve has the following form:

$$N \cdot \sigma^{5.171066} = 2.6058212 \cdot 10^{17} \quad \text{or} \quad \sigma = 2.33325 \cdot 10^{3} \cdot N^{-0.193384}.$$

The special test-pieces (Fig. 2.87) have been manufactured to analyse the fatigue resistance characteristics of the skin with a hole filled with unloaded shear rivet OCT1 34040-79 5 mm in diameter.

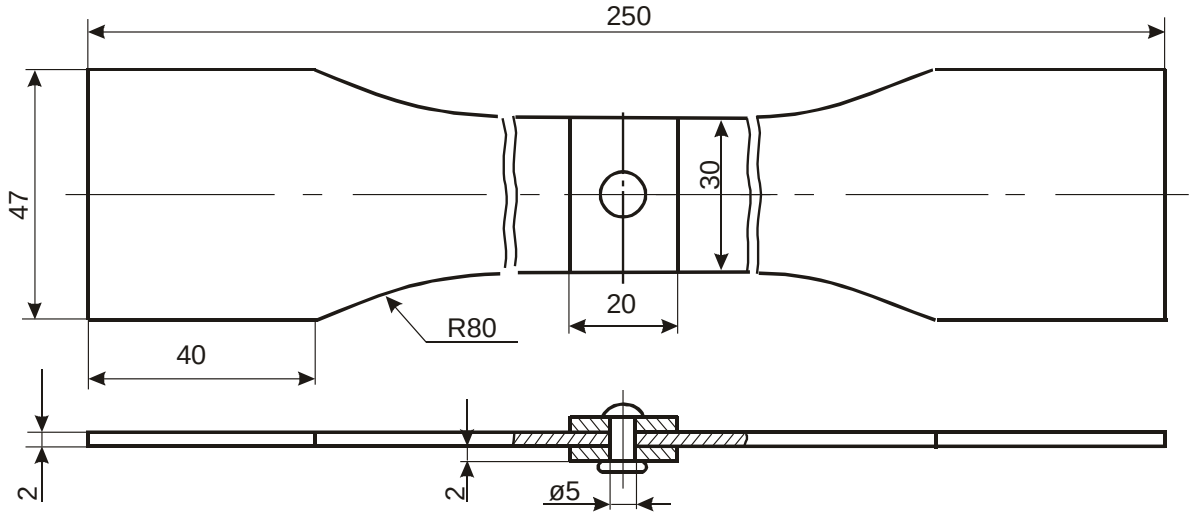

Fig. 2.87. Test-pieces of plates of Д16АТл2 sheet with unloaded hole filled with rivets-11 OCT1 34040-79

The skin and the straps have been manufactured by milling along the contour of Д16АТл2 sheet anodized by "НХ" according to the series production procedure. The plates have been chamfered 45°×0.1-0.2 mm along the perimeter.

OCT 34040-79 rivet 5-11 holes have been drilled by means of the drill 5.05 mm in diameter. The holes have been chamfered 120×0.1-0.2 mm along the perimeter. The rivetes have been unriveted using КП-204 press. Snap rivet heads 2.5±0.1 mm in depth have been formed in the process of riveting.

The test-pieces have been subject to fatigue tests using УРМ-2000 machines at a frequency of 40 Hz and a cycle ratio of R_σ=0.1 at three levels of load application corresponding to $\sigma_{\delta 0}^{gr} = 228$, 196, 165, 165 MPa.

The fatigue test results of the skin test-pieces with a hole filled with uncountersunk rivet are illustrated in Fig. 2.88.

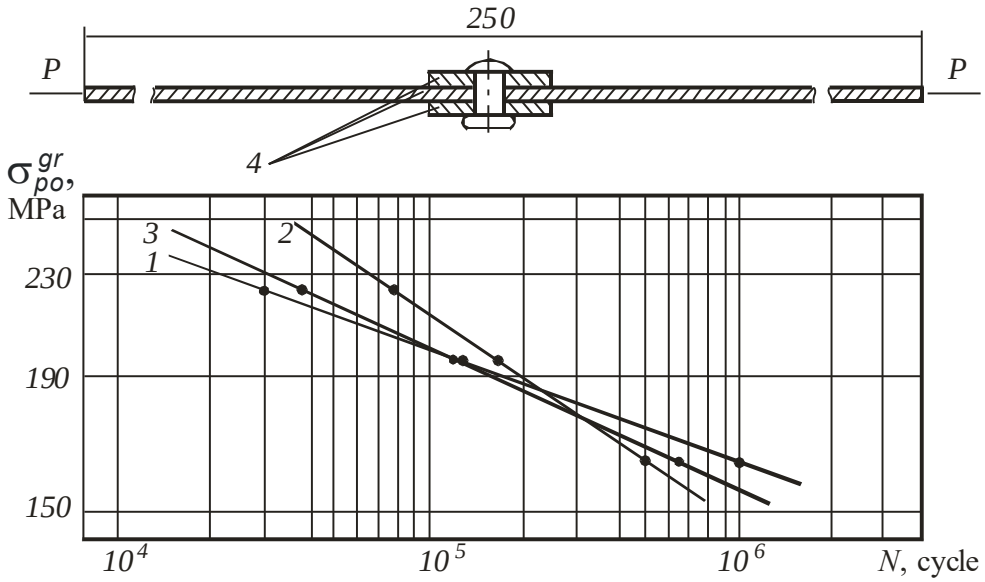

Fig. 2.88. Fatigue curves of the plate from Д16АТл2 sheet with unloaded hole filled with rivets 5-11 ОСТ 2. 34040-79: 1 – failure from hole wall; 2 – failure under strap;
3-1+2; 4 – plate and strap from Д16АТл2 sheet

The test-pieces have been divided into two groups following the fatigue test result analysis of the plates from Д16АТл2 with unloaded hole filled with the rivet 5-11 ОСТ 2. 34040-79 in compliance with the fracture pattern.

The first group involves test-pieces failed due to the combined action of the geometric stress concentration and fretting-corrosion in the contact zone between the rivet shank and the hole wall. The cracks were developed from the hole wall followed by offset from the rivet axis to be 0.65-1.5 mm.

The second group involves the test-pieces failed because of fretting-corrosion along the joint faces in the contact zone of strap and plate. The crack in seventy percent (70%) of test-pieces was developed in the plate cross-sectional planes within the hole zone. Areas of crack origination were located at a distance of 5 mm to 12.6 mm from the longitudinal axis of the test-pieces. The rest test-pieces have been failed along the plate at the points of its contact with the straps along cross-sectional planes beyond the hole zone. The distance between the hole center and the crack origination zone along the axis parallel to the axis of load application is 7.0-7.5 mm while along the axis directed across the plate fatigue curve from Д16АТл2 sheet with unloaded holes filled with rivet 5-11 ОСТ1 34040-79 has the following form.

The expression of fatigue curve of plate made of Д16АТл2 sheet with unloaded holes filled with rivet 5-11 ОСТ 1 34040-79 has the following form:

$$N \cdot \sigma^{8.3785} = 1.989085 \cdot 10^{24} \quad \text{or} \quad \sigma = 7.9439 \cdot 10^2 \cdot N^{-0.193}.$$

The expression of the plate fatigue curve from Д16АТл2 sheet with

unloaded holes filled with rivet 5-11 OCT1 34040-79 in failure of joint faces as a result of fretting-corrosion has the following form:

$$N \cdot \sigma^{11.0436} = 2.40729 \cdot 10^{30} \quad \text{or} \quad \sigma = 5.637 \cdot 10^{2} \cdot N^{-0.09055}.$$

The expression of the plate fatigue curve from Д16АТл2 sheet with unloaded holes filled with rivet 5-11 OCT1 34040-79 in failure of joint faces as a result of fretting-corrosion has the following form

$$N \cdot \sigma^{6.03083} = 1.20099 \cdot 10^{19} \quad \text{or} \quad \sigma = 1.4577 \cdot 10^{3} \cdot N^{-0.165815}.$$

Additional researches have been performed to analyse the fatigue resistance characteristics of the skin with a hole filled with unloaded shear rivet OCT1 34040-79 4 mm in diameter. The special test-pieces (Fig. 2.89) have been manufactured for testing.

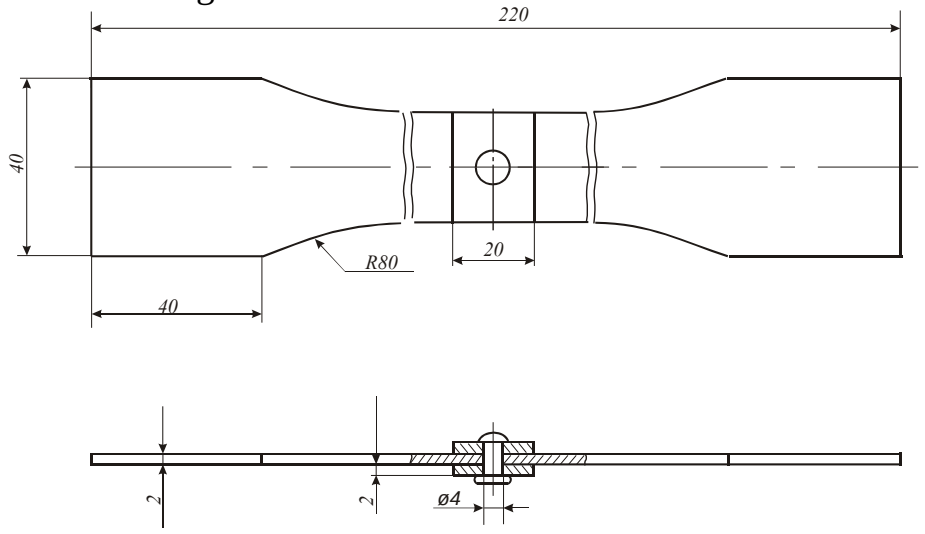

Fig. 2.89. Test-pieces of plates from Д16АТл2 sheet with unloaded hole filled with
rivet 4-11 as specified in OCT1 34040-79

The skin and the strap have been manufactured by milling along the contour of Д16Атл2 sheet anodized by "НХ" according to the series procedure. The plates have been chamfered 45°×0.1-0.2 mm along the perimeter.

OCT1 34040-79 rivet 4-11 holes have been drilled by means of the drill 4.05 mm in diameter. The holes have been chamfered 120°×0.1-0.2 mm along the perimeter. The rivets have been unriveted using КЛ-204М press. Snap rivet heads 2.0±0.1 mm in depth have been formed in the process of riveting.

The test-pieces have been subject to fatigue tests using УРМ-2000 fatigue test machine at a frequency of 40 Hz and a cycle ratio of R_σ=0.1.

The fatigue test results of the skin test-pieces with a hole filled with uncountersunk rivet are illustrated in Fig. 2.90.

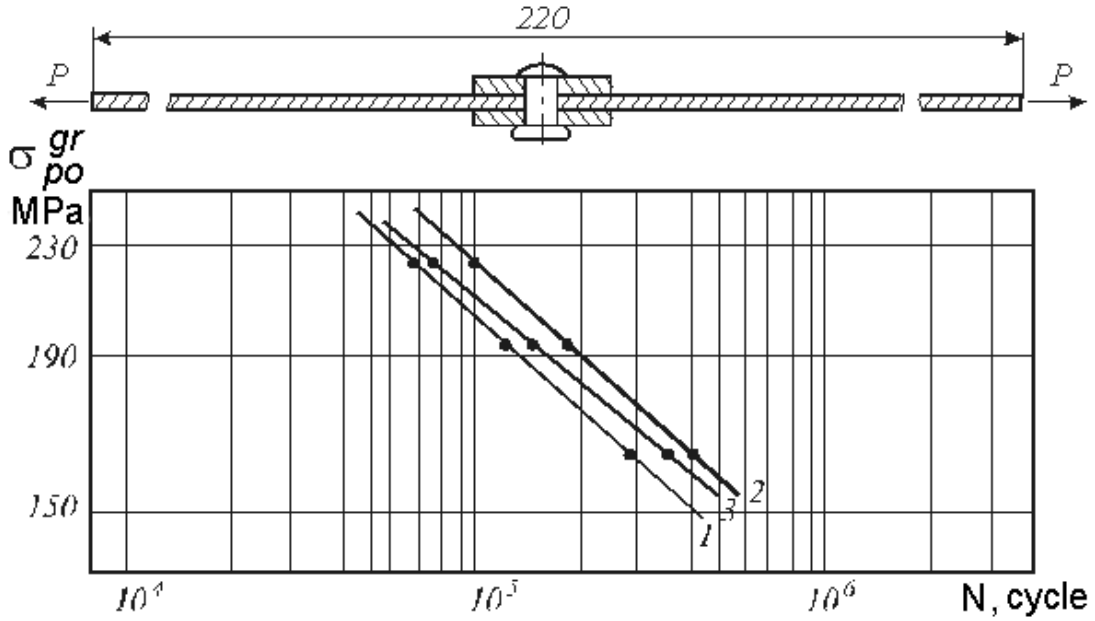

Fig. 2.90. Fatigue curves of plate of Д16АТл2 sheet with unloaded hole filled with 11 OCT1 34040-79 rivets 4-11

The test-pieces have been divided into two groups following the fatigue test result analysis of the plates from Д16АТл2 with unloaded hole filled with the rivet 4-11 OCT1 34040-79 in compliance with the fracture pattern.

The first group involves test-pieces failed due to the combined action of the geometric stress concentration and fretting-corrosion in the contact zone between the rivet shank and the hole wall. The cracks were developed from the hole wall followed by offset from the rivet axis to be 05. – 1.2 mm.

The second group involves the test-pieces failed because of fretting corrosion along the joint faces in the contact zone of strap and plate. The crack in twenty five percent (25%) of test pieces was developed in the plate cross-sectional plane within the hole zone. Areas of crack origination were located at a distance of 3 mm to 7 mm from the longitudinal axis of the test-piece. The rest test-pieces have been failed along the plate at the points of its contact with the straps at the plate cross-sectional planes beyond the hole zone. The distance between the hole center and the crack origination zone along the axis directed across the load applied is 3-7 mm.

Expression of the plate fatigue curve of Д16АТл2 sheet with unloaded holes filled with OCT1 34040-79 rivet 4-11 has the following form

$$N \cdot \sigma^{5.0567} = 5.7748 \cdot 10^{16} \quad \text{or} \quad \sigma = 2.064 \cdot 10^{3} \cdot N^{-0.1978}.$$

Expression of the plate fatigue curve from Д16АТл2 sheet with unloaded holes filled with OCT1 34040-79 rivet 5-11 in case of failure from joint action of the geometric stress concentration and fretting-corrosion in the contact zone of the rivet shank and the hole wall has the following form:

$$N \cdot \sigma^{4.6724} = 6.63 \cdot 10^{15} \quad \text{or} \quad \sigma = 2.433 \cdot 10^{3} \cdot N^{-0.214}.$$

Expression of the plate fatigue curve from Д16АТл2 sheet with unloaded holes filled by ОСТ1 34040-79 rivet 5-11 in case of failure from fretting corrosion along the joint faces in the contact zone of the strip and the plate has the following form:

$$N \cdot \sigma^{4.5772} = 5.84699 \cdot 10^{15} \quad \text{or} \quad \sigma = 2.7836 \cdot 10^{3} \cdot N^{-0.2185}.$$

2.5. METHOD IN FATIGUE LIFE PREDICTION OF PLATES WITH HOLE

The aircraft wing life time is specified by the service life of the wing panel longitudinal joints. The rest structural irregularities are designed for their service life to meet or exceed the life time of the wing panel longitudinal joints [196, 290].

Aircraft life tests have demonstrated that the fatigue life of the wing panel longitudinal joints from Д16чТ material coincides with the cylindrical hole that is described by an expression generally having the form of: $N \cdot \sigma_{gr.0}^{m} = C$.

Where $\sigma_{gr.0}$ – nominal stress in gross section of structural component brought into zero-to-tension stress cycle, m and C – experimental, determinative constants with an allowance made for the material life properties and type of the irregularity zones.

It this case, it has been found that the dependence describing service life for the test pieces from Д16чТ alloy has the following form [376, 414].

$$N = 3 \times 10^{9} \sigma_{eqv}^{-4}, \tag{2.7}$$

and for test pieces from В95пчТ2 alloy [2]

$$N = 4.14 \times 10^{8} \sigma_{eqv}^{-3.5} \tag{2.8}$$

In formulae (2.7), (2.8) the equivalent stresses have the units [xgf / mm^2].

Change of hole parameters and shape in the plate result in change of local deflected mode characteristics and, hereupon, fatigue life before crack occurrence. Developed methods of structural member life time analysis with the holes are based on determination of the efficient stress concentration factors. It should be noted that the experiment-calculated dependencies used for life time prediction of the structural members according to the nominal stresses and made from the same material of different thickness and semi-product require experimental investigations in great scope for determination of m and C factors. These methods are used to predict the fatigue resistance at the stage of draft design.

The researches [437-441] have shown that the life time analysis of the irregular shaped structural components is feasible to perform on the basis of the local deflected mode characteristics. Lifetime analysis method according to local

deflected modes has been developed to provide high accuracy of calculation. It is based on determination of the local deflected mode concentration as well as on the use of the smooth test-piece fatigue characteristics.

Fatigue life prediction method of structural components with the geometric concentrator in the form of a hole on the basis of the energy criteria and the local elastoplastic deflected mode characteristics as well as fatigue resistance of the standard plate with a hole has been proposed and presented hereinafter by the author.

This method involves:

1. Determination of the local maximum elastoplastic stresses and deformations on the geometric concentrator contour of the plate with a hole of the model under investigation with an allowance made for the loading history by the use of the finite element method realized in the system of the ANSYS engineering analysis.

2. Analysis of the maximum zero-to-tension stresses and deformations of the fatigue cycle according to Oding's formula in the basic and investigated test-pieces.

3. Analysis of stressing level effect on the change of the energy criteria ($\sigma_{eqv.loc.0} \times \varepsilon_{eqv.loc.0}$) in the test pieces.

4. Determination of the fatigue resistance experimental characteristics of the standard plates with a hole made of the material under research.

5. Parameter determination of the experiment-calculated dependence in life prediction of the plate basic test-pieces on the basis of the energy criteria.

6. Analysis of the predicted life time of the test-piece under investigation.

Let’s discuss the structural zone with a free hole. Local deflected mode characteristics of the plate test-pieces with parallel and countersunk holes analysed using ANSYS system of engineering analysis [474] to determine fatigue characteristics of these zones are illustrated in Fig. 2.91, 2.92.

With an account taken for the plate symmetry and external load application condition, 1/4 part of the model with the corresponding fastening conditions were the subject of analysis. Zero movement along Y and Z components has been selected to limit the model movement along Y and Z axis for every unit lying on the plate end surface at the point of the external load application. Symmetry conditions [Fig. 2.93] have been selected for the units of the finite-element mesh lying in OX and OY planes.

The finite-element model of the plate with a hole consists of the solid eight-units elements SOLID 45 presented in ANSYS system [474]. Totally, the model contains 1500 finite elements. The equivalent stress pattern of the plate with the countersunk hole is illustrated in Fig. 2.94.

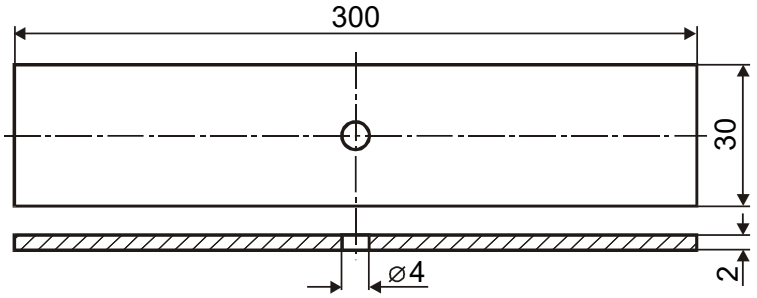

Fig. 2.91. Test-piece structure of plate with cylindrical hole

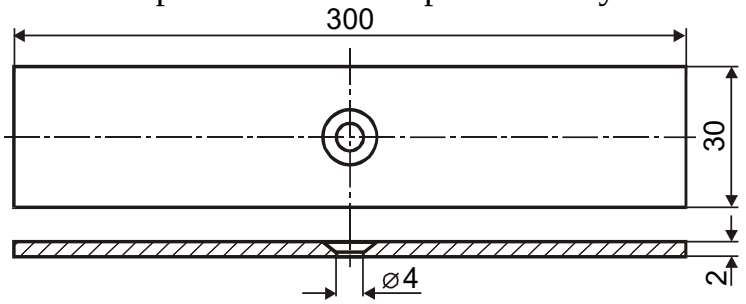

Fig. 2.92. Test-piece structure of plate with countersunk hole

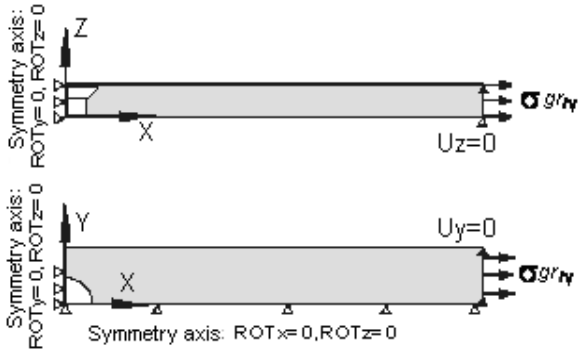

Fig. 2.93. Analytical model of plate with hole

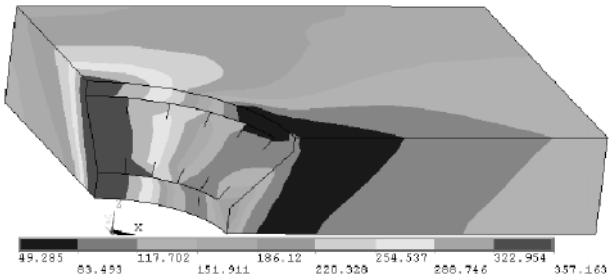

Fig. 2.94. Equivalent stress pattern of plate with countersunk hole

1) Axis of symmetry

The analysis results of the local deflected mode are illustrated in Fig. 2.95 in the form of dependencies $\sigma_{eqv.loc.0} \times \varepsilon_{eqv.loc.0}$ from σ_0^{gr}.

The fatigue curves of the plate with cylindrical and countersunk free holes in the coordinates $\sigma_{eqv.loc.0} \times \varepsilon_{eqv.loc.0}$ from N are illustrated in Fig. 2.96.

The fatigue curve for the plate with the cylindrical hole has been taken from TsAGI (ЦАГИ) works. The points specifying the lifetime of the plate with a countersunk hole have been determined under the assumption that the fatigue of the plate with the cylindrical hole is twice higher than the fatigue of the plate with the countersunk hole to 80% depth of the plate thickness [246].

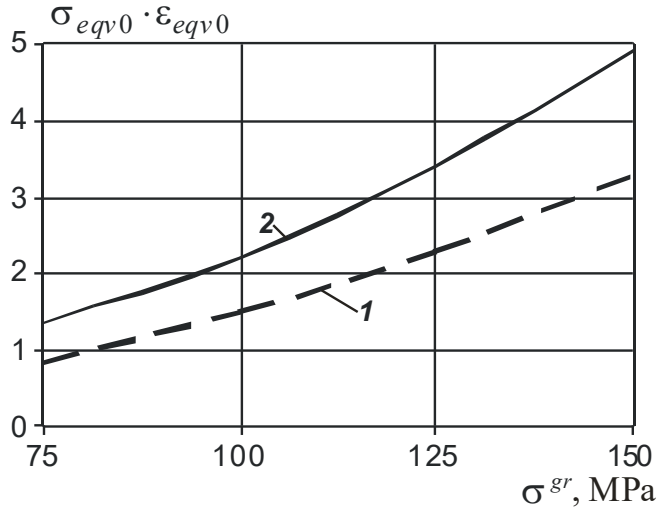

Fig. 2.95. Dependence of local stresses and deformation product at the most loaded point on the contour from nominal stresses σ_0^{gr} for plate:
1 – with free cylindrical hole; 2 – with free countersunk hole

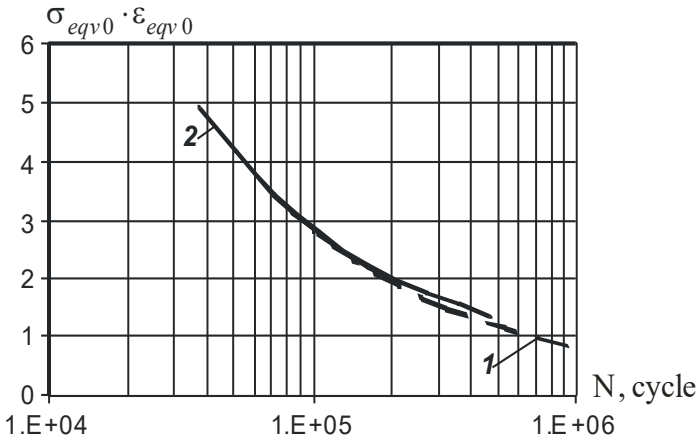

Fig. 2.96. Plate fatigue curves in coordinate $N = f(\sigma_{eqv.loc.0} \times \varepsilon_{eqv.loc.0})$;
1 – with free cylindrical hole; 2 – with free countersunk hole

Obtained experimental fatigue curves of plate with cylindrical hole are approximated by the expression

$$\left(\sigma_{eqv\,0} \times \varepsilon_{eqv\,0}\right)^{m_{exp}} N = C_{exp}, \qquad (2.9)$$

where m_{exp}=1.8528; c_{exp}=6.91619×10^5.

Coincidence of the fatigue curves in these coordinates allows to assume that the constant $C_э$ in the expression (2.9) would be equal to the plates with the regarded hole shapes provided that the local deflected modes are specified by the energy criterion equal to the product of the maximum equivalent zero-to-tension stresses and deformations. According to the available life curve of the plate with the cylindrical hole and with the account taken for coincidence of the constant C,

we get an expression for predicting the lifetime of the plate with a countersunk hole (Fig. 2.96):

$$N_2 = N_1 \times \left(\frac{\left(\sigma_{eqv.loc.0} \times \varepsilon_{eqv.loc.0}\right)_P}{\left(\sigma_{\acute{y}eqv.loc.0} \times \varepsilon_{eqv.loc.0}\right)_C} \right)^{m_{exp}}, \qquad (2.10)$$

where N_2 – lifetime of plate with countersunk hole; N_1 – lifetime of plate with cylindrical hole; $\left(\sigma_{eqv.loc.0} \times \varepsilon_{eqv.loc.0}\right)_P$ – product of local stresses and deformations of plate with cylindrical hole; $\left(\sigma_{eqv.loc.0} \times \varepsilon_{eqv.loc.0}\right)_C$ – product of local stresses and deformations of the plate with countersunk hole.

Fatigue test and analysis results of the plate life with cylinder-conic and cylindrical holes are illustrated in Fig. 2.97.

Lifetime analysis of the plate with the cylindrical and countersunk holes of Д15АТл5 alloy shows that the plate fatigue strength with the cylindrical hole is two times higher than the fatigue strength of the plate with the countersunk hole to 80 % depth from the plate thickness [246].

The lifetime of the plate with the countersunk hole (See Fig. 2.97) obtained by analysis is also two times less than the lifetime of the plate with the cylindrical hole that makes it possible to note the satisfactory correspondence to the analysis and experiment results.

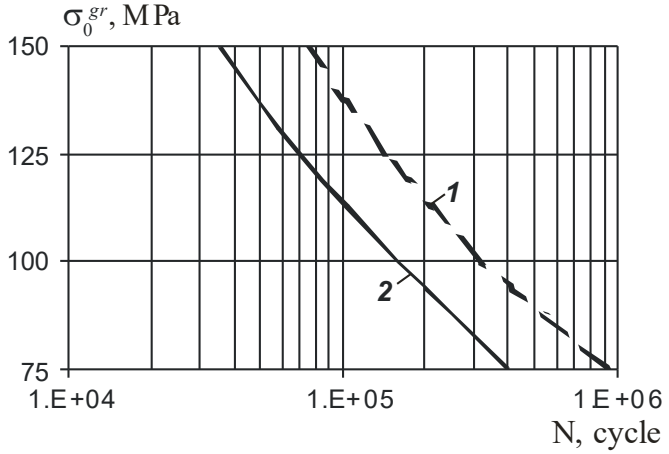

Fig. 2.97. Plate fatigue curves in coordinates $N = f(\sigma_0^{gr})$:
1 – with free cylindrical hole (experiment); 2 – with free countersunk hole (analysis)

2.6. METHOD IN LIFETIME PREDICTION OF SHEAR JOINTS MADE WITH AXIAL AND RADIAL INTERFERENCE OF HEXAGON-HEADED BOLTS

The aim and goal of this method is fatigue life time prediction of the shear bolted joints made with elastoplastic radial and axial interference under their cyclic loading in the zones of probable failure resulting from both geometric stress concentration and contact pressures causing development of fretting

corrosion.

The life time prediction method of modified models of shear bolted joints with the axial and radial interference of bolts is based on the damaging action equivalence hypothesis until crack occurence from the total specific deformation energy concentration factor at the mostly loaded zones of the modified joint members in the standard plate with a hole filled with bolts with axial and radial interference according to one and the same procedure and of the identical materials as well as basing on the analysis of their contact interaction characteristics. Allowance is made in analysis for the change of the deflected mode characteristics in the joint members made with the elastoplastic interference after external load application.

The lifetime prediction method of the shear bolted joints made with interference contains the following stages:

1. Analysis of the structurally-technological parameters of the shear bolted joints made with the elastoplastic axial and radial interference.

2. Selection of shear bolted joint standard test-pieces with their effect on the joints lifetime to be analysed. Manufacture of standard test-pieces according to the series manufacturing procedure.

3. Subjection of standard test-pieces to fatigue tests and analysis of their fatigue strength characteristics approximation of test results by analytical expressions and fatigue curve construction according to the nominal zero-to-tension stresses.

4. Analysis of the local deflected mode characteristics in the zones of stress concentration and contact pressures in the members of the test piece parts joined by the use of the finite element method. Determination of the specific energy criteria concentration factors and contact pressure values in correspondence to the mating surfaces of the joint parts with an allowance made for the change of the deflected mode after the first loading cycle.

5. Lifetime prediction of the modified joint on the basis of the accepted criteria with an allowance made for the change of the design factors.

The standard plate test pieces with unloaded hole filled with bolts 8-24-К$_д$-ОСТ131103-80 making single, – two, and three-row shear joints and installed with radial interference of 1 % d_b and axial tightening P_t = 10 kN, further denoted as 1, 2, 3, 4 respectively (Fig. 2.98) to test and approve the proposed method basing on the analysis (stage 1) of the available design-engineering parameters of the aircraft structures [285] bolted joints at stage 2.

At stage 3 the fatigue test results of the standard plate test-pieces with unfilled hole (1_o), with a hole filled with bolt having an interference (1_{int}) and with interference and tightening ($1_{int+tight}$) as well as double-shear joints (2, 4) have been approximated by the analytical expressions of the following type

$$N \cdot \left(\sigma_0^{gr}\right)^m = C,$$

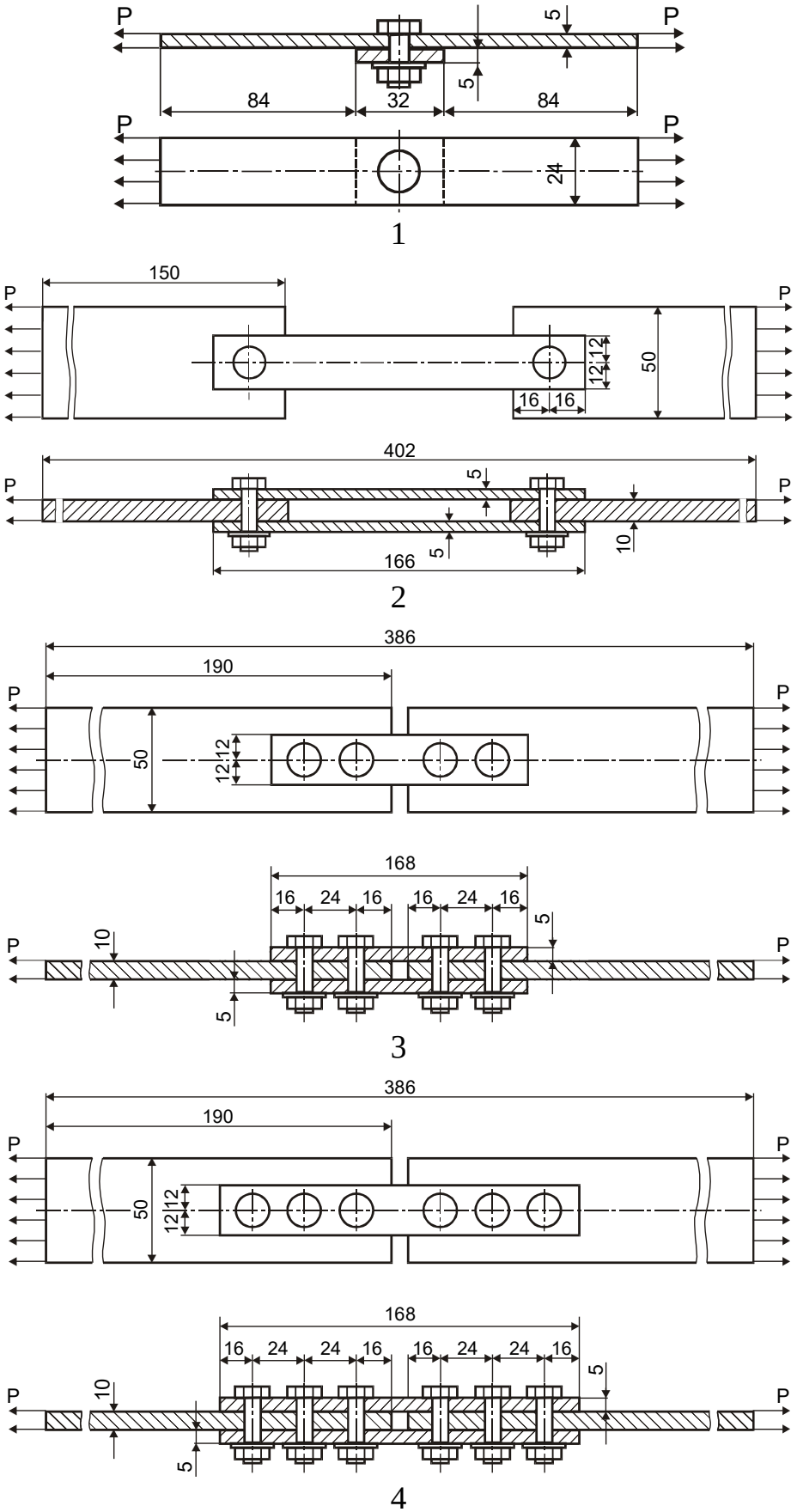

Fig. 2.98. Analysed test-pieces of shear bolted joints

where σ_0^{gr} – nominal stresses in gross section of the structural member reduced to zero-to-tension stress cycle; m and C – constants determined by the fatigue test results of the structural component data (Fig. 2.99).

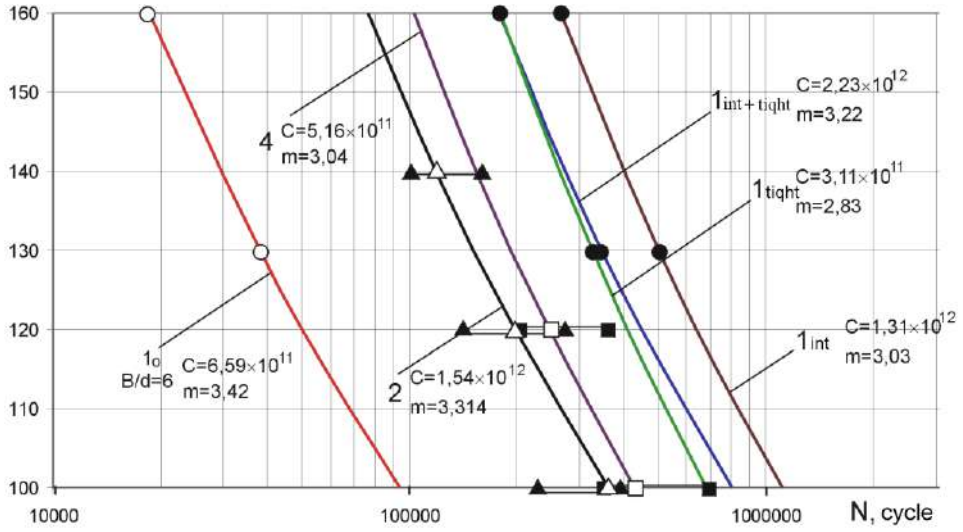

Fig. 2.99. Fatigue curves of standard test-pieces plotted by means of test results approximation

It has been found that failure of the standard test-pieces of joints performed with a radial interference and axial tightening under cyclic application of the tensile load from geometric stress concentration occurs just at the upper loading level. Mainly, the test-pieces failed in the zones of the fretting-corrosion development along the mating surfaces of the joint members proving the need for the fatigue lifetime estimation of the shear bolted joints with interference both in the zones of stress concentration and the zones of the probable fretting-corrosion development.

The finite element models of the analysed test-pieces (Fig. 2.100) consisting of the volumetric eight units elements SOLID45 and contact elements of the second order CONTA173, TARGE170 available in the ANSYS database have been created at stage 4 using the system of engineering analysis ANSYS [474] to determine the deflected mode characteristics in the joint element. To reduce calculation time, 1/4 part of the model has been examined in correspondence to attachment conditions. The external load has been simulated by applying pressure to the model end surfaces.

The members of the studied test-piece joints have been subjected to the analysis of the deflected mode characteristics under modelling the external tensile stress at a value of 100, 120 and 140 MPa. The cross-section of the connecting strap in the stress concentration zone of the extreme range of the analysed test-pieces (Fig. 2.101) has been studied as a zone of the probable fatigue failure from the geometric stress concentration.

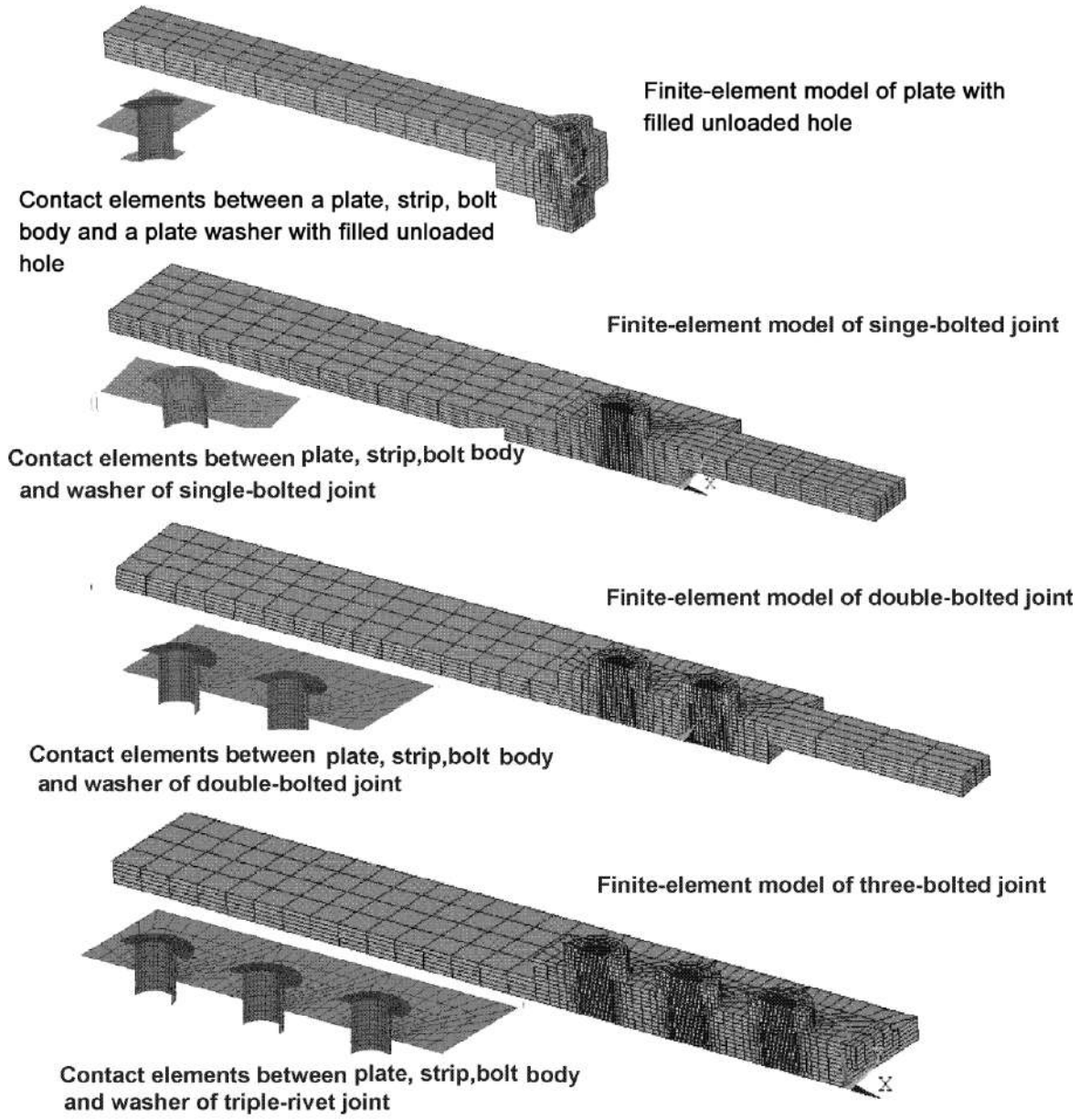

Fig. 2.100. Finite-element models of test-pieces shear bolted joints under examination

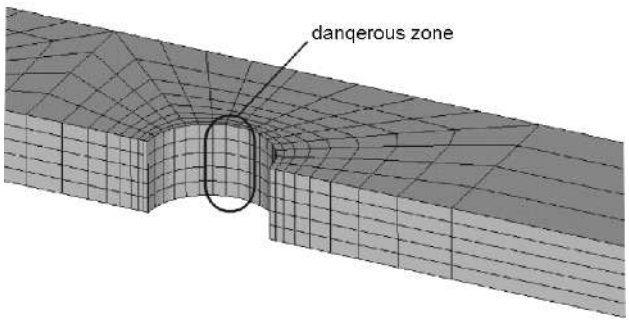

Fig. 2.101. Zone of probable fatigue failure from geometric stress concentration

The stresses and deformations have been determined after setting bolts with interference and tightening in holes followed by application of the external tensile loading as well as after total unloading to reveal the nature of the deflected mode change in dangerous zone (Fig. 2.102).

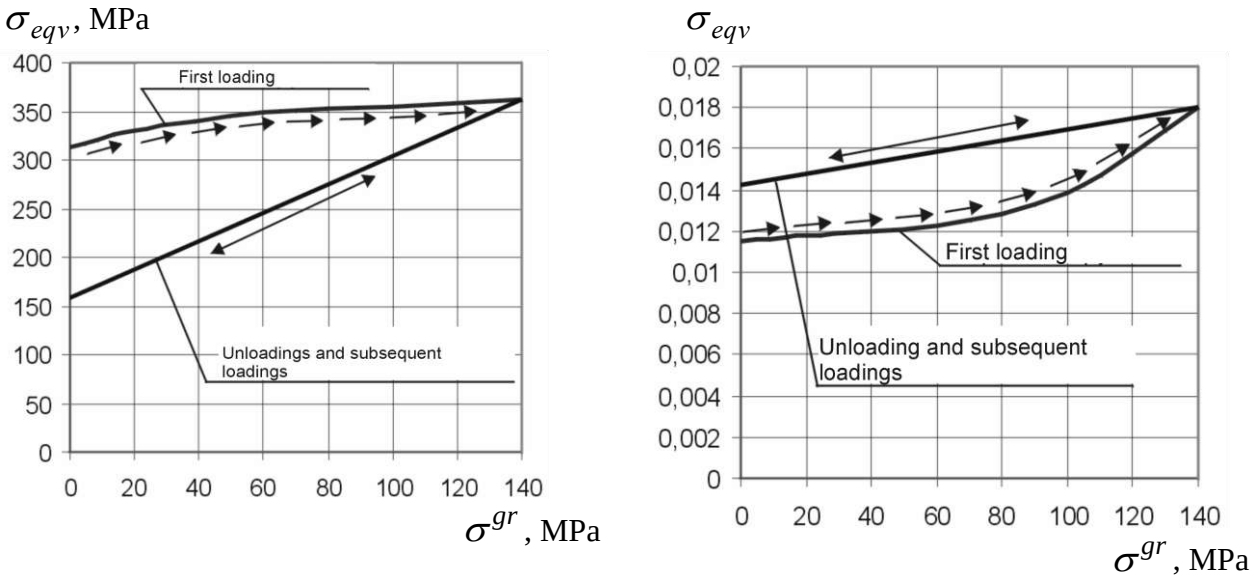

a b

Fig. 2.102. Change of residual equivalent: a – stresses; b – deformation in studied zone of single-shear bolted joint after application of external tensile stress of σ^{gr}=140 Mpa

As illustrated in Fig. 2.102, the elastoplastic interference effect is reduced with reference to the stresses (residual equivalent stresses are reduced by half under unloading) just under the second cyclic loading of the single joint test-piece by the tensile load corresponding to (σ^{gr}=140 MPa).

It this case, residual equivalent deformations are increased by 24%. Under subsequent cyclic loading, dependence between the equivalent stresses and deformations at σ^{gr}<140 MPa will have a linear nature (under progressive accumulation of the residual deformations), that is, will have the stabilized values. It enables to operate the product of the zero-to-tension stress cycle as a criterion proportional to the total specific deformation energy in the local zone.

Fig. 2.102 shows values dependence of the product maximum values ($\sigma_{eqv} \cdot \varepsilon_{eqv}$) in the elements of the studied joint test-pieces under the change on the external tensile loading.

As illustrated in Fig. 2.103, the maximum values of the product $(\sigma_{\sigma 0} \times \varepsilon_{\sigma 0})_{max}$ in the local zones do not always sufficiently reflect change of the fatigue characteristics of the observable single-joint test pieces under cyclic loading at their separate consideration.

The nature of the stress change along the cross section of the members produces a significant influence on the life time of the joints under cyclic loading. The data available in the scientific publications shows that the limit of the metals fatigue when tested under non-homogeneous stress condition is higher than under homogeneous stress state condition [187].

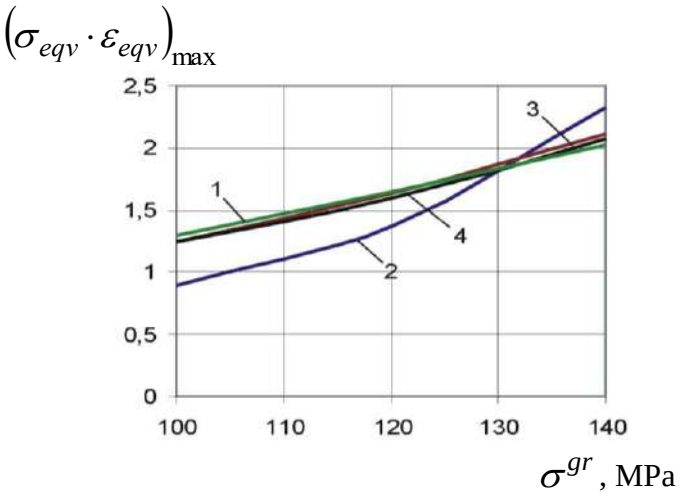

Fig. 2.103. Influence of external tensile loading on value of maximum product value $(\sigma_{eqv} \times \varepsilon_{eqv})_{max}$ in the members of the joint test pieces under study

The distribution of the equivalent stresses and deformations with reference to the strap thickness and width in cross section along the hole axis in the strap (path L1 and L2, Fig. 2.104) has been a subject of the study with their values reduced to the equivalent zero-to-tension stresses according to Oding's formula:

$$\sigma_0 = \sqrt{2\sigma_a \sigma_{\max}}\ ;\ \varepsilon_0 = \sqrt{2\varepsilon_a \varepsilon_{\max}}\ ,$$

where σ_a – amplitude of stresses acting in the structural components; σ_{max} – maximum stress values acting in the structural components.

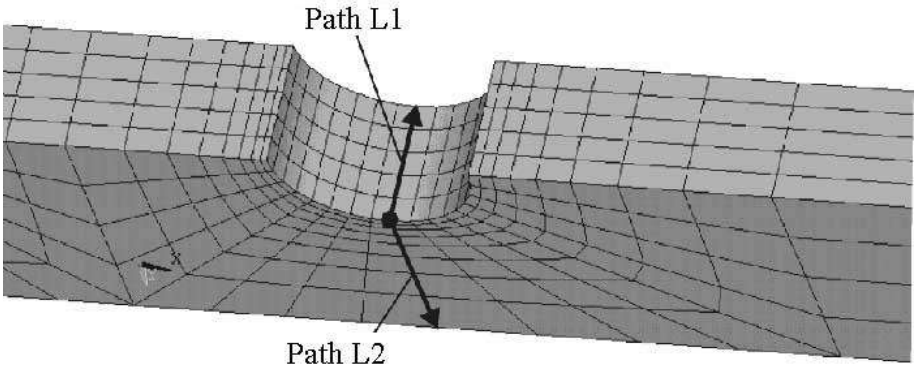

Fig. 2.104. Paths used for determination of $\sigma_{eqv0} \cdot \varepsilon_{eqv0}$ values

Fig. 2.105 Illustrates distribution nature of $\sigma_{eqv0} \cdot \varepsilon_{eqv0}$ with reference to the strap thickness and width in stress concentration zone.

As shown in Fig. 2.105, irregularity in distribution of value $\sigma_{eqv0} \cdot \varepsilon_{eqv0}$ along the strap thickness has been observed in the zones of holes for installation of bolts due to the bending of a bolt. Under external tensile stress of σ^{gr} <140 MPa, maximum value of $\sigma_{eqv0} \cdot \varepsilon_{eqv0}$ exceeds minimum one in 1.8 time in a single-row joint test piece and in 1.4 time in the test pieces of the two-

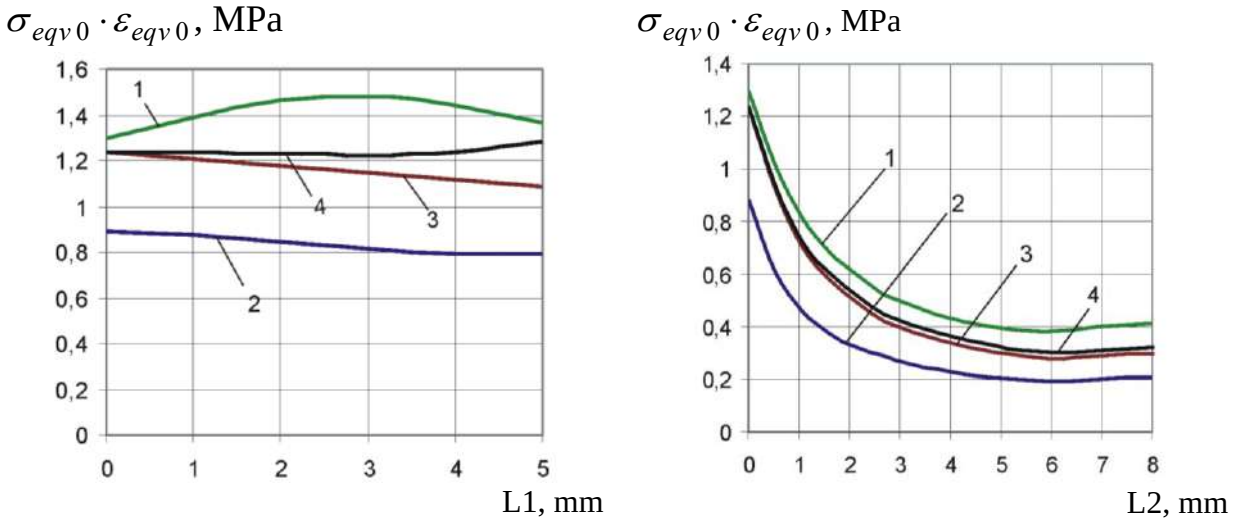

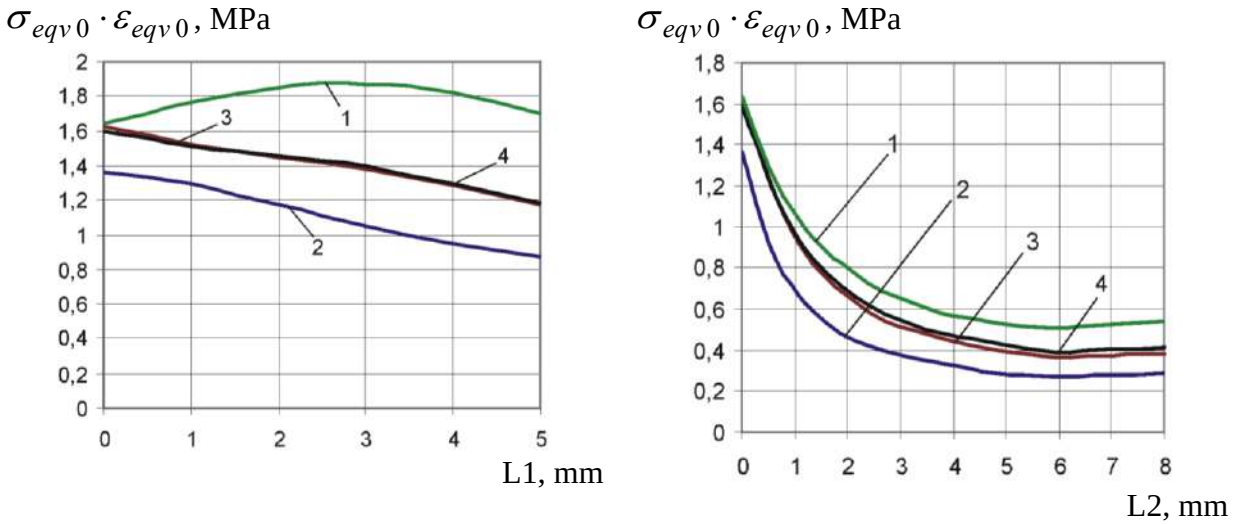

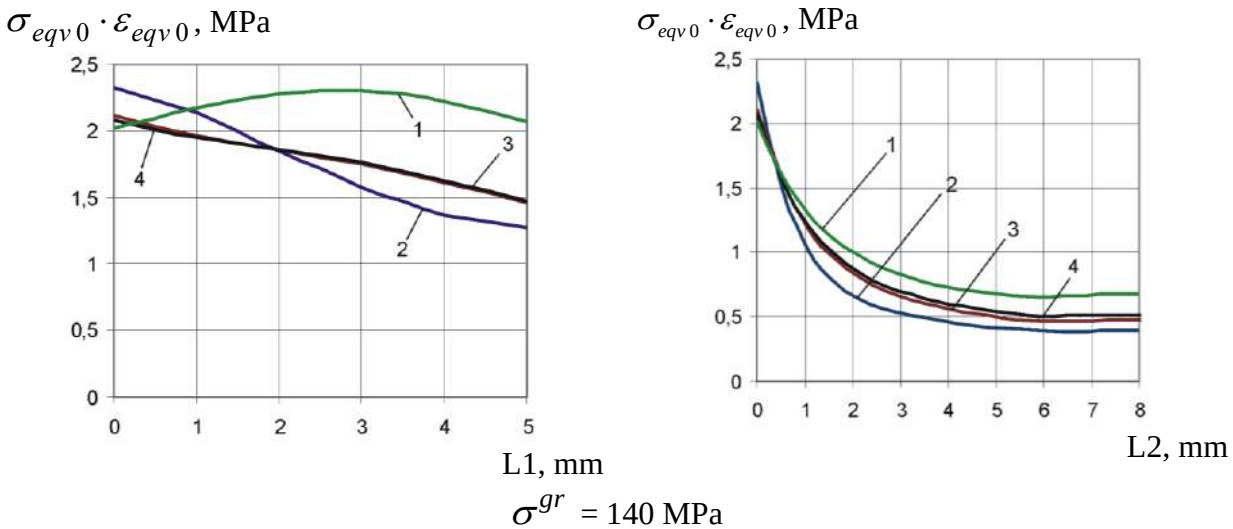

Fig. 2.105. Distribution of value $\sigma_{eqv0} \cdot \varepsilon_{eqv0}$ along width and thickness of joint strap

row and three-row joints. Irregularity of product value distribution $\sigma_{eqv0} \cdot \varepsilon_{eqv0}$ in the plate with the filled unloaded hole lies in decrease of values on the lower and upper surface due to the effect of the bolt tightening. Maximum value of $\sigma_{eqv0} \cdot \varepsilon_{eqv0}$ along the plate thickness exceeds the minimum one in 1.12 time and σ^{gr} =140 MPa.

The distribution irregularity coefficients of the value $\sigma_{eqv0} \cdot \varepsilon_{eqv0}$ with regard to the thickness [L1] and a concentration factor of value $\sigma_{eqv0} \cdot \varepsilon_{eqv0}$ regarding to width [L2] of the joint strap in the zone of the extreme row have been introduced for qualitative account of deflected mode irregularity degree in the zone of the probable fatigue failure:

$$\theta = \left[\frac{\left(\sigma_{eqv0} \cdot \varepsilon_{eqv0}\right)_{max}}{\left(\sigma_{eqv0} \cdot \varepsilon_{eqv0}\right)_{m}} \right]_{L1}; \; k = \left[\frac{\left(\sigma_{eqv0} \cdot \varepsilon_{eqv0}\right)_{max}}{\left(\sigma_{eqv0} \cdot \varepsilon_{eqv0}\right)_{m}} \right]_{L2},$$

Where $\left(\sigma_{eqv\,0} \cdot \varepsilon_{eqv\,0}\right)_{\max}$ – maximum value of $\sigma_{eqv\,0} \cdot \varepsilon_{eqv\,0}$;

$\left(\sigma_{eqv\,0} \cdot \varepsilon_{eqv\,0}\right)_{cp} = \dfrac{\int_{0}^{L1(L2)} \left(\sigma_{eqv\,0} \cdot \varepsilon_{eqv\,0}\right) dL_i}{L_i}$ – medium integral value of $\sigma_{eqv\,0} \cdot \varepsilon_{eqv\,0}$ in regard to the thickness (width) of the joint strap.

Fig. 2.105 shows dependence of θ and k coefficients as well as values of their product θ·k in the zone of probable fatigue failure from the level of the external tensile stress σ^{gr}, MPa.

For single row joint in change of σ^{gr} from 100 MPa to 140 MPa, the coefficient θ increases from 1.06 to 1.33 and *k* from 2.94 to 3.55. The value of product $\theta \cdot k$ in change of σ^{gr} from 100 MPa to 140 MPa increases from 3.13 to 4.74.

For two-row and three-row joints, the coefficients θ and k change with reference to σ^{gr} increase not so intensively as it is true for a single row joint. And the value of the product θ·k lies within the limits of 2.6…3.

Concentration factors and irregularity coefficients of value $\sigma_{eqv0} \cdot \varepsilon_{eqv0}$ (Ref. Fig. 2.106) obtained are required for the prediction of the fatigue life time depending on geometric stress concentration in the elements of the modified test-piece resulting from the fatigue tests of the base test-piece. A zone of joint strap interaction has been considered and a distribution nature of contact pressures along the contact surface (Fig. 2.107) has been determined to predict life time of the joint members in the zone of the fretting-corrosion (stage 5).

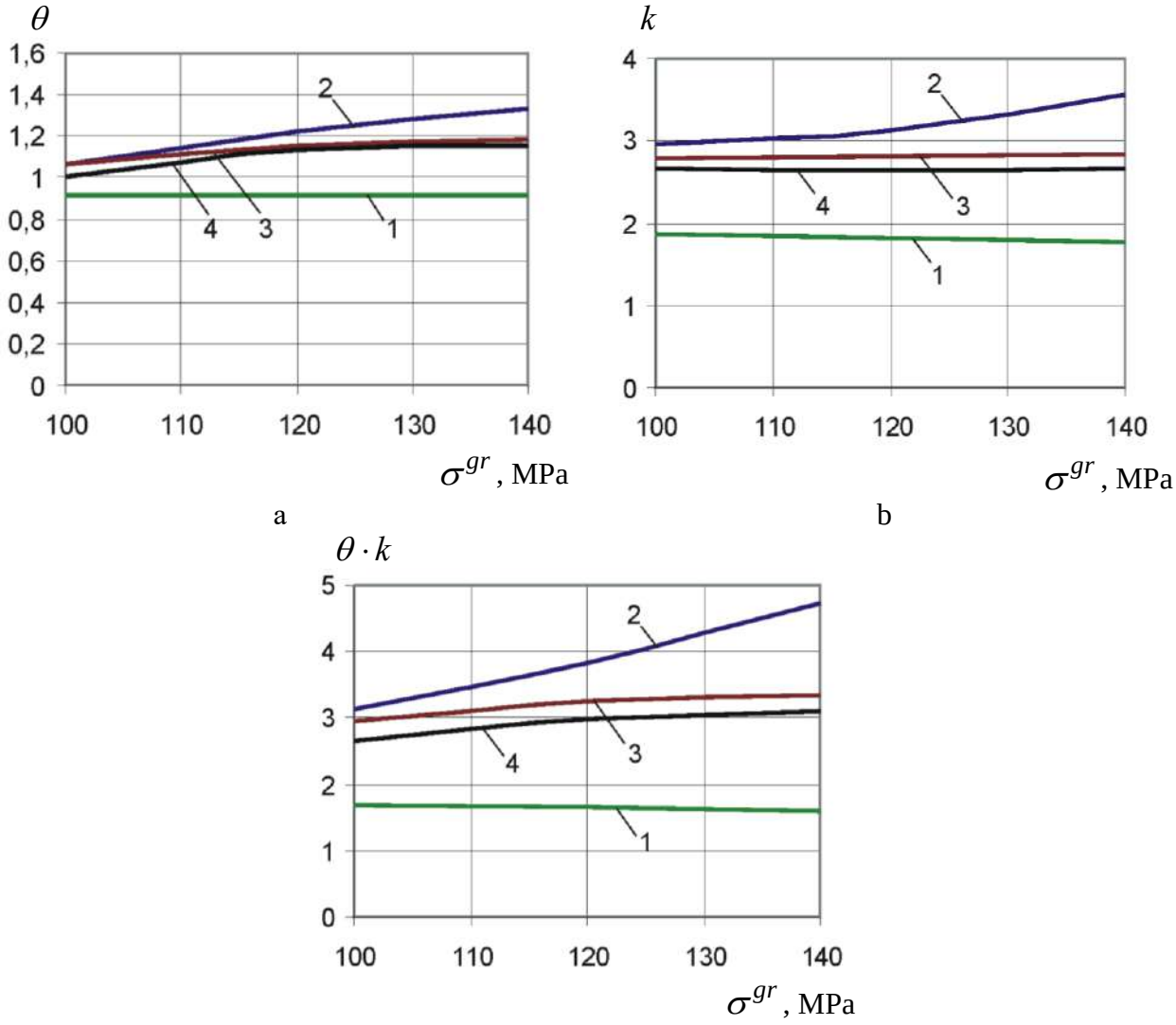

Fig. 2.106. Influence of external tensile stress σ^{gr} on irregularity coefficients $\sigma_{eqv0} \cdot \varepsilon_{eqv0}$ regarding to thickness (a); concentration factors $\sigma_{eqv0} \cdot \varepsilon_{eqv0}$ regarding to width (b); $\theta \cdot k$ product value (c)

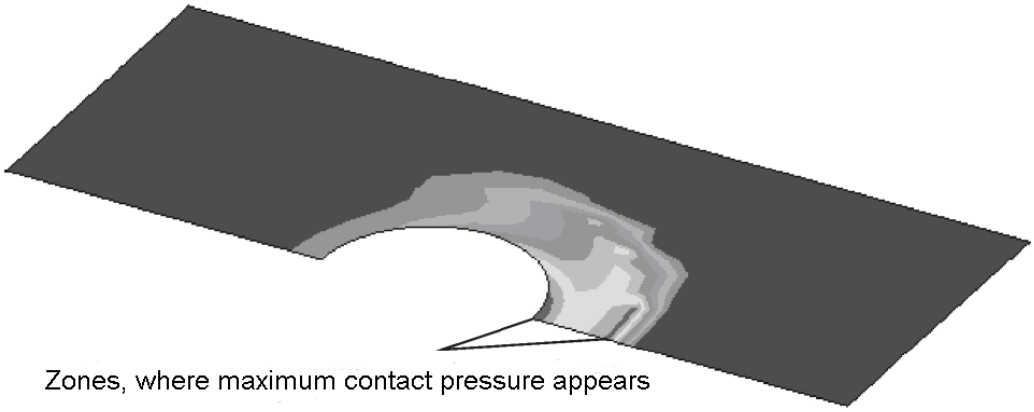

Fig. 2.107. Nature of contact pressure distribution between the strap and bolt washer under action of tensile load in joint

Degree of contact pressure distribution irregularity between the washer and the strap due to the bolt bending (Ref. Fig. 2.107) has similar nature for every examined test-piece of shear bolted joints. Fig. 2.108. demonstrates a value change dependence of maximum contact pressure values between the bolt head and the strap under σ^{gr} change in test-pieces of standard joints.

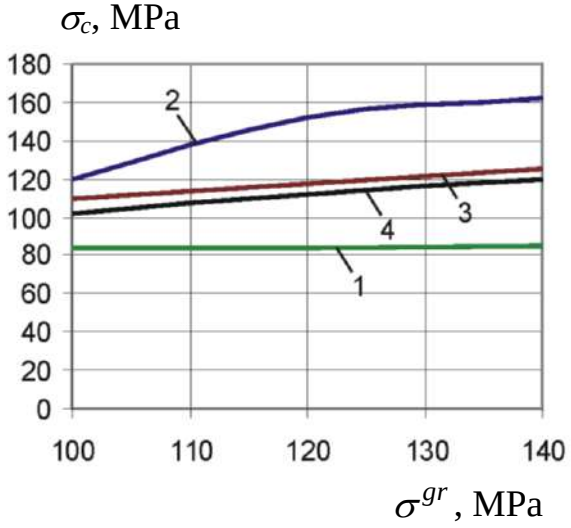

Fig. 2.108. Influence of loading level (σ^{gr}) on value of maximum contact pressures between the strap and bolt head

It is obvious from Fig. 2.108 that increase of row numbers from one to two will decrease a maximum value of acting contact pressures between a washer and a strap approximately by 23%. With the increase of row numbers from two to three, the maximum contact pressures insignificantly decrease.

In plate with a hole filled with bolt, the maximum contact pressures between a washer and a plate are not practically changed with reference to a value following increase of external load within the range under study being approximately 84 MPa.

Obtained characteristics of the local deflected mode allow to start predicting the fatigue resistance characteristics of the test-pieces under study in the concentration zone of the energy criteria value:

$$N_m = \frac{C_b}{\left(\sigma_0^{gr}\right)^m \left[\frac{(\theta \cdot k)_m}{(\theta \cdot k)_b}\right]^t},$$

where σ_0^{gr} – nominal stress in “gross” section of the structural component reduced to zero-to-tension stress cycle; m and C_b – constants for approximation of base test-pieces fatigue curve determined by the results of the fatigue tests; t=0.8 – irregularity influence degree factor of the deflected mode in changing from the base test-pieces (index “b”) to the modified one (index "m") a test-pieces of the plate

with a hole filled with a bolt with interference has been selected as a base one.

The fatigue curves of the test-pieces under study have been plotted in Fig. 2.109 on the basis of calculation according to the formula (2.11) – for the zones of the geometric stress concentration and according to formula (1.1) – for the zones of the fretting corrosion initiation.

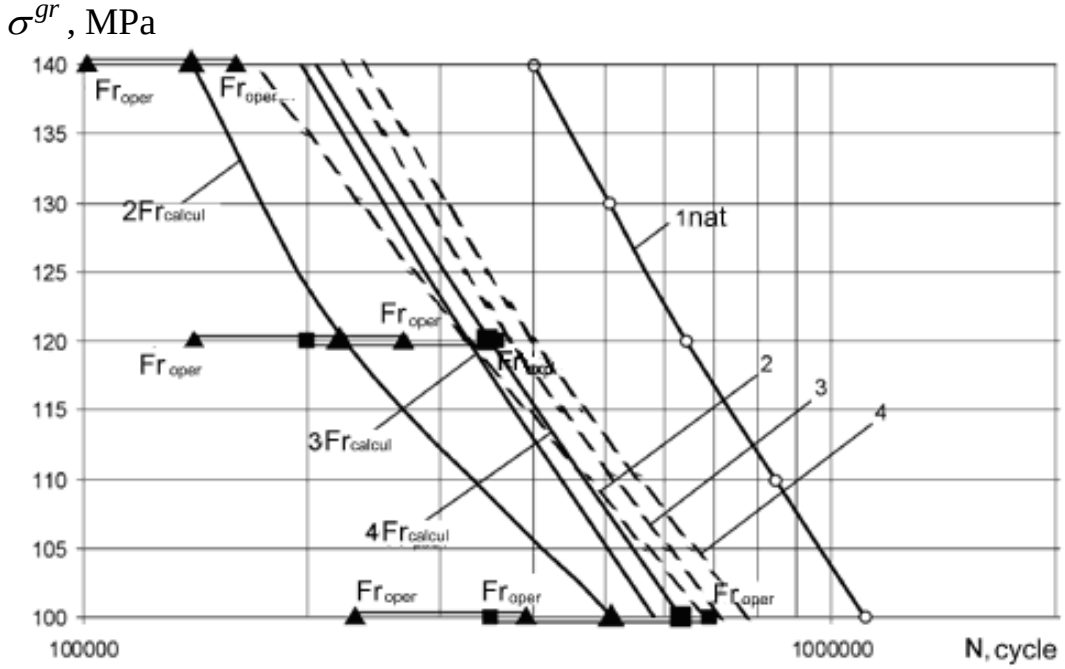

Fig. 2.109. Fatigue curves for test-pieces under study:
—○— – fatigue basis curve of the plate with a hole filled with bolt with interference; — — — – fatigue curves of the shear bolted joint test-pieces under study calculated in compliance with (2.11); fr_{calc}– curves limiting-corrosion determined according to (1.1.); ■ $^{fr_{exp}}$, ▲ $^{fr_{exp}}$ – plotted points of failure due to fretting-corrosion under test

It is obvious from this figure that the failure of the components from the fretting corrosion at the lower level of loading occurs well before failure from the geometric stress concentration in the zones of bolts installation, that is, the fretting corrosion limits the positive influence of the elastoplastic interference on the joint life time.

It should be noted that the proposed method has been tested in the life time analysis of the modified test-piece on the basis of the base one just in case of modification involving change of the row numbers. The authors analyse application of this method under wide variation of the joint parameters (value of elastoplastic interference under installation of bolts, thickness of the jointed components, diameters of the fasteners).

Following the results of the researches performed we may come to the following conclusions:

1. The method of predicting the life time characteristics of the bolted joints with the radial and axial interferences has been developed on the basis of the fatigue resistance characteristics of the local deflected mode and contact interaction of the standard test-piece members of the shear bolted joints.

2. Under study of the deflected mode characteristics in the members of the shear bolted joints in the zones of stress concentration, it has been found that the residual deformations and stresses after the first cycle of the external loading take values unequal to the initial ones due to interference and tightening resulting in change of stress amplitude and deformation values acting in the local zones.

3. Concentration factor of the full deformation specific work $\sigma_{eqv0} \cdot \varepsilon_{eqv0}$ including irregularity of the deflected mode in the local zone has been taken as a criteria influencing on the life time of the joints made with interference.

4. The nature of contact pressure changes between the joint members in the process of the loading has been found and the dependence of their maximal values on the values of the external tensile load and number of rows has been determined.

5. The suggested method has been tested in analysis of the life time of the shear bolted joints made with radial and axial interferences under change of the row numbers. The calculated fatigue curves obtained have been compared with the results of the experiments performed. Fair coordination of the analysis and the experiment results has been established.

2.7. CONCLUSIONS

1. New concept, principles and methods of integrated design and computer-aided modelling of aircraft assembly structures using CAD/CAM/CAE UNIGRAFICS and CAD/CAE ANSYS system have been developed.

2. Method in creation of master-geometry, space distribution models and parametric analytical master copies of aircraft assembly structures have been developed. The method has been tested and implemented in computer-aided modelling AN-140, AN-74TK-300, AN-148 aircraft assembly structures.

3. Method in analysing the design-engineering parameters on the local deflected mode characteristics of the aircraft assembly structure regular zone elements using ANSYS system has been developed with the account made for geometric, physical nonlinearities and contact interaction of structural members.

4. Fatigue resistance characteristics of the standard models of the aircraft assembly structure regular zone have been obtained by the experimental way. Criterion analysis and experimental dependencies have been developed for predicting the life time of the assembly structures regular zones.

5. Life time prediction method of aircraft assembly structure high-life time zones on the basis of the energy criteria has been developed with an allowance made for fretting-corrosion and joint manufacturing techniques.

Section 3
INTEGRATED DESIGN METHOD AND ACHIEVEMENT OF ASSIGNED SERVICE LIFE OF AIRCRAFT ASSEMBLY STRUCTURE SHEAR BOLTED JOINTS

Development of integrated design techniques of aeronautical engineering using CAD/CAM/CAE/PLM computer-aided integrated systems and information support of an aircraft life cycle creates the necessary prerequisites to provide their competitiveness on the world market of the aviation freight services due to achievement of the aircraft performance, ecological and economic characteristics corresponding to international standards specified by the Customer.

The aircraft integrated design involves the integrated design and modelling of the aircraft structure joints. The integrated design and modelling algorithm of structure shear bolted joints is illustrated in Fig. 3.1. It contains initial data for creation of joints, joint design of the assigned service life with minimum mass, joint manufacturing procedure, service life and air pressure test, computer-aided modelling and engineering analysis of the joint deflected mode, development of service life achievement methods under laboratory tests and operation conditions, development of the design, manufacturing operation and maintenance publications and repair manuals using computer systems.

The purpose of the integrated design and computer-aided modelling of the aircraft assembly structure joints using CAD/CAM/CAE/PLM is the determination of joints structural parameters, their manufacturing procedure providing specified level of static strength, scheduled service life, tightness, external surface quality under minimum mass of the joints and fatigue quality exceeding the level achieved before.

Implementation of this purpose is achieved by the development of new concept with reference to: materials used; advanced fasteners; structures of joints; fastener installation techniques; new design-engineering methods of local deflected mode characteristic analysis and fatigue resistance of joint members; methods of fatigue crack growth delay; application of integrated design system; modelling and engineering analysis; information support of their life cycle.

Combining the new design and engineering solutions in regard to the fasteners, engineering installation techniques and structural features of the joints with the computer aided methods of three-dimension modelling, we get the new concept of integrated design of aircraft assembly structure joints comprising development of the analytical standard of aircraft structural joint based on coordinated application of:

– parametric analytical three-dimensional standards of joint members and aircraft structures;

– analysis method of influence of joint members design and engineering features on characteristics of its solid local deflected mode;

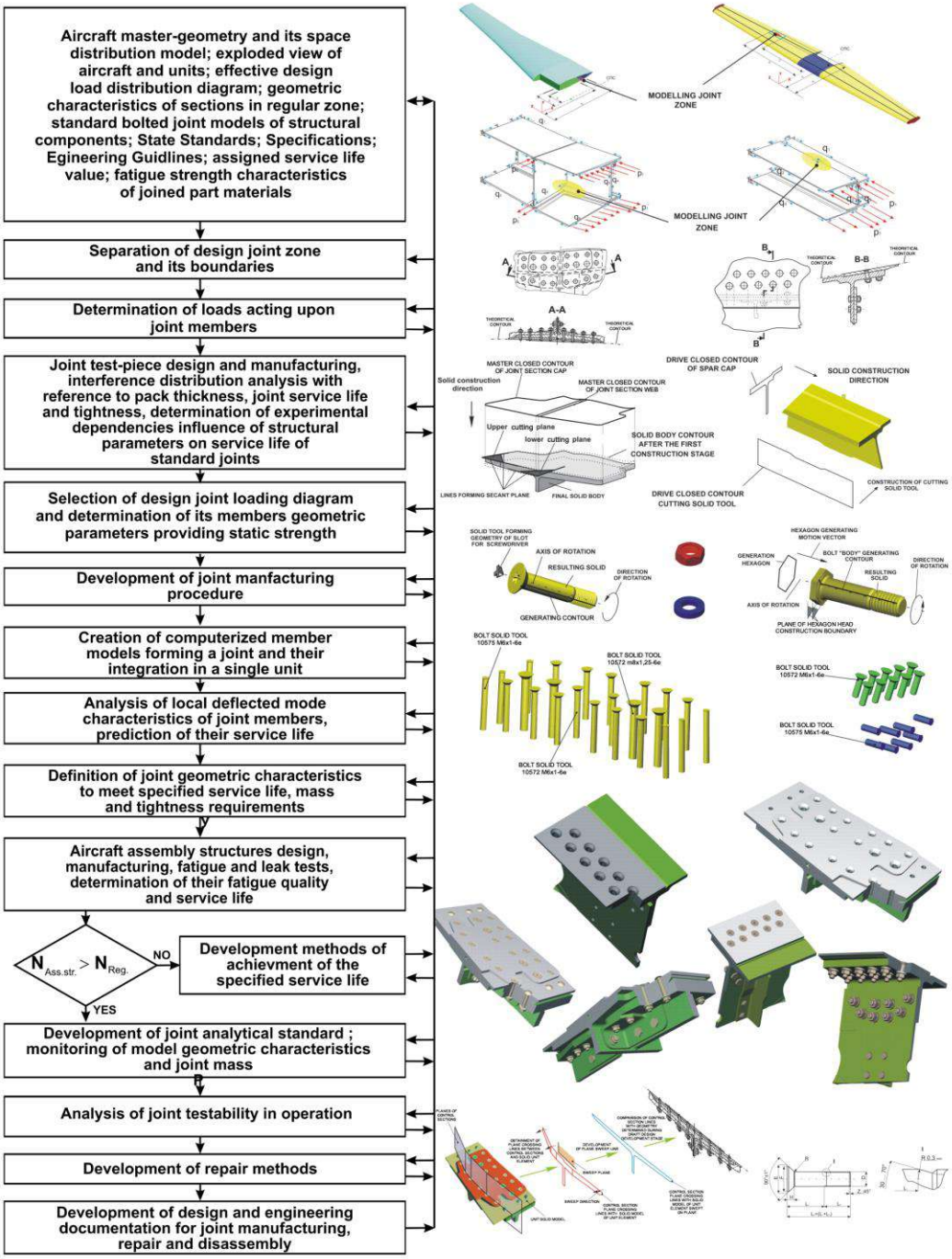

Fig. 3.1. Integrated design and modelling method of aircraft assembly structure shear bolted joints with assigned durability members

– analysis method of influence of joint members design and engineering features on characteristics of its fatigue strength;

– selection method of joint design and engineering parameters providing specified characteristics of static strength, fatigue durability, tightness and

external surface quality under minimum joint mass;

– method of fatigue crack growth delay to extend service life and provide flight safety.

Provision of specified characteristics of aircraft structure joints has required the development of integrated analysis method of the design and engineering factor influence on characteristics of the local deflected mode of the joint members (Fig. 3.2).

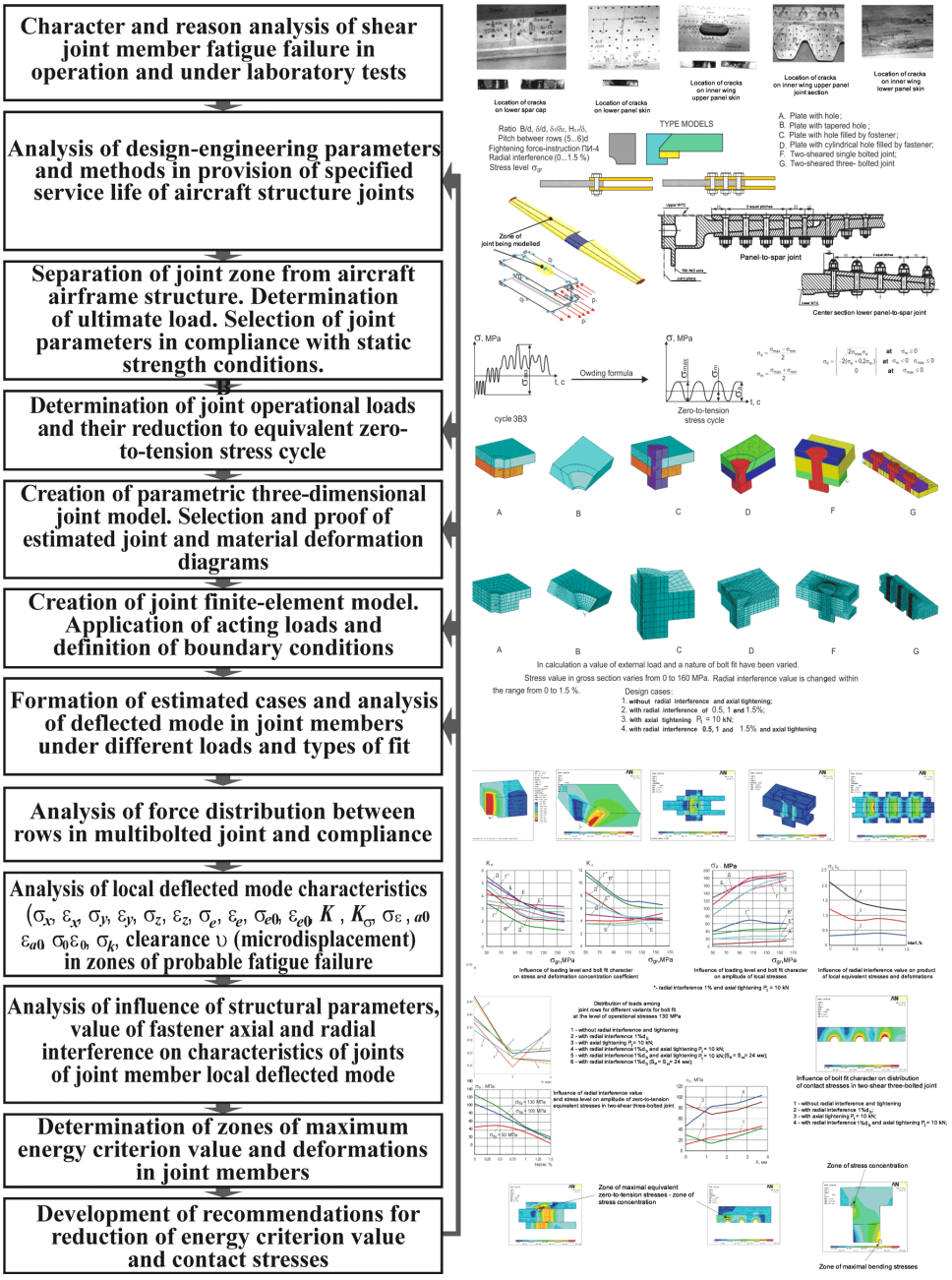

Fig. 3.2. Integrated analysis method of design and engineering parameters influence on characteristics of local deflected mode in shear bolted joints members

3.1. INTEGRATED ANALYSIS OF BOLT INSTALLATION PROCEDURE AND LOADING LEVEL INFLUENCE ON CHARACTERISTICS OF LOCAL DEFLECTED MODE IN MEMBERS OF DOUBLE-SHEAR SINGLE-ROW COUNTERSUNK BOLTED JOINT USING ANSYS ENGINEERING ANALYSIS SYSTEM

Determination of fatigue strength characteristics of aircraft structure shear bolted joints by the calculated-experimental method is based on determination of the local deflected mode condition characteristics in the joint members within the zones of their probable fatigue failure due to concentration caused by normal and contact stresses as well as on the basis of the fatigue life curves of the plate with hole standard bolted joint filled with bolt according to the specified procedure and characteristics of local deflected mode in the hole zone [169].

Fig. 3.3 Illustrates the fragment of AN-12 aircraft wing panel with structure failure caused by the concentration of stresses in the installation zones of the countersunk bolts. It is obvious from this figure that the crack formation is initiated by the countersunk holes for installation of the countersunk bolts and design-engineering parameters of the joint.

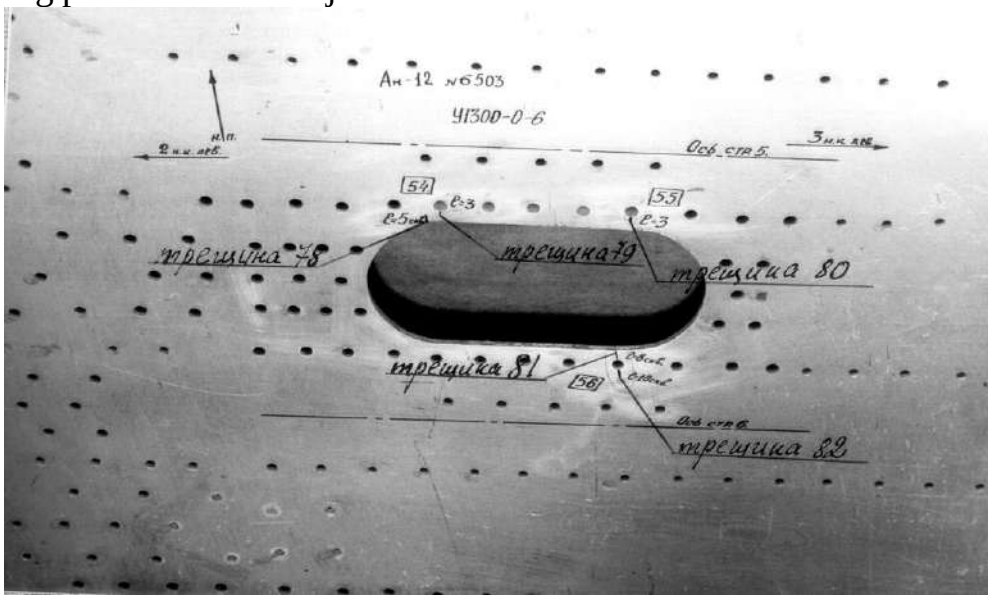

a

b

c

Fig. 3.3. Damage to AN-12 aircraft wing panel structure in zone of countersunk bolted joint installation: a) – wing panel appearance; b, c) – damaged joint area appearance

To provide specified operability characteristics of the shear bolted joints the analysis algorithm of the design-engineering parameters influence on the volumetric local deflected mode members of the shear bolted joints using CAD/CAM/CAE ANSYS system (Fig. 3.4) has been developed. Its testing has

been conducted using the models of the shear bolted joints.

The analysed model of the single-row double-shear bolted countersunk joint involves a centre plate with dimensions 150×50×10 mm and two straps with dimensions of 166×24×5 mm connected with bolt 8 mm in diameter with the countersunk head. Geometric dimensions of joint model are illustrated in Fig. 3.5.

The material of the plate and the straps is Д16АТ aluminium alloy with a modulus of elasticity E=70000 MPa and a Poisson ratio equal to 0.3. The multilinear model with a kinematic law of strength development has been selected to describe the plate and strap material behavoiur.

Bolt material is 30ХГСА steel with modulus of elasticity E=210000 MPa and Poisson's ratio equals to 0.3. A linear – elastic behaviour of the bolt material described by the Hooke's law has been used for analysis.

Analysis of the local deflected mode in the joint members under external tensile stress has been performed using ANSYS engineering analysis system for the following variants of the upper and lower straps joined with center plate using a bolt:

1) without axial and radial interferences;

2) with radial interference of 1% d_b;

3) with axial tightening of $Ð_t$ = 10 kN;

4) with radial interference of 1% d_b axial tightening of $Ð_t$ = 10 kN.

The tensile load has been applied to the plate. In the analysis they have been assumed to be equal to: A) $Ð_{pl}$ = 0 N; B) $Ð_{pl}$ = 12000 N; C) $Ð_{pl}$ = 24000 N; D) $Ð_{pl}$ = 31200 N; E) $Ð_{pl}$ = 38400 N. These loads in the plate gross section have been in correspondence to the following nominal stresses: A) σ_{pl}^{gr} =0 MPa; B) σ_{pl}^{gr} = 24 MPa; C) σ_{pl}^{gr} = 48 MPa; D) σ_{pl}^{gr} = 62.4 MPa; E) σ_{pl}^{gr} = 76.8 MPa. The nominal $\sigma_{str}^{gr.calcul}$ design stresses in strap gross section were equal to: A) $\sigma_{str}^{gr.calcul}$ = 0 H; B) $\sigma_{str}^{gr.calcul}$ = 50 MPa; C) $\sigma_{str}^{gr.calcul}$ = 100 MPa; D) $\sigma_{str}^{gr.calcul}$ = 130 MPa; E) $\sigma_{str}^{gr.calcul}$ = 160 MPa.

1/4 model with corresponding fastening conditions has been subject to analysis with the allowance made for the test piece symmetry and a nature of the external load application. Zero displacements along Z-component have been assigned to limit model displacement along Z-axis for every unit locating on the plate end surface at a point of the external load application. The model planes of symmetry have been used to limit X and Y components of displacement vector (Fig. 3.6).

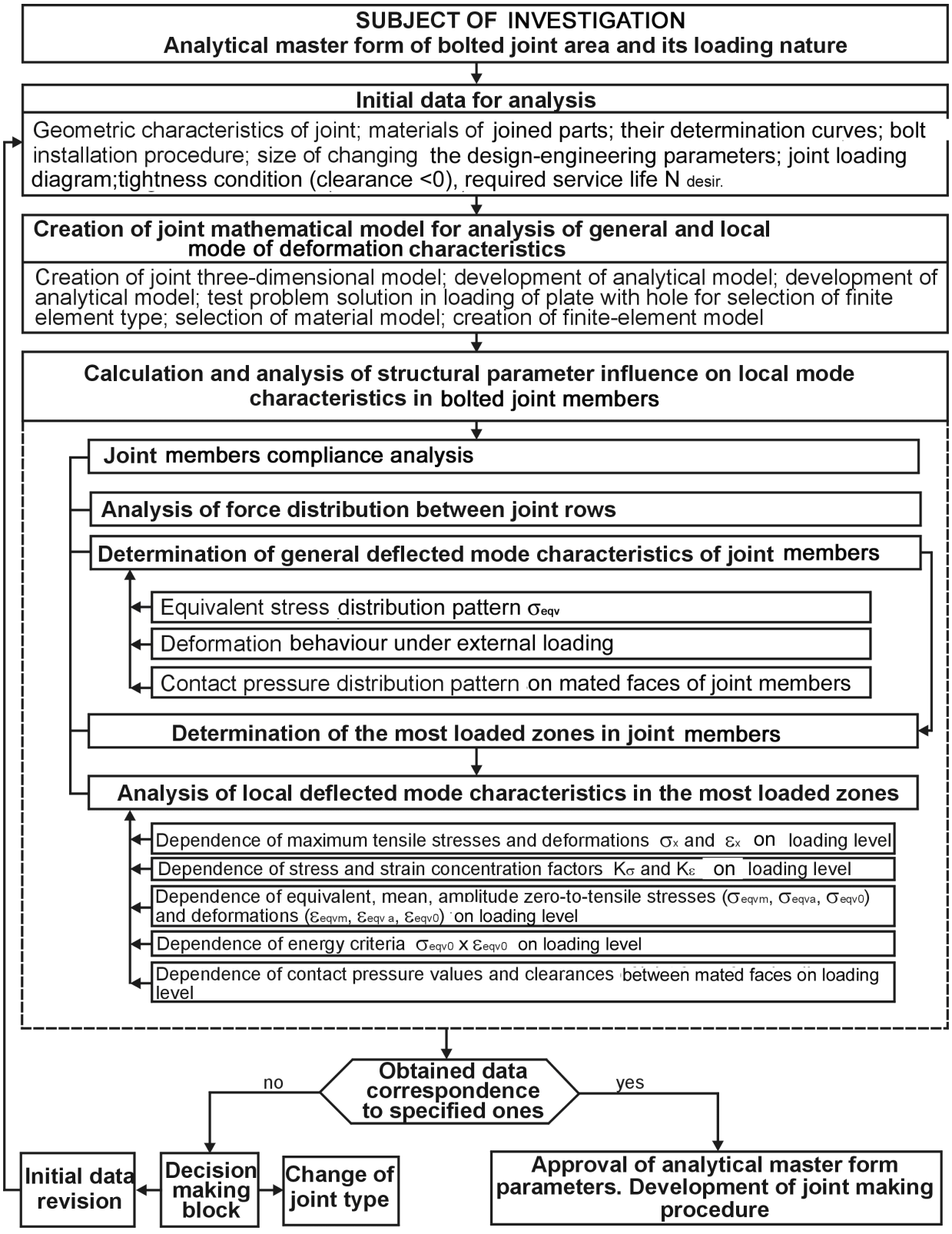

Fig. 3.4. Analysis algorithm of design-engineering parameters influence on volumetric local deflected mode of shear bolted joints members

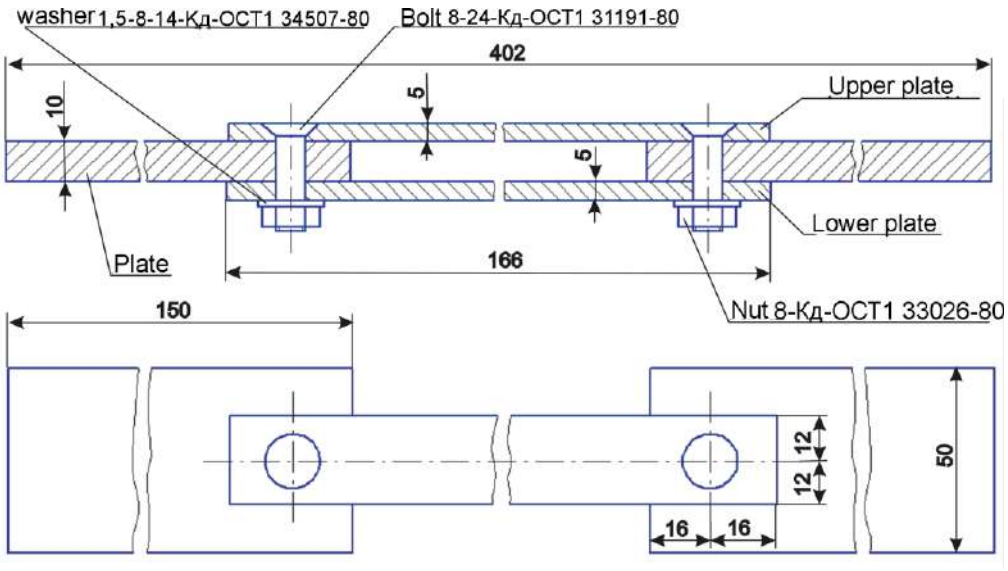

Fig. 3.5. Geometric model of double-shear single-row countersunk bolted joint

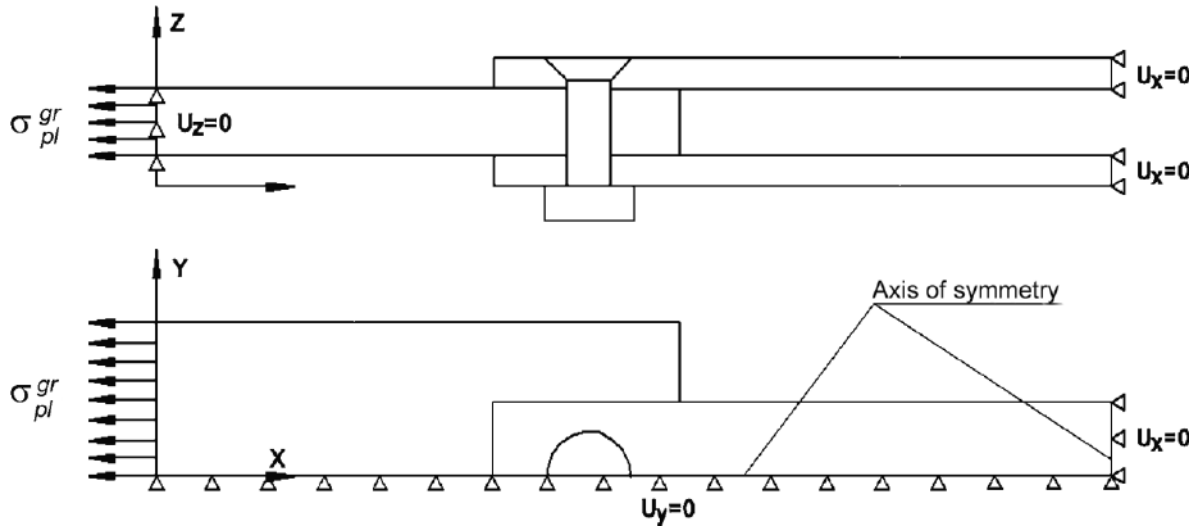

Fig. 3.6. Analytical model of double-shear single-row countersunk bolted joint

The finite-element model (Fig.3.7, 3.8) consists of volumetric eight unit members SOLID 45 as well as contact members CONTA 173 and tightening members PRETS 179 presented in ANSYS system [474].

The radial interference of modelling has been realized in the contact algorithm using the effect of "initial penetration" of the bolt body to the hole wall. The "surface-to-surface" model has been selected and coulomb elastic friction model with a friction coefficient of 0.15 has been used for modelling of the contact interaction. The bolt axial tightening and pre-stressed condition in the joint members caused as a result of axial tightening application have been modelled using a special tightening element PRETS 179.

Preliminary meshed bolt has been "dissected" in two parts and along the units of the finite elements lying in the dissected section and special tightening

elements PRETS 179 have been generated by means of insertion. Due to the solution of the finite-element problem the local deflected mode has been subject to analysis in the plate, strap and bolt from an action of radial interference, axial tightening and their joint action under conditions of joint uniaxial tension. Fig. 3.9, 3.10 show the nature of the test piece deformation and distribution field of the equivalent stresses in the joint members under the action of the external load $\sigma_{pl}^{gr} = 48$ MPa ($\sigma_{incl}^{gr.calcul} = 100$ MPa).

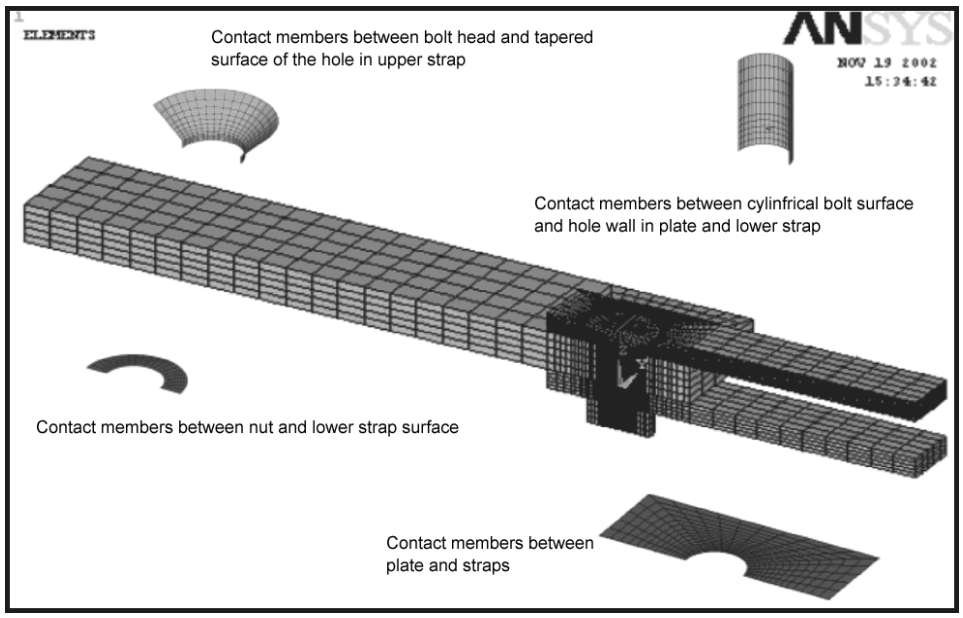

Fig. 3.7. Finite-element model of double-shear single-row countersunk bolted joint

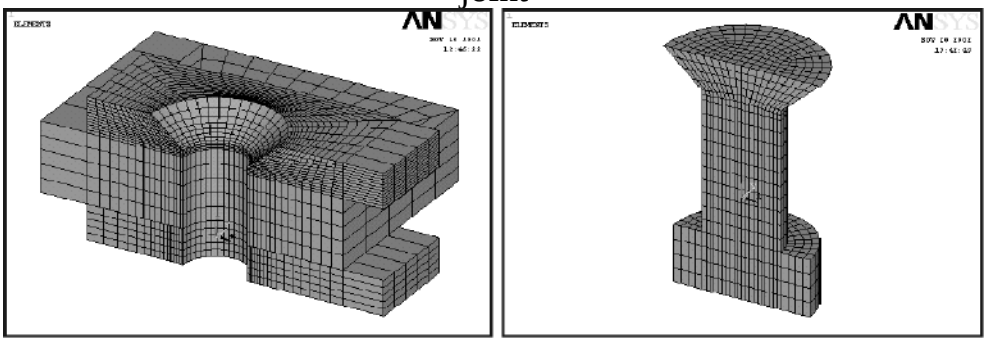

a b

Fig. 3.8. Fragments of finite-element model: a – plate and straps; b – bolt with a nut

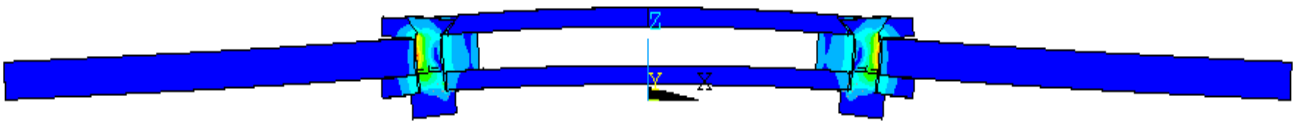

Fig. 3.9. Nature of test-piece deformation under action of external load $\sigma_{pl}^{gr} = 48$ MPa ($\sigma_{str}^{gr.calcul} = 100$ MPa) (displacement range – 20:1)

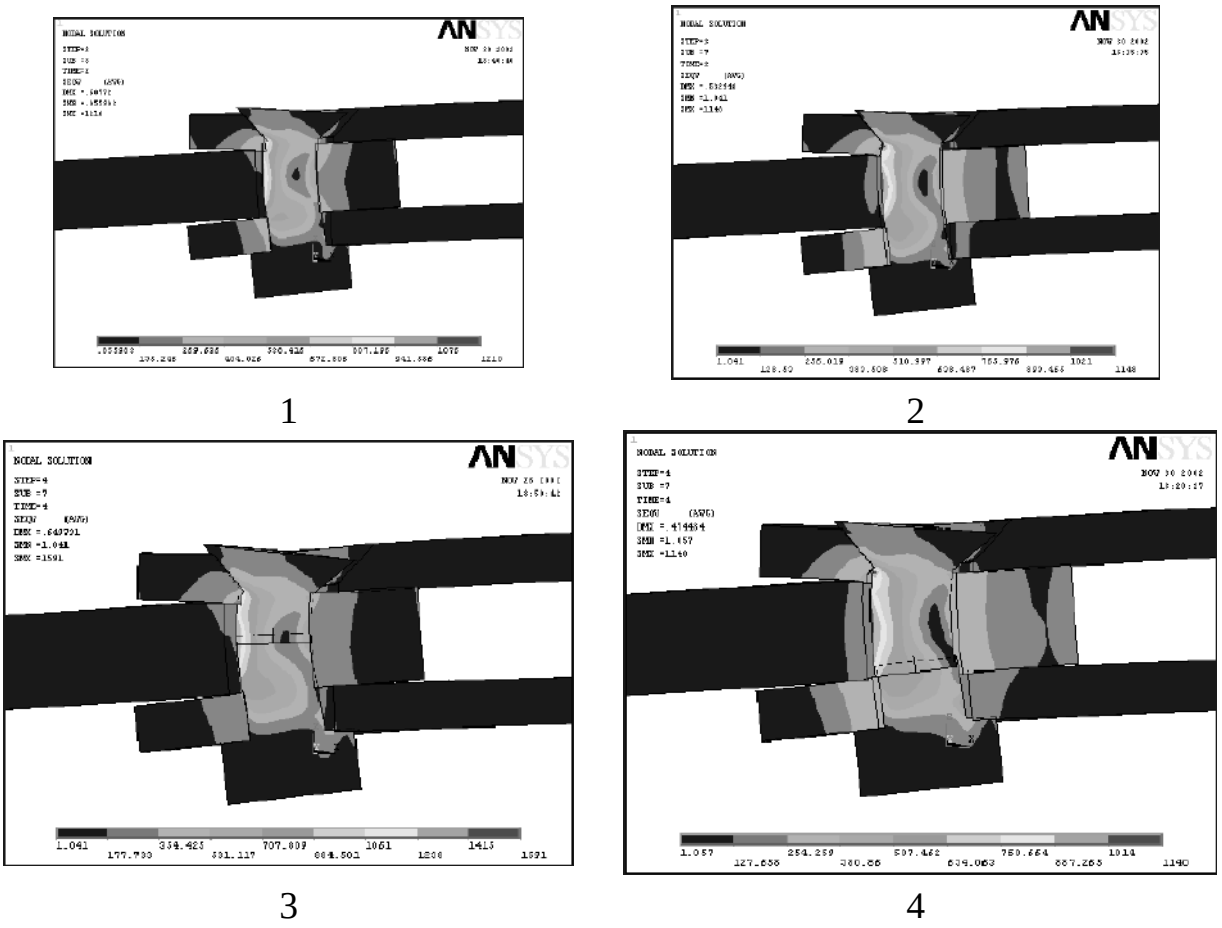

Fig. 3.10. Nature of equivalent stress distribution σ_{eqv} in joint members under loading level of $\sigma_{pl}^{gr} = 48$ MPa ($\sigma_{str}^{gr.calcul} = 100$ MPa) and nature of joint members deformation under different variants of bolt installation (displacement range – 20:1)

It is obvious that the bolt works in shear and bending in case of the external tensile load application to the joint. Fig. 3.11 demonstrates the distribution field σ_z in the bolt under tensile load application to the action zones of maximum tensile stresses in the bolt body.

From Fig. 3.11 we notice that the cylindrical portion and the field of bolt shank transition to the countersunk head are the most loaded zones on the bolt body.

Dependencies of tensile load distribution σ_z in the most loaded zones (path N (Fig. 3.12) on the nature of bolt installation and level of external loading σ_{pl}^{gr} (Fig. 3.13) have been derived to obtain more accurate information.

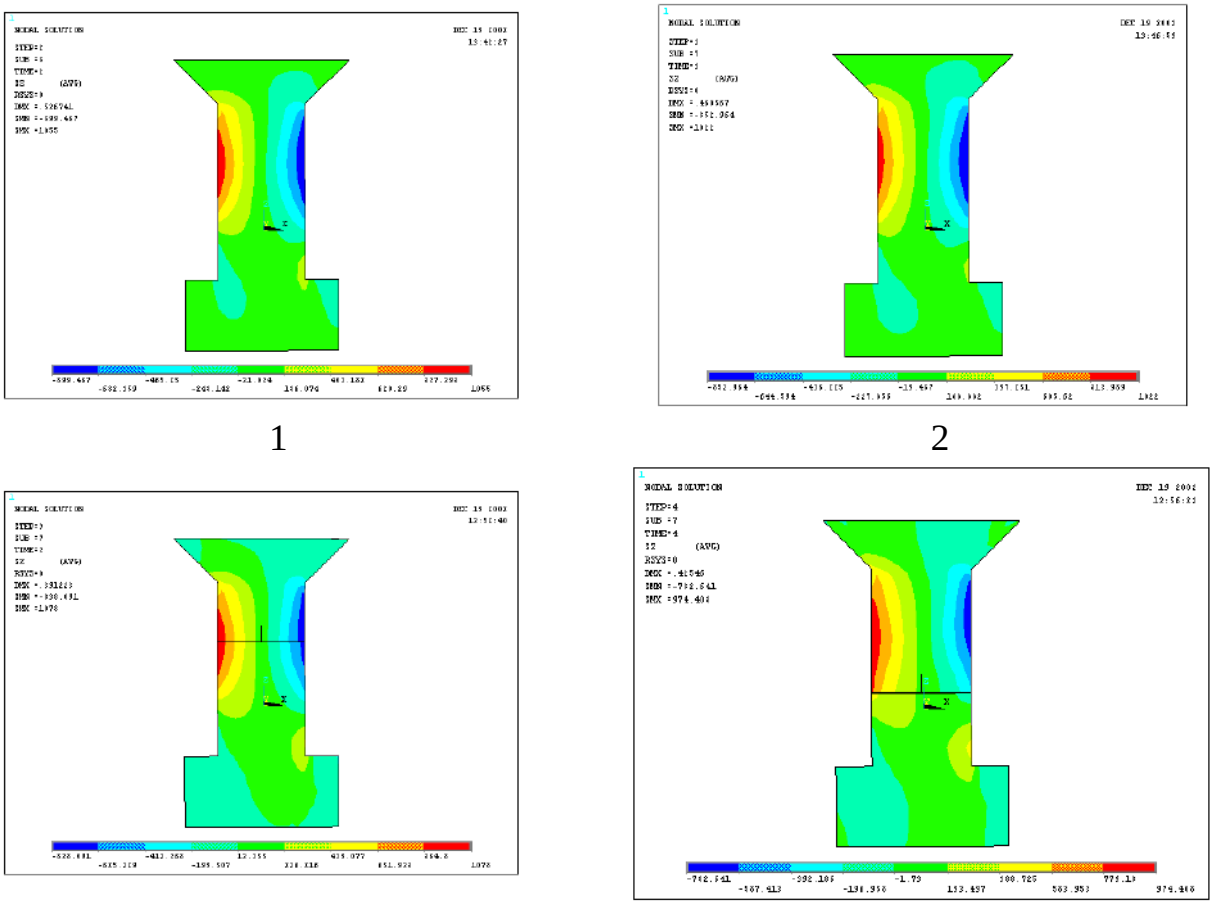

1 2

3 4

Fig. 3.11. Normal stress distribution field σ_z in bolt under different installation variants and external loading level $\sigma_{pl}^{gr} = 48$ MPa ($\sigma_{str}^{gr.calcul} = 100$ MPa)

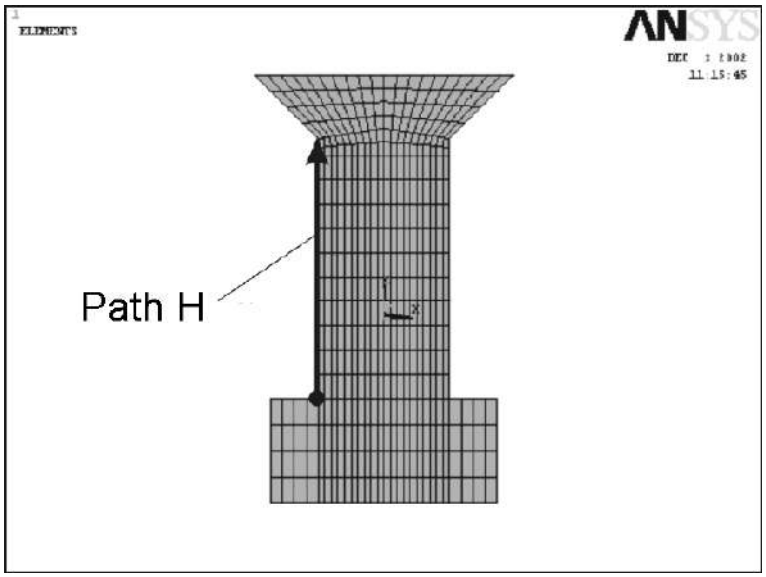

Fig. 3.12. Display of path H for deriving distribution of normal stresses σ_z, MPa

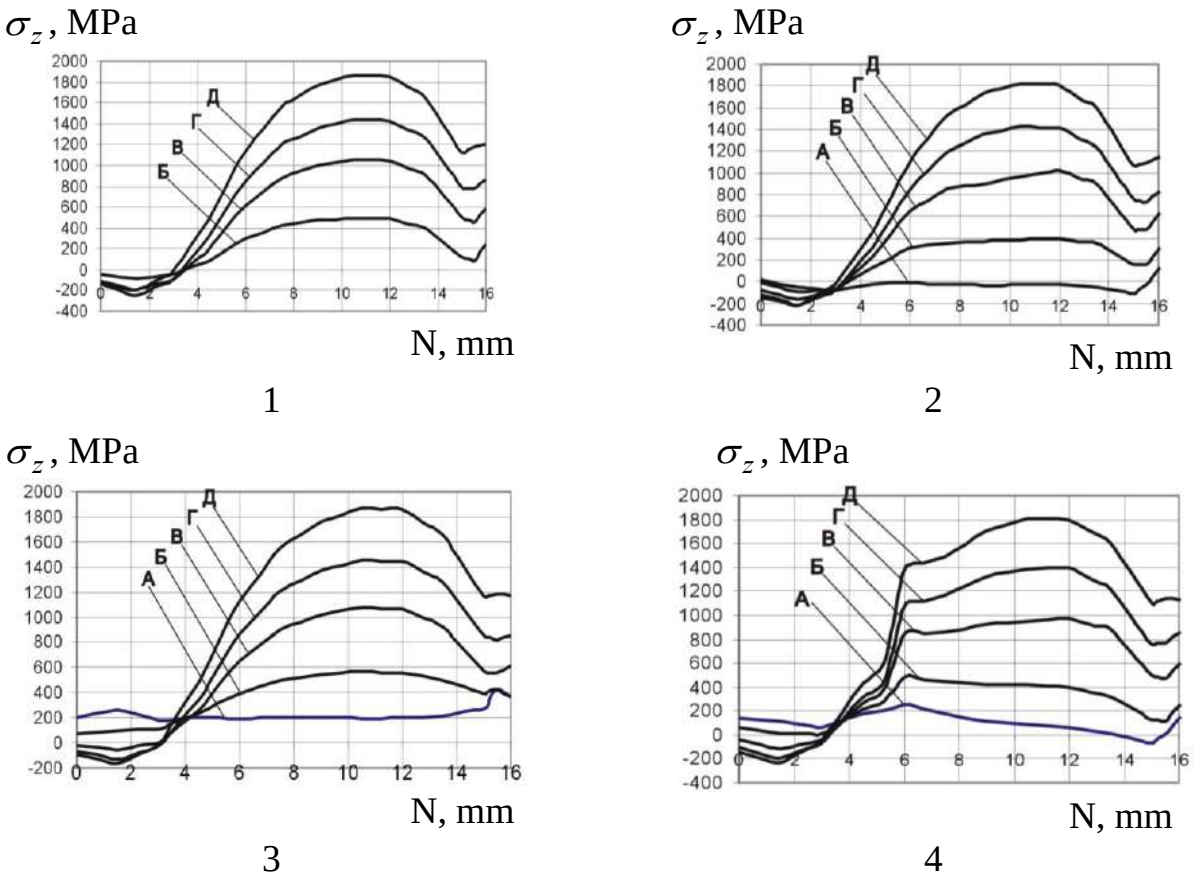

Fig. 3.13. Influence of external loading level (σ_{pl}^{gr}) and nature of bolt installation on distribution of normal stresses σ_z along the length of bolt cylindrical portion (path H)

Analysis of normal stress distribution σ_z in the bolt body shows that the bolt zone is the most extended zone located in the joint longitudinal section. The value of maximum values σ_z is determined by the level of the joint loading to be significantly reduced under bolt radial interference.

Difference in interaction nature between the upper and lower straps with the countersunk bolt results in reveal of their different compliance, and consequently, to different deformation value under application of tensile loads to the plate (see Fig. 3.9, 3.10). It results in redistribution of stresses, that is, loads transmitted through the upper and lower straps. Fig. 3.14 shows the influence of the external tensile load level applied to the plate on the redistribution of stresses in regular portion of the upper and lower straps.

The difference in value transmitted by the load straps can reach 20 %. It has been found that the nature of the bolt fit produces insignificant influence on the redistribution of loads between the joint straps.

During analysis of the local deflected mode maximum equivalent $\sigma_{eqv\,max}$ and maximum tensile stresses $\sigma_{x\,max}$ have been determined in the plate and the

straps. Nature of the equivalent stress distribution in the upper strap is illustrated in Fig. 3.15.

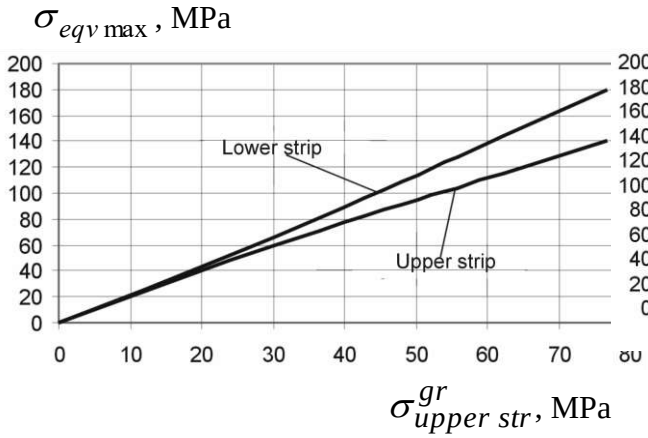

Bolt installed without axial and radial interferences

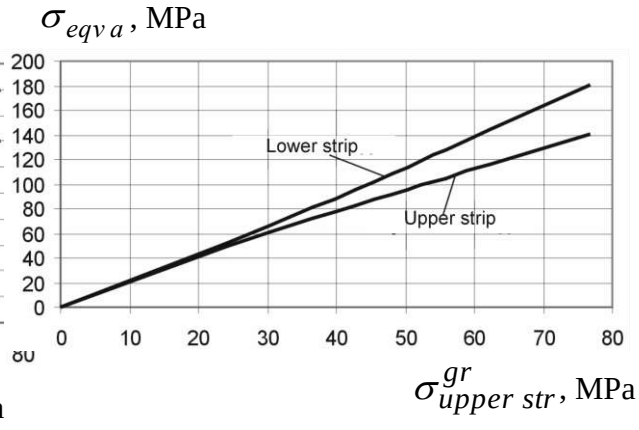

Bolt installed with radial interference of $1\%d_b$

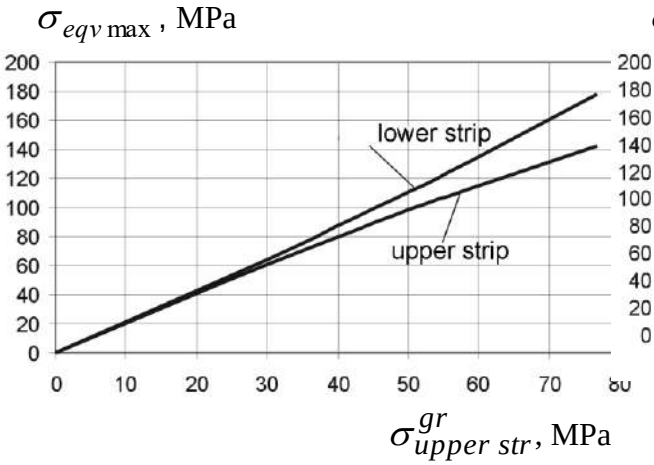

Bolt installed with axial tightening of P_t = 10 kN

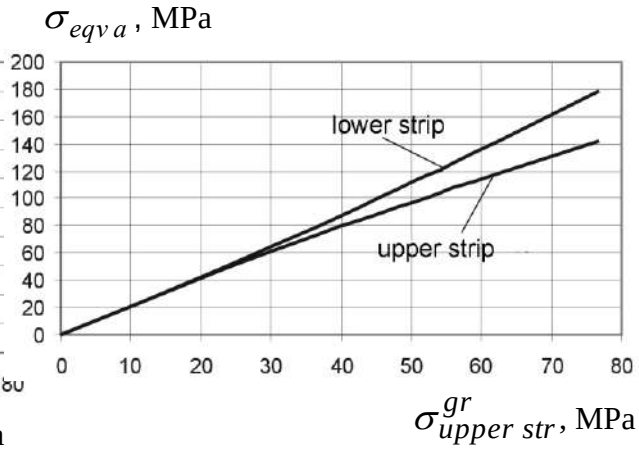

Bolt installed with radial interference $1\%d_b$ and axial tightening of P_t= 10 kN

Fig. 3.14. Influence of external tensile load level applied to plate on redistribution of stresses in regular portion of upper and lower straps

Under known maximum equivalent stresses in the upper strap in every case of the model loading (σ^{gr}_{pl} 24,48,64 and 72 MPa) and values of initial equivalent stresses (from tightening of P_t=10 kN, from radial interference of 1%d_b and from combined action of radial and axial tightening) we can calculate the equivalent amplitude $\sigma_{eqv\,a}$, mean $\sigma_{eqv\,m}$ stresses at points with maximum values of equivalent stresses $\sigma_{eqv\,max}$. Zero-to-tension stresses under asymmetry load cycle have been determined according to Oding's formula.

$$\sigma_{eqv\,0} = \sqrt{2\sigma_{eqv\,max}\,\sigma_{eqv\,q}}\ .$$

The dependencies $\sigma_{eqv\,max}\,\sigma_{eqv\,q}$, $\sigma_{eqv\,m}$ and $\sigma_{eqv\,0}$ on the level of the

external load application (σ_{pl}^{gr}) are illustrated in Fig. 3.16. It is obvious that application of axial tightening P_t=10kN in combination with the radial interference 1% d_b significantly reduces amplitude equivalent stresses $\sigma_{eqv\ a}$. Under $\sigma_{upper\ str}^{gr}$85 MPa at points with maximum amplitude stresses, $\sigma_{eqv\ a}$ are practically equal to zero.

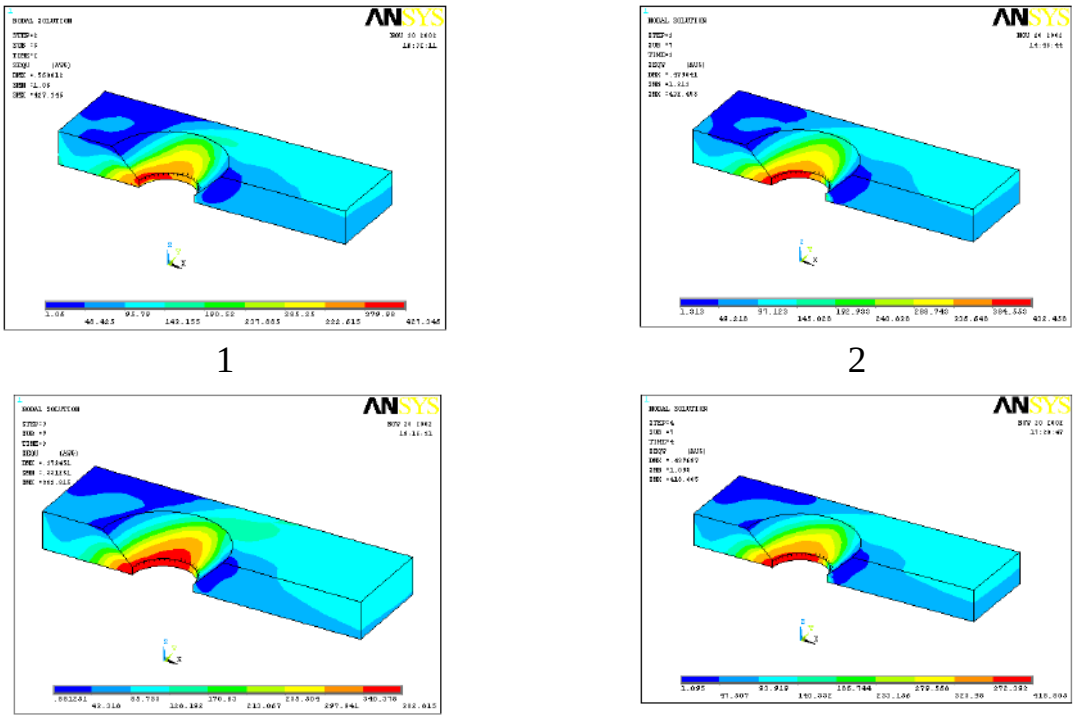

Fig. 3.15. Nature of equivalent stress distribution in upper strap under different variants of bolt installation and level of external loading σ_{pl}^{gr} = 48 MPa

($\sigma_{str}^{gr.calcul}$ = 100 MPa)

Comparing the results of radial and axial interference application, we may notice the following: in case of bolt installation with axial tightening P_t=10kN and radial interference of 1% d_b under $\sigma_{upper\ str}^{gr}$130 MPa the effect of combined application of radial and axial interference for reduction of amplitude stresses is reduced to zero.

The analysis of the local deflected mode calculation results in upper strap has shown the following:

1. In bolt installation without axial and radial interferences the zone of maximum tensile stresses is located in the transition area of the conical hole to the cylindrical one being outside the plane of cross section from the countersinking axis in the line of the upper strap regular portion. Initiation zone of maximum equivalent stresses $\sigma_{eqv\ max}$ in upper strap is located in the transition area of the

conical hole to the cylindrical one and the zone $\sigma_{eqv\,max}$ is shifted along the hole arc at 10… 15 degrees in level increase of the external load σ^{gr}.

2. In case of bolt installation with the radial interference of 1% d_b, the zone of maximum tensile stresses is located on the surface of the hole countersunk portion in the upper strap. Followed by the growth of σ^{gr}, the zone of maximum tensile stresses is shifted to the transition boundary of the conical hole to the cylindrical one. Maximum equivalent stresses σ_{eqv} are initiated on the cylindrical hole surface in the upper strap. Followed by the growth of the applied external tensile load σ^{gr}, the initiation zone $\sigma_{eqv\,max}$ is shifted to the transition area of the hole conical portion to the cylindrical one to be displaced approximately at 15 degrees along the transition edge arc of the cylinder to the cone.

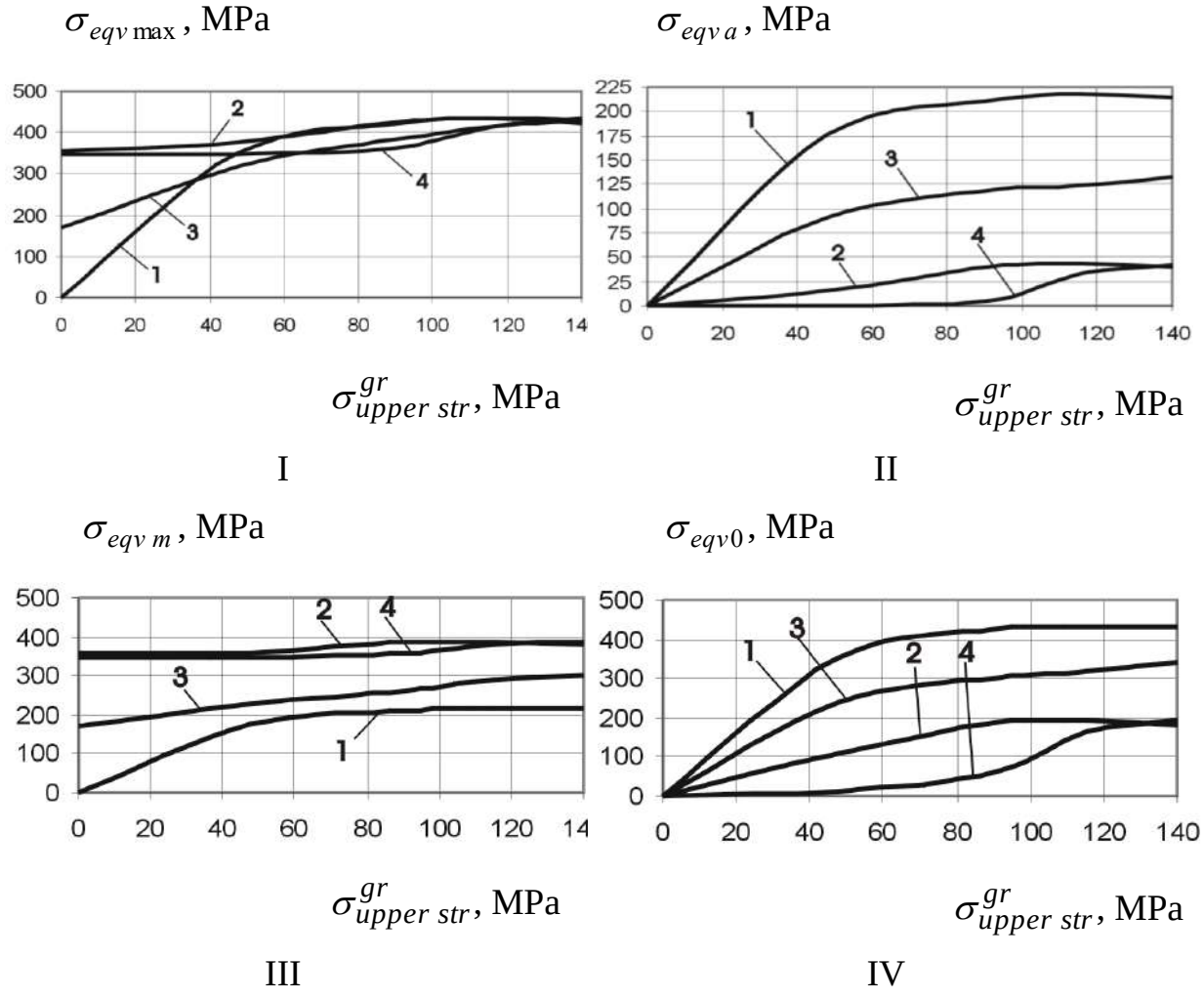

Fig. 3.16. Influence of loading level $\sigma^{gr}_{upper\ str}$ and nature of bolt installation on values of: I – maximum equivalent stresses in upper strap; II – amplitude equivalent stresses in upper strap; III – mean equivalent stresses in upper strap; IV – zero-to-tension equivalent stresses in upper strap

3. Under axial tightening of the bolt P_t =10 kN, the zone of the maximum tensile stresses is located at the lower edge of the hole in the upper strap to be shifted to the transition boundary by the conical load applied. Followed by the growth of $\sigma^{gr}_{upper\ str}$, the maximum equivalent stresses are shifted within the range of 10 degrees along the transition edge arc of conical portion to the cylindrical one.

4. Under axial tightening of bolt P_t = 10 kN and radial interference of 1% d_b, the behaviour of the maximal tensile stress zone practically corresponds to the case of bolt installation with a radial interference of 1% d_b. The zone of maximum equivalent stresses is located on the hole lower edge in the upper strap. Followed by the growth of σ^{gr}, it is shifted to the transition area of conical hole to the cylindrical one and is located approximately at 10 degrees from the plane longitudinal section of the hole countersinking axis.

The influence of the load level $\sigma^{gr}_{upperstr}$ and the nature of the bolt fit on the characteristics ε_{eqvmax}, ε_{eqva}, ε_{eqvm}, ε_{eqv0} as well as product of $\sigma_{eqv0} \cdot \varepsilon_{eqv0}$ have been subjected to analysis (Fig. 3.17, 3.18).

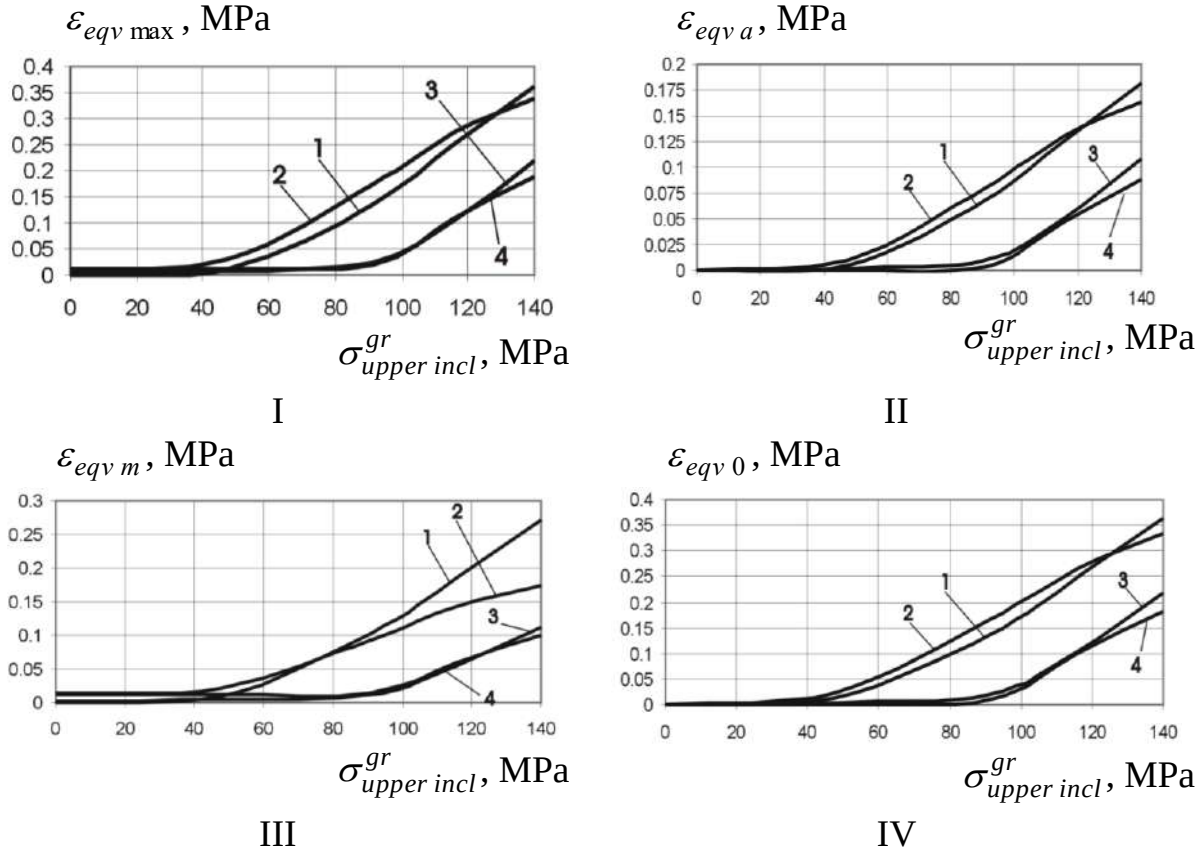

Fig. 3.17. Influence of load level $\sigma^{gr}_{upper\ str}$ and nature of bolt installation on values of: I – maximum equivalent deformations in upper strap; II – amplitudes of equivalent deformations in upper strap; III – mean equivalent deformations in upper strap; IV – maximum zero-to-tension equivalent deformations in upper strap

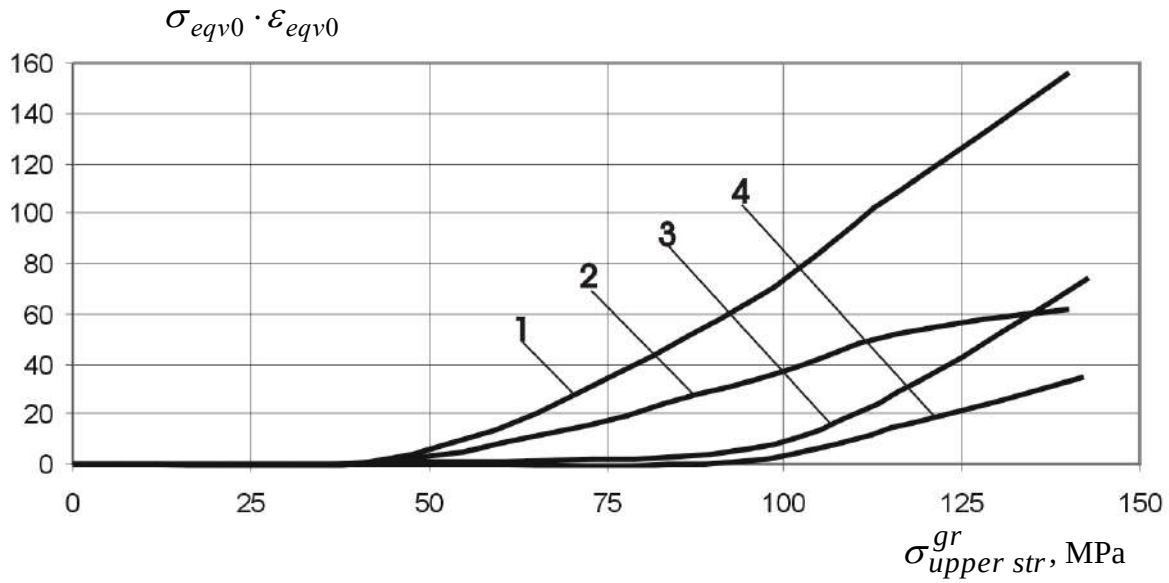

Fig. 3.18. Influence of load level $\sigma^{gr}_{upper\ incl}$ and nature of bolt installation on product value of zero-to-tension equivalent stresses and deformations in upper strap

From Fig. 3.17, 3.18 it is obvious that application of radial interference of 1% d_b and axial bolt tightening P_t=10 kN significantly reduces the amplitude of the maximum deformations in a single-row double-shear bolted joint.

The nature of contact pressure distribution between the bolt and hole wall in the upper strap, plate and the lower strap is illustrated in Fig. 3.19, 3.21, 3.23. The major part of the tensile load is transmitted to the upper strap through the cylindrical portion of the hole. The contact pressures in this zone have high concentration level under every variant of bolt installation (Fig. 3.19).

The concentration factor of contact pressures θ between the contacting surfaces is used as one among criteria of durability estimation. It can be found by the following formula.

$$\theta = \sigma_{c\,max} / \sigma_{shear}, \qquad (3.1)$$

where $\sigma_{c\,max}$ – maximum value of contact pressures between the surfaces, MPa; σ_{shear} – mean value of contact pressures along the mated surface, MPa.

Values of contact pressure concentration factor θ depending on the nature of bolt installation and the external loading application level have been calculated for surfaces of contact: "bolt – upper strap", "bolt – plate", "bolt – lower strap ". Dependence of loading level effect $\sigma^{gr}_{upperstr}$ and nature of bolt installation on the value of contact pressure concentration factor between mating surfaces of the bolt and upper strap is shown in Fig. 3.20.

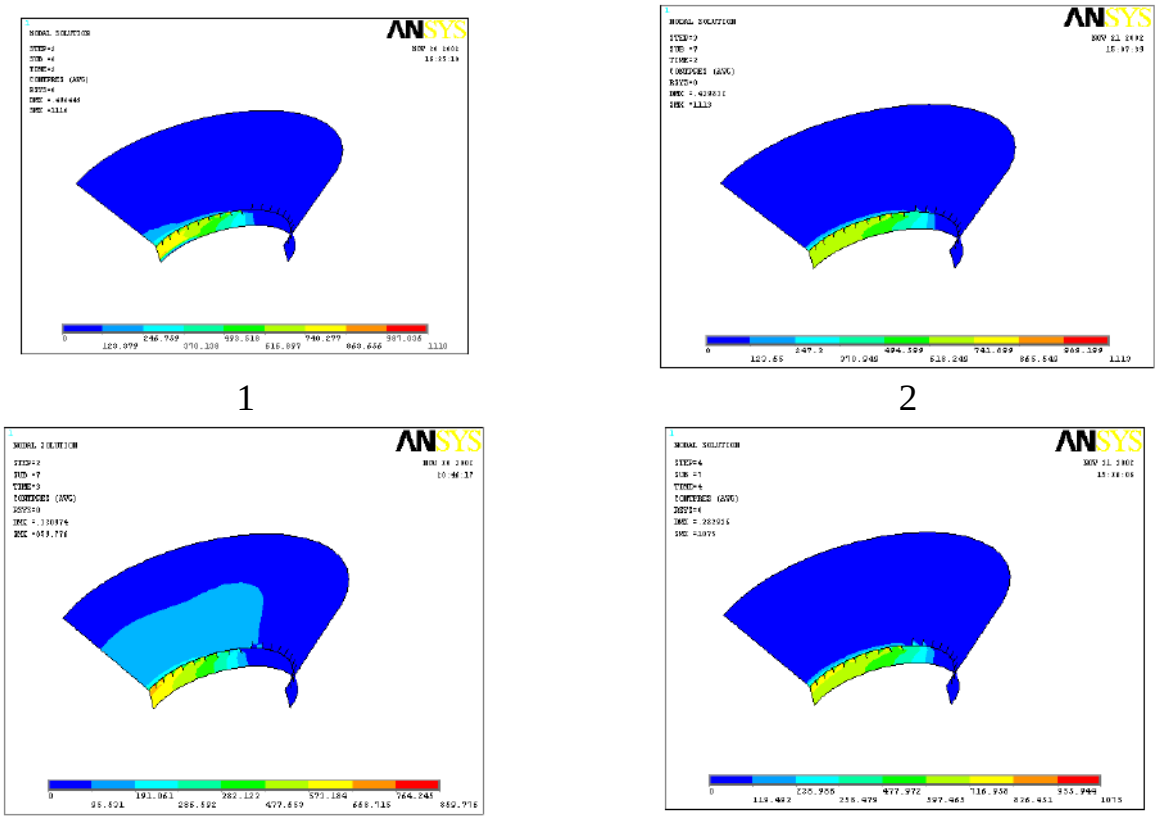

Fig. 3.19. Contact pressure distribution field between the bolt head and hole wall in the upper strap with various variants of bolt installation and external loading level σ_{plate}^{gr} = 48 MPa (σ_{str}^{calc} = 100 MPa)

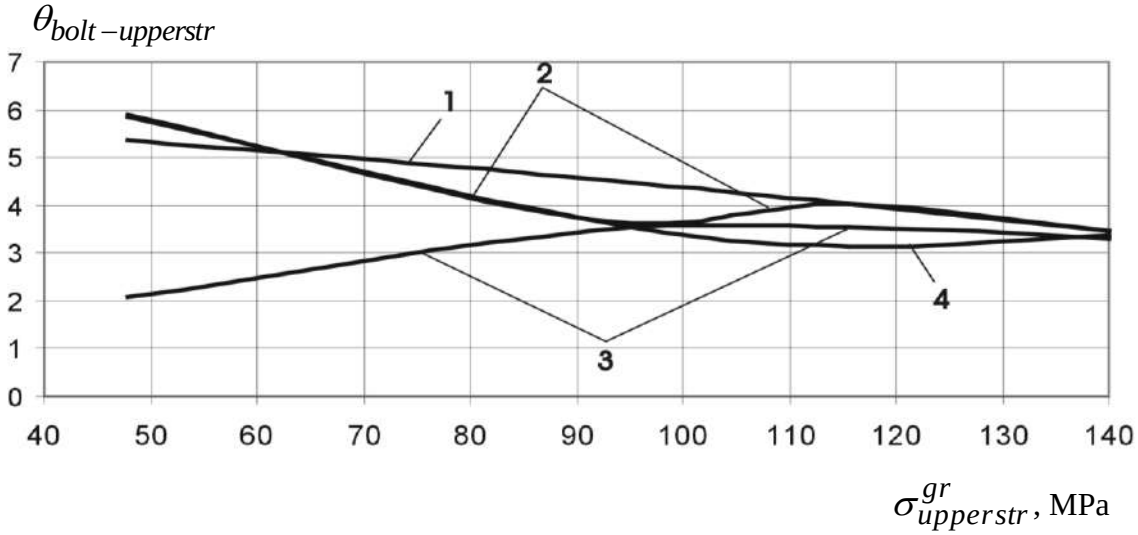

Fig. 3.20. Dependence of loading level $\sigma_{upperstr}^{gr}$ and nature of bolt installation effect on the value of contact pressure concentration factors between the bolt head and upper strap

When analysing the dependence of external loading effect on contact pressure concentration factor between the bolt and the hole wall in the upper strap (Fig. 3.20), it should be noted that application of axial interference P_t = 10 kN provides the minimum factor θ = 2…3.5 at $\sigma^{gr}_{upperstr}$ < 95 MPa. For external loading $\sigma^{gr}_{upperstr}$ > 95 MPa the minimum contact pressure concentration factor during bolt with axial interference and radial interference installation is θ = 3.1…3.5.

The contact pressure distribution field between bolt body and hole wall in a plate (Fig. 3.21) shows that the contact pressure concentration zone is located near the hole edges because of bolt bending in the longitudinal plane.

The contact pressure concentration factor was calculated for the contact surface between bolt body and hole wall in the plate by formula (3.1). The relation of loading level effect σ^{gr} and the nature of the bolt installation on the value of contact pressure concentration factors between bolt body and hole wall in the plate is shown in Fig. 3.21 – 3.24.

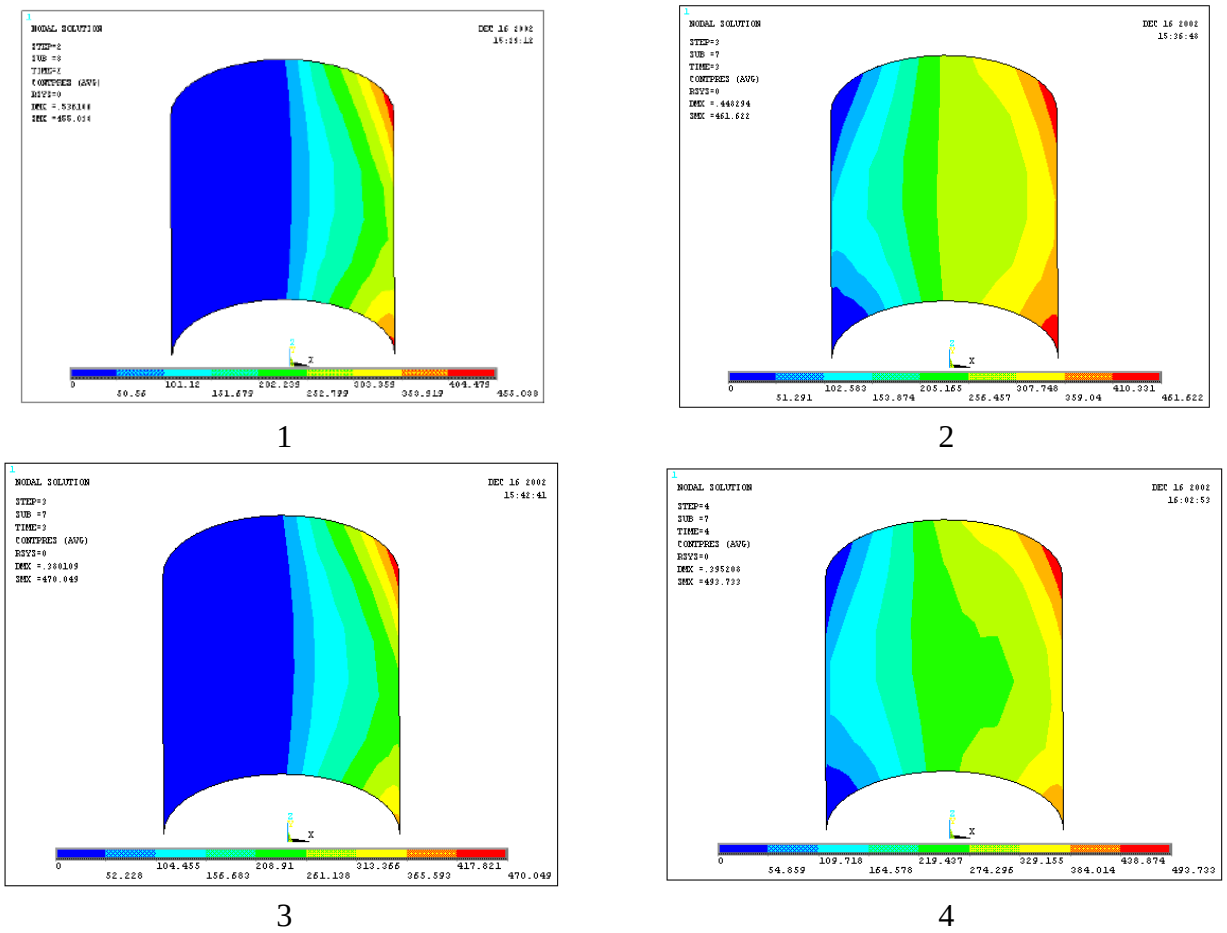

Fig. 3.21. Contact pressure distribution field between the bolt body and hole wall in the plate for various versions of bolt installation and external loading level (σ^{gr}_{pl} = 48 MPa, $\sigma^{calc.gr}_{str}$ = 100 MPa)

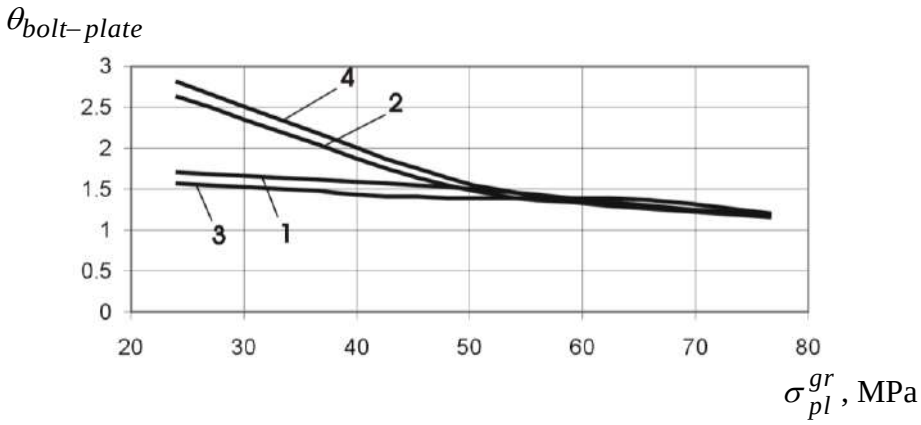

Fig. 3.22. Loading level effect of σ_{pl}^{gr} and nature of bolt installation on the value of contact pressure concentration factors between bolt body and hole wall in the plate

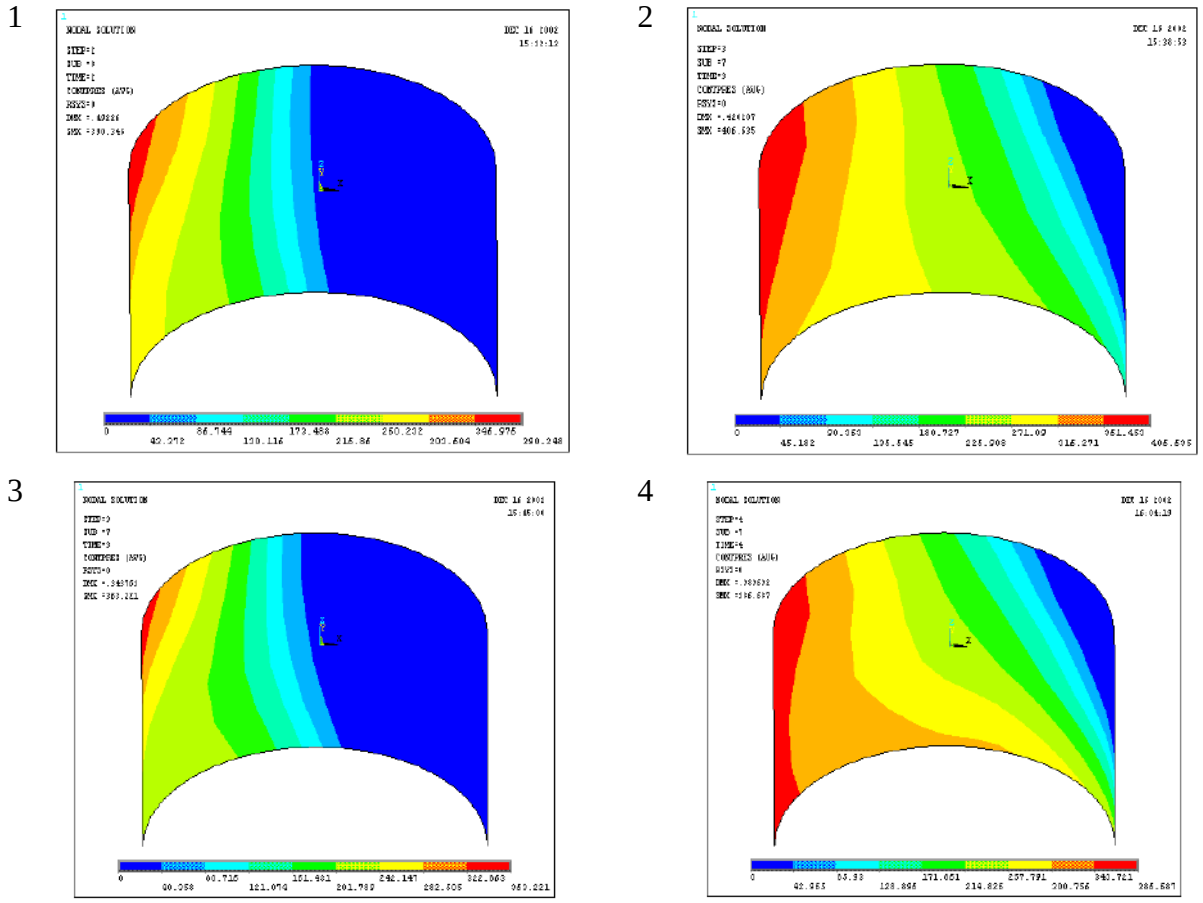

Fig. 3.23. Contact pressure distribution field between the bolt body and hole wall in the lower strap for various versions of bolt installation and external loading level σ_{pl}^{gr} = 48 MPa ($\sigma_{str}^{calc.gr}$ = 100 MPa)

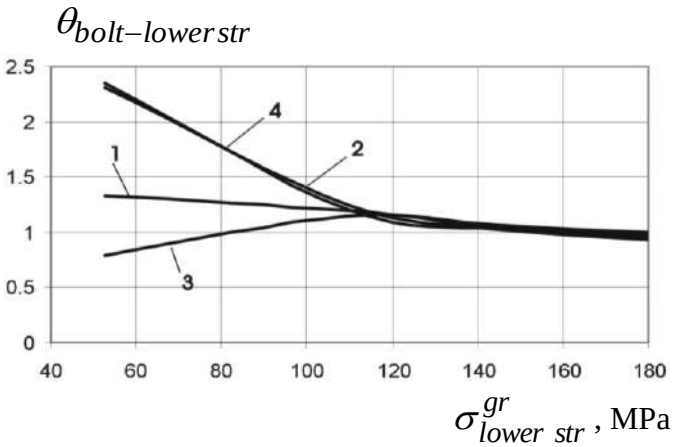

Fig. 3.24. Loading level effect σ^{gr} and the nature of bolt installation on value of contact pressure concentration factors between bolt body and hole wall in the lower strap

For representation of contact pressures between bolt body and joint members the following paths were selected (Fig. 3.25): L1, L2 – in longitudinal section of the hole axis; L3 – in cross section of hole axis; L4 – along cylindrical hole in the upper strap (Fig. 3.26 – 3.34).

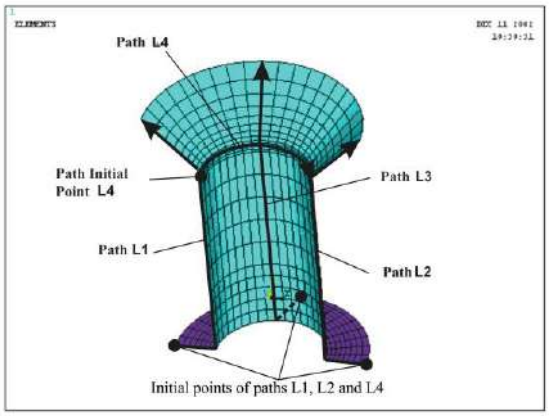

Fig. 3.25. Representation of paths along which contact pressures and clearances between mating surfaces are distributed

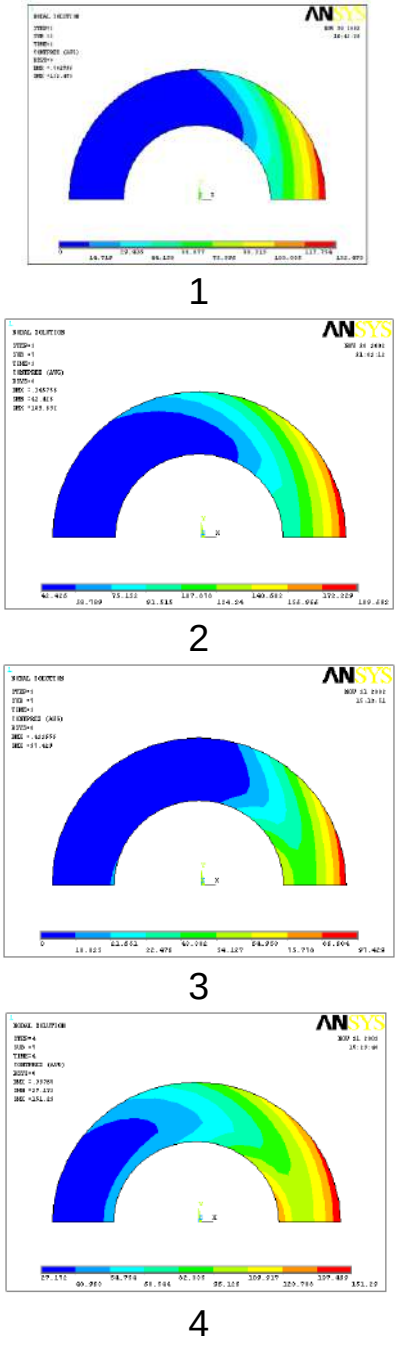

Fig. 3.26. Contact pressure distribution field between the screw nut body and lower strap for various versions of the bolt installation and external loading level σ^{gr}_{pl} =48 MPa

($\sigma^{calc.gr}_{str}$ = 100 MPa)

The bolt is installed without radial and axial interferences

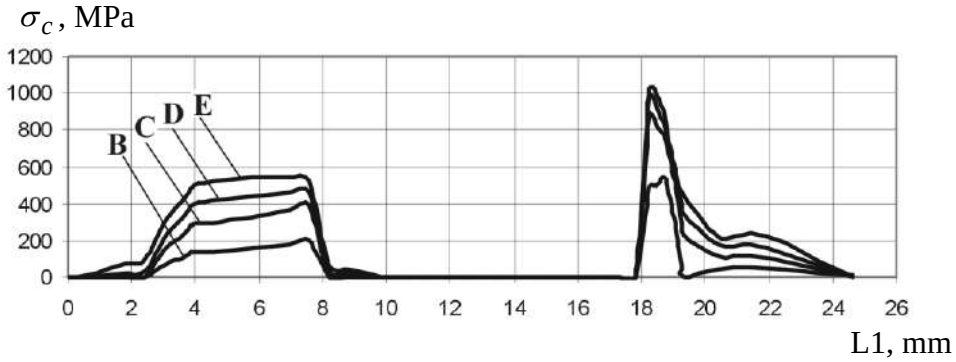

The bolt is installed with radial interference 1% d_b

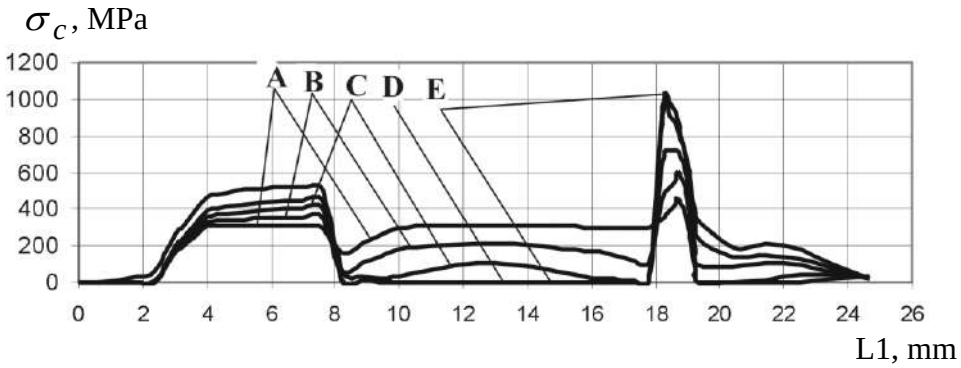

The bolt is installed with axial tightening P_t = 10 kN

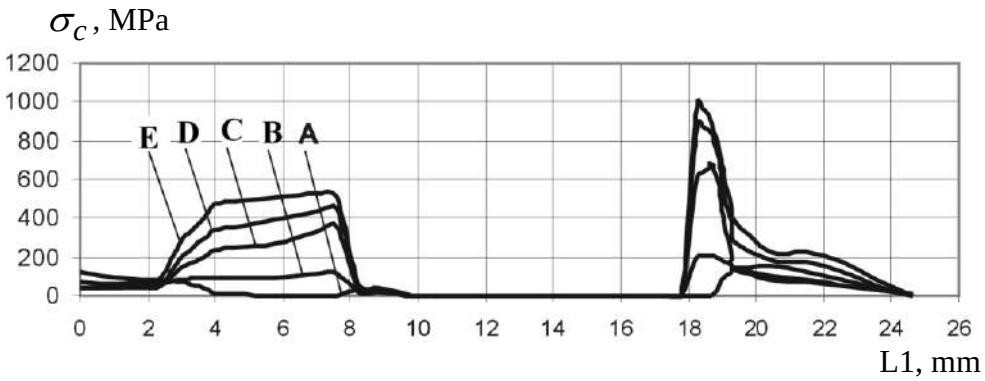

The bolt is installed with radial interference 1% d_b and axial tightening P_t = 10 kN

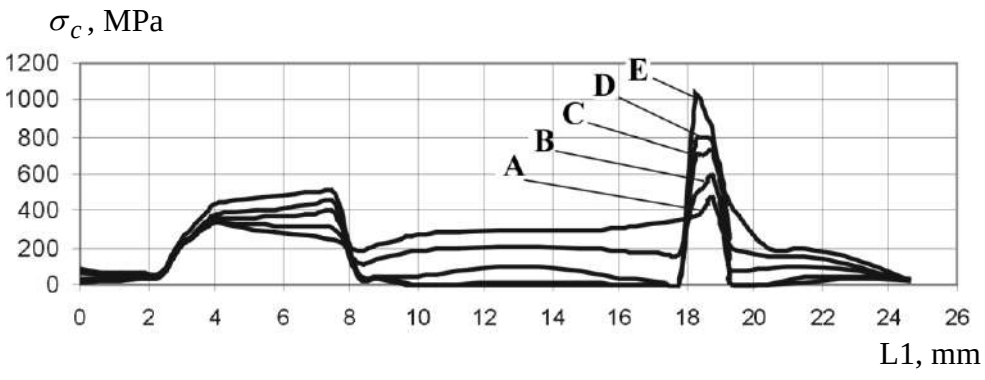

Fig. 3.27. Effect of external loading application level and the nature of bolt installation on contact pressure distribution between the bolt body and pack along path L1

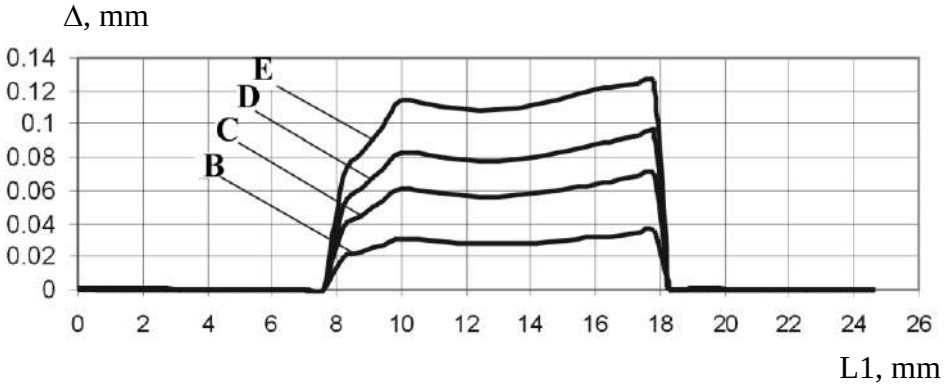

The bolt is installed without radial and axial interferences

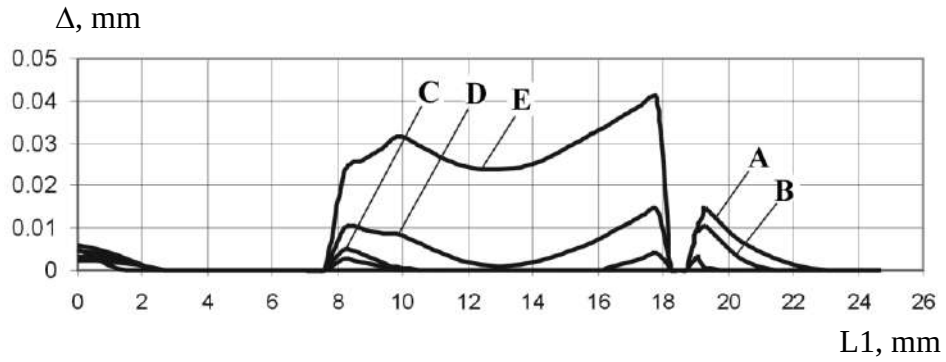

The bolt is installed with radial interference 1% d_b

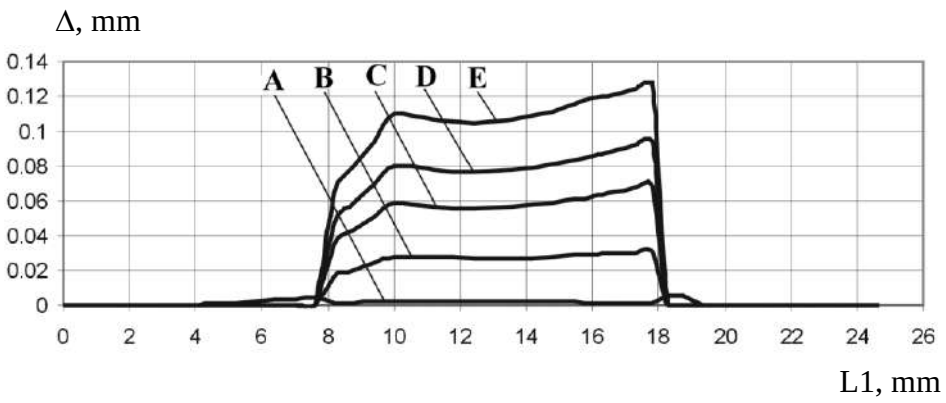

The bolt is installed with axial tightening P_t = 10 kN

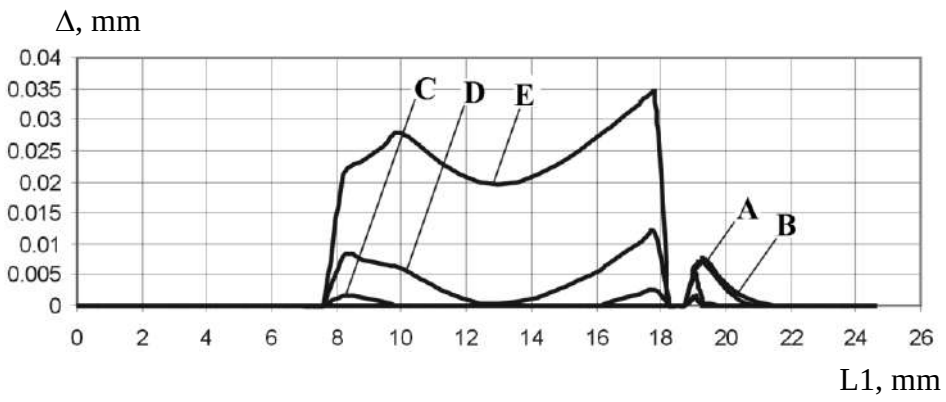

The bolt is installed with radial interference 1% d_b and axial tightening P_t = 10 kN

Fig. 3.28. Effect of external loading application level and the nature of bolt installation on clearance distribution between the bolt body and pack along path L1

The bolt is installed without radial and axial interferences

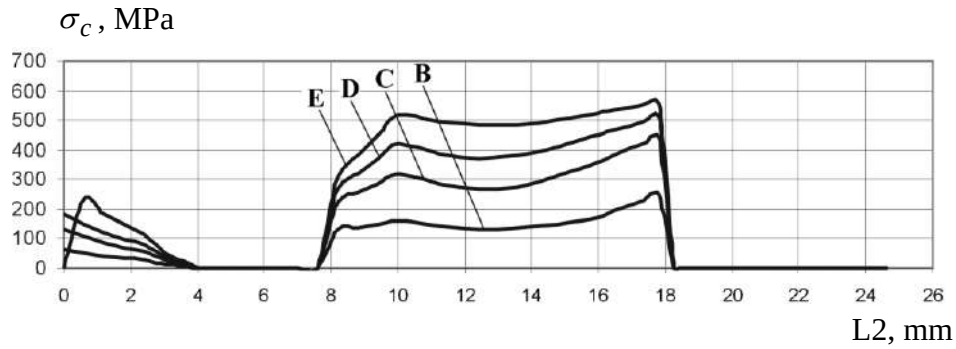

The bolt is installed with radial interference 1% d_b

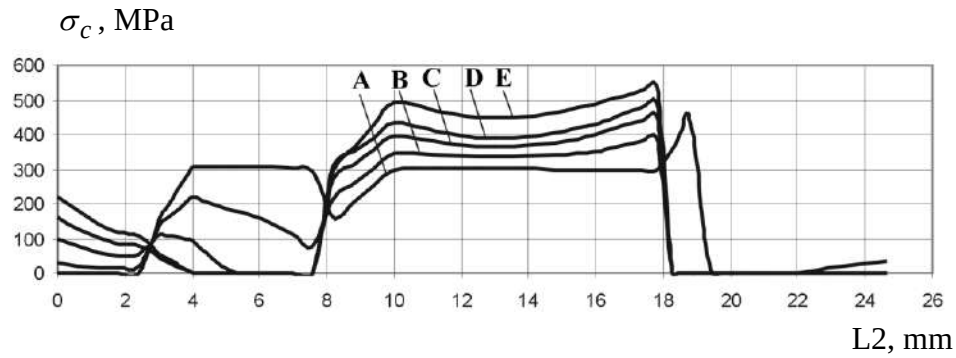

The bolt is installed with axial tightening P_t = 10 kN

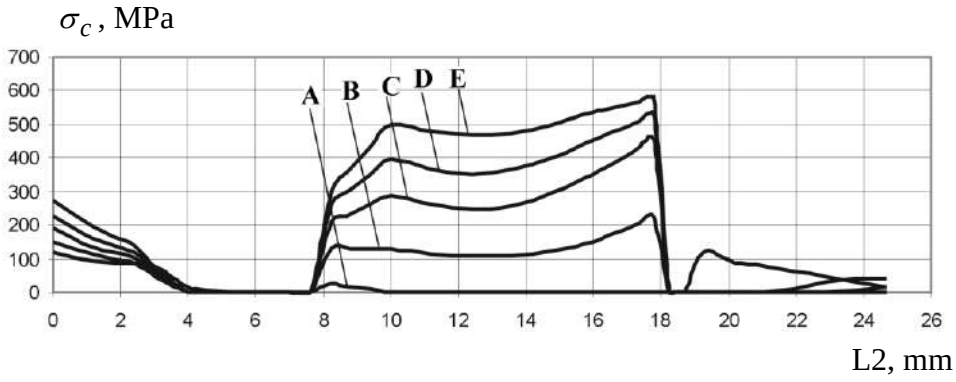

The bolt is installed with radial interference 1% d_b and axial tightening P_t = 10 kN

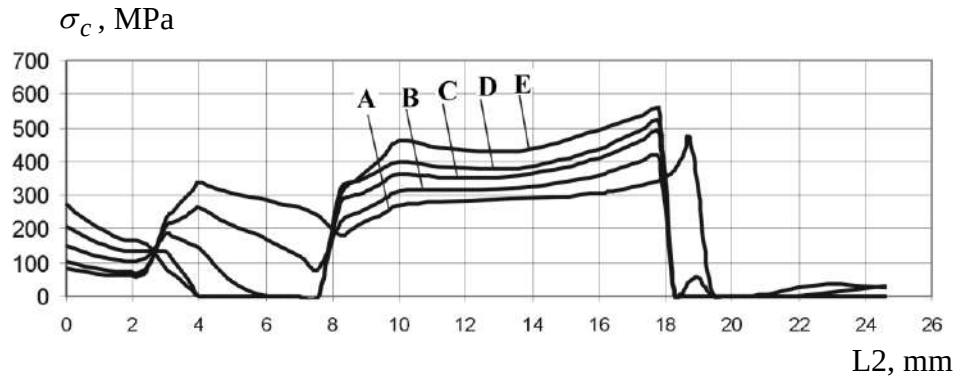

Fig. 3.29. Effect of external loading application level and the nature of bolt installation on contact pressure distribution between the bolt body and pack along path L2

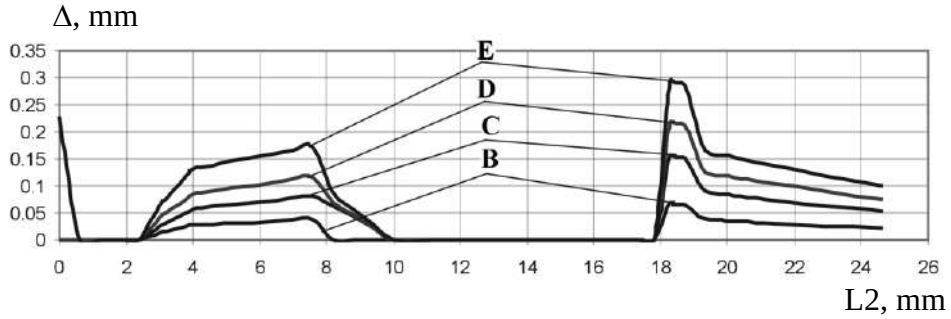

The bolt is installed without radial and axial interferences

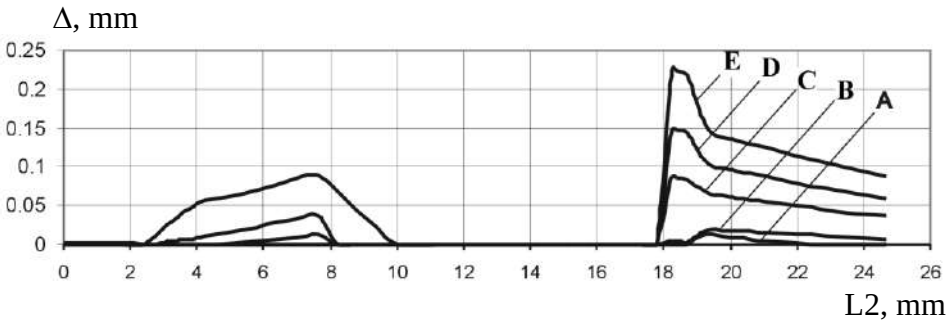

The bolt is installed with radial interference $1\% d_b$

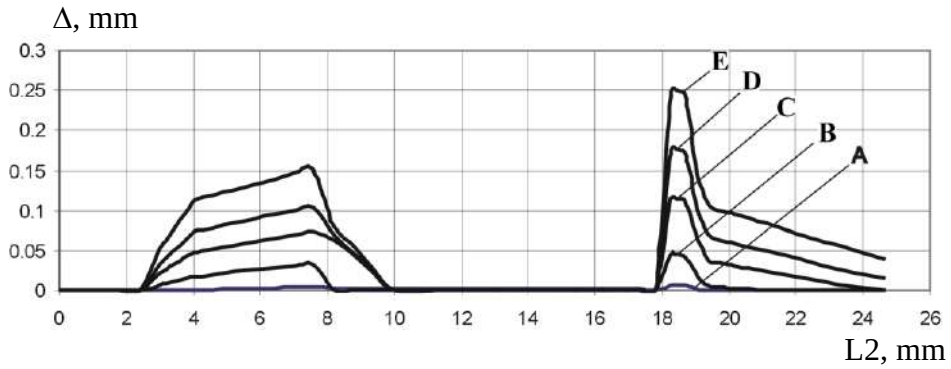

The bolt is installed with axial tightening P_t = 10 kN

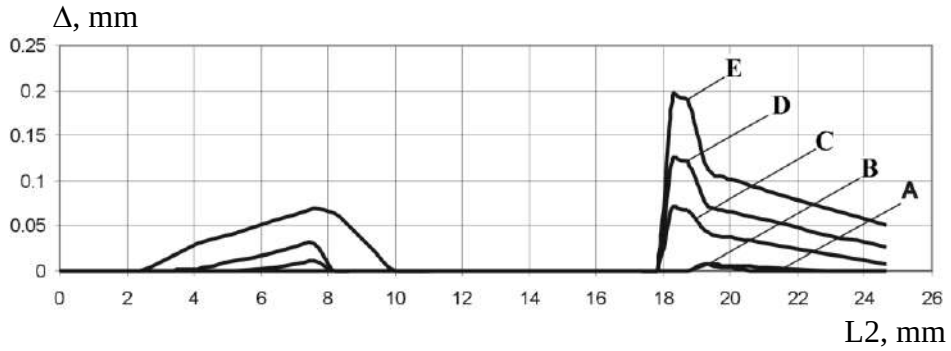

The bolt is installed with radial interference $1\% d_b$ and axial tightening P_t = 10 kN

Fig. 3.30. Effect of external loading application level and the nature of bolt installation on contact clearance distribution between the bolt body and pack along path L2

Contact pressure concentration factor in case of radial interference application of 1 % d_b considerably increases at σ_{pl}^{gr} < 50 MPa. With external loading level of σ_{pl}^{gr} > 50 MPa the contact pressure concentration factor between the bolt and hole wall for various versions of bolt installation is practically at one level ($\theta_{bolt-plate}$=1.2…1.5).

Fig. 3.23 shows that maximum contact pressures zone between bolt body and hole wall in the lower strap is located near the hole edge mating the central plate surface, owing to the bolt bending Fig. 3.30 shows when tensile load is applied to the 3D model of the bolted joint, the maximum clearances in size originate between cylindrical surfaces of the bolt and upper strap. The positive effect from the radial interference usage is the decreasing of the clearance value (by 0.75 mm at loading level D in comparison with version of the bolt installation without radial and axial interference). Joint use of radial interference of 1% d_b and axial tightening P_t = 10 kN reduces the clearance value formed between the bolt and upper strap by 1 mm at external loading level D in comparison with the version of the bolt installation without radial and axial interferences.

Relations of clearance value between bolt installed with radial interference and axial tightening P_t = 10 kN, and the upper strap from radial interference value (in percentage of d_b) and external loading level application $\sigma_{upperstr}^{gr}$ (see Fig. 3.31) have been obtained.

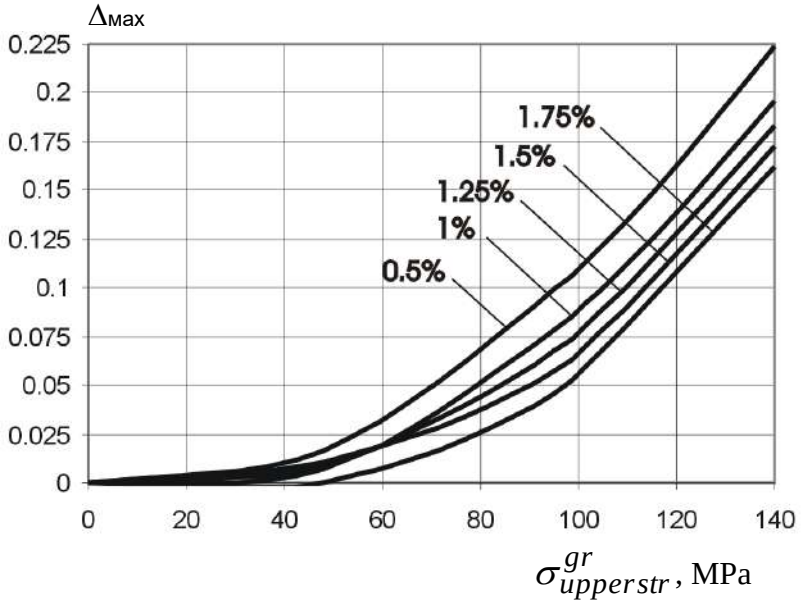

Fig. 3.31. Effect of external loading application level on the clearance value between the bolt body and hole wall in the upper strap at axial tightening of P_t = 10 kN and different values of bolt radial interference (within 0.5 to 1.75 % d_b)

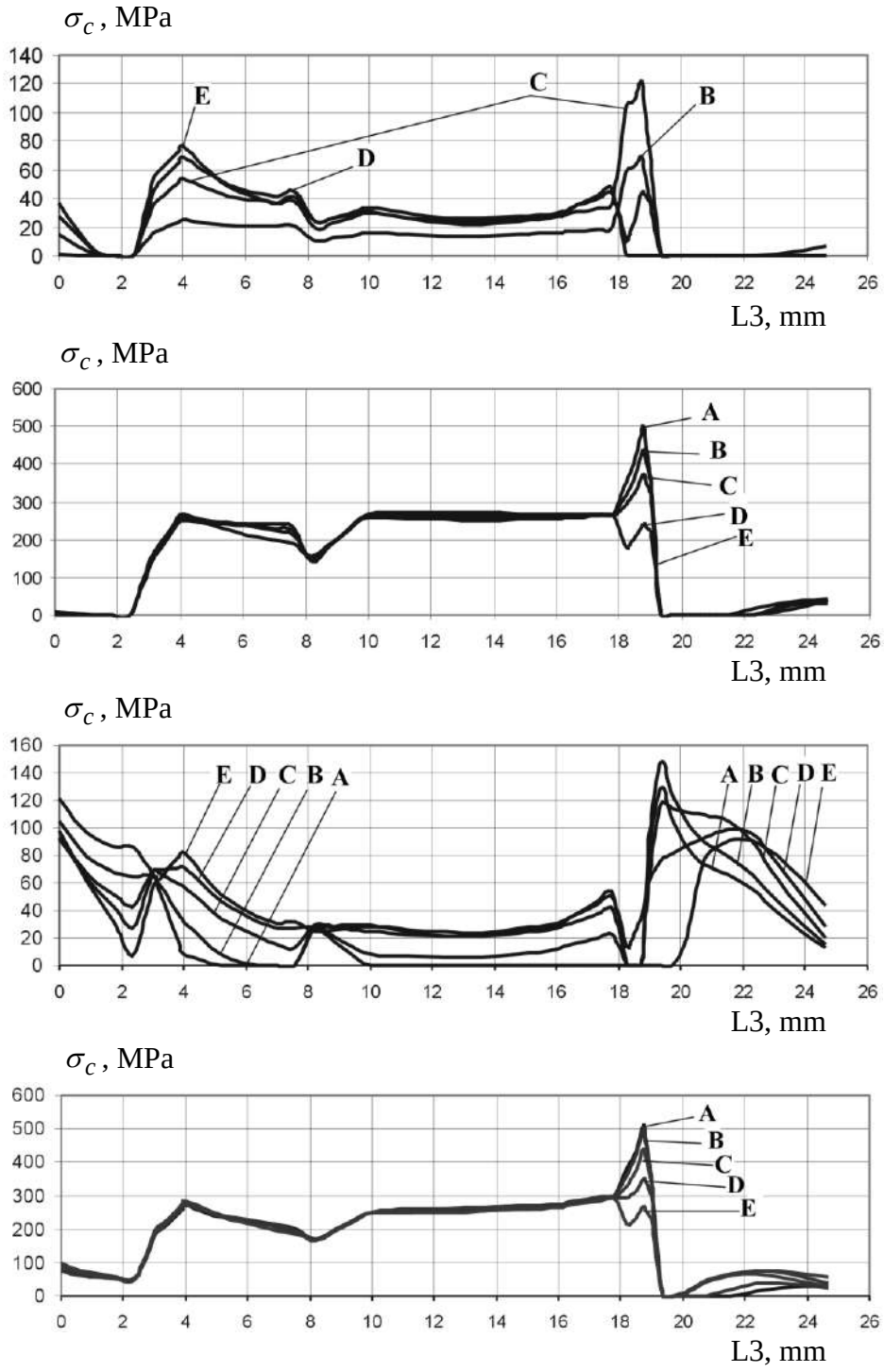

The bolt is installed without radial and axial interferences

The bolt is installed with radial interference 1% d_b

The bolt is installed with axial tightening P_t = 10 kN

The bolt is installed with radial interference 1% d_b and axial tightening P_t = 10 kN

Fig. 3.32. Effect of external loading application level and nature of bolt installation on contact pressure distribution between bolt body and pack along path L3

Combined radial interference of 1.75 % d_b usage with axial tightening P_t = 10 kN enables to prevent the clearance between the bolt and the upper strap

at external loading level of $\sigma_{upperstr}^{gr}$ < 50 MPa. Increase of radial interference from 1 up to 1.75 % d_b enables to reduce the clearance value between the bolt and hole wall in the upper strap in 1.5 times (at $\sigma_{upperstr}^{gr}$ = 100 MPa).

During installation of the bolt **without radial and axial interferences** and the external loading application maximum contact pressures originate between bolt and cylindrical surface of counterbore in the upper strap in longitudinal direction (path L1) and exceed the values of contact pressures between bolt body and hole wall in the lower strap practically twice.

The maximum values of clearances between bolt body and hole wall (at σ_{pl}^{gr} =24 MPa Δ = 0.055 mm; at σ_{pl}^{gr} = 76.8 MPa Δ = 0.3 mm) arise in the area of a cylindrical surface of hole in the upper strap in longitudinal section (path L2). Clearances between the bolt body and the lower strap are at level Δ = 0.025 mm (σ_{pl}^{gr} =0 MPa) and Δ = 0.14 mm at σ_{pl}^{gr} = 0 MPa, the clearance between the bolt body and the plate is at level Δ = 0.03 mm (σ_{pl}^{gr} = 24 MPa) and Δ = 0.11 mm (σ_{pl}^{gr} = 72 MPa).

If the bolt **with a radial tightening 1% d_b** is installed, the maximum contact pressures (σ_c = 500…600 MPa) arise between the bolt body and the upper strap in a longitudinal direction (path L1). Contact pressures (path L1) between bolt and the lower strap are at level σ_c =300 MPa (σ_{pl}^{gr} =0 MPa) and σ_c=500…550 MPa

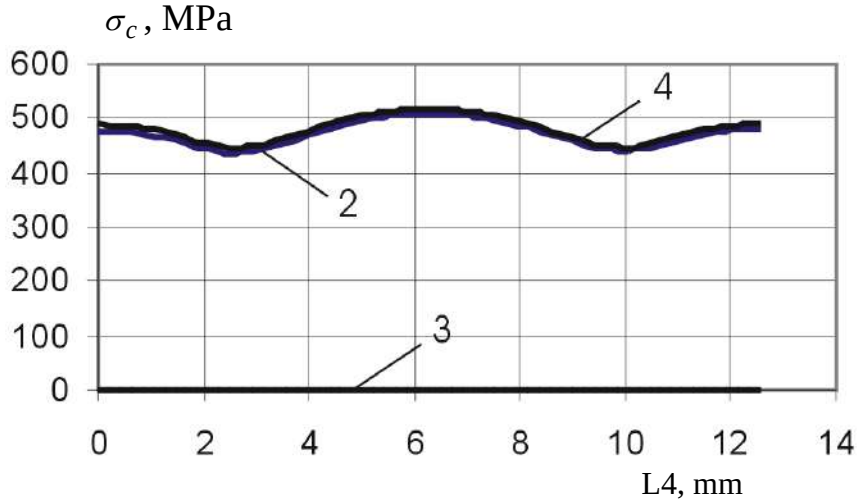

Fig.3.33. Effect of bolt fit nature on value of contact pressures between the bolt head and upper strap along path L4

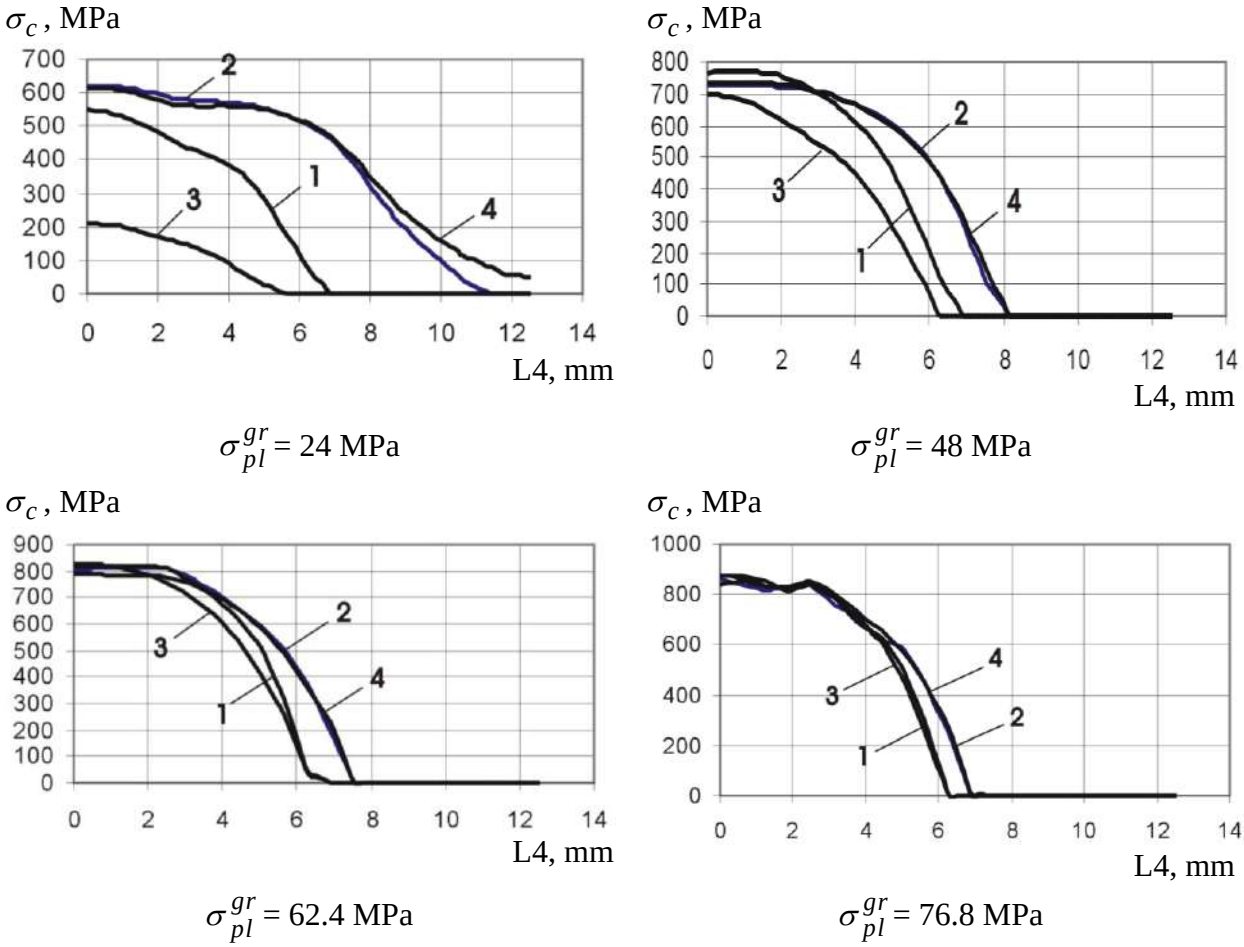

Fig. 3.34. Effect of loading level σ^{gr} and nature of bolt installation on the value of contact pressures between bolt head and upper strap along path L4

(σ_{pl}^{gr} = 76.8 MPa). The maximum contact pressures arise between the plate and the bolt in longitudinal section on path L2 (σ_c=300 MPa at σ_{pl}^{gr}=0 MPa and σ_c=450…550 MPa at σ_{pl}^{gr}=76.8 MPa).

The maximum clearance between the hole wall and bolt body arises in the zone of cylindrical part of the hole in the upper strap (Δ=0.075 mm at σ_{pl}^{gr}=48 MPa and Δ = 0.225 mm at σ_{pl}^{gr}=76.8 MPa). At σ_{pl}^{gr}=24 MPa the clearance between bolt body and hole wall does not appear. The clearance between bolt and hole walls in a plate and the lower strap starts to arise at σ_{pl}^{gr}>62.4 MPa.

When the bolt **with axial tightening P_t = 10 κN** is installed in longitudinal section (path L1) between bolt and a cylindrical portion of hole in the upper strap, maximum contact pressures appear (to 1000 MPa at σ_{pl}^{gr} = 76.8 MPa). Contact

pressures of lower level (σ_c=100 MPa at σ_{pl}^{gr}=24 MPa and σ_c=500 MPa at σ_{pl}^{gr}=76.8 MPa) emerge between the bolt body and the hole wall in the lower strap. Value of contact pressures between the bolt and hole wall in a plate is at level σ_c=100…200 MPa (σ_{pl}^{gr}=24 MPa) and σ_c = 470 … 550 MPa (σ_{pl}^{gr}=76.8 MPa) on path L2.

The size of clearances between bolt body and hole wall takes the maximum value (Δ = 0.05 mm at σ_{pl}^{gr} = 24 MPa and Δ = 0.25 mm at σ_{pl}^{gr} = 76.8 MPa) in the zone of the hole cylindrical part in the upper strap in longitudinal section (path L2). Clearances have smaller level (Δ=0.025 mm at σ_{pl}^{gr}=24 MPa and Δ=0.11 mm at σ_{pl}^{gr} = 76.8 MPa) between bolt and hole wall in the lower strap. The clearance between bolt and hole wall in the plate is at level Δ = 0.03 mm at σ_{pl}^{gr} = 24 MPa and Δ = 0.115 mm at σ_{pl}^{gr} = 76.8 MPa.

In case when the bolt **with axial tightening Pt = 10 κN and radial interference 1%** ***d*** is installed the contact pressures between the bolt body and cylindrical surface of hole in the upper strap is equal to σ_c=440 MPa at σ_{pl}^{gr}=0 MPa and σ_c=1000 MPa at σ_{pl}^{gr}=76.8 MPa. Contact pressures are created between bolt and hole wall in the lower strap at level σ_c=250…350 MPa at σ_{pl}^{gr}=0 MPa and σ_c=450…500 MPa at σ_{pl}^{gr}=76.8 MPa. Contact pressures between bolt body and hole wall in a plate are σ_c = 300 MPa at σ_{pl}^{gr} = 0 MPa and σ_c = 450 … 550 MPa at σ_{pl}^{gr} = 76.8 MPa.

Clearances between cylindrical portion of the hole in the upper strap and bolt body are Δ = 0.07 mm at σ_{pl}^{gr} = 48 MPa and Δ = 0.2 mm at σ_{pl}^{gr} = 76.8 MPa. The size of clearances between bolt and hole wall in the lower strap is Δ = 0.05 mm at σ_{pl}^{gr} = 76.8 MPa (at σ_{pl}^{gr} <62.4 MPa the clearance is not formed). Between the bolt body and hole wall in a plate Δ = 0.02 mm at σ_{pl}^{gr} = 76.8 MPa (under external loading σ_{pl}^{gr}<62.4 MPa the clearance between bolt and hole wall in a plate does not arise).

In Fig. 3.35 – 3.38 results of the analysis of contact interaction of a plate with the upper strap are shown.

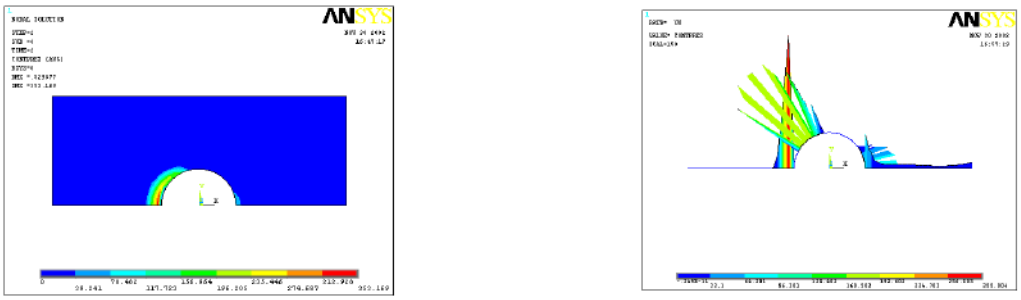

1

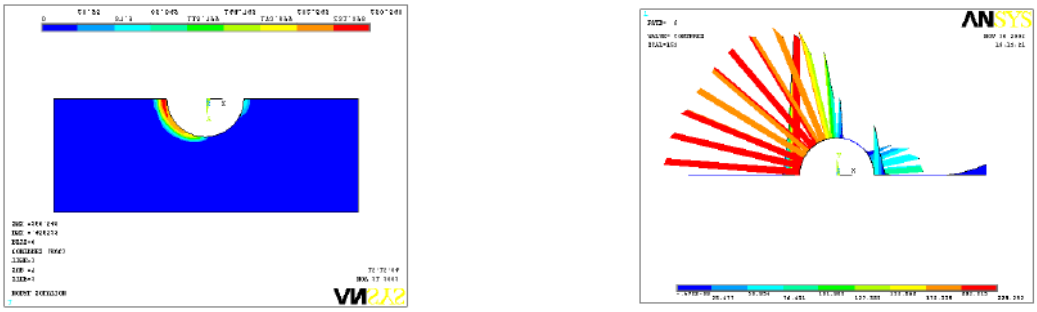

2

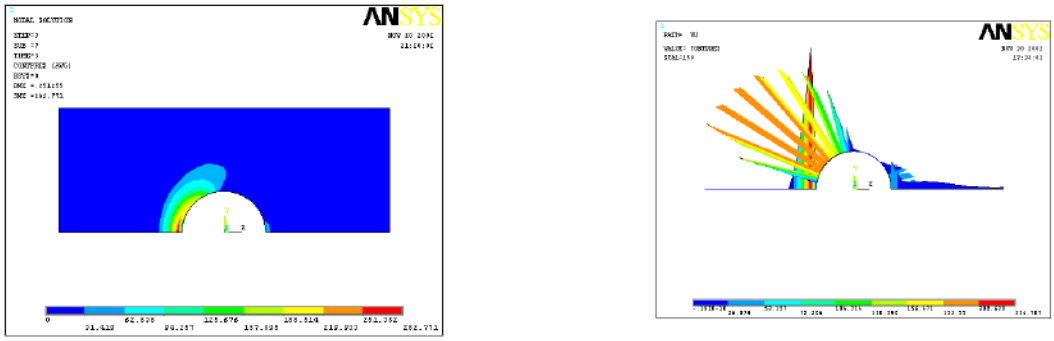

3

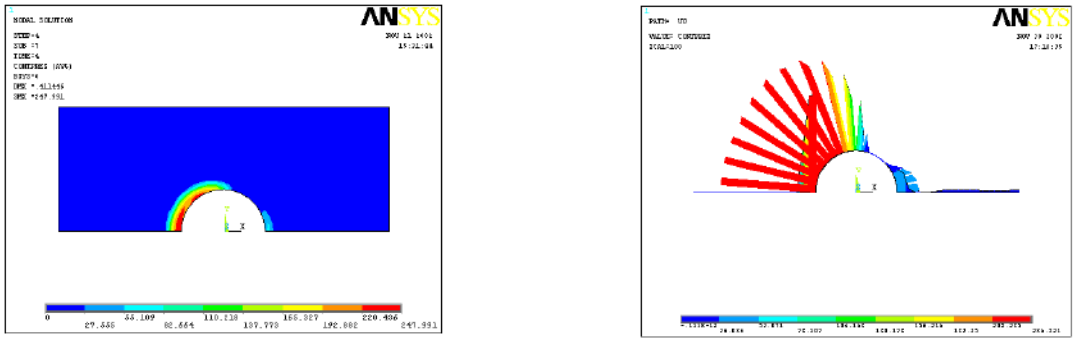

4

Fig. 3.35. Contact pressure distribution field between the upper strap and plate and contact pressure distribution diagram along the surface edge of the upper strap contacting with a plate at different ways of bolt installation and external loading σ_{pl}^{gr} = 48 MPa

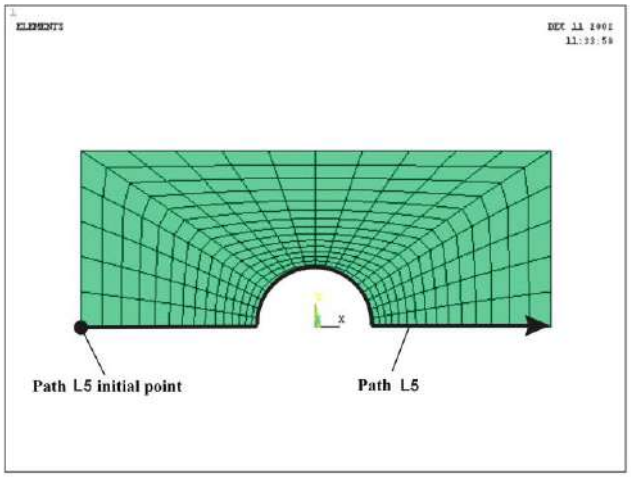

Fig. 3.36. Image of path L5 along which contact pressures between mating surfaces of upper strap and plate are distributed

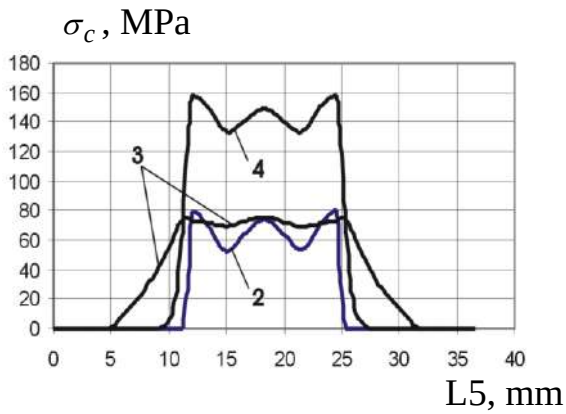

Fig. 3.37. Influence of bolt fit type on value of contact pressures between bolt head and upper strap along path L5

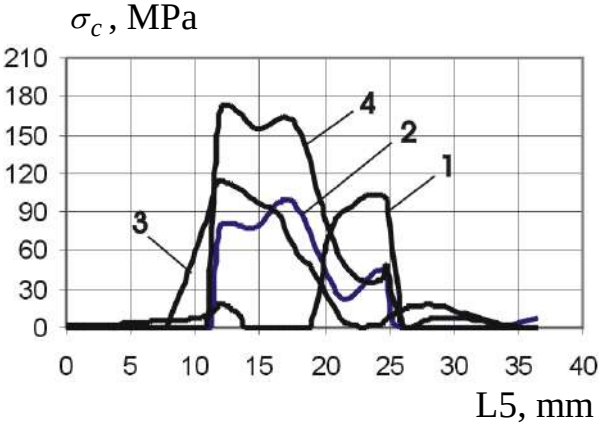

σ_{pl}^{gr} = 24 MPa

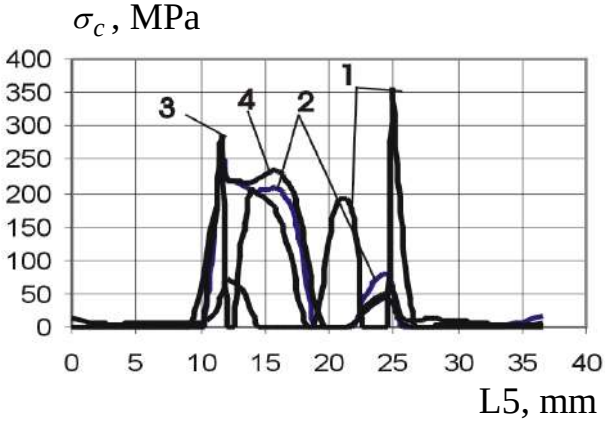

σ_{pl}^{gr} = 48 MPa

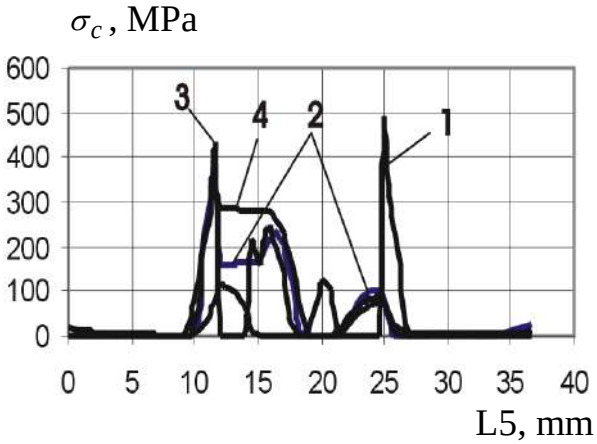

σ_{pl}^{gr} = 62.4 MPa

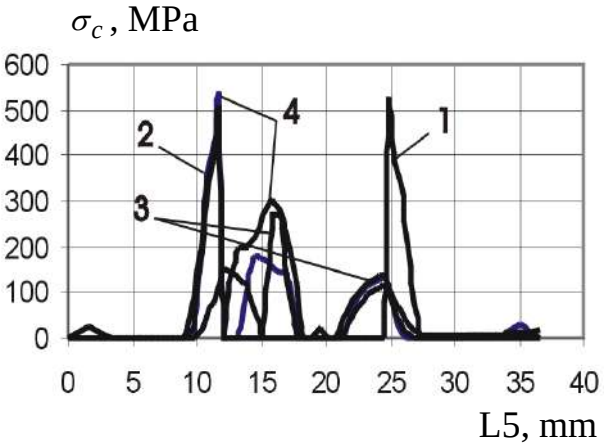

σ_{pl}^{gr} = 76.8 MPa

Fig. 3.38. Influence of stress level σ^{gr} and nature of bolt installation on the value of contact pressures between a plate and the upper strap on path 5

The durability of investigated joint is determined by intensity of fretting corrosion to its members. The tested specimens in most cases failed in sections on plate edge, and also, in section on body edge in the zone of countersink for embedded socket countersunk bolt head in zones of intensive fretting corrosion growth. Fig. 3.39 shows the distribution field of relative displacements of contacting plate surfaces with the upper strap and bolt with a wall countersunk hole in the upper strap during the bolt fit with a radial interference 1% d_b and axial tightening P_t = 10 kN.

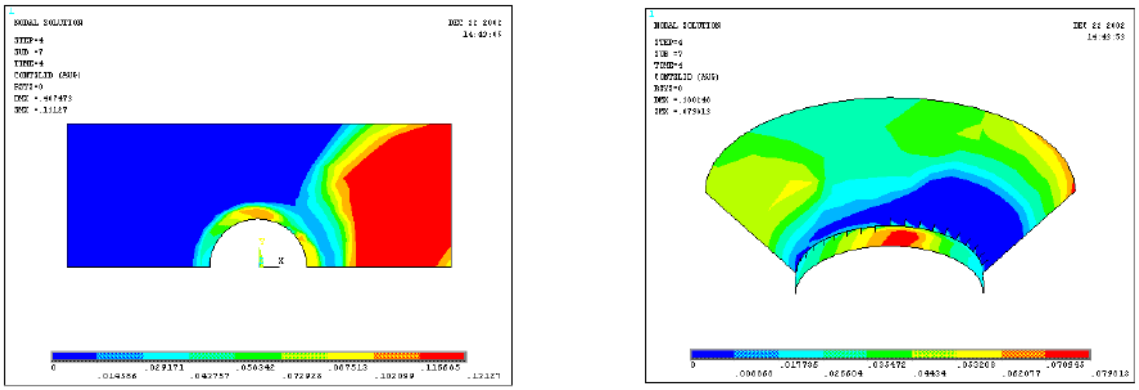

a b

Fig. 3.39. Nature of relative displacement distribution of contacting surfaces: a – plates with the upper strap; b –bolt with hole wall in the upper strap at σ_{pl}^{gr} = 48 MPa (σ_{str}^{calc} = 100 MPa)

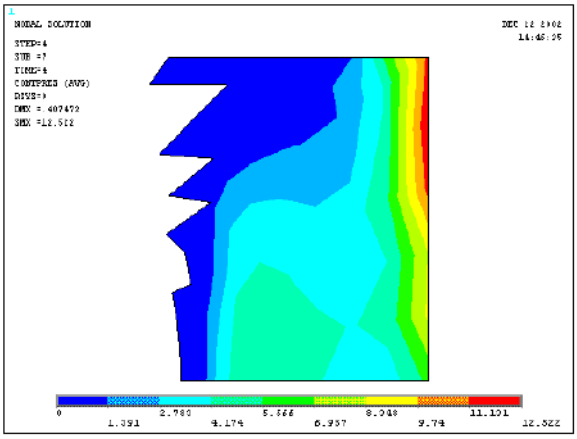

Fig. 3.40. Nature of disposition of contact pressure distribution between the plate and the upper strap in section on plate edge at σ_{pl}^{gr} =48 Mpa ($\sigma_{str}^{calc.gr}$ = 100 MPa)

From Fig. 3.39, 3.40 we can see that calculation of the local mode of deformation in joint members confirms interference concentration of relative displacements and contact pressures in failure zones of experimental specimens by fretting-corrosion.

It is possible to draw the following conclusions from these investigations:

1. The investigations enabled to develop the integrated analysis method of influence of structurally-technological parameters and stress level on characteristics of the local mode of deformation by means of the engineering analysis system CAD\CAE ANSYS, including specifying the maximum values of zero-to-tension equivalent stresses and deformations both in elastic and in plastic areas, values and nature of contact pressure distribution between mating joint members, contact pressure irregularity coefficient, sizes of clearances while changing the external stress level using fits with elastoplastic radial and axial interferences.

2. The integrated analysis method is approved in the course of the modelling experiment directed on specifying the local mode of deformation characteristics of double-shear single-row countersunk bolt joint made of aluminium alloy Д16аТ. In this case it is determined that application of axial and radial interferences of countersunk bolts facilitates the reduction of maximum zero-to-tension equivalent stress amplitude and maximum zero-to-tension equivalent deformations at operational level σ_{pl}^{gr} =100…130 MPa accordingly in 2 … 2.5 times and in 2 … 4 times in comparison with analogous characteristics in the joint executed without radial interference and tightening.

3.2. The influence analysis of bolt installation technology and stress level on the local mode of deformation characteristics in double-shear three-row countersunk joint members

The given method is also approved during analysing influence of bolt installation technology and stress level on the local mode of deformation characteristics in double-shear three-row countersunk joint members consisting of the central plate (190×50×10 mm) and two straps (168×24×5 mm) connected with three bolts 8 mm in diameter with countersunk head. The geometrical dimensions of this model are shown in Fig. 3.41.

Straps and plates are made of aluminum alloy Д16АТ with the elasticity modulus E = 70000 MPa and the Poisson's ratio which equals 0.3. To describe the material response of the plate and strap the polylinear model with the kinematic law of hardening is chosen.

Bolt material is 30ХГСА steel, modulus of elasticity E = 210000 MPa, Poisson's ratio equals 0.3. In calculations the linearly-elastic material response of the bolt was taken described by Hooke's law.

During this analysis the large deformation effect by inclusion of the NLGEOM option was considered. For the nonlinear solution the option of including the complete Newton-Raphson method was chosen. Change of load timing steps is automatic (AUTOTS, ON). The solver type is previous connected iterative with accuracy 1E-5 and multiplier 3 (EQSLV, PCG, 1E-5,3). The

maximum number of iterations is 1500 (NEQIT, 1500), linear search is included (LNSRCH, ON).

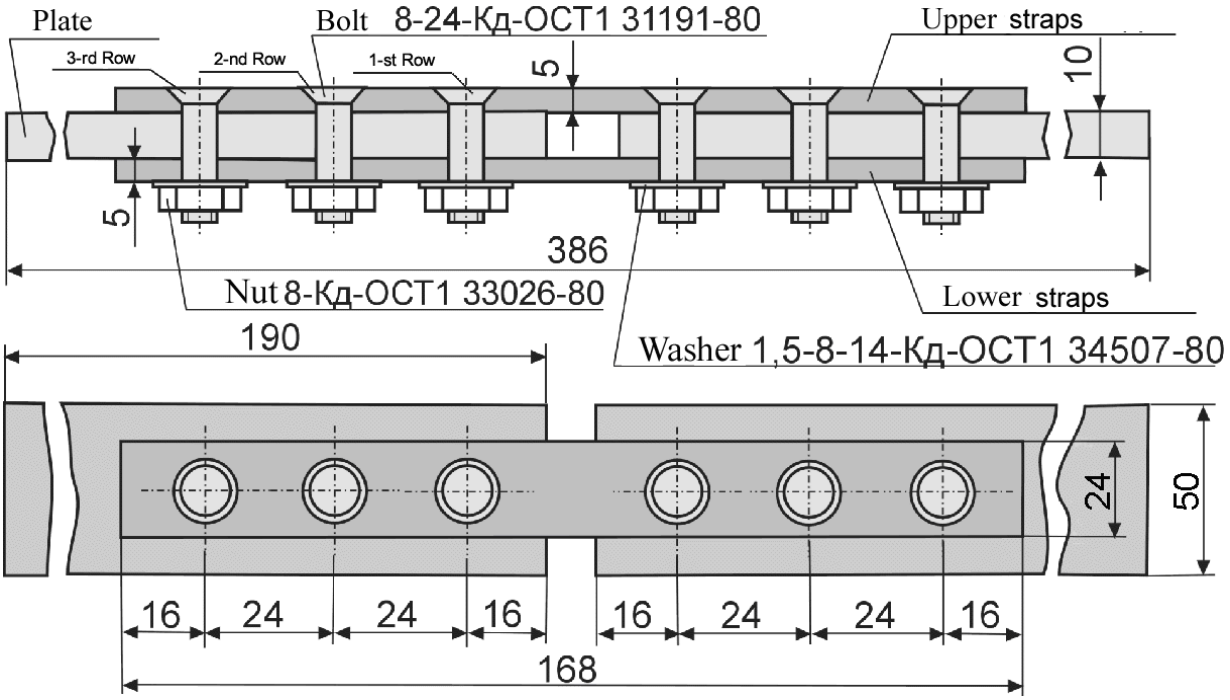

Fig. 3.41. Geometrical layout of double-shear three-row countersunk joint

Calculation of the local mode of deformation in joint members under external extension strain was carried out by means of ANSYS engineering analysis system for the following variants of the bolted joint of the upper and lower straps with the central plate:

1) without axial and radial interferences;

2) with radial interference 1% d_b;

3) with axial tightening P_t = 10 kN;

4) with radial interference 1% d_b and axial tightening P_t = 10 kN.

The stretch force was imposed to a plate. In calculations they were considered as equal: a) P_{pl}=0 N; b) P_{pl}=12000 N; c) P_{pl}=24000 N; d) P_{pl}=31200 N; e) P_{pl}=38400 N. This force in plate gross section corresponded to the nominal stress: a) σ_{pl}^{gr}=0 N; b) σ_{pl}^{gr}=24 MPa; c) σ_{pl}^{gr}=48 MPa; d) σ_{pl}^{gr} = 62.4 MPa; e) σ_{pl}^{gr}=76.8 MPa. In plates gross section the nominal calculation stress corresponded to: a) $\sigma_{str}^{calc.gr}$ =0 N; b) $\sigma_{str}^{calc.gr}$=50 MPa; c) $\sigma_{str}^{calc.gr}$=100 MPa; d) $\sigma_{str}^{calc.gr}$=130 MPa; e) $\sigma_{str}^{calc.gr}$=160 MPa.

Considering symmetry of the specimen and kind of the external stress application, during calculation only 1/4 model was considered under

corresponding gripping conditions. During the restriction of model displacement along axis Z for all joints laying on the plate end surface in the point of the external stress application zero displacement along Z component were set. Restrictions for X and Y components of a displacement vector were set on symmetry model planes. (Fig. 3.42). In the design model it was taken that the bolt body washer and nut represent the whole volume from bolt material.

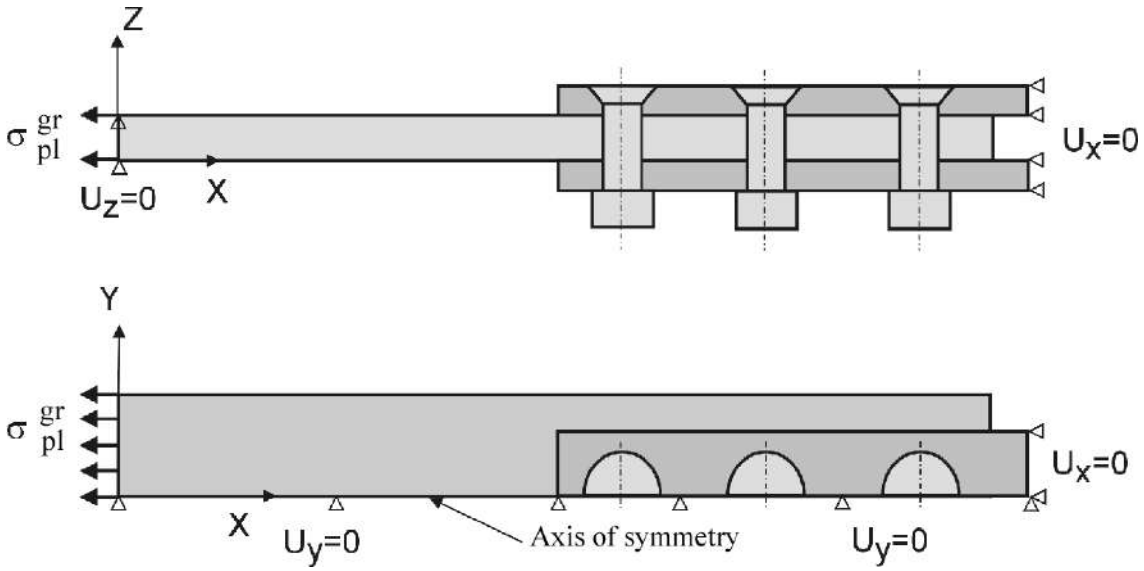

Fig. 3.42. Design model of double-shear three-row countersunk bolt joint

The finite element representation model (Fig. 3.43, 3.44) consists of volumetric eight-node elements SOLID45, and also contact elements CONTA173, TARGE170 and the tightening elements PRETS179 presented in the system ANSYS [474].

The radial interference was modelled by means of realization of "initial penetration" effect in contact algorithm by bolt body into hole wall. For the modelling of contact interaction the contact model "surface into surface" was chosen and also the elastic Coulomb friction model with friction coefficient 0.15 was used. The axial interference of bolt and prestressed condition in joint members, which arises as a result of the axial interference application, was modelled using the special tightening member PRETS179. Preliminarily meshed bolt was "dissected" into two parts, and on junctions of the finite elements lying in dissected section, special tightening members PRETS179 were generated by the way of insertion. Contact members CONTA173 and TARGE170 were generated on contact surfaces of a plate with the upper and lower straps and bolts with hole walls in a pack.

At the first stage of the mode of deformation of joint members analysis the deformation nature and distribution of equivalent stresses in joint members were considered at level of external extension strain $\sigma_{str}^{calc.gr}$ = 100 MPa (Fig. 3.45, 3.46).

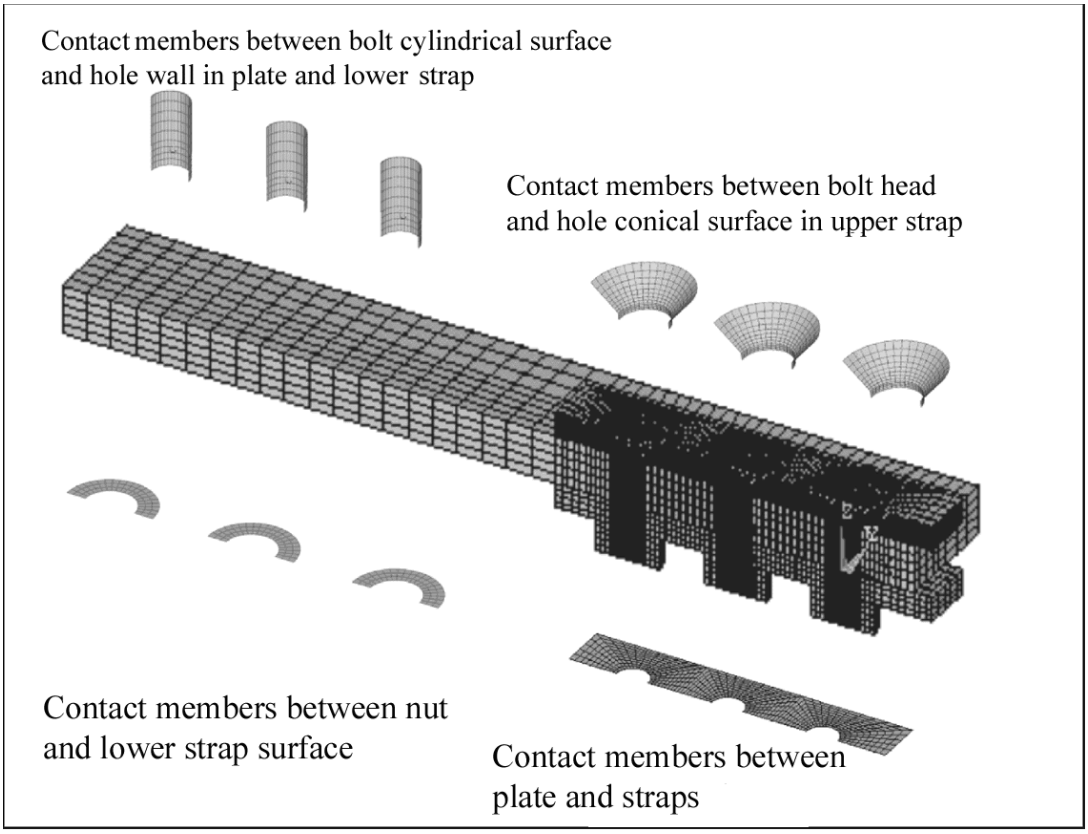

Fig. 3.43. The finite element representation model of double-shear single-row countersunk bolt joint

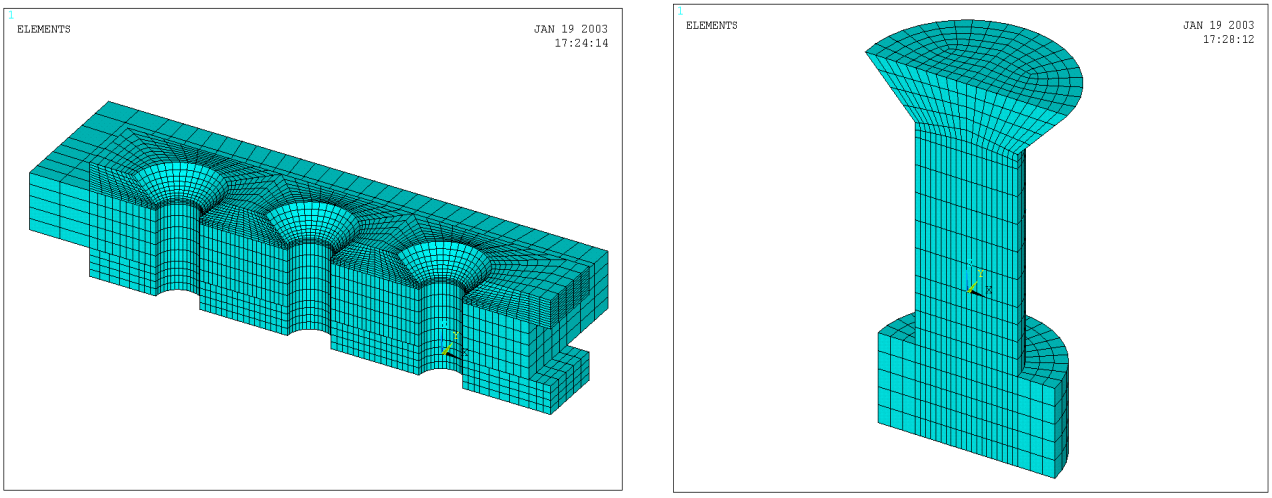

a b

Fig. 3.44. Fragments of the finite element representation model: a – is a plate with straps; b – is bolt with a nut

As a result of different compliance of the upper and lower straps the stress transfer in the joint occurs with eccentricity which leads to the bending joint. (see Fig. 3.45).

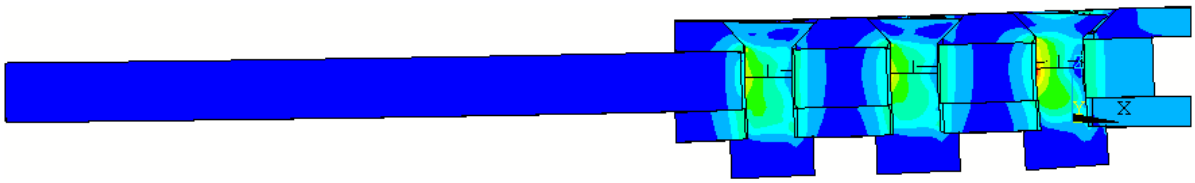

Fig. 3.45. Deformation nature of joint members under external tensile stress $\sigma_{str}^{calc.gr}$ = 100 MPa (displacement scale – 20:1)

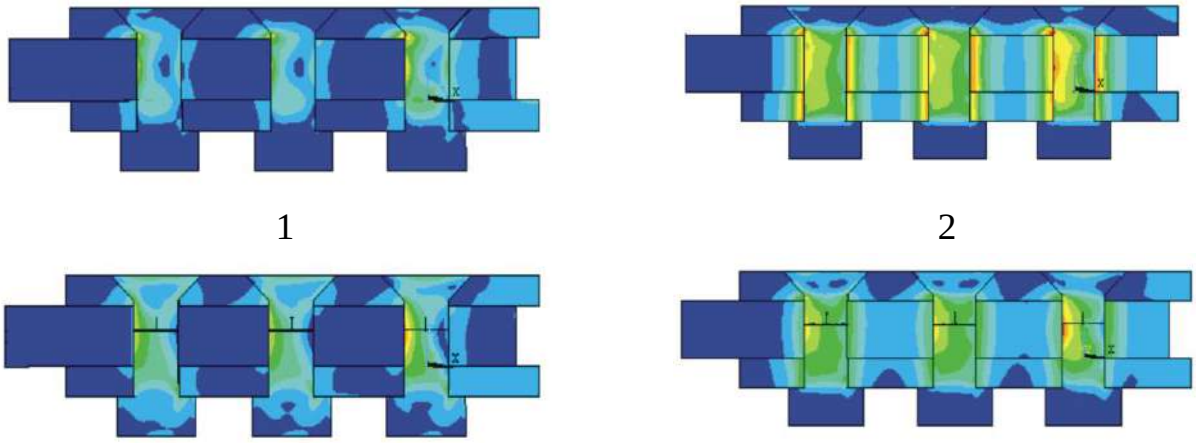

Fig. 3.46. Nature of equivalent stresses distribution in joint members at stress level σ_{pl}^{gr} = 48 MPa ($\sigma_{str}^{calc.gr}$ = 100 MPa)

In Fig. 3.46 we can see that the most intensive equivalent stresses in joint members arise in zones of their connection with countersunk bolts. It is notable that as a result of the external tensile stress application the bolt works in bending, and the most intensive bending stresses appear in bolt body of an extreme row. In works [114 – 116, 118, 119, 121, 143, 159, 160, 162, 164-166, 168] the results of the analysis of local mode of deformation characteristics in the members of three-row countersunk and non-countersunk shear bolted joints are represented in part.

The analysis of contact pressure distribution between a plate and joint straps under the condition of different kinds of bolt installation is listed below (Fig. 3.47, 3.48).

The most intensive contact pressures between a plate and straps arise in zones of holes for bolt installation. For quantitative estimation of these values in Fig. 3.49 the path, on which values of contact pressures between a plate and straps (Fig. 3.50, 3.51) will be deduced, is shown.

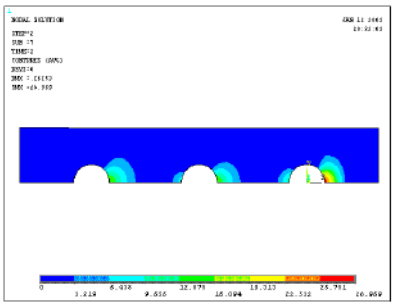

1

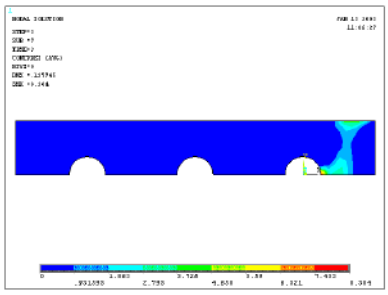

2

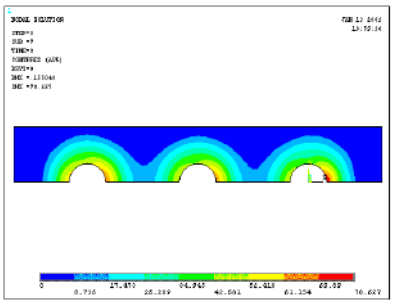

3

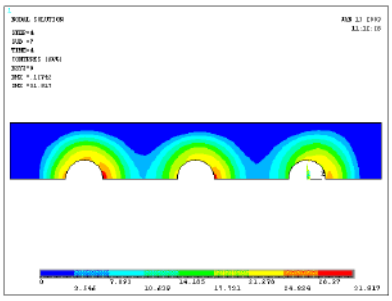

4

Fig. 3.47. Contact pressures distribution field between the lower strap and the plate with various bolt installation and external stress level

σ_{pl}^{gr} =48 MPa ($\sigma_{str}^{calc.gr}$ =100 MPa)

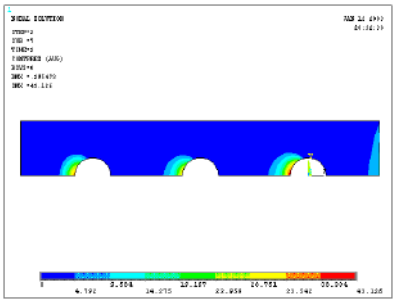

1

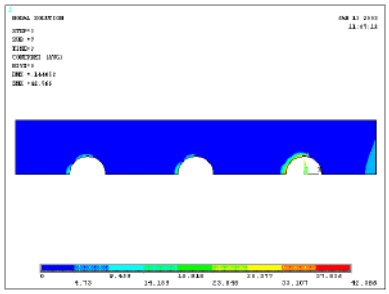

2

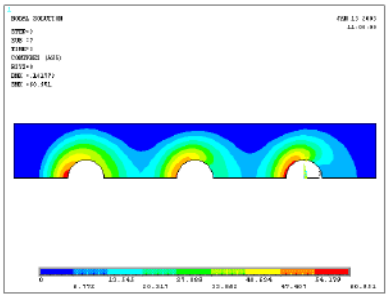

3

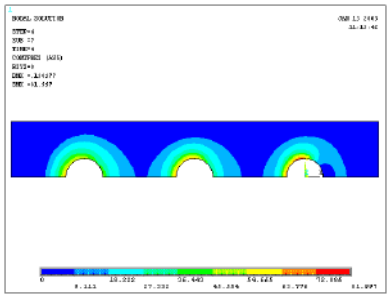

4

Fig. 3.48. Contact pressures distribution field between the lower strap and the plate with various bolt installations and external stress level

σ_{pl}^{gr} =48 MPa ($\sigma_{str}^{calc.gr}$ =100 MPa)

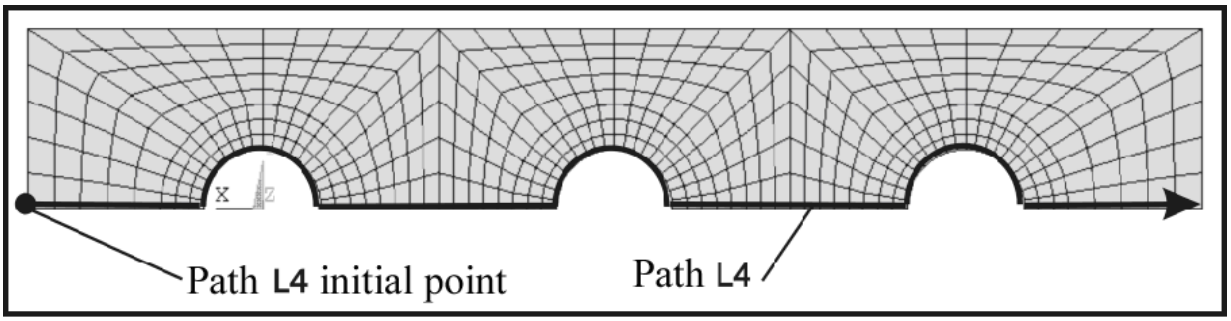

Fig. 3.49. The display of path L4 on which values of contact pressures between mating surfaces of a plate and straps are deduced

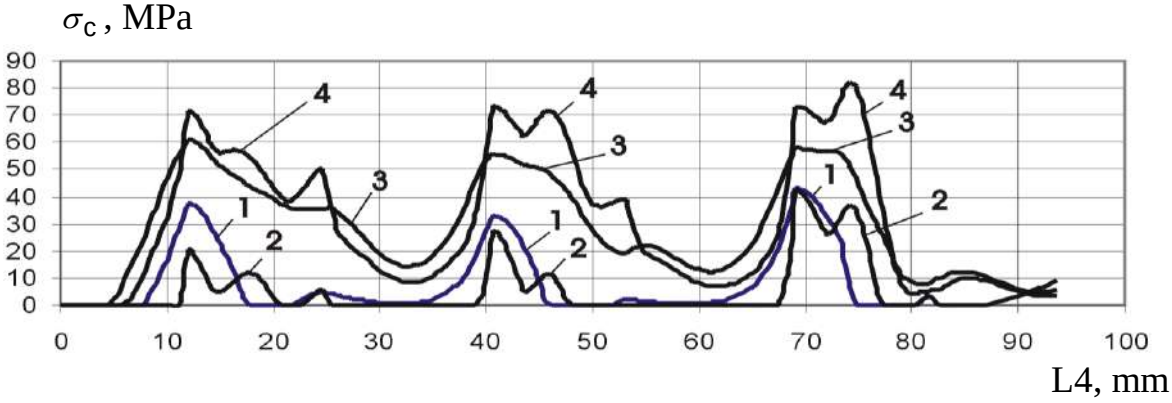

Fig. 3.50. Nature of bolt installation type influence on contact pressures distributions between a plate and the upper straps under external stress level σ_{pl}^{gr} = 48 MPa

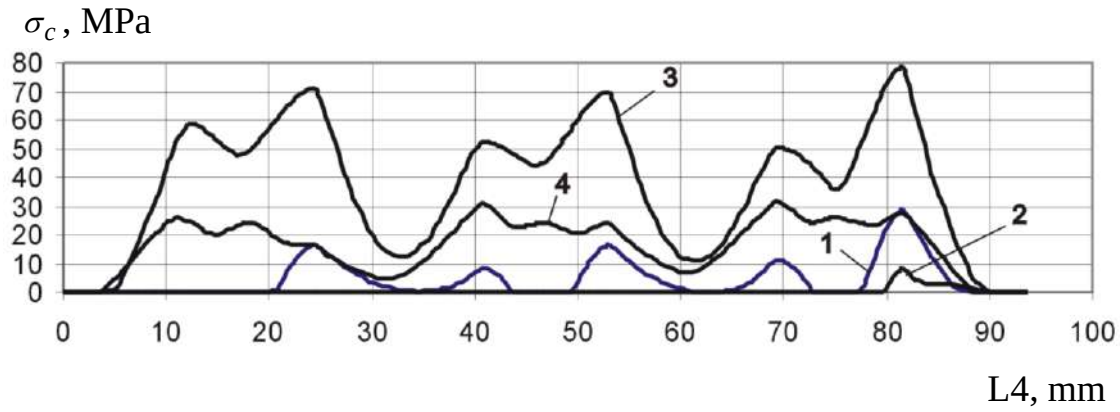

Fig. 3.51 Nature of bolt installation type influence on contact pressures distribution between the lower strap and the plate under external stress level σ_{pl}^{gr} =48 MPa ($\sigma_{str}^{calc.gr}$ =100 MPa)

As seen from Fig. 3.50, 3.51, contact pressures between plate and upper strap reach maximum under the bolt installation with a radial interference 1%d_b and axial tightening P_t = 10 kN in the hole zone for installing the first row of countersunk bolts (σ_c = 83 MPa). Between a plate and the lower strap contact

pressures reach maximum in the hole zone of the first row of countersunk bolts and reach values of σ_c = 80 MPa.

From these investigations it is possible to draw the following conclusions:

1. If the bolt without radial and axial interferences is installed, the maximum contact pressures arise between the bolt and cylindrical portion of hole in the upper strap and reach value of 450 MPa under stress $\sigma_{str}^{calc.gr}$ = 100 MPa. The clearance size between bolt body and hole wall in a plate reaches 0.15 mm ($\sigma_{str}^{calc.gr}$ = 100 MPa); between the upper strap and bolt – 0.05 mm; between bolt and the lower strap it equals 0.05 mm. It should be noted that formation of clearances between bolt of extreme row and hole wall in a package begins practically at once with applying external tensile strain.

2. If the bolt with radial interference $1\% d_b$ and external stress level $\sigma_{str}^{calc.gr}$ = 100 MPa is installed, contact pressures between bolt and wall of cylindrical portion of hole in the upper strap reach 500 MPa, and clearance size is equal to 0.036 mm in the zone of a cylindrical portion of hole in the upper strap (in this case nearby the beginning of countersinking the clearance between bolt head and hole wall is not formed owing to the bend of bolt and the upper strap). Between the bolt and the hole wall in a plate and the lower strap the clearance is not formed. As a result of bending the bolt and the joint as a whole, contact pressures between the bolt and the hole wall in a plate reach 290 MPa near the lower edge of hole in a plate, between the bolt and the lower strap they reach 250 MPa.

3. If the bolt with axial tightening P_t =10 kN and external stress $\sigma_{str}^{calc.gr}$ =100 MPa is installed, contact pressures between the bolt head and hole wall in a plate reach value of 100 MPa, and the clearance between the bolt and the upper strap exists only in the zone of cylindrical part of the hole in the strap. Contact pressures between the bolt and the hole wall in a plate reach value of 150 MPa, and sizes of clearances are equal to 0.01 mm. Between the bolt and the lower strap contact pressures are at the level of 240 MPa, and clearances are equal to 0.015 mm.

4. If the bolt is installed with radial interference $1\% d_b$ and an axial tightening P_t = 10 kN and operational level of external stress value, contact pressures between bolt and hole wall in the upper strap reach 490 MPa, between bolt and hole wall in a plate – 280 MPa, between bolt and hole wall in the lower strap – 240 MPa. The clearance between bolt body and hole wall in a package at operational level of external stress is not formed.

5. Comparing the calculation results of clearances between the bolt body and hole wall in the upper strap, it is necessary to should be noted that during the bolt installation with axial tightening and radial interference in single-row joint the

clearance is formed at $\sigma_{str}^{calc.gr}$ =100 MPa, but in three-row joint at $\sigma_{str}^{calc.gr}$ =130 MPa and is practically twice as little as (0.005 and 0.01 mm respectively). Under the stress of $\sigma_{str}^{calc.gr}$ = 130 MPa the clearance size between bolt and the upper strap is equal to 0.05 mm at single-row joint and 0.019 mm – at three-row joint.

6. It is determined that application of axial and radial interferences facilitates to prevent formation of clearances between a countersunk bolt and hole wall in a package at stress operational level of the joint made of aluminum alloy Д16АТ. Using of radial and axial interferences of countersunk bolts allows to lower the amplitude of maximum zero-to compression equivalent pressures in 3.5 times at stress operational level in comparison with a variant of bolt installation without radial and axial interferences. The use of elastoplastic interference in combination with an axial tightening also allows to achieve leakproofness of the joint under external operating load.

3.3. INVESTIGATION OF DURABILITY OF STANDARD COUNTERSUNK BOLTED JOINTS MODELS

3.3.1. Durability of double-shear single-row bolted joints

Durability investigation of double-shear single-row bolted joints specimens (Fig. 3.52) is carried out during cyclic tension.

The connected parts of specimens working under tension were made of anodized «НХ» Д16АТл10 sheets, and straps with thickness $\delta_1 = \delta_2$ – of Д16АТл5 sheet. The joint was performed with steel countersunk bolts 5015А and titanic bolts ОСТ 1.12086-77. Nominal diameter of bolts was 8 mm.

Bolts were pressed in hole by R-10 machine. The insertion force of steel bolts 5015А was 8 kN, titanic bolts ОСТ 1.12086-77 – 18 kN. While pressing-in, the bolts with the radial interference 0.8 – 1.2%d_b were installed (where d_b is a diameter of bolt body).

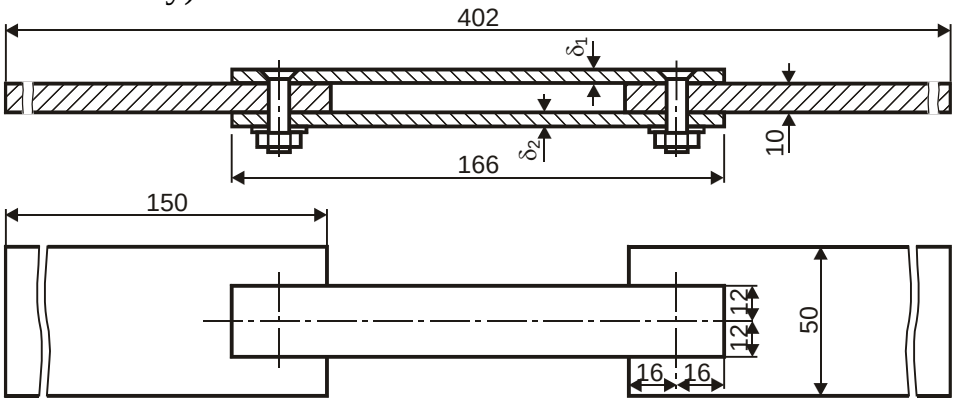

Fig. 3.52. Double-shear single-row bolted joints specimens

Tightening the nuts was carried out with torque wrench: in the beginning by the torque $M_{nut\,torq}$=25 N·m, then unloading was carried out to $M_{nut\,torq}$ = 0 N·m and a final tightening of nuts $M_{nut\,torq}$ = 20 N·m according to OCT 1.00017-77.

Fatigue tests of specimens were conducted on hydraulic pulsator ЦДМ-10Пу at five levels of cyclic loading with frequency of 13 Hz, cycle asymmetry ratio R_σ = 0.1 and maximal cyclic loading P_{max} = 35, 30, 25 and 20 kN (σ_{p0}^{gr} = 138, 119, 99 and 79 MPa respectively).

At loadings level P_{max}=35 kN two specimens were tested, at P_{max}=30 kN three specimens, at P_{max}=25 кN – four specimens, at P_{max}=20 кN – eight specimens.

The majority of the tested specimens failed on straps of Д16АТл5 sheet in sections on plates edge made of Д16АТл10 sheet in a zone of intensive fretting corrosion growth. In two specimens which achieved the level of 203700 loading cycles before failure and 226300 loading cycles before failure at P_{max}=30 kN (σ_{p0}^{gr}=119 MPa) and at P_{max}=25 kN (σ_{p0}^{gr} = 99 MPa) respectively, fatigue cracks developed in straps, in section on a plate edge made of Д16АТл10 sheet and in section on edge of bolt body in a zone of countersunk socket for embedded countersunk bolt head.

In two specimens, which achieved the level of 217100 and 569000 loading cycles at P_{max}=30 kN and P_{max}=25 kN respectively, fatigue cracks developed in sections of plates made of Д16АТл5 sheet along the hole axis for bolts.

Results of fatigue tests are presented in Fig. 3.53, curve 3. Points of curves are calculated by average values N at each loading level, the intervals of values dispersion for each type of specimens are also shown on the graph.

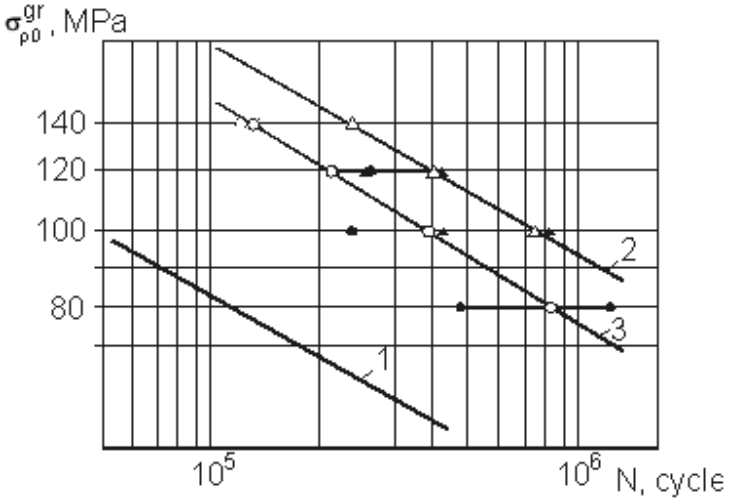

Fig. 3.53. Fatigue curves:

1 – plate with countersunk hole, anodized; 2 – plate filled with a countersunk bolt with radial interferences Δ=(10,2) % d_b) and axial ($M_{nut\,torq}$=20 N·м); 3 – single-row double-shear joint with radial and axial interferences

Expression for fatigue curve of double-shear single-row joints specimens with straps in $\delta_1 = \delta_2 = 5$ mm thickness at their failure in strap zone caused by the fretting-corrosion is as the form

$$N_{fr} \cdot \sigma^{3.2977} = 1.48473 \cdot 10^{12} \quad \text{or} \quad \sigma = 4.90852 \cdot 10^3 \cdot N^{-0.303242}.$$

According to tests results the coefficient $k_{bear.fr}$ for bolted joints made with bolts with a countersunk head is defined, under specimens failure caused by intensive action of fretting corrosion between the strap and plate:

$$k_{bear.fr} = \frac{4.90852 \cdot 10^3 \cdot N^{-0.303242}}{5.16829 \cdot 10^3 \cdot N^{-0.29213}(B/d)} = 0.35097 \cdot N^{0.0111},$$

And the coefficient k_t under specimens failure caused by the fretting corrosion and in section of hole for a bolt was also defined:

$$k_{bear} = \frac{7.62293 \cdot 10^3 \cdot N^{-0.32519}}{5.16829 \cdot 10^3 \cdot N^{-0.29213}(B/d)} = 0.5177 \cdot N^{0.0219}.$$

3.3.2. Durability of double-shear three-row countersunk joints with straps of equal thickness

The durability test of specimens of three-row counetrsunk joints was carried out (Fig. 3.54).

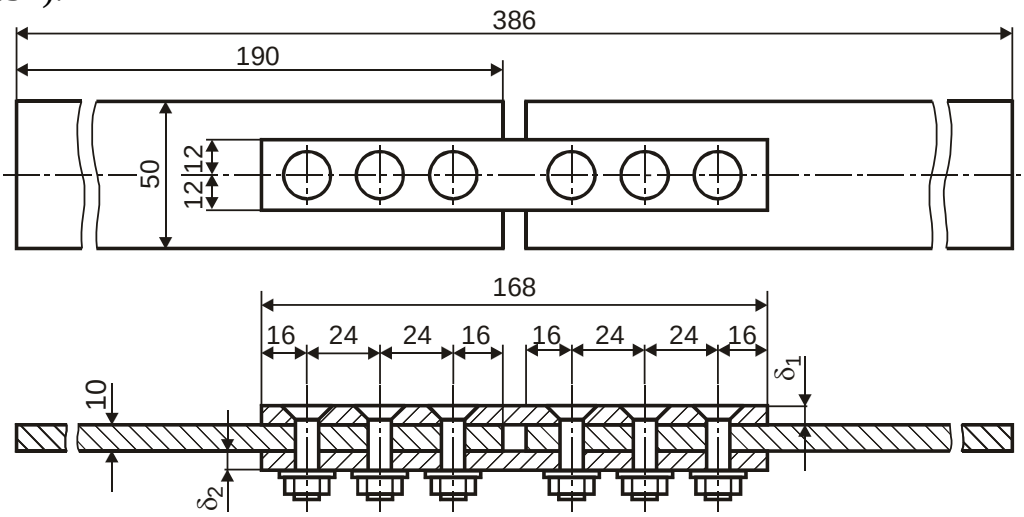

Fig 3.54. Specimens of double-shear three-row joints

Connected parts were made of sheet of Д16АТ material in 10 mm nominal thickness, straps were made of sheet of Д16АТ material in $\delta_1 = \delta_2 = 5$ mm nominal thickness.

Parts being connected were anodized with "НХ".

The joint was made with titanic bolts ОСТ1.12086-77 8 mm in diameter.

Bolts were pressed in holes by machine R-10. The prepressing force of bolts was 18 kN. The placing of bolts with the radial interference equal to 0.8 –

1.2% d_b (where d_b is a bolt body diameter) was provided during pressing.

Tightening the nuts was carried out with torque wrench: in the beginning with the torque equals 25 N·m, then unloading was carried out to $M_{nut\ torq}$ = 0 N m and final tightening of nuts to 20 N ·m according to OCT 1.00017-77.

Fatigue tests were carried out on a hydraulic pulsator ЦДМ-10Пу at levels of cyclic loading with frequency 13 Hz in stress ratio R_σ = 0.1 and the maximum cyclic loadings $P_{\max}$ equal 35, 30, 25, 20 and 17.7 kN (σ_{p0}^{gr} = 138, 119, 99, 79 and 70 MPa).

At each level of loadings four specimens were tested.

All tested specimens failed on straps in area of part tips located in the middle in a zone of intensive fretting corrosion on mating surfaces.

Results of fatigue tests are presented in Fig. 3.55, curve 4. Points of curves are calculated by average values of *N* at each loading level, intervals of values dispersion for each type of specimens are also shown on the graph.

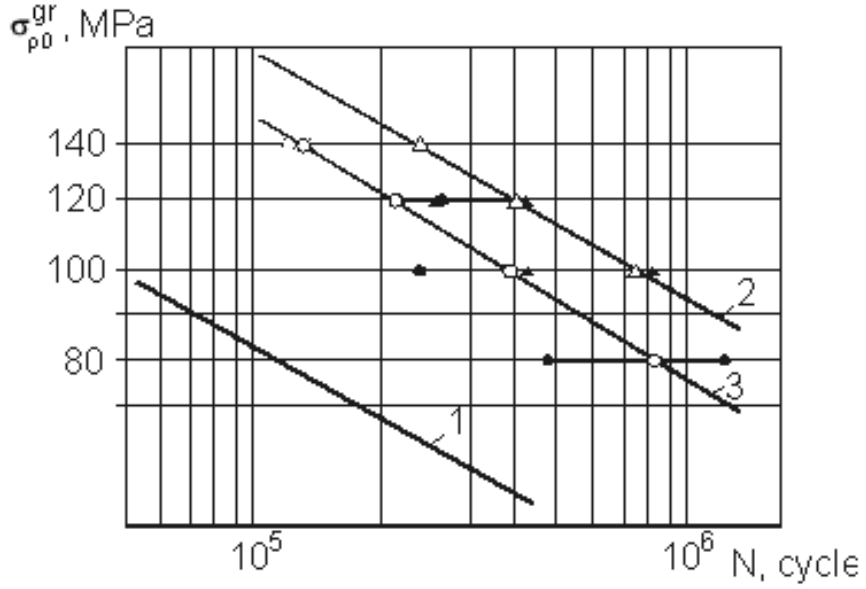

Fig. 3.55. Fatigue curves:
1 – anodized plate with a countersunk hole; 2 – plate with hole filled with a countersunk bolt with radial and axial interferences; 3 – single-row double-shear joint with radial and axial interferences; 4 – three-row double-shear joint with radial and axial interferences

The expression for fatigue curve of double-shear three-row joint specimens with plates $\delta_1 = \delta_2$ = 5 mm is the following

$$N_{fr} \cdot \sigma^{3.066} = 5.95009 \cdot 10^{11} \text{ or } \sigma = 6.92393 \cdot 10^3 \cdot N_{fr}^{-0.326158}.$$

Results of calculation and experiment are reduced in Tables 3.1.

Tables 3.1

$P_{\max}$, N	P_0^{gr}, N	$\sigma_{\partial 0}^{gr}$, MPa	N_{calc}, cycle	$N_{\exp}$, cycle	$\Delta = \frac{\lvert N_{\exp} - N_{calc} \rvert}{N_{\exp}} \cdot 100$
30 000	28 460	119	230 900	257 600	10.4%
25 000	23 720	99	398 000	452 800	12.1%
20 000	18 970	79	775 000	904 500	14.3%
17 700	16 790	70	1 116 000	1 311 000	14.9%

From calculation the convergence of calculation results with experimental data is obvious.

Results of investigations are presented in Fig. 3.56.

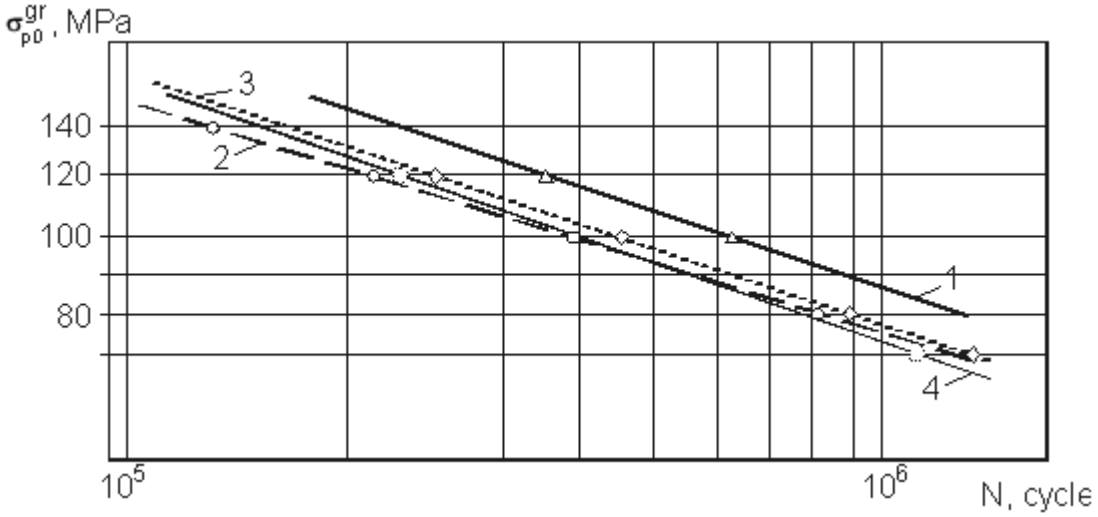

Fig. 3.56. Fatigue curves:
1 – plates with hole filled with countersunk bolt with interference and tightening; 2 – plates of single-row double-shear countersunk joint; 3 – plates of three-row double-shear countersunk joint (curve obtained by results of experiment); 4 – calculated fatigue curve of plates of three-row double-shear joint with interference and tightening

Experiment-calculated dependence is developed by the results of the carried out investigations for predicting fatigue of multi-row countersunk double-shear bolted joints executed with axial and radial interferences.

3.4. Design procedure of force distribution between rows in shear bolted joints of aircraft structures by means of ANSYS engineering analysis system

Shear bolted joints between themselves are one of standard joints of airframe structural members. Designing such joints includes force determination transferred by each bolt in multi-row joints [456].

Existing experimental-calculated methods [209, 236, 446, 459, 475, 477] allow to determine quantitative and qualitative nature of force distribution between bolts in multi-row shear joints. Force method is applied to them, design models in which bolt is considered as a bem lying on elastic basis can also be applied (Fig. 3.57).

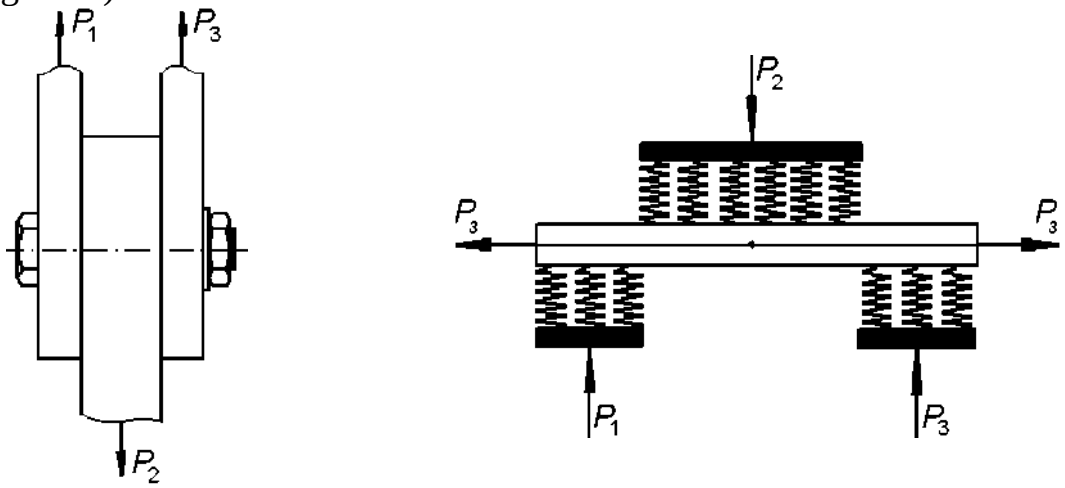

Fig. 3.57. Single-bolted shear joint and interactions diagram of its members

However, similar problems are solved in flat setting without taking into consideration the volume contact interaction of joint members and their influence on change of the local mode of deformation in members. For account of structurally-technological features of connected members the program finite element packages are usually used allowing to solve a problem in spatial setting taking into consideration non-linear dependence "loading – displacement" [474]. The given technique is applicable to standard models of joints. But during the calculation of effort distribution in multi-row shear joints of real power airframe members of on personal computers necessary time for performance of calculations exceeds 24 hours. It takes a lot of considerable machine time to solve the problems with contact interaction of joint members.

For the majority of the developed design procedures of force distribution on rows of shear joint it is necessary to determine the values of relative displacement of members of the single-row joint, including the following deformations: bearing stress of hole walls $\delta_{h.bear}$, bearing stress of bolt walls $\delta_{b.bear}$, bend and shift of bolt $\delta_{b.bend}$ and $\delta_{b.shift}$ respectively.

Many experts carried out experimental investigations in order to determine the influence of applied load on the value of relative displacement of joint members.

In the work [446] the specimens of single-bolted joints were tested (Fig. 3.58). On the central plate along the line of bolt axis the bracket A was set on the glue, in which two dial gauges B were built in. Plungers of dial gauges were rested against a cross-beam C, which was fixed to external strips along the line of bolt axis.

Displacement values were measured from two sides of the specimen to reduce experimental error.

In the work [84] joint compliance was determined by means of the appliance shown in Fig. 3.59.

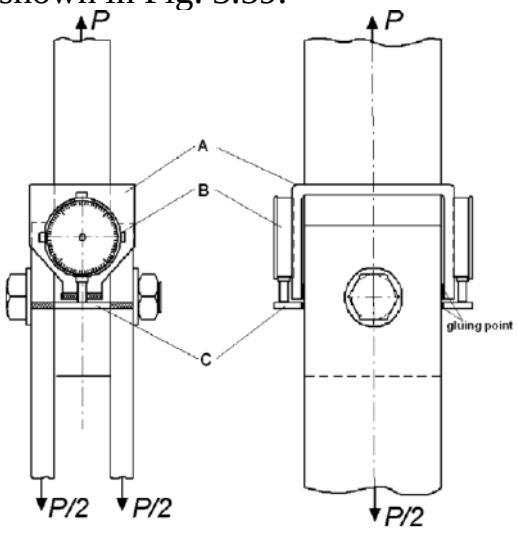

Fig. 3.58. Specimen for determination of relative displacement of connected plates

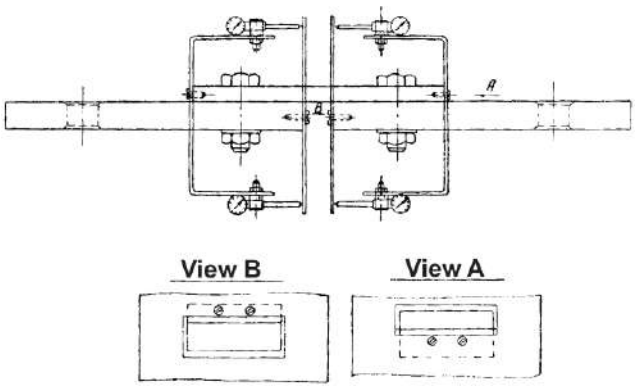

Fig. 3.59. Diagram of the appliance for determination of joint compliance

In this case the displacements caused by turn of the free plates ends were considered. The half-sum of paired indicators readings determined relative displacements of free ends of bolted joints members of the specimen corresponding to the next loading stage.

Known Swift's empirical dependence for definition of joint connection compliance with specified geometrical parameters and material properties of joint members is presented:

$$C = \frac{5}{E_3 d_3} + 0{,}8\left[\frac{1}{E_1\ d_1} + \frac{1}{E_2\ d_2}\right], \qquad (3.2)$$

where E_1, E_2 and E_3 are moduli of the elasticity connected members and fasteners; h_1, h_2 – thicknesses of connected members; d_3 is fastener diameter.

However dependence (3.2) determines value of joint compliance only in an elastic zone of loading and does not consider the way of bolt installation in hole. Therefore for solving each specific calculation task of force distribution between rows it is required to carry on tests of specially made specimens and to define the nature of external loading influence and fastener type on dependence "loading – displacement" of single-row joint.

The purpose of this investigation is the development of design procedure of joint compliance and force distribution between rows in shear bolted joints of aircraft structures under elastic and elastoplastic deformation by means of ANSYS engineering analysis system without carrying out experimental

investigations.

To realize this purpose ANSYS system was used to investigate the external loading influence and nature of bolt installation on the mutual displacement value of connected members of single-bolt double-shear joints (Fig. 3.60) consisting of dural (Д16Т) central plate 10 mm in thickness and 50 mm in width and two steel (30ХГСА) plates 5 mm in thickness and 50 mm in width connected with a bolt ∅16 mm in diameter made of 30ХГСА steel. Considering the geometrical symmetry of the specimen in the design diagram (Fig. 3.61) 1/4 the model with corresponding conditions of fastening was considered.

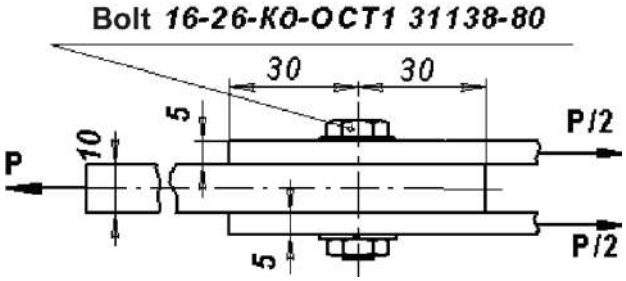

Fig. 3.60. Geometrical model of single-bolt double-shear joint specimen executed to determine fastener compliance

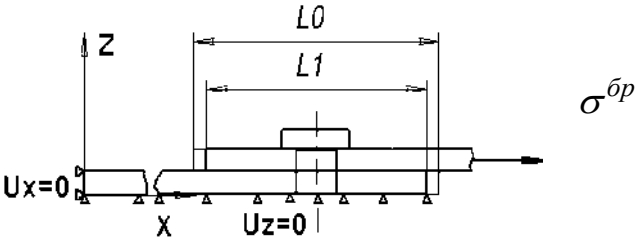

Fig. 3.61. Design diagram of single-bolt double-shear joint

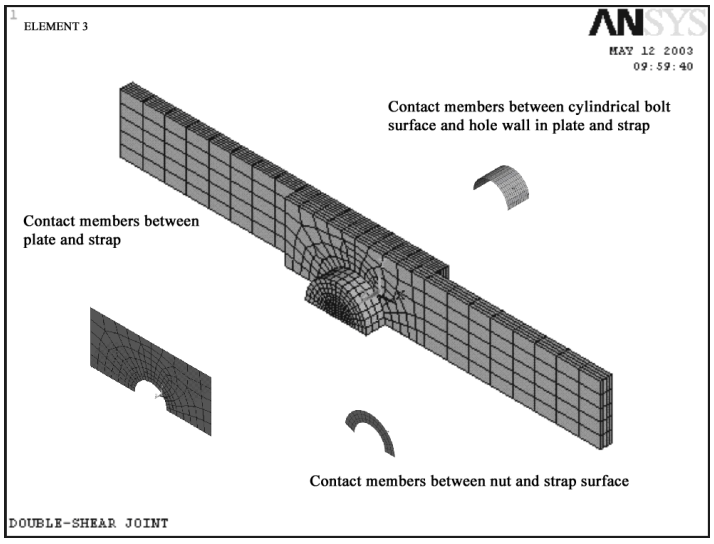

Fig. 3.62. The finite element model of single-bolt double-shear joint specimen

During the process of calculation the contact interaction of bolt body and hole walls in a package, the central plate and straps, bolt nut and strap nut was considered. The finite element model (Fig. 3.62) of the joint consists of volumetric eight-nodal members SOLID45, contact members CONTA173, TARGE170 and tightening elements PRETS179 presented in system ANSYS [474].

Relative displacement of free end surfaces was defined by difference $\Delta = L0 - L1$. Measurements of relative displacements of connected plates were carried out along relative displacements of free end surfaces of connected members (see Fig. 3.61).

The influence of external loading value and bolt installation method into hole on the nature of joint compliance change was investigated. The following variants

of bolt installation were considered: 1 – without radial and axial interferences; 2 – with radial interference 0.5% d_b; 3 – with radial interference 0.75% d_b; 4 – with radial interference 1 % d_b; 5 – with axial tightening 50 kN; 6 – with axial tightening 100 kN; 7 – with radial interference 0.75% d_b and axial tightening 100 kN.

Fig. 3.63 shows the nature of external tensile stress influence and the type of bolt installation method on the relative displacement of joint members of single-bolt double-shear joints for variants of bolt installation specified above.

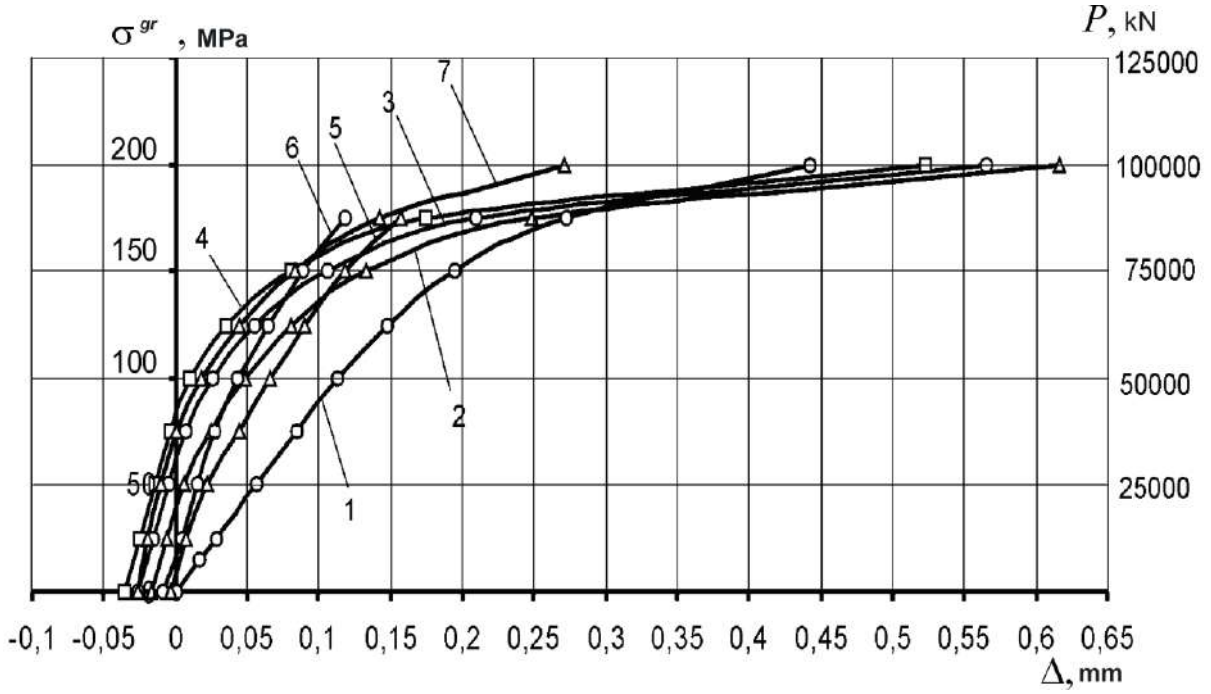

Fig. 3.63. The influence of loading level (P, H) and bolt installation method on the value of relative displacement of single-bolt double-shear joint members

As is seen from this figure, the bolt installation method makes substantial impact on change of connected plates mutual displacement nature under loading in comparison with the variant of bolt installation without interference and clearance. For quantitative estimation of this influence the joint compliance depending on value of external loading was calculated:

$$C = \delta\Delta / \delta P,$$

where $\delta\Delta$ is an increment of relative displacement of joint members, mm;
δP is an increment of external loading, N.

In Fig. 3.64 – 3.69 the influence of external loading value and bolt installation method on the joint compliance change nature is shown.

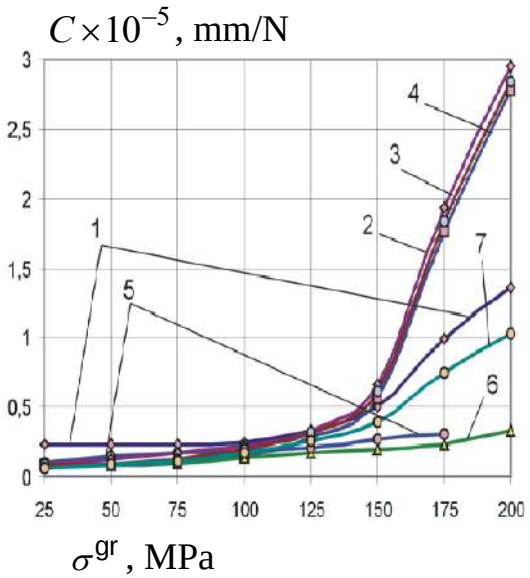

Fig. 3.64. The influence of external loading level(σ^{gr}) and bolt installation method on the value of single-bolt double-shear joint

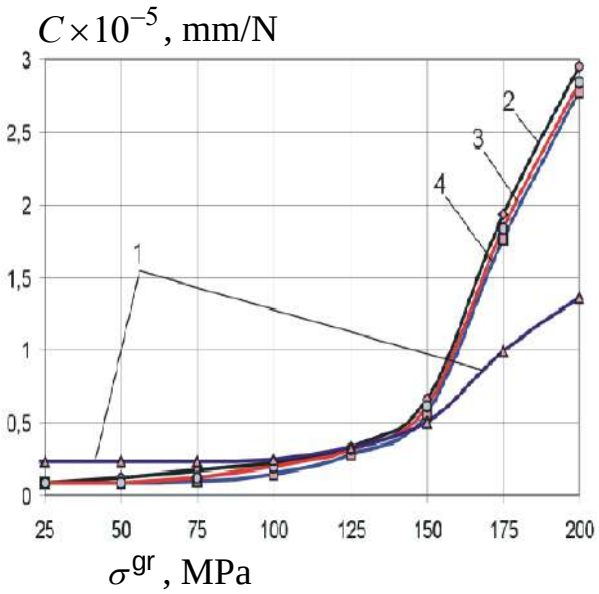

Fig. 3.65. The influence of external loading level(σ^{gr}) and the value of radial interference % d_b on the value of flexibility of single-bolt double-shear joint

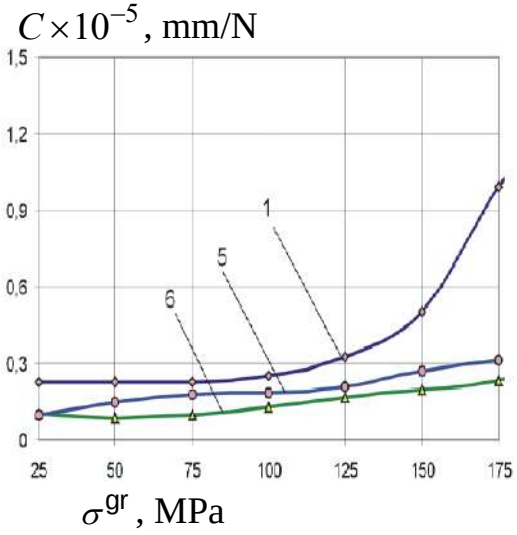

Fig. 3.66. The influence of external loading level(σ^{gr}) and the extent of axial tightening P_t on the value of single-bolt double-shear joint compliance

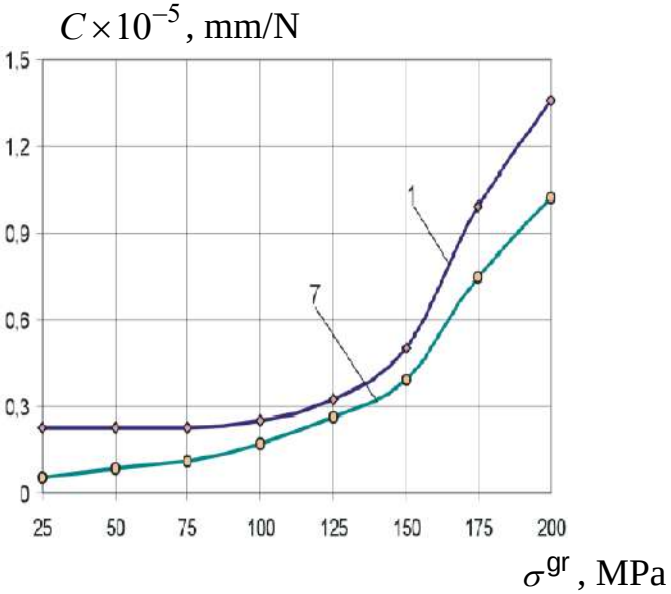

Fig. 3.67. The influence of combined application of axial and radial interferences on the value of joint compliance when changing the external loading level (σ^{gr})

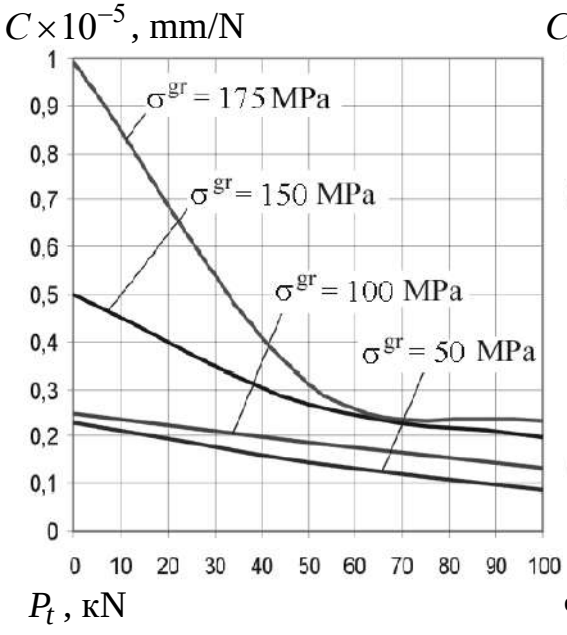

Fig. 3.68. The influence of external loading level(σ^{gr}, MPa) and the extent of axial tightening on the value of single-bolt double-shear joint compliance

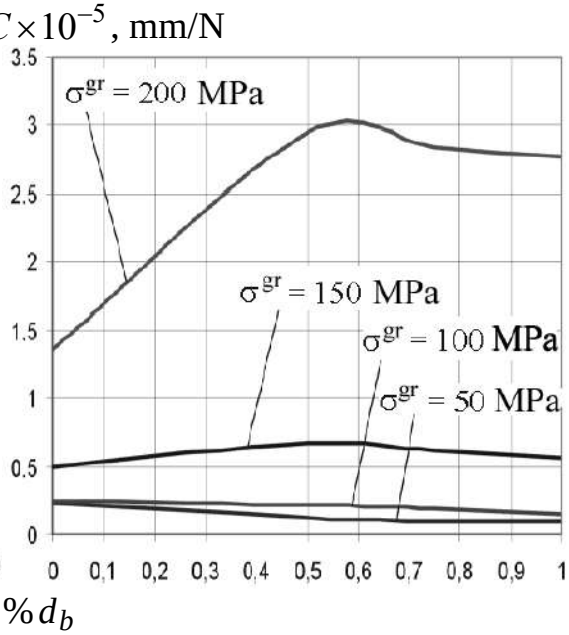

Fig. 3.69. The influence of external loading level(σ^{gr}, MPa)and the extent of radial interference $\%d_b$ on the value of single-bolt double-shear joint compliance

Application of radial interference increases the angle of slope of curve $P=f\backslash(\Delta)$ on a linear section (see Fig. 3.63), and consequently, decreases joint compliance. At the level of external loading σ^{gr} = 25 MPa the radial interference reduces the joint compliance in 2.5 times. With further increase of external loading, the value of a radial interference 0.5 … 1% d_b practically does not influence the change of joint compliance. For σ^{gr} > 150 MPa the use of a radial interference 0.5 … 1 % increases the value of joint compliance in two times.

The axial tightening reduces the bolted joint compliance. At the level of external loading σ^{gr} = 100 MPa the axial tightening 100 kN reduces joint compliance in two times in comparison with joint compliance with bolt installed without radial and axial interferences. As the level of external loading increases, the joint compliance with bolt installed with axial tightening 50 … 100 kN slightly changes.

With combined application of an axial tightening 100 kN and a radial interference of 0.75 % d_b, the joint compliance is 1.4 times lower in comparison with joint compliance with bolt installed without radial and axial interferences.

The compliance of straps connection with the central plate in an elastic loading zone for the variant of bolt installation without elastoplastic interference is equal to $2.27\cdot10^{-6}$ mm/n. This value was compared with the compliance value calculated by the Swift's formula:

$$C = 0.5\left[\frac{5}{E_3 \cdot d_3} + 0.8\left(\frac{1}{E_1 \cdot d_1} + \frac{1}{E_2 \cdot d_2}\right)\right] =$$

$$= 0.5\left[\frac{5}{200000 \cdot 16} + 0.8\left(\frac{1}{70000 \cdot 5} + \frac{1}{200000 \cdot 5}\right)\right] = 2.324 \cdot 10^{-6} \text{ мм/Н}.$$

As is seen, the compliance values obtained by this formula and as a result of solving the finite element problem, differ by 2.3 %, and they can be used for obtaining dependences "loading – displacement" calculations by the finite element method of without expensive specimens tests.

Knowing the dependence of compliance change on external loading for single-bolted joint, it is possible to determine the force distribution nature in multi-row bolted joint having the corresponding geometrical dimensions. At number of rows more than five it is reasonable to replace each fastener with the link adequately reflecting joint flexibility with a real fastener. In ANSYS system this link can be presented by member COMBIN39 having properties of a non-linear spring, for which the deformation rule is set in advance. In this case it corresponds to the deformation nature of single-bolted joint.

For the specified member one degree of freedom is chosen (for example, along axis X, in a direction of action arising in force combination). While selecting an option of one degree of freedom of a member the spatial position of nodes "i" and "j" of the COMBIN39 member is of no significance. The only requirement to the selection of their placing is conformity of member deformation to the chosen rule, i.e. if the deformation rule from external tensile loading is chosen for the member, then there will be no response of the member during its compression. Nodes "i" and "j" of COMBIN39 member are connected with nodes of joint model (Fig. 3.70), lying in sections at distance of a half-pitch from the holes axis, by the equations of combined displacement moving along axis X. In addition, special element COMBIN39 works in tension, as is shown in Fig. 3.70.

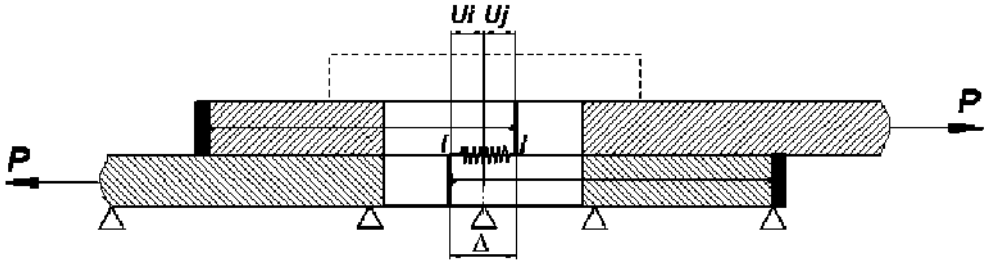

Fig. 3.70. Determination of relative displacement of single-bolted joints connected plates and modeling it by special member COMBIN39

The design procedure of force distribution between rows in a joint includes:

1. Creation of three-dimensional model of a design with bolted joints included into it in CAD-system.

2. Determination of the dependence "loading – displacement" for each available fastening connection with taking into consideration the fastener

installation type. For this purpose it is necessary to have results of an experimental investigation of corresponding specimens of joints or to determine the joint compliance by means of ANSYS system.

3. Development of the design diagram, selection of finite elements type and specifying material properties, creation of corresponding finite element model of the structure, generating special elements COMBIN39 with the specification of properties and inclusion of all necessary options, the applying of operating loads and specifying the respective conditions of fastening.

4. Problem calculation and the analysis of force distribution nature on rows of fasteners.

As object of investigation for developing the design procedure of force distribution between rows the specimen of eight-row double-shear bolted joint is chosen (Fig. 3.71), as the central plate connected to the upper and lower straps by □∅16 mm bolts. Thickness of a plate and straps is 10 and 5 mm respectively, width is 50 mm.

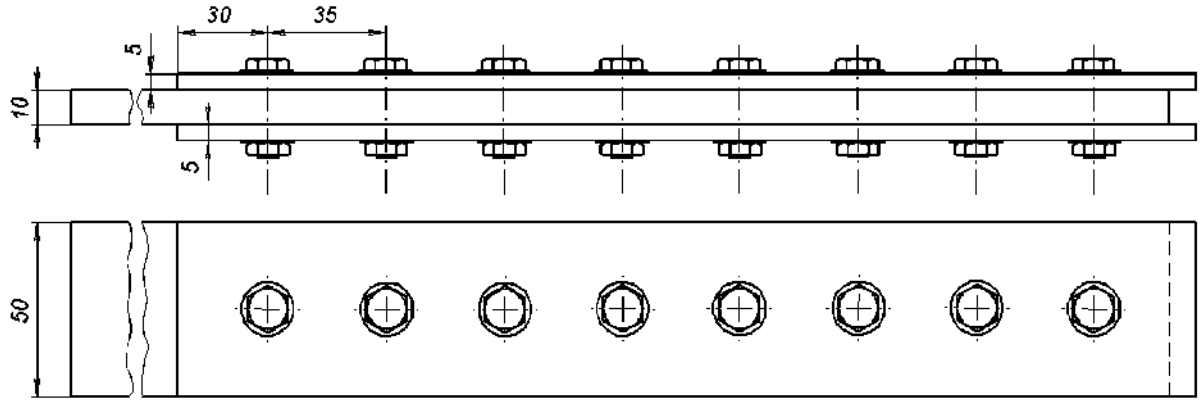

Fig. 3.71. Geometrical model of double-shear eight-row bolted joint

Material of the central plate is Д16Т alloy with the modulus of elasticity E = 70000 MPa. For the account of plastic properties of a material of the central plate non-linear dependence "pressure – deformation" [11] is set.

Bolts, the upper and lower straps are made of 30ХГСА steel (modulus of elasticity is E = 200000 MPa, the Poisson's ratio is μ□= 0.3). The material behavior of the upper and lower straps under loading is described by Hooke's law.

The solution of problem of the eight-row double-shear specimen of bolted joint loading by offered technique demands initial dependence "effort – moving" for modelling connection of joint members with bolt. In the process of the problem's formulation, the deformation rule of elements COMBIN39 was chosen in accordance with the nature of compliance change under loading of the single-row bolted joint at bolt installation without radial and axial interferences (see Fig. 3.63). As 1/4 part of the model with corresponding conditions of its fastening was considered at the numerical solving of joint loading problem (Fig. 3.72), the compliance rule change of element COMBIN39 was set as $P/4 = F(\Delta)$.

The finite element representation model (Fig. 3.73) for calculation of force between bolts in eight-row double-shear bolted joint consists of volumetric eight-node elements SOLID45 and special elements with properties of the nonlinear spring COMBIN39, presented in ANSYS system [474].

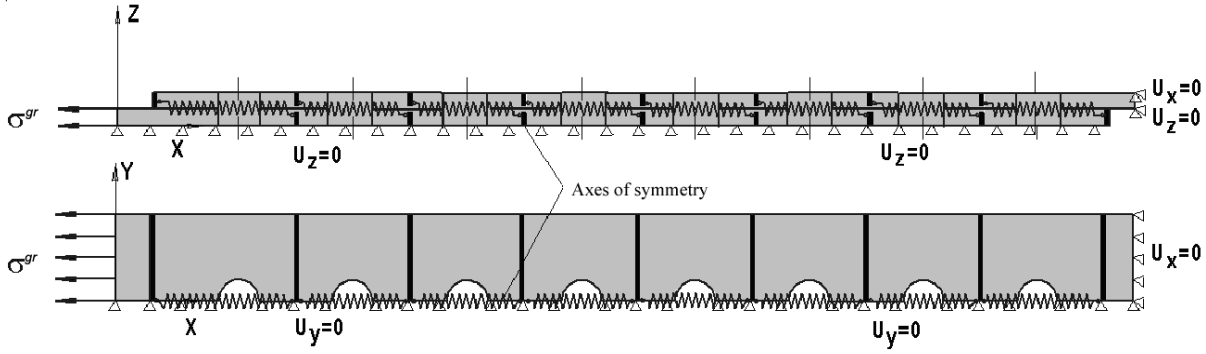

Fig. 3.72. The calculation diagram of double-shear eight-row bolted joint

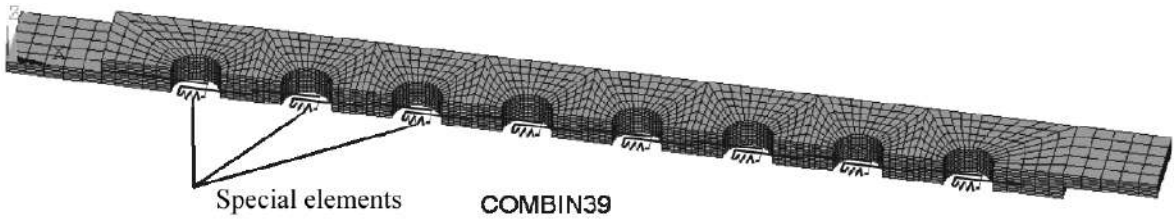

Fig. 3.73. The finite element model of double-shear eight-row bolted joints for solving the problem with special elements CONBIN39, presented in the form of the equations of combined deformations

Force distribution calculation on rows was carried out under the external tensile stresses applied to the central plate: P = 12500 … 50000 N. Stresses σ^{gr}=25…100 MPa correspond to these forces.

Among output data of special element CONBIN39 there is a possibility of determination the effort operating on the element. As a result of solving the finite-element problem of double-shear eight-row bolted joint model loading using the special element COMBIN39 the dependence of influence of external tensile stress level σ^{gr} on the force distribution nature between rows of bolts was obtained. Theoretical force distribution can be found in elastic area by the dependences offered in work [446]. Comparison of force distribution nature on rows on the basis of results of theoretical calculation and solution of finite element problem at external loading level σ^{gr}=25…100 MPa is shown in Fig. 3.74. For external loading σ^{gr} = 100 MPa dependences of force distribution on rows as a result of solving the finite element problem using compliance rules change in the cases of fastener installation with radial interference 1%d_b, with axial tightening 100 kN and without using elastoplastic interference (Fig. 3.74,) are constructed.

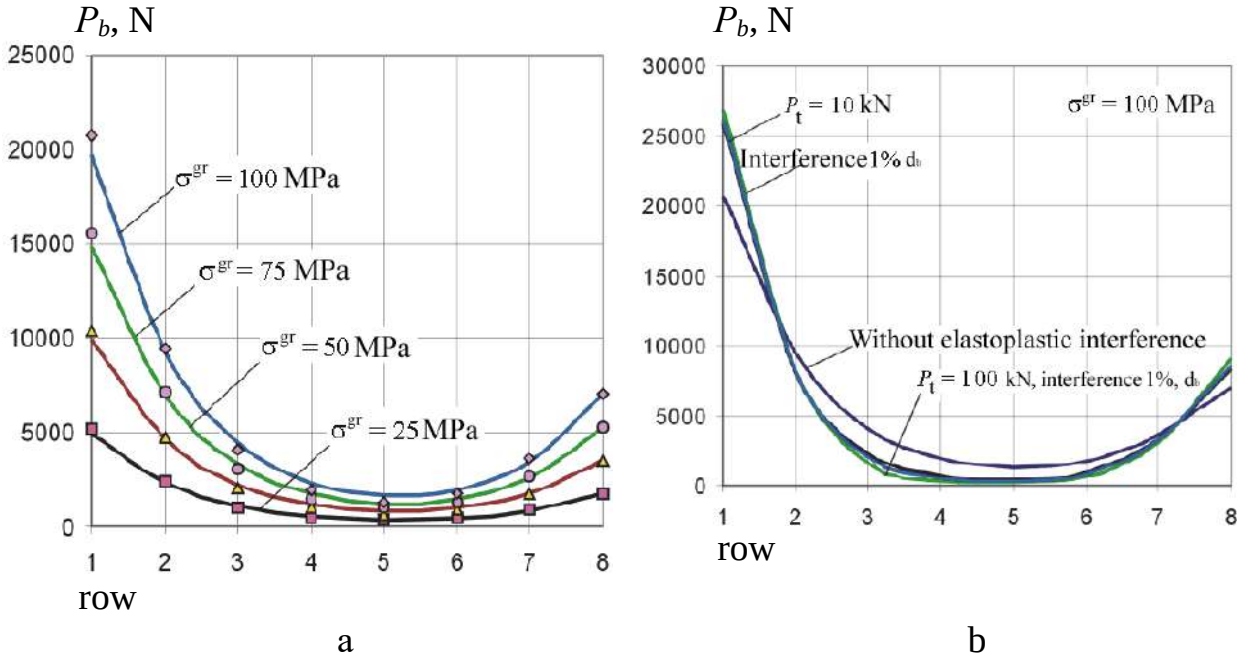

Fig. 3.74. Influence of external loading level σ^{gr} on effort distribution on rows. Theoretical effort distribution is designated by lines, calculation by finite element method using COMBIN39 element is designated by points

As seen from Fig. 3.74, the design procedure of force on rows with reference to the double-shear eight-row bolted joint specimen demonstrates the result having divergence with the theory no more than 4.5 % regarding force on extreme row bolt. During bolt installation with axial and radial interferences in double-shear joint the extent of extreme rows workload increases, and this may reduce radial interference efficiency for increasing endurance of multi-row joints.

From the results of these investigations the following conclusions can be drawn:

1. The definition technique of compliance and force distribution on rows in shear bolted joints is offered. The influence of loading level on the specimen of double-shear eight-row bolted joint on the force distribution nature on rows is investigated. The offered design procedure of force distribution in multi-row bolted joints combines relative simplicity of problem statement with computing power of finite element pack without using contact elements which increase the calculation time.

2. Using a radial interference during bolt installation reduces joint compliance on the elastic section of loading. The axial tightening of bolt in considered joint also reduces its compliance. The application of bolt installation into the package hole with radial interference $1\% d_b$ and axial tightening P_t = 100 kN increases irregularities of inequality of force distribution on rows and extreme row workload of the considered specimen in 1.25 times.

3. The developed design procedure of force distribution between bolts of multi-row shear joint is the component of integrated designing method of aircraft structural joints of the specified service life.

3.5. THE FORECASTING METHOD OF INFLUENCE OF STRUCTURALLY-TECHNOLOGICAL PARAMETRES OF SHEAR COUNTERSUNK BOLTED JOINTS ON THEIR DURABILITY

Objective of this investigation is development of forecasting method of aircraft structural members durability on the basis of fatigue resistance characteristics of standard specimens of countersunk bolted joints and calculation of local full specific energy of deformation on the components of the local mode of deformation obtained by means of finite element method (FEM).

The method contains the following stages:

1. The analysis of structurally-technological parameters of shear countersunk bolted joints.

2. Selection of standard specimens of countersunk bolted joints and their parameters. Manufacture of specimens using the corresponding technology.

3. Investigation of characteristics of fatigue resistance of standard specimens. Carrying out fatigue tests of standard specimens. Approximation of test results of by analytical expressions and plotting of fatigue curves on nominal zero-to-tension stresses.

4. Calculation of characteristics of the local mode of deformation in members of standard specimens and the modified joint. Determination of full specific energy of deformation in critical zones of members.

5. Forecasting of joint durability with the account of parameters changes of structural irregularities.

On the basis of the analysis of applicable shear countersunk bolted joints parameters the following standard specimens (Fig. 3.75) and their geometrical characteristics (hereinafter designations in figures correspond to numbering of standard specimens listed below) are selected:

1) plate with a countersunk hole filled with countersunk bolt 5015A with radial interference 1% d_b and axial tightening 10 kN;

2) double-shear single-row countersunk joint with bolt 5015A installed with a radial interference 1% d_b and axial tightening 10 kN;

3) double-shear three-row countersunk joint with bolts 5015A installed with radial interference 1% d_b and axial tightening 10 kN.

On the basis of fatigue tests results [372] of considered bolted joints standard specimens (Fig. 3.76), factors m and C for the analytical expressions of fatigue curves calculated by nominal stresses (Tables 3.2) were determined.

Table 3.2

Values of calculation-experimental factors m and C for standard specimens

Standard specimen	$N \cdot \sigma_{gr.0}^{m} = C$	
	m	C
The plate with countersunk hole filled with a countersunk bolt	3.386	4.15×10^{12}
Single-row countersunk bolted joint (failure on the upper strap)	2.941	1.86×10^{11}

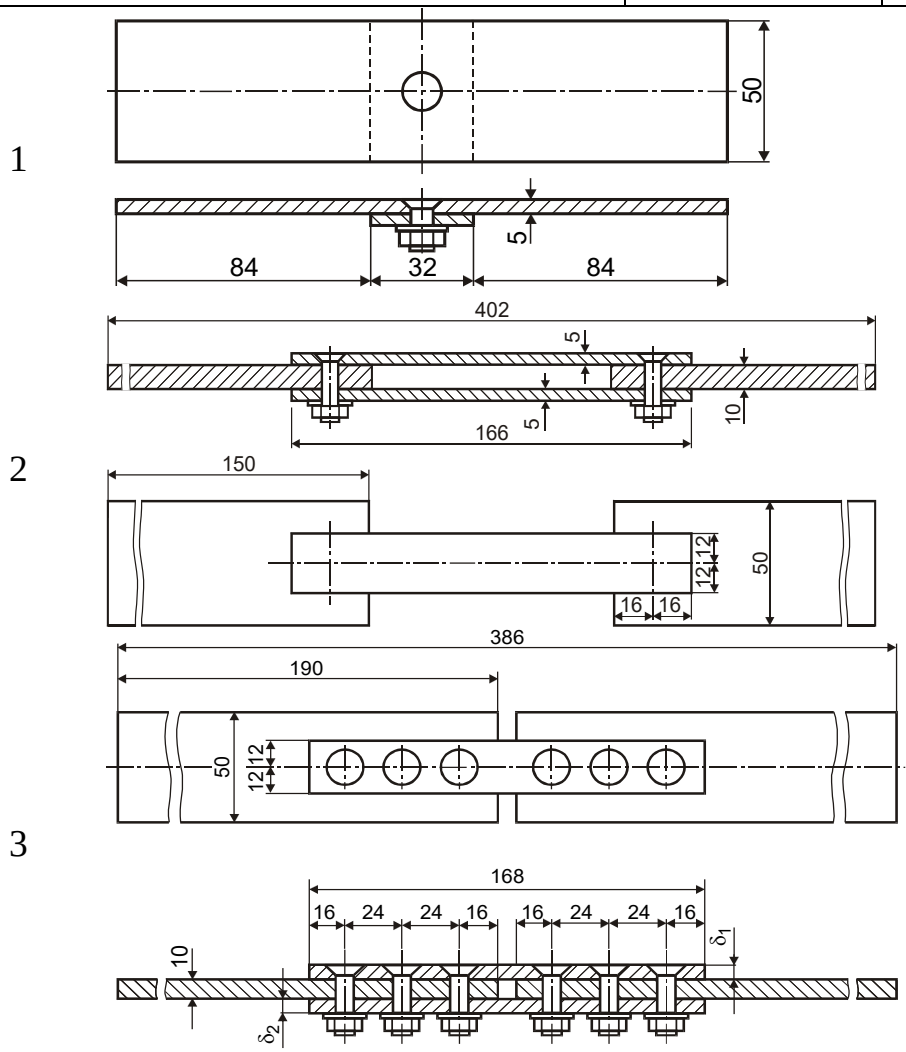

Fig. 3.75. Standard specimens of countersunk bolted joints

For forecasting three-row double-shear countersunk bolted joint durability the calculation of the local mode of deformation characteristics in members of standard specimens by means of ANSYS engineering analysis system [474] has been carried out. Local equivalent stresses and deformations in the most loaded points near to hole are reduced to zero-to-tension stress cycle according to the Oding's formula (Fig. 3.77, a, b).

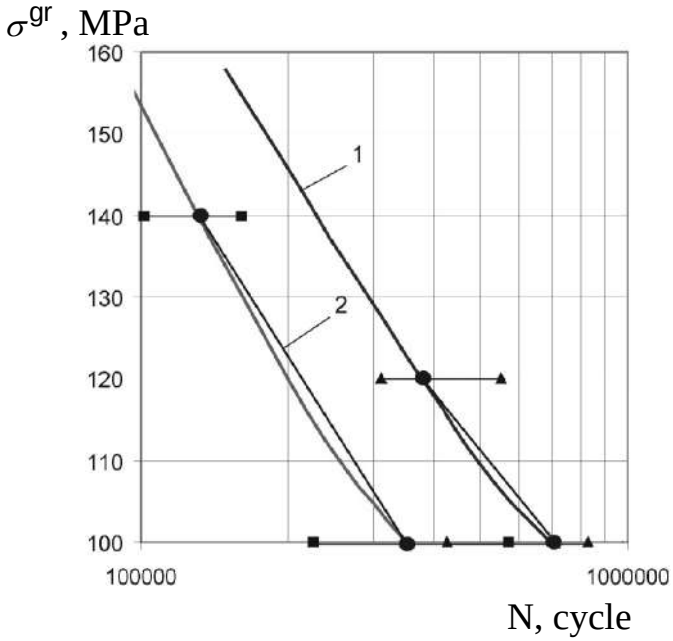

Fig. 3.76. Curves of cyclic durability and spread of experimental points during fatigue tests

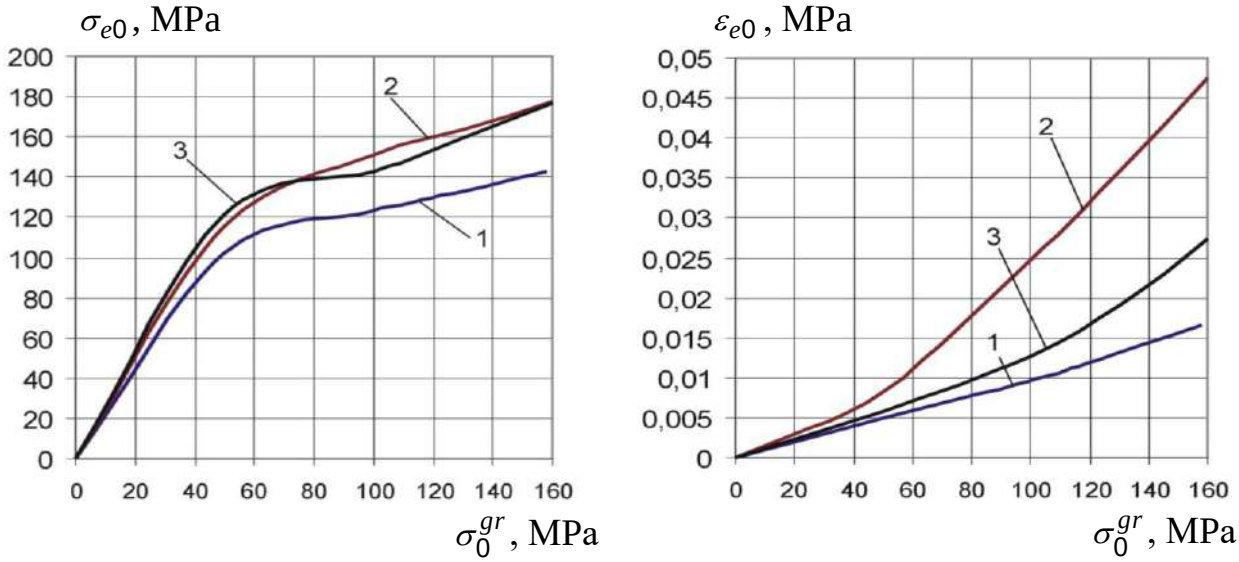

a b

Fig. 3.77. Influence of external tensile stress σ^{gr}, MPa, on the value of the local equivalent: a – stresses, b – deformations reduced to zero-to-tension stress cycle according to the Oding's formula

In Fig. 3.78 the dependences $\sigma_{e0} = f(\varepsilon_{e0})$ for standard and smooth specimens are shown.

As is shown in this figure, design data of standard specimens influence the dependence $\sigma_{e0} = f(\varepsilon_{e0})$.

Specific energy of deformation of the specimen was determined in a probable fatigue failure zone – the transition of a conic portion of hole in cylindrical in section along bolt axis. Full specific energy of deformation develops from elastic W_{elast} and plastic W_{plast} components (Fig. 3.79) and is equal to the area limited by the curve $\sigma_{e0} = f(\varepsilon_{e0})$ and an abscissa axis:

$$W = \int_0^{\varepsilon_{e0}} \sigma_{e0} d\varepsilon_{e0}$$

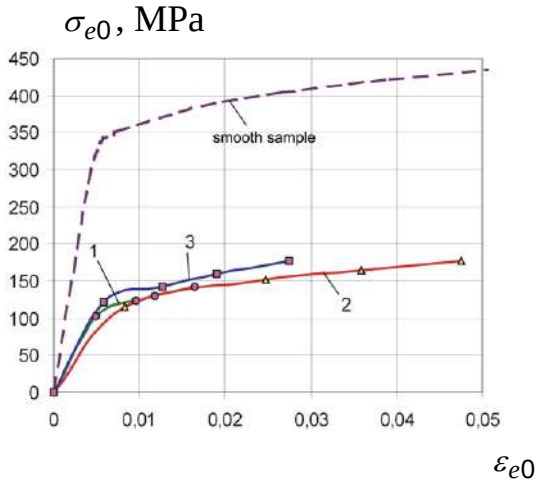

Fig. 3.78. Ratio between local equivalent zero-to-tension stresses σ_{e0} and deformations ε_{e0} in dangerous zones of standard specimens

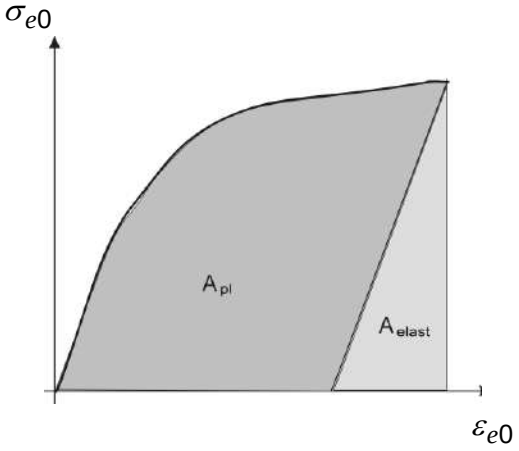

Fig. 3.79. Dependence $\sigma_{e0} = f(\varepsilon_{e0})$ determining full specific work of deformation in a local zone

By numerical integration of the dependences shown in Fig. 3.78, values of full specific works of deformation in dangerous zones of investigated specimens were obtained during change of σ_0^{gr} value, MPa (Fig. 3.80).

Durability of the modified (three-row) specimen was calculated using the expression

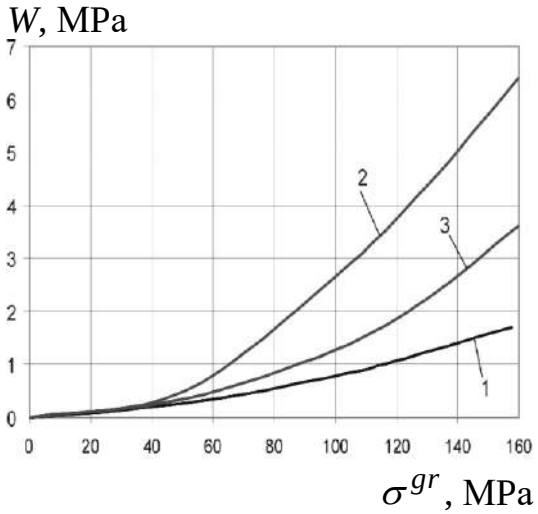

Fig. 3.80. Value of full specific deformation work in probable fatigue failure zones of standard specimens

$$N_m = \frac{C_b}{\left(\sigma_{á\,0}^{gr}\right)^m \left(W_m / W_b\right)^k}, \qquad (3.3)$$

where W_b, W_m and c is full specific work of deformation in the most loaded zone near the hole of the basic and modified specimens respectively and fault probability rate coefficient expressed by the ratio of works of the modified specimen deformation in comparison with basic one.

As is seen from Fig. 3.81, value of full specific energy of deformation in a local zone is maximal when the specimen of single-row double-shear countersunk bolted joint is loaded, and minimal when a plate with hole filled with a countersunk bolt is loaded. Hence, the approximate estimation of influence of design parameters on durability of similar joints is possible at the calculation stage of full specific deformation energies.

While forecasting durability of the three-row joint specimen the fatigue curve of a plate with countersunk hole filled with unloaded countersunk bolt is accepted as a basic curve. Factor $k = 0{,}585$ of transition from a basic curve to fatigue curve of single-row double-shear countersunk joint has been determined. Forecasting durability of three-row joint was carried out with the assumption of factor invariability k (see Fig. 3.81).

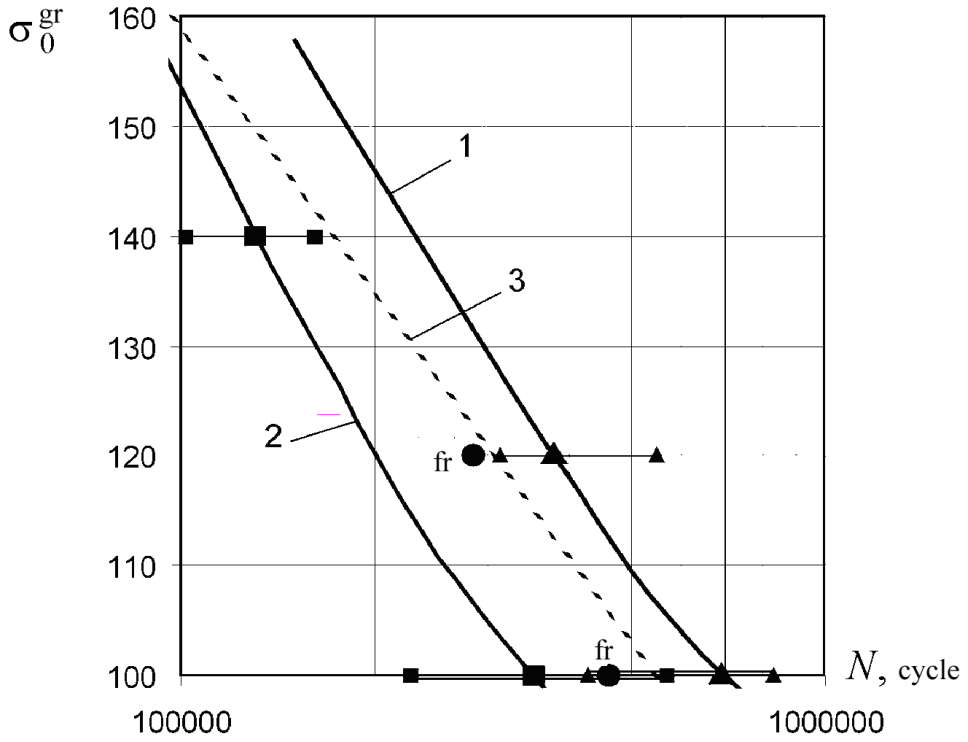

Fig. 3.81. Fatigue curves of the standard specimens, plotted by results of tests and by calculation. Spread points of test results and failures caused by fretting corrosion (fr) of three-row bolted joint specimen are marked

From results of the carried out investigations it is possible to draw following conclusions:

1. The forecasting method of shear bolted joints durability on the basis of fatigue tests results of standard specimens and calculation of the local mode of deformation characteristics in probable fatigue failure zones of joint members has been developed. Dependence allows to consider structurally-technological features of irregularities zones and influence of their changes on fatigue characteristics.

2. The durability of three-row double-shear countersunk bolted joint on the basis of tests of standard specimens of a plate with filled unloaded countersunk hole and single-row double-shear countersunk bolted joint is forecasted.

3.6. PROCEDURES FOR CREATION OF COMPUTER MODELS OF BOLTED JOINTS OF AIRCRAFT ASSEMBLY STRUCTURES USING UG SYSTEM

The basis of preservation of the assigned aircraft aerodynamic characteristics during its manufacture is provision of theoretical contour (TC) of its units coming out in the airstream. Recently the tendency to the further toughening of requirements for deviations of forms and the sizes of units from the theoretical contour is accurately traced. We will consider the creation technology of analytical standards using UNIGRAPHICS system of standard bolted joints on an example of assembly of technological shear joint of the second spar of the average transport plane taking into account the breaking of an aerodynamic contour. Design feature of this assembly is that the direct spar of the wing center section is joined with a descending spar (the angle of wing cross-section V is negative) of a wing console part, deflected from a normal to the aircraft plane of symmetry back along the flight on the angle of 15°.

The attachment assembly (Fig. 3.82) is formed by the power strap 1, skin 2, joint profile 3, wing center section spar 4, outer wing panel (OWP) spar 5, wing center section angle 6 and outer wing panel angle 7. Attachment of these parts is carried out by means of bolts with countersunk heads ∠90 OCT 1 10572-72 with threads M6x1-6e – 8, M8x1.25-6e – 9; bolts with reduced plano-convex head OCT 1 10575-72 with thread M6x1-6e – 10; bolts with reduced hexahedral head OCT 1 10570-72 with thread M8x1.25-6e – 11, and also low hexahedral-nuts OCT 1 12140-78 with threads M6x1-4H5H – 12 and M8x1.25-4H5H – 13. Washers because of assembly features are not standard members.

The technology of joint assembly suggests such a sequence of operations: skin panels installation in the assembly device and their fixing; installation of joint profile in the assembly device and its fixing; installation of the wing center section spars and outer wing panel (OWP) in the assembly device and their fixing; installation of angles in the assembly device and their fixing; combined drilling of holes for fasteners in assembly parts; installation of fasteners.

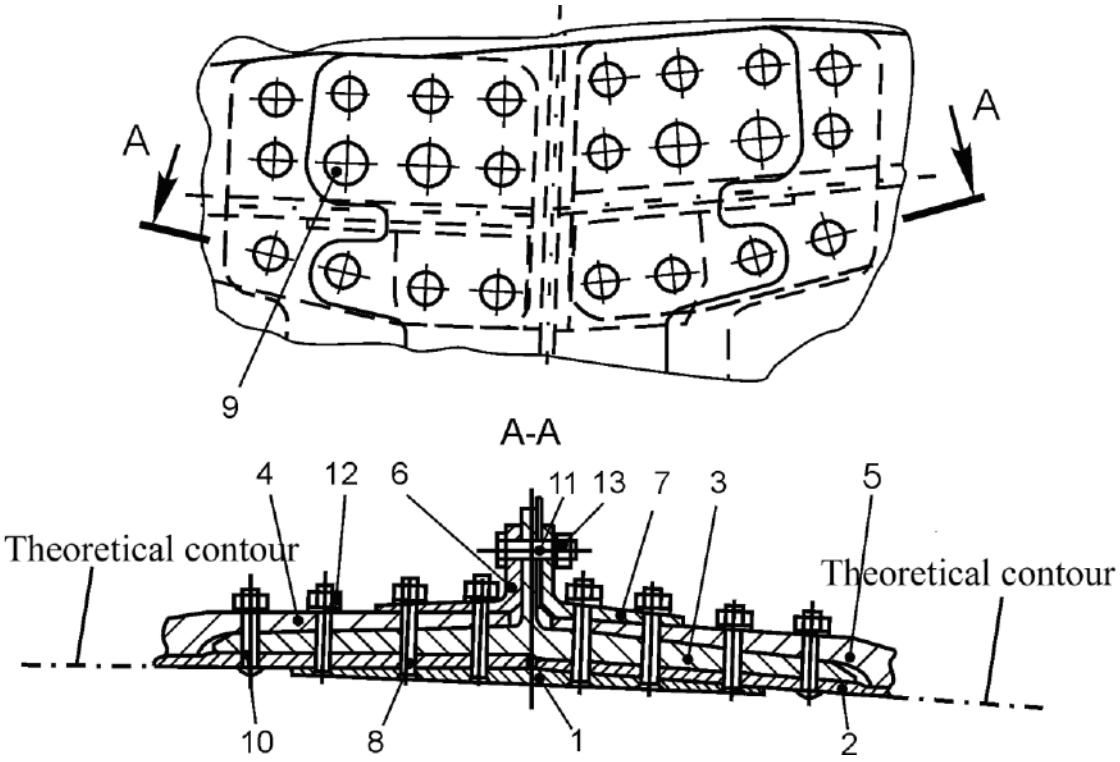

Fig. 3.82. The general view of the modelled assembly

Joint parts of assembly are made by treatment on the milling machine with numerical control (NC).

It is reasonable to begin the construction of the analytical standard of bolted joint with construction of analytical standards of skins in the location of assembly which are created according to the analytical standard of theoretical wing surface.

The next stage is the construction of a joint profile flange, as it is an integral connecting member for all other parts. The specified configuration of object turns out as a result of its "dissection" by the planes setting flange thickness and its inclination (Fig. 3.83), and removals of superfluous parts. The web anet is plotted to the constructed anet of joint profile flange, and with the help of Boole addition operation an integral object can be obtained. The place of flange and wall joint is rounded by radius R5.

The remained parts of assembly are modelled similarly as a whole. The offered diagram of construction of entering assembly components allows to realize high accuracy of conjugation of two next parts.

Analytical standards of fasteners (bolts with countersunk head) are executed by rotation of a generating contour round the fixed axis. Then tool blank, specifying geometry of grooves for a screw-driver (Fig. 3.84), is “subtracted” from the made blank. The creation of the analytical standard is finished by the generation of necessary facets and rounding off radii.

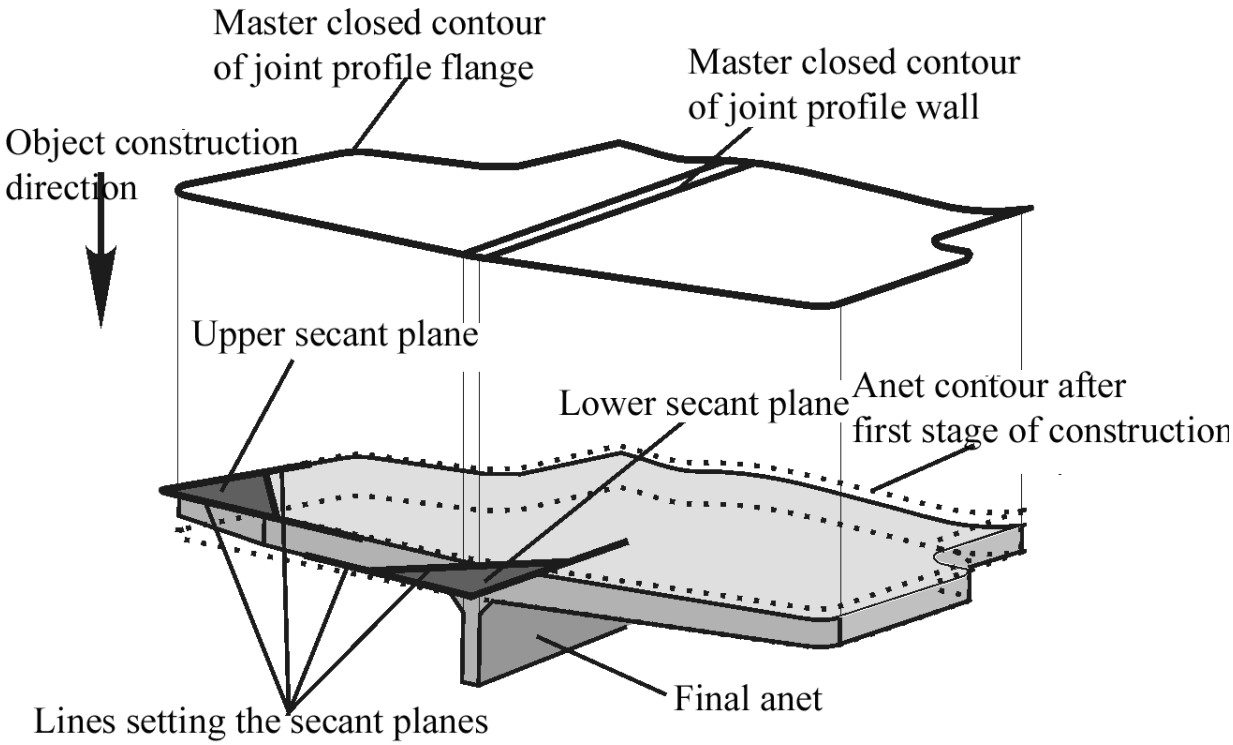

Fig. 3.83. The creation diagram of the analytical standard of a joint profile

Analytical standards of nuts and washers are carried out by translational motion of hexahedron and circles along axial line on specified distance. To produce the facet at nut end faces (it is similar for hexagon bolt heads) the set of the lines, describing by itself its configuration, is created. By the method of rotation of the obtained contour the tool blank is created. The carried out Boole operation of subtraction of tool blank from the basic one allows to obtain the required configuration of nut (hexagon bolt head) (Fig. 3.85).

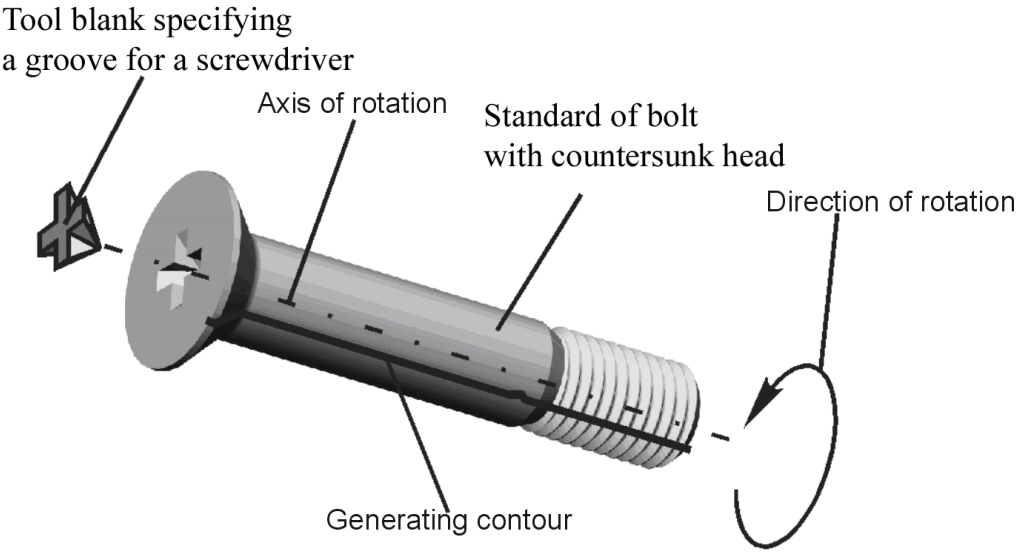

Fig. 3.84. Construction of the analytical standard of bolt with a countersunk head

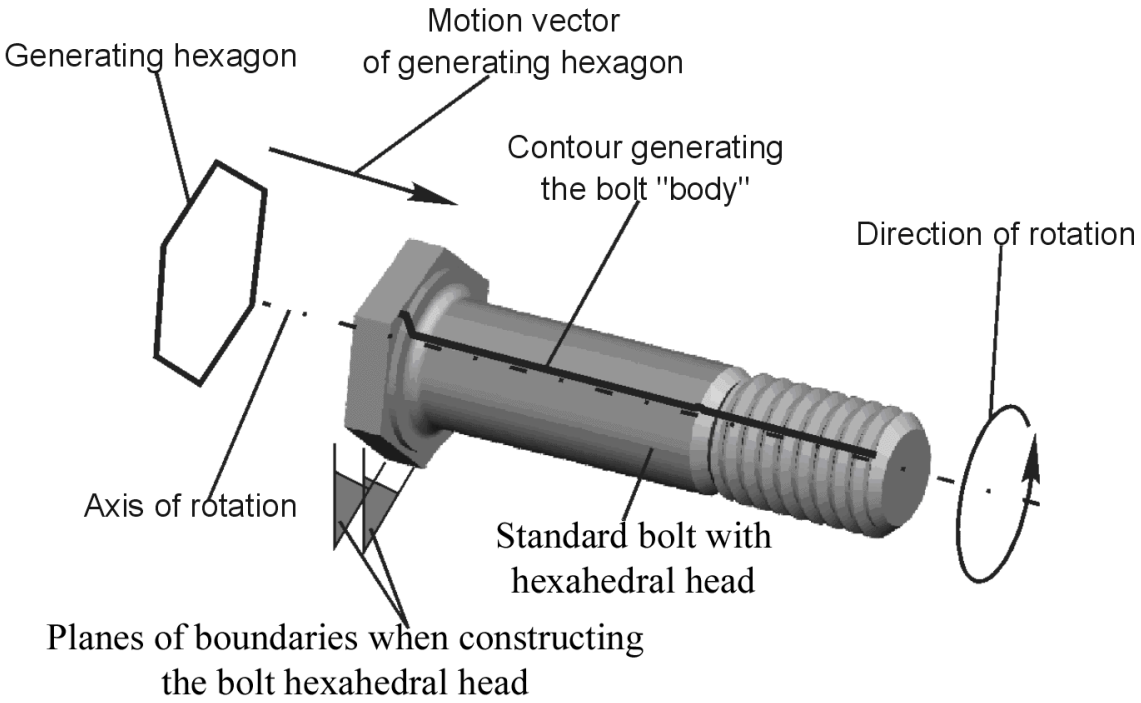

Fig. 3.85. Construction of the analytical standard of bolt with a hexahedral head

Bolt-mounting holes with hexahedral and plano-convex heads are "stitched" directly with bolt itself with the cut off head. Bolt-mounting holes with a countersunk head are carried out with a special blank, which is a body of rotation with a cone (angle with vertex ∠90°) on the end. The representation of tool standards of bolts is presented in Fig. 3.86.

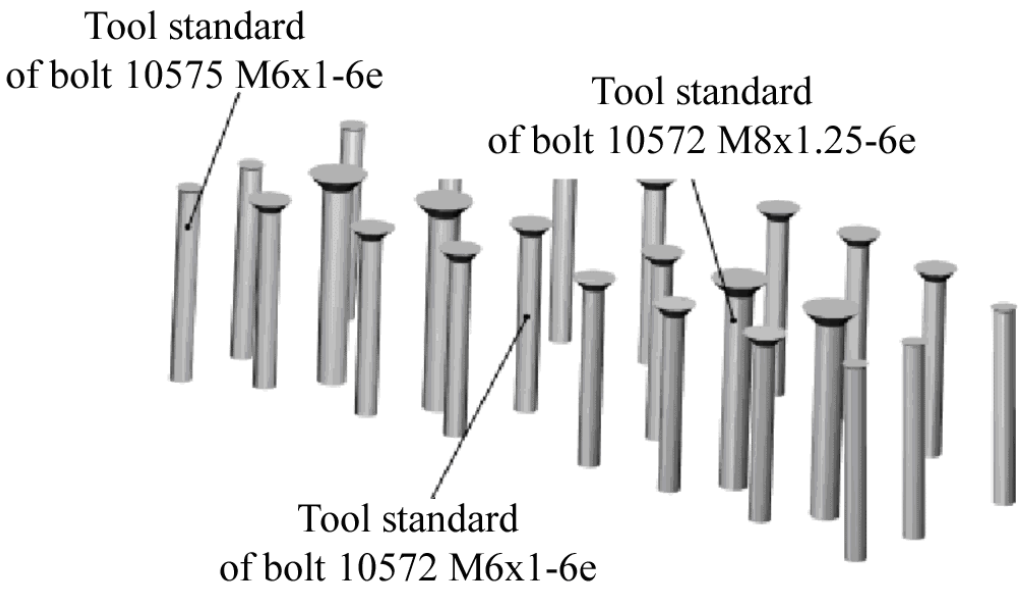

Fig. 3.86. The representation of tool standards of bolts

Having executed operation of subtraction of tool standards from blanks of parts, we will obtain the analytical standard of the considered assembly with holes for fasteners (Fig. 3.87).

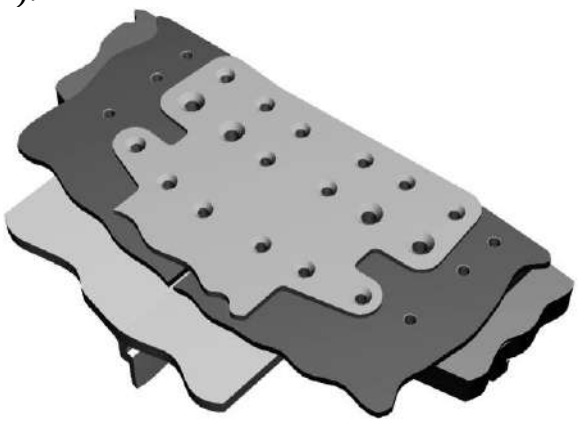

Fig. 3.87. Assembly blank with holes for fasteners

By uniting analytical standards of parts and fasteners we obtain the joint presented in Fig. 3.88.

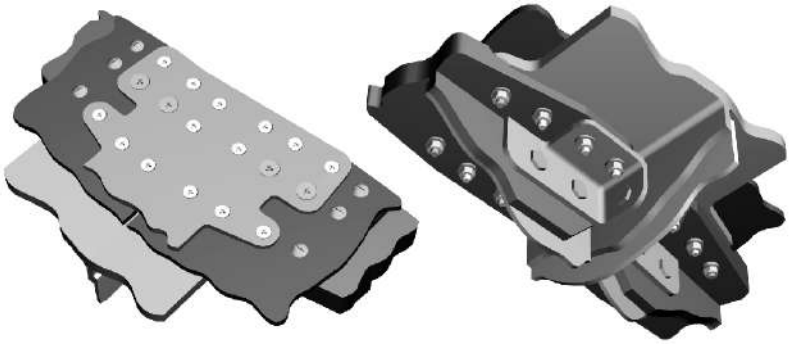

Fig. 3.88. The analytical standard of assembly of wing center section spar and OWP attachment

The stated above principles of creation of bolted joints anets were used while creating presented below bolted joints anets of spar web and flange (Fig. 3.89) and fitting joint of wing center section panels and OWP panels (Fig. 3.90).

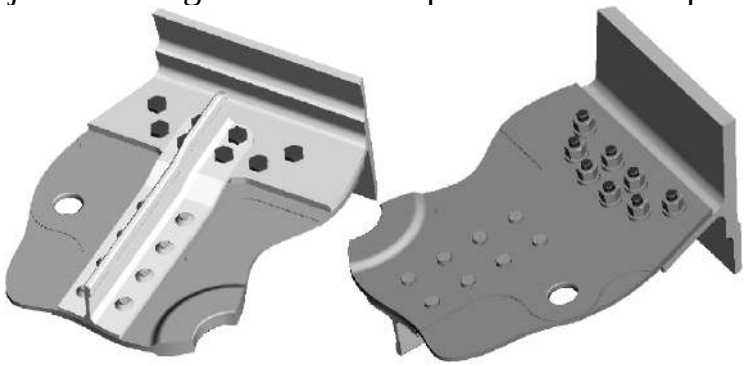

Fig. 3.89. Analytical standard of bolted joint of spar web and flange

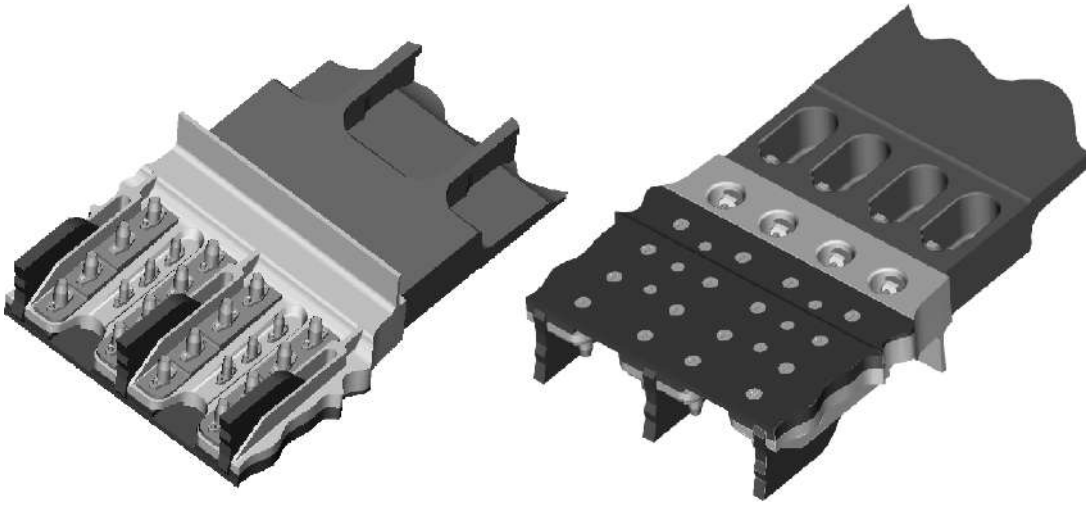

Fig. 3.90. The analytical standard of fitting joint of wing center section and OWP panels

The executed constructions of fitting joint have one feature which distinguishes it by construction from earlier considered example. It is that forming of an insert under bolt head and nut fitting is necessary, because curvilinear surfaces of slot do not allow them to provide dense mating contact, and, accordingly, the required level of tightening. It is formed on the basis of the curves setting geometry of a slot in the panel, by means of which the high quality of interface of the given surfaces (the unified data carrier is used) is reached.

The offered technology of creation of bolted joints allows to model rather complete objects for computer systems of technological preparation of manufacture and engineering analysis. Anets, created by UNIGRAPHICS system, can serve as primary sources of information for other moduli (CAM/CAE). Input of the created models to external systems is carried out by means of universal communication formats IGES, STEP type etc. All realized constructions are parametrical, that allows later on to change freely the configuration of members ts and ways of their joint. It is especially important at the stage of assembly geometry selection while designing it.

3.7. CONCLUSIONS

1. The method and the block–diagram of the integrated designing and modelling of shear bolted joints by means of UNIGRAPHICS and ANSYS systems are offered.

2. The method of the influence analysis of structurally-technological parameters on characteristics of the volumetric local mode of deformation of shear bolted joint members with taking into consideration physical, geometrical and contact non-linearities by means of ANSYS integrated analysis system has been considered. The analysis method is approved while calculating characteristics of the local mode of deformation in standard single-row and multi-

row shear joint members executed with elastoplastic radial interference and tightening. The change of local specific energy of deformation, contact pressures and clearances when changing the loading level is investigated. This allows to predict characteristics of assigned durability in concentration zone of specific energy of deformation and contact pressures. The change of clearances sizes between joint members under of loading change has been examined; this is a basis for designing the tight joints.

3. Experimentally we have obtained fatigue resistance characteristics of bolted joints upon which main dependences for durability calculation of these specimens have been developed.

4. The new design procedure of force distribution between rows in shear multi-row bolted joints of assembly structures by means of ANSYS system on the basis of joint compliance calculation has been developed. Influence of radial interference on change of joint compliance and increase of extreme rows load in joints with radial interference is established.

5. The new forecasting method of influence of structurally-technological parameters of shear countersunk bolted joints on their durability taking into account value change of full specific energy of deformation in probable fatigue failure zones and intensive development of fretting corrosion has been offered. The technique is approved while calculating durability and its change for standard bolted joints.

6. The technique of creating the computer models of bolted joints of aircraft assembly structures by means of UNIGRAPHICS system has been developed, allowing to conduct parametrical modelling of joints in the course of iterative designing of joints.

Section 4

NEW STRUCTURALLY-TECHNOLOGICAL SOLUTIONS FOR SHEAR BOLTED JOINTS OF AIRCRAFT ASSEMBLY STRUCTURES

The set durability level, crack toughness and tightness of aircraft structural members joints define type of fastener, its embodiment, radial interference, bolt installation method, joint structural parameters, coating type, fretting corrosion and stress corrosion protection type, unloading procedure of a joint extreme row.

Radial interference up to $1.2\% d_b$, during installing the steel and titanic bolts with diameter 5 – 12 mm, is recommended according to condition restrictions of corrosion cracking resistance for joints made of aluminum alloys and considering mechanical tolerance in the industry.

Holes are made in accordance with H7 and H9 for the joints with radial elastoplastic interference. Meanwhile tolerances for diameter of fastener rod smooth portion specified in the industry-specific standard (OCT) for fasteners provide the interference field along bolt cylindrical portion.

Fasteners with interference are installed according to PTM 1.4.1121-82 (NIAT, 1982) "Implementation of bolted joints with elastoplastic interference in the packs made of aluminum alloys".

The distance between hole axes must correspond to not less than three bolt diameters, the distance from hole axis to joint edge must correspond to not less than two bolt diameters in the shear bolted joints with radial elastoplastic interference. The used bolts must have geometric parameters corresponding to the OCT for them. Countersunk bolted joint feature is radial interference effectiveness decrease and countersink depth increase. Fatigue failure of countersunk bolted joints begins in the countersunk seat area and in the area of intensive fretting corrosion development along contact areas of connected parts. That is why we should provide radial interference in the countersunk seat area, its surface strengthening, fretting corrosion intensiveness decrease, increase of joint tightness and resistance to fretting corrosion and stress corrosion using structural-technological methods and to reach the set durability level of countersunk shear bolted joints. We can solve this task by modification of the countersunk bolt head providing local radial interference in the countersunk seat area while assembling. And we can also use additional technological procedures promoting fatigue durability increase of joints with such bolts (Fig. 4.1).

Since multi-row shear joint fatigue failure, as a rule, occurs in the area of fasteners extreme row, then one of the ways to increase durability of such joints is to decrease their extreme row load applying unloaded holes, stay gaskets, stickable edge plates, part local thickening.

Conic surface of a countersunk insert bolt head is produced as an annular collar 1, with annular grooves 2 at the head butt and under the head near the bolt body being filled with sealant.

A.c. 649894

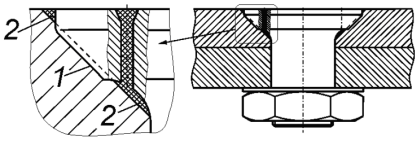

The countersunk insert bolt head and socket for it are cylindrical; near-butt portion of an insert head has side conic annular collar 1 or offset 2; surface annular groove 3 filled with sealant

A.c. 627252

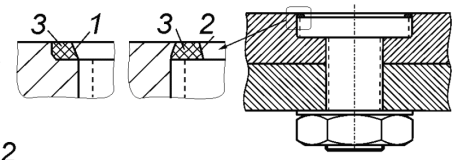

The countersunk insert bolt head is triple-cone, the angle of the first cone is less than the countersinking angle of a hole in a joint component, the angle of the second cone equals it the angle of the third cone is more than it.

A.c. 781422

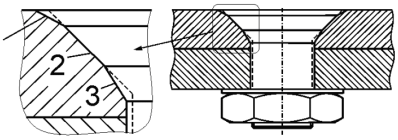

The countersunk insert bolt head is double-cone, countersinking is cylindrical-conic, joints: *a* - detachable with sealant in the annular hollow, *b* - one-piece with radial interference along the body and insert head.

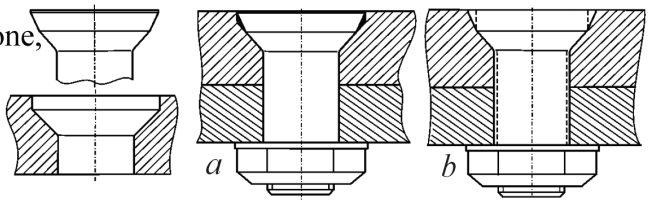

The strip is glued to the joint part in the area of the first row of fasteners.
The strength of the strip material is equal or more than that of the part material.

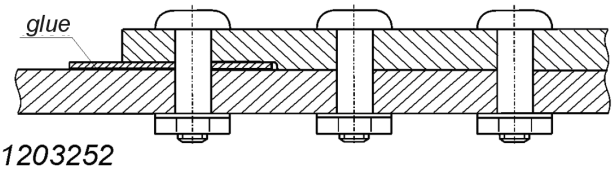

A.c. 1203252

In the joint parts in front of and behind the first row of holes for fasteners, the through holes 1 and blind holes 2 are made. These holes are filled with sealant 3 or with pins 4 installed with radial interference.

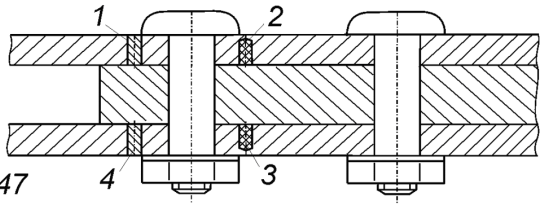

A.c. 1303747

The holes in strips for the first row of fasteners are produced with conic cavities 1 located on the side of joint strips contact surface.

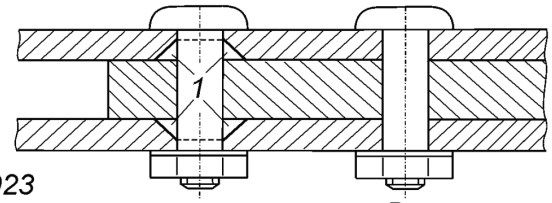

A.c. 1754923

The loading of parts with static load, which corresponds to operating load, and which is unloaded after the formation of a hole and placing of fasteners in that hole with radial interference.

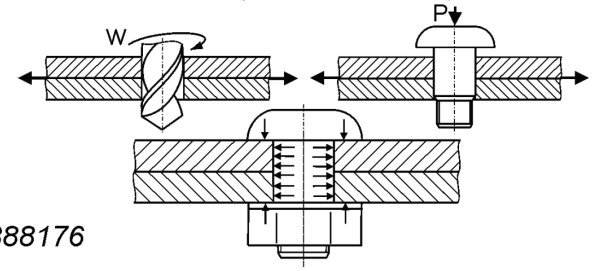

A.c. 1388176

Fig. 4.1. New structurally-technological solutions increasing cyclic durability and tightness of shear bolted joint of aircraft structures

4.1 JOINT DURABILITY BY INCREASE METHOD BY APPLYING TRIPLE-CONIC COUNTERSUNK BOLTS

Local interference in the transitional areas of countersunk seat increases fatigue durability of countersunk joint. Thereby, it is reasonable to apply countersunk bolts with modified head which provide guaranteed interference along all pack thickness. The modification is a countersunk bolt with triple-cone head (Fig. 4.2). Head cone angles are made as increasing ones, beginning from the bolt rod, and middle cone apex angle is equal to seat conicity angle. The bolt head provides radial interference in the seat area adjacent to the external component surface by means of the external cone lateral surface. The internal cone lateral surface provides radial interference in the area where hole conic part turns into cylindrical one. The total height of bolt countersunk head is equal to the head height of countersunk bolt corresponding to OCT 1.31043-79 and intended for installation with elastoplastic radial interference.

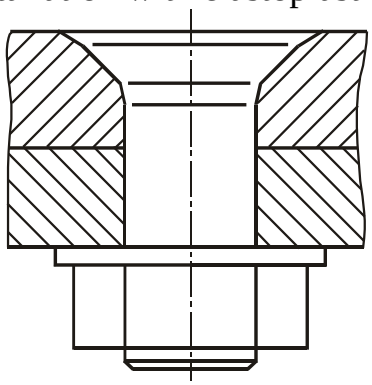

Fig. 4.2. Countersunk bolt modification

Bolt geometrical parameters are selected from the condition of the 1% radial interference in respective seat areas (Fig. 4.3 and 4.4). Parameters of plain and thread bolt portions, lead-in part geometry and temporary tail sizes are set according to OCT 1. 31043-79. Temporary tail detachable neck diameter is determined subject to additional draw axial force necessary for elastoplastic interference in the countersunk seat.

Application effectiveness of local interference of countersunk bolts with triple-conic head has been analysed during fatigue test of shear countersunk joint specimens, as follows:

Double-shear single-bolted (Fig. 4.5);

Double-shear multi-bolted with initial failure (Fig. 4.6).

As a basis for comparison, we take serial countersunk bolts with normal 5015A and diameter 8 mm. They are installed with the 1% radial interference in the holes with maximum diameter 7.9 mm.

Countersunk double-shear single-bolted joint specimen is the joint of plates made of Д16АТл5 alloy. Fatigue tests of the given specimens are carried out on the ЦДМ-10Пу test machine at asymmetrical tension cycle with asymmetry parameter R_σ = 0.1 and frequency of cycling 14 Hz.

The results (Fig. 4.7) show that the application of modified bolts with local interference (curve 2) increases specimen fatigue durability in 4.3 times in comparison with the specimens assembled with bolts 5015A with local interference (curve 1) at the cyclic stress level with σ_{max}^{gr} = 125 MPa.

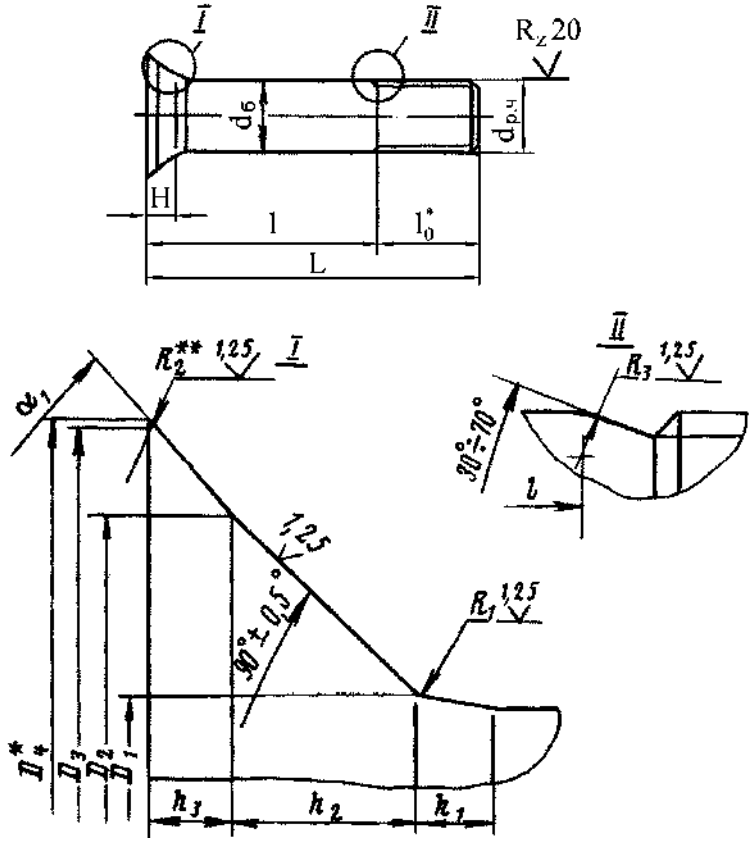

Fig. 4.3. Geometrical parameters of triple-conic countersunk head:
* – reference sizes; ** – sizes provided with tools

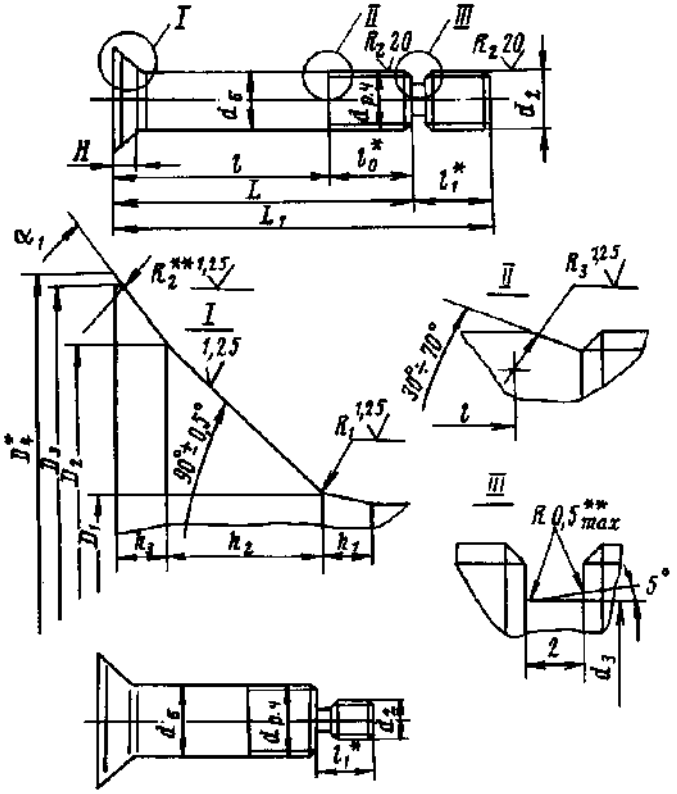

Fig. 4.4. Geometrical parameters of triple-conic countersunk head bolt:
* – reference sizes; ** – sizes provided with tools

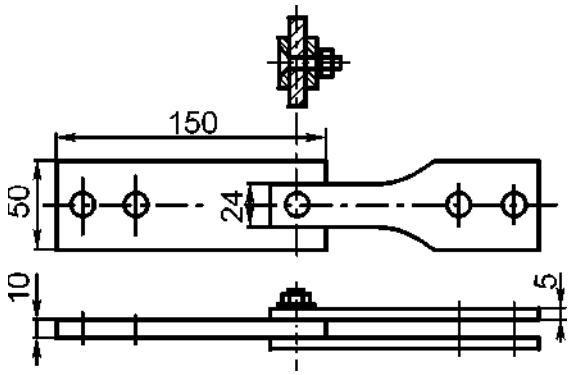

Fig. 4.5. Double-shear countersunk joint specimen

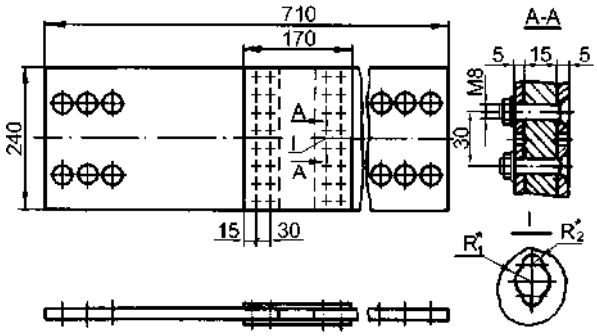

Fig. 4.6. Double-shear bolted joint specimen with initial failure

Specimen fatigue durability with local interference of modified bolts increases only in two times in comparison with the analogous basic specimens on the lower cyclic stress level (σ_{max}^{gr} = 83 MPa).

This is explained by the fact that the factor determining the durability was fretting corrosion of joint member interface surface on the lower cyclic stress level.

Countersunk multi-bolted joint specimens were carried out as double-shear bolted joint of two central plates with two straps made of Д16АТл5 alloy. The initial strap failure was made as the hole with diametrical half-circle cutout in the specimen. The specimens were tested on the МУП-200 facility at asymmetrical tension cycle R_σ = 0.6.

The test data given in Fig. 4.8 (1 – the 5015A bolts; 2 – modified bolts) show that application of modified bolts with local interference increases multi-bolted joint fatigue durability in 2.6 times in comparison with usual countersunk bolts.

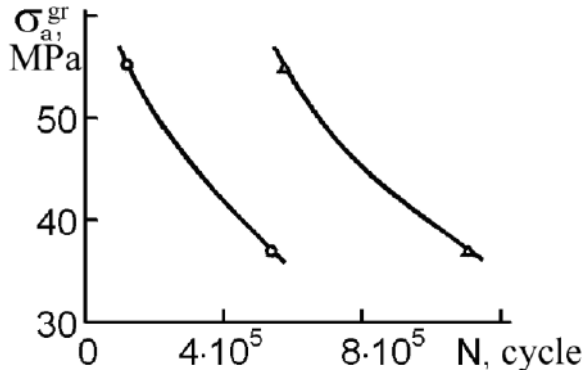

Fig. 4.7. Modified bolt installation influence on single-bolted joint durability

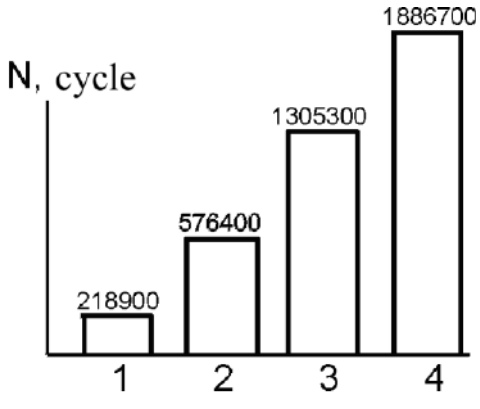

Fig. 4.8. Modified bolt installation influence on multi-bolted joint durability

4.2. APPLICATION OF GLUE FILM TO INCREASE DURABILITY OF COUNTERSUNK JOINTS WITH LOCAL INTERFERENCE

The ВК-9 glue is used to eliminate interface surface fretting corrosion of joint with local interference. The glue is applied along joint interface surfaces. Glue film effectiveness is proved with help of fatigue tests of single – and multi-bolted shear joint specimens.

Fig. 4.9 (1 – without glue; 2 – with ВК-9 glue) shows the results of fatigue tests carried out on single-bolted countersunk joints with local interference on the ВК-9 glue (see Fig. 4.5).

The ВК-9 glue has eliminated fretting corrosion of interface surface and increased fatigue durability at the lower load level in 2.5 times in comparison with the durability of analogous specimens assembled without glue.

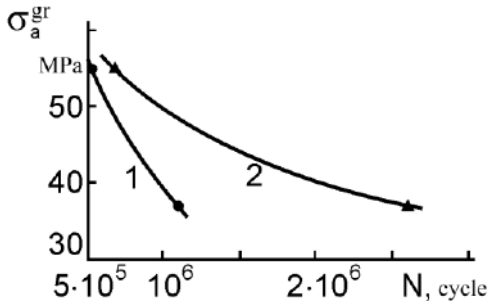

Fig. 4.9. Glue film effectiveness in single-bolted countersunk joints

The application of the ВК-9 glue on the interface surfaces has increased durability of multi-bolted joints (see Fig.4.6.) assembled with bolts of normal 5015A with 1% interference in 5.9 times in comparison with the durability of analogous specimens assembled without glue (see Fig. 4.8, 3 – bolt 5015A + the ВК-9 glue). The glue film has increased durability of joints assembled with modified bolt local interference in 3.3 times in comparison with the specimen durability with modified bolts and without the glue (see Fig. 4.8, 4 – modified bolt 5015A + ВК-9 glue).

Combined application of modified bolts with local interference and glue film on the interface surfaces provides durability increase in 8.6 times in comparison with durability of the analogous specimens assembled without glue but with the 5015A countersunk bolts and 1% radial interference.

The influence of bolt and glue film local interference on the rate of fatigue crack propagation is investigated in the cyclic load of countersunk shear multi-bolted joint specimens (see Fig. 4.6).

The multi-bolted joint specimen had the initial failure as the concentrator along the strap axis (circular hole 4 mm in diameter with diametrical half-circle cutouts 1 mm in radius).

The joint specimens were tested on the МУП-200 facility at asymmetrical tension P_{max}/P_{min} = 150000/90000 N (σ_{max} = 85 MPa) and cycling frequency of 200 cycle/min.

The specimen failure development has the following periods (Fig. 4.10):

0 – 1 – loading till crack formation 1 mm in length on the concentrator

tops;

1 – 2 – crack propagation from 1mm in length to the length equal the distance to the first bolt hole wall ;

2 – 3 – crack delay on the first bolt hole;

3 – 4 – crack propagation from the first to the second bolt hole;

4 – 5 – crack delay on the second bolt hole;

5 – 6 – crack propagation from the second to the third bolt hole .

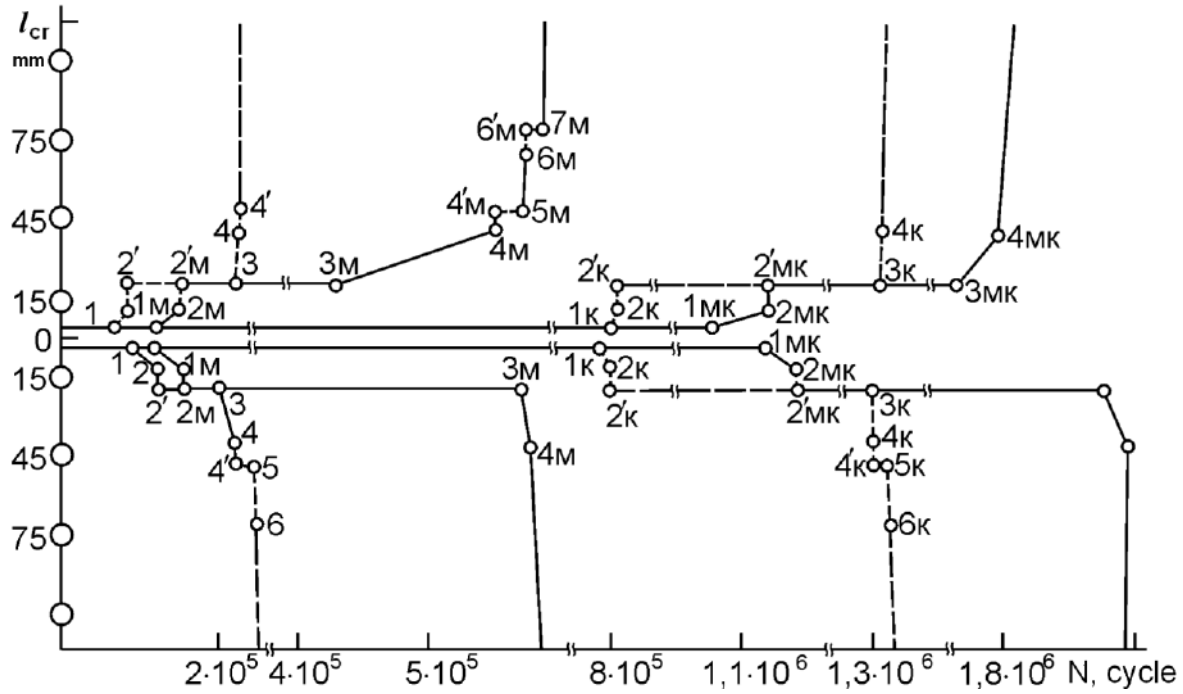

Fig. 4.10. Fatigue crack propagation rate in the specimen of multi-bolted countersunk joint

The duration of the period of crack propagation 1 mm in length in the specimens with usual bolts was equal to 130000 – 160000 cycles regardless of bolt type. The crack propagation rate was equal to 0.5 – 0.66 mm/kcycle on the 1 -2 periods, and the delay period on the first bolt hole was 54000 – 74000 cycles. The crack propagation rate increased rapidly on the following sections, since the specimen net-section area decreased appreciably (stress in the net-section increased) during the continuous cyclic loading.

The application of the modified bolt with local interference has no influence on the initial period of crack propagation in the specimen under consideration with the initial failure. The period does not virtually change as well as in the specimens with usual countersunk bolts.

The mean crack propagation rate decreased to 0.29 – 0.45 mm/kcycle on the 1-2 periods. This fact is explained by the influence of the local interference in the bolt area. It is significant to note that the modified bolts with local interference increase considerably the crack delay period on the hole. The delay period is equal, in this case, to 250000 – 390000 cycles that exceeds in five times the same

period of joints with the usual bolts.

The joints with BK-9 glue have the same crack propagation characteristic as well as the joints with the usual bolts. The duration of crack propagation 1 mm in length of increased at the expense of the bolt unloading with glue film. If the joints without glue had the duration equal to 130000 – 160000 cycles, the duration of the joints with glue on the interface surfaces increased to 800000 – 1 000000 cycles, i.e. in six times. It is significant that the crack velocity decreased on the 1-2 application periods of modified bolts with local interference and glue. So the specimens with usual bolts had the velocity equal 0.5 – 0.66 mm/kcycle, the velocity of the modified bolts was equal to 0.29 – 0.45 mm/kcycle and the velocity of the modified bolts and glue was 0.13 – 0.29 mm/kcycle.

Glue BK-9 has increased the crack delay period on the hole in the joints with the usual bolts to 497000 – 499000 cycles, i.e. in 6-7 times. And using modified bolts with local interference increased this period to 745000 – 841000 cycles, i.e. in 11 – 18 times in comparison with the joints with usual bolts without glue.

4.3. APPLICATION OF DISCHARGE HOLES TO INCREASE BOLTED JOINT DURABILITY

We propose to cut out additional discharge holes with smaller diameter in the shear bolted joint near the extreme bolt hole and locate them in front of and behind the basic hole along the line of load action on the joint part.

Let us use the following terminology while locating the discharge holes along the line of resultant load action on the joint:

discharge hole behind the extreme bolt (BDH) — when the discharge hole is behind the bolt on the side contacting with the joint part;

discharge hole in front of the extreme bolt (FDH) — when the discharge hole is in front of the bolt on the side of acting load on the joint.

A few variants of discharge holes are designed in respect to the shear bolted joints (Fig. 4.11):

1 – through discharge hole (BDH);

2 – discharge hole (FDH) filled with the unriveted rivet, BDH is through;

3 – discharge hole (BDH) is recess, (FDH) is filled with the unriveted rivet.

You can find the geometrical parameters of discharge holes in Fig. 4.11.

Discharge holes provide decrease of stress concentration on the edge of the hole filled with the bolt and the bolt load rate relative to the hole walls in the sheet as a result of joint compliance. That must result in the joint durability increase.

The influence of the (BDH) discharge hole diameter d_{dh} and the size of clearance between the basic and discharge hole (BDH) C_{dh} on the bolt compliance is experimentally studied. Empirical dependence is obtained:

$$C_b^{dh} = \tilde{N}_b \left[1 + 0{,}8 \left(\bar{d}_b \right)^{0{,}75} \left(1 - \bar{\tilde{N}}_{sh} \right)^{1{,}5} \right], \qquad (4.1)$$

where $\bar{d} = d_{dh}/d_b$, $\bar{C}_{dh} = C_{dh}/d_b$.

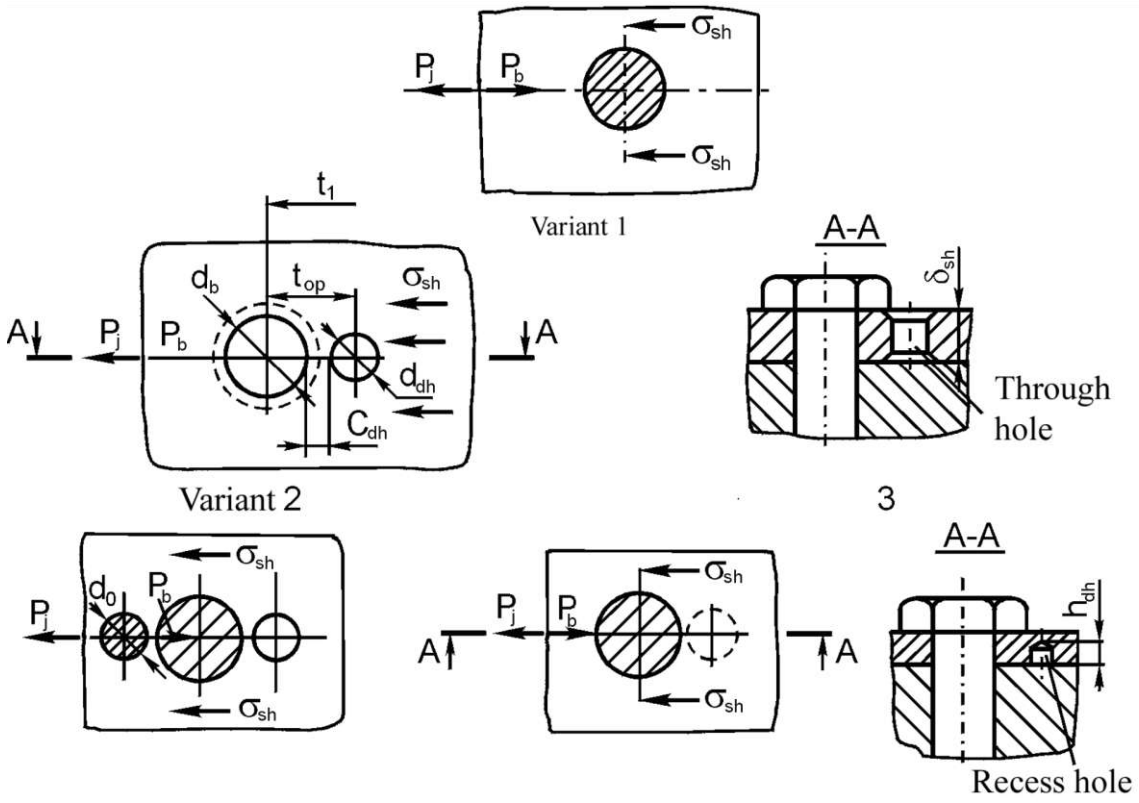

Fig. 4.11. Geometrical parameters of discharge holes

Increase of the first row bolt compliance results in its loading decrease. The calculation of force distribution along the bolt rows should be carried out subject to changed bolt compliance according to (4.1). Besides, additional hole increases sheet section compliance t_1 between bolts where the hole is located (Fig. 4.11):

$$a_1 = \frac{\gamma}{E_{sh}}\left[\frac{t_1 - d_{dh}}{B_{sh}\delta_{sh}} + \frac{d_{dh}}{(B_{sh} - d_{dh})\delta_{sh}}\right],$$

where γ = 1.2.

Recess additional hole (Fig. 4.11, variant 3) provides the joint tightness. The depth of recess hole is chosen according to the proportion:

$$h_{dh} = \delta_{sh} - 1 \text{ mm}.$$

Comparative fatigue tests of specimens of triple double-shear bolted joints with BDH – through discharge hole (Fig. 4.12) are carried out to identify rational geometrical parameters of discharge holes. Fatigue tests are carried out twice.

The first time. BDHs, through discharge hole d_{dh} = 4 mm in diameter was made in the specimens. The spacing length between basic and discharge holes was equal to C_{dh} = 0.5; 0.8; 1; 1.5; 2; 2.5; 3; 4 mm or $\bar{C}_{dh}$ = 0.083; 0.133; 0.166; 0.25; 0.333; 0.416; 0.5; 0.66 mm.

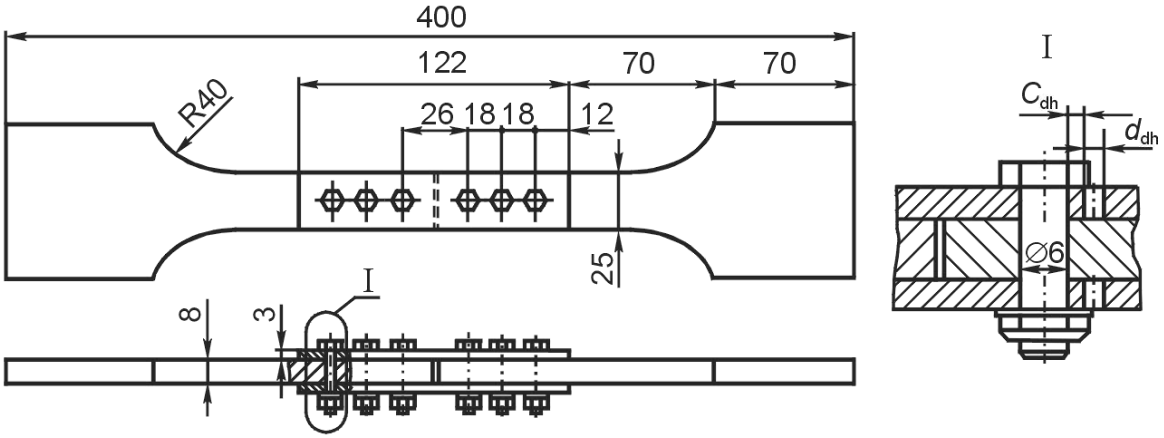

Fig. 4.12. Three-row double-shear bolted joint specimen

The second time. BDH, through discharge holes with the spacing length C_{dh}=1 mm was made. The discharge hole diameter was equal to d_{dh}=2, 3, 4, 5, 6 mm or $\bar{d}_{dh}$=0.333; 0.5; 0.666; 0.833; 1.

The test specimens are made of Д16АТ alloy. Bolts with normal 5009А-6-24, nut with normal 3373А-6 and washers with normal 3404А-6-12-1, 5, bolt fit according to H7/p6 were used. And bolt tightening corresponds to ОСТ 1.00017-77 and is equal to M_t=8 N·m.

The specimens were tested on the ЦДМ-10Пу hydraulic pulsator with the frequency of cyclic loading f=12.5 Hz. The level of cyclic loading is P_{max}/P_{min}=21500/4300 N/N and equal maximum zero-to-tension stress cycle $\sigma_{max\,0}$=128 MPa. Four specimens of each discharge hole variants have been tested. The specimens of triple double-shear bolted joints without discharge holes have been tested to compare.

Fig. 4.13 shows the influence of the spacing length between the basic and discharge holes $\bar{C}_{dh}$ and discharge hole diameter $\bar{d}_{dh}$ on the increase of the joint fatigue life.

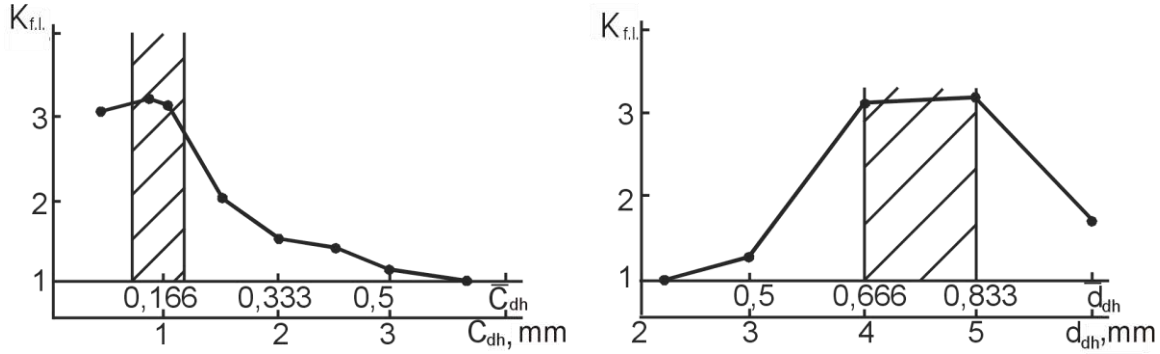

Fig. 4.13. Influence of discharge hole parameters on the joint durability

Analysis of the fatigue test results shows that the maximum increase of

fatigue life ($K_{f.l.}$ = 3) is obtained when discharge holes have the following geometrical parameters:

$$\overline{d} = d_{dh}/d_b = 0.65\ldots0.85;\ \ \overline{C}_{dh} = C_{dh}/d_b = 0.13\ldots0.2.$$

Experimental studies of different discharge hole variant effectiveness on cyclic durability of multi-row bolted joints with rational geometrical parameters

$$\overline{C}_{dh} = 0.13\ldots0.2 \text{ or } \overline{d}_{dh} = 0.65\ldots0.85$$ were carried out.

We used double-shear four-row joint (DFJ) without discharge holes (Fig. 4.14, a) and DFJ with BDH — through discharge hole (Fig. 4.14, b), front discharge hole (DH) filled with the unriveted rivet (Fig. 4.14, c); DFJ with BDH — recess discharge hole (Fig. 4.14, d), the depth of recess hole was equal to h_{dh} = 2.5 mm, front DH was filled with the unriveted rivet.

The produced BDHs — through discharge holes — had the following geometrical parameters: C_{dh} = 1 mm ($\overline{C}_{dh}$ = 0.167); d_{dh} = 4.5 mm ($\overline{d}_{dh}$ = 0.75). The front discharge holes had d_{dh} = 5 mm ($\overline{d}_{dh}$ = 0.83) and C_{dh} = 1 mm ($\overline{C}_{dh}$ = 0.167). Rivets were used to fill holes according to OCT 1.34040-79 with their further riveting, manufactured and closing head milling.

Bolts with normal 5009A-6-24, bolt fit H7/p6, bolt tightening M_t =8 N·m were used to assembly the specimens. Bolts according to normal OCT 1.11856-77 installed in the holes with interference Δ_{int} =1% d_b were used to assembly double-shear four-row joint (DFJ) with and without BDHs.

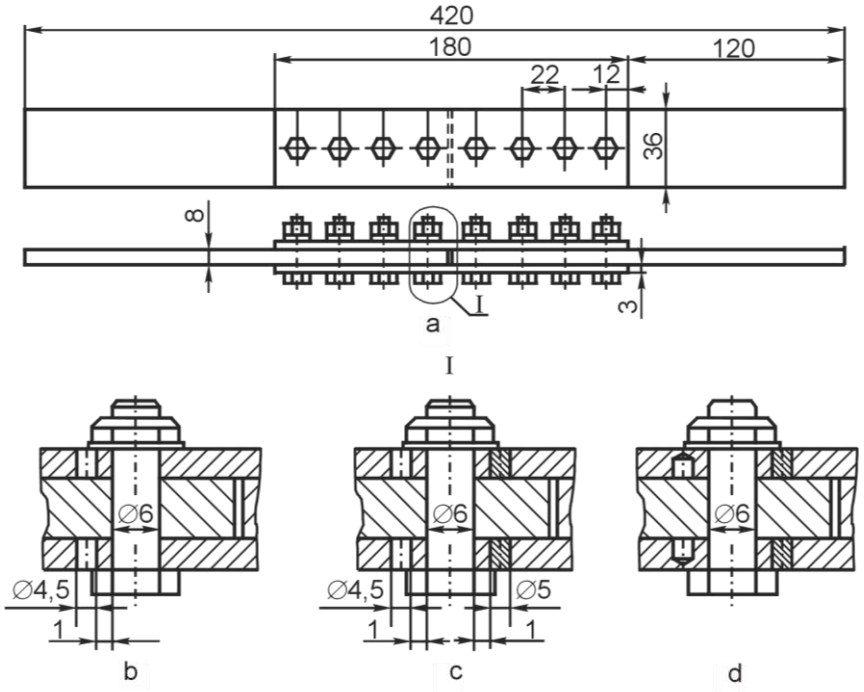

Fig. 4.14. Double-shear four-row joint specimen

All specimens were tested on the ЦДМ-10Пу hydraulic pulsator with the

frequency of cyclic loading f =12.5 Hz.

The specimens were tested on three levels of cyclic loading P_{max}/P_{min} = 39290/7850, 31350/6250, 20600/4100 N/N or $\sigma_{max\,0}$ = 168, 134, 88 MPa.

Fig. 4.15 shows the curves of the specimen number of cycles to failure.

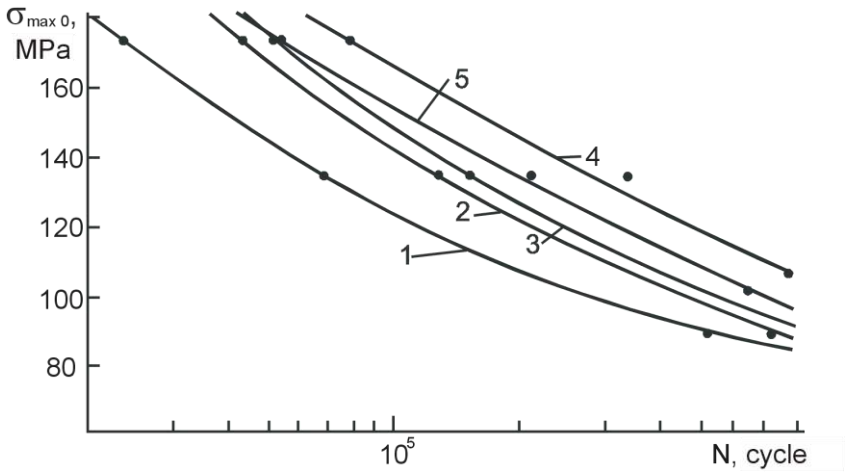

Fig. 4.15. Specimen fatigue test results: 1 — without discharge holes; 2 — with one-sided BDH; 3 — with two-sided BDH, the front DH filled with the unriveted rivet; 4 — one-sided BDH, bolts with the interference Δ_{int} =1% d_b; 5 — without discharge holes, bolt interference Δ_{int} =1% d_b

The analysis of the fatigue tests shows that all discharge hole variants increase fatigue life of shear bolted joints.

So the durability increases for four-row double-shear joints on the level $\sigma_{max\,0}$=134 MPa:

in ~1.9 times when two-sided through discharge holes with FDH filled with the unriveted rivet (see Fig. 4.15, curves 1, 3) are used;

in ~1.8 times when one-sided through discharge hole is used (see Fig. 4.15, curves 1, 2).

Thus, we recommend to execute the following discharge hole variants for multi-row bolted joints (more than three rows): one-sided through (recess) BDH; through (recess) BDH + pressure testing in front of the hole that increases its number of cycles to failure in 1.6 – 2.0 times when joint assembling labour increases minimally.

4.4. THE USE OF DISCHARGE GASKETS TO INCREASE SHEAR BOLTED JOINT LIFE

We recommend sticking the gaskets made of stronger material than connected plate material (Fig. 4.16) on the contacting surfaces of connected parts in the area of extreme bolts to increase bolted multi-row joint durability. While loading the joints the stuck gasket takes part in load perception. Thereby, it discharges connected plates along the section weakened by the first hole row

made for fasteners.

Two variants of discharge gasket installation in multi-row joints are designed:

1) the first row bolts are installed with interference along all thickness of connected pack including the gasket (Fig. 4.16, b, variant Gs1);

2) bolts 1 (Fig. 4.16, c, variant Gs2) are installed with the gap in part 2, for which this bolt row is the first one relative to the applied load, and with interference in sympathetic connected part 3 and gasket 4.

Gasket is stuck to the part, for which this bolt row is the first one, for all structural joint variants. When the gasket is stuck in this way, it increases the area of connected sheet along the section of the first hole row and decreases thereby the level of the cyclic tensile stress σ_e in the area of probable sheet fatigue failure. Bolt installation with the gap in the part, for which it is the first one, allows to exclude the bolt rod contact with the part body on the operating level of cyclic loading and to transfer load from the part to the part through the stuck gasket connected with the bolt. In this case the application of the gasket can have maximum effect because bearing stress is absent along the hole wall in the sheet.

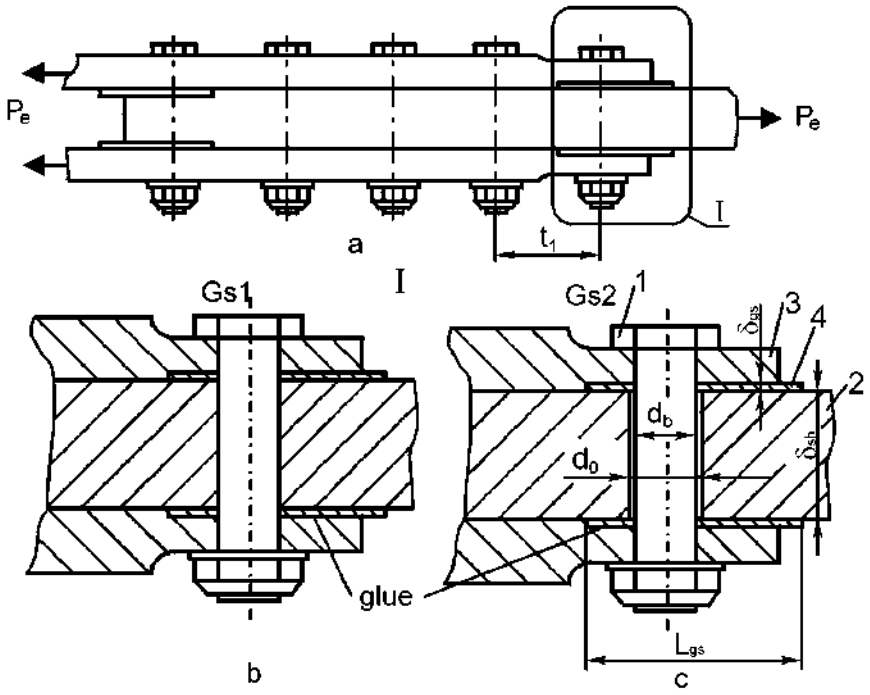

Fig. 4.16. Structure of discharge gaskets in multi-row joint

The gap between the hole wall and fastener rod are chosen and the bolt is switched in use according to the traditional diagram of multi-row bolted joint on the load level close to the static failure.

The value of the reduced stresses of the joint with the stuck gaskets according to work [403] is as follows:

$$\sigma_{gs}^{red} = K_{bear}^{red}\sigma_{bear}^{red} + K_{tens}^{red}\sigma_{tens}^{red} + K_{bend}^{red}\sigma_{bend}^{red}, \qquad (4.2)$$

where $K_{bear}^{red}, K_{tens}^{red}, K_{bend}^{red}$ – experimentally determined damage factor according to normal bearing, tensile and bend stress; $\sigma_{bear}^{red}, \sigma_{tens}^{red}, \sigma_{bend}^{red}$ – bearing stress along the bolt hole wall, tension in the sheet behind the bolt, sheet bend in the area where the gasket is glued.

The joints with glued gaskets have the same number of cycles to failure as the plates with the holes filled with bolts according to the same technology of their installation have:

$$\sigma_{gs}^{red} = \sigma_{pl} = \grave{a}N^{m}, \qquad (4.3)$$

where a, m – experimentally determined constants of cyclic durability curve.

Geometrical parameters of joints without gaskets, satisfied static joint strength condition, are necessary to determine geometrical parameters of gasket. We use method of successive approximations for the further design of joint with gasket. It is reasonable to set initial gasket thickness equal δ_{gs}=0.2…0.3 δ_{sh} from the proximal one according to assortment. Gasket width is in the row

$$2C_{dh} \le B_{gs} \le t. \qquad (4.4)$$

Gasket length is determined by lifting properties of glue film:

$$L_{gs} = \left(K_{gs}P_b\right) / B_{gs}\tau_{gl}, \qquad (4.5)$$

where P_b is primarily determined for joints without gasket.

We can take in the first approximation

$$K_{gs} = K_b \frac{\delta_{gs}E_{gs}}{\delta_{sh}E_{sh}}. \qquad (4.6)$$

We should note that stuck gasket has influence on the force distribution over the bolt rows. That is why it is necessary to recalculate the force distribution over the bolt rows with gaskets according to the methodology of works [411, 446] after the approximate estimation of gasket geometrical parameters. And we should take into account the rigidness variation of sheet area to which the gasket is glued:

$$a_1 = \frac{\gamma}{E_{sh}B_{sh}}\left[\frac{L_{gs}}{\delta_{sh} + K_{gs}E_{gs}/E_{sh}\delta_{gs}} + \frac{t_1 - L_{gs}}{\delta_{sh}}\right]. \qquad (4.7)$$

Gasket thickness is determined after the force estimation on the first bolt row of joint with gasket.

$$\delta_b = \left(K_{gs}P_b\right) / d_b\sigma_{bear}^{gs}. \qquad (4.8)$$

Discharge gaskets provide decrease of tensile stress in the plates

$$\sigma_{sh}^{red} = \frac{P_{\tilde{n}} - P_b}{B_{sh}\left(\delta_{sh} + K_{gs}\delta_{sh}\right)}, \qquad (4.9)$$

decrease of bearing stress over bolt hole wall:

$$\sigma_{bear}^{red} = \frac{P_b}{d_b\left(\delta_{sh} + K_{gs}\delta_{sh}\right)}. \qquad (4.10)$$

When gasket geometrical parameters and joint stressed state parameters have been determined, joint number of cycles to failure is estimated using the values of reduced stresses (4.2) with account of (4.3). If joint number of cycles to failure is less than the specified, it is necessary to increase the connected sheet thickness. And when joint number of cycles to failure is considerably less than the specified one (over 30 – 50%), it is necessary to increase the gasket thickness from the nearest greater assortment thickness as well. Then we repeat the calculation of the new gasket parameters and joint stressed state parameters according to – (4.10), until we obtain number of cycles equal the set value.

The choice of Gs2 gasket geometrical parameters (Fig. 4.16) has its peculiarities. The geometrical parameters (thickness)of the gasket, its material mechanical parameters and glue film lifting features determine fastening connection compliance for clearance between hole wall and bolt. Since the glue shear modulus G_{gl} is by order of magnitude smaller than gasket and bolt material modulus of elasticity, glue film lifting features generally determine fasten connection compliance for the joint with gasket Gs2:

$$C_b = 1/G_{gl}B_{gs}\,. \qquad (4.11)$$

Therefore, it is necessary for force distribution calculation along the bolt row to take into account formula (4.11), while determining in what follows gasket geometrical parameters, stressed state parameters and joint cyclic durability according to formulas (4.4) – (4.10). The clearance between connected sheet and bolt is determined from the relation

$$\Delta_{clear} = \frac{d_0 - d_b}{2} = C_b P_b. \qquad (4.12)$$

The experimental investigation of the developed method efficiency was carried out on the double-shear four-row joint specimen (Fig. 4.17).

The specimen is in a butt joint of plates made of Д16АТ л. 8.0 alloy and two-sided straps made of Д16АТ л. 3.0 alloy. Bolts with normal 5009А-6-24, the 3373А-6 nuts and the 3404А-6-12-1.5 washers were used for the assembly. The bolt fit was according to H9/h8, bolt tightening was M_t = 8 N·m.

Three variants of double-shear four-row joint specimens: without gaskets (basic variant) in Fig. 4.17, a; with glued gaskets of Gs1 variant in Fig. 4.17, b; with gaskets while installing the extreme bolts with the clearance in the middle plate body (variant Gs2 in Fig. 4.17, c) were tested.

The gaskets were made of 30ХГСАл.0.5 material and stuck to connected parts with glue ВК-9.

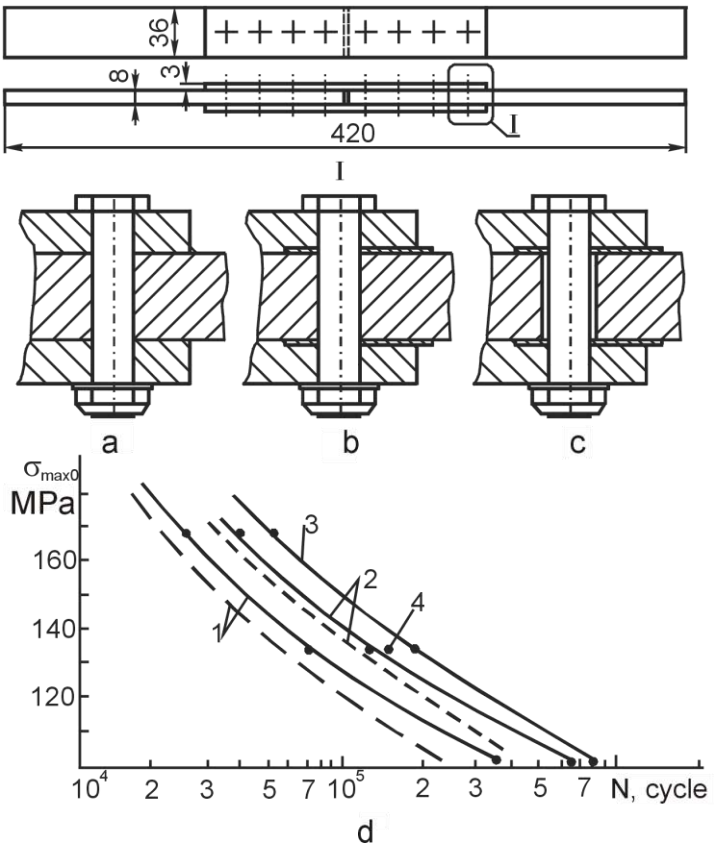

Fig. 4.17. Double-shear four-row joint specimen and fatigue test results

The specimens were testes on ЦДМ-10Пу hydraulic pulsator at cyclic loading frequency f = 12.5 Hz on three cyclic loading levels P_{max}/P_{min} =39200/7850, 31350/6270, 20600/4100 N; this data corresponds to maximum normal stress of zero-to-tension stress cycle $\sigma_{\max 0}$ = 168, 134, 88 MPa.

Five specimens were tested on every level of the cyclic loading. The curves of the tested specimen cyclic durability are given in Fig. 4.17, d: where 1 — basic specimen test; 2 — with gasket Gs1; 3 — with gasket Gs2; 4 — with gasket Gs2 at load cycle asymmetry parameter R_σ =0.5. Failure of all specimens occurred on the first (internal) row of bolt-holes of joint straps.

The analysis of fatigue test results shows that application of discharge gaskets provides increase of specimen cyclic life in 1.6 – 2.1 times.

Calculation of the specimen cyclic life is carried out according to the methodology of work [409] with formulas (4.2), (4.3). While calculating the basic curve of plate cyclic durability with the holes filled with bolt fit according to H7/h6 was used:

$$\sigma_{pl} = 1334N^{-0,1881}, K_{bear} = 0,089N^{0,132}.$$

The calculation results with gaskets Gs1 are given in Table 4.1. Estimated curves of basic specimen cyclic life and cyclic durability of specimens with gaskets Gs1 are given in Fig. 4.17, d (dotted curve).

Table 4.1

Results of double-shear four-row joint fatigue tests

$\sigma_{\max 0}$, MPa	$P_{\max 0}$, H	$P_{b,}$ H	P_{sh}, H	σ_{bear}, MPa	σ_{sh}, MPa	K_b	$N_{calc,}$ cycle	N_{exp}, cycle
168	37000	1036	2664	51	130	0.28	31100	38200
134	29500	826	2124	41	104	0.28	111200	124300
88	19400	543	1397	26,5	68	0.28	410700	570100

4.5. LIFE INCREASE METHODS OF ASSEMBLY PANEL JOINTS WITH BREAK PROFILE

Efficiency of constructive ways of shear joint durability increase is approved on specimens of the reattachment of single-stringer panels with break profile. Development and manufacture of specimens are carried out taking into account constructive, power and technological features of cross-section shear bolted joints of aircraft wings.

Standard members of similar joints are panel skin, stringer, break profile: (reattachment profile), reattachment fittings, and fasteners. The regular part of single-stringer panels — skin with attached stringer was invariable during the structure development of all specimen constructive variants.

The Д16Т л. 5.0 sheet material having in stringer joining place 50 mm in width of and 5 mm in thickness and mechanically milled on both sides of the stringer web to the thickness equal 3 mm was used to produce the skin. The Пр315-3 profile of Д16Т ones was used to produce the stringer. The width of the specimen is 120 mm; the area of panel regular part is 710 mm^2. Reattachment fittings are made by mechanical milling of the Д16Т material.

Six variants of specimen embodiment are developed and produced.

Variant 1 (Fig. 4.18). The specimen consists of break profile 1, skin 8 with riveted stringer 7 and reattachment fittings 3, 4, connected to the profile with help of bolts 2 with the 5013A-6-26 normal and to the skin with bolts 5 with the 5004A-5-20 and 5013A-6-20 normal. Bolts fit in holes is on H7/h6, bolt tightening corresponds to OCT 1.00017-77 and is equal to 5 N·m for bolts 5 mm in diameter and 8 N·m for bolts 6 mm in diameter.

Variant 2 (Fig. 4.19). The specimen structure differs from the specimen structure of variant 1 in the fact that bilateral discharge holes are executed in the places of probable fatigue failure (the first bolt rows of joint); forward discharge holes 2 (in relation to loading operating in a part) in the skin panel are made as recess ones with the open surface turned to the stringer and reattaching profile. Discharge hole 3 and hole 1 in the skin are executed as through ones in the BDH butt profile. Diameter of through and blind discharge holes are equal to d_{dh}=4 mm, depth of blind holes are h_{dh}=4.5 mm ($\bar{h}_{dh}$ = 0.9). Rivets are applied to fill holes according to OCT 1.34040-79, rivets are blind and closing heads are

milled after unriveting.

Variant 3 (Fig. 4.20). Reattaching fitting structure grasping panel stringer only for edge is changed in comparison with the specimen structure of variant 1. Bolts with the OCT 1.11856-76 and OCT 1.11857-76 normal (countersunk) are applied to assemble the specimens. The bolts are seated in hole with interference $\Delta_{int} = 1\% d_b$, the bolt tightening corresponds to OCT 1.00017-77.

Variant 4 (Fig. 4.21). The specimen structure differs from the specimen structure of variant 1 in the fact that discharge gaskets 1 are glued in the places of probable fatigue failure (the first bolt rows of joint). The gaskets are made of the 30ХГСА material 0.5 mm in thickness and glued to connected parts with the ВК-9 glue.

Variant 5 (Fig. 4.22). The specimen structure differs from the specimen structure of variant 1 in the fact that reattaching fitting rigidity changes along their lengths that allows reducing loading degree of the joint first rows. The inclusion zone in perception of loading part of reattaching the stringer panel with fitting is spaced. The discharge gaskets 1, 2, 3 made of the 30ХГСАлО.5 material are stuck in the places of probable fatigue failure.

Variant 6 (Fig. 4.23). The stringer panel is connected to the reattaching profile without the reattaching fittings. Bolts with interference $\Delta_{int} = 1\% d_b$ are applied to assemble the joint. Uncountersunk bolts with interference $\Delta_{int} = 1\% d_b$ and discharge gaskets 1 are applied in the places of probable fatigue failure.

Specimens of all embodiment variants are tested on the МУП-50 hydraulic fatigue machine at the maximum stress level of zero-to-tension stress cycle in the specimen regular part $\sigma_{\max 0}$ = 128 MPa at cyclic loading frequency f =6 Hz.

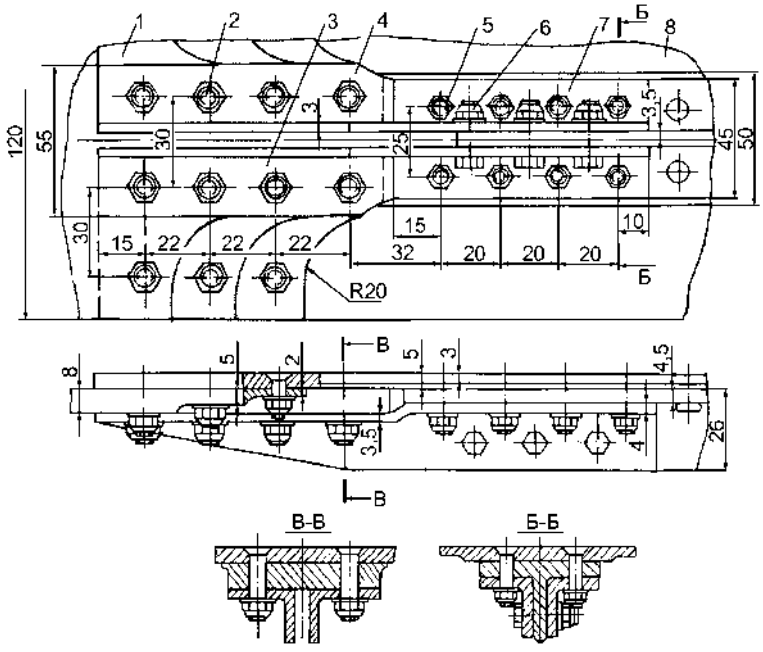

Fig. 4.18. Specimen of stringer panel-to-break profile joint (variant 1)

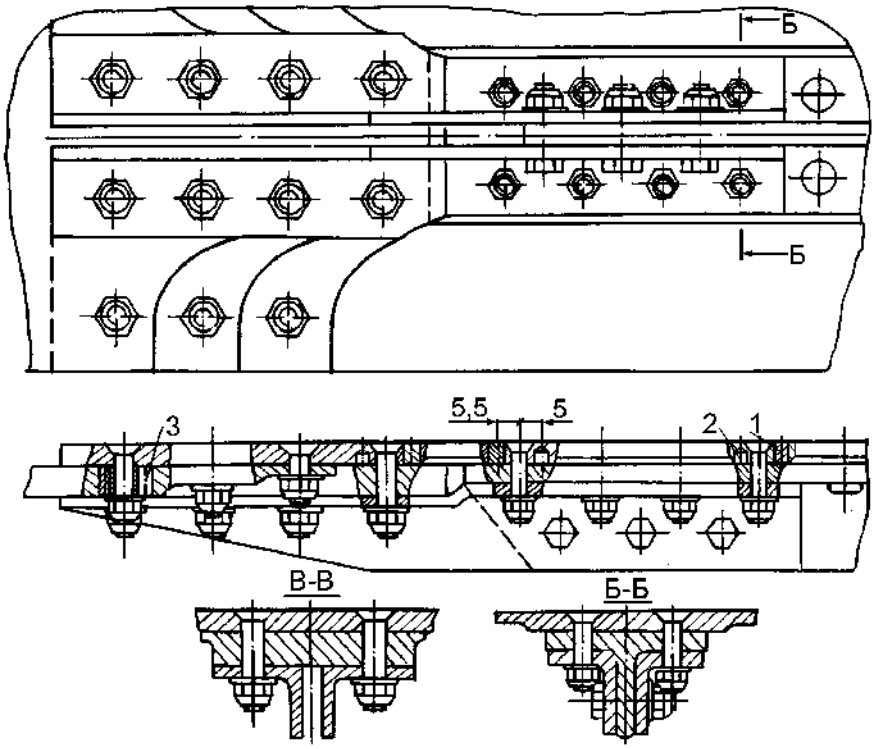

Fig. 4.19. Specimen of stringer panel-to-break profile joint (variant 2)

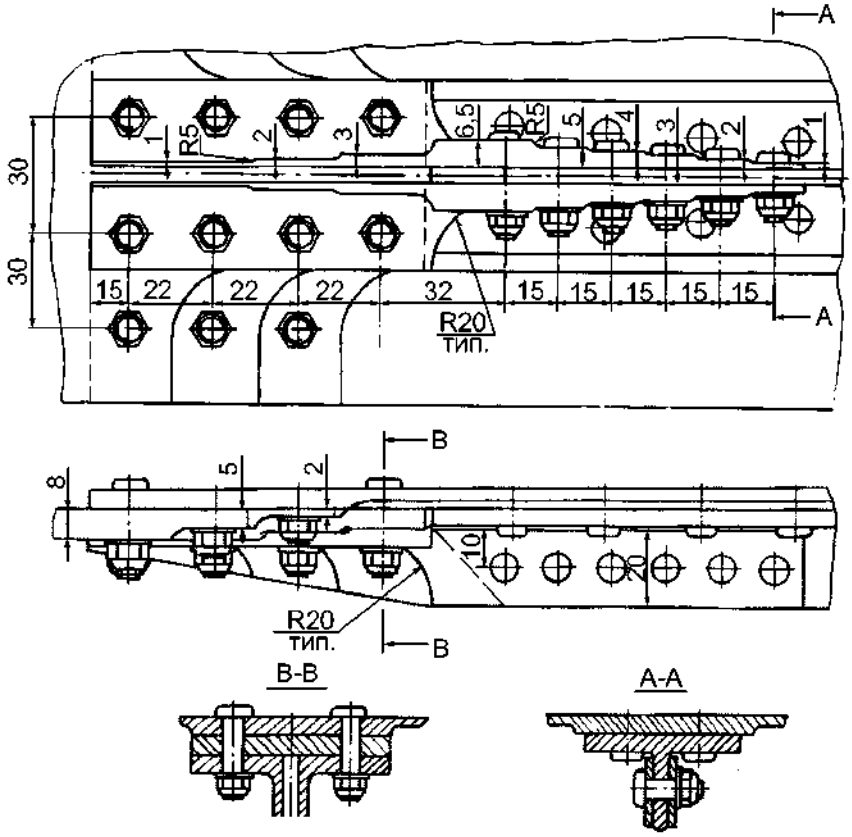

Fig. 4.20. Specimen of stringer panel-to-break profile joint (variant 3)

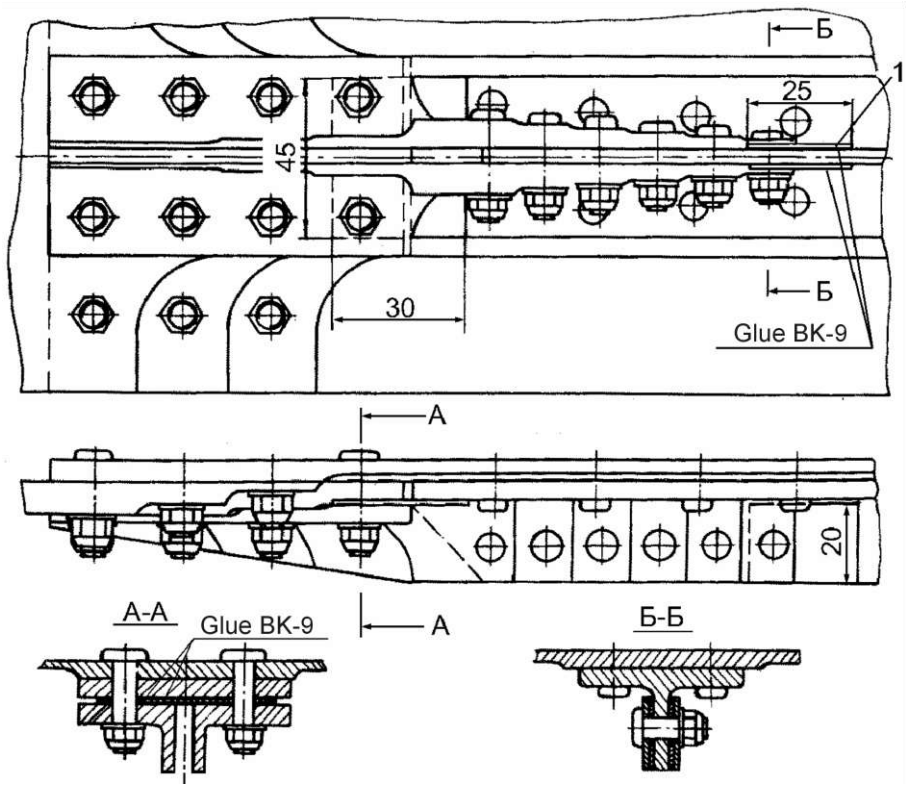

Fig. 4.21. Specimen of stringer panel-to-break profile joint (variant 4)

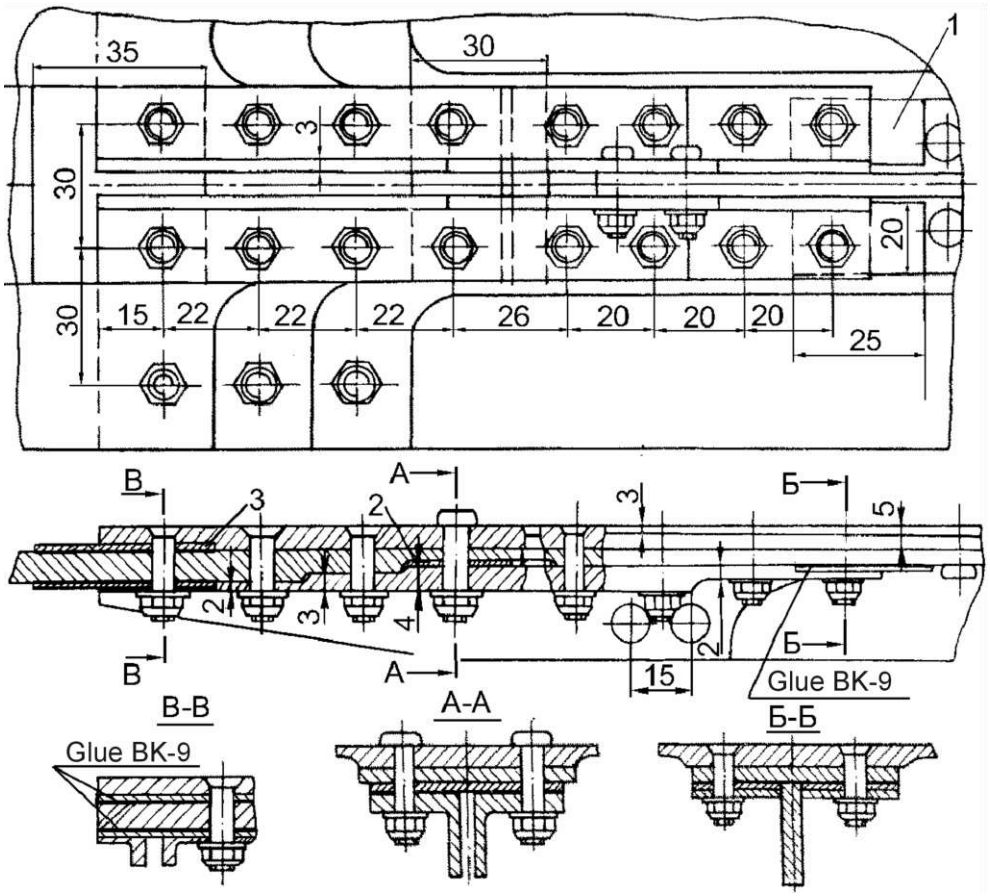

Fig. 4.22. Specimen of stringer panel-to-break profile joint (variant 5)

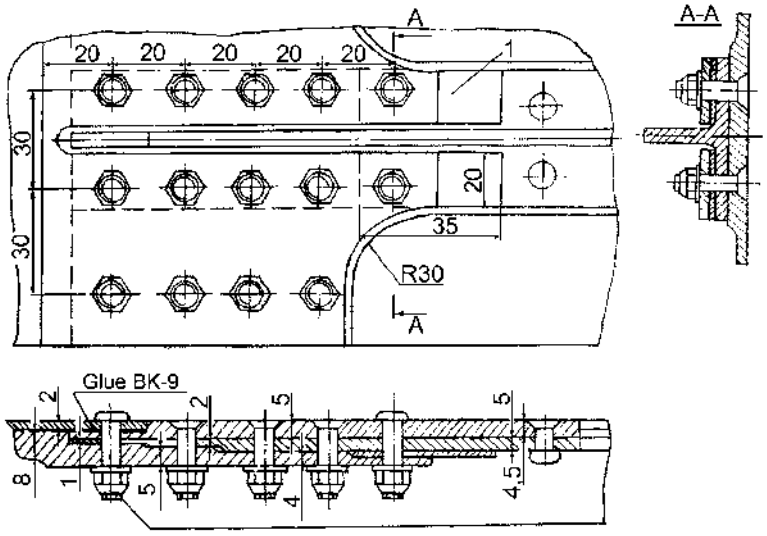

Fig. 4.23. Specimen of stringer panel-to-break profile joint (variant 6)

Four specimens of each variant have been tested. Carried out fatigue tests revealed four zones of specimen fatigue failures (Fig. 4.24).

Table 4.2 shows the results of fatigue tests and the zones of specimen fatigue failures.

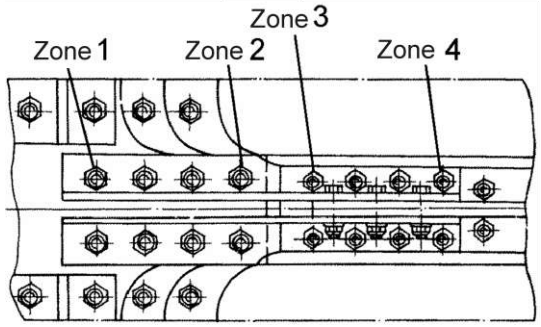

Fig. 4.24. Zones of fatigue cracks initiation

Table 4.2

The results of specimen fatigue test

Variant	N, cycle (failure zone) Specimen number				N_m	$N_{calc}^{zone\,3}$	S
	1	2	3	4			
1	63700 (1)	70600 (2)	81300 (3)	106400 (4)	78900	70200	0.0966
2	76500 (1)	98300 (2)	124700 (3)	158600 (4, 2)	114500	103300	0.1012
3	74300 (4)	89700 (4)	108300 (3)	121400 (3)	96700	88900	0.0937
4	104600 (2)	127300 (3)	160000 (2)	230200 (2)	155800	161300	0.1184
5	127100 (1)	144800 (1)	173200 (3)	210500 (2)	160900	143500	0.0852
6	240400 (1)	293100 (4)	362700 (1)	475600 (4)	332100	301100	0.1271

The analysis of fatigue test results shows that the developed ways increase cyclic life of reattaching place structure of assembled stringer panels with reattaching profile. So, for example, bilateral through and blind holes made in places of probable fatigue failure (variant 2, see Fig. 4.19) have provided the cyclic life increase of the base specimen (variant 1, see Fig. 4.18) approximately in 1.45 times. Application of discharge gaskets in places of probable structure fatigue failure (variant 4, see Fig. 4.21) has provided cyclic durability increase of analogous structure specimen (variant 3, see Fig. 4.20) approximately in 1.6 times.

Joint cyclic live of variants 5 and 6 are greater than the joint life of the base specimen and approximately in 2 and 3.8 times respectively.

The given stresses in specimens are calculated according to expression (4.2).

Cyclic life curves of plate with the holes filled with bolts are used as base ones:

– for bolt fit according to H7/h8

$$\sigma_{pl} = 1334N^{-0.188};$$

– for bolt fit with interference $\Delta_{int} = 1\% d_b$

$$\sigma_{pl} = 298N^{-0.1442}.$$

Damage factors received experimentally were used to calculate:

– for bolt fit according to H7/h8

$$K_{bear} = 0.09N^{0.13},\ K_{bend} = 0.316N^{0.024};$$

– for bolt fit with interference $\Delta_{int} = 1\% d_b$

$$K_{bear} = 0.086N^{0.126},\ K_{bend} = 0.302N^{0.022}.$$

Bending stresses along the joint length are estimated due to the methodology of the paper [25]. We take K_{sh} =0.9 while estimating the specimens with discharge holes and glued gaskets.

The results of the estimation are given in Tab. 4.2. They (N_{calc}) conform to test data satisfactorily.

We have compared the joint effectiveness according to the panel masses of variants 5 and 6 with the base specimen. For this action we calculated masses of connected parts, gaskets, glue and fasteners:

$$M_{j.var.1} = 840 \text{ g},\ M_{j.var.5} = 650 \text{ g},\ M_{j.var.6} = 610 \text{ g}.$$

comparison test for the mentioned variants was value:

$$\overline{m}_N = \frac{\Delta m}{N},$$

where N – joint cyclic durability; $\Delta m = M_j - M_{reg}$, where M_j – joint absolute mass; M_{reg} – mass of the regular panel part along the connection length (as if the joint is absent).

Mass of the regular panel part along the joint length is ($l_{j.var.1}$= 183 mm, $l_{j.var.5}$=177 mm, $l_{j.var.6}$=110 mm, area of the regular panel zone F_{reg} =710 mm^2):

$$M_{j.var.1}=470 \text{ g};\ M_{j.var.5}=358 \text{ g};\ M_{j.var.6}=222 \text{ g}.$$

Thus:

$$\overline{m}_{N\,var.1}= 5.95\cdot10^{-3} \text{ g/cycle};\ \overline{m}_{N\,var.5}= 1.81\cdot10^{-3} \text{ g/cycle};$$

$$\overline{m}_{N\,var.6}= 1.29\cdot10^{-3} \text{ g/cycle}.$$

The analysis of the calculation results shows that variant 6 (see Fig. 4.23) has the best mass efficiency from all offered constructive variants of stringer reattaching.

4.6. POLYMERIC FILLER INFLUENCE ON DURABILITY OF SINGLE-SHEAR BOLTED BIAS JOINTS

Mating part surfaces must have snug fir to each other that is provided by machining with further part scraping before assembly to provide fatigue life and survivability of shear bolted joints.

Surface adjustment by scraping is labour intensive process after which it is possible to achieve mating surfaces fit no more than 70 … 80 % of full contact zone size.

Camber of the part surface while assembling leads to occurrence of gaps in the contact zone and reduction of contact area (RCA) of mating parts. Bending stresses and increase of contact stress concentration occur while tightening the bolts and seating them with radial interference in the joints with gaps and reduction of contact area in the connected parts.

Intensity of fretting corrosion increases and joint durability decreases when contact stress and bending stress increase during the joint cyclic loading.

Serial coverings such as anodizing and primer coating of the ФЛ-086 type do not remove negative influence of fretting corrosion and technological tolerances on the fatigue life of the shear bolted joints. That is why we propose to cover the qualitatively treated surfaces of parts with surface waviness with the help of polymeric fillers to eliminate gaps between connected surfaces of metal parts and their direct contact along the mating surfaces.

Fillers ЗП-1, ЗП-2, ЗП-2М, ЗП-3, В3-27 and others made on basis of the К4С, ВК9, ВК-27 and different Е fillers in the form of titanium dioxide, chrysotile asbestos, disulphide molybdenum, chopped glass fiber and alumina are used as compensators of mechanical tolerances for the part shear joints made of

aluminum alloys. In this case joints can be detachable and permanent [215, 218].

When fillers are used scraping labour intensive process is eliminated, intensity of fretting corrosion decreases and durability increases. Polymeric fillers also provide increase of joint tightness.

Polymeric filler introduction provides considerable results in the aircraft industry.

Owing to that polymeric fillers of the ЗП-2 type remove additional stresses, increase the contact area of mating joint member surface, approximately to 100%, decrease access of oxygen and moisture from air, they should essentially decrease intensity of fretting corrosion and increase of bolted bias joints durability especially when axial and radial bolt interferences are used.

Fatigue tests of bias joint models (Fig. 4.25) have been carried out for experimental check of the given hypotheses. The ЗП-2М polymeric filler was spread on the anodized surfaces.

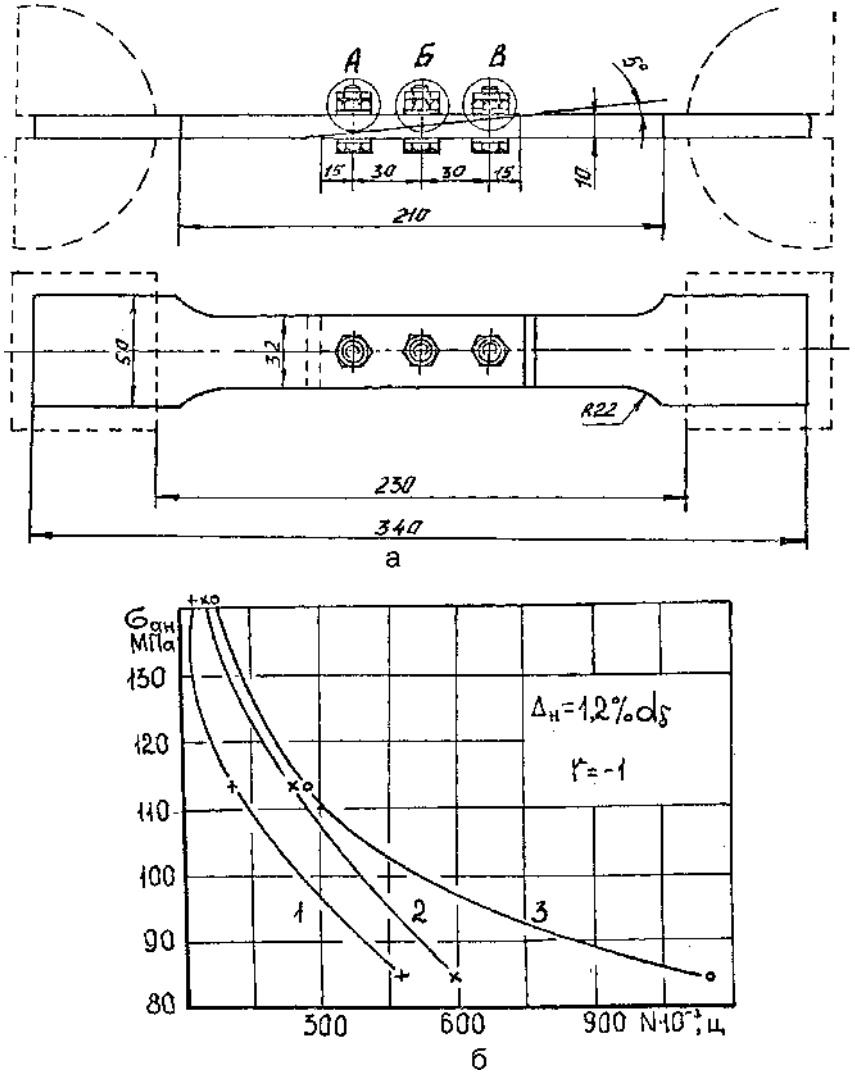

Fig. 4.25. Specimen of single shear bias joint with smooth mating surfaces and influence on its fatigue life of the ЗП-2М polymeric filler:
1 – anodization+ ФЛ-086; 2 – anodization; 3 – anodization + ЗП-2М

As you see from Fig. 4.25 (b) at $\sigma_{àn} = 141.5$ MPa polymeric filler has practically no influence on durability of bias joint with radial interference equal to $\Delta_{int} = 1.2\% d_b$.

Durability of the joint increased in 1.6 times at $\sigma_{àí} = 113$ MPa in comparison with joint durability with coating “anodization + the ФЛ-086 primer”.

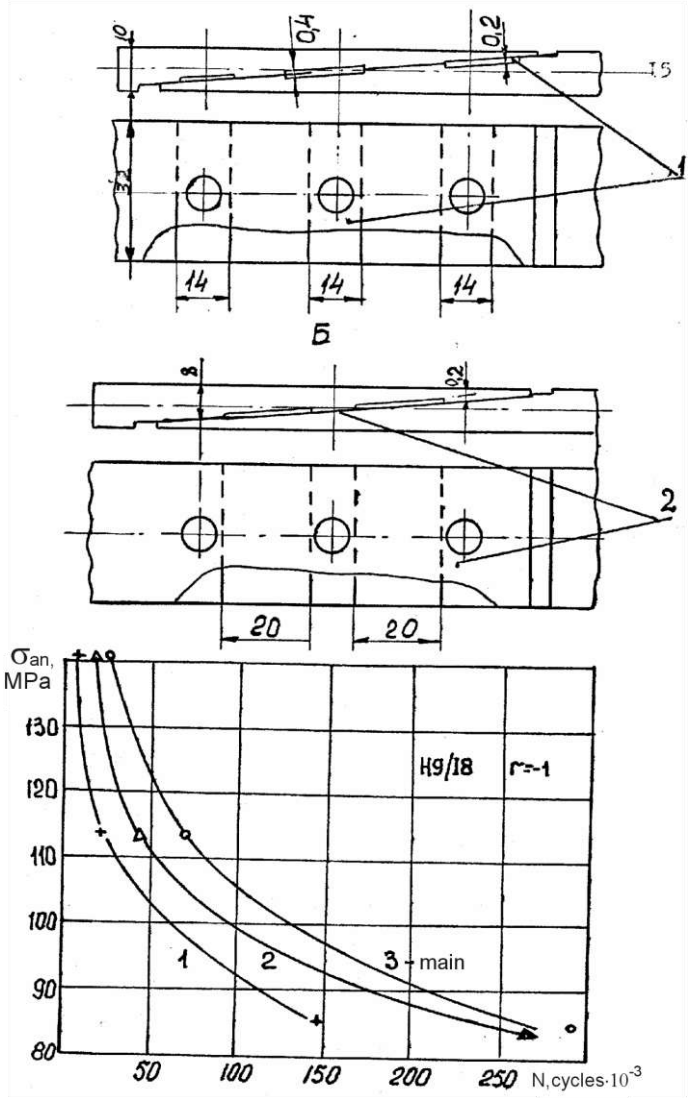

Fig. 4.26. Production tolerance influence in the form of gaps (1) and RCA (2) on bias joint durability

The 3П-2М filler permitted to increase bias joint durability more than in 2 times at $\sigma_{aн} = 85$ MPa. This fact is explained by that, firstly, filler removes fretting corrosion on the mating surfaces, secondly, it sticks joint members and thereby considerably discharges holes in this case.

Fatigue tests of bias joint models with gaps and the reduced contact area (RCA) (Fig. 4.26) have been conducted for investigation of the 3П-2М polymeric filler influence on durability of bias joints with production tolerance characterized by mating surfaces nonstraightlinearity.

Specimens both with gaps and with RCA were made in two variants: with sliding bolt fit (H7) and with radial interference equal to $1.2\% d_b$. Fatigue test results of bias joints with production tolerance and polymeric filler are given in Fig. 4.27 and 4.28.

Fig. 4.27 presents average numbers of cycles before bias joint damage with sliding bolt fit with smooth mating surface (curve 2), with gaps (curve 1) and with gaps while spreading the 3П-2 (curve 3) and 5П-2М (curve 4). Comparing the curves 1 and 3 you can see that polymeric filler has increased durability of bias joint with gaps in 3.6 times at $\sigma_{aн}$ = 141.5 MPa and in 3.7 times at $\sigma_{aн}$ =113 MPa and in 2.3 times at $\sigma_{aн}$ = 85 MPa.

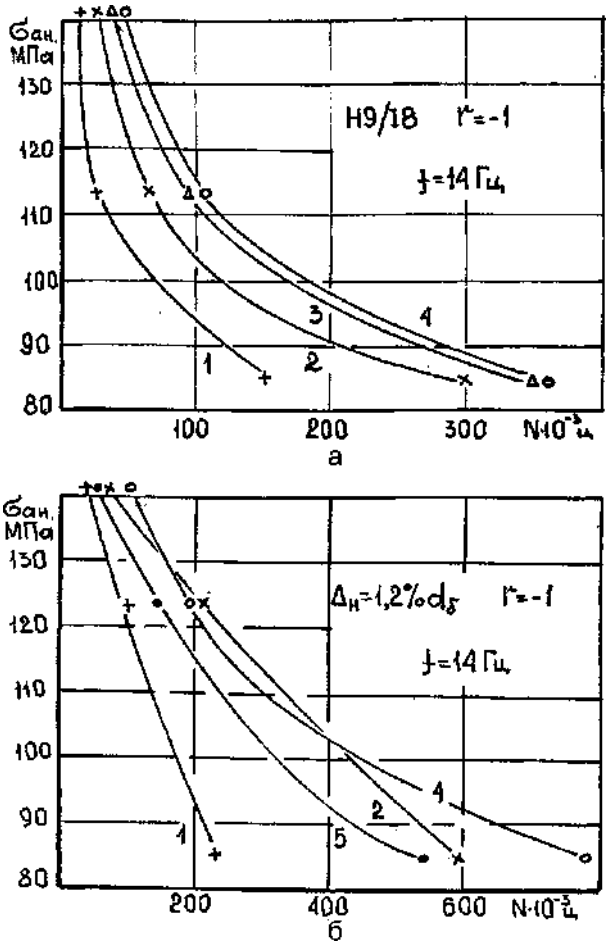

Fig. 4.27. Polymeric filler influence on bias joint durability with sliding bolt fit (a) and radial interference (b): 1 – with gaps; 2 – smooth contact surfaces; 3 – gaps + 3П-2; 4 – gaps + + 3П-2М; 5 – gaps + 3П-3

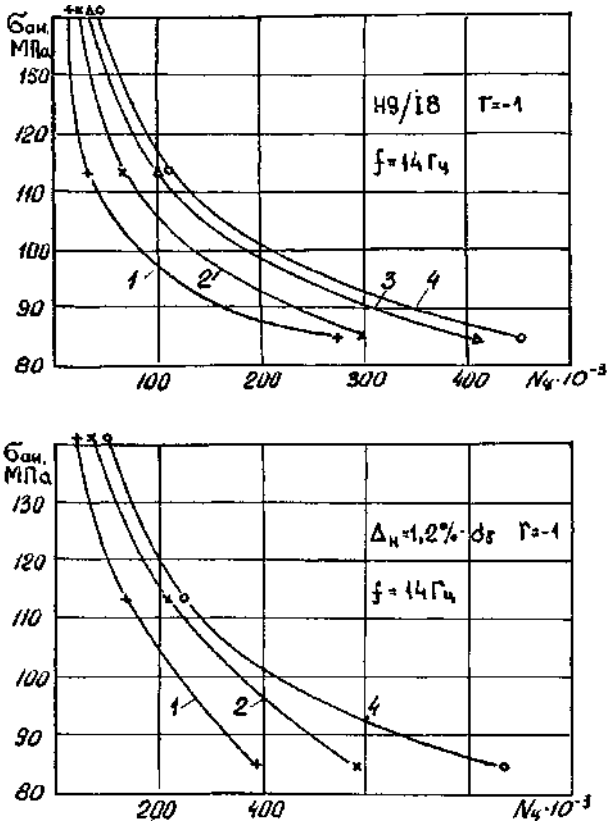

Fig. 4.28. Filler influence on fit joint durability: 1 – reduction of contact area (RCA);
2 – smooth mating surfaces;
3 – RCA + 3П-2;
4 – RCA + 3П-2М

The comparison of curves 2 and 4 shows that durability of the specimen with gaps and 3П-2М is even slightly greater than durability of the specimen with smooth mating surface. It results from several causes. Firstly, 3П-2М removes fretting corrosion, secondly, contact area approximates to 100% when filler is used. And it is especially necessary to note the third cause: the gaps between bolts and hole walls are filled with the polymeric fillers during assembling the specimens with sliding bolt fit. It tells on fatigue life of bias joint favourably.

Results of tests showed that the 3П-2 and 3П-2М fillers as compensators of production tolerance is quite effective in the single shear bias joints.

The polymeric filler increased durability in 1.5 times at $\sigma_{à\,n}$ = 141.5 MPa, in 2.1 times at $\sigma_{à\,n}$=113 MPa and in 3.5 times at $\sigma_{à\,n}$ = 85 MPa in joints with production tolerance such types as gaps at bolt fit with interference 1.2%d_b. You

can see it from comparison of curves 1 and 2 (see Fig. 4.27).

The comparison of curves 2 and 4 shows that durability of the joint with gaps and ЗП-2М is greater than durability of the joint with smooth mating surface. It results from that: fretting corrosion on the mating surfaces, which is practically removed when filler is used, has considerable influence on the durability

The curve 4 represents average numbers of cycles before damage of the specimens with gaps, on mating surfaces of which the ЗП-3 polymeric filler developed on the basis of the ВК-9 glue by Siberian bureau of NIAT is spread. It is evidently that the ЗП-3 fillers is an effective compensator of production tolerance on the mating surfaces of bias joints.

The ЗП-2М filler in the joints with RCA has permitted to increase durability of joint with sliding bolt fit in 1.8 times at $\sigma_{à í}$ = 141.5 MPa, in 2.5 times at $\sigma_{a н}$ = 113 MPa and in 1.4 times at $\sigma_{a н}$ = 85 MPa (curves 1 and 3, see Fig. 4.28). Fatigue life of specimens with RCA and ЗП-2М is also greater than durability of joints with smooth mating surface in 1.3 – 1.5 times.

When bolts were fitted with interference the polymeric filler has increased fatigue life of joints with RCA in 1.8 times at $\sigma_{a н}$ = 141.5 MPa, in 1.6 times at $\sigma_{a н}$ = 113 MPa and in 2.2 times at $\sigma_{a н}$ = 85 MPa (see curves 1 and 2, Fig. 4.28).

When stress is equal to $\sigma_{a н}$ = 85 MPa joint life with RCA and ЗП-2М is as well slightly greater than durability of joint with smooth mating surface without coating (curves 2 and 3).

The analysis of the damaged specimens showed that fatigue cracks originate, as a rule, in section along the hole axis. Several specimens had damages in these zones on boundaries of groove and smooth surface of joint members. When loads were heavy, damages occurred in section along hole axis, when load was low damages occurred in zone of bending stresses generated by eccentricity of force transfer from one member to another one.

Failures of polymeric filler layer did not occur. Thus, fatigue tests showed high efficiency of polymeric fillers as means of maintainability and durability increase of bias joints.

Full-sized bias joint the structure of which is given in the Fig. 4.29 was tested for investigation of possible replacement of scraping by spreading the ЗП-2 polymeric filler layer in Tu (Ty)-134 aircraft joints.

This joint is applied when stabilizer spar caps are connected with power section

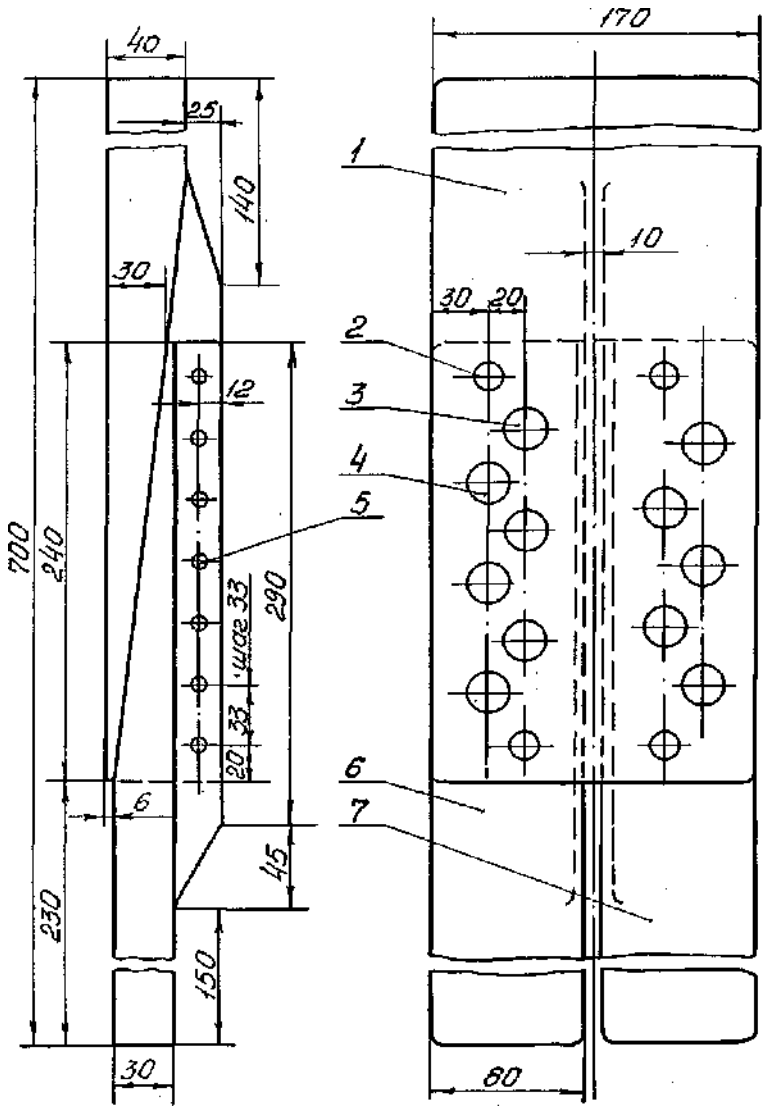

Fig. 4.29. Specimen of full-sized bias joint

The joint consists of three basic members: T-section cap I and two straps (spar cap) of angle section 6 and 7. Chamfer angle of joint members is equal to 6°.

Members of full-sized joint are made by milling of the РС ПК-11295-Д16Т section. Scraped specimens have the mating areas along the wedge and vertical cap equal to not less than 80 % of all mating area according to the specifications. Parts 1, 6 and 7 are anodized.

Bolt holes preparation and nut tightening is carried out according to the manufacturing instruction 323Н0. Bolts with normal 709НС are fitted on the ФЛ-086 crude primer Пл during the fitting.

The polymeric filler on the mating surfaces of unscraped joint members was spread in 0.6 mm nominal thickness.

Fatigue tests of full-sized bias joint with scraped mating surfaces and with polymeric filler layer are carried out on the МУП-200 fatigue machine with frequency equal to 3.33 Hz under asymmetric cyclic loading with cycle

asymmetry factor r =0.15.

The joint has been tested on two loading levels $P_{\max}/P_{\min} = (50/7)\cdot 10^3$ and $(30/7)\cdot 10^3$ daN. The loading equal to $50\cdot 10^3$ daN corresponds to half theoretical static breaking force under tension.

Applied loading corresponds to nominal stresses

$\sigma_{\max}$ = 109.5 and 64.4 MPa, $\sigma_{\min}$ = 63 and 37 MPa and $\sigma_{a\,н}$ = 46.5 and 27.4 MPa in section on the first bolt row in joint members 6 and 7.

Results of fatigue tests of full-sized bias joint are given in Fig. 4.30. Straight line 1 represents average numbers before damages of joints with scraped surfaces, straight line 2 shows number of joint with filler layer.

As we can see interseam compensation of production tolerances in full-sized bias joint does not only reduce but on the contrary increases joint durability.

This can be explained by the following: the contact area on mating surfaces is close to 100% when filler is applied and it favourably affects durability of bias joints.

On the other hand, as the analysis of the damaged specimen showed intensive fretting-corrosion develops on joined surfaces of joints without filler. Fretting-corrosion practically does not occur on mating surfaces of specimens with filler.

Fatigue cracks both on specimens with filler and on scraped joints originate from the section along hole axis, i.e. in the place of the maximum stress concentration.

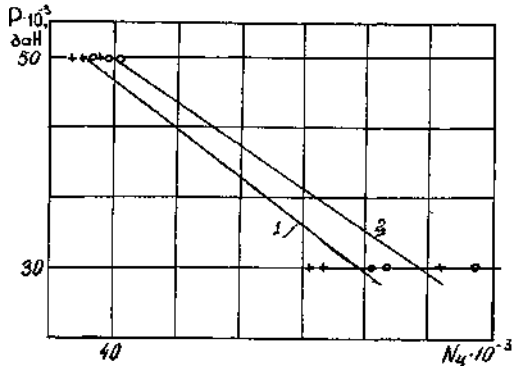

Fig. 4.30. Influence of polymeric filler on fatigue life of full-sized bias joint: 1 – scraped joint; 2 – joint with the ЗП-2 polymeric filler

That is why though fretting-corrosion elimination makes positive impact on joint durability but it is not so considerable.

Fretting-corrosion developed on specimens of both types on the internal hole surface and on bolts.

Unlike plane-parallel shear joints with bolts with the countersunk heads, the damage of which begins most often with fatigue cracks occurrence in transition zone of countersunk conic hole portion in cylindrical one, fatigue cracks propagation in bias joints on all specimens without exception began on mating surface. Bending stress caused by force transfer eccentricity from one joint member to another one explains this phenomenon in the shear bias joints.

The tested specimens can be divided according to the fatigue failure nature into three groups:

Fatigue cracks originated on mating surface in section along hole axis of the second bolt row of 7 joint member in specimens of the first group. They developed up to member damage. 75 % specimens had such damage nature.

19 % specimens had more complete damages. At first the fatigue crack occurred and developed on the hole axis of extreme bolt in the member edge 1. The crack stopped growing after reaching the certain size. But fatigue cracks occurred in section along the hole axis of the second bolt row of member 1. They developed up to cap damage.

Only 6 % specimens were damaged in section along hole axis of the first bolt row of member 7 (such fatigue failure nature is typical for plane-parallel shear joints).

Visible difference in nature of fatigue crack propagation in specimens with filler and in scraped joints was not revealed.

The polymeric filler layer during the cyclic loading was not damaged. Signs of wear of filler layer were not revealed. Actually measured thickness of a filler layer between joined surfaces was equal to from 0.3 to 0.5 mm.

Thus, experimental investigations have shown that polymeric fillers are quite satisfactory means to increase maintainability of shear bias joints working in the cyclic loading conditions.

4.7. LIFE INCREASE OF SINGLE–SHEAR JOINTS ON THE RIGID PROFILE BY MEANS OF LOCAL STRAPS THICKENING IN THE EXTREME ROW ZONE

Influence of fitting the bolts in extreme rows with triple-cone countersunk head with gap in forming the part lapping edge on joint durability on the rigid profile is investigated (Fig. 4.31).

Specimens were made of the Д16Т-ПР315-7 T-section and two plates made of the Д16АТл5 sheet, anodized according to the serial technology.

Plates were connected to the profile with cadmium bolts made of the 30ХГСА 5015А-8-26 steel. The bolts were installed on sliding fit for the first (base) joint variant.

Bolts with triple-cone countersunk head with interference equal to 0.8 – 1.2 % in bolt body diameter were installed along all rows of specimens of the second joint variant.

Bolt-holes were consistently machined with the drill in 7.7 mm diameter and by the 7.9 А3 and 8 А3 (8Н9) reamer. The first row bolt holes in the section were made 9 mm in diameter (Fig. 4.31, pos. 1, 2).

Triple-cone head bolts were pressed with force of 800 daN, after that prepressing with force of 2000 daNwas carried out.

Nut tightening was carried out with torque wrench, torque was equal to 1.3 daN·m for the first and second joint variants and 0.3 daN·m for the first row bolts of the second joint variant.

Fatigue tests were carried out on one loading level with P_{max} =4000 is daN ($\sigma_p^{бр}$ =125 MPa), with cycle asymmetry factor R_σ =0.1 and frequency f =12 Hz on the ЦДМ-10Пу hydraulic pulsator (Fig. 4.31).

The analysis of results showed that fatigue life of bolted joints of parts made of the Д16АТл5 sheet the extreme rows of which were installed with gap in the joining profile and the extreme row bolts tightening was carried out with the torque equal to 0.3 daN·m was increased at an average in 1.9 times in comparison with fatigue life of joints without gaps, in which fastener nut tightening was equal to 1.3 daN·m.

The given specimens were damaged in the operating zone of bending stress owing to the considerable eccentricity of loading transfer.

Further fatigue life of single-shear bolted joints can be increased by means of local thickenings of connected plates on the lapping edge.

The specimens modelling the joint of lower aircraft wing panels (Fig. 4.31, b) were designed to analyze the influence of installed extreme rows of fasteners with gap in the part forming the lapping edge and having local thickening in the zone of this row on the fatigue life of bolted joints. Fasteners holes were drilled and turned in two transitions after that chamfer was removed and connected parts were degreased. After bolt installation on sliding fit the nuts were tightened with torque M_{torq} = 2 daN·m and then full unloading and final tightening of nuts to M_{torq} =1.3 daN·m were carried out.

The following variants of structural and production versions of joint specimens were considered:

- basic variant — three – row joint with smooth plates (Fig. . 4.31, pos. 2.1);
- variants of joint specimens which have in the first row the thickening equal to 1.5 mm made by the overhanging plate from the upper side (Fig. 4.31, pos. 2.2), lower (Fig. 4.31, pos. 2.4), symmetrically from each side along 0.75 mm (Fig. 4.31, pos. 2.3);
- basic variant of joint specimens and variants with thickening in which radial gap between bolt bodies and hole walls (Fig. 4.31, pos. 2.5 – 2.7) is executed along the first row to decrease its loading level in the joining section; holes of the extreme rows in the joining section are made with the drill 9 mm in diameter.

Fatigue tests have been carried out with maximum cyclic loading P_{max} = 4000 daN ($\sigma_p^{áð}$ = 125 MPa), cycle asymmetry factor R_σ = 0.1, frequency f = 12 Hz on the ЦДМ-10Пу hydraulic pulsator. From three to five specimens of each type have been tested (see Fig. 4.31).

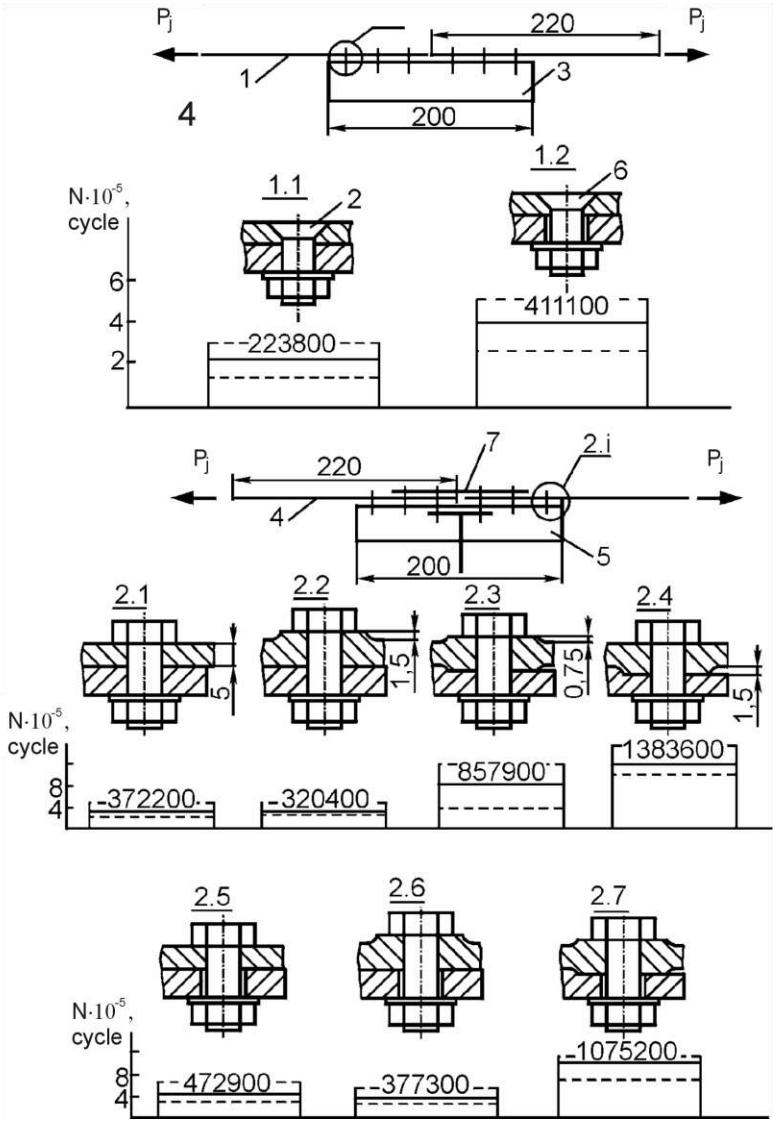

Fig. 4.31. Specimens of joints with the rigid profile: 1 – plate made of the Д16АТл5 sheet; 2 – 5015-8-25 bolt; 3, 5 – the Д16Т-Пр315-7 profile; 4 – Д16Т plate; 6 – three-cone countersunk head bolt; 7 – strap

The analysis of results has shown that the fatigue life of single-shear bolted joints can be increased on the average in 3.7 times using the thickening in the package along the first bolt row (to the nearest to edge of the joining profile) in 2.3 times using the symmetric thickening and in 2.9 times using the symmetric thickening and gaps between bolt bodies of the first row and hole walls in the joining section.

When you use joints with reinforcement along the first row inside the pack or symmetrically relatively to loaded part, they become safely damageable. As strap damage (Table 4.3) that can be revealed visually preceded the specimen damage in a whole in six specimens from ten tested ones. Besides, even if plateswere damaged along the radius transition behind the first bolt row (this phenomenon was observed in five from ten specimens), the specimen continued to

operate (operating time equal to from 24800 to 163400 cycles of loading was observed).

Table 4.3

Results of fatigue tests and thickness of specimen straps of bolted joints on the rigid profile

Specimen variant	Specimen number, cycle	δ, mm	Strap number, cycle
with symmetrical thickening (Fig. 4.31, pos. 2.3)	460000 853300 1260300	2.5 – 2.6 2.5 – 2.6 2.5 – 2.6	Without damage 711500 964000
with thickening downward (Fig 4.31, pos. 2.4)	1203800 1408700 1460400 1461400	2.4 2.5 2.85 2.85	700000 Without damage Without damage –
with symmetrical thickening and gap (Fig.. 4.31, pos. 2.7)	778900 1199400 1247400	2.8 2.0 2.5 – 2.6	660000 593400 964000

4.8. CONCLUSIONS

1. The countersunk bolt structure with three-cone countersunk head providing the increase of joint durability with the radial interference in 2 – 4 times has been designed on the basis of integrated designing method and achievement of regulated durability of shear bolted joints of aircraft assembly structures.

2. It is shown that spreading the BK-9 glue on mating surfaces of shear joint parts while their assembling by means of bolts with the modified countersunk head increases durability in 2 – 6 times in comparison with joint durability with local tightness but without glue.

3. Structurally-technological methods have been developed to increase fatigue life of lateral shear bolted joints of airframe members by unloading the zones of probable fatigue failure due to discharging holes, gaskets, straps, local thickening.

4. The ways to increase shear bias joints life have been proposed.

5. To increase life the way of part connection including the loading of connected parts by static tensile load, the value and direction of which correspond to operational loading, formation of holes in the stretched part for fasteners, bolt fit with radial interference after which preload is removed.

6. The developed ways of part connection increase their durability in 1.5 – 4 times.

Section 5
INTEGRATED DESIGNING METHOD AND ACHIEVING ASSIGNED DURABILITY OF SHEAR RIVETED JOINTS OF AIRCRAFT ASSEMBLY THIN-WALLED STRUCTURES

The purpose of the riveted joints integrated designing process is to determine their parameters, development of design and production publications for joints, their monitoring in operation and repair on the basis of experimental-calculated analysis (methods) of their strength, local mode of deformation, fatigue strength, maintainability, new design-manufacturing solutions and modelling with using computer integrated systems.

5.1. INTEGRATED DESIGNING METHOD AND MODELING STANDARD RIVETED JOINTS OF AIRCRAFT ASSEMBLY STRUCTURES

Procedure and algorithm diagram of integrated designing and modelling the standard riveted joints of aircraft assembly structures is shown in Fig. 5.1.

The following initial data for joint designing are necessary: surface analytical model of the aircraft and its units; exploded view of the aircraft major components; distribution diagrams of acting assumed loads; geometrical characteristics of primary member sections in the structure regular area; models of standard riveted joints of primary members; regulations (Standards, Manuals, Guiding Materials); assigned service life time of the joint regular area; fatigue characteristics of the materials of parts to be joined and standard joints.

The purpose of designing the transverse and longitudinal riveted joints of the airframe primary members for assumed levels of ultimate and operational loads is to determine the parameters of such joints providing execution of the specified requirements with minimal mass of the joint parts.

Let’s consider the procedure of creating the solid models of standard riveted joints using, as an example, joints of the passenger aircraft cylindrical fuselage section, in particular, longitudinal joint in place of frame-to-stringer attachment by means of a knee.

The assembly model is developed in the solid modelling module of the UNIGRAPHICS system.

Prior to develop the model perform the following operations:

– select the assembly to be developed in the unit surface model (fuselage for considered case, Ref. Fig. 5.2);
– determine loads acting upon the section;
– make a joint draft (Ref. Fig. 5.2);
– calculate geometrical parameters of the joint.

The fuselage theoretical contour is the base for any constructions. Primary structural members (frames, stringers, skin) are created inside the fuselage as equidistant: at first – skin, then frame and stringers. The knee model as a member

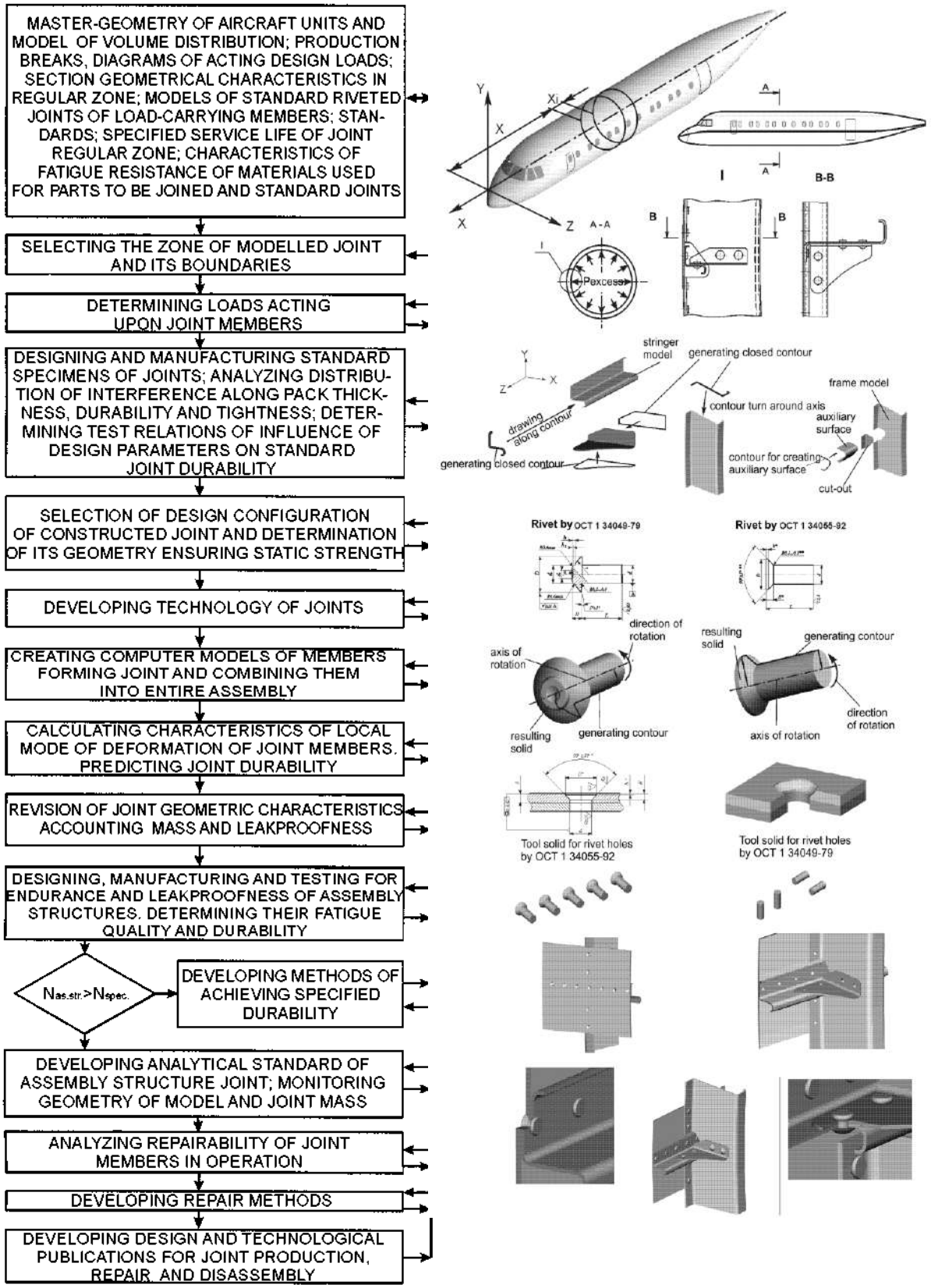

Fig. 5.1. Method of integrated designing and modeling standard riveted joints of aircraft assembly structures

of technological compensation is developed at the last stage (theoretically holes in frame and stringers in places of their attachment to knee are drilled while assembling in situ, thus technological deviations accumulated while assembling are compensated).

The assembly has such specific features as countersunk and normal riveted joints; various shape of parts assembled and various processes of their manufacturing.

Frame and stringer have Z-shaped structural sections (it is assumed that frame is round). Knee is made of angle bar. Knee-to-frame and knee-to-stringer joints use normal rivets, Skin-to-frame and skin-to-stringer joints use countersunk rivets.

Modeling process may be divided into several conventional stages:

– development of models of the joint parts (Stringer, Frame, Knee, Skin);
– combination of parts into section;
– «drilling» holes;
– modeling the rivets and their installation into the holes.

The set of curves created in the UNIGRAPHICS system in compliance with obtained draft is the basis for model creation (Ref. Fig. 5.2).

Solid models being a part of the assembly are created by method of moving closed contour along the forming curve.

The set of curves being components of the stringer profile is placed in plane XY (Ref. Fig. 5.3). Stringer model is created while moving the contour along the axis Z.

Skin model is constructed in the similar way.

While modelling the frame the generating contour is not drawn along the axis as it was made for other parts. The model is obtained by rotation of generating contour with respect to axis Z (Ref. Fig. 5.3).

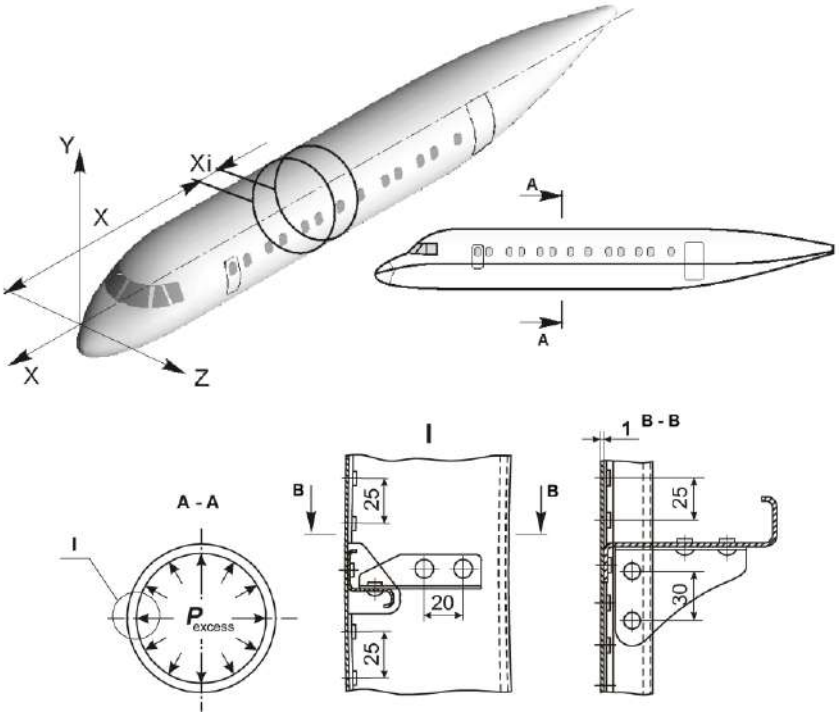

Fig. 5.2. Assembly draft

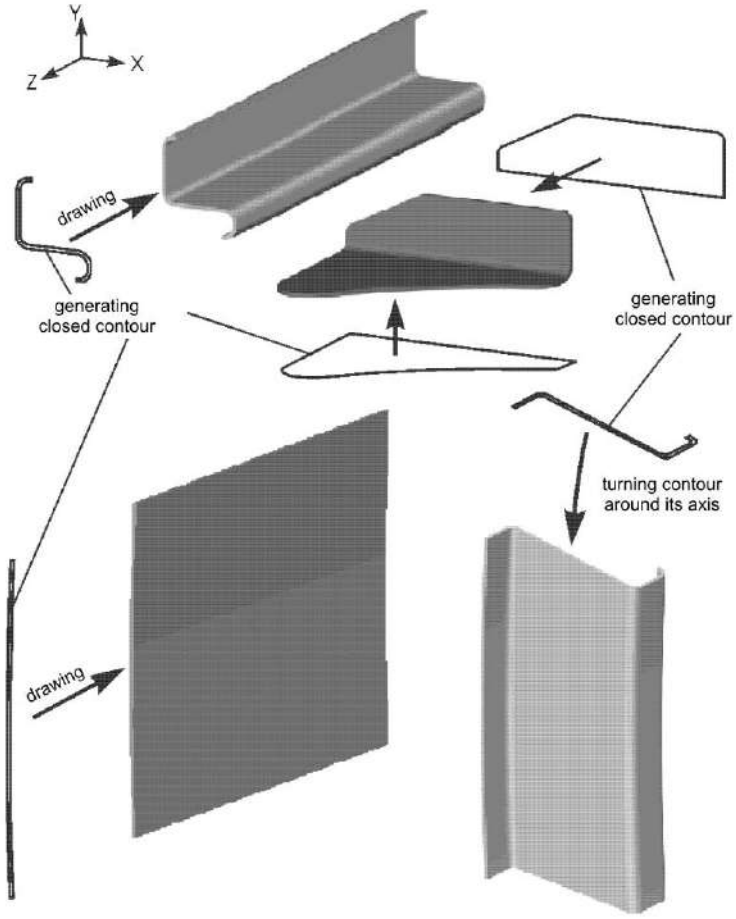

Fig. 5.3. Modelling parts being components of section

Next operation of modelling the frame is construction of cutout for stringer. To make the cutout it is necessary to construct auxiliary surface, which is developed along the cutout contour (Ref. Fig. 5.4).

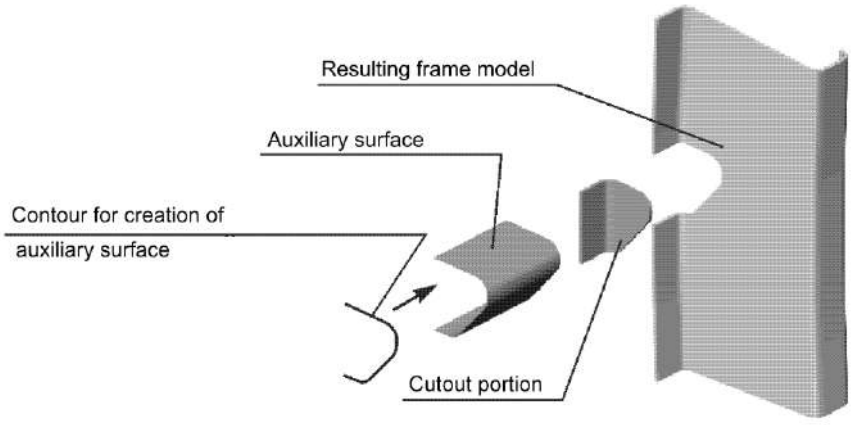

Fig. 5.4. Modelling cutout in frame model

Thereafter the frame model is divided by the obtained surface onto two

portions and useless portion is eliminated.

Knee model may be obtained by two ways:

– to create angle bar model similar to model of stringer, for example, and then to cut the vertical and horizontal planes of the angle bar so as to obtain knee model;

– to create separately models of vertical and horizontal planes of knee, to join them and to make rounding of the required radius between the surfaces.

Let us use the second method. Because it does not include time-taking cut-out operation. Therefore, first draw vertical and horizontal contours along the Y and Z axes correspondingly, and then join obtained solids and round edge between them with suitable radius.

Next step in the section modelling is joining all parts into the entire section that may be accomplished using function “transformation” (all solids are created in a single coordinate system that is why it is not difficult to coordinate them in space).

For obtaining the complete model it is necessary to make holes and install rivets into them.

5.1.1. Modelling the rivets

Fig. 5.5 and 5.6 show rivets used in the developed assembly: Fig. 5.5 represents normal riveted joint (in the considered assembly it is knee-to-frame and knee-to-stringer joints), and Fig. 5.6 shows countersunk rivets for skin-to-stringer and skin-to-frame joints. The following positions are enumerated in Figures: 1 – rivet shank; 2 – compensator; 3 – manufactured rivet head.

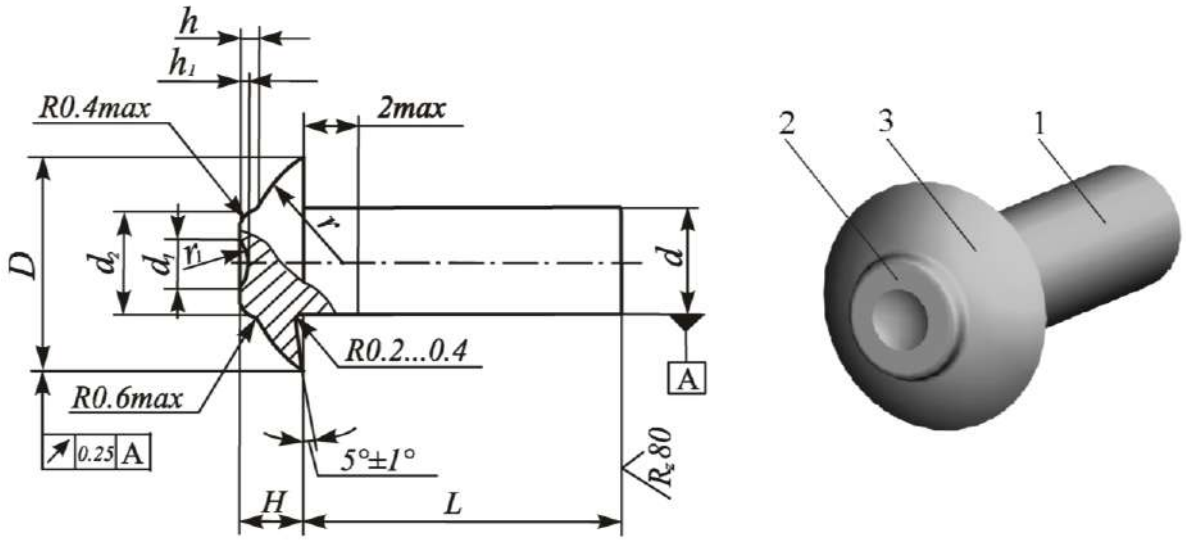

Fig. 5.5. Flat-round head rivet and compensator by OCT 1 34040-79

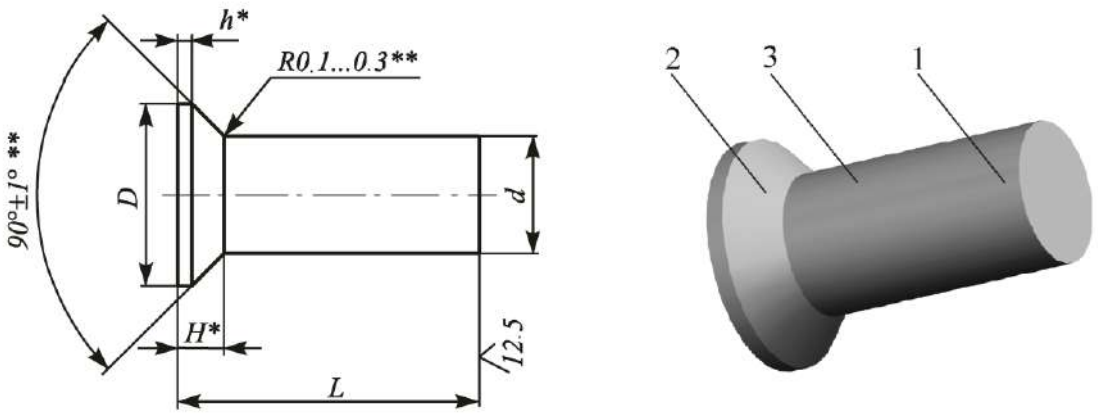

Fig. 5.6. Countersunk rivet with cylindrical compensator by OCT 1 34055-92

Rivet model is obtained by rotation of generating contour around the rivet axis (contour is constructed according to the rivet drawing).

It should be noted that rivet model made in compliance with the drawing (Fig. 5.5 – 5.7) does not coincide with the rivet model in joint due to the following reasons:

1. While riveting the shape of the set head is changed because the compensator is upset.

2. Rivet shank is deformed (shank diameter is 0.05 mm less than hole diameter) and interference in the joint is provided.

3. Closing rivet head is shaped, which is barrel-shaped and has its own diameter and depth.

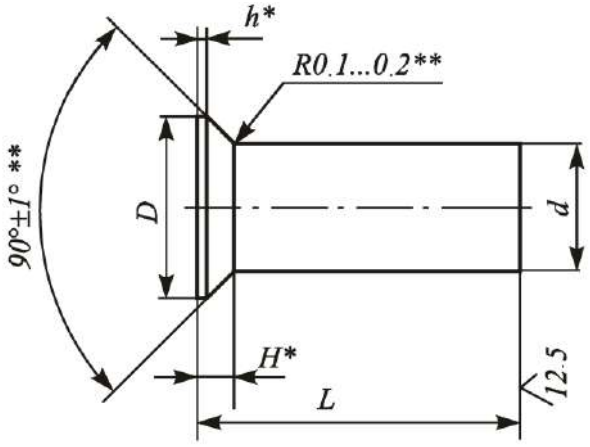

Fig. 5.7. Rivet having reduced depth of countersunk head
with cylindrical compensator by АНУ 0314

Hole for riveting made by OCT 1 34055-92 may be of two versions: for thick and thinner skins (Ref. Fig. 5.8, 5.9). For riveting thicker skins the hole has a cylindrical portion, for riveting thinner skins the cylindrical portion is not provided.

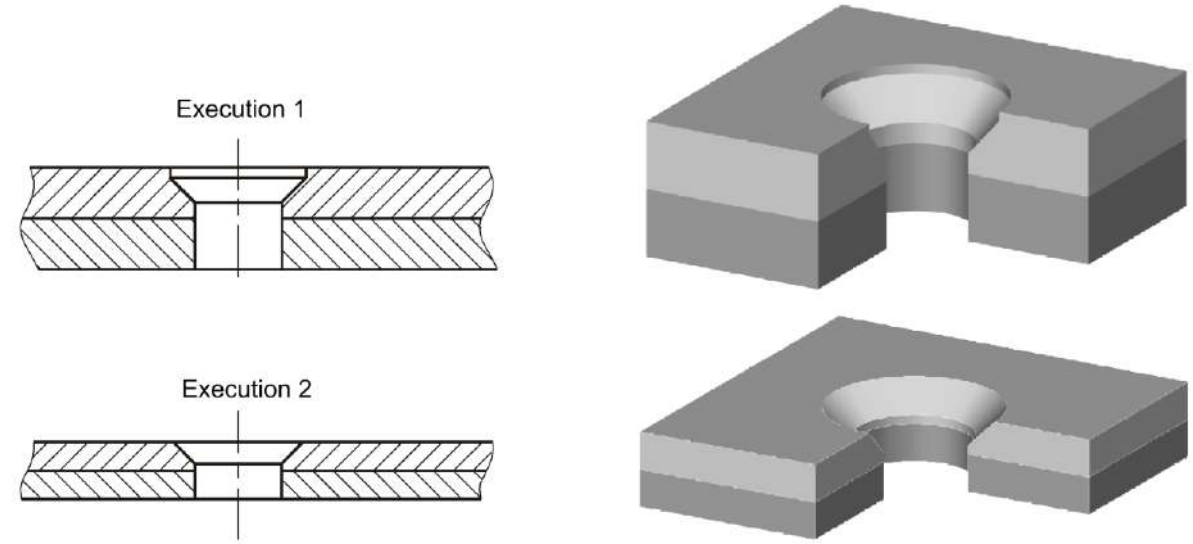

Fig. 5.8. Holes for riveting by OCT 1 34055-92

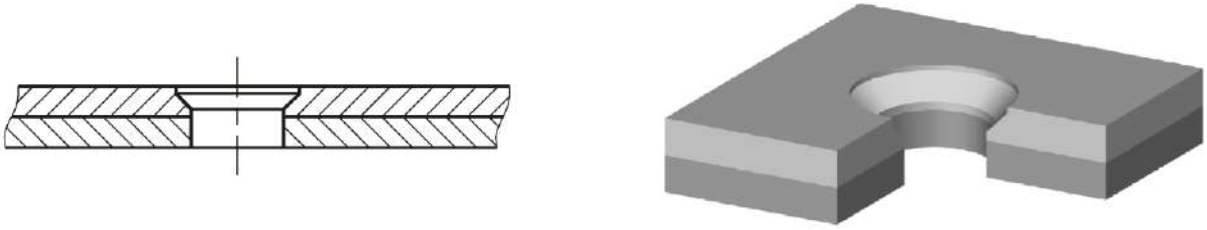

Fig. 5.9. Holes for riveting by АНУ 0314

In the first case the rivet is installed with interference at the hole cylindrical portion provided before riveting, and then, after riveting, interference is formed along all the pack thickness.

In the second case the compensator extension is milled after riveting (Ref. Fig. 5.10). Extension of countersunk rivet head is allowed to be of 0.05 mm maximum. Similar method of obtaining the countersunk joint (with milling the heads after riveting) has some disadvantages:

– tightness of joint is impaired;
– joint interference reduces;
– while milling scratches appear on skin, which reduce the joint service life as well as of the entire aircraft;
– while milling the rivet shank is deformed and eccentricity of load application appears that also reduces the structure life time.

In Kharkov Aviation Institute the rivets with decreased depth of set head and cylindrical compensator have been developed (Ref. Fig. 5.7) for riveting the countersunk joints of thin skins (it is possible to rivet skins having thickness less than 1 mm), in which the compensator is calculated so that there is no necessity in milling the set heads after riveting, and hole for such rivet has a cylindrical portion (see Ref. Fig. 5.9), therefore durability and tightness increase. Formation

of riveted joint of thin skins using rivets being in compliance with АНУ 0314 is represented in Fig. 5.11.

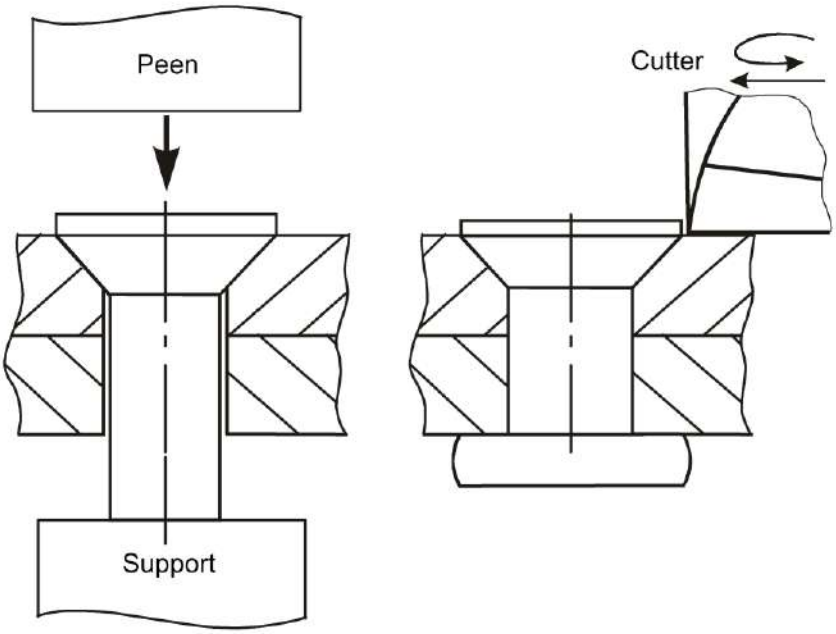

Fig. 5.10. Riveting thin skins using rivets by OCT 1 34055-92

When riveting with rivets being in compliance with OCT 1 34040-79 the compensator becomes a part of the rivet shank, and with correctly selected mode of riveting provides that set head is shaped as a portion of sphere i.e. segment (Ref. Fig. 5.12).

After creation of models rivets are placed in file containing developed section and required number of rivet models is created in places shown on the drawing by copying.

For general joint view it is not necessary to show holes (because place under a rivet is not visible), but it is necessary for studying how to make riveted joints and for subsequent application of model in the modules CAM and CAE.

Holes for normal rivets are developed using the “hole” option (hole diameter and centre point of the hole should be specified). Obtained joint including installed rivet is shown in Fig. 5.13.

Hole for rivet may be made in other way: tool solid (copy of hole for rivet) is subtracted out of the part model. It is evident that cylinder is the tool solid for development of holes for normal rivet (Ref. Fig. 5.14).

For creation of holes for countersunk rivets the other type of tool solid is applied (Fig. 5.15).

Tool solids are made in the same way as rivet models; the difference lies in that for tool solid the generating contour is taken from drawing of the holes for rivets (Ref. Fig. 5.8, 5.9).

After subtraction of tool solids out of part models the model of joint without rivets is obtained (Fig. 5.16).

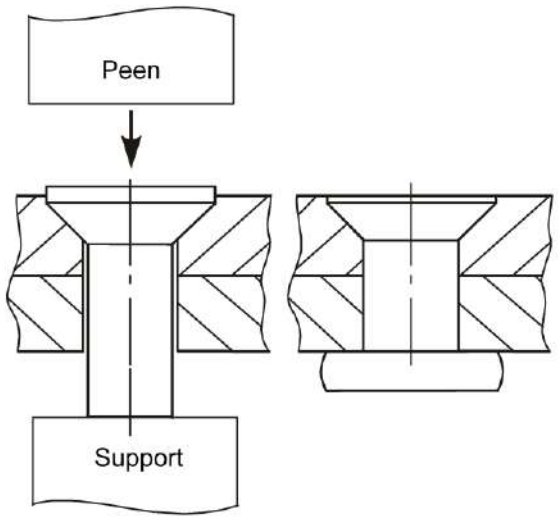

Fig. 5.11. Shaping riveted joint of thin skins using rivets by АНУ 0314

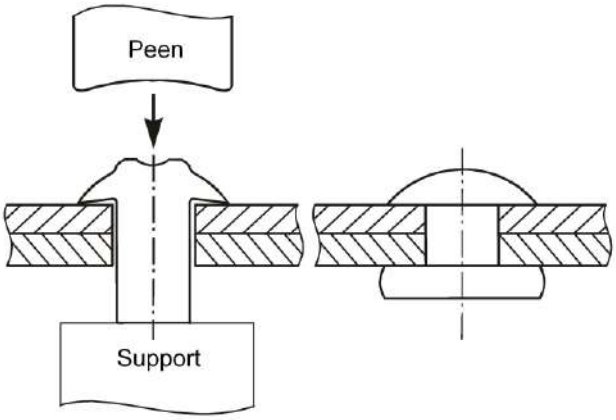

Fig. 5.12. Shaping riveted joint using rivets by ОСТ 1 34040-79

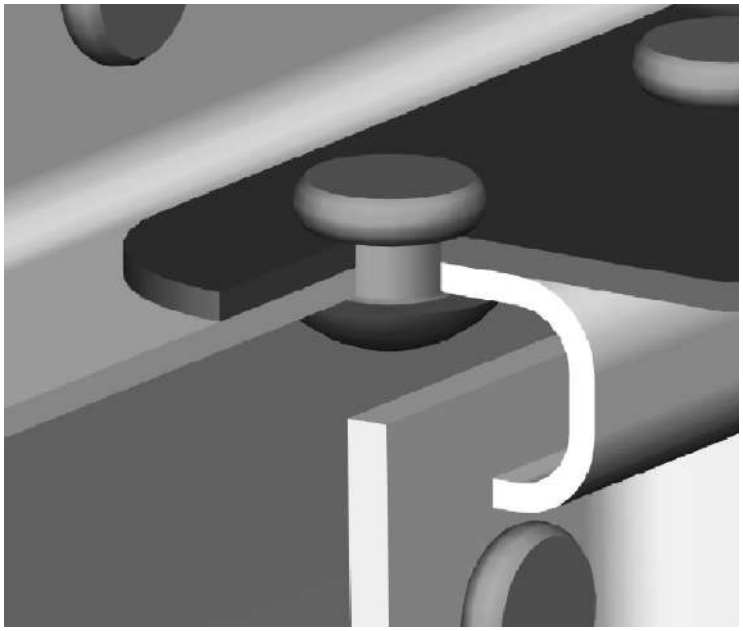

Fig. 5.13. Knee-to-stringer joint

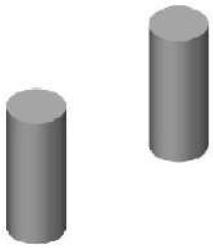

Fig. 5.14. Tool solids for normal rivets

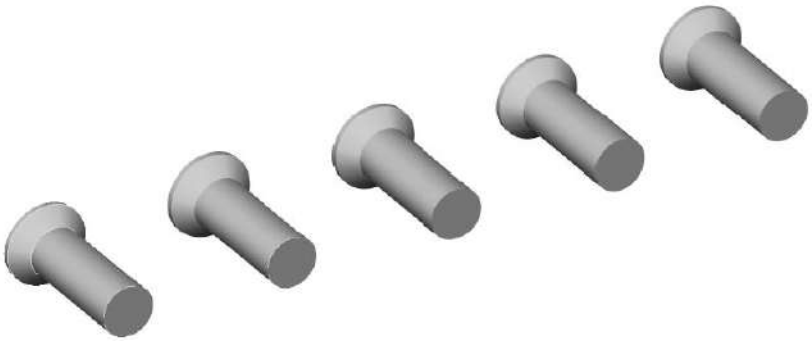

Fig. 5.15. Tool solids for countersunk rivets

Now it is necessary to install rivets into holes that may be made by placing the developed rivet models into obtained holes creating closing heads of rivets in this case. The model of riveted joint is completed (Fig. 5.16).

Thus several parts mutually coordinated with minimal errors have been obtained. Any part being a member of the joint may be taken out of the joint model, module CAM allows to develop the program of its manufacturing, and module CAE allows to get characteristics of joint under load applied.

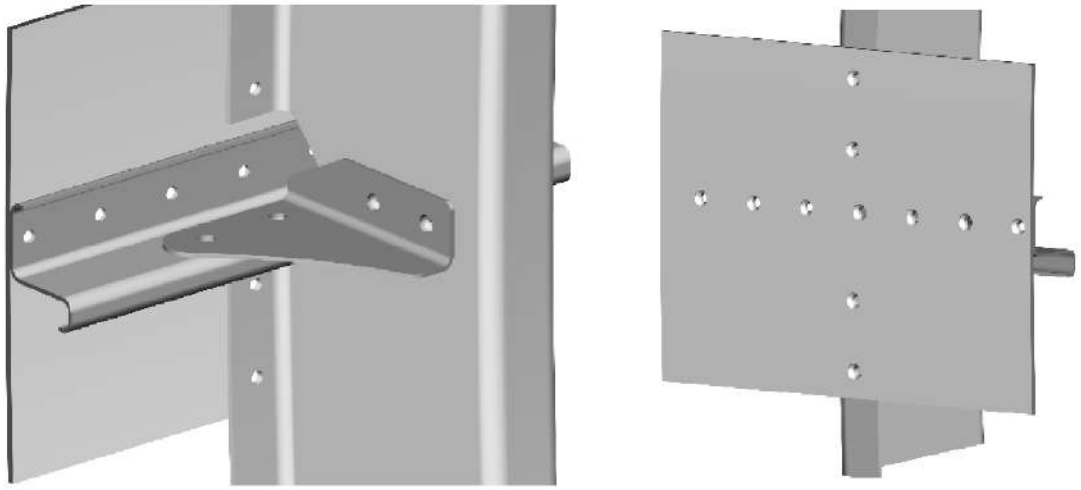

Fig. 5.16. Joint model without rivets

According to the similar procedure the model of transport aircraft spar section was developed (draft of the joint is shown in Fig. 5.18, completed model is represented in Fig. 5.19, 5.20). The following positions are designated in Fig. 5.18: 1 – upper spar cap; 2 – spar web; 3 – spar cap; 4 – rivets; 5 – lower spar cap.

In this section the parts have more complicated shapes in comparison with fuselage section considered in detail; theses are: spar caps and stiffener. But while developing the stiffener model it was divided into several parts, then model of each part was made, and at the end all models were combined into one entire model.

While modelling caps the complexity was in modeling the places of joint with stiffener (reinforcing the cap). First, the model with stiffener constant height equal to height of place to be reinforced was made, and then the “excess” portions were cut off.

Rivets in this section are the same as used in the fuselage section considered before.

Technical requirements applied for shear joints include ensuring static strength, durability and maintainability, which are the limitations while selecting their parameters.

As an efficiency criterion, while designing aircraft separate structural members o and their joints, the criterion of structure minimal mass was used. Therefore, the objective of designing the joints lies in selection of parameters ensuring minimal mass at given static strength, durability, tightness and outer surface quality.

Fig. 5.17. Joint model

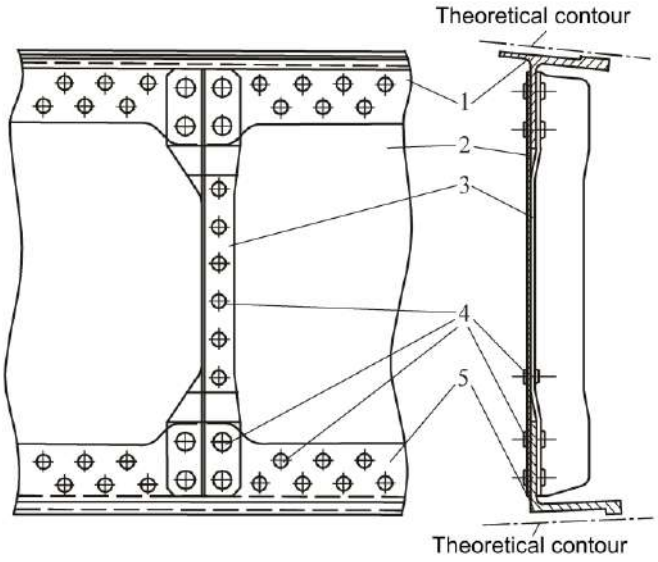

Fig. 5.18. General view of spar section

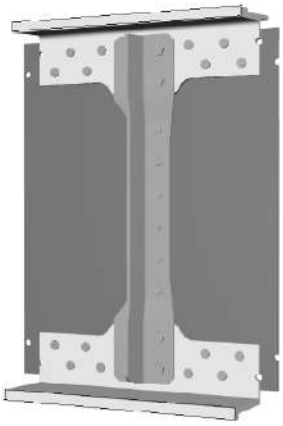

Fig. 5.19. Model of spar section

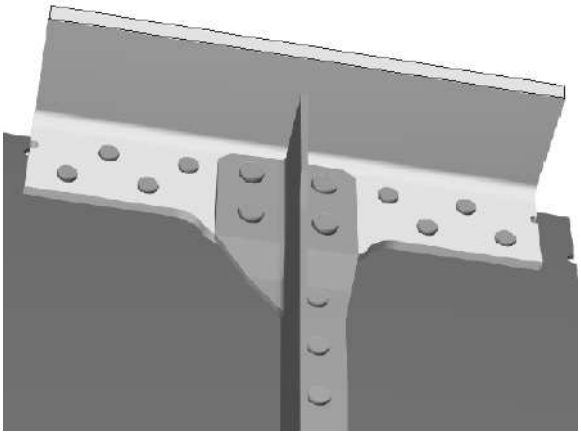

Fig. 5.20. Model of spar section

5.2. PROCEDURE OF DESIGNING SKIN RIVETED JOINTS OF SPECIFIED DURABILITY AT STAGE OF DRAFT DESIGN

Let us assume that design calculation on selection of parameters of skin and its reinforcing members has been accomplished. This implies selection of load-carrying structure, production breaks, materials, directive stresses, and also determination of geometrical parameters of regular zone. Despite the fact that materials are selected at earlier design stages, their selection is accomplished taking into account service life characteristics, which are mainly determined by joint durability and other structural irregularities.

Design procedure of skin riveted joints of specified durability at design draft stage is shown in Fig. 5.21.

While selecting materials for structures with high mass efficiency the specific indices are used, which are determined for each loading case. For example, specific strength of structure loaded with tensile or compression stresses without buckling is characterized by ratio of material ultimate strength to its density:

$$\sigma_{\text{ult}}/\rho \text{ or } \sigma_{0.2}/\rho;$$

For compressed bars and other members under general buckling the specific modulus of elasticity determined as ratio of material modulus of elasticity to its density is used:

$$E/\rho;$$

When analyzing plates in compression and in shear under local buckling the specific modulus of elasticity is determined by formula

$$E^{1/3}/\rho.$$

It is proposed to use concept of specific durability in the form of ratio of maximum stresses of zero-to-compression stress cycle for plate having a hole on base, for example, 10^5 stress cycles to the damage divided by the material density:

$$\sigma_{\max 0}/\rho.$$

Every specific factor characterizes not only mechanical characteristics of alloy, but mass characteristics too, which finally determine mass of structure. Specific factors, which are called as material weight perfection factors, are widely used for comparison of weight efficiency of various alloys and selection of reasonable material.

It is reasonable to compare material weight perfection on chart plotted in coordinates “loading – mass”, because change of loading may affect on operating conditions, and, therefore, formulas for specific factors. It is the most evident while analyzing structural members in compression or shear that is under conditions at which buckling is probable.

Let us consider change of mass of compressed reinforced skin of unit area ($\overline{m}$), which is analyzed as plate, edges of which are hinge pivoted in relation to

knife-edge compressing load per unit length (T). Let us assume that plate width is a = 200 mm.

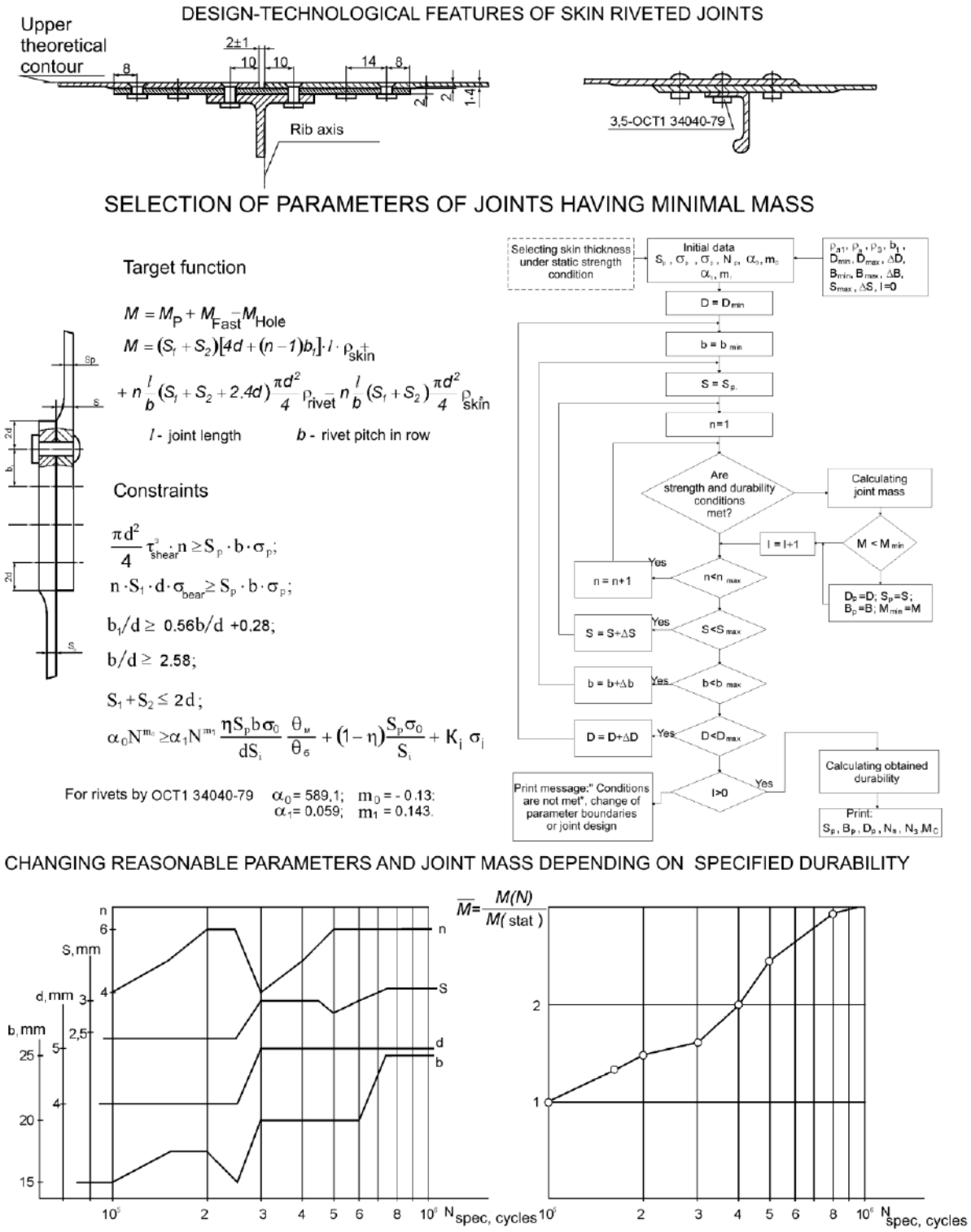

Fig. 5.21. Design procedure of skin riveted joints of specified durability at draft design stage

Using formulas $\sigma_{\text{ђр}} = \dfrac{kE}{(a/s)^2}$ and $T = \sigma_{\text{ђр}} \cdot s = \dfrac{kEs^3}{a^2}$, $s = \sqrt[3]{\dfrac{Ta^2}{kE}}$ is determined. Mass of the skin area unit is written as $\overline{m} = s\rho$, here s – plate thickness. With increasing load the plate thickness increases and it's buckling critical stress also rises. When critical stress reaches value of $\sigma_{0,2}$, then plate thickness is calculated by formula $s = T/\sigma_{0,2}$. On chart (Fig. 5.22) the corresponding load level is marked with figure 1 for material Д16Т and with figure 2 for material В95Т.

As it is evident on chart, the alloy В95Т is more preferable then alloy Д16Т for compressed skin. Insignificant advantage of material Д16Т within the range of loading from 0 to level equal to 1 is clarified by difference in material density by 3.5 %. Within the range for comparison of materials it is necessary to use weight efficiency factors written for plate under local buckling, – $E^{1/3}/\rho$. Within the range beginning from level of loading equal to 2 and higher the comparison should be accomplished using weight efficiency factors written for plate under compression without buckling, that is $\sigma_{0,2}/\rho$. Within the range from the 1st to 2nd loading levels the comparison of materials using weight efficiency factors is impossible, and materials may be compared using charts of "load – mass" relation only.

Fig. 5.23 illustrates the comparison of the materials with respect to weight efficiency factors written for time-variable tensile load; the materials are compared taking into account fatigue characteristics. It is evident that material Д16Т is more preferable within the full range of loads. The same conclusion is proved by durability curves represented in Fig. 5.24.

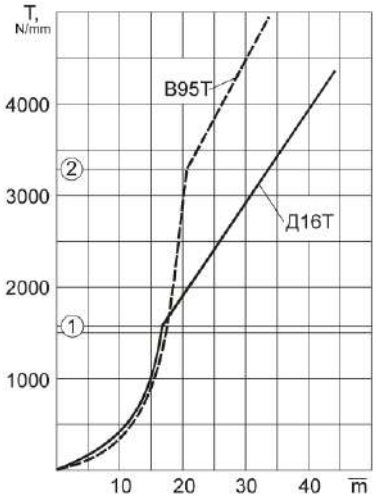

Fig. 5.22. Mass comparison of different materials for plate under compression

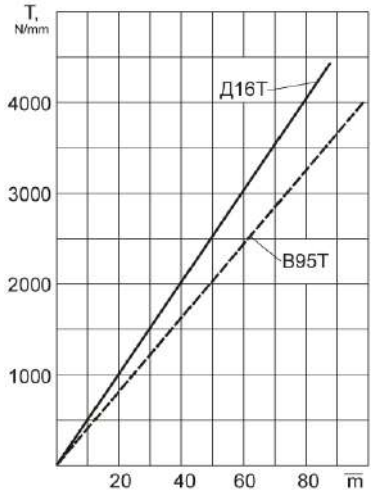

Fig. 5.23. Mass comparison of different materials for plate having hole being under action of alternate loads

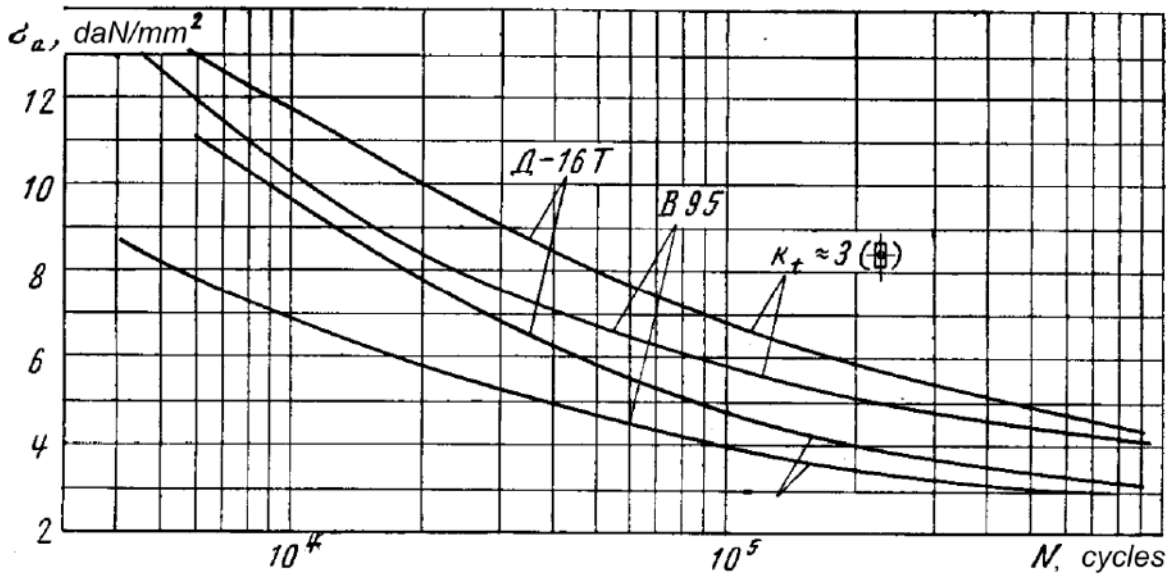

Fig. 5.24. Fatigue charts of plates having hole
and panels made of Д16Т and В95Т alloys

Moreover, material sensitivity to accumulation of fatigue damage is characterized by coefficient equal to ratio of fatigue strength on the base of 10^5 cycles of loading to ultimate strength.

Therefore, for lower surface of load-carrying member, which, as a rule, determines the wing service life, the most appropriate is the application of aluminum-copper alloy Д16Т and alloys based on it.

These alloys have been tested in practice. They have good characteristics of durability and persistence; have low sensitivity to concentrators and internal stresses appearing while assembling. High-purity alloys (for example, Д16чТ and others) improve the above mentioned properties. The most reasonable alloy for upper panels of load-carrying structure is the alloy on the aluminium–zinc basis, such as В95 and its modifications. Application of these alloys having mechanical characteristics exceeding proper characteristics of Д16Т alloys by about 20%, and, therefore, having higher characteristics of weight perfection, gives great economy of mass in ensuring the static strength. But their application must be matched with the service life requirements, because their durability indices and characteristics of alloys persistence based on В95Т are greatly lower than those of alloys based on Д16Т. For example, the index of sensitivity to fatigue damage accumulation of alloys based on В95Т is lower by 15% than that of alloys based on Д16Т.

After selection of reasonable material the calculations for reducing loading cycles to zero-to-compression stress cycles are accomplished according to Owding’s formula:

$$\sigma_0 = \begin{cases} \sqrt{2\sigma_a \sigma_{\max}} & at \quad \sigma_m \geq 0; \\ \sqrt{2}\left(\sigma_a + 0{,}2\sigma_m\right) & at \quad \sigma_m \leq 0 \; and \; \sigma_{\max} \geq 0; \\ 0 & at \quad \sigma_{\max} < 0. \end{cases}$$

Then zero-to-compression stress cycle equivalent to flight loading spectrum is determined by implemented damage:

$$\sigma_{eqviv} = \sqrt[4]{\sum_{i=1}^{k} n_i \cdot \sigma_{0i}^4} \; .$$

Therefore, the initial data for selection of the skin lateral joint parameters are taken on the basis of materials and their mass, strength, fatigue characteristics, values of design and operating stresses, geometrical parameters of members to be joined in regular zone and value of specified durability.

By tradition, the next designing stage is the selection of the joint parameters such that static strength is ensured.

In this work it is proposed to select joint parameters such that required static strength and durability are ensured, therefore it is the difference from traditional calculation methods. On the basis of analysis of structurally-technological features of skin lateral joints of the existing aircraft it is assumed that joint under development will be single-shear made by fasteners working in shear arranged in 2 – 6 rows. As fasteners the rivets are used. Rivet diameters are selected among standard series of diameters (2.6; 3; 3.5; 4; 5 and 6 mm), rivet pitch in row is about from 4 to 10*d*, between rows – from 3*d* to 5*d* and is changed discretely with 2.5 mm interval. Skin in the joint area may have local thickening for compensation of damaging influence of fastener holes, and skin thickness in the thickened area is also changed discretely and gets values divisible by 0.1 mm.

To write down joint mass (Fig. 5.25) it is necessary to mention its overall dimensions: joint length is assumed to be equal to reinforcing stringer pitch, and width is assumed to be equal to coupling zone of joined parts. Let's write joint mass:

$$M = M_P + M_{FAST} - M_{hole},$$

here M_P – mass of parts to be joined; M_{hole} – mass of material removed while drilling holes for fasteners; M_{FAST} – mass of fasteners.

Taking into account designations assumed for geometrical joint parameters it is possible to write mass components:

$$M = \left(S_1 + S_2\right)\left[4d + (n-1)b_1\right] \cdot l \cdot \rho_{л} + n\frac{l}{b}\left(S_1 + S_2 + 2{,}4d\right)\frac{\pi d^2}{4}\rho_{з} - n\frac{l}{b}\left(S_1 + S_2\right)\frac{\pi d^2}{4}\rho_{л},$$

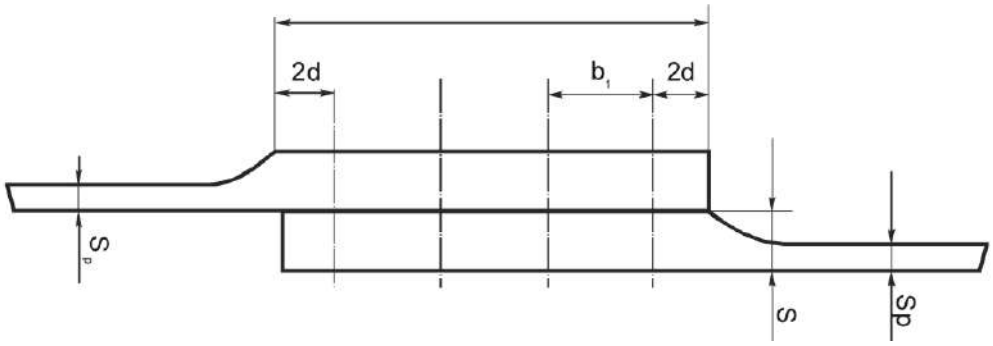

Рис. 5.25. Skin overlapping single-shear joint

here S_i – skin thickness in joint area; d – fastener diameter; n – number of joint rows; b – pitch of fasteners in row; b_1 – pitch of rows; l – joint length; ρ_{skin}, ρ_{rivet} – material density of skin and fastener accordingly.

It is evident that joint mass is a function of coupled parts thickness, joint length, fastener diameter, fastener pitch in row and between rows, bridge sizes and also of material density of coupled parts and fasteners. To determine the joint parameters it is necessary to solve the optimization problem under limitations applied to design parameters. The following conditions are assumed as limitations:

– static strength of fasteners in shear and of sheet in crumpling:

$$\frac{\pi d^2}{4}\tau^{3}_{shear}\cdot n \geq S_p \cdot b \cdot \sigma_{calc},$$

$$n \cdot S_1 \cdot d \cdot \sigma_{collapse} \geq S_p \cdot b \cdot \sigma_{calc};$$

– static strength in shear of sheet along bridges between fasteners:

– when fasteners are arranged as on a chess-board:

$$b_1 / d \geq 0.56 b / d + 0.28;$$

– when fasteners are arranged in line:

$$b / d \geq 2.58\ ;$$

– maintainability (ensuring more even interference along the pack thickness):

$$S_1 + S_2 \leq 2d\ ;$$

– ensuring specified fatigue life:

$$\alpha_0 N^{m_0} \geq \alpha_1 N^{m_1} \frac{\eta S_p b \sigma_0}{d S_i} + (1-\eta)\frac{S_p \sigma_0}{S_i} + 0.5\sigma_{bend}.$$

Here $\tau^{з}_{shear}$ – ultimate stress of rivet material in shear; σ_{calc} – calculated failure stresses in skin regular zone; σ_0 – maximum stresses of zero-to-compression stress cycle, equivalent to load operating spectrum in damageability; η – degree of fastener first line loading, that is share of loading, which is taken by the first row; σ_{bend} – bending stresses in zone of analyzed joint row caused by eccentricity of load transmission; α_0, m_0, α_1, m_1 – experimental coefficients of relation on joint durability calculation, determined by results of fatigue tests of plate specimens with filled unloaded hole and single-row joint.

When joint is made of material Д16Т by means of rivets by ОСТ1 34040-79 then $\alpha_0 = 3.72 \cdot 10^3$, $m_0 = -0.2265$. When rivets by ОСТ1 34052-85 are used then $\alpha_0 = 2.31 \cdot 10^3$, $m_0 = -0.2069$. In both cases $\alpha_1 = 0.063$, $m_1 = 0.153$.

Analysis of influence of joint parameters on its mass shows the following.

If a bridge is larger than minimal permissible value ($2d$), then structure becomes heavier and its static strength and durability are not enhanced. Increased thickness of the second part to be coupled (with unchanged thickness of the first part) and pitch between fastener rows results in increasing joint mass, and also does not essentially affect its fatigue and strength characteristics. That is why while designing the joint having minimal mass the parameters b_1 and S_2 must be minimal and taking into account strength, fatigue and technological limitations.

Next group of parameters contains skin thickness in joint zone, number of rows, and fastener pitch in row and fastener diameter. Influence of these parameters is not uniquely. For example, with increasing fastener diameter the joint mass increases and its strength and fatigue characteristics enhance. That is why, while selecting the parameters S_1, b and d, it is necessary to find compromise solution, and these parameters in particular are taken as to be optimized while searching minimum of mass.

Scanning is chosen as optimization method – the method of searching the global extremum. According to the method procedure the domain of objective function determination is divided into a number of sub-domains, in the center of each of them the objective function value is calculated, and optimal solution is chosen by means of comparison. Optimization numerical computing is selected because the objective function and limitations are non-linear functions of design parameters and the design parameters themselves are discretely variable values. Application of analytical methods in such case is not reasonable.

The reasonable parameters of joints were calculated using a computer. The calculation program block-diagram is presented in Fig. 5.27.

Calculations are made as follows. After the initial data input the parameters are cyclically looked through. In this case all combinations of the parameters are analyzed with their variations from minimal to maximum values.

For each parameter combination only after checking every limitation the

joint mass is computed and compared with current minimum. Joint parameters ensuring minimal mass, when all limitations are met, are considered as rational. Then, for the joint rational parameters the durability design value is computed, which exceeds specified value due to discrete variation of parameters.

For approbation of the calculation procedure and functioning the program the calculation of rational parameters of a number of lateral riveted joints was made with the following initial data: σ_p = 400 MPa, σ_0 = 150 MPa, S = 2 mm. Calculation results are represented in Fig. 5.26 in relation to value of the specified durability.

It is evident that ensuring relatively low level of fatigue endurance (100000 cycles of loading) requires changing the parameters got from conditions of static strength: it was necessary to increase skin thickness from 2 to 2.4 mm. Further increasing the specified durability causes change of every joint parameter.

Change of joint parameters related with ensuring durability specified level results from increase of structure mass, but at each level of specified durability the rational combination of parameters was selected, which ensures the structure minimal mass (Fig. 5.27).

When the joint parameters are determined then the model of the full determination of the joint zone using the CAD\CAM\CAE systems is made and the local mode of deformation in the joint members is analyzed using the ANSYS engineering analysis system.

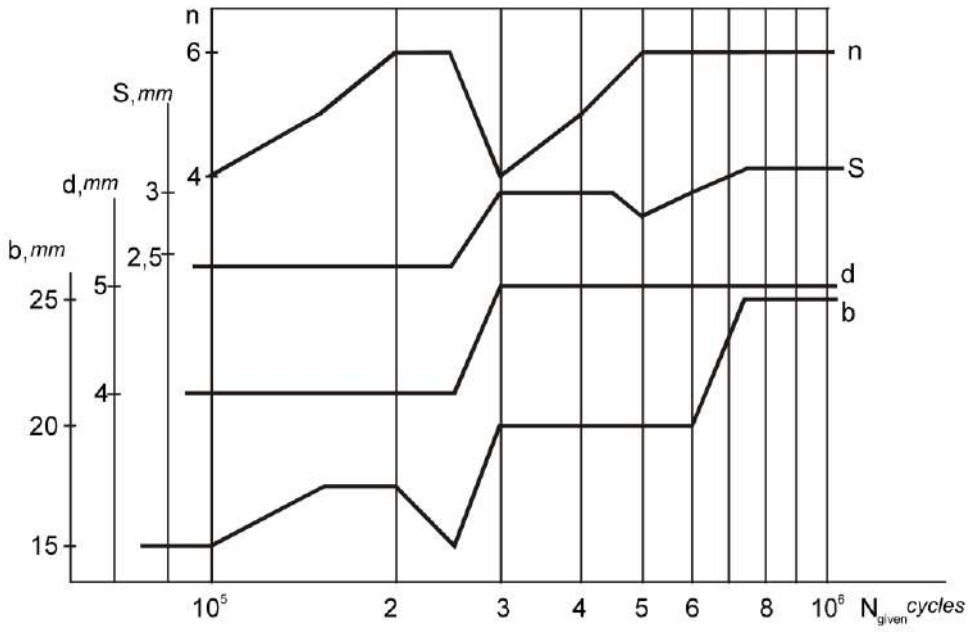

Fig. 5.26. Variation of joint rational parameters
in relation to specified durability

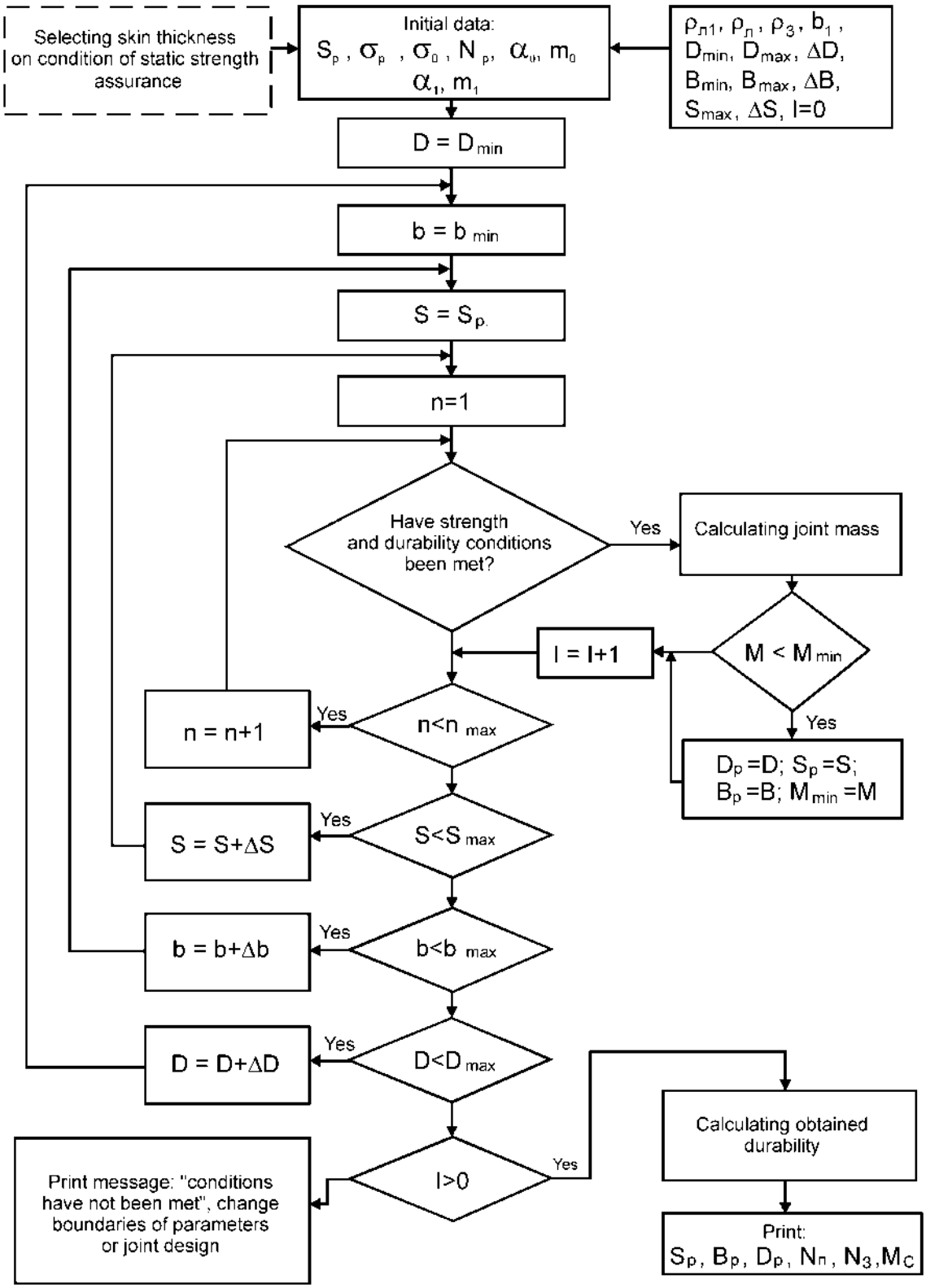

Fig. 5.27. Block diagram of rational parameter calculation of joint specified durability

5.3. Analysis of influence of structural and technological parameters on characteristics of riveted joint local mode of deformation

Analysis algorithm of influence of structural and technological parameters on characteristics of riveted joint local mode of deformation is shown in Fig. 5.28.

The procedure has been approved while calculating the durability of plates having enlarged hole filled with riveted countersunk rivet АНУ 0314 and rivet АНУ 0309, of single-shear three-row countersunk riveted joint performed by using rivets АНУ 0314 and АНУ 0309, and also while analysing influence of dimension deviations appearing in manufacturing the rivets according to ОСТ 1-34040-79 Industry Standard and making holes for rivet installation on distribution of radial interference along the pack thickness after riveting.

5.3.1. Analysis of characteristics of local mode of deformation in three-row single-shear joint members made with rivets by АНУ 0309 and by АНУ 0314

Geometrical parameters of shear joint are represented in Fig. 5.29.

Taking into account the specimen symmetry and nature of external load application in calculation only a half of model is analyzed under the adequate fastening conditions.

To limit model displacement along axes Y and Z for all nodes lying on end surfaces of plates, zero displacements for Y and Z components were given. Symmetry conditions were given along axis X (Fig. 5.30). There are two possible variants of plate attachment: 1st – rigid attachment of plate ends, 2nd – hinged attachment of plate ends. In the first case left and right plates are attached along axis X along the entire strap surface, in the second case – only along the plate ends. Tensile forces for both cases are applied to the end of the right plate.

Finite-member model (Fig. 5.31) consists of volumetric eight-node members SOLID45, second-order contact members TARGE170 and CONTA173 arranged between mating surfaces represented in ANSYS system. Total number of members in model is 19822.

Fig. 5.32, 5.33 show specimen deformation nature and distribution field of equivalent stresses in the joint members after riveting process and under action of external tensile forces corresponding to stresses σ^{tens} = 150 MPa.

It should be noted that distribution of residual equivalent stresses, and also equivalent stresses after application of tensile forces has irregular nature. The highest values were observed in plates not in the zones contacting with rivet, but at distance of 1.5...2.5d_z from the rivet axis. These zones are more expressed in the plate from the side of rivet snap head and lie on the plate surface. Here stress values are within the range of 340...380 MPa. It is also evident that after riveting in plates between rows stresses appear, which change rivet loading.

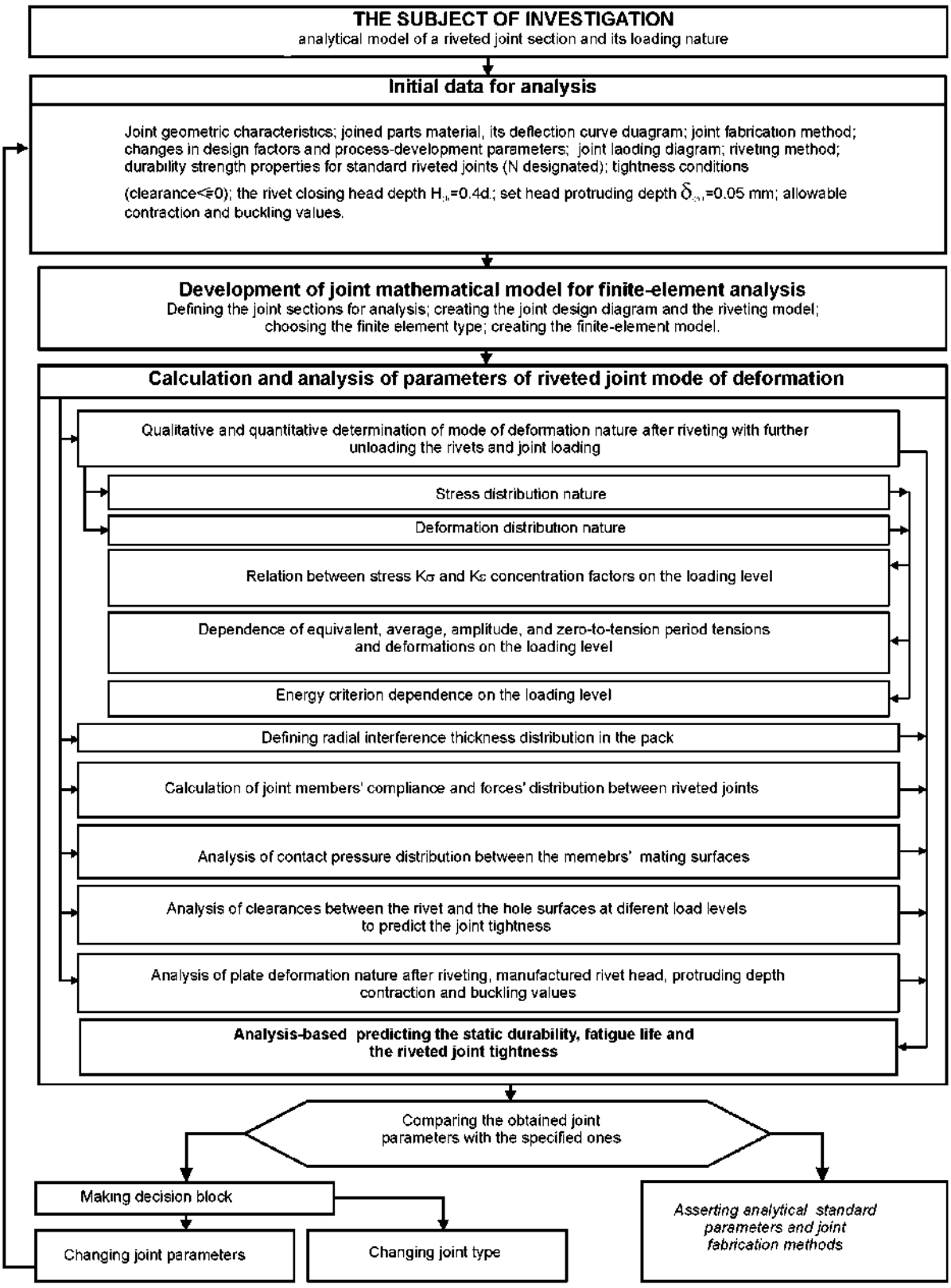

Fig. 5.28. Analysis procedure of influence of structural and technological parameters on characteristics of riveted joint local mode of deformation

To analyze local mode of deformation the zones of the highest equivalent stresses were selected (Fig. 5.34, 5.35) in the plate with enlarged holes for countersunk head (let us name it as plate No. 1), and also in the plate from the side of rivet snap heads (let us name it as plate No. 2).

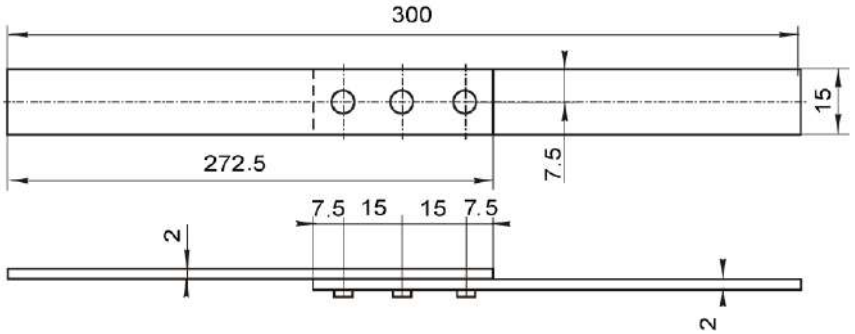

Fig. 5.29. Specimen of single-shear three-row riveted joint

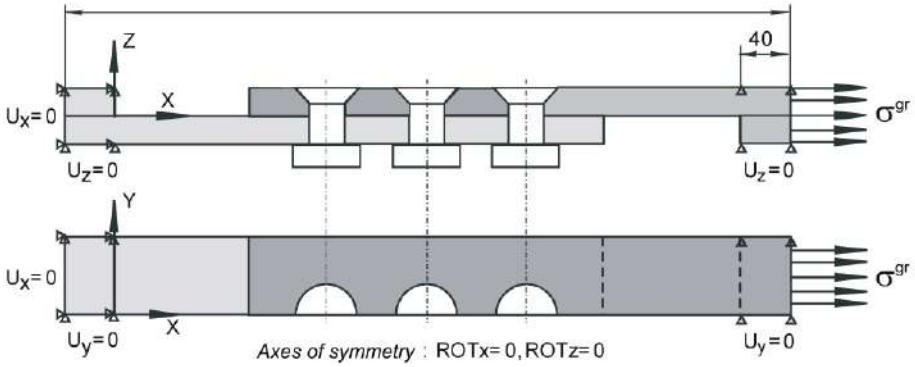

Fig. 5.30. Design diagram of single-shear three-row riveted joint

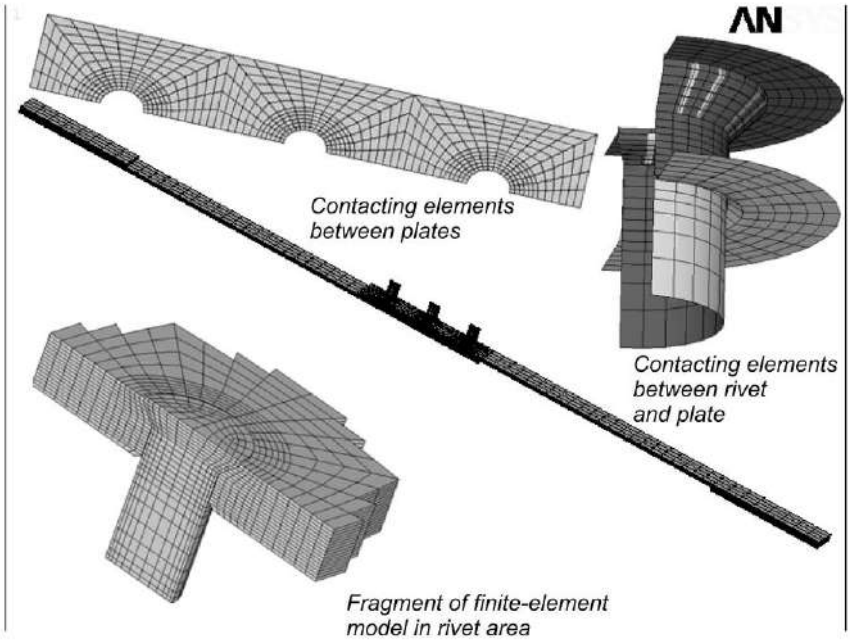

Fig. 5.31. Finite-element model of single-shear riveted joint

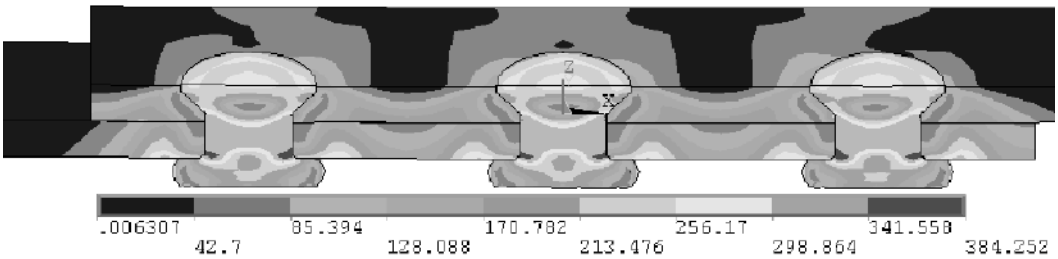

a

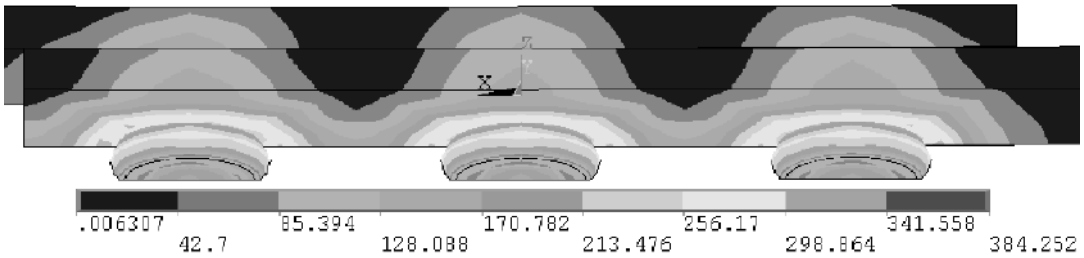

b

Fig. 5.32. Distribution field of equivalent stresses in pack after riveting process:
a – view at angle of 30^0 as viewed from manufactured head;
b – view at angle of 30^0 as viewed from snap head

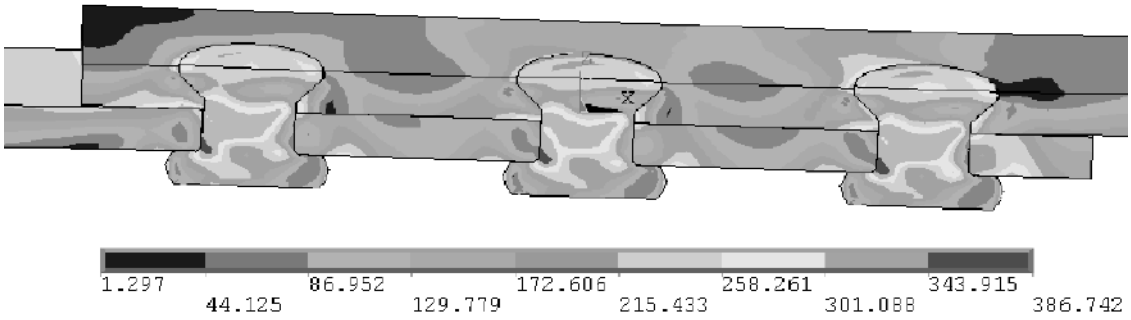

a

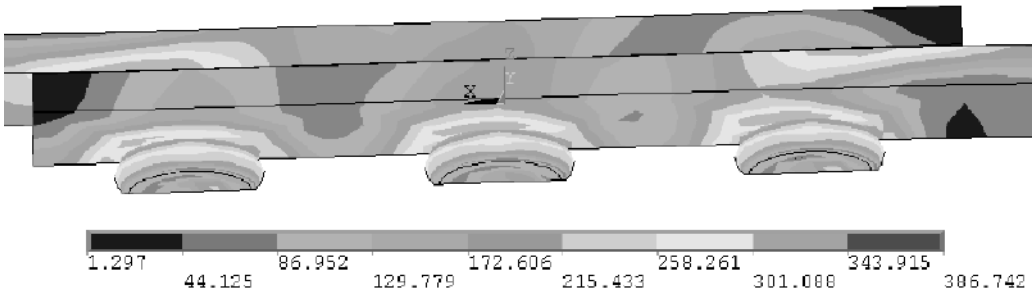

b

Fig. 5.33. Distribution field of equivalent stresses in pack after riveting process due to action of tensile forces corresponding to stresses σ^{tens} = 150 MPa:
a – view at angle of 30^0 from the side of set head;
b – view at angle of 30^0 from the side of snap head

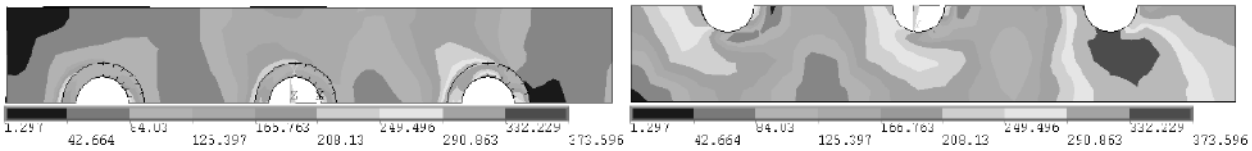

a b

Fig. 5.34. Distribution field of equivalent stresses in plate with enlarged holes for countersunk head after riveting under action of tensile force corresponding to stresses σ^{gr} = 150 MPa:
a – view from set head; b – view from contact with lower plate

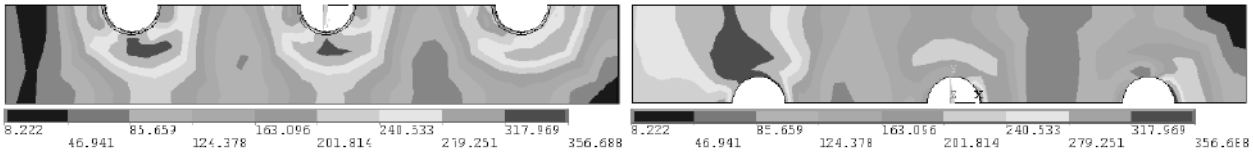

a b

Fig. 5.35. Distribution field of equivalent stresses in plate from the side of snap rivet heads after riveting under action of tensile forces corresponding to stresses σ^{gr}= 150 MPa: a – view from the side of contact with upper plate; b – view from snap head

Enumerate rivets from the left to the right. For further analysis select the most dangerous portions of the plates: for plate No. 1 they are in the third row zone of rivets, for plate No. 2 they are in the first row zone of rivets.

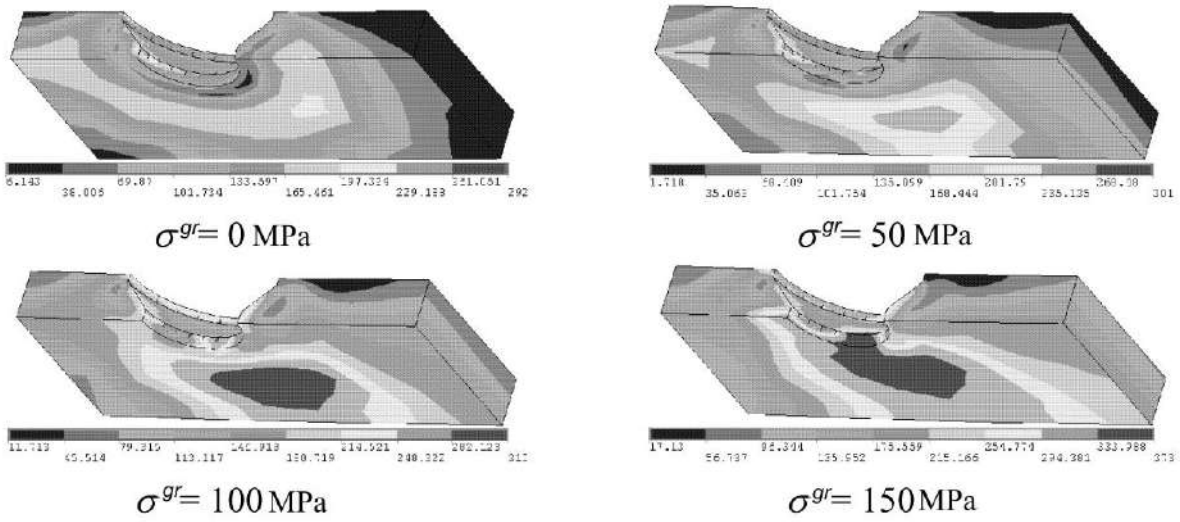

Fig. 5.36. Distribution nature of equivalent stresses σ_{eqv} in plate No. 1

Distribution nature of equivalent stresses σ_{eqv} in plate No. 1 for various versions of loading σ^{gr} is shown in Fig. 5.36.

The plate is looked from the side of contact with plate No. 2, because maximum stresses are observed from this side. It is evident that the most dangerous section is the section set at angle of about 15^0 with respect to the lateral

direction along the rivet axis, and the most dangerous zone is the zone of transition of cylindrical portion into conical one, where equivalent stresses reach value of 315 MPa under action of tensile loads corresponding to σ^{gr} = 100 MPa. Fig. 5.37, 5.38 represent graphs of distribution of normal σ_x and equivalent stresses and deformations in this section for various versions of loading. Hereinafter the following parameters are enumerated as: 1 – σ^{gr} = 0 MPa, 2 – σ^{gr} = 25 MPa, 3 – σ^{gr} = 50 MPa, 4 – σ^{gr} = 75 MPa, 5 – σ^{gr} = 100 MPa, 6 – σ^{gr} = 125 MPa, 7 – σ^{gr} = 150 MPa.

Under action of tensile force the plates are deformed and bending stresses appear in them due to availability of eccentricity. For estimation of bending stresses the nature of distribution of longitudinal stresses lengthwise the plate No. 1 was analyzed from the side of rivet snap head and from the contact with plate No. 2 (Fig. 5.39) along paths L1 and L2 (Fig. 5.40). Nature of the plate deformation under action of bending stresses is shown in Fig. 5.41, 5.42.

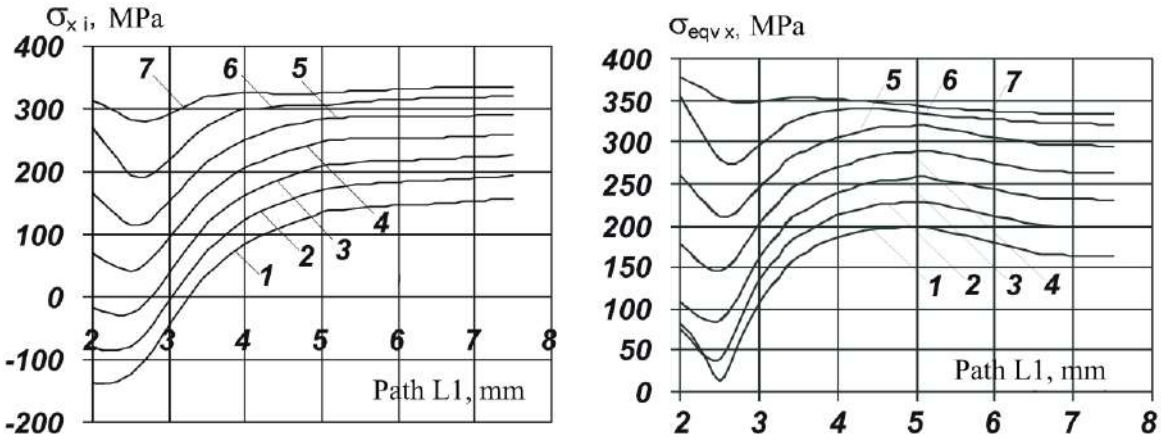

Fig. 5.37. Distribution of normal and equivalent stresses along rivet axis in section of plate No. 1

Analysis of stresses σ_x shows that maximum bending stresses appear in the zone of the first row under the rivet head. Their value is in 2.2 - 4 times higher than nominal stresses created by tensile force.

Relations of σ_{max}, σ_a, σ_m, σ_0, and also of ε_{max}, ε_a, ε_m and ε_0 in plate No. 1 for equivalent and longitudinal stresses with respect to external load application level corresponding to stresses σ^{gr} are shown in Fig. 5.43, 5.44. Influence of loading level σ^{gr} on variation of concentration factor σ_x and tensile deformation ε_x is shown in Fig. 5.45. Influence of loading level σ^{gr} on product of multiplication $\sigma_{eqv\,0} \times \varepsilon_{eqv\,0}$ is shown in Fig. 5.46.

Analysis of tightness is performed by analyzing the nature dependence of contact pressures distribution and values of gaps appearing between rivet and plates with respect to loading level σ^{gr} (Fig. 5.47). Fig. 5.48 shows paths in the pack thickness along which the dependences were plotted.

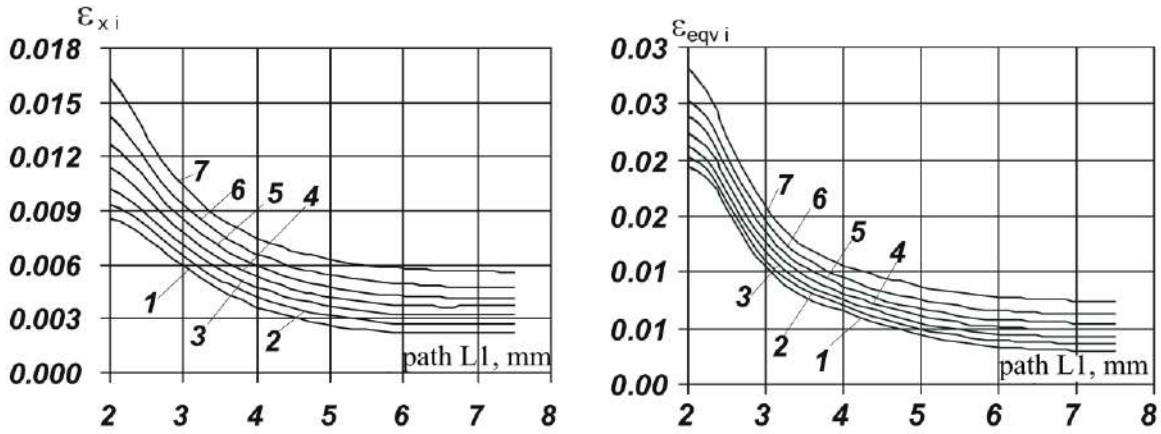

Fig. 5.38. Distribution of normal and equivalent deformations along rivet axis in section of plate No. 1

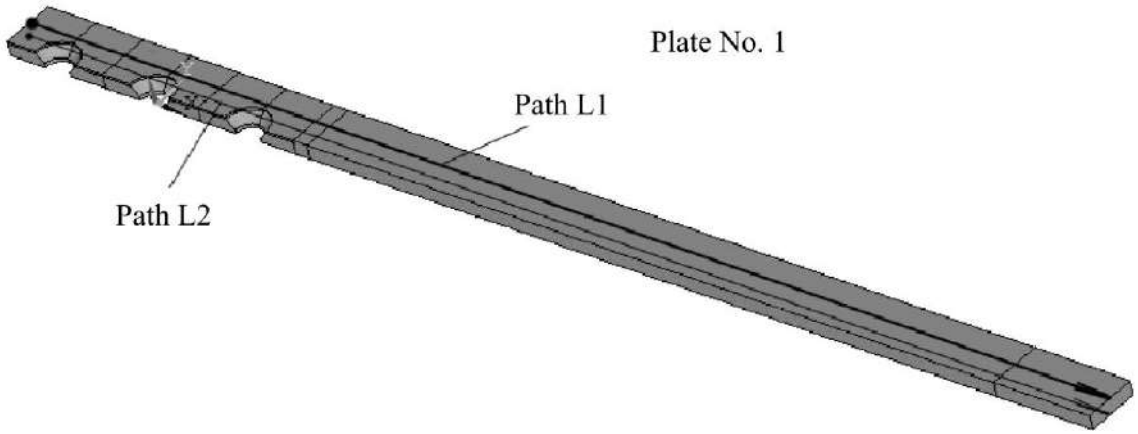

Fig. 5.39. Representation of paths L1, L2 of stress distribution σ_x

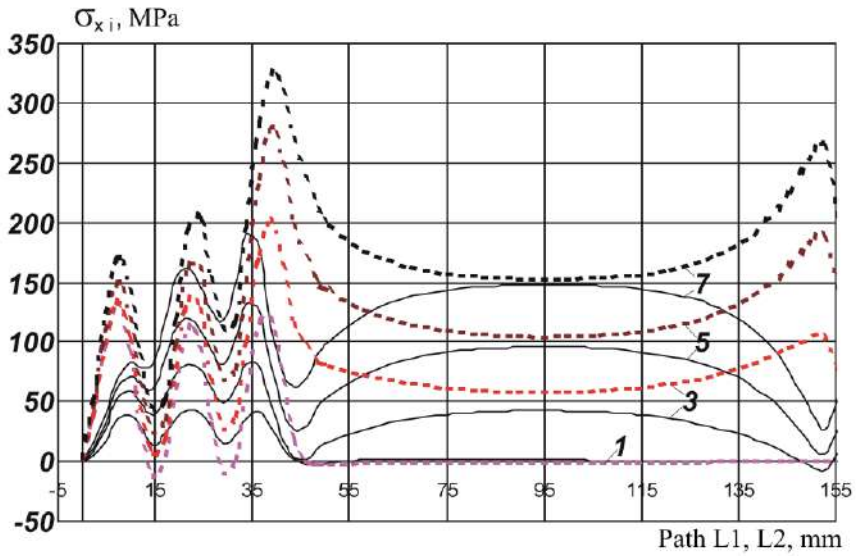

Fig. 5.40. Distribution nature of longitudinal stresses σ_x along paths L1 (solid line) and L2 (dotted line)

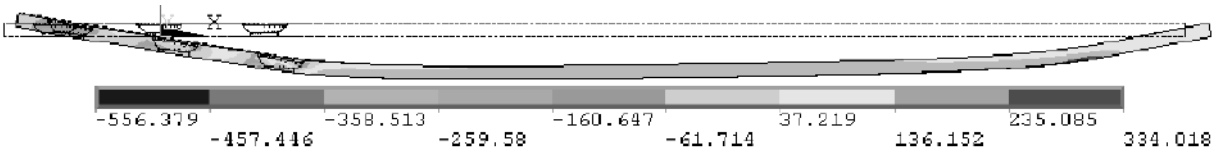

Fig. 5.41. Deformation of plate No. 1 under action of bending stress (scale of displacement – 5:1). Rivet is not shown

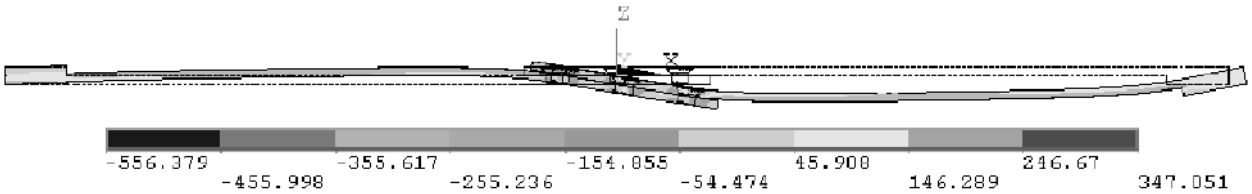

Fig. 5.42. Deformation of both plates under action of bending stress (scale of displacement – 5:1). Rivet is not shown

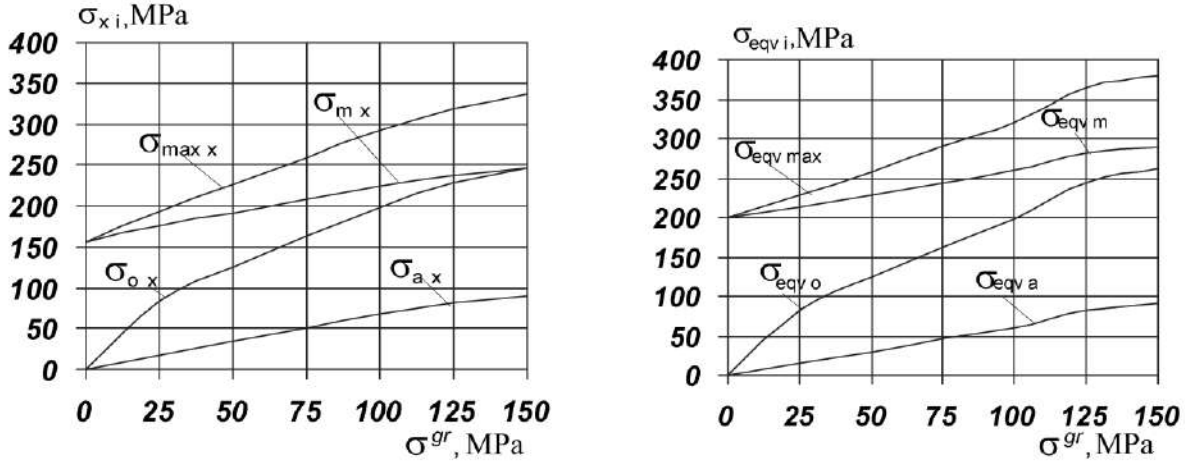

Fig. 5.43. Influence of external loading level σ^{gr} on σ_{max}, σ_a, σ_m and σ_0

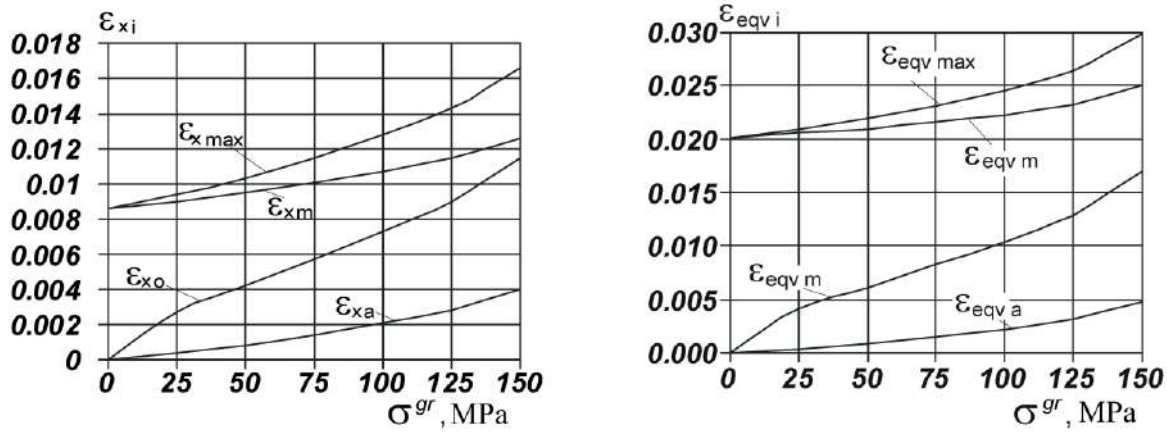

Fig. 5.44. Influence of external loading level σ^{gr} on ε_{max}, ε_a, ε_m and ε_0

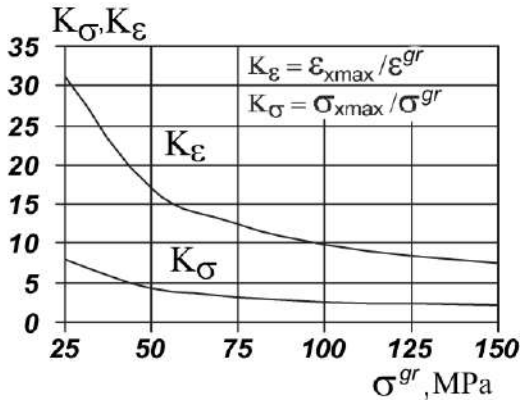

Fig. 5.45. Influence of loading level σ^{gr} on variation of concentration factor of tensile stresses σ_x and tensile deformations ε_x

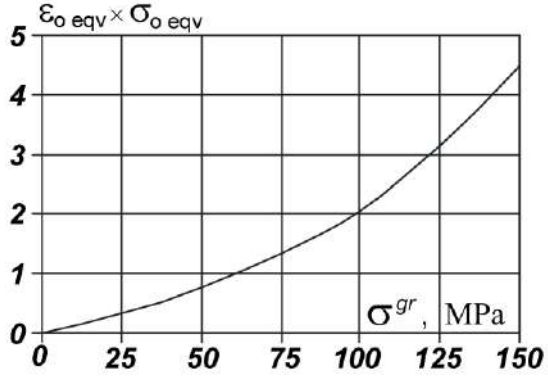

Fig. 5.46. Influence of loading level σ^{gr} on product of multiplication $\sigma_{eqv\,0} \times \varepsilon_{eqv\,0}$

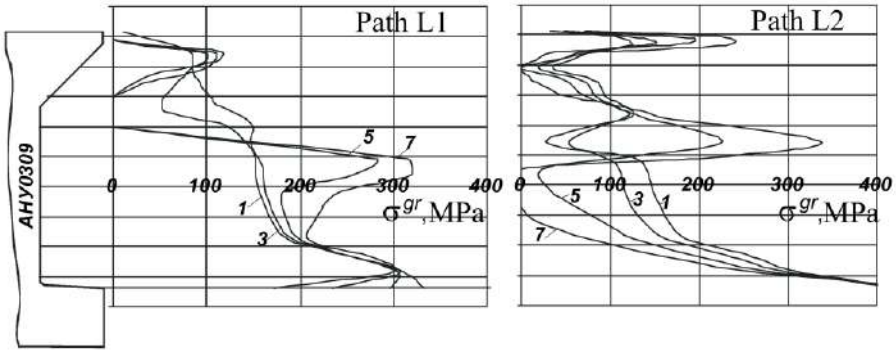

Fig. 5.47. Influence of loading level on contact pressure distribution between rivet body and pack along paths L1, L2

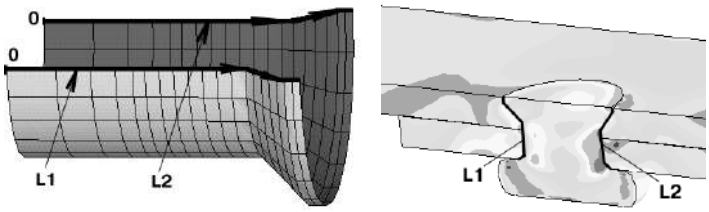

Fig. 5.48. Representation of path along which contact pressure distribution and values of gaps between interfaced surfaces are derived

Distribution of contact pressure is irregular that is due to both the riveting process itself and bending the rivet while applying tensile forces.

Gaps between the rivet and the plate appear due to application of tensile forces corresponding to stresses σ^{gr} = 100...150 MPa and do not exceed value of 0.058 mm within local zone. That proves the joint tightness within the full range of considered tensile stresses.

Analysis of mode of deformation of plate No. 2 in the zone of the first row of rivets is performed in the same way and is not represented further.

It is also necessary to consider distribution of contact pressure between plates. It is known that while riveting the pack swells and in fact plates contact only in area fitting closely to the rivet. Fig. 5.49 shows paths along which the graphs of contact pressure distribution are plotted (Fig. 5.50, 5.51).

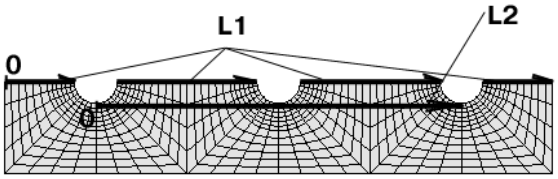

Fig. 5.49. Paths along which contact pressure distributes between plates are derived

Measuring value of contraction Δ_c and buckling Δ_b in longitudinal direction was performed for the second row of riveting. Value of contraction Δ_c was 0.04 mm and value of buckling Δ_b was 0.041 mm.

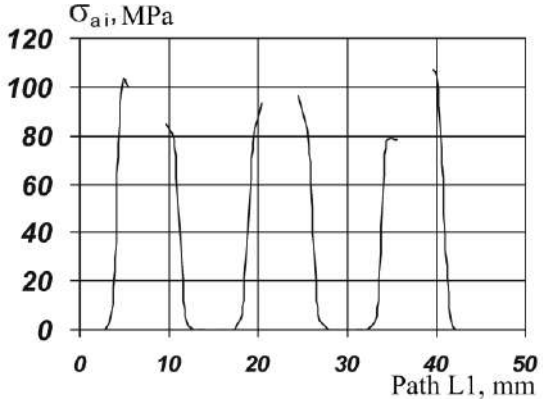

Fig. 5.50. Distribution of contact pressure between plates along path L1

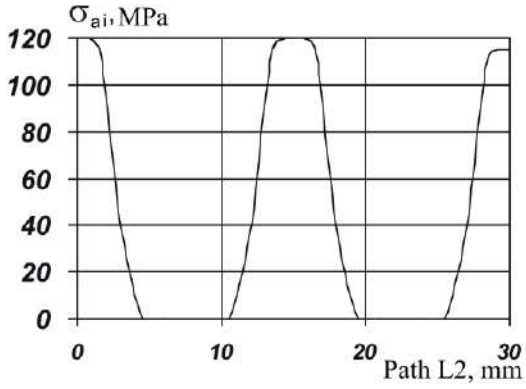

Fig. 5.51. Distribution of contact pressure between plates along path L2

Fig. 5.52 shows nature of specimen deformation and distribution field of equivalent stresses in plates after riveting of each rivet, but before application of tensile load.

Fig. 5.52. Nature of plate deformation after riveting each rivet (scale of displacement is 10:1). Rivet is not shown

Fig. 5.53 shows the results of analysis of characteristics of local mode of deformation in members of three-row single-shear joint made with rivet АНУ0314.

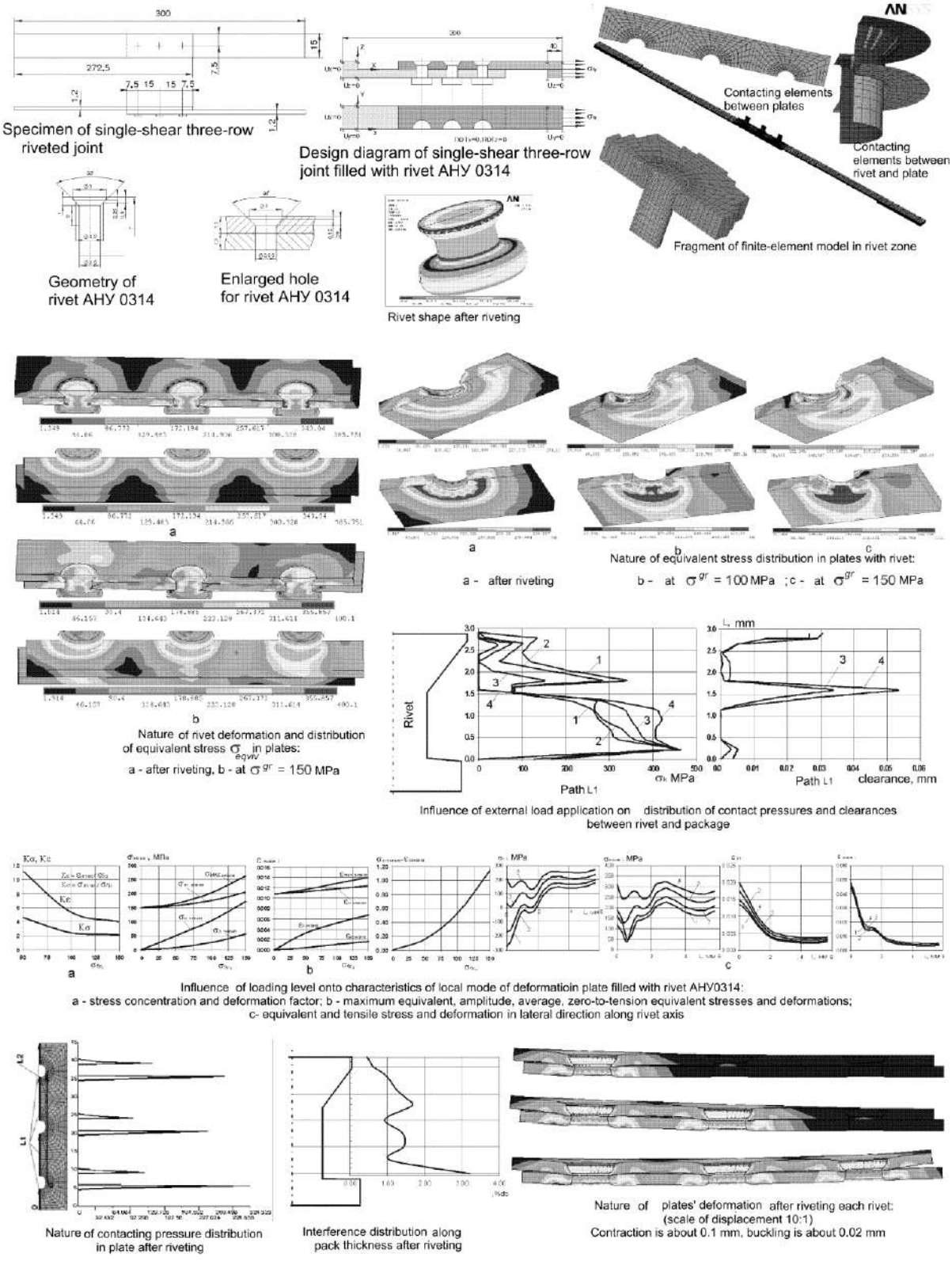

Fig. 5.53. Analysis of characteristics of local mode of deformation in members of three-row single-shear joint with rivet AHУ 0314

5.4. DESIGN PROCEDURE OF FORCE DISTRIBUTION BETWEEN ROWS OF SHEAR RIVETED JOINT

Design algorithm of force distribution between rows of shear riveted joint is shown in Fig. 5.54.

The ANSYS engineering analysis system allows computing force distribution for rivet rows in two methods.

First method lies in determination of distribution field of tensile stresses σ_x, which has irregular nature in sections between rivet rows (Ref. Fig. 5.54) of the upper and lower plates. Calculation of forces between rows of riveted joint is performed by multiplying averaged integral values of stresses σ_x in each section by value of the plate section area:

$$P_{plate_i} = \int_F \sigma_{xi} dF .$$

Calculation of force distribution between rivet rows is made according to formula:

$$P_{rivet\,i} = P_{plate\,i} - P_{plate\,(i+1)},$$

here i – row (cross-section) number, $P_{rivet\,i}$ – force transmitted by i^{-th} rivet.

$$R_i = \frac{P_{rivet\,i}}{P},$$

here R – share of force taken by i^{-th} rivet.

The second method lies in replacing the model of countersunk rivets with special members COMBIN39 (Fig. 5.55) having properties of non-linear springs. Deformation law of COMBIN39 member is given in table by six-seven points and corresponds to nature of mutual displacement of plates of single-row single-shear riveted joint having adequate geometrical dimensions. One of output option for element COMBIN39 is determining forces acting upon it.

Connection ensured with the fastener is replaced with element COMBIN39 and forces acting upon the element are taken as equal to these acting upon the rivet.

Results of calculations according to the proposed methods and their comparative analysis are represented in Fig. 5.54.

5.5. PROCEDURE OF ANALYZING AFFECT OF DIMENSION DEVIATIONS OCCURRING WHILE MANUFACTURING RIVETS AND MAKING HOLES FOR RIVET INSTALLATION ON DISTRIBUTION OF RADIAL INTERFERENCE ALONG PACK THICKNESS AFTER RIVETING

One of the most important parameters determining quality of the riveted joint is radial interference realized while riveting. Its numerical values and nature of distribution over thickness of the pack are used as integral characteristic, which may give possibility to predict static strength, fatigue durability, tightness and corrosion resistance of riveted joint. Minimal value of radial interference in riveted joint should exceed 0.4% of $d_з$ or equal to it. Algorithm of the method using the CAD/CAE

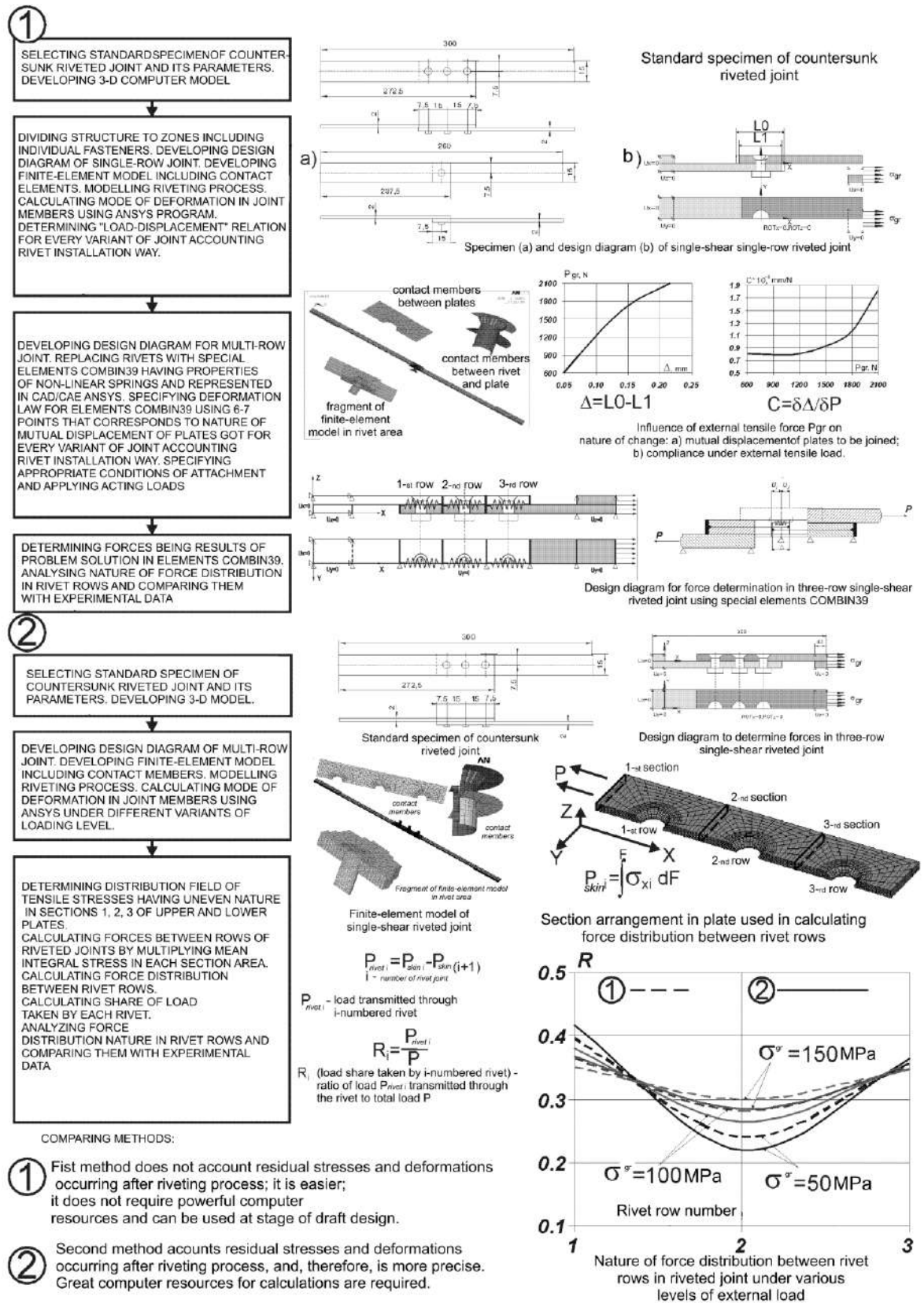

Fig. 5.54. Design procedures of force distribution between rows of shear-riveted joint

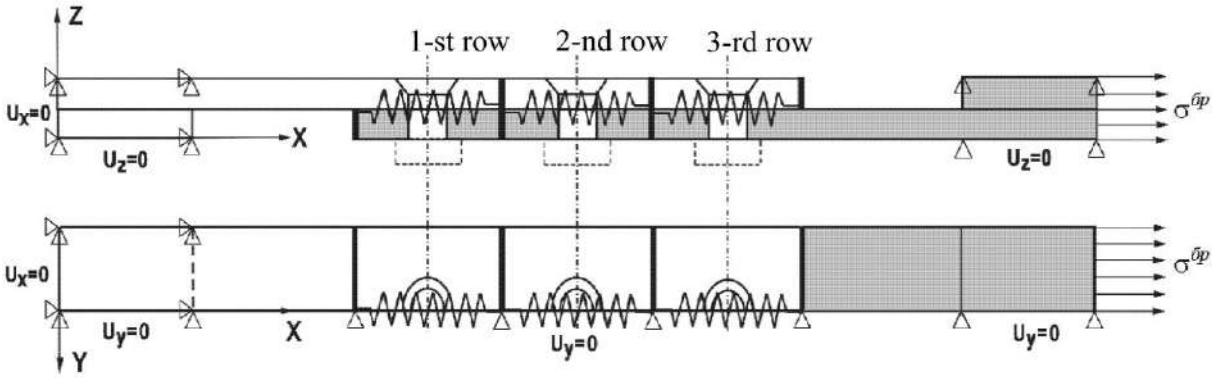

Fig. 5.55. Design diagram for determining forces in three-row single-shear riveted joint

ANSYS system analyzing influence of technological deviations occurring while manufacturing rivets, hole drilling on distribution of radial interference along the pack thickness on the plate having a hole mode of deformation is represented in Fig. 5.56. The rivet conforming to OCT1-34040-79 was selected for analysis.

5.6. PROCEDURES OF PREDICTING INFLUENCE OF STRUCTURALLY-TECHNOLOGICAL PARAMETERS OF COUNTERSUNK RIVETED JOINTS ON THEIR DURABILITY

When calculating durability of structural members one should determine the set of variable forces acting upon the joint and reduce them to the equivalent once and then to zero-to-compression cycles correspondingly:

$$\Delta\sigma_{eqv} = \sqrt[4]{\sum n_i \Delta\sigma_i^4}\,, \qquad \sigma_0 = \sqrt{2\sigma_a\sigma_{\max}}\,,$$

where σ_a – amplitude of the stresses acting in the structural members of the equivalent loading cycle; $\sigma_{\max}$ – maximum stress in structural members of the actual equivalent loading cycle.

It is known that durability under cyclic loading of the aircraft structural members may be determined using the following formula:

$$N\left(\sigma_0^{gr}\right)^m = C\,, \tag{5.1}$$

Where σ_0^{gr} – nominal stresses in gross-section of structural member reduced to the zero-to-compression stress cycle; m and C – constants determined by the fatigue test results of these members.

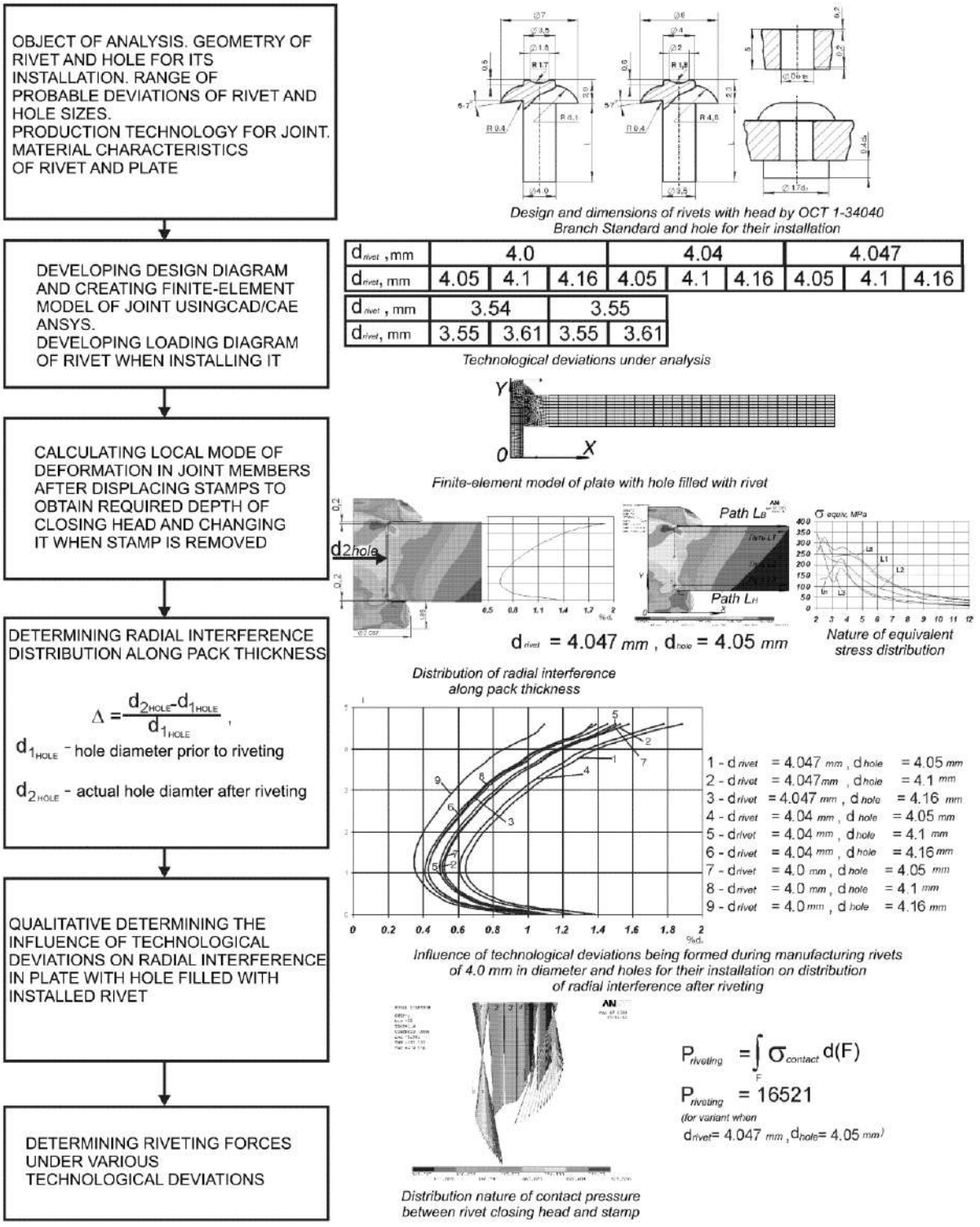

d_{rivet} ,mm	4.0			4.04			4.047		
d_{rivet}, mm	4.05	4.1	4.16	4.05	4.1	4.16	4.05	4.1	4.16

d_{rivet} , mm	3.54		3.55	
d_{rivet}, mm	3.55	3.61	3.55	3.61

Fig. 5.56. Analysis procedure of influence of dimension deviations being formed while manufacturing rivets and drilling holes for rivet installation on distribution of radial interference along pack thickness after riveting

Formula (5.1) gives possibility to calculate durability of different structural irregularities by fatigue test results but does not allow to take into account changing durability characteristics due to modification of structural members (such as changing geometry, fastener type, assembling technology) without additional fatigue tests.

To predict joint durability the total mode of deformation must be determined and standard specimens shall be put to fatigue tests.

When calculating joint durability the principle of superposition is used with dividing the loading into one passing along the sheet and taken by the fastener. In this case complicated loading close to holes is represented in the form of sum of the simplest cases of loading plate with a hole and single shear joint. According to this the reduced stress may be obtained in the joint section:

$$\sigma_{red}(f(N)) = K_{bear}(f(N))\sigma_{bear} + \sigma_{sheet} + K_{bend}(f(N))\sigma_{bend},$$

where σ_{sheet} – nominal stress produced by the loading passing in the sheet; σ_{bear} – bearing stress produced by loading taken by the fastener; K_{bear} – bearing ratio; σ_{bend} – bending stress.

But such method for accounting influence of assembly technology on joint durability requires more precise determination of the coefficients being components of the formula. It is used for revealing critical joint member sites from the fatigue durability point of view at stage of draft design. Number of cycles to failure is calculated on the basis of statistical data that requires experimental tests in case of structural or technological modifications of the joint.

Predicting influence of structural parameters on durability of the structural members is accomplished on the basis of characteristics' analysis of local mode of deformation in the critical sites of joints. But when using this method change of local mode of deformation of the member while assembling is not taken into account and the method itself is based on the test results of smooth specimens.

It also should be taken into account that calculation of durability of structural members shall be accomplished not only in the zone of geometrical concentrators of stresses but also in the zone of possible intensive development of fretting-corrosion on contact surfaces of parts to be loaded.

On the basis of test results the following analytical equation has been obtained for calculation of durability of structural members when they are damaged in the zone of fretting-corrosion due to variable tensile loading:

$$\sigma_{à\ fr} = 2.34(\sigma_{ult} - \sigma_m)^{0,63}\left[0.64 + 43.3(lg\ N)^{2,1}\right] - 4.068(lg\ N)^{0,92K_{ï}}\ \sigma_C^{0,32}K_m K_{fc}, \quad (5.1)$$

Where $\sigma_{a\,fr}$ and σ_m – correspondingly amplitude and average values of cyclic nominal tensile stresses in structural members in the zone of fretting-corrosion, MPa; σ_{ult} – ultimate strength of aluminum alloy, MPa; σ_C – contact stresses in the part in the zone of fretting-corrosion, MPa; N – number of cycles up to failure; K_C –

factor taking into account influence of coatings on reducing amplitudes of stress at the specified durability; $K_{II} = 1$ – for clad sheet articles; $K_{II} = 0.86$ – for anodized articles; $K_C = 0.89$ – for anodized articles coated with primer ФЛ-086; K_m – factor taking into account changed shape of contact; $K_m = 1$ – for rectangular shape of contact; $K_m = 1.36$ – for other shapes of contact; K_{fc} – factor taking into account influence of radial interference on change of limiting value of maximum zero stresses. Value lies within the range of 0.95…0.90.

The purpose of the analysis is to develop procedure of predicting structural member durability on the basis of the fatigue resistance characteristics of the standard specimens of the countersunk riveted joints and calculation of local total specific deforming work per component of the local mode of deformation, which were obtained using finite element model.

Algorithm of the proposed procedure is represented in Fig. 5.57.

On the basis of analyzing parameters of the shear countersunk riveted joints applied the standard specimens and their geometrical characteristics were selected (hereinafter positions on figures correspond to enumeration of the standard specimens shown below):

1) plate with enlarged hole filled with riveted rivet by ОСТ 1 34055-92 (АНУ0309);
2) single-shear three-row countersunk riveted joint made with rivets by ОСТ 1 34055-92 (АНУ0309).

Having available fatigue test results of such types of joints (Fig. 5.58) and assuming durability of joints made with rivets by ОСТ 1 34055-92 (АНУ0309) as basic, the following task is set forth: to predict durability of these specimens but with rivets by АНУ0314 with reduced depth of the countersunk head.

Taking into account the fatigue test results the coefficients m and C for analytical formulas of the fatigue curves were calculated using nominal stresses (5.1) (Ref. Table 5.1).

Table 5.1

Fatigue Curve Experimental Coefficients of Riveted Joint Standard Specimens

Standard Specimen	$N\left(\sigma_0^{gr}\right)^m = C$	
	m	C
Plate with enlarged hole filled with rivet by АНУ0309	6.2010585	6.1007996E+18
Single-shear three-row riveted joint made with rivets by АНУ0309	2.8488924	6.5912688E+10

To predict fatigue durability of standard specimens made with rivets by АНУ0314, the calculation of characteristics of local mode of deformation using engineering analysis system ANSYS was made. Local equivalent stresses and deformations in the most loaded points close to the hole were reduced to the zero-to-compression loading cycle according to Owding's formula (Fig. 5.59, a, b).

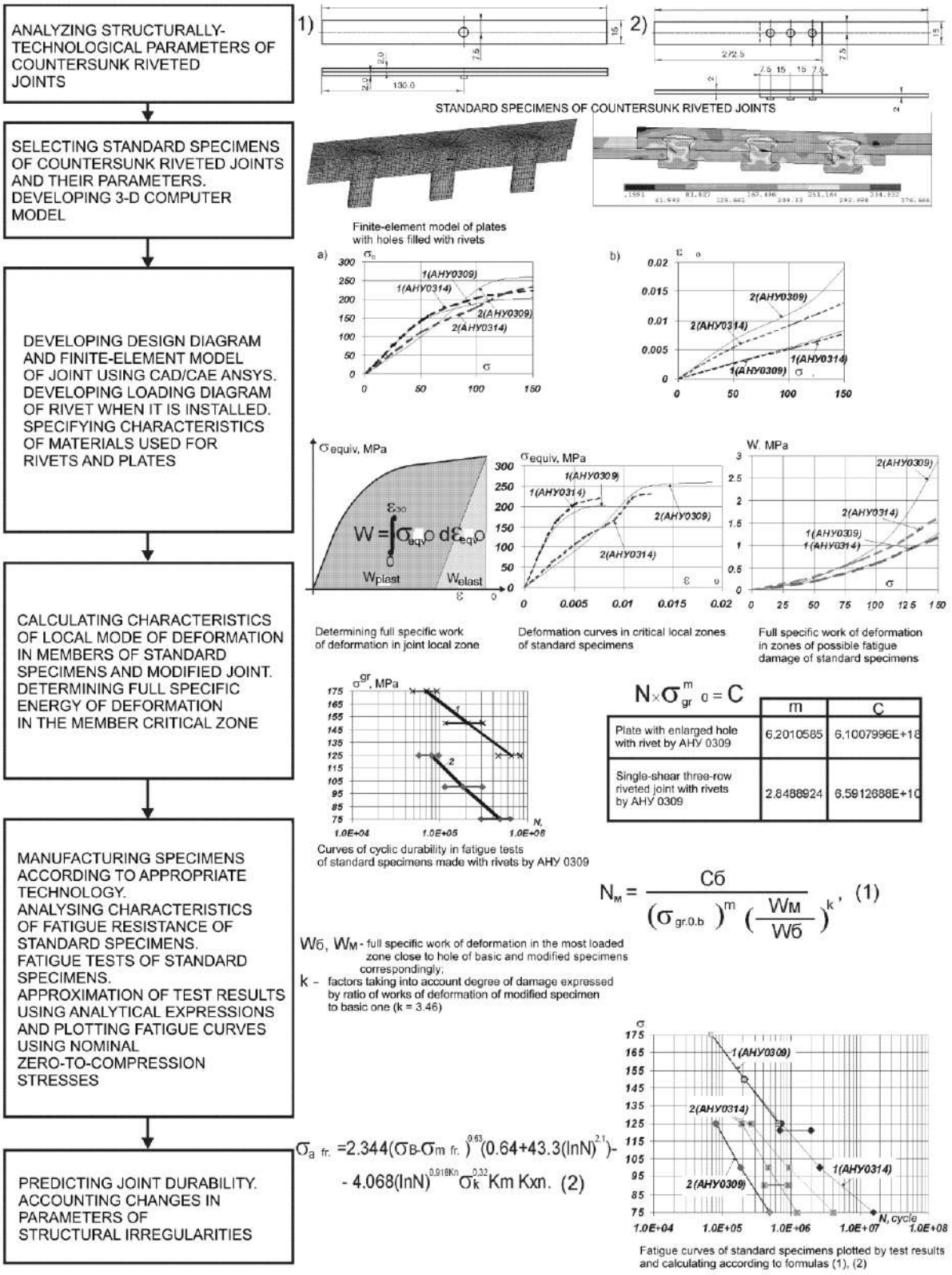

Fig. 5.57. Procedure of predicting influence of structurally-technological parameters of countersunk riveted joints on their durability

As it is evident from Fig. 5.60, constructive parameters of standard specimens affect the relation $\sigma_{eqv0} = f(\varepsilon_{eqv0})$.

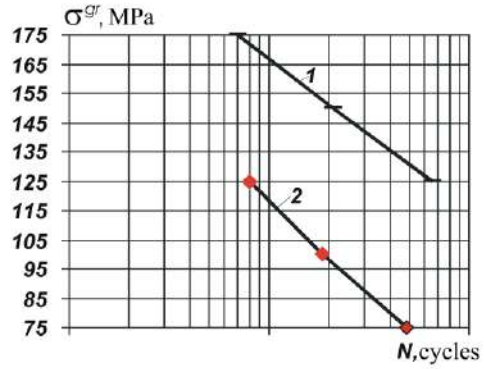

Fig. 5.58. Curves of cyclic durability under fatigue tests of standard specimens made with rivets АНУ0309

In Fig. 5.60 the relations $\sigma_{equiv0} = f(\varepsilon_{equiv0})$ are shown for the considered standard specimens.

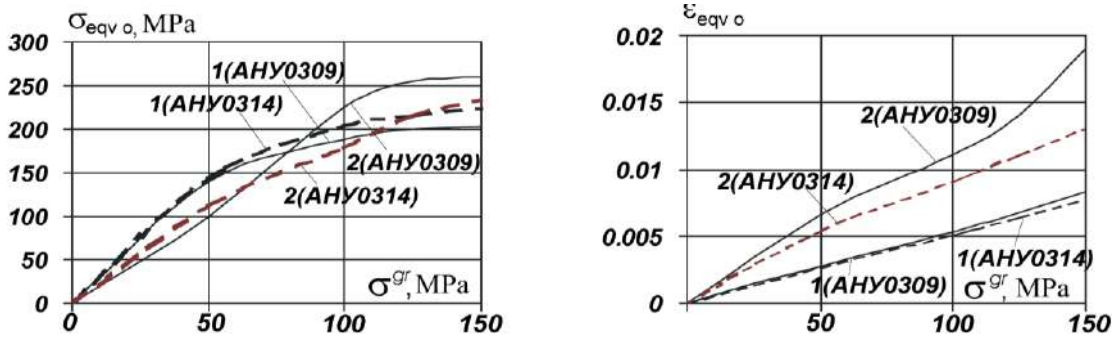

a b

Fig. 5.59. Influence of External Tensile Load σ^{gr}, MPa, on Local Equivalent: a – stresses; b – deformations reduced to zero-to-compression loading cycle according to Owding's formula

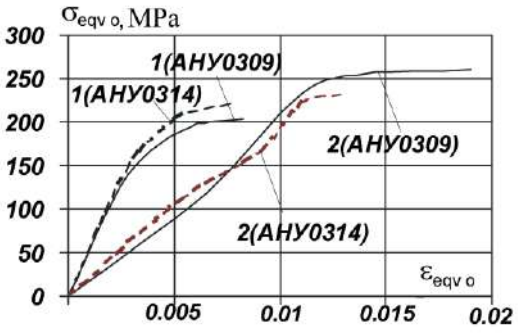

Fig. 5.60. Relations between local equivalent zero-to-tension stresses σ_{eqv0} and deformations ε_{eqv0} in critical zones of standard specimens

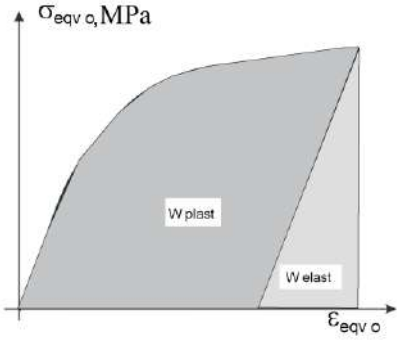

Fig. 5.61. Relation $\sigma_{eqv0} = f(\varepsilon_{eqv0})$, determining total specific work of deformation in local zone

Specific energy of the specimen deformation was determined in the zone of probable fatigue failure – transition of the hole tapered portion into the cylindrical one in the section along the rivet axis. Total specific energy of deformation consists of elastic W_{elast} and plastic W_{plast} components (Fig. 5.61) and equals square limited with curve $\sigma_{eqv0} = f(\varepsilon_{eqv0})$ and abscissa axis:

$$W = \int_0^{\varepsilon_{eqv0}} \sigma_{eqv0} d\varepsilon_{eqv0} .$$

By means of numerical integrating the relations shown in Fig. 5.60, values of total specific work of deformation in the critical zones of specimens under test were obtained with changing σ_0^{gr}, MPa (Fig. 5.62).

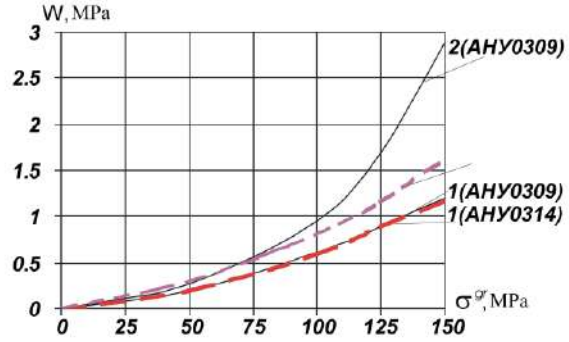

Fig. 5.62. Total specific work of deformation in zones of probable fatigue failure of standard specimens

Durability of standard specimens made by means of rivet by АНУ0314, was calculated according to formula

$$N_m = \frac{C_b}{(\sigma_{gr.0b})^m \left(\left(\frac{W_m}{W_b} \right)^k \right)}, \qquad (5.2)$$

where W_b, W_m and k – total specific work of deformation in the most loaded zone close to the hole in the basic and modified specimen correspondingly and coefficient taking into account extent of damage expressed by ratio of work of deformation in the modified specimen in comparison with basic one.

As it is evident from Fig. 5.62, value of total specific energy of deformation in the local zone is approximately equal to specimens with non-loaded hole filled with rivets by АНУ0309 and АНУ0314 that is proved by the fatigue test results. In case of single-shear three-row countersunk riveted joint total specific energy of deformation has the same values only up to value of tensile load corresponding to σ^{gr} = 75 MPa. With further increase of tensile load for the specimen with rivets by АНУ0309 more intensive increasing of total specific energy of deformation was observed in comparison with the specimen with rivets by АНУ0314. Therefore, approximate estimation of influence of constructive parameters on durability of

such joints is possible at calculation stage of total specific energy of deformation.

While predicting specimens' durability using rivets by АНУ0314, the fatigue curve of plate having enlarged hole and filled with rivet by АНУ0309 was assumed as basic curve. According to formula (5.2) knowing durability of standard specimens made with rivets by АНУ0309, it is possible to determine coefficient $K = 3.463$ of transition from basic curve to fatigue curve of the single-shear three-row countersunk riveted joint. Predicting durability of standard specimens made with rivet by АНУ0314 was accomplished with assumption of coefficient k invariability (Fig. 5.64).

As evident predicted durability for specimen with filled non-loaded hole lies within area of results obtained in tests. For three-row single-shear joint the design durability lies higher than test values. This proves the fact that failure occurs due to fretting-corrosion, which reduces joint durability. Calculation is accomplished by formula (5.1).

Values σ_c and σ_{bend} were determined in plate with enlarged holes in the area of utmost rivet row at the border with the second plate (Fig. 5.63).

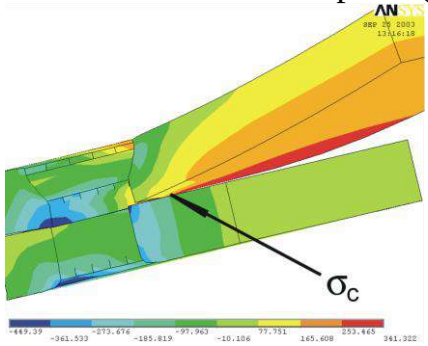

Fig. 5.63. Nature of deformation and distribution of stress σ_x in area of the utmost row of three-row single-shear joint made with rivet by АНУ0314. Deformation scale – 7:1

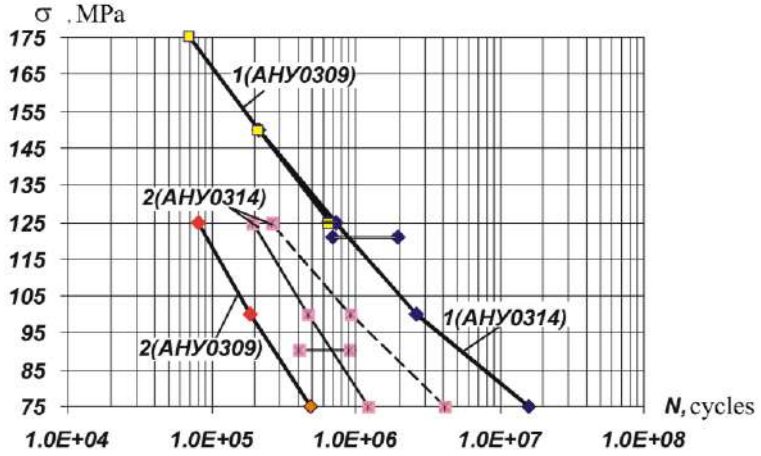

Fig. 5.64. Fatigue curves of standard specimens plotted according to test results and through calculations by formulas (5.1), (5.2)

In Fig. 5.64 fatigue curves for standard specimens made with rivet by

АНУ0309 have been obtained experimentally. Design durability of the specimen with non-loaded hole filled with rivet by АНУ0314 lies within the range of test values and coincides with fatigue curve of the specimen made with rivet by АНУ0309. For three-row single-shear specimen made with rivets by АНУ0314, two fatigue curves are represented. Solid line represents predicted durability calculated by formula (5.2) in section along the hole axis. Dotted line indicates predicted durability calculated within the zone of intensive fretting-corrosion according to formula (5.1). Its values lie within the range of test value spread.

5.7. Conclusions

1. Method of integrated designing, 3-D modeling and reaching specified durability of shear riveted joints of aircraft assembly structures using CAD/CAM/CAE UNIGRAPHICS and ANSYS systems has been proposed.
2. Procedure of computer-aided modeling of fuselage and wing spar assembly sections made with advanced rivets has been developed.
3. Procedure of integrated designing process of skin riveted joints at stage of sketch design allowing to select joint rational parameters for the specified durability and minimal mass has been proposed.
4. Analysis procedure of influence of design and technological parameters on characteristics of local mode of deformation in the riveted joint members accounting plastic deformations in rivets while riveting and contact interaction of joint members has been developed.
5. Characteristics of local mode of deformation in members of three-row single-shear joint made with new countersunk rivets has been analyzed using ANSYS system.
6. New design procedures of load distribution between rows of shear riveted joint using ANSYS system taking into account riveting production process has been proposed.
7. Analysis procedure of influence of dimension deviations occurring while manufacturing rivets and drilling holes on radial interference distribution along the pack thickness after riveting allowing to estimate influence of technological deviations on the joint operability has been developed.
8. New procedure of predicting influence of design and technological parameters of countersunk riveted joints onto their durability taking into account variation of specific energy of deformation in the zones of probable fatigue failure has been proposed.

Section 6
NEW STRUCTURAL AND TECHNOLOGICAL SOLUTIONS FOR SHEAR RIVETED JOINTS OF AIRCRAFT THIN-WALLED ASSEMBLY STRUCTURES

Riveted joints of load-carrying members of aircraft structures are critical places in airframe responsible for ensuring its strength, service life, tightness, corrosion resistance and quality of external surface.

Important problem while riveting airframe operated under corrosive conditions is to provide high quality of its external surface, durability and tightness along thickness of the pack of assembly parts. Technologies used at aviation enterprises on mechanical cleaning of protruding rivet heads do not provide assured meeting the requirements of specifications and require essential costs for head milling and restoring protective coating. That is why the development of modified rivets and also technology of their installation ensuring required extension of rivet set head after riveting without mechanical cleaning is the very important problem.

The author has proposed several design-technological solutions (Fig. 6.1) increasing cyclic durability, tightness and quality of external surface of shear riveted joints of aircraft structures.

6.1. STRUCTURALLY-TECHNOLOGICAL METHODS OF FATIGUE DURABILITY INCREASE OF SINGLE-SHEAR RIVETED JOINTS BY UNLOADING THE UTMOST ROWS

In longitudinal and transverse single-shear riveted joints of wing and fuselage, skin-to-stringer tip joints, repair straps-to-load carrying members of airframe joints operational load is transmitted with eccentricity in relation to section of regular zone of load-carrying structure.

Eccentricity in load transmission causes appearance of bending stresses in parts to be assembled. In the zone of utmost rows, which are the most loaded, in multi-row joint they increase stress concentration that assists in decreasing fatigue durability of single-shear joints. On the basis of analysis of mode of deformation of single-shear joint plates the following methods to increase its fatigue durability has been developed:

- in the utmost rows the rivets are installed with clearances in the part forming the edge of overlapping and with interference in the second part to be joined;
- additional row of rivets is installed at the overlapping edge, so tips of connected parts are involved in taking bending moment and do not work in shear;

Rivet set head butt includes straight circular cylindrical compensator with diamater equal to cylindrial portion of a countersunk primary head.

Пат. 2066003

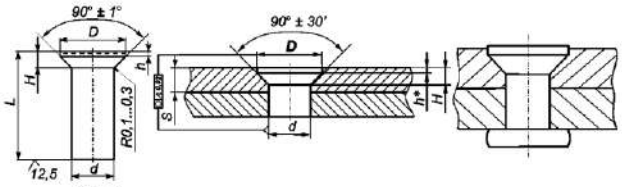

Joint rivets have reduced countersunk set head with cylindrical compensator placed on the head butt.

(АНУ 0314)

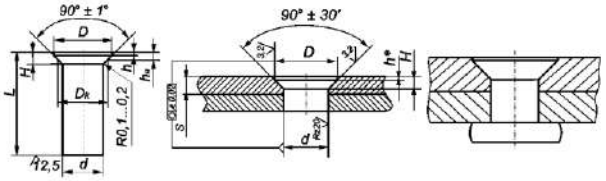

Joint rivets a plane compensator in truncated cone shaped adjacent to the set head with smaller base.

(АНУ 0310)

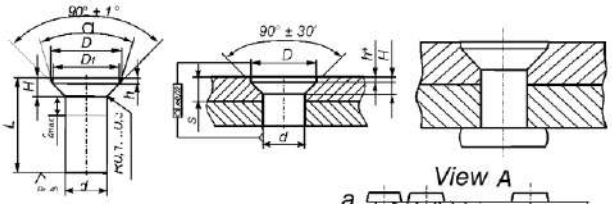

Additional rivet row with standard (a), segmental (b) c-stepped (c) set heads is installed overlapping at the joint edge at distance of ahalf pivot diameter.

A.c. 978649

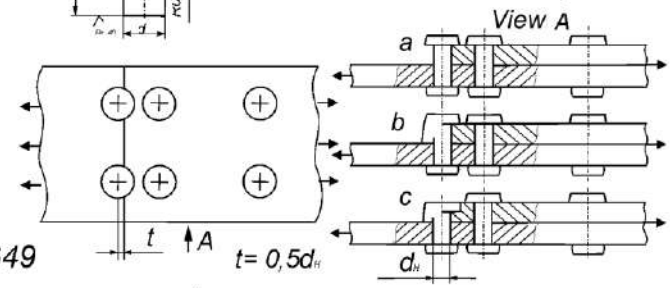

Shear joint shank ends are additionally attached to the mating parts with fasteners installed with a shank end clearance and the radial interference in mating part.

A.c. 1010325

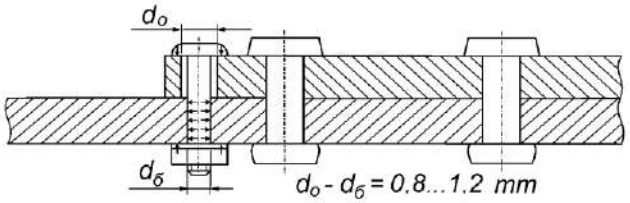

The extreme rivets in the skin and left stringer are installed with a stringer grip clearance and with the skin radial interference. The rivet closing heads may be countersunk and cone.

A.c. 1418524

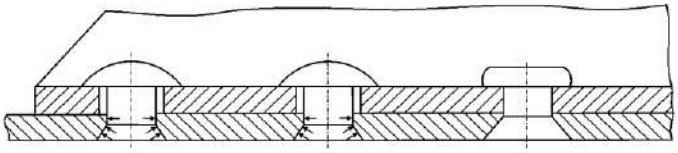

The shank end edge of the joined part is attached to the loaded part near the location where the cantilever head edges are leant against the additional strap attached to the mating part. The fastener bars are installed with hole clearances at the junction of the strap and the shank end edge with radial interference in loaded part.

A.c. 1186844

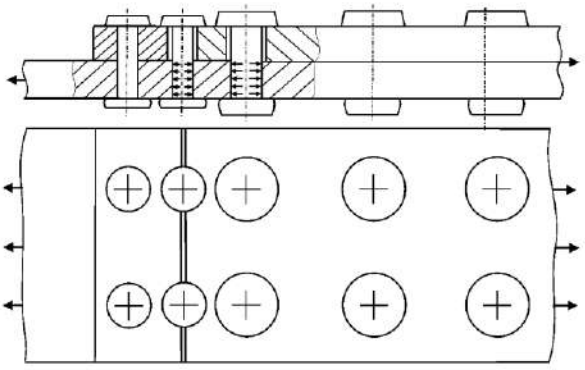

Fig. 6.1. New design-technological methods increasing cyclic durability, tightness and external surface quality of shear riveted joints of aircraft structures

It was proved that unloading the utmost rows of single-shear joints practically does not affect the breaking load of such joints under their tensile static loading. For example, analysis of test results of five-row overlapped joints (Fig. 6.2) shows that clearance between rivet shank and hole wall in the part forming overlapping edge within the tested range of clearances while testing for breaking load under tensile static loading practically does not affect because spread of breaking loads lies within the range of permissible error.

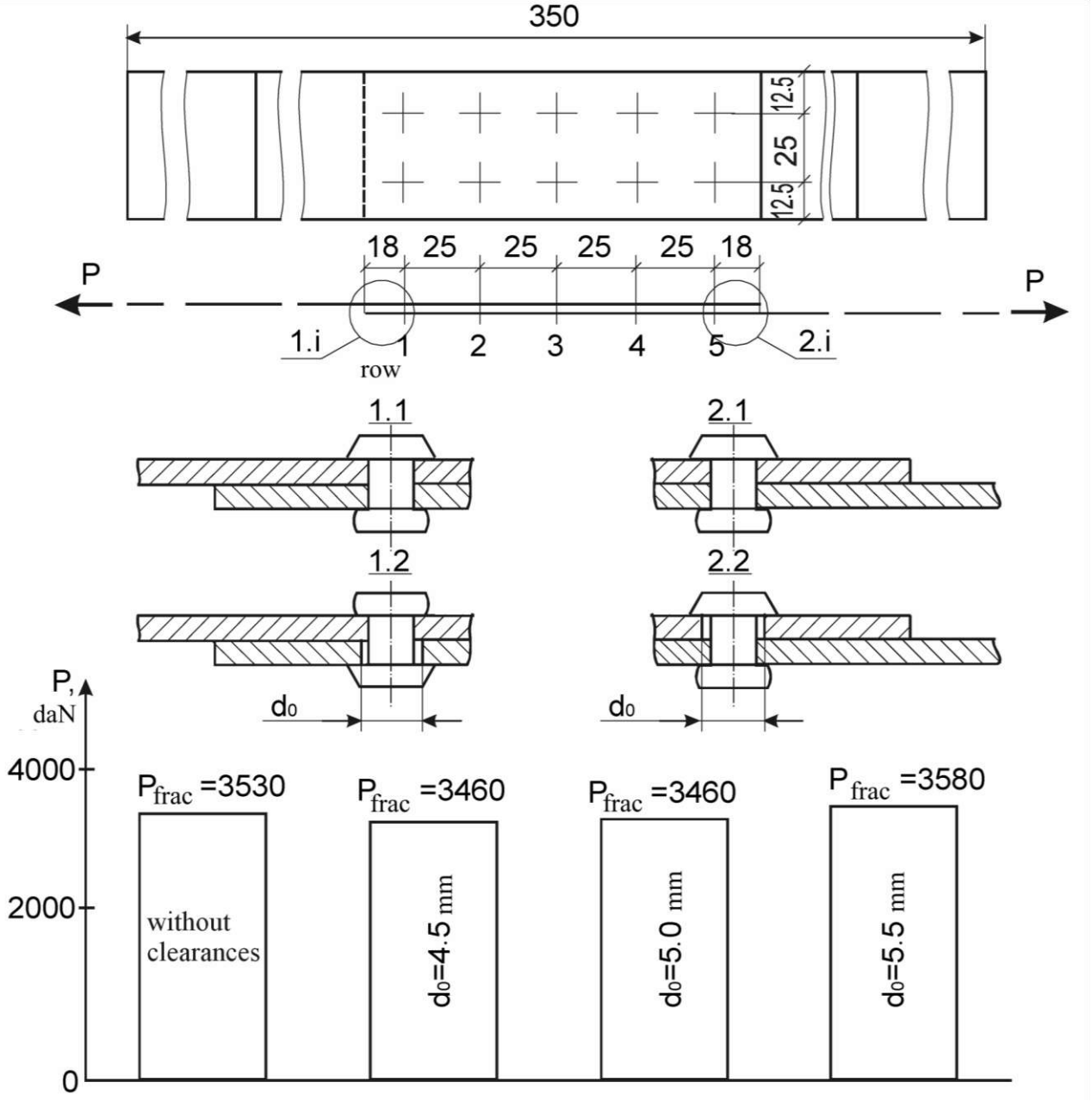

Fig. 6.2. Influence of hole diameter on breaking load of five-row overlapped riveted joint under its static loading

6.1.1. Influence of clearances between rivet shanks in the utmost rows and hole walls in parts forming overlapping edge on fatigue durability of five-row overlapped joints

Influence of clearance between rivet shanks and hole walls in tips of parts to be joined with overlapping on joint fatigue durability was made on specimens of five-row overlapped riveted joint. Joint was made with rivets АНУ 0300-4-9, installed according to serial technology without unloading for basic variant of specimen execution 1.1, 2.1 (Fig. 6.3).

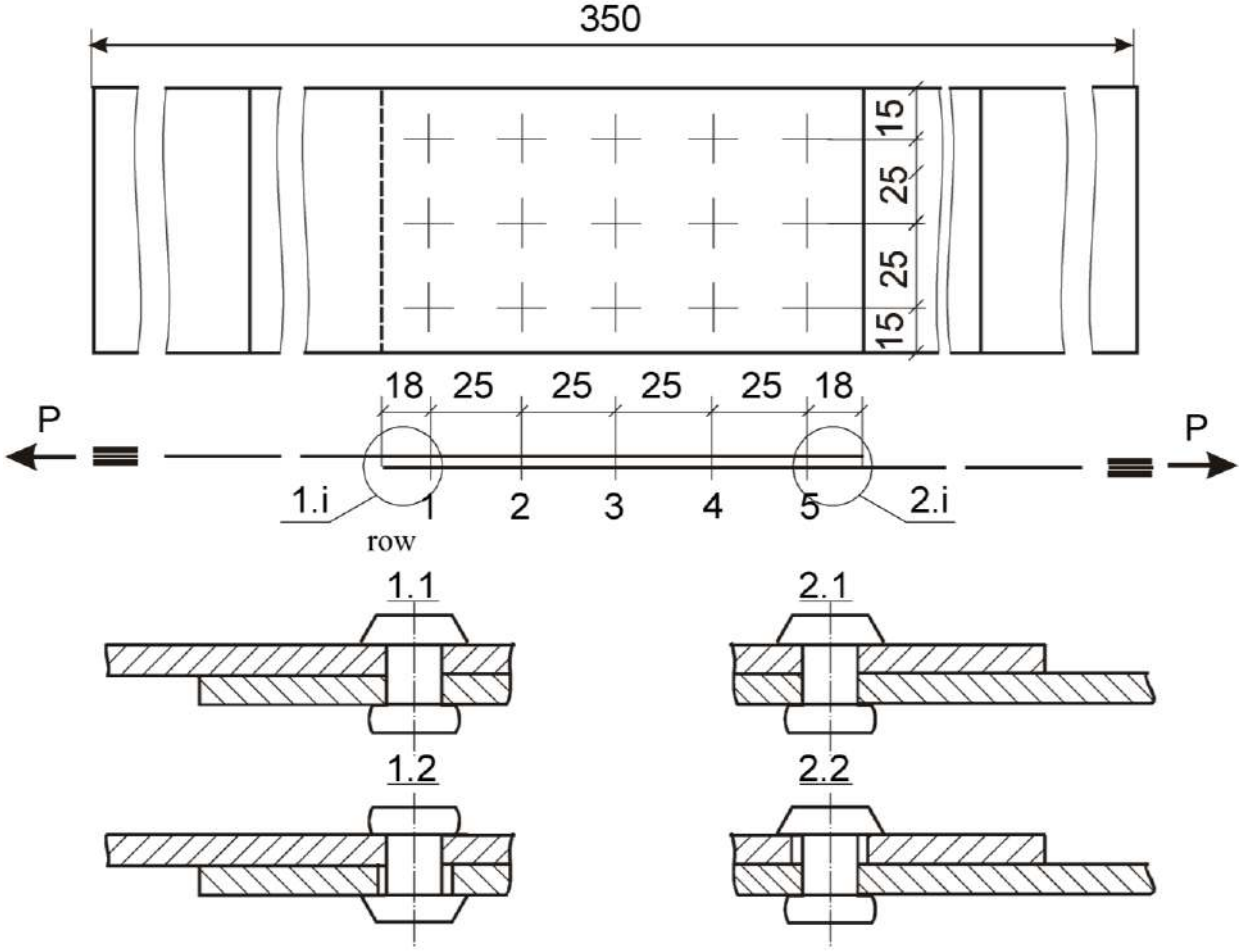

Fig. 6.3. Variants of five-row overlapped joints execution

After drilling holes of ∅4.1 mm for rivets of ∅4.0 mm the holes in tips of parts to be joined were enlarged to diameters of 4.5; 4.8; 5.0; 5.2; 5.5 mm for the second variant of specimen 1.2, 2.2 execution (Ref. Fig. 6.2). Then holes were chamfered over perimeter in 0.1…0.2 mm depth at angle of 120°, parts were degreased and rivets were installed. Rivet set heads were inserted from the side of larger holes. Depth of snap heads was equal to half the rivet shank diameter.

Test results are shown in Fig. 6.4 and Fig. 6.5.

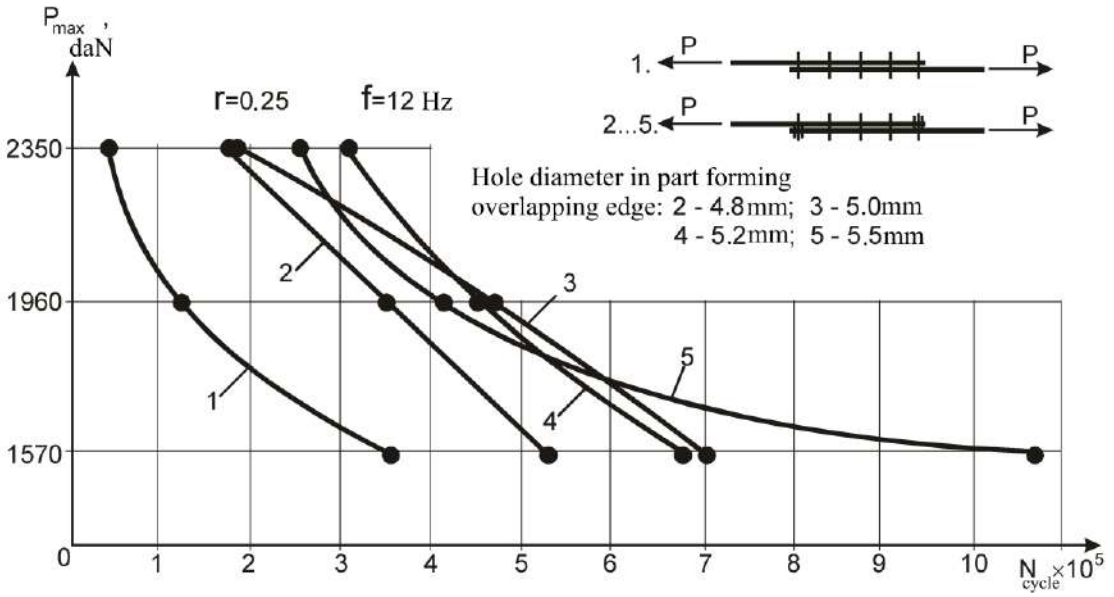

Fig. 6.4. Relation between fatigue durability of five-row overlapped joint specimens
and applied load for different hole diameters

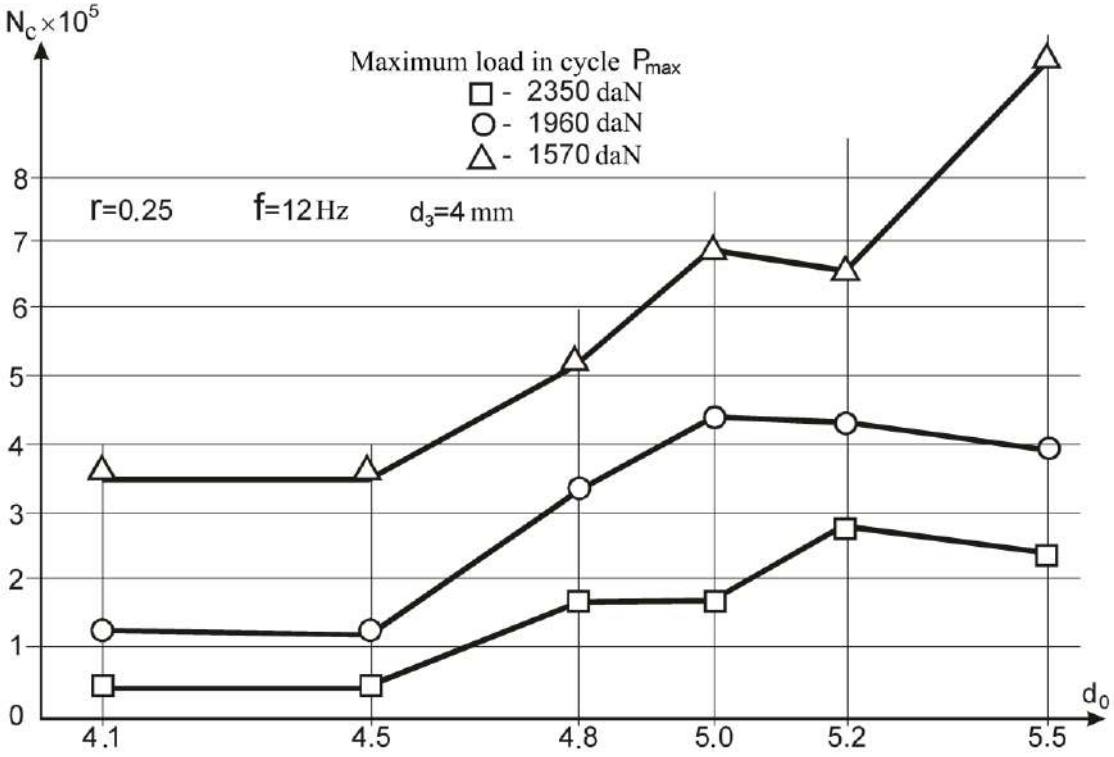

Fig. 6.5. Relation between fatigue durability of five-row overlapped joint specimens and hole diameter in part forming overlapping edge,
thus ensuring installation with clearance of rivets in the utmost rows

Analysis of fatigue test results shows that when holes in the part forming the overlapping edge have 4.5 mm in diameter the fatigue durability of the five-row overlapped joint in fact does not change. This shows that holes of such diameter do not ensure required clearance between shank of the installed rivet and hole wall in the part forming the overlapping edge.

Stable increasing fatigue durability was obtained after enlarging holes of ∅4.8…5.5 мм in the parts to be joined in 1.5…6 times in average in comparison with specimen fatigue durability, in which rivets were installed without clearances.

Influence analysis of installing a washer from the side of the hole of larger diameter in the part forming overlapping edge was made for specimens of five-row riveted overlapped joint.

Joints were made in parts of Д16АТВл2 material joined by means of rivets АНУ 0300-4-9, which were installed without clearances for the fist basic variant of making the joint specimens 1.1 (Fig. 6.6).

The utmost rows of rivets of the second variant of making the specimens 1.2 were installed with clearance in the part forming the overlapping edge. Clearance was ensured by enlarging the holes with drill in the part forming the overlapping edge of 5.2 mm. Set heads were arranged from the side of holes having smaller diameter.

Prior to riveting from the side of the holes having lager diameter the washers made of 30ХГСА material in 0.9…1.0 mm thickness of with inner diameter of 4.1…4.3 mm and outer diameter of 8.7…8.9 mm were installed. In the utmost rows the rivets АНУ 0300-4-10 were put. Depth of closing head of any rivet after riveting was equal to one-half the diameter of its body.

Fatigue tests were carried out under one level of loading with maximum cyclic load P_{max}=1960 daN. The fatigue test results are represented in Fig. 6.6.

Analysis of fatigue test results shows that fatigue durability of five-row overlapping joints, the utmost rows of which are installed with clearances in the part forming overlapping edge using washers, increases in 4.1 times in comparison with fatigue durability of joints without clearances.

6.1.2. Influence of coating parts to be joined while riveting the utmost rows with clearances in part forming overlapping edge on fatigue durability of single-shear joints

Sheet articles of aircraft structures are forwarded to assembling after anodizing, and in some cases of anodizing with the following coating with primer of ФЛ-086 grade.

In such case it is necessary to evaluate influence of installation of the utmost row rivets with clearances in the part forming overlapping edge with the availability of coatings on the parts to be joined, which are applied by anodizing or anodizing with the subsequent application of primer of ФЛ-086 grade.

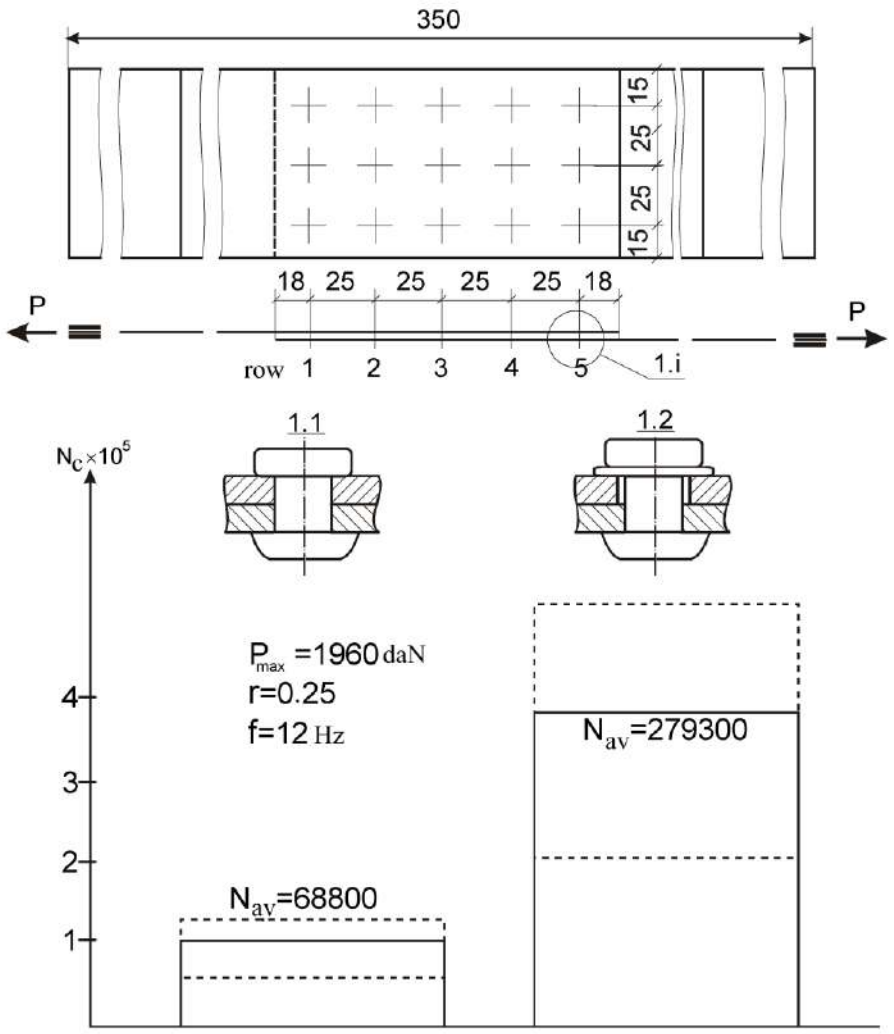

Fig.6.6. Influence of installation of the utmost rivets of five-row joint with clearance in the part forming overlapping edge using washers

Influence of coating on fatigue durability of single-shear overlapping joints when the utmost rivets are installed with clearances in the part forming overlapping edge was analyzed for five-row riveted joints of sheet articles HX anodized and plated with primer ФЛ-086, HX anodized with subsequent assembling with sealing compound УЗОМЭС-5, and also joints of sheet articles in delivery condition.

Each joint plated with the coating listed below was manufactured and tested in two variants:

– basic (first) variant of joints made without clearances (1.1, 1.2 in Fig. 6.7);

– second variant made by rivets АНУ 0300-4-9, placed in the parts forming overlapping edge with clearance, the clearance is ensured by enlarging holes in tips of joined parts up to 5 mm in diameter (1.2, 2.2 in Fig. 6.7).

Fatigue tests were carried out at three levels of loading P_{max}=2350, 1960 and 1570 daN. The fatigue test results are shown in Fig. 6.7 and 6.8.

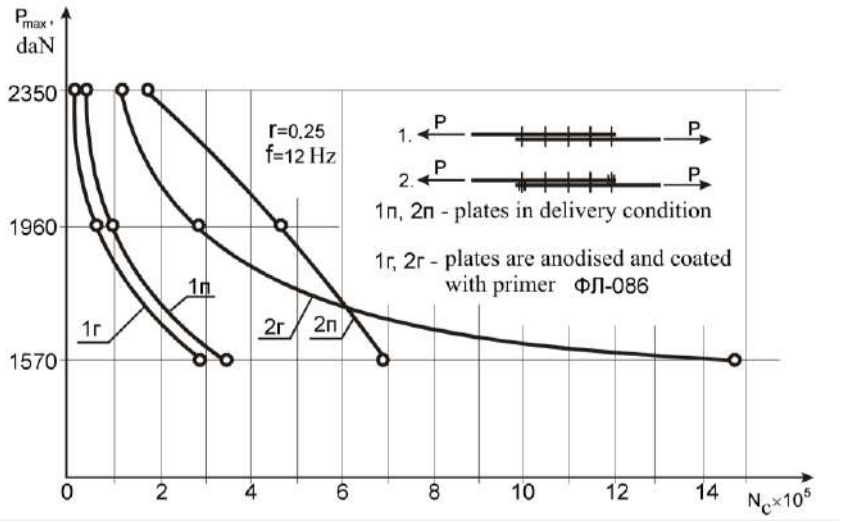

Fig. 6.7. Fatigue test results of specimens of five-row riveted joints of parts anodized and coated with primer ФЛ-086, and also in state of delivery, utmost rows of fasteners were installed with clearance into the parts forming overlapping edge

Analysis of fatigue test results shows that installation of rivets in the utmost rows of single-shear joints with clearance in the part forming the overlapping edge is an effective means to increase fatigue durability of such joints with the availability of coatings on joined parts used in tests.

The fatigue durability of joint specimens when clearances are provided between rivet shanks and hole walls in the part forming overlapping edge increases in 1.7...6.7 times on the average in comparison with fatigue durability of joint specimens made without clearances with the availability of serial coatings.

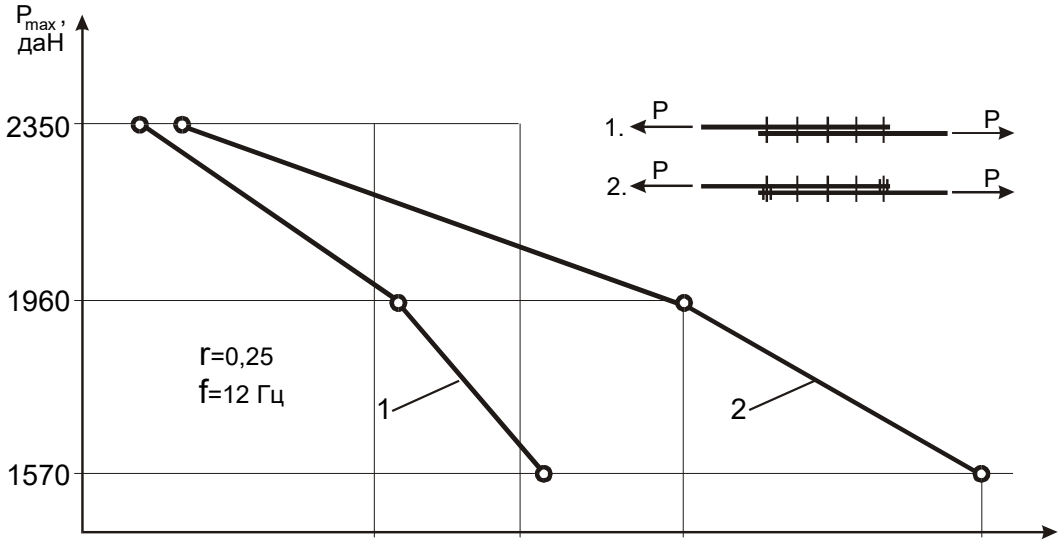

Fig. 6.8. Fatigue tests results of five-row riveted overlapping joint specimens with rivets in the utmost rows installed with clearances into the parts forming overlapping edge assembled using УЗОМЭС-5 sealing compound applied to surfaces to be joined

6.1.3. Influence of additional rivet row with stepped set head on fatigue durability of single-shear joints

To analyze the rivets having stepped set head (Fig. 6.9) with regard to fatigue durability of riveted joints the specimens of overlapping joints have been made and tested.

For additional rivets in parts being joined forming overlapping edge the grooves having 4.4 mm in width and 7 to 10 mm in length have been made for rivet installation with one and two abutments on set head correspondingly. The groove center lines coinciding with the line of main row rivet axes. Holes in the mating part were drilled up to diameter of 4.1 mm on the groove axis flush to the edge and in its center for installation of rivets having single or two abutments on set head accordingly.

Specimens of overlapping joint comprise two sheets made of material Д16АТВл2, interconnected with rivets of АНУ 0300-4-9 grade, located in five rows for basic (first) variant of their execution (1.1, 2.1 in Fig. 6.3). On the edge of overlapping of specimens of the second and third variants of execution the additional stepped rivets having single abutment (1.3, 2.3 in Fig. 6.10) and with two abutments and two parallel flats (1.4, 2.4 in Fig. 6.10) on set head were installed accordingly.

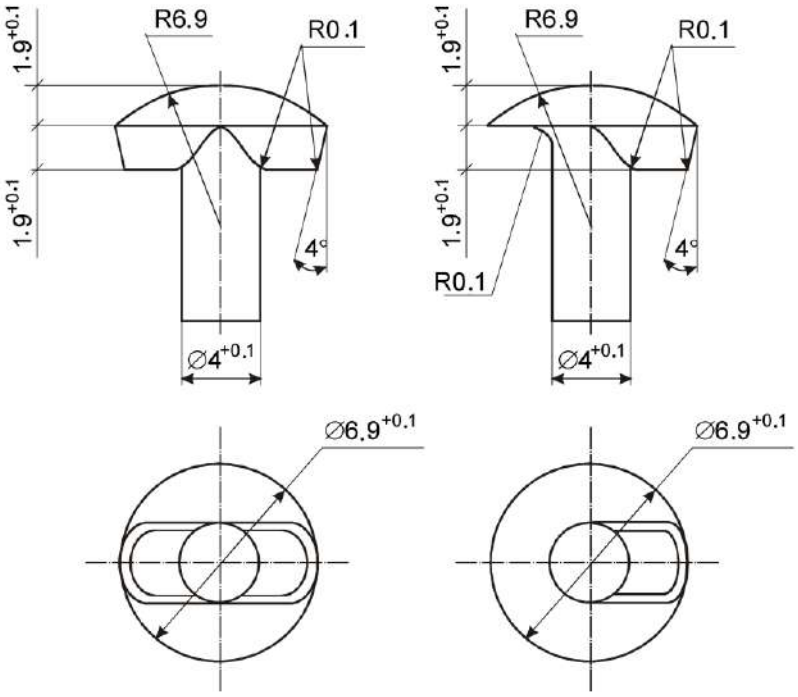

Fig. 6.9. Special rivets of pre-production batch with convex-plane head and two (one) lugs

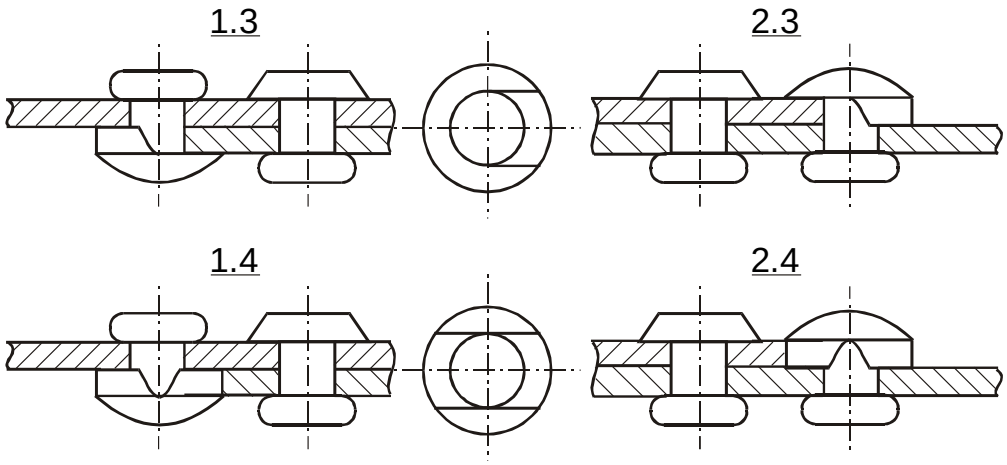

Fig. 6.10. Variants of execution of
five-row overlapping riveted joint specimens

Fatigue tests were carried out at three loading levels with maximum cyclic loading P_{max}=2350, 1960 and 1570 daN. Test results are represented in Fig. 6.11.

Analysis of results shows that installation of additional rows of stepped rivets at the overlapping edge increases the fatigue durability of five-row riveted joints in 2.3...2.4 times on average when installing rivets with two parallel flats and two abutments on set head, and increases the fatigue durability in 1.4...2.5 times when installing rivets with one abutment on set head in comparison with the fatigue durability of specimens without additional rivets.

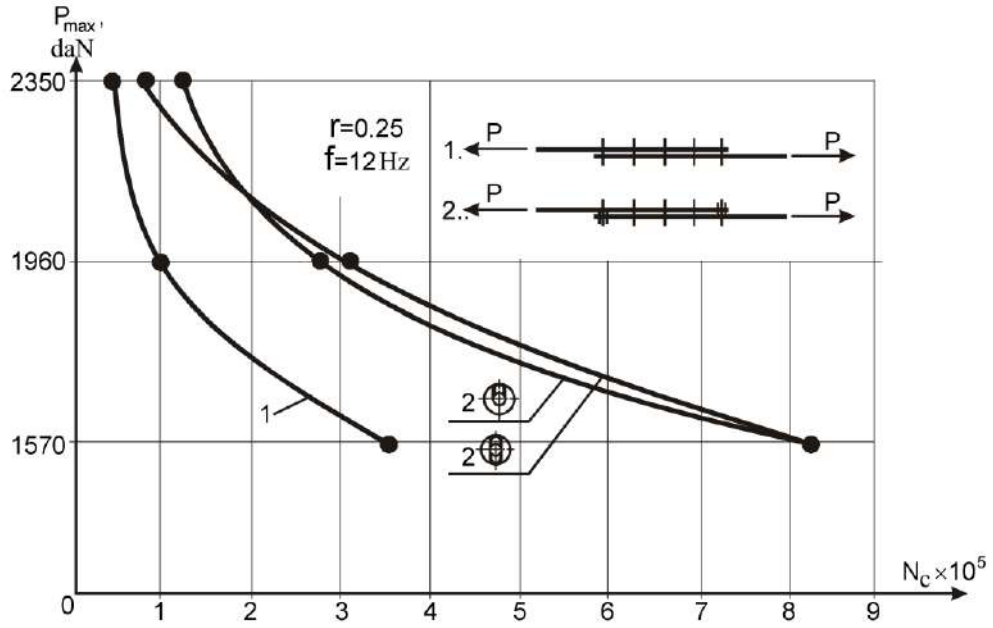

Fig. 6.11. Fatigue test results of five-row riveted joint specimens
with installation of additional stepped rivet rows on overlapping edge

6.1.4. Influence of Additional Row of Fasteners on Fatigue Durability of Joints Having Operating Time

While detecting the zones with low fatigue durability in single-shear joints it is reasonable to modify them by means of installation of additional row of fasteners at the overlapping edge.

Analysis of influence of installing the additional row of fasteners on joint fatigue durability having operating time was made on specimens in five-row overlapped riveted joint. Joints of parts made of Д16АТВл2 material were made using АНУ 0300-4-9 rivets (Fig. 6.12).

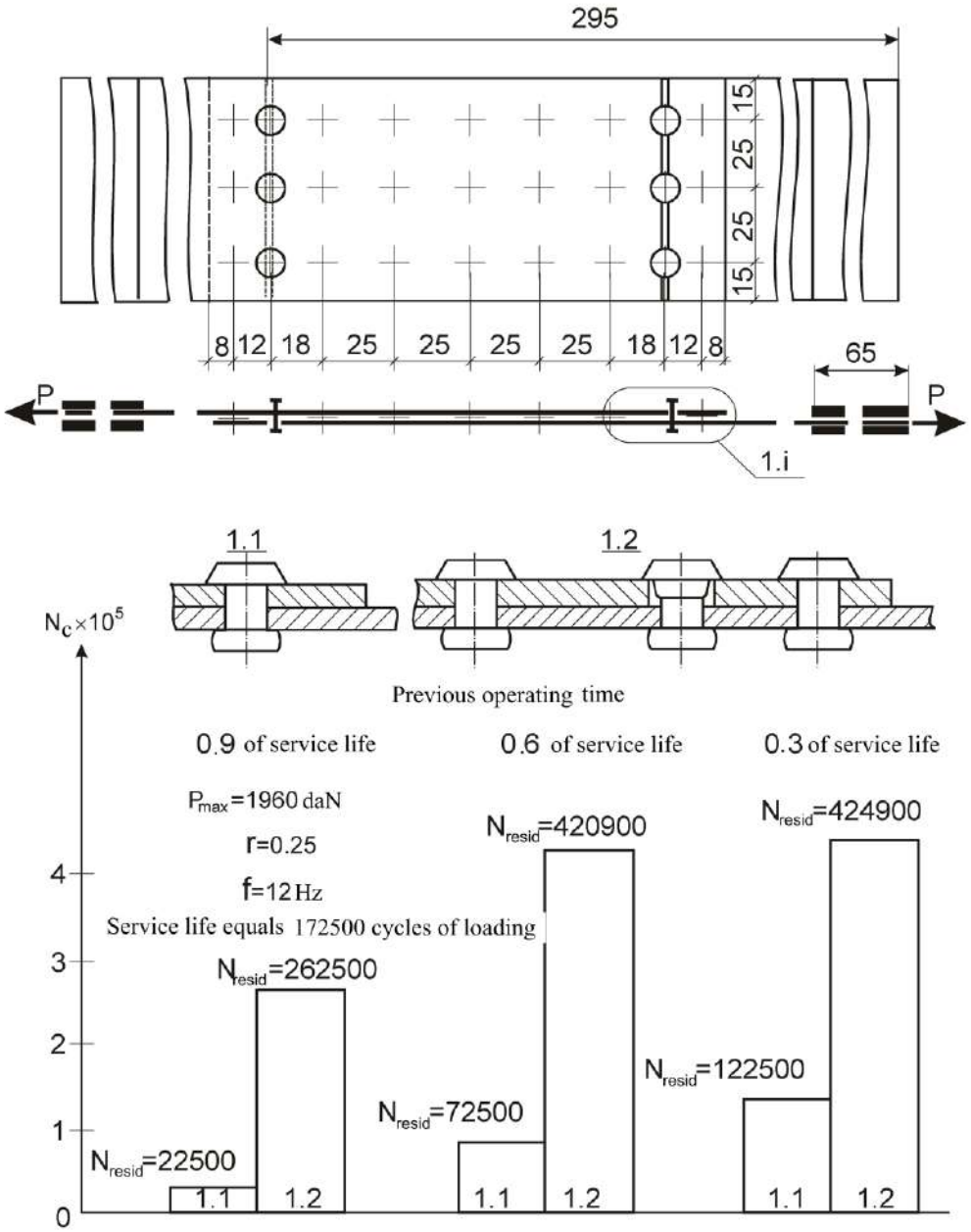

Fig. 6.12. Influence of additional row of fasteners installed on overlapping edge on fatigue durability of single-shear joints having operating time

To clarify influence of the additional row of fasteners and riveted technological strap on joint fatigue durability having operating time, the specimens with full fatigue durability under maximum load in cycle equal to 172500 on average, were tested in 50000, 100000 and 150000 cycles, that is, have an operating time equal to 0.3, 0.6, 0.9 of the joint service life accordingly. After such operating time at the overlapping edge the technological strap having 20 mm in thickness equal to thickness of the part forming the overlapping edge was riveted to the sheet. At joint of the technological strap and the part forming the overlapping edge the additional row of rivets АНУ 0300-4-9 was installed with clearance on joint and radial interference in other part to be joined 1.2 (See Fig. 6.12). The clearance was provided by drilling the parts to be joined at the place of joint with 5 mm in diameter drill. Drilling depth was set by means of drill limiting stop.

To clarify influence of the additional row of fasteners and riveted technological strap on joint fatigue durability having operating time, the specimens with full fatigue durability under maximum load in cycle equal to 172500 in average, were tested in 50000, 100000 and 150000 cycles, that is, have an operating time equal to 0.3, 0.6, 0.9 of the joint service life accordingly. After such operating time at the overlapping edge the technological strap having 20 mm in thickness equal to thickness of part forming the overlapping edge was riveted to the sheet. At joint of the technological strap and part forming the overlapping edge the additional row of rivets АНУ 0300-4-9 was installed with clearance on joint and radial interference in other part 1.2 to be joined (See Fig. 6.12). The clearance was provided by drilling parts to be joined at place of joint with 5 mm in diameter drill. Depth of drilling was set by means of drill limiting stop.

After assembling the joint the fatigue tests of specimens were continued at the previous level of cyclic load.

Fatigue test results on determination of the specimen residual durability of five-row overlapped riveted joints having operating time equal to 0.3, 0.6, 0.9 of service life are shown in Fig. 6.12.

Analysis of specimen fatigue test results of five-row overlapped riveted joints having operating time equal to 0.3, 0.6, 0.9 of service life has revealed that when installing the additional row of fasteners on the overlapping edge with riveted technological strap, their residual durability increases in average in 3.5, 5.8 and 11.7 times accordingly in comparison with durability of specimens tested without method increasing their residual durability.

6.1.5. Analysis of unloading efficiency from utmost rows of multi-row single-shear overlapped specimens, and also skin-to-stringer tip joints

Tests proved that installation of fasteners in the utmost rows with clearance in the part forming the overlapping edge, their fatigue durability increases on average as follows:

– in 1.5…6.0 times for five-row overlapped joints;
– in 2.2…3.0 times for three-row joints on strap;
– in 2.3 times for four-row overlapped joints and in 1.9 times if countersunk rivets are used;
– in 2.6…4.2 times for four-row joints with strap;
– in 1.2…1.9 for four-row overlapped joints with strap, in which rivets of the utmost rows were installed with clearance next the nearest rivets;
– in 5.9…31.6 times for skin-to-stringer joint in comparison with fatigue durability of joints without loads applied to their utmost rows.

Fatigue tests were performed for joint specimens, in which the utmost rows were installed with clearance in the part forming the overlapping edge assembled with primer УЗОМЭС-5 applied to joined surfaces, anodized "НХ" and coated with primer ФЛ-086, and also specimens assembled of parts in state of delivery. It was shown that while making clearances between rivet shanks and hole walls in the part forming the overlapping edge, the joint fatigue durability increases in average in 1.7…6.7 times with the availability of used coatings.

Installation of additional rows of fasteners at the overlapping edge of single-shear joints, which involve tips of parts to be joined into taking bending moment and not working in shear, increases fatigue durability as follows:

– overlapped riveted joints – in 2.3...3 times in average;
– skin-to-tip stringer joints – in average in 3.9…4.8 times in comparison with joint fatigue durability without additional fasteners.

It was proved that installation of additional fasteners at the overlapping edge of joints having operating time 0.3, 0.6, 0.9 of service life with technological strap under the rivet head increases the joint residual durability in average on 3.5, 5.8 and 11.7 times accordingly.

The technology of joint manufacture has been developed and approved for joints, in which the utmost rows are installed with clearance in the part forming the overlapping edge and joints with additional rows of fasteners using rivets with stepped set head, and also standard fasteners, tools and equipment used in industry.

6.2. RIVETS FOR LONG-LIFE COUNTERSUNK RIVETED JOINTS

Countersunk rivets are widely used while assembling thin-wall aircraft structures.

There are known rivets consisting of cylindrical shank, tapered set head and compensator in the form of concentric protrusions and pits at the end of the set head or in the form of truncated cone coaxial with the rivet shank leaning against the set head butt with the larger base, diameter of which equals the shank diameter, in the form of cylinder having diameter equal to the rivet diameter, coaxial with the rivet shank and located on the set head butt.

There is known rivet comprising a shank and a countersunk set head consisting of a tapered portion adjacent to the shank and cylindrical portion located above with

compensator on the butt in the form of concentric protrusions having different depth and pits with different depth.

As it was said above this rivet possesses low manufacturability index. For its manufacturing by upset process it is necessary to have a punch with specially profiled working surface according to the compensator shape. Because of the fact the compensator is formed in punch and the rest portion of a set head is formed in the die then high quality of the rivet could not be ensured because in practice working equipment is misaligned in upsetting machines. That is why such defect as compensator displacement with respect to the shank axis while upsetting is known. Moreover features of contact of flat butt of rivet billet and punch profiled surface may cause eccentric compression of billet accompanied, as a rule, with its longitudinal bend. As a result, plastic deformation of billet is asymmetric, metal excessively flows into the space between the punch and die forming non-standardized burr, but cavities intended for compensator and set head remain partially unfilled. Thus accuracy of specified shape and dimensions of compensator and set head of the analyzed rivet while upsetting is low, that makes worse joint reliability made with such rivets, in particular, their tightness and fatigue durability could not be assured. The compensator structure also adversely affects the joint reliability. Thus, shape and dimensions of compensator of the analyzed rivet (or its analogues) are such that plastic deformation of the rivet shank and compensator begins practically simultaneously. The further upsetting process is unstable and in case of eccentric application of riveting force, a defect in the form of displacement of the set head with respect to rivet shank appears and worsens joint quality and reliability.

Development of new design of rivet is directed as to enhance manufacturability and quality of rivets obtained by upsetting that is reached by possibility to form compensator in die using punch with flat working surface as to enhance quality and reliability of riveted joint due to the fact the shape and dimensions of the set head and rivet compensator are stable and correspond to specified values with high accuracy.

Such technical result is reached in the way that rivet comprising shank and set head in the form of truncated circular cone adjacent to shank with its smaller base and cylinder interfaced with the cone of larger base and located at the compensator butt, the latter is made in the form of circular right cylinder, in which diameter equals diameter of countersunk set head.

Execution of compensator as an integral part of cylindrical portion of the set head ensures possibility to manufacture rivet by upsetting under minimal costs of working tools, because it is sufficient to use an ordinary punch with flat working surface, as rivet is fully formed in die without difficulty. With that misalignment of die and punch in the upsetting machine does not affect on accuracy of given parameters of the countersunk set head and punch. Moreover, rivet billet upset with flat punch under conditions of eccentric compression possesses higher longitudinal stability, which also improves rivet quality because the process of plastic

deformation is close as much as possible to axially symmetric. Therefore, proposed design of rivet allows simplifying its production technology by upsetting and enhancing quality due to high precision of parameters. All said above proves high manufacturability of developed rivet with compensator.

Assembling the parts using rivets with small errors of shape, mutual position of surfaces and dimensions of its set head ensures filling enlarged hole with rivet material installed with radial interference that increases reliability and quality of riveted joint, in particular, joint tightness and fatigue durability.

Fig. 6.13 represents overall view of the rivet, Fig. 6.14 represents the rivet put into a hole made in pack of parts, Fig. 6.15 shows joint of parts.

Rivet comprises shank 1 and countersunk set head 2 consisting of tapered portion 3 and interfaced cylindrical portion 4 with compensator 5 on the butt. Structural parameters of rivets having various diameters, normal and shortened depth of countersunk heads were chosen using the CAD/CAM/CAE UNIGRAPHICS system.

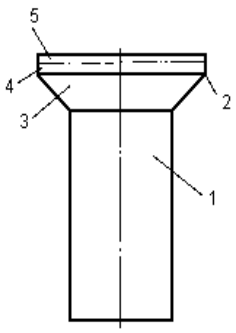

Fig. 6.13
Overall view of rivet

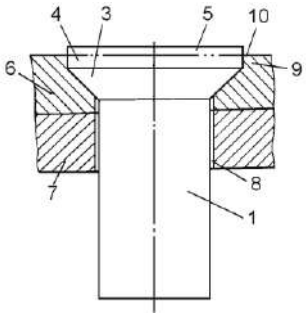

Fig. 6.14
Rivet put into a hole made in pack of parts

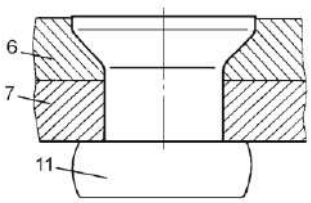

Fig. 6.15
Joint of parts

Riveted joint of the parts is made as follows.

In the pack consisting of parts 6 and 7 hole 8 is made, in which socket 9 for rivet countersunk set head 2 is made. Distinguishing feature of socket 9 is presence of cylindrical portion 10 in it, corresponding to cylindrical portion 4 of countersunk set head 2, diameter of which equals the diameter of the socket cylindrical portion or is 0.05...0.1 mm lager. Rivet is put in hole 8, in so doing portions 3 and 4 of set head 2 fill socket 9, and compensator 5 extends over the surface of part 6. After that shank 1 and countersunk set head 2 of the rivet are subjected to plastic deformation by pressing or shock, as a result hole 8 and socket 9 are filled and closing head 11 is formed.

As real parameters of the rivet are stable and correspond to the given values with high precision, then before riveting clearances between shank 1 and hole walls 8, and also between cylindrical portion 4 and mating cylindrical portion 10

of socket 9 are minimal and their values vary in fact within tolerances of hole 8 and socket 9 . That is why the radial interference in joint is realized along the entire pack width while riveting with high reliability, including cylindrical portion of socket 9 that enhances riveted joint quality, in particular, its tightness and fatigue durability.

6.2.1. Design of new countersunk rivets with cylindrical compensator

After riveting to ensure quality of the outer surface (extension of rivet set head after riveting should not exceed 0.05 mm) the excessive compensator of the set head is milled that increases labor inputs of assembly works and worsens quality of skin surface and panels in the form of local cuts deteriorating corrosion protection and creating additional stress concentrators on skin surface in the zone of rivet set head location.

To eliminate such disadvantages the design of countersunk rivets with cylindrical compensator has been developed (Fig. 6.16), in which the compensator was chosen so that after riveting the set heads should not be milled, and the countersunk sockets for rivets have also cylindrical portion corresponding to the cylindrical portion of the rivet countersunk head.

The distinguishing feature of modern aircraft manufacturing is wide use of thin skins in airframe unit structures. For example, fuselage skin of the AN-140 passenger aircraft has thickness of (0.3…0.4)d, where d – diameter of rivet shank, connecting skin to airframe members and between themselves.

Decreasing the skin thickness created problem in ensuring quality of countersunk riveted joints, because available advanced long-life fasteners for countersunk riveting have depth of set head equal to 0.4d. Therefore, application of ordinary technology of countersunk riveting inevitably causes countersinking in skin and, as a result, a defect in joint known as “sharp knife”. Such joints are unacceptable for modern aircraft structures due to very low characteristics of fatigue resistance and tightness.

The majority of the aircraft production companies solve such a problem applying rivets with shortened depth of countersunk set head and compensator. Shape of such rivets is similar to the rivet shape with normal depth of countersunk set head, and depth is decreased by decreasing the diameter of the set head or increasing its angle. Also such technical solutions are possible; in particular one of them is applied at the ANTONOV ASTC.

It lies in the following. Rivets with standard depth of the countersunk set head of 0.4d are used, but sockets for heads made in skin are of the decreased depth equal to 0.25d approximately. After riveting the portions of the set heads excessively extending beyond the skin surface are eliminated mechanically, for example, by milling.

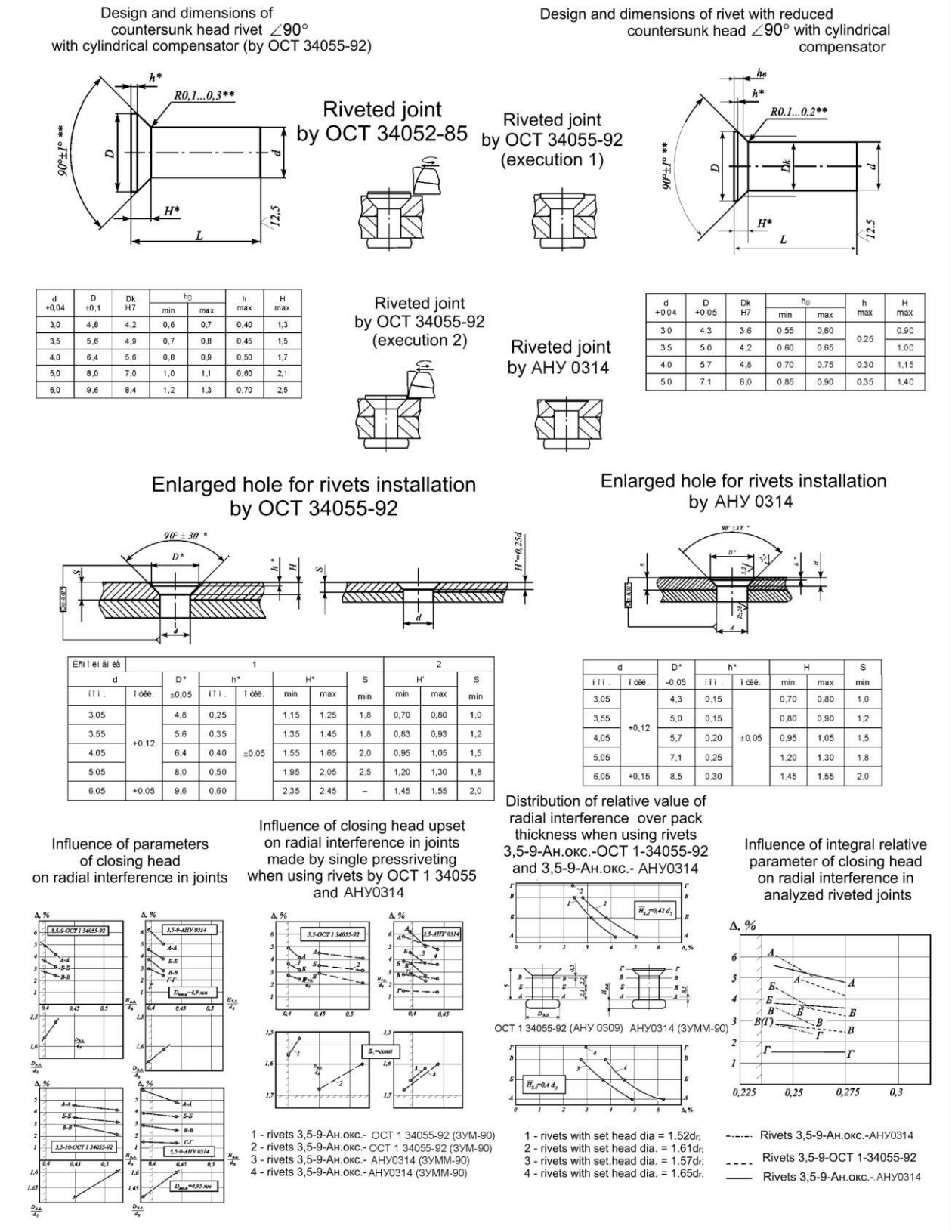

d +0,04	D ±0,1	Dk H7	h min	h max	h max	H max
3,0	4,8	4,2	0,6	0,7	0,40	1,3
3,5	5,6	4,9	0,7	0,8	0,45	1,5
4,0	6,4	5,6	0,8	0,9	0,50	1,7
5,0	8,0	7,0	1,0	1,1	0,60	2,1
6,0	9,6	8,4	1,2	1,3	0,70	2,5

d +0,04	D +0,05	Dk H7	h min	h max	h max	H max
3,0	4,3	3,6	0,55	0,60	0,25	0,90
3,5	5,0	4,2	0,60	0,65		1,00
4,0	5,7	4,8	0,70	0,75	0,30	1,15
5,0	7,1	6,0	0,85	0,90	0,35	1,40

Ëñíîâíîé	1							2		
d		D*	h*		H*		S	H'		S
íîì.	íóìèí.	±0,05	íîì.	íóìèí.	min	max	min	min	max	min
3,05	+0,12	4,8	0,25	±0,05	1,15	1,25	1,8	0,70	0,80	1,0
3,55		5,6	0,35		1,35	1,45	1,8	0,83	0,93	1,2
4,05		6,4	0,40		1,55	1,65	2,0	0,95	1,05	1,5
5,05		8,0	0,50		1,95	2,05	2,5	1,20	1,30	1,8
6,05	+0,05	9,6	0,60		2,35	2,45	–	1,45	1,55	2,0

d		D*	h*		H		S
íîì.	íóìèí.	-0,05	íîì.	íóìèí.	min	max	min
3,05	+0,12	4,3	0,15	±0,05	0,70	0,80	1,0
3,55		5,0	0,15		0,80	0,90	1,2
4,05		5,7	0,20		0,95	1,05	1,5
5,05		7,1	0,25		1,20	1,30	1,8
6,05	+0,15	8,5	0,30		1,45	1,55	2,0

Fig. 6.16. Design of new countersunk rivets with cylindrical compensator

Considered structurally-technological solutions are widely used in manufacturing, but they could not be classified as long-life for thin packs. This is because of the early concept of creating long-life countersunk riveted joints according to which the rivet set head must contain excessive volume of material in the form of compensator. While riveting the compensator penetrates the pack so the parts to be joined are hardened along the hole surface, especially on the portion of the enlarged socket.

As at that time application of thin skin in the units was limited, then development of design of countersunk rivets with compensator was performed for medium and thick packs. The following rule has been developed: the more radial interference in joint, the higher its fatigue durability. This was the reason why rivets were taken for manufacturing, available compensator of which volume tenfold exceeds the required amount. In this case quality of the outer surface of the riveted structures was forcedly ensured by additional laborious operations of milling the set heads after riveting and their corrosion protection. But goal set to increase service life justifies the means to achieve it.

When thin-wall structures found wide use in aircraft manufacturing, then the solution was made to standardize existing countersunk rivets, which were obtained by method of similarity. Their main distinguishing feature was the shortened depth of the set head. Other specialists fighting for the idea of unifying aircraft manufacturing just modified joints by means of decreasing the countersinking socket depth for countersunk rivet set heads. But these solutions were proposed and later on introduced without taking into account one distinguishing feature of thin skin – inclination to warping in the form of contraction or buckling in the zones around fasteners. Such residual deformations greatly exceed specified values when there is large clearance between skin surface and set surface while joining the parts.

Analyzing existing solutions it is easy to see that applicable riveted joints form contractions and buckling under condition that such clearance is present. That is why riveted structures of thin skin are named as “quilt or “quilting”. Such phenomenon not only worsens quality of the outer surface but adversely affects its reliability because occurring residual deformations and tensile stresses reduce fatigue durability of the countersunk riveted joints.

Everything said above proves that problem of development of long-life countersunk riveted joints of thin skins is still actual. There are several directions for search and investigation:

1) development of new design of countersunk-headed rivets;

2) development of new methods of riveting;

3) rework of existing technologies of countersunk riveted joints of thin skins.

Accumulated experience of investigation performed in “KhAI” together with leading specialists of ANTONOV ASTC, KSAMC, KiAPO, «Tupolev» ASTC, TAPO, TsAGI, UkrNIIAT and others allows developing the technology for long-

life countersunk riveted joints of thin skins while keeping other important factors of quality and reliability.

The solution includes application of the new rivet design having smaller set head ∠90° with cylindrical compensator and method of riveting. Rivet for thin skins was designed on the basis of principles and recommendations given in technical publications. Design and dimensions of the rivet made of B65 alloy were the base for development of АНУ 0314 ANTONOV ASTC standard. shape and dimensions of the enlarged socket for set head of the newly designed rivet were developed (АНУ 0502 plant standard) also. Method of riveting and other features of making joints are represented in Production Manual No. 140 ТИ 36-30-96.

Design of the socket, rivet (See Fig. 6.16) and joint production technology must ensure specified extension of the rivet set head beyond the socket before and after riveting required radial interference and its distribution along the pack thickness, given durability level and tightness of joints using developed rivet during operation. It is necessary to note that rivet is inserted with interference over the countersunk cylindrical portion, that greatly assists in getting required interference after riveting.

Complex of scientific-research works including analyzing radial interference, static strength, durability and tightness of joints together with developed rivets has been performed.

While analyzing static strength the pulling and shearing tests were performed under static loading. Static strength of the specimen was determined in the way of its continuous loading up to failure. To provide sufficient (mean) accuracy of results no less than three specimens of each kind of being investigated riveted joints were tested.

The specimen plate blanks were made out of sheets of aluminum alloy Д16АТ, which were anodized «НХ» under conditions ensured by the KSAMC.

The holes for rivets were drilled by the special machine. Two-stage drill having nominal diameter of the second stage equal to 3.05 mm applied in batch production at KSAMC was used for drilling the holes.

Holes for set heads of rivets ОСТ 1 34055-92 were made with core drills having diameter of the working section equal to 4.8 mm, and for rivets АНУ 0314 with the core drills having the diameter of the working section equal to 4.15 mm were used.

The specimens were loaded with machine ZD-10. All tested specimens with heads working in separation and shear were broken due to change of the shape of the rivet set heads.

Analysis of the static test results of the rivet operation in separation has shown that static strength of joints made with rivets ОСТ 1 34055-92, inserted in the holes with reduced depth of countersinking and joints made with rivets АНУ 0314 of 3 mm in diameter are practically equal. Squeezing force of sheets while operation of

joints with rivets АНУ 0314 and ОСТ 1 34055-92, working in shear lies within range of squeezing force for sheets with rivets ЗУ-120 and ЗУ-90 (Refer to: Reference Data and Design Procedures of Static Strength. Riveted Joint Design: 002.МР-74; К.: КМЗ, 1974. – 149 р.)

Analysis of static test results of rivets working in shear has shown that static strength of joints with rivets АНУ 0314 installed according to the developed technology is 1.07 times higher than the static strength of joints with rivets ОСТ 1 34055-92 installed according to the technology specified in ТИ 36-21-86.

One of the comparative tests of riveted joints performed to estimate efficiency of applied rivets or riveting technology are the unriveting tests, in which the fits realized in the joints are monitored especially with presence or absence of interference.

Such tests are performed according to the known procedure of measuring geometrical parameters of holes before riveting and upset rivets taken out of stack as it is specified in Branch Standard ОСТ 1 34041-79.

Values and distribution of radial interference were analyzed on technological specimens of the riveted joints with rivets 3,5-9(10)-Ан.Окс-ОСТ 1 34055-92 made according to the technology of riveting thin skins in the "AN" articles according to Production Manual ТИ 36-21-86, and also with rivets 3,5-9-Ан.Окс-АНУ 0314 according to the developed technology.

Traditionally in the "AN" articles the countersunk rivets having standard depth of set head equal to ($0.4d_r$) are used. In thin skin the holes for set heads of such rivets are made of reduced depth equal to about $0.25d_r$, here d_r – rivet shank diameter, and after riveting the set heads are milled. As a result structural-technological parameters of the realized joints greatly change that affects adversely the joint quality. When rivets with crown-shaped compensator by ОСТ 1 34052-85 and rivets with cylindrical compensator by ОСТ 1 34055-92 are used, then it is necessary for high-quality and reliable joint to ensure that socket for countersunk rivet head would have a cylindrical portion. But existing technology of riveting thin skins realizes joints without cylindrical portion in the zone of the countersunk socket. Such joints differ a little from joints made with standard countersunk rivets such as ЗУ-90°. Moreover the following consequence results from the reduced depth of the enlarged sockets in applicable joints such as less length of the rivet shank tail extended out of the hole, which is the part for creation of the closing head.

As a result, when pack thickness of the parts to be joined is close to ($(1...1.5)d_r$), then it is impossible to increase the degree of the closing head upsetting to the value of its diameter exceeding $1.6d_r$, because in that case the depth realized is less than minimal allowable value equal to $0.4d_r$.

To widen the technological capabilities of the assembly process the specialists have to use the rivets with more length that reduces mass efficiency of the riveted joints. To estimate the influence of such solution onto the radial

interference the following two versions of the base technology of the single impact riveting were analyzed: with rivets 3,5-9-Ан.Окс-ОСТ 1 34055-92 and rivets 3,5-10-Ан.Окс-ОСТ 1 34055-92.

The distinguishing feature of the developed riveting technology of thin skins is the application of rivets with decreased countersunk set head ∠90° having cylindrical compensator according to Plant Standard АНУ 0314 and performing enlarged sockets in the holes with tool, in which nominal diameter of the cylindrical cutting portion is less than that of the rivet set head. Graphical interpretation of obtained results is shown in Fig. 6.16.

Newly designed joints were approved for technological specimens made and tested under laboratory conditions in KhAI. As the basic version the thin skin riveting technology was accepted used at the ANTONOV ASTC. In particular, rivets complying with OCT 1 34055-92, used in the AN-140 aircraft airframe were tested. It was determined that radial interference in joints with rivets complying with АНУ 0314 exceeds interference in joints complying with OCT 1 34055-92.

In aircraft manufacturing great experience is accumulated in determining the fatigue strength characteristics of mechanical joints. While developing newly designed rivets or new technological processes of riveted joints the Branch Standard OCT 1 00872-77 prescribes comparative fatigue tests, which should be performed using laboratory technological specimens of the base and proposed solutions (riveted joints used while assembling thin skins of the AN articles, for example AN-140, are accepted as basic version).

Tests concerning determination of durability of the riveted joint specimens with rivets complying with АНУ 0314 (ЗУММ-90°) and with OCT 1 34055-92 were conducted under their regular tensile loading with frequency of 40 Hz to the specimen breaking using testing machine УРМ-2000.

The fatigue strength of the standard specimens of shear joints (complying with 2-OCT 1 00872-77) and specimens with filled unloaded holes were analyzed.

Blanks of the technological specimens were made of Д16АТ material as anodized sheet in 1.2 mm thickness.

The 3.5 mm in diameter and 7 mm in length rivets were used.

Joints were made by single press riveting method with pack being prepressed with the КП-204М press.

Test results are represented in Fig. 6.17.

Analysis of the results shows that developed rivets АНУ 0314 with regard to fatigue durability criterion are not worse than basic rivets corresponding to OCT 1 34055-92 when inserting them into the sockets having smaller depth.

The specimens made for checking the interference over the joint height with rivets being in compliance with OCT 1 34055-92 and АНУ 0314 were used to check local tightness.

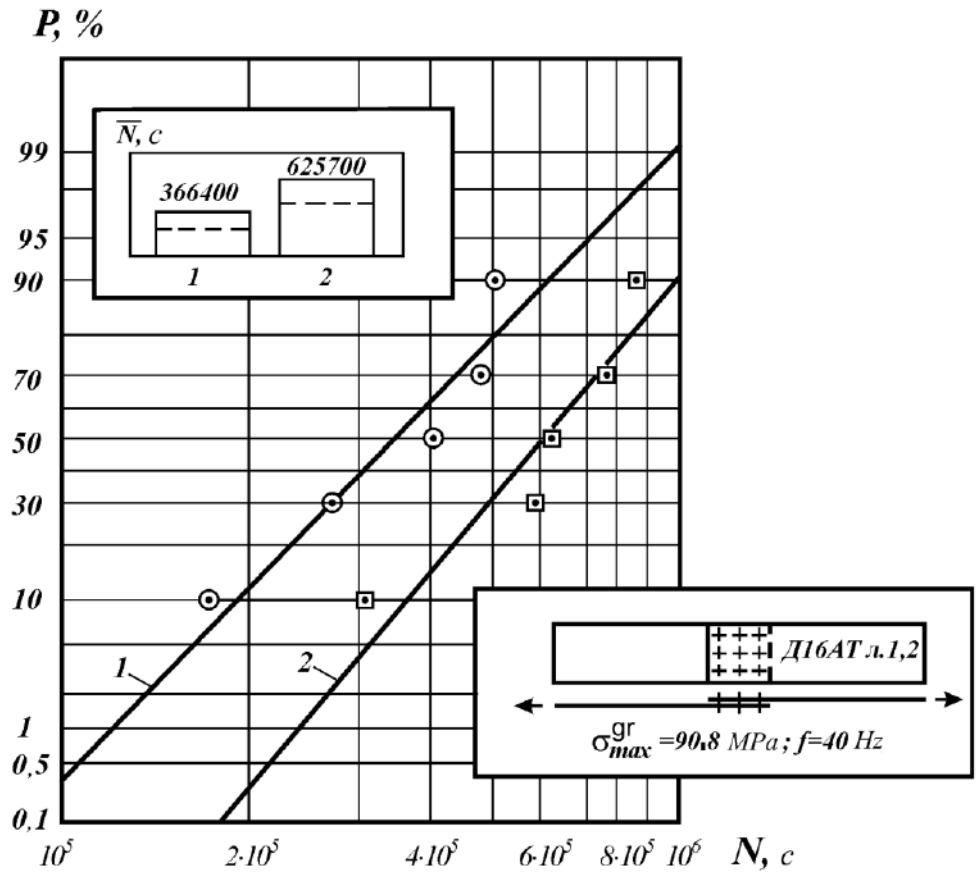

Fig. 6.17. Relations of lognormal distribution functions of fatigue crack life of single-shear riveted joint specimens of thin skins: 1 – rivet 3,5-7-Ан.Окс-by ОСТ 1 34055-92; 2 – rivet 3,5-7-Ан.Окс-by АНУ 0314

To analyze general tightness the temporary specimens in the form of plate made of sheet of material Д16АТл1.2 with straps made of material Д16АТл2 having dimensions of (18×20) mm «НХ» anodized according to batch production procedure were used in shop conditions of KSAMC.

While testing tightness within the kerosene medium the special device comprising bath, sealing gasket and system of pipes for kerosene delivery was made. Excessive pressure of (0.03 ±0.005) MPa [(0.3 ±0.05) kg/cm^2] was created by the compressor. The specimens were held for a half an hour in bath in kerosene, which contacted with rivets from the side of the set heads without excessive pressure. Then the specimens were loaded by the ЦД 10/90 machine with loads creating in the specimen cross-section the stepped variation of stress with step of 25 MPa in gross section having held the specimens under each load value for 3 minutes under excessive pressure of kerosene from the side of rivet set heads.

Kerosene leakage was detected by change of chalky coating applied before

tests from the side of the rivet set heads.

While testing rivets OCT 1 34055-92 the first case of leakage was registered under load of 1581 daN (250 MPa), leakage in the area of every rivet was detected under load of 1739 daN (275 MPa). While testing rivets АНУ 0314 the first case of leakage was detected under load of 1265 daN (200 MPa), leakage in the area of every rivet was registered under load of 1739 daN (275 MPa).

Analysis of leakage test results has shown that integrally tightness of joints made with rivets АНУ 0314 in fact equals to tightness of joints made with rivets ОСТ1 34055-92. But probability of penetration of aggressive medium from the side of the set heads of rivets ОСТ1 34055-92 when used for riveting thin-sheet skins is higher than of joints made with rivets АНУ 0314.

Comparing obtained results allows to make a conclusion that countersunk riveted joints of thin skins made according to new technology may be classified as long-life ones.

According to the primary joint quality criteria they are not worse than the most advanced riveted joints used in the branch of industry. But riveted joints with the rivets complying with АНУ 0314 have incontestable advantage. The skin outer surface quality is ensured directly while riveting without application of additional very laborious finishing operations. In this case required specifications are met not only in criterion of extension of the rivet countersunk set head beyond the skin but also in value of the skin contraction in the zones of the fastener points. “Quilt” effect is practically absent, and this creates good base for increasing competitive ability of the riveted structures of the thin skins.

6.3. Countersunk-head rivet with compensator and efficiency of its application in standard joints

At present countersunk riveted joints are made:

– with rivets having a set head in the form of tapered cone known as ЗУ rivets, for example, rivets conforming to Standard ОСТ 1 34087-80;
– rivets having compensator at the end of set head (ЗУКК, АНУ 0305, ЗУК, ЗУКМ, ЗУКС, ЗУГ, ЗУГБ);
– normal rivets and soft-collar rivets (ЗС, УЗ), riveted according to «ПЗГ» method.

Riveted joints with the ЗУ rivets are the most manufacturable, and distinguishing features of the set head allow manufacturing rivets by cold upsetting under minimal costs of working tools. The flat end of the set head, moreover, ensures rivet axial stability while its plastic deforming that, in its turn, allows excluding such defect as displacement of closing head with respect to shank under application of eccentric riveting force.

But the ЗУ rivets and joints based on them possess several essential disadvantages.

For example, while riveting the set head of the ЗУ rivet practically is not subject to plastic deformation. Radial interference in the joint is provided mainly with the upset shank tail material flowing into the hole that does not ensure high reliability of the joint, in particular, tightness and fatigue durability, especially for large and medium thickness of parts to be riveted.

As the set head of the ЗУ rivet is not subject to plastic deformation then values of the set head extension given in Specification of the article may be realized only in the way of the rivet selection.

It is difficult to realize such technology under conditions of the batch production. That is why while manufacturing the articles, on outer surface of which very high requirements are imposed and in case of installation of the ЗУ rivet, the rivet set heads are milled after riveting.

Rivets with compensator ensuring higher characteristics of tightness and fatigue resistance in comparison with the ЗУ rivets also require essential complication of joint technology, as in the case, for example, when soft-collar rivets or normal rivets are used.

There are the following disadvantages of the known rivets with compensator:

1) material volume of the compensator is excessive so that after riveting to ensure required quality of the skin outer surface it is necessary to perform additional laborious finishing operations, such as, milling set heads (Fig. 6.18) and restoring corrosion-resistant coating removed while milling;

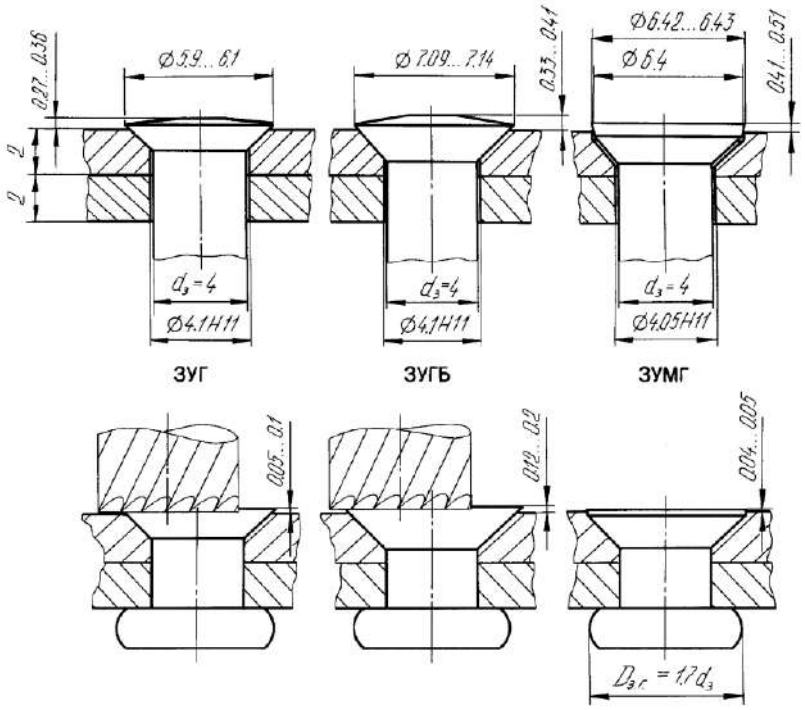

Fig. 6.18. Parameters of riveted joints with rivets conforming to Branch Standard ОСТ 1 34117-91 (ЗУГ(ZUG)), ЗУГБ (ZUGB) and ЗУМГ (ZUMG) having standard diameter of 4 mm

2) compensator parameters are such that plastic deformation of the rivet shank and its set head begins in practice simultaneously, as a result, upsetting process is sensitive to eccentricity of riveting force application (that frequently explains occurring defect in joints made with such rivets, which lies in displacement of the set head with respect to rivet shank);

3) while manufacturing rivets by means of cold upsetting the rivet compensator is formed in the punch cavity, and it is impossible to preclude misalignment of working tools, then the upsetting process is accompanied with such rivet defects as displacement of compensator with respect to rivet axis and improper shape of the set head, and also low accuracy of the given parameters of the set head, especially its diameter;

4) unriveting the known rivets with compensator in thin packs, as a rule, is accompanied with contraction of parts that worsens quality of the external surface and presents difficulties in milling set heads to the required value of their extension without skin damage.

To eliminate the abovementioned disadvantages the countersunk rivet with flat compensator in the form of truncated cone (Ref. Fig. 6.19) placed at the end of the rivet set head over its entire surface was developed.

In this case in joint before riveting the compensator is partially inserted into the socket for the set head, and the socket is made with a cylindrical portion. Rivets, primary structural parameters of which are represented in Fig. 6.19, are shortly named as ЗУМГ (rivet ЗУ modified tightness) (АНУ 310).

Processing technology of the ЗУМГ rivet upsetting with modified compensator 4 mm in diameter has been performed at the Taganrog Aviation Scientific Technical Complex (TASTC) and at the Kharkov State Aircraft Manufacturing Company (KSAMC). After upsetting the rivets were subject to heat treatment, tumbling and anodic oxidation. Processing technology of the rivet upsetting with the modified compensator proved reality and possibility of manufacturing the rivets with compensator in the form of truncated cone using existing equipment of the serial production.

Performed works have shown that while manufacturing the mounting for upsetting dies for the ЗУМГ rivets it is necessary to pay attention to metal quality, which is used for manufacturing mounting, because if there are defects in the material then possibility of spilling in the edge zone of the conical hole while the rivet upsetting exists due to higher impact loads in the indicated zone at the moment of filling the inset hole in the zone of its tapered portion with increased wire length used for formation of the rivet set head. When checking the rivet quality pay attention to presence of flash on the set head, which may appear if length of wire consumed for formation of the set head is excessive. In the presence of flash perform the check of the set heads for absence of flash after the tumbling operation.

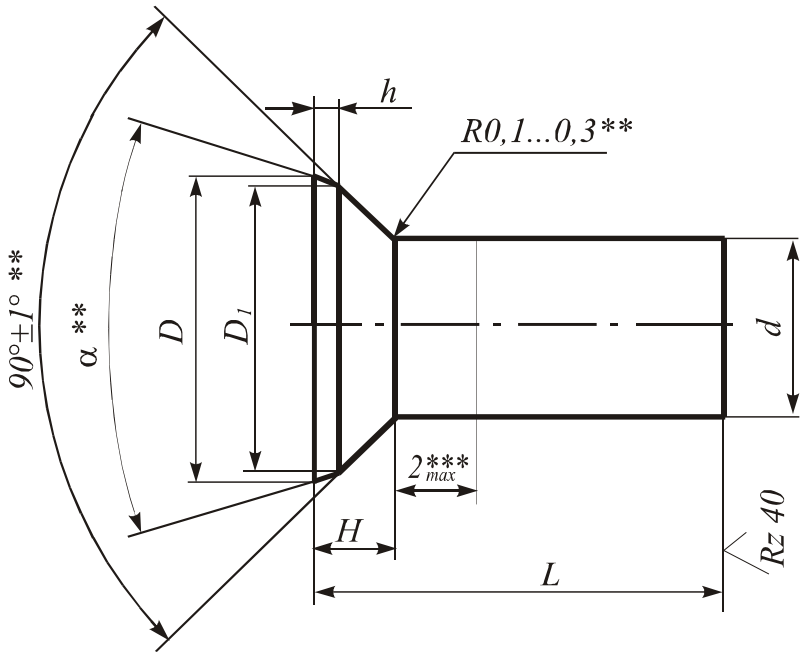

d	D_1		α	*D*		h	H
Extreme Deviation +0.05	Nominal Value	Extreme Deviation	Extreme Deviation +30'	Nominal Value	Extreme Deviation		Extreme Deviation –0.05
3.0	4.8	+0.05	14°	4.9	0.05	0.4	1.3
3.5	5.6		12° 30'	5.7		0.45	1.5
4.0	6.4		11° 30'	6.5		0.5	1.7
5.0	8.0		9° 30'	8.1		0.6	2.1
6.0	9.6	+0.06	8°	9.7	+0.06	0.7	2.5

Fig. 6.19. Design and Dimensions of Rivet ЗУМГ: * – reference dimension; ** – dimensions are ensured with tool; *** – for length of 2 mm it is allowed to increase shank diameter up to 0.04 mm for $d \leq 5$ mm and up to 0.06 mm for $d = 6$ mm

At KSAMC the batch of rivets having 4 mm in nominal diameter and 9 and 10 mm in length was upset. At TASTC three batches of rivets having 4 mm in nominal diameter and 9, 10 and 14 mm in length were upset.

Analyzing values and nature of the radial interference distribution over the pack thickness for joints made with countersunk rivets, specifically, rivets ЗУГ (complying with ОСТ 1 34117-91), ЗУГБ and ЗУМГ (modified rivets complying with ОСТ1 34087-80) for base riveting technology according to ТР 1.4.1220-83 and developed technology, was accomplished in compliance with the accepted measuring procedure of the unriveted rivet diameter taken out of the pack. As the

specimen technological plates for analysis the plates made of Д16АТп5 sheet 4.7…4.8 mm thick were used (Fig. 6.20).

Riveting was performed by press КП–204М. Diagram representing measurement of rivets after their extraction is shown in Figs 6.21 – 6.23. Measurements were accomplished with indicating gage in special device (Fig. 6.24).

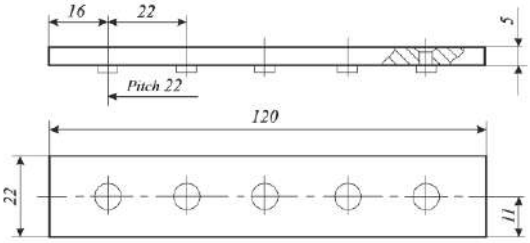

Fig. 6.20. Specimen for analyzing values of radial interference and local tightness in joint made in plate of Д16АТ alloy sheet having 5 mm in nominal thickness

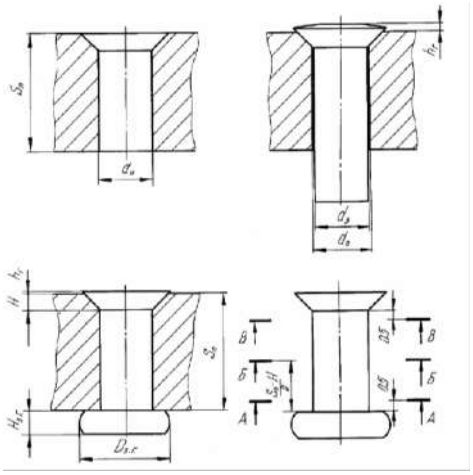

Fig.6.21. Diagram representing process of measuring joint parameters when ЗУГ rivets used

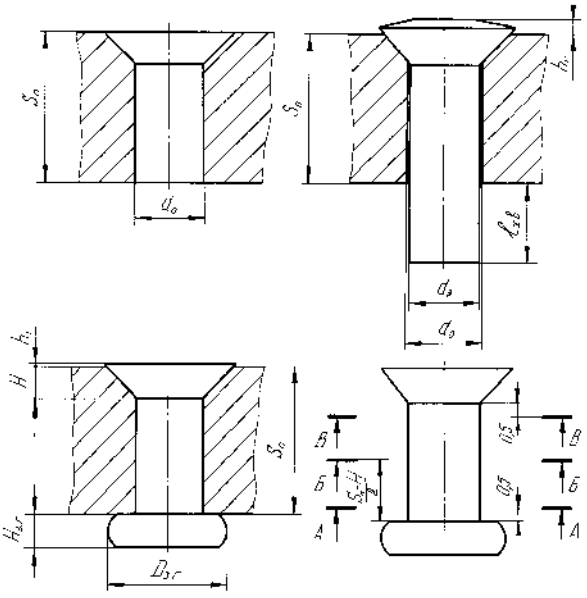

Fig. 6.22. Measuring joint parameters with rivets ЗУГБ

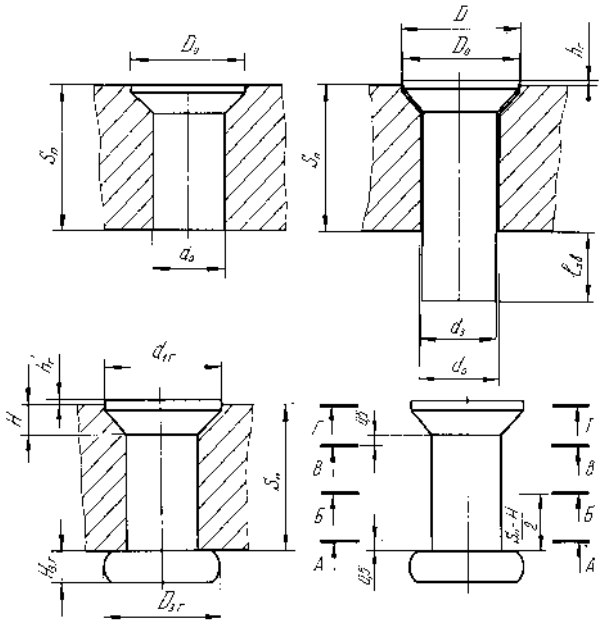

Fig. 6.23. Measuring joint parameters with rivets ЗУМГ

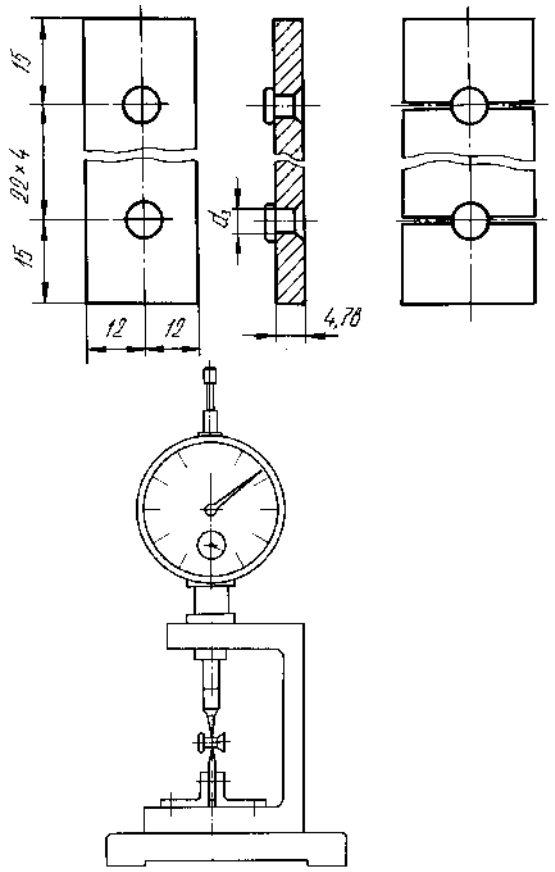

Fig. 6.24. Device used for measuring diameters of unriveted rivets

Value of radial interference (Δ) was determined by formula

$$\Delta = \frac{d_{ji} - d_0}{d_0} \cdot 100\%,$$

where d_{ji} – rivet diameter within the measured cross-section after unriveting and rivet separation from the pack, mm; d_0 – hole diameter in the pack before unriveting, mm.

Results of measuring the rivet parameters and parameters of joints before and after riveting, and also values of radial interference in the joints for analyzed combinations of their design-manufacturing parameters and riveting methods are represented in Fig. 6.25.

While analyzing the following was established: when using rivets ЗУМГ the radial interference is realized in joints, value of which is 2.3 times higher than interference value lengthwise the rivet shank complying with ОСТ1 34117-91 and 1.8 times higher interference value lengthwise the rivets ЗУГБ. Radial interference over depth of the cylindrical cap of the rivet ЗУМГ realized in such case equal from 1.9 to 2.7%*D* must assist to enhance durability and tightness of riveted joints with rivets ЗУМГ.

At present while manufacturing airframe different rivet designs with compensator for countersunk joints are used. Comparison of fatigue characteristics

of skin-to-stringer joints using such rivets shows that any known rivet possesses nearly the same efficiency. In this connection it is reasonable to perform comparative fatigue tests of joints with the developed rivets ЗУМГ and joints with known types of long-life countersunk rivets.

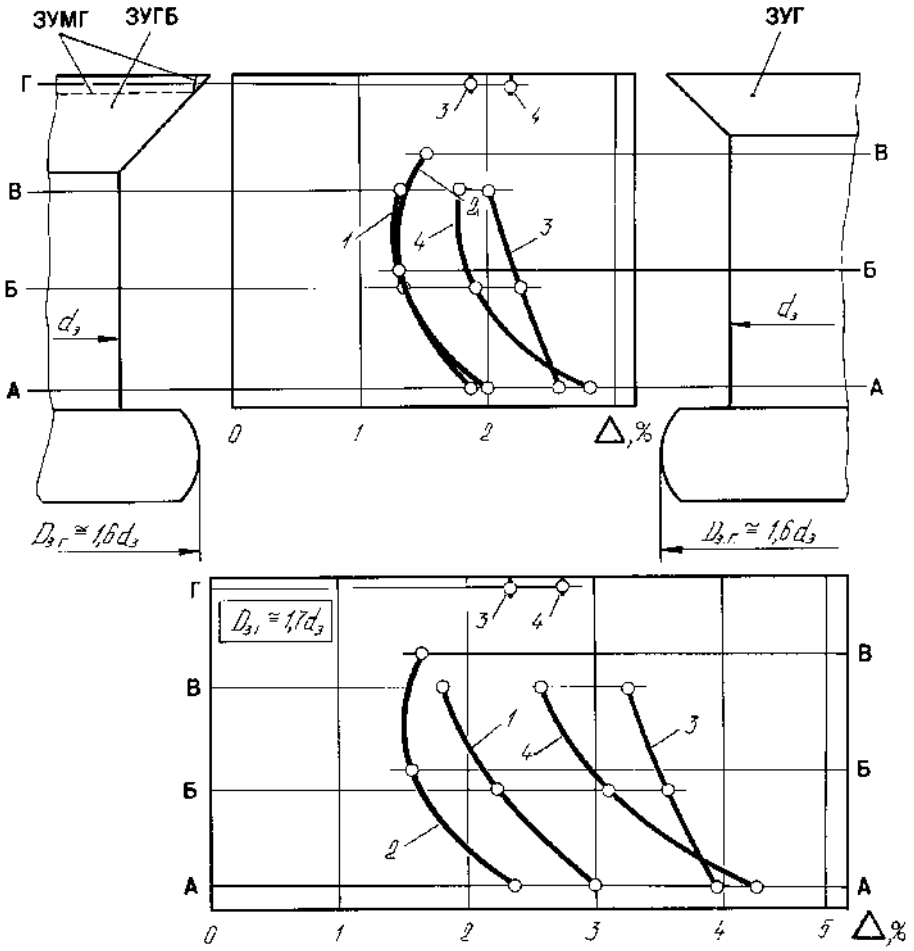

Fig. 6.25. Radial interference in countersunk riveted joints using rivets ЗУГ (ZUG) and ЗУГБ (ZUGB) according to technology as specified in ТР 1.4.1220-83 and rivets ЗУМГ (ZUMG) according to developed technology: 1 – rivets ЗУГБ (ZUGB), rivet hole diameter – 4.1H11 mm; 2 – rivets ЗУГ (ZUG)(ОСТ 1 34117-91), rivet hole diameter – 4.1H11 mm; 3 – rivets ЗУМГ (ZUMG) (KSAMC), rivet hole diameter – 4.1H11 mm; 4 – rivets ЗУМГ (ZUMG) (KSAMC), rivet hole diameter – 4.05H11 mm

As at the Taganrog Aviation Scientific Technical Complex while riveting the rivets complying with ОСТ1 34117-91 (ЗУГ) and ЗУГБ, then these rivets may be chosen as the basic ones for comparative fatigue tests.

To perform comparative fatigue tests of the countersunk riveted joints made in the way of single press riveting taking into account recommendations the temporary specimens were made according to ОСТ 1 00872-77 (Fig. 6.26), which model standard riveted joints of the aircraft structural members.

To analyze fatigue durability of plate specimens made of Д16АТл2 sheet with unloaded filled hole the following joints were made:

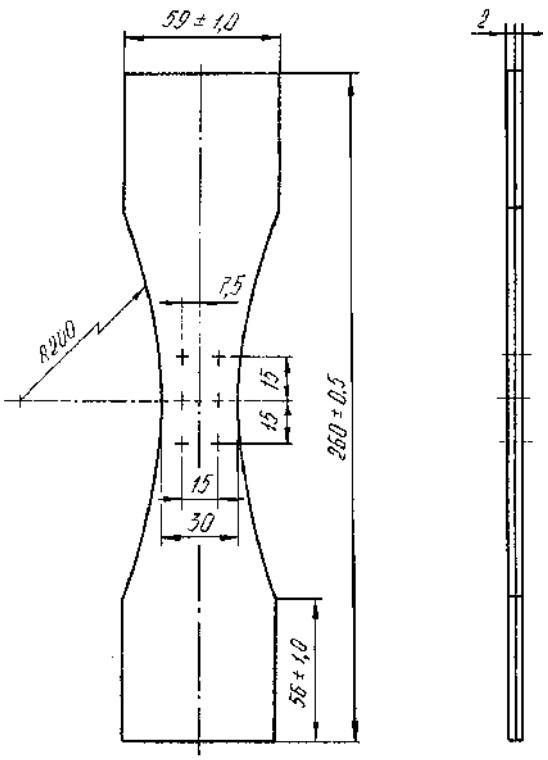

Fig. 6.26. Plate specimen with filled unloaded hole

– riveted joints using rivets 4-9-Ан.Окс-ОСТ1 34117-91 (ЗУГ), made in the way of single press riveting by press machine КП-204М along the travel ensuring diameter of the closing heads equal to 6.7...6.8 mm, depth of closing heads equal to $H_{c.h}$ = (1.75...1.8) mm and extension of the set heads after riveting h_{head} = (0.04...0.05) mm;
– riveted joints using rivets 4-9-Ан.Окс-ЗУГБ, made in the way of single press riveting by press machine КП-204М along the travel ensuring diameter of the closing heads equal to 6.7...6.8 mm, depth of closing heads equal to $H_{c.h}$ = (1.8...1.9) mm and extension of the set heads after riveting h_{head} = (0.06...0.07) mm;
– riveted joints using rivets 4-9-Ан.Окс-ЗУМГ made in the way of single press riveting by press machine КП-204М along the travel ensuring diameter of the closing heads equal to 6.7...6.8 mm, depth of closing heads equal to $H_{c.h}$ = (1.75...1.8) mm and extension of the set heads after riveting h_{head} = (0.04...0.05) мм.

Totally 15 specimens were made for fatigue testing the plates with filled unloaded hole (Ref. Fig. 6.26). Fatigue tests were performed by the machine УРМ-2000 at level of cyclic loading with maximum reduced zero-to-compression stress equal to 137 MPa and frequency of 40 Hz within the “gross” section. Fatigue test results statistically processed are represented in Fig. 6.27.

Analysis of the fatigue test results shown that cyclic durability of the plate specimens with filled unloaded hole when using rivets ЗУМГ practically equals the joints durability with rivets ОСТ1 34117-91 (ЗУГ) and increases in 1.46 times on average in comparison with the joints durability with rivets ЗУГБ made according to technology specified in ТР 1.4.1220-83.

To perform comparative fatigue tests of countersunk riveted joints made in the way of single press riveting, the temporary specimens were made (Fig. 6.28), which model standard shear riveted joints of the aircraft structural members.

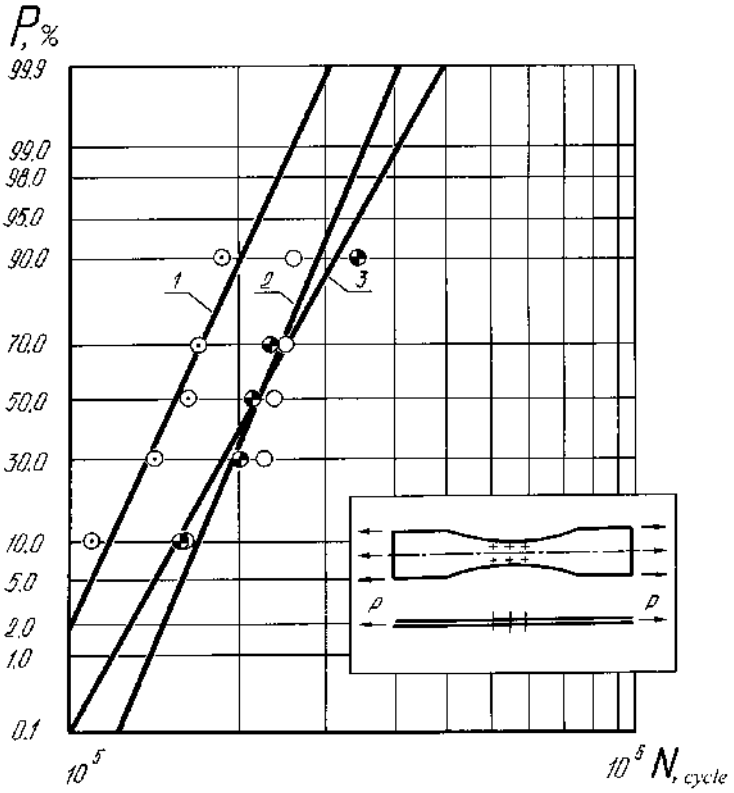

Fig. 6.27. Lognormal distribution functions of riveted joint specimens made according to technology applied for articles operated under corrosion environment conditions:

1 – ⊙ – Rivets 4-9-Ан.Окс-ЗУГБ (ZUGB);

2 – ○ – Rivets 4-9-Ан.Окс-ОСТ 1 34117-91 (ЗУГ (ZUG));

3 – ◓ – Rivets 4-9-Ан.Окс-ЗУМГ (ZUMG) (KSAMC)

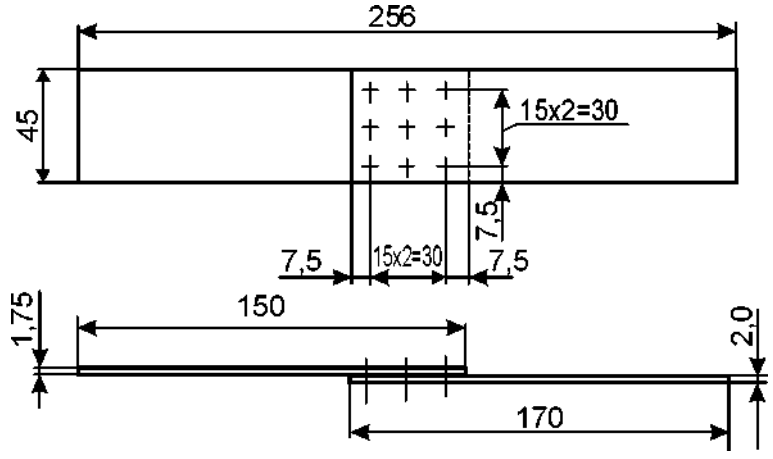

Fig. 6.28. Specimen of three-row overlapped riveted joint made of Д16чАТл2 sheet

To analyze fatigue durability of the plate specimens made of Д16АТл2 sheet with filled unloaded hole the following specimens were made:

– joints using rivets 4-9-Ан.Окс-ОСТ1 34117-91 (ЗУГ), made in the way of single press riveting on press machine КП-204М along travel ensuring diameter of closing heads equal to 6.7...6.8 mm, depth of closing heads equal to $H_{c.h}$ = (1.8…1.9) mm and extension of set heads after riveting h_h = (0.02...0.05) mm;
– joints using rivets 4-9-Ан.Окс-ЗУГБ, made in the way of single press riveting on press machine КП-204М along travel ensuring diameter of closing heads equal to 6.7...6.8 mm, depth of closing heads equal to $H_{c.h}$ = (1.9...1.95) mm and extension of set heads after riveting h_h = (0.08...0.12) mm;
– joints using rivets 4-9-Ан.Окс-ЗУМГ, made in the way of single press riveting at the press machine КП-204М along travel ensuring diameter of closing heads equal to 6.7...6.8 mm, height of closing heads equal to $H_{c.h}$ = (1.9...2.0) mm and extension of set heads after riveting h_h = (0.04...0.05) mm.

Totally 57 specimens were made for fatigue tests of overlapped shear joints (see Ref. Fig. 6.28)

Fatigue tests were performed by machine УРМ-2000 at level of cyclic loading with maximum reduced zero-to-compression stress equal to 118.2, 82.7 and 59.1 MPa and frequency of 40 Hz within the “gross” section.

Statistically processed results of the fatigue test are represented in Figs 6.29, 6.30.

Analysis of the fatigue test results shows that specimen cyclic durability of single-shear overlapped joints using rivets ЗУМГ increases in 1.97...3.4 times on average and in 1.6...2.7 times in comparison with durability of analogous joints using rivets ЗУГБ and ЗУГ at tested levels of cyclic loading with c σ_{max} = 118.2, 82.7 and 59.1 MPa.

The purpose of checking the joints for leakage is to test the tightness of riveted joints made with rivets 4-10-Ан.Окс-ОСТ1 34117-91, 4-10-Ан.Окс-ЗУГБ and 4-10-Ан.Окс-ЗУМГ in presence of corrosive medium from the side of the rivet set heads.

For riveted joints of the airframe structural members working in contact with sea medium it is very important to ensure tightness of zone contacting with penetrating medium from the set head side and members to be joined including joint heightwise because, even when joint is leakproof in general, then penetration of sea water to a portion of the riveted rivet depth from the set head side may cause corrosion damage and joint failure.

It is possible to check the joints for leakage in the presence of corrosive medium represented in the form of sea water using painting method.

While testing tightness of the riveted joints using painting method after unriveting the paint having high penetrative ability was applied from the closing head side so t6o overlap boundary of rivet-hole contact on 1...3 mm (Fig. 6.31).

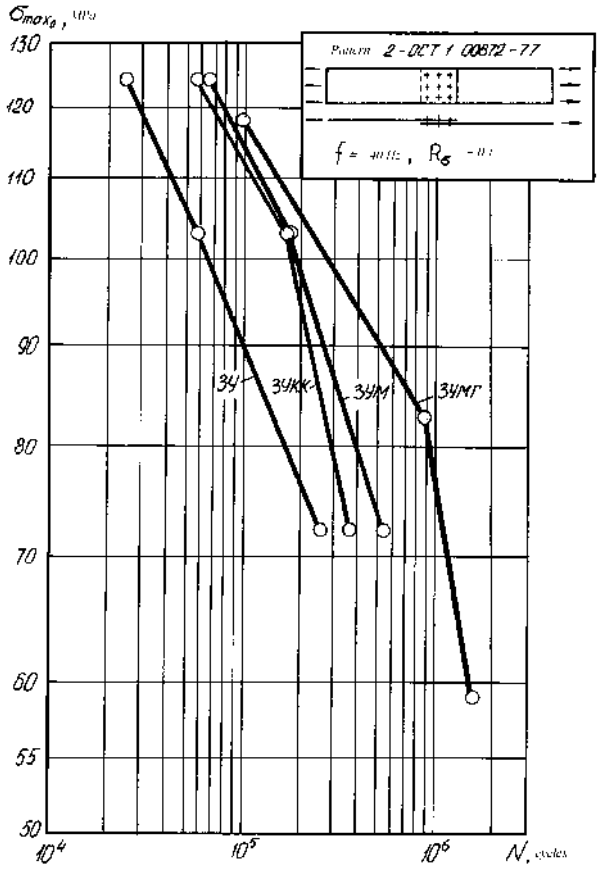

Fig. 6.29. Stress-cycle diagrams of riveted joint specimens assembled using method of single press riveting: rivet standard size – 4-9-Ан.Окс; specimen material – Д16АТл2 sheet – Ан.Окс.; production process of riveting using rivets ЗУ is specified in ПИ-249-78; production process of riveting using rivets ЗУКК and ЗУМ is specified in ТИ 36-21-86; ЗУМГ – in ТР 1.4.1220-83

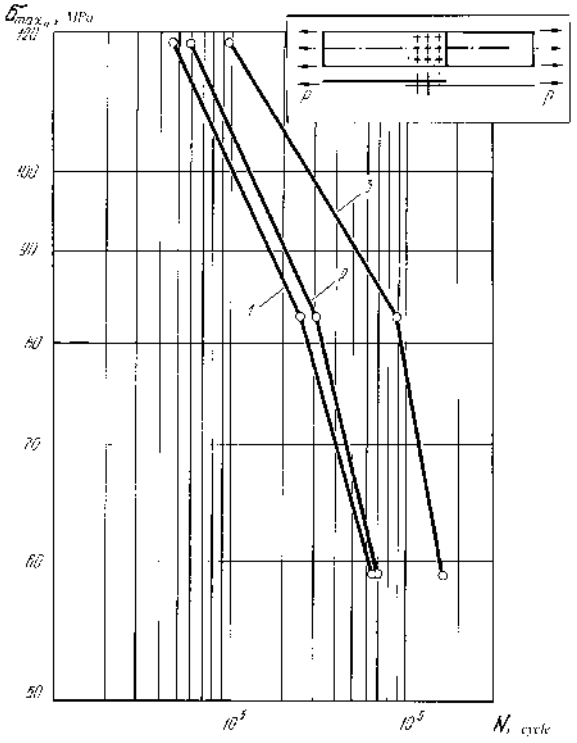

Fig. 6.30. Stress-cycle diagrams of riveted joint specimens (type 2 – ОСТ 1 00872-77) assembled according to technology used under presence of corrosive medium: 1 – rivets 4-9-Ан.Окс-ЗУГБ; 2 – rivets 4-9-Ан.Окс-ОСТ 1 34117-91 (ЗУГ); 3 – rivets 4-9-Ан.Окс-ЗУМГ; f = 40 Hz; R = 0.1

When paint dried out the specimens were cut along rivet axes and joint tightness was determined visually on traces of paint on the hole walls and on rivets.

Comparative tests for tightness of countersunk riveted joints made by single press riveting with rivets ЗУГ, ЗУГБ and ЗУМГ, when contacting with penetrative medium from the side of the closing heads, were made on the plate specimens with filled unloaded hole.

To perform experiment the special specimens were made (see Ref. Fig. 6.20) made of Д16АТл5 sheet with rivets ЗУГ (ОСТ1 34117-91), ЗУГБ and ЗУМГ.

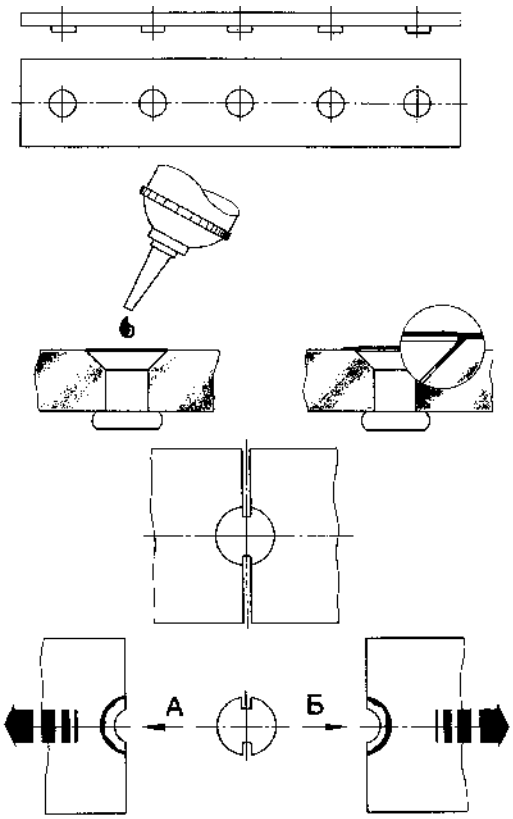

Fig. 6.31. Diagram explaining check of riveted joints for leakage using paint with high penetration ability

To check plate joints made of the Д16АТл5 sheet with filled unloaded hole the following joints were made:

– joints with rivets 4-10-Ан.Окс-ОСТ1 34117-91 made by single press riveting by press machine КП-204М along travel ensuring diameter of the closing heads equal to 6.4 and 6.8 mm when rivets were inserted in the hole with diameter equal to 4.13 mm;
– joints with rivets 4-10-Ан.Окс-ЗУГБ made by single press riveting by press machine КП-204М along travel ensuring diameter of the closing heads equal to 6.4 and 6.8 mm, when rivets were inserted in the hole with diameter equal to 4.13 mm;
– joints with rivets 4-10-Ан.Окс-ЗУМГ made by single press riveting on press machine КП-204М along travel ensuring diameter of the closing heads equal to 6.4 and 6.8 mm when rivets were inserted in the hole with diameter equal to 4.08 mm and hole with diameter equal to 4.13 mm.

8 specimens were made for checking the joints for leakage using paint with high penetrative ability. As a paint the red penetrating fluid “К” intended for dye penetrant flaw detection was used complying with Standard ТУ 6-10-750-79.

Test results for leakage using painting method are represented in Fig. 6.32.

It is evident that when inserting rivets ЗУГ and ЗУГБ in compliance with ТР 1.4.1220-83 and drilling holes for rivets with drill having 4.1 mm in diameter and forming rivets while riveting (where d_r – rivet shank diameter) the paint from the side of set head penetrates to the depth equal to 100% of the set head depth. Thus, when using rivets ЗУГ and ЗУГБ it is impossible to exclude penetration of corrosive medium along the set head depth, and, therefore, corrosion damage of the joint is possible.

When using rivets ЗУМГ while drilling holes for rivets with drill having diameter both 4.1 mm and 4.05 mm and forming closing head having diameter of 1.6 and 1.7d_r the paint penetrated to the height not exceeding height of cap in the form of truncated cone at the set head.

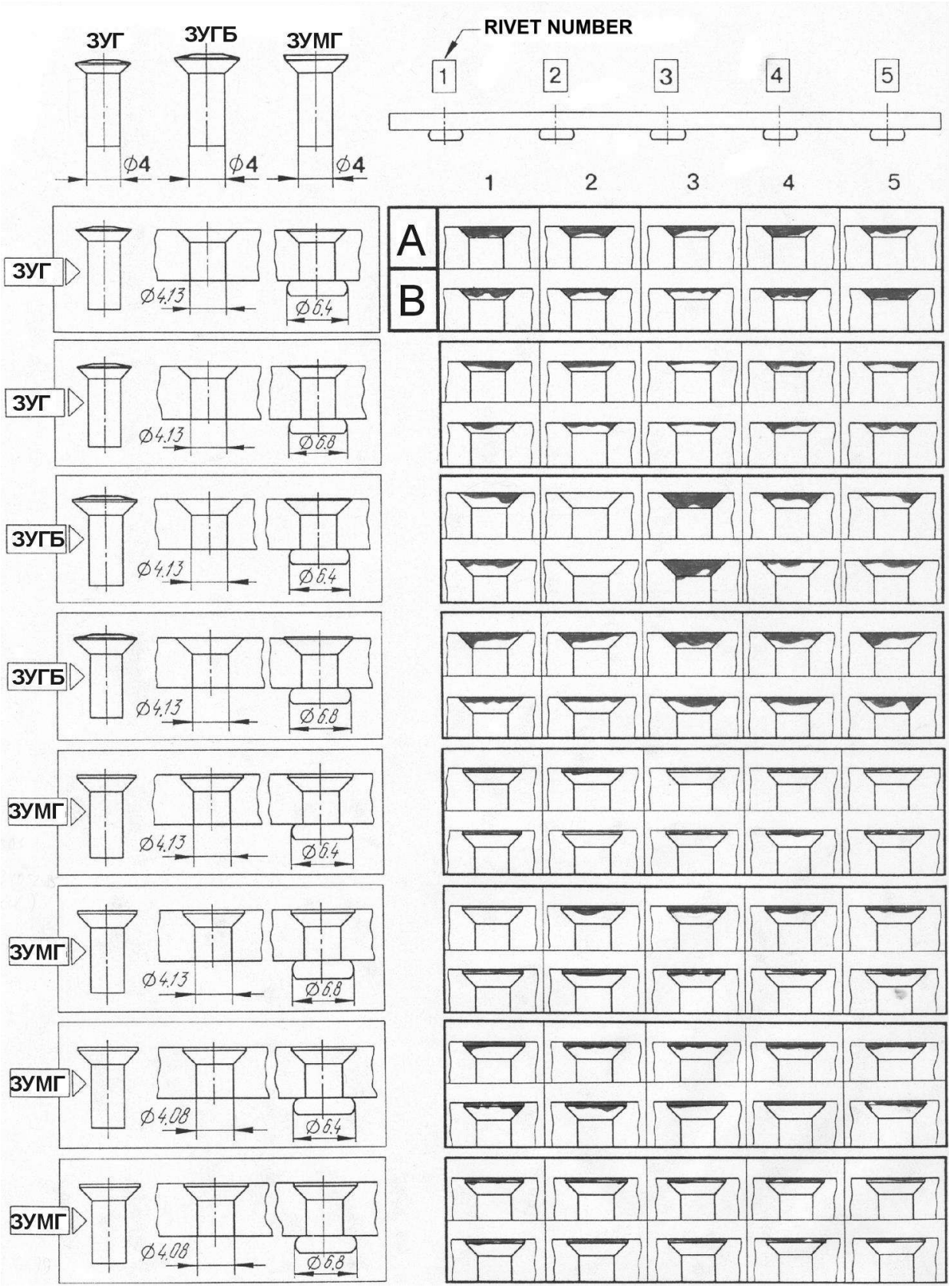

Fig. 6.32. Nature of paint penetration to walls of holes filled with rivets

Analysis of test results has shown that joint tightness using rivets ЗУМГ in

the presence of corrosive medium from the set head side is higher than tightness of riveted joints using rivets ЗУГ and ЗУГБ, due to the presence of the cap on the rivet set head assisting in forming barrier to corrosive medium from the set head side.

According to degree of tightness all units may be divided into three groups:

1) tightness requirements are not claimed;

2) leakage of working medium through joint is not allowed;

3) leakage of working medium through joint is allowed and standardized.

For units of the second group the qualitative estimation of tightness is the most applicable. The estimation criterion is “tight joint” and “untight joint” irrespectively to leakage amount. As working medium air or kerosene may be used. Leak tests for may be performed under static loading with excessive pressure, repeatedly-static loading with excessive pressure. diagram of static loading with excessive pressure of kerosene from the side of rivet closing heads with simultaneous cyclic loading creating operational stress level in the joint members.

Comparative leak tests for of the countersunk riveted joints made by single press riveting with rivets ЗУГ, ЗУГБ and ЗУМГ under contact of penetrating medium from the side of closing heads were performed for plate specimens with filled unloaded hole simulating stringer-to-skin joint in the area of integral fuel tank (Fig. 6.33). Kerosene was used as working medium.

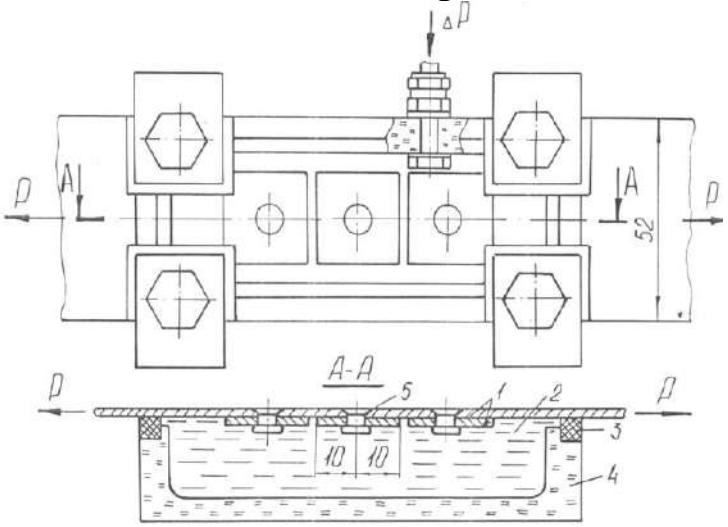

Fig. 6.33. Device used in test of riveted joint for leakage

For tests special specimens were made (Fig. 6.16). Skins and straps of the specimens while using rivets ЗУГ were made of the Д16АТл2 sheet, while using rivets ЗУГБ and ЗУМГ were made of the Д16АТл2.5 sheet. Sheet thickness was selected on the basis condition to provide maximum similarity of specimens for comparative leak tests, including cylindrical cap thickness in the transition zone of the hole cylindrical portion into conical.

Skin-to-strap joints were performed using rivets ЗУГ (ОСТ 1 34117-91), ЗУГБ and ЗУМГ.

For testing tightness of joints made of the Д16АТл2 sheet with filled unloaded hole the joints with rivets 4-9-Ан.Окс-ОСТ1 34117-91 were made by single press riveting by the press machine КП-204М along travel ensuring the closing head diameter equal to 6.6...6.8 mm, closing head depth equal to $H_{c.h}$ = (1.7...1.8) mm and extension depth of closing heads after riveting h_h = (0.04...0.07) mm.

For testing tightness of joints made of the Д16АТл2.5 sheet with filled unloaded holes the joints with rivets 4-9-Ан.Окс-ЗУГБ were made by single press riveting by the press machine КП-204М along travel ensuring the closing head diameter equal 6.6...6.7 mm, closing head depth equal $H_{c.h}$ = (1.85...1.95) mm and extension depth of closing heads after riveting h_h = (0.08...0.15) mm; the joints with rivets 4-9-Ан.Окс-ЗУМГ, made by single press riveting by the press machine КП-204М along travel ensuring the closing head diameter equal to 6.6...6.8 mm, closing head depth equal to $H_{c.h}$ = (1.85...1.95) mm and extension depth of closing heads after riveting h_h = (0.04...0.06) mm.

For maximum account of real operating conditions while leak testing the specimens were tested in cyclically loaded grips of testing machine of the УРМ-2000 type. Special rectangular cap made of organic glass was installed using rubber gaskets to deliver kerosene to the specimen from the closing head side (See Fig. 6.33). Through connection installed on the cap wall inner cavity was filled with kerosene and connected with compressor, which creates excessive pressure of (0.3 ±0.05) daN/cm^2 while testing. The specimen was covered with chalk solution before testing to detect leakage. Leakage appearance was detected by darkening chalk solution from the rivet set head side.

Analysis of leak test results under cyclic loading has shown that specimens with rivets ЗУГ (ZUG) and ЗУМГ (ZUMG) did not lose leakproofness up to 1,000,000 cycles of loading. Two specimens with rivets ЗУГБ (ZUGB) were destroyed at 930,000 and 1,000,000 cycles of loading correspondingly. In this case leakproofness was lost after 25,000...30,000 cycles of loading after appearance of fatigue crack. The third specimen was removed from tests after 500,000 cycles of loading to ensure possibility of leak testing under static loading.

Analysis of leak test results under static loading has shown that specimens with rivets ЗУГ lost their leakproofness under maximum stresses within the “gross” section equal to 133...212 MPa, with rivets ЗУГБ (ZUGB) at 155...194 MPa and with rivets ЗУМГ (ZUMG) at 155...291 MPa. Statistical processing the leak test results under static loading has shown that average stresses of joint leakproofness lost with rivets ЗУГ (ZUG), ЗУГБ (ZUGB) and ЗУМГ (ZUMG) is about 156, 175 и 222 MPa correspondingly. It is evident that average stresses of joint leakproofness lost with rivets ЗУМГ (ZUMG) is in 1.4 and 1.3 times higher than average stresses of joint leakproofness lost with rivets ЗУГ (ZUG) and ЗУГБр (ZUGBr).

6.4. RIVETING METHOD AND TECHNOLOGY AS FACTOR INCREASING RIVETED JOINTS ERVICE LIFE AND THEIR EXTERNAL SURFACE QUALITY

It should be noted that riveting method and technology also essentially affects the riveted joint service life and their external surface quality. For analysis the press riveting device described in inventor's certificate No. 1765966 (Fig. 6.34) was selected.

Essence of the device: die contains setting punch 1 made in the form of anvil 2 with flat working surface 3 and shank 4. The anvil and shank are separated with collar 5. On the anvil with the possibility of axial motion along slide fit the clamping bushing 6 is installed, spring-loaded by means of spring 7 with respect to the edge. Surface of the working end of the clamping bushing is positioned above the anvil working surface. On the latter the flat washer 8 is installed, in this case the anvil diameter equals the washer diameter. Clamping bushing 6 on the area located above setting punch 1 has conical inner surface 9, depth of which equals extension of the working end surface of clamping bushing over working surface of anvil 3.

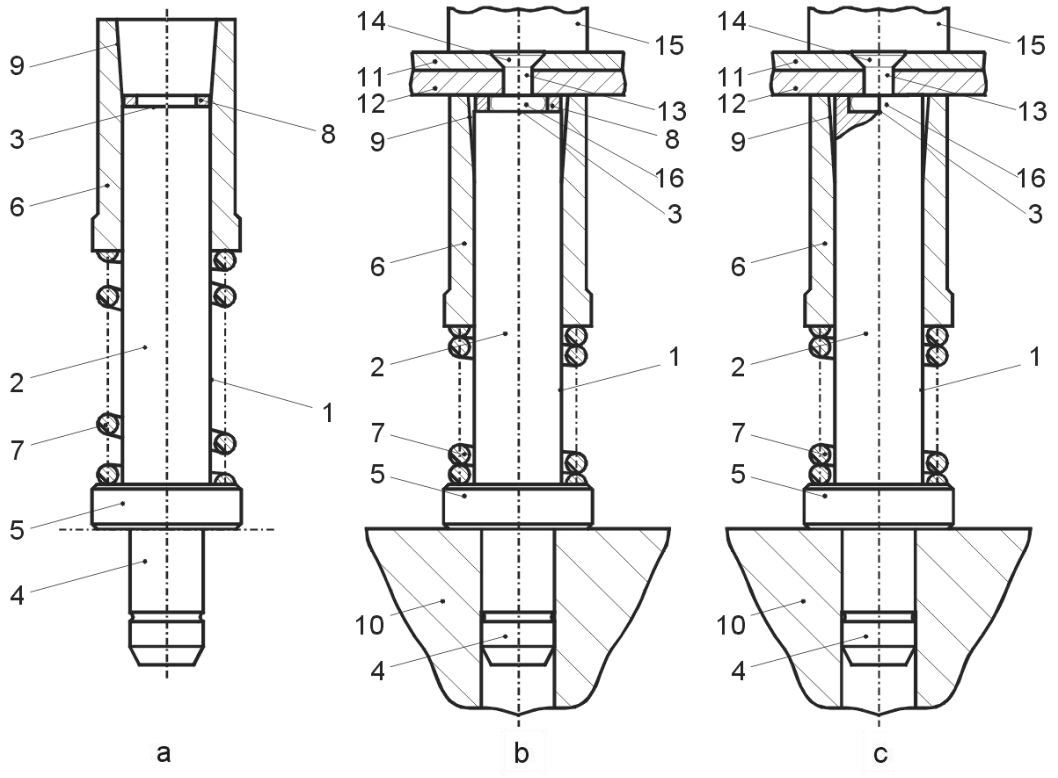

Fig. 6.34. Design of press tool for single press riveting

Distinguishing feature of the proposed press tool lies in the fact that relative freedom of technological washer motion in the plane perpendicular to the riveting axis is achieved not by increasing the anvil diameter in comparison with the washer diameter resulting in increasing overall dimensions of the press tool

members and its steel intensity, but by increasing the inner surface diameter of the clamping bushing on the area protruding over the anvil working surface.

Continuous increase of the clamping bushing inner surface diameter beginning from the setting punch end realized in the conical inner surface provides not only possibility to displace the washer in proportion to the upsetting rivet set along the die axis, but, together with equality of anvil and washer diameters and also interfacing the clamping bushing with anvil using slide fit allows self-alignment of the washer coaxially to the anvil while the joint unloading.

As the die modification it is possible to use the device shown in Fig. 6.34, c. Its distinguishing feature is that in the anvil a recess equal to the closing head depth and diameter exceeding maximum diameter of the rivet closing head is made.

6.5. Conclusions

On the basis of principles and methods of integrated designing and achieving regulated durability of shear riveted joints of the assembly structures the following ways were developed:

1. New design-technological methods of unloading the utmost rows of multi-row shear riveted joints providing enhanced durability of standard joints in 2.3…6 times.

2. Design of new countersunk rivets with cylindrical or cylindrical-tapered compensators intended for joining medium and thin aircraft skins ensuring required characteristics of durability, tightness and quality of the joint external surface without milling the rivet set heads after riveting.

3. Method and procedure of riveting with cylindrical or cylindrically-tapered compensators ensuring required depth of the rivet closing heads while riveting.

Section 7

NEW STRUCTURALLY-TECHNOLOGICAL METHODS AND THE WAYS OF FATIGUE CRACKS GROWTH DELAY TO PROLONG THE SERVICE LIFE OF THE ASSEMBLY THIN-WALLED STRUCTURES

To provide reliability and flight safety the prolongation of structure service life is one of the actual problems facing designers and technologists in aircraft industry.

There are stress concentrators in each structure where fatigue cracks arise.

To prolong the airframe service life, members of which have fatigue cracks of subcritical size, it is advisable to develop and apply the ways of cracks growth delay and restoring of bearing ability of the structural damaged members [196, 290].

As a method of fatigue cracks delay the research of the local mode of deformation influence in members with a crack, caused by fasteners installation with interference in the holes made in crack apexes is offered.

7.1. INVESTIGATION OF HOLE OVALITY AND MODE OF DEFORMATION IN PLATE WITH FATIGUE CRACK

Loading of structure with a fatigue crack leads to displacement of crack edges from each other, in particular, to crack opening and due to this the holes cease to be round (Fig. 7.1).

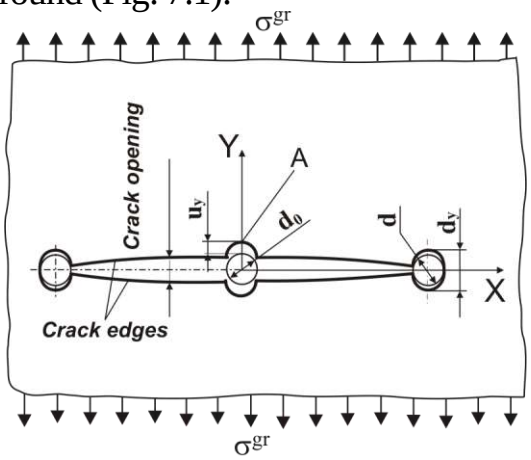

$\vartheta_i = u_{yi} = (d_{yi} - d_i)/2$

Fig. 7.1. Diagram of ϑ Hole Ovality Made in Crack Apexes and in the Middle of Fatigue Crack Midpoint

Hole ovality must be generally determined according to formula:

$$\vartheta = \frac{d_y - d_0}{2}.$$

According to Fig. 7.1 the value $(d_y - d_0)/2$ is equal to the greatest displacement u_y of point of a hole contour along the crack trajectory. Calculations were made for uniaxial loaded models of sheet parts with central located concentrators (hole, fatigue crack) (Fig. 7.2).

To choose needed radial interference of fasteners it is necessary to determine the ϑ holes ovality value along the crack trajectory to provide the guaranteed radial interference under operational loadings.

As for geometrical and power symmetry in the design model, we considered only 1/4 plate (and also 1/2 fasteners installed in apex and along the length of a fatigue crack) (Fig. 7.3). Fatigue crack was modelled by groove t = 0.1 mm width.

Action of the plate rejected parts was replaced by corresponding connections (boundary conditions). External loading was modeled by applying to free edge end of quarter plate uniformly distributed, directed along longitudinal axis of plate of tensile load which is equivalent to σ^{gr} to fatigue crack and level of the σ^{gr} external loading to transfer (opening $2 \cdot u_y$) crack ends and the ϑ hole ovality made in the crack apex and in the middle of its length, in plate from Д-16Т.

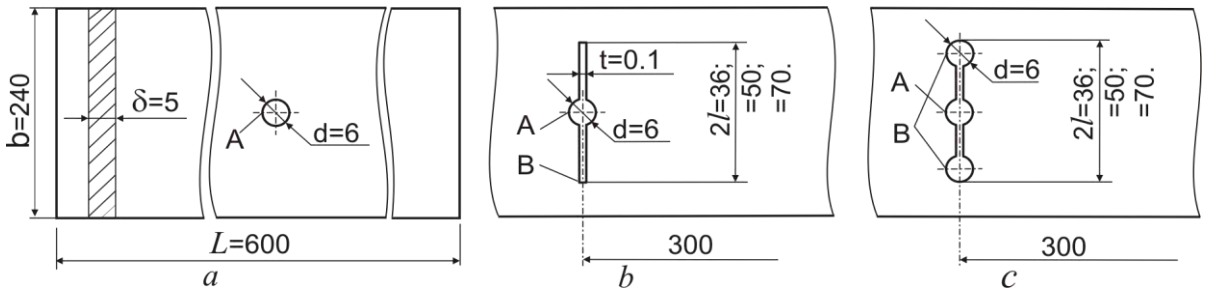

Fig. 7.2. Models of Sheet Parts:
a – plate with hole located centrally; b – plate with developing crack; c – plate with crack and holes; d = 6 mm, in crack apexes

It is assumed in calculations that plate is made of Д16АТ aluminum alloy (coefficient of elasticity $E = 7.2 \cdot 10^4$ MPa, Poisson's factor $\mu = 0.3$), elasto-plastic deformation is described by deformation curve $\sigma - \varepsilon$ [11]. Bolts and nuts are made of 30ХГСА steel ($E = 2.1 \cdot 10^5$ MPa, μ = 0,3) and deformed only elastically. Friction coefficient between adjacent surfaces of plate and fasteners was equal to $f_{fric} = 0.15$.

The $2 \cdot l$ length influence was investigated by calculated method. To decrease time and increase calculation accuracy in areas of expected high gradients of stresses and deformations in a plate a number of areas (6 substructures) with various grid step of finite-element breakdown (Fig. 7.4) marked on the design diagram.

Finite-element grid was formed of the Solid82 flat quadrangular elements [474]. In material characteristics of finite elements the curve of material deformation was modelled by a smooth curve using five points. The obtained finite-element model of the plate with applied loadings and boundary conditions is shown in Fig. 7.5.

Results of calculations [167] are presented in the form of diagrams (Fig. 7.6) of dependences of the A point and the B point displacements on stress value σ^{gr} for various crack lengths. Calculation is coordinated with experimental data that proves possibility and expediency of definition of the mode of deformation in aircraft design members having fatigue cracks by using of the ANSYS 5.3 system.

During investigation, the system of value designed definition of crack opening and the hole ovality executed in apex and along crack length depending on crack length and loading level is developed and adjusted. These data are necessary to choose the values of a radial interference Δ_d of the fasteners installed

in these holes (Table 7.1, for σ^{gr} = 100 MPa).

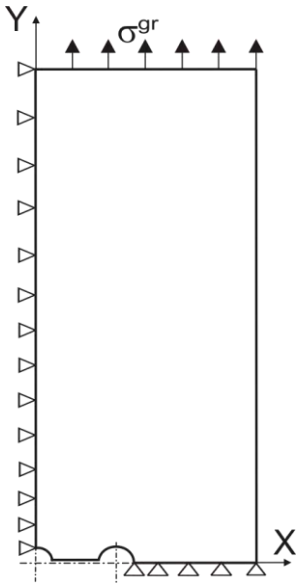

Fig. 7.3. Design Diagram of Plate with Crack

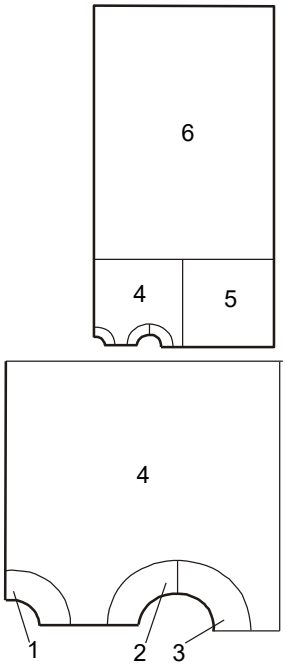

Fig. 7.4. Breakdown Scheme of Plate With Crack on Finite-Element Substructures: 1, 2, 3…6

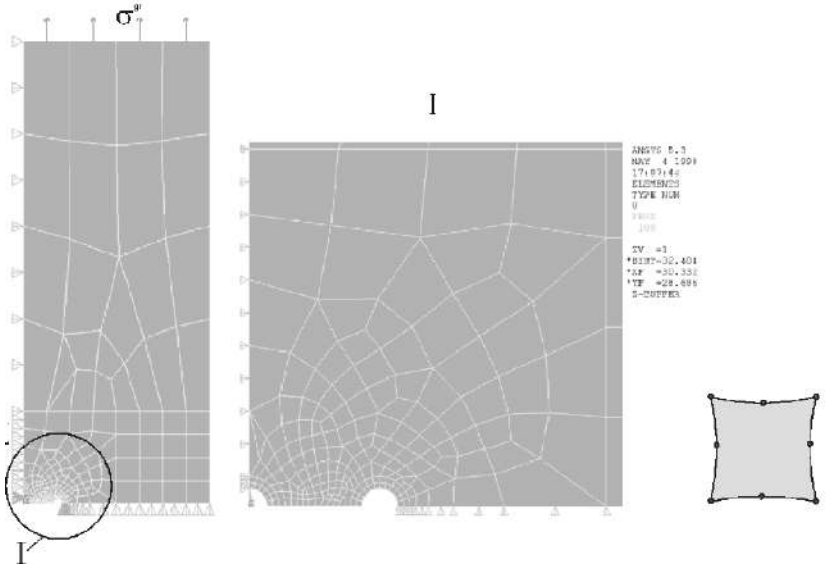

Finite Element Type: Plane 82, 2-D element, 8-node, Freedom degrees: UX, UY

Fig. 7.5. Finite-Element Model of Plate with Applied Loadings and Boundary Conditions

The character was revealed and the degree of stress distribution non-uniformity concerning nominal stress in "gross" section (σ^{gr}) and "net" section (σ^{net}) was calculated using data received by means of the ANSYS 5.3 system about the mode of deformation of the plate with centrally located concentrator (hole or crack). For this purpose $K_{\sigma^{gr}}$ and $K_{\sigma^{net}}$ stress concentration coefficients

were determined (Fig. 7.7).

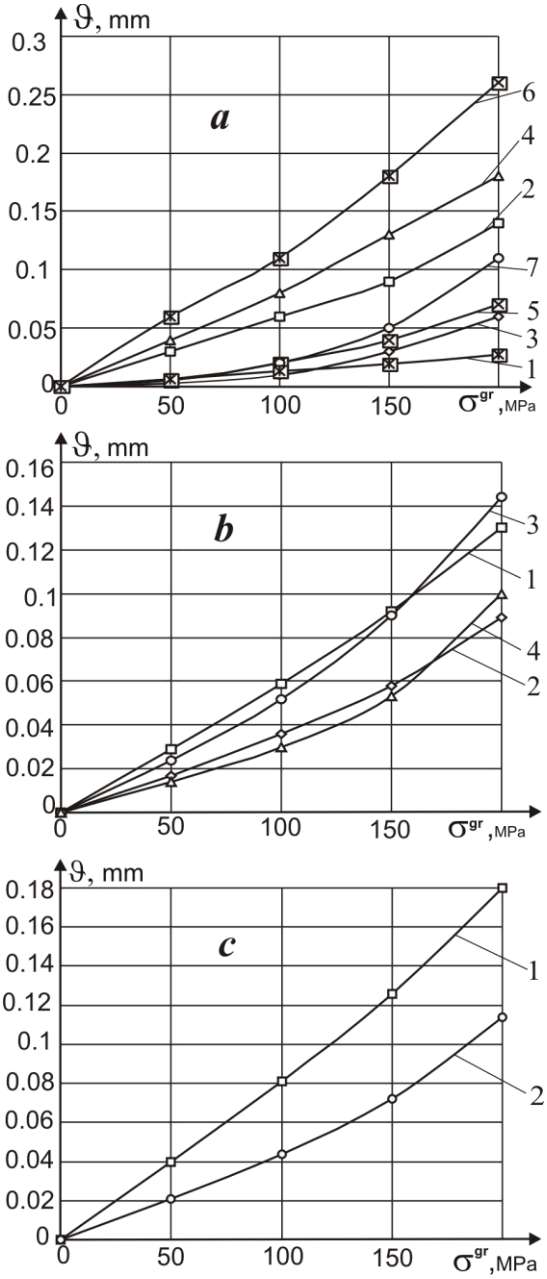

Fig. 7.6. Dependence of hole ovality on the σ^{gr} stresses and crack length in a plate of Д16АТ: a – without holes in crack apexes 1, 2, 4, 6 – point A ($2l = d_0$, 36, 50, 70 mm); 3, 5, 7 – point B ($2l$ = 36, 50, 70 mm); b – holes, ∅6 mm, in crack apexes ($2l$ = 36 mm) 1*, 3** – point A; 2*, 4** – point B; * – calculation, ** – experiment; c – hole, ∅6 mm, in crack apexes ($2l$ = 50 mm), 1 –

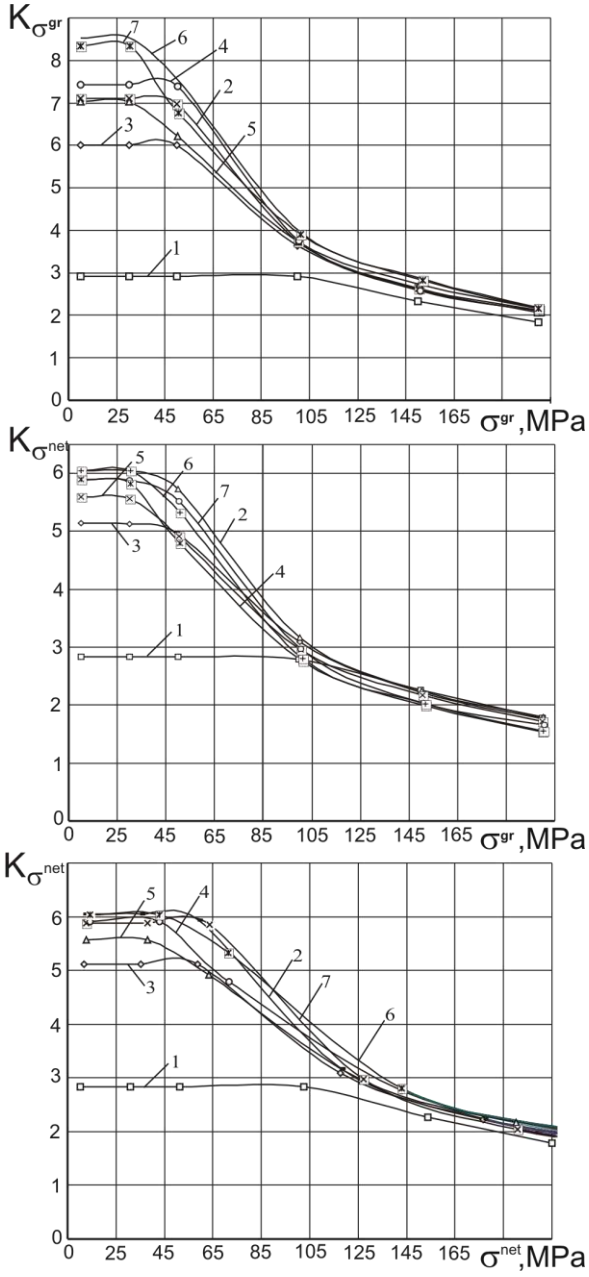

Fig. 7.7. Dependence of Stress Concentration Coefficients on Loading Level and Crack Length in Plate of Д16АТ:

$$K_{\sigma^{gr}} = \sigma_{max} / \sigma^{gr};\ K_{\sigma^{net}} = \sigma_{max} / \sigma^{net};$$

$$\sigma^{net} = \sigma^{gr} F^{gr} / F^{net};\ F^{gr} = b\delta;$$

$$F^{net} = (b - 2l)\delta.$$

1, 2, 3, 4, 5, 6, 7 – $2l = d_0$, = 36*, = 36**, = 50*, = 50**, = 70*, = 70** mm

point A; 2 – point B

Table 7.1

Influence of Crack Length on Holes Ovality and Needed Radial Interference Value

$2 \cdot l$, mm	d_0	36	50	70
ϑ, mm (point A)	0.01	0.06	0.08	0.12
$\overline{\Delta}_{dA} = 2 \cdot \vartheta_A / d_A + 1{,}0$, %	1.03	3.0	3.7	5.0
ϑ, mm (point B)	0.01	0.036	0.044	0.054
$\overline{\Delta}_{dB} = 2 \cdot \vartheta_B / d_B + 1{,}0$, %	1.03	2.2	2.5	2.8

The analysis of the obtained results shows that hole performance, ∅6 mm, in crack apex reduces the stress concentration coefficients in 115 … 12 times for fatigue cracks, $2 \cdot l \le 80$ mm length, at loading level corresponding to $\sigma^{gr} \le 100$ … 150 MPa.

7.2. Influence of the tightening bolts installed in holes made in fatigue crack apexes on local mode of deformation of plate

The investigation of efficiency of bolts installation with an axial interference in crack apexes is carried out by calculation (by means of ANSYS 5.3).

As an investigation object the plate with centrally located crack was accepted, in apexes of which the holes ∅6 mm, are made and the OCT 1 31132-80 bolts and the OCT 1 33026-80 nuts with axial interference (Fig. 7.8) are installed.

In the design diagram (Fig. 7.9) the bolt and the nut are modeled by monolithic fastener. To create three-dimensional finite-element model (Fig. 7.10 – 7.12) of plate and fastener the finite elements [474] were chosen: PLANE 42 – flat four-node, SOLID 45 – volumetric eight-node and CONTAC49 – volume linear contact element.

To estimate the efficiency of bolt installation with axial interference in fatigue crack apex the axial interference value influence on the $K_{\sigma^{gr}}$ stress concentration coefficient, σ_a amplitude, σ_m mean and $\sigma_{\max}$ maximum tensile stresses in the range of the operational loadings corresponding to σ^{gr} = 10... 200 MPa was analyzed (Fig. 7.13 to Fig. 7.21).

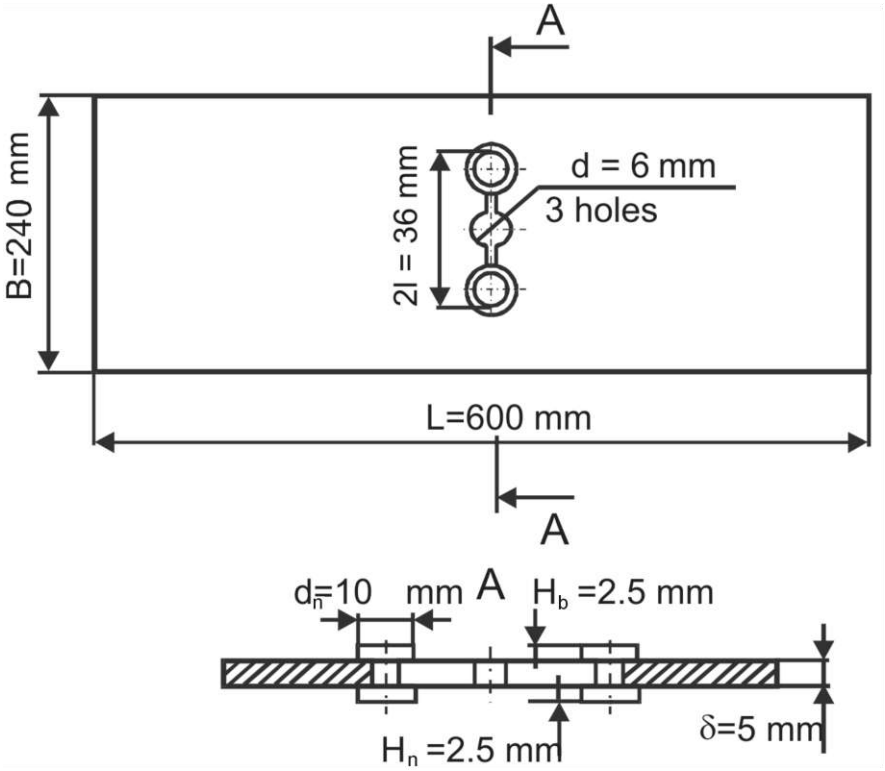

Fig. 7.8. Geometrical Model of Plate with Crack with the Holes, ∅ 6 mm, in Their Apexes and Bolts With Axial Interference are Installed

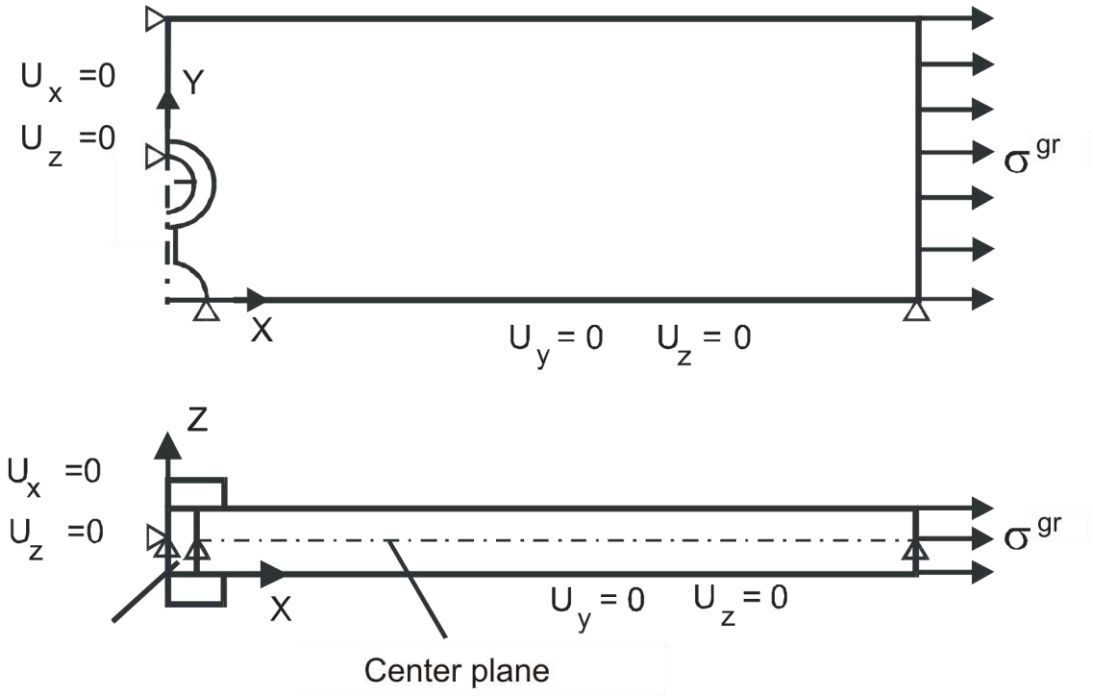

Fig. 7.9. Design Diagram of Plate With Central Hole, Crack and holes Made in Crack Apex

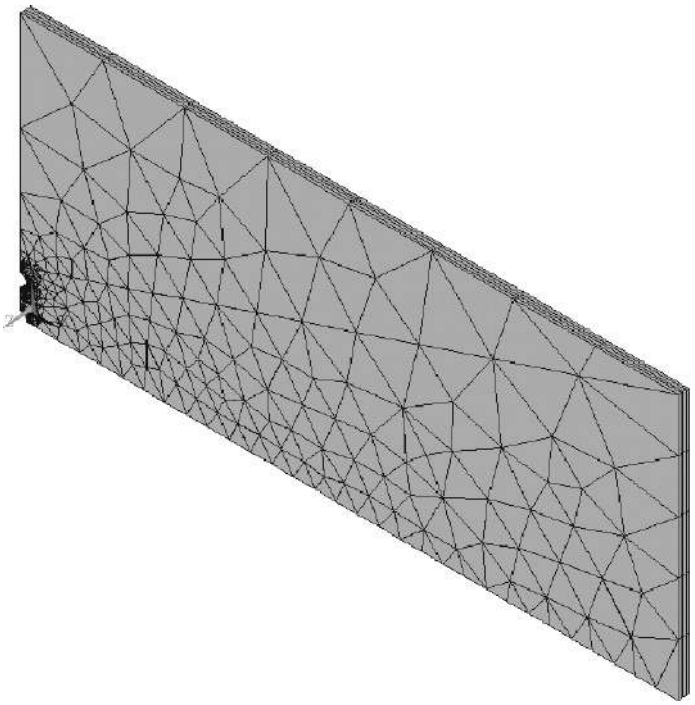

Fig. 7.10. Finite-element model of the plate with the central hole and crack with holes in its apexes

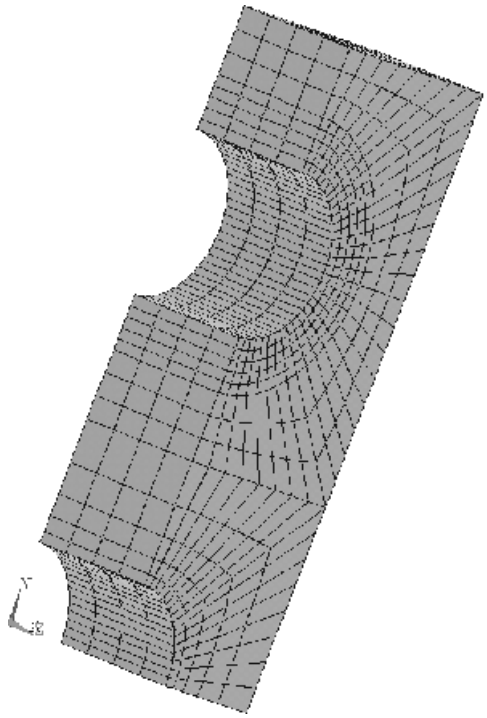

Fig. 7.11. Finite-element grid in fatigue crack area

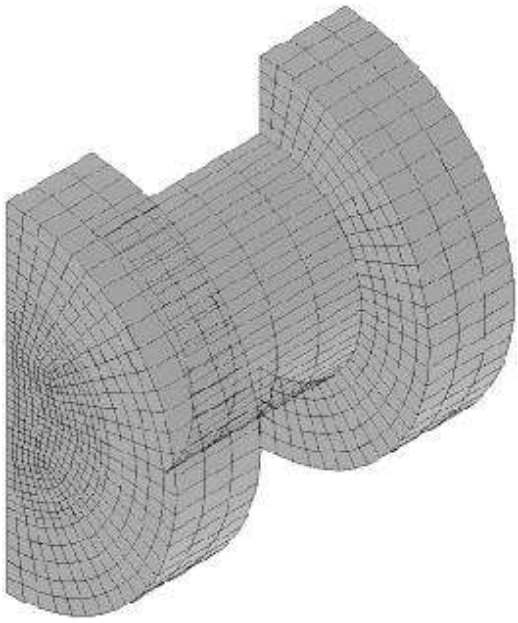

Fig. 7.12. Finite-element model of fastener

In Fig. 7.14 and 7.15: 1 – σ_c = 0 MPa, 2 – σ_c = –100 MPa, 3 – σ_c = –190 MPa.

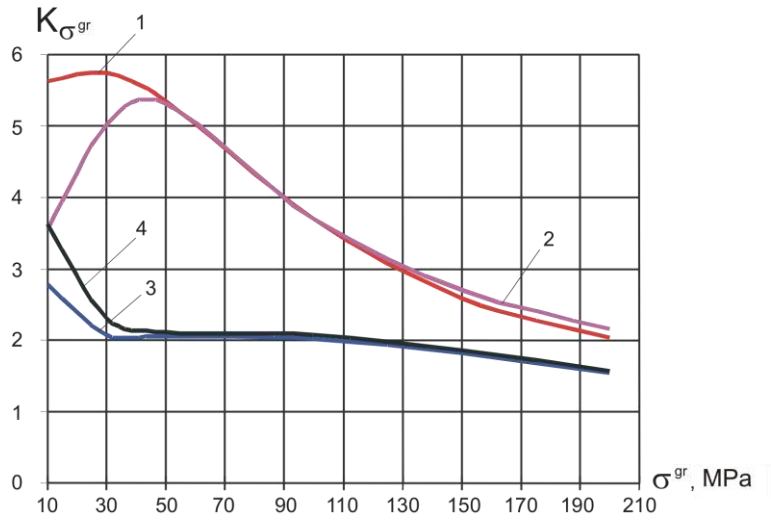

Fig. 7.13. Loading level influence (σ^{gr}) on the $K_{\sigma^{gr}}$ stress concentration coefficient:
1 – σ_c = 10 MPa; 2 – σ_c = – 55,5 MPa; 3 – σ_c = –100 MPa; 4 – σ_c = –190 MPa

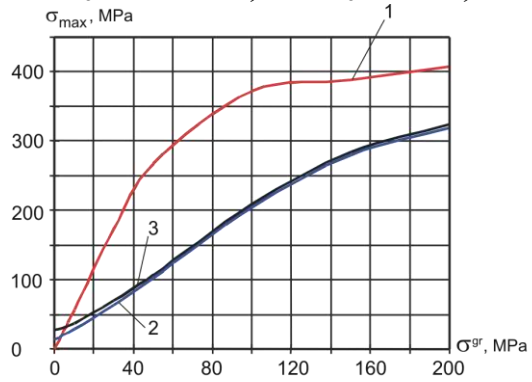

Fig. 7.14. Loading level influence on (σ^{gr}) the σ_{max} maximum stresses

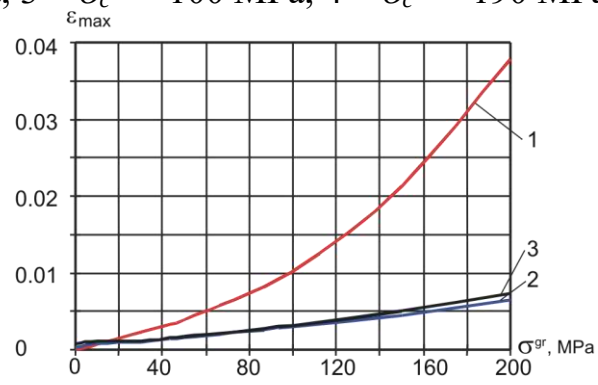

Fig. 7.15. Loading level influence (σ^{gr}) on the ε_{max} maximum deformations

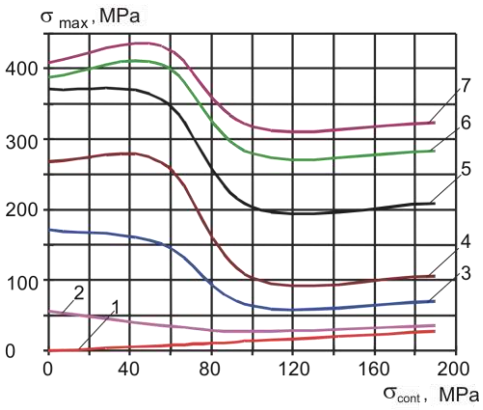

Fig. 7.16. Influence of σ_{cont} contact stresses on σ_{max} maximum stresses

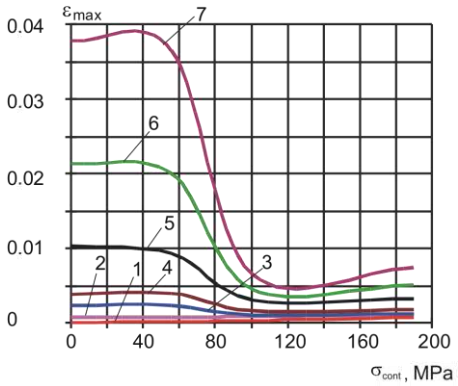

Fig. 7.17. Influence of σ_{cont} contact stresses on ε_{max} maximum deformations

In Fig. 7.16 and 7.17: 1 – σ^{gr} = 0 MPa, 2 – σ^{gr} = 10 MPa, 3 – σ^{gr} = 30 MPa, 4 – σ^{gr} = 50 MPa, 5 – σ^{gr} = 100 MPa, 6 – σ^{gr} = 150 MPa, 7 – σ^{gr} = 200 MPa.

The analysis of calculation results shows the following:

– the axial interference of the bolt installed in a hole in crack apex displaces the maximum value of σ_x tensile stress and σ_1 main stress from a hole web by 5…8 its diameters, thus the area near a hole web is unloaded and plate near-surface layers are compressed on greater value than the middle ones;

– the bolts location with an axial interference in the crack apexes reduces the $K_{\sigma^{gr}}$ stress concentration coefficient in 1.3 … 2.8 times and reduces amplitude of σ_a tensile stresses in 1.3 … 4 times.

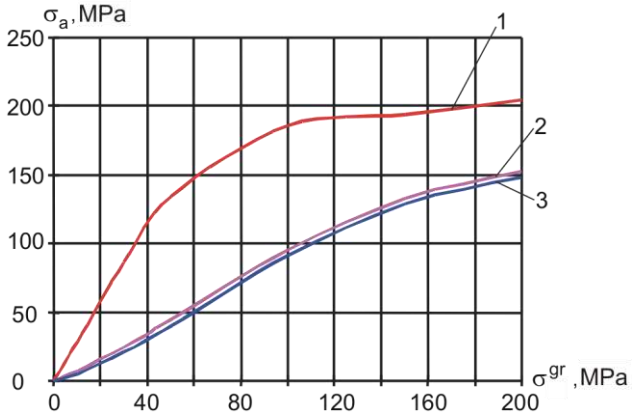

Fig. 7.18. Loading level influence (σ^{gr}) on σ_a stress amplitude

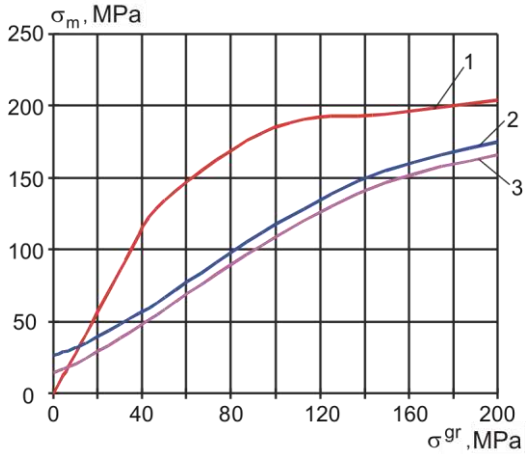

Fig. 7.19. Loading level influence (σ^{gr}) on σ_m mean stresses

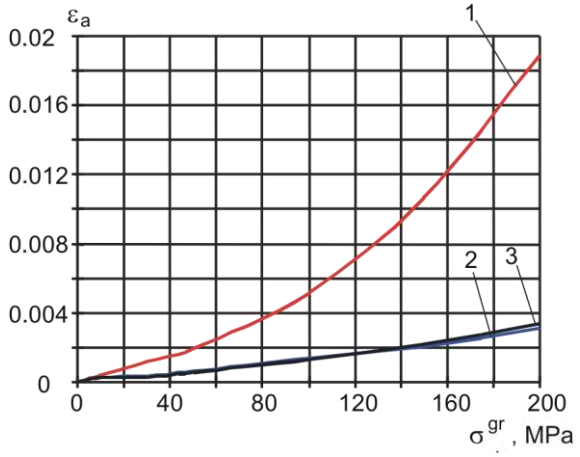

Fig. 7.20. Loading level influence (σ^{gr}) on the ε_a deformation amplitude

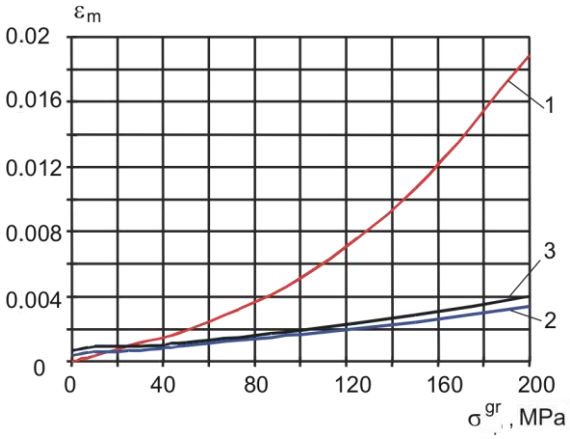

Fig. 7.21. Loading level influence (σ^{gr}) on the ε_m mean deformations

In Fig. 7.18 –7.21: 1 – = 0 MPa, 2 –σ_{cont} –100 MPa, 3 – σ_{cont} = –190 MPa.

The carried out investigation of the mode of deformation in sheet parts with cracks shows that it is reasonable to make holes in crack apexes (and along its

length) and to fill these holes with fasteners with radial interference to increase durability of thin-walled aviation structures with fatigue cracks.

7.3. INFLUENCE OF BOLT RADIAL INTERFERENCE ON MODE OF DEFORMATION OF PLATE WITH FATIGUE CRACK AND HOLES MADE ALONG ITS LENGTH

The investugation of influence of radial interference of bolts installed in holes made in the crack apexes and in the middle of its length on the mode of deformation of plate [163] is carried out (by calculation using ANSYS 5.3 system). Plate and bolt modelling is executed by the PLANE42 four-node finite elements [474]. Surface interaction of the bolt body and the hole webs are modelled by the CONTACT48 flat contact elements [474]. As a whole the plate model consisted of twelve substructures which formed the areas with high (near to crack and holes) and low density of finite elements splitting (Fig. 7.22).

Calculations are carried out for loading levels σ^{gr} = 10, 30, 50, 100, 150 and 200 MPa numbered accordingly Fig. 7.22 and Table 7.2.

Table 7.2

Loading level influence on value of required radial interference

$\overline{\Delta}_{dA}$, %	0.5	1.0	1.5
$\overline{\Delta}_{dB}$, %	0.35	0.75	1.1

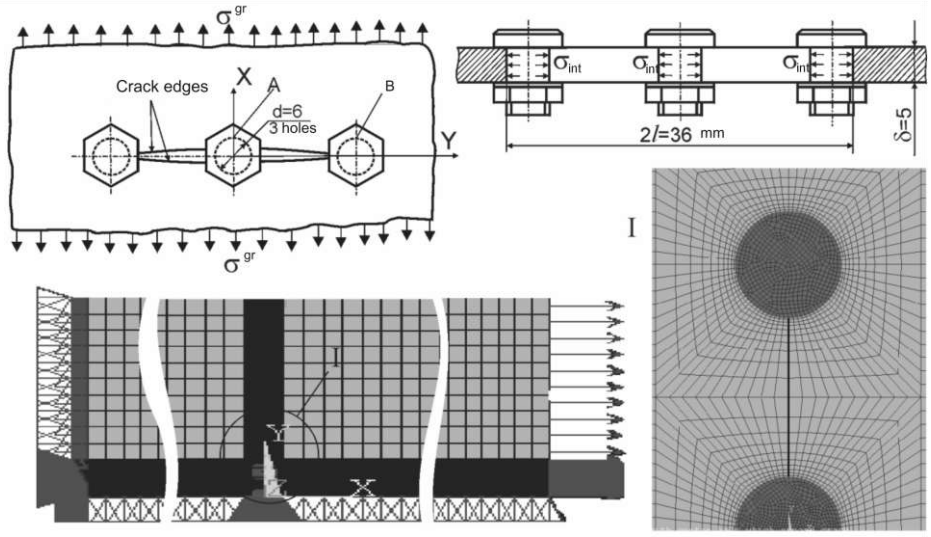

Fig. 7.22. Modelling of the plate with center crack with bolts installed with radial interference in crack apexes

The results of design of the mode of deformation (for $\overline{\Delta}_{dA}$ = 1.5 % and $\overline{\Delta}_{dB}$=1.1 %) are selectively shown in the form of diagrams of stress distribution (σ_x, $\sigma_{y)}$ and deformations (ε_x, ε_y) along lateral (X = 0, Y_1 = 18, Y_2 = 120 mm) axis of symmetry of the plate (Fig. 7.23).

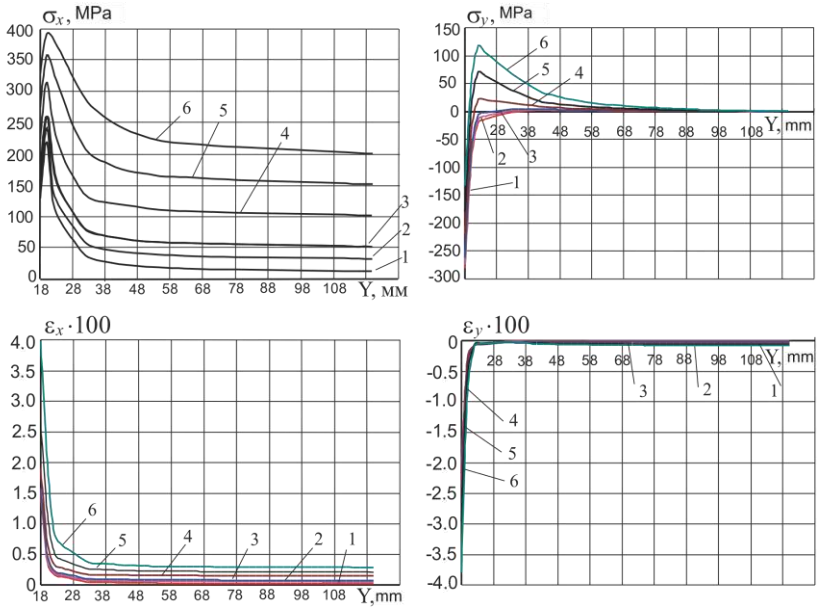

Fig. 7.23. Distribution of normal stress (σ_x, σ_y) and deformations (ε_x, ε_y) along the lateral axis of symmetry of the plate made of Д16АТ with fatigue crack with bolts installed with radial interference $\overline{\Delta}_{dA}$ = 1.5 %, $\overline{\Delta}_{dB}$=1.1% in crack apexes (and on the middle of length)

It is confirmed by design investigation of mode of deformation of the plate with fatigue crack, that bolt installed with radial interference in the hole in crack apex displaces σ_x maximum tensile stress from the hole web (Fig. 7.24). The displacement value in direction of crack development makes ~35 % of the hole diameter. The area adjoining to the hole web is unloaded owing to presence of the plasticity area caused by installation of the bolt with radial interference into the hole.

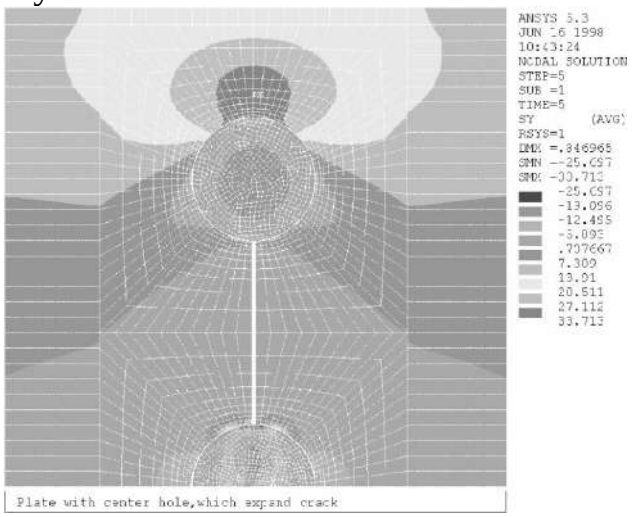

Fig. 7.24. Map of circumferential stress distribution in fatigue crack area at level of stress σ^{gr} = 100 MPa and at radial interference value of bolt installed in crack apex, δ = 0.35 %

To estimate the bolts installation efficiency with radial interference in fatigue crack apex the $\overline{\Delta}_{dB}$ value radial interference influence on the $K_{\sigma^{gr}}$ and $K_{\sigma^{net}}$ stress concentration coefficients, σ_a amplitude, σ_m mean, σ_{max} maximum tensile and σ_0 zero-to-tension stresses in a range of the operational loadings corresponding to σ^{gr}=10... 200 MPa (Fig. 7.25 to 7.31) has been analyzed.

At σ^{gr} = 10... 200 MPa the σ_a stress amplitude owing to bolt installation with radial interference in crack apex of the bolt is decreased in an area adjoining to the hole web in 2 … 3.8 times.

Bolts installation with a radial interference in crack apexes reduces the σ_0 zero-to-tension stress cycle in critical section of the plate in 1.9... 3 times.

Similar results differing only numerically are also obtained [163] for tangential stresses (τ_{max}, τ_a, τ_m, τ_0) and deformations (ε_{max}, ε_a, ε_m, ε_0) (Ref. Fig. 7.2 – 7.34).

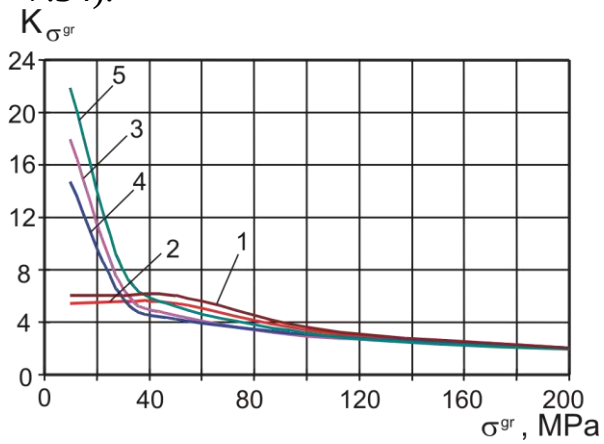

Fig. 7.25. Influence of loading level (σ^{gr}) on $K_{\sigma^{gr}}$ stress concentration coefficient in cases:

1 – holes without filling;
2 – holes with filling (value of radial interference δ = 0%);
3 – value of radial interference of bolt installed in center hole – δ = 0.5%, in crack apex – δ = 0.35%;
4 – value of radial interference of bolt installed in center hole – δ = 1%, in crack apex – δ = 0,75%;
5 – value of radial interference of bolt installed in center hole – δ = 1.5%, in crack apex – δ = 1.1%;

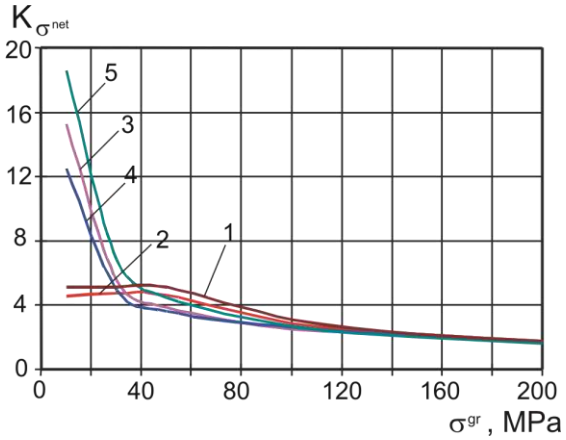

Fig. 7.26. Influence of loading level (σ^{gr}) on $K_{\sigma^{net}}$ stress concentration coefficient in cases:

1 – hole without filling;
2 – holes with filling (value of radial interference δ = 0%);
3 – value of radial interference of bolt installed in center hole – δ = 0.5%, in crack apex – δ = 0.35%;
4 – value of radial interference of bolt installed in center hole – δ = 1%, in crack apex – δ = 0.75%;
5 – the value of radial interference of bolt installed in central hole – δ=1.5%, in crack apex – δ = 1.1%;

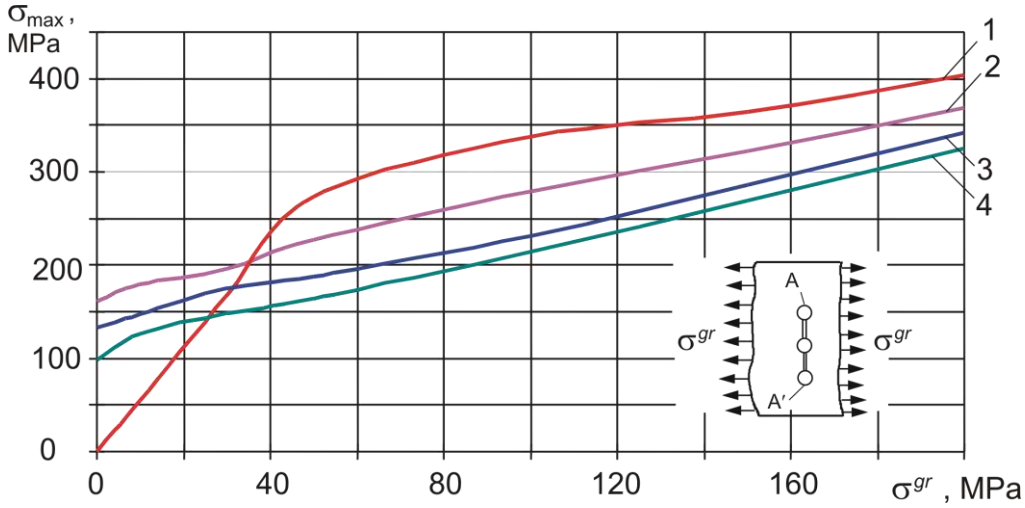

Fig. 7.27. Influence of loading level (σ^{gr}) on the maximum normal stress on hole edge in cases: 1 – value of radial interference δ = 0%; 2 – value of radial interference of bolt installed in center hole – δ = 0.5%, in crack apex – δ = 0.35%; 3 – value of radial interference of bolt installed in center hole – δ = 1%, in crack apex – δ = 0.75%; 4 – value of radial interference of bolt installed in central hole – δ =1.5%, in crack apex – δ =1.1%

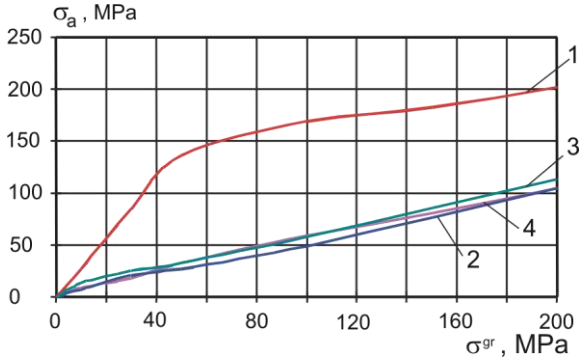

Fig. 7.28. Influence of loading level (σ^{gr}) on stress amplitude on hole edge (points A and A′) in cases: 1 – value of radial interference δ = 0%; 2 – value of radial interference of bolt installed in central hole – δ = 0.5%, in crack apex – δ =0.35%; 3 – value of radial interference of bolt installed in center hole – δ = 1%, in crack apex – δ = 0.75%; 4 – value of radial interference of bolt installed in center hole – δ = 1.5%, in crack apex – δ = 1.1%

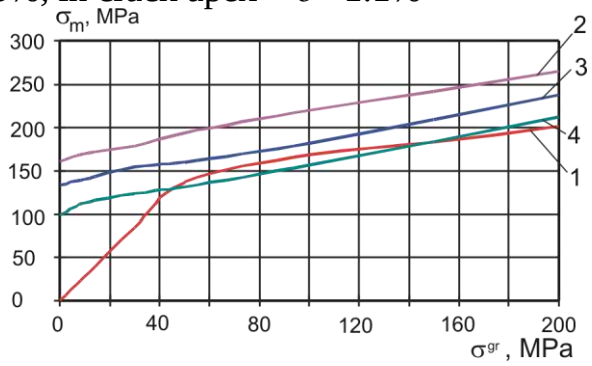

Fig. 7.29. Influence of loading level (σ^{gr}) on mean stress on hole edge (points A and A′) in cases: 1 – value of radial interference δ = 0%; 2 – the value of radial interference of bolt installed in center hole – δ =0.5%, in crack apex –δ = 0.35%; 3 – value of radial interference of bolt installed in center hole – δ = 1%, in crack apex – δ = 0.75%; 4 – value of radial interference of bolt installed in center hole – δ = 1.5%, in crack apex – δ =1.1%

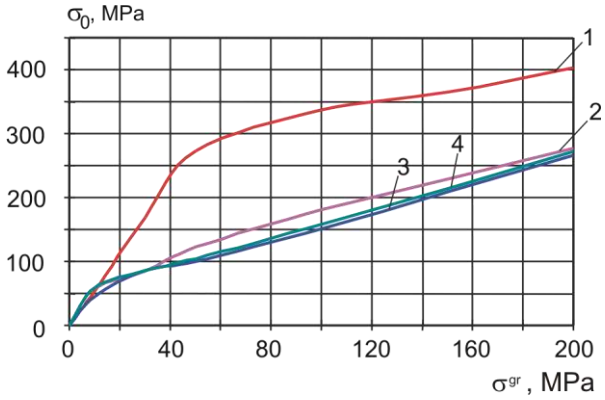

Fig. 7.30. Loading level influence(σ^{gr}) on stresses of equivalent zero-to-tension cycle σ_0 in cases:
1 – value of radial interference $\delta = 0\%$;
2 – value of radial interference of bolt installed in center hole – $\delta = 0.5\%$, in crack apex – $\delta = 0.35\%$; 3 – value of radial interference of bolt installed in center hole – $\delta = 1\%$, in crack apex – $\delta = 0.75\%$; 4 – the value of radial interference of bolt installed in center hole – $\delta = 1.5\%$, in crack apex – $\delta = 1.1\%$

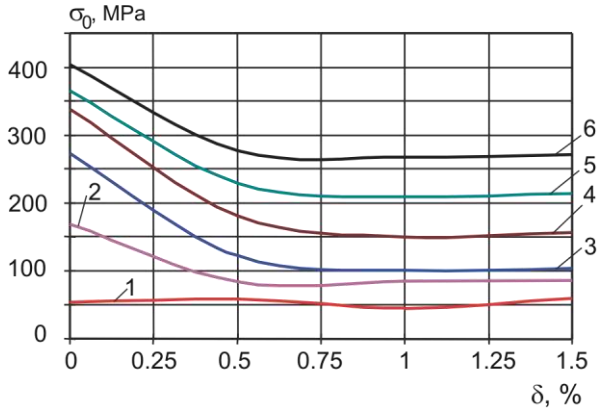

Fig. 7.31. Influence of radial interference value on stresses of equivalent σ_0 zero-to-tension cycle:

1 – $\sigma^{gr} = 10$ MPa;

2 – $\sigma^{gr} = 30$ MPa;

3 – $\sigma^{gr} = 50$ MPa;

4 – $\sigma^{gr} = 100$ MPa;

5 – $\sigma^{gr} = 150$ MPa;

6 – $\sigma^{gr} = 200$ MPa

Fig. 7.32. Influence of loading level (σ^{gr}) on maximum relative deformations: 1 – value of radial interference $\delta = 0\%$; 2 – value of radial interference of bolt installed in central hole – $\delta = 0.5\%$, in crack apex – $\delta = 0.35\%$; 3 – value of radial interference of bolt installed in central hole – $\delta = 1\%$, in crack apex – $\delta = 0.75\%$; 4 – value of radial interference of bolt installed in center hole – $\delta = 1.5\%$, in crack apex – $\delta = 1.1\%$

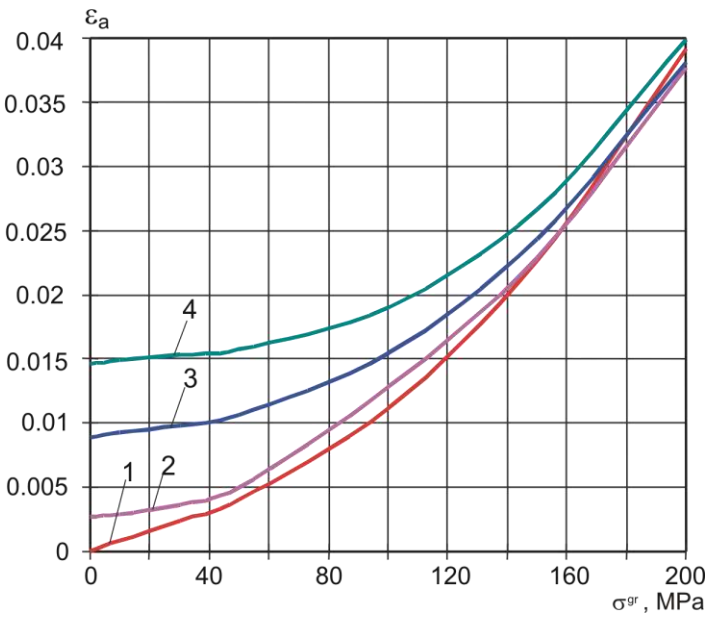

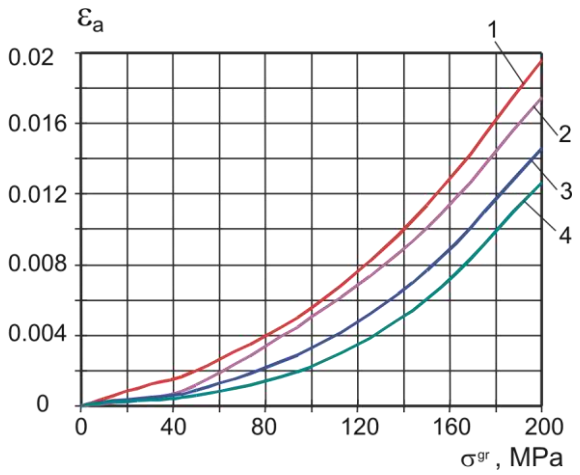

Fig. 7.33. Influence of loading level (σ^{gr}) on the amplitude of relative deformation in cases:
1 – value of radial interference δ = 0%;
2 – value of radial interference of bolt installed in central hole – δ = 0.5% in crack apex – δ = 0.35%;
3 – value of radial interference of bolt installed in central hole – δ = 1% in crack apex – δ = 0.75%; 4 – value of radial interference of bolt installed in center hole – δ = 1.5% in crack apex – δ = 1.1%

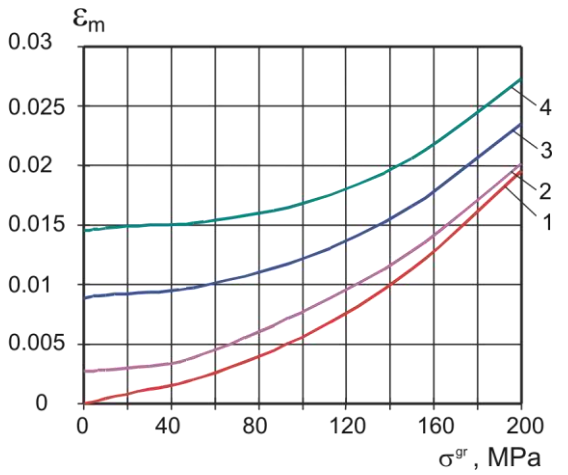

Fig. 7.34. Influence of loading level (σ^{gr}) on average relative deformation in cases:
1 – value of radial interference δ = 0%;
2 – value of radial interference of bolt installed in central hole – δ = 0.5% in crack apex – δ = 0.35%;
3 – value of radial interference of bolt installed in central hole – δ = 1% in crack apex – δ = 0.75%; 4 – value of radial interference of bolt installed in center hole – δ = 1.5% in crack apex – δ = 1.1%

Calculations are carried out for the 1, 2, 3 … 6 loading levels providing σ^{gr} = 10, 30, 50, 100, 150 and 200 MPa and for values of the axial interference providing σ_c =–55, –100, –190 MPa.

It is obtained that the installation of bolts with radial interference in crack apex promotes decrease of stress concentration coefficient at stress levels $\sigma^{gr} \le 100$ MPa in comparison with concentration coefficient in the plate with the unfilled holes by 7...15%. If the σ^{gr} stress is increased to 200 MPa, then the coefficients tally with the $K_{\sigma^{gr}} \approx 2$ and $K_{\sigma^{net}} \approx 1.7$ values.

Radial interferences of $\overline{\Delta}_{dA}$ = 1.5 % (along the bolt installed in central hole) and $\overline{\Delta}_{dB}$ = 1.1 % (along the bolt installed in hole in crack apex) at σ^{gr} =40...200 MPa reduce the maximum stress σ_{max} on hole contour by 20 … 40 %.

7.4. INTEGRATED FATIGUE CRACK GROWTH DELAY METHODS BY MEANS OF BOLTS INSTALLED IN CRACKS TIPS WITH RADIAL INTERFERENCE AND TIGHTENING

7.4.1. Influence of radial interference of bolt installed in crack apex on plates fatigue durability

To determine the efficiency of the radial interference as means of creating the residual stresses promoting crack growth delay, the experimental investigation of fatigue durability of plates different in width and thickness of aluminium alloys with cracks of different length in apexes of which the holes are made and the bolts with radial interference are installed in these holes.

Plates of the Д1АТ l. л. 2.5 aluminium alloy had B width equal to 200 mm in working portion. The fatigue crack, $2l_0 = 40 \pm 1$ mm long, was grown in plates from center concentrator applying uniaxial cyclic loadings with frequency f=10.2 Hz. The 5009A-6 bolts with the geometrical radial interference equal to 0, 1, 2 % of bolt diameter but without interference were pressed in the holes made in crack apexes. When bolts were installed, further fatigue tests of plates for N_{res} residual durability were carried out under the same cyclic loadings corresponding to σ_{max}^{gr}=100 MPa, σ_{min}^{gr}=40 MPa, σ_{max0}^{gr}=75 MPa to complete failure of plates.

Results of residual durability tests of plates of Д1АТ л.2.5 with crack of $2l_0$=40 mm are shown in Table 7.3.

Plates of В95пч АТ1СВ л. 5 alloy in working portion have width B = 240 mm. The crack 30 mm long was grown from centrally located concentrator. The holes in ∅6 mm were drilled in crack apexes, the «Joe»-bolts (ОСТ 1.11200-73) with radial interference were installed in these holes, then plates were tested for durability under the loadings corresponding to σ_{max}^{gr} = 134 MPa, σ_{min}^{gr} = 71 MPa, σ_{max0}^{gr} = 87 MPa to their complete failure. Residual durability test results of plates of В95пч АТ1СВ л. 5 are shown in Table 7.4. («Joe»-bolts with the radial interference installed in crack apexes).

The crack 35 mm long was being grown in plates made of Д16АТ л.2 alloy with width B=186 mm, and the 5009A-6 bolts without interference were installed in crack apexes. Then the fatigue tests of plates were being carried out at σ_{max}^{gr}=140 MPa, σ_{min}^{gr} = 85 MPa, σ_{max0}^{gr} = 82,2 MPa to failure.

Table 7.3

Test results on residual durability of plates of Д1АТ л. 2.5 with crack $2l_0$ = 40 mm long

N_i	Residual durability			
	Crack apexes are not drilled	Bolts with radial interference $\overline{\Delta}$		
		$\overline{\Delta} = 0$	$\overline{\Delta} = 1\%$ of bolt diameter	$\overline{\Delta} = 2\%$ of bolt diameter
N_1	9600	16700	27000	113400
N_2	10200	17300	31500	119700
N_3	11700	18100	35900	129200
N_4	12500	20600	43600	148200
N_5	13100	22800	57000	159500
N_{av}	11400	19100	39000	134000

Table 7.4

Test results on residual durability of plates of В95пч АТ1СВ л. 5

N_i	Residual durability			
	Crack apexes are not drilled	«Joe»-bolts with radial interference $\overline{\Delta}$		
		$\overline{\Delta} = 0$	$\overline{\Delta} = 1\%$ of bolt diameter	$\overline{\Delta} = 2\%$ of bolt diameter
N_1	2700	12000	82500	164900
N_2	2700	14100	65600	181700
N_3	2900	14600	51400	234500
N_4	3900	178000	53800	267500
N_5	4700	22600	46000	290500
N_{av}	3400	16200	59900	227800

Test results of on residual durability of plates made of Д16АТ л. 2 with the crack of $2l_0$ = 35 mm are shown in Table 7.5.

The influence of installation of «Joe»-bolts (∅6 mm, ОСТ 1. 1200-73) with radial interference in crack apexes $2l_0$ = of 30 mm long on residual durability of the plate made of Д16АТ л. 2 at σ_{max}^{gr}=134 MPa, σ_{min}^{gr}=71 MPa, σ_{max0}^{gr}=87.2 MPa was investigated.

Test results on residual durability of plates made of Д16АТ л. 2 are shown in Table 7.6.

The analysis of test results shows that the radial interference of bolt diameter of 1

% along the hole web made in crack apex has increased fatigue durability of plates of Д1АТ л. 2,5 in 2 times, plates from Д16АТ л. 2 – in 2.3 – 6 times, plates from В95пч АТ1СВ л. 5 – in 3.7 times. The radial interference increase to 2 % of bolt diameter has increased residual durability of the same plates in 7.0; 15.5 and 14.0 times accordingly.

Table 7.5

Test results on residual durability of plates made of Д16АТ л. 2 with crack of $2l_0$=35 mm

N_i	Residual durability	
	Bolt without interference	Bolt with interference 1 %
N_1	5800	12300
N_2	5900	13700
N_3	6300	15200
N_4	6800	16300
N_5	7100	17500
N_{av}	6400	15000

Table 7.6

Test results on residual durability of plates made of Д16АТ л. 2

N_i	Residual durability			
	Crack apexes are not drilled	Bolts with radial interference $\overline{\Delta}$		
		$\overline{\Delta}=0$	$\overline{\Delta}=1\%$ of bolt diameter	$\overline{\Delta}=2\%$ of bolt diameter
N_1	4700	12300	60700	182500
N_2	5400	12800	78100	206600
N_3	5500	13400	87800	210000
N_4	5900	15600	95500	233500
N_5	6300	16900	11600	268400
N_6	6900			
N_{av}	5800	14200	87600	220200

So, it is possible to delay the crack growth and essentially to increase residual durability of plates with cracks by means of installation the bolts with two-sided and one-sided accesses with the radial interference equal to 1 – 2 % in the holes made in crack apexes.

7.4.2. Influence of nuts tightening on the bolts installed in crack apexes on fatigue durability of plates

The experimental investigation of fatigue durability of plates with center crack, in tips of which the bolts with axial interference of nuts are installed, was carried out to reveal the efficiency of nut tightening as a means of creating residual stresses, fastening of the crack edges, creating friction forces preventing crack opening and in whole as means of crack growth delay with apexes drilled.

Fatigue tests were carried out on specimen of plates with width of 200 mm made of Д1АТ л. 2,5 material. The 0.6 mm holes of were made in apexes of the initial center crack $2l_0$ = 40 mm long and the 3315А-6-К bolts were installed along the H9/h8 sliding fit with axial interference of 3315А-6-К nuts corresponding to M_{torq} = 0, 5, 8 N·m. The 3401 А-1.5-5-12 washers were installed under the nuts and bolt heads.

Tests were carried out at σ_{max}^{gr} =100 MPa, σ_{min}^{gr} = 40 MPa, σ_{max0}^{gr} = 75 MPa.

Test results of influence of interference on residual durability of plates made of Д1АТ л. 2,5 are shown in Table 7.7.

Table 7.7

Influence of interference on residual durability of plates made of Д1АТ л. 2,5

N_i	Residual durability		
	M_{torq} = 0	M_{torq} = 5 N·m	M_{torq} = 8 N·m
N_1	16700	107000	214700
N_2	17300	130800	231200
N_3	18100	158400	238300
N_4	20600	176500	353500
N_5	22800	192600	389000
N_{av}	19100	153100	285300

The analysis of test results shows that the nut tightening has increased the residual durability of plates with center crack in 8 times at M_{torq} = 5 N·m and in 15 times at M_{torq} = 8 N·m for bolts in ∅ 6 mm.

7.4.3. Influence of tensile loading under action of which the fasteners are installed in crack apexes on plates residual durability

Efficiency of radial interference of fasteners in plates with cracks can be increased in case of the holes made in crack apexes and fasteners installed in these holes if the static loads acting on the plate and opening the crack. This loading is removed only after installation of fasteners. Applying on structure with crack the tensile static loads which open the crack while the holes are made on the crack ends and the fasteners are installed in these holes promotes that at the next cyclic

loading of structure the crack opening and as consequence increasing of the hole diameter in direction loading action does not lead to considerable reduction of the radial interference because the material is already deformed in crack apexes by static loading and the round hole executed in the elastodeformed material is filled by the rod of the fastener.

The experimental investigation of efficiency of this method of fasteners installation in crack apexes has been carried out on uniaxially loaded plates with width of 280 mm made of Д16АТ л. 2 with two lengths of the center cracks: $2l_0$=30 and 58 mm.

After growing, the crack has been grown for one of the specified lengths the plate was loaded with static loading of 0, 5, 75 kN stretching the crack that corresponds to σ_{stat}^{gr} = 0, 9, 134 MPa. The holes, ∅6 mm, were made in crack apexes under load and the bolts made of BT-16 titanic alloy were installed in these holes with 1 % geometrical radial interference. The further fatigue tests were carried out under cyclic loadings σ_{max}^{gr} = 134 MPa, σ_{min}^{gr} = 71 MPa, σ_{max0}^{gr}=87.2 MPa.

Test results of determining the influence of stress level opening the crack with bolt installation on residual durability of plates are shown in Table 7.8.

Table 7.8

Influence of stress level on residual durability of plates

Length of Initial Crack $2l_0$	N_i	Residual Durability		
		σ_{stat}^{gr} = 0	σ_{stat}^{gr} = 9 MPa	σ_{stat}^{gr} = 134 MPa
30	N_1	29300	180000	271600
	N_2	36000	194000	298000
	N_3	39800	203200	302700
	N_4	42800	205300	312800
	N_5	49000	210500	324000
	N_{av}	39400	198600	305400
58	N_1	8900	15800	136900
	N_2	9700	16000	144700
	N_4	13100	16700	172300
	N_5	13400	17400	191300
	N_{av}	11400	16400	158500

The analysis of fatigue test results shows that the application to plates of the static loading equal to the maximum cycle loading during the process of making holes in apexes of the centrally located crack and installation of bolts in these holes with 1 % radial interference have increased plates residual fatigue durability in 8 – 14 times.

7.4.4. Ways of fatigue cracks growth delay by installing the fasteners with the elastoplastic radial interference and tightening in their area

Industrial FCGDMs are developed on the basis of carried out investigations:

– installation of the fasteners with radial interference and axial interference in the holes made in crack apexes (Fig. 7.35);

– loading of structure area with the crack prior to making the holes in crack apexes by the tensile and opening effort to crack and the effort is removed after installation of fasteners in the holes with radial interference and axial tightening;

– number of holes performed along the crack length where consecutively the fasteners with elastoplastic radial interference and their subsequent axial tightening are installed from the middle of crack length to its apex inclusively.

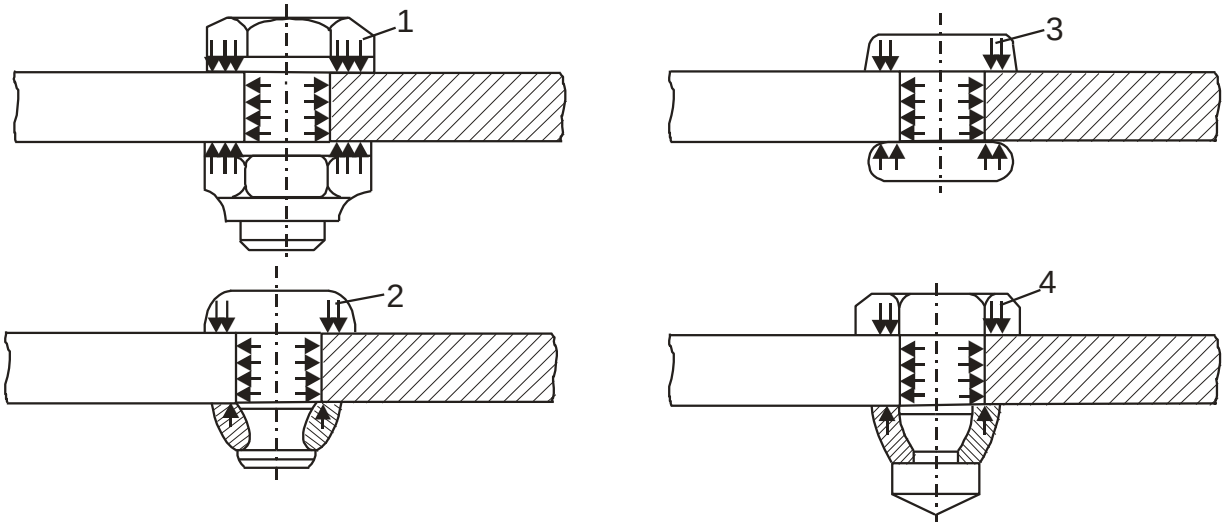

Fig. 7.35. Fatigue cracks growth delay methods:
1 – bolt with two washers and nut; 2 – bolt-rivet; 3 – rivet; 4 – «Joe»-bolt

Efficiency of the industrial FCGDMs developed for the radial interference and tightening obtained during installation of standard fasteners according to serial assembly technique using the standard drilling and countersinking tool which are applied in aircraft industry and the equipment and also devices for bolt press-in, tightening of nuts on bolts, formations of snap rivet heads etc. was investigated.

Experimental investigations of efficiency of the first of developed industrial specifications are carried out on the plates made of Д1АТ л. 2,5, Д16АТ л. 2, Д16АТ l. 5 and В95пч АТ1СВ л. 5 aluminium alloys.

The holes, $\varnothing\ 5.95^{+0.02}_{-0.0}$ mm in dia., were made in apexes of center cracks and the 5009А-6-К bolts with radial interference $1.2^{+0.0}_{-0.2}$ % of bolt diameter were

pressed in the obtained hole and the 3315A-6-K nuts were tightened to M_{torq}=8 ±0.8 N·m. The 3404A-1,5-6-12 washers are installed under bolt heads and nuts. Efficiency of the first way of crack growth delay of the at installation in crack apexes of rivets (OCT 1. 34040-79) was investigated. Snap heads depth is 0.3-0.4 d_{riv}.

Test results on plate residual durability after the industrial specification application are shown in Table 7.9 to 7.12.

Table 7.9

Residual durability of plates made of Д1АТ л. 2,5 (B = 200 mm) with the center crack

N_i	Residual durability		
	Holes ∅ 6 mm	Holes, 5009A bolts with 1% radial interference and tightening M_{torq} = 8 N·m	Holes, rivets (6-9-OCT 1. 34040-79)
N_1	16700	249500	393300
N_2	17300	376800	483300
N_3	18100	414300	520200
N_4	20600	543200	541700
N_5	22800	531700	
N_{av}	19100	423000	484400

Table 7.10

Residual durability of plates made of Д16АТ л. 2 (B = 186 mm) with the center crack ($2l_0$ = 35 mm)

N_i	Residual durability	
	Holes ∅ 6 mm	Holes, the 5009A bolts with 1% radial interference and tightening M_{torq} = 8 N·m
N_1	5800	271000
N_2	5900	247800
N_3	6300	302800
N_4	6800	311 700
N_5	7100	374600
N_{av}	6400	301600

Table 7.11

Residual durability of plates made of Д16АТ л. 2 (B=280 mm) with the center crack ($2l_0$ = 30 and 58 mm)

Length of initial crack $2l_0$, mm	N_i	Residual durability	
		Holes ∅ 6 mm	Holes, the 5009A bolts with 1% radial interference and tightening M_{torq} = 8 N·m
30	N_1	4700	365100
	N_2	5400	366300
	N_3	5500	416700
	N_4	5900	494 100
	N_5	6300	
	N_6	6900	
	N_{av}	5800	410600
58	N_1	5700	100900
	N_2	6300	101300
	N_3	6500	105000
	N_4	7000	111000
	N_5	8300	126200
	N_6	–	134000
	N_7	–	136200
	N_{av}	6800	116400

Table 7.12

Residual durability of plates made of Д16АТ л. 5 and В95пч АТ1СВ л.5 (B = 240 mm) with the center crack ($2l_0$ = 30 mm)

Specimen material	N_i	Residual durability	
		Holes ∅ 6 mm	Holes, the 5009A bolts with 1% radial interference and tightening M_{torq} = 8 N·m
Д16АТ л. 5	N_1	26700	303600
	N_2	27100	352100
	N_3	28000	37500
	N_{av}	27300	343600
В95п.ч. Т1СВ Л. 5	N_1	12000	276000
	N_2	14100	281800
	N_3	14600	290500
	N_4	17800	308200
	N_5	22600	339900
	N_{av}	16200	299200

The values of residual durability (σ_{max}^{gr} = 100 MPa, σ_{min}^{gr} = 40 MPa) of plates made of Д1АТ л. 2,5 (B = 200 mm) with the center crack are given in Table 7.9; the residual durability (σ_{max}^{gr}=140 MPa, σ_{min}^{gr}=85 MPa) of plates made of Д16АТ л. 2 (B=186 mm) with the center crack ($2l_0$=35 mm) are given in Table 7.10; the residual durability (σ_{max}^{gr}=134 MPa, σ_{min}^{gr}=71 MPa) of plates made of Д16АТ л.2 (B=280 mm) with the center crack ($2l_0$ = 30 and 58 mm) are given in Table 7.11; the residual durability (σ_{max}^{gr}= 134 MPa, σ_{min}^{gr} = 71 MPa) of plates made of Д16АТ л.5 and В95п.ч. АТ1СВ л.5 (B = 240 mm) with the center crack ($2l_0$ = 30 mm) are given in Table 7.12.

Experimental investigations of efficiency of the second of the developed industrial specification are carried out on plates made of Д16АТ л.5 and В95пч АТ1СВ л. 5 with the center located cracks.

When the holes were made in crack apexes the plate was loaded with static tensile efforts σ_{stat}^{gr} = 0, 40, 60, 120, 180, 210 MPa which open the crack and were removed after installation of ∅6 mm fasteners of with 1 % radial interference and tightening. The 5009А-6-К bolts with the 3315А-6-К nuts and the 3404А-1, 5-6-12 washers or ∅6 mm «Joe»-bolts, (18-ОСТ 1.11200-73) were used as fasteners. The holes, $\varnothing 5.9^{+0.02}_{-0.0}$ mm dia., were made under «Joe»-bolts, $\varnothing 5.98^{+0.0}_{-0.02}$ mm dia.

Fatigue tests results of plates on residual durability are shown in Table 7.13 and 7.14.

The values of plates residual durability made of Д16А-Т л.5 (B = 240 mm) with the center crack ($2l_0$ = 30 mm) at σ_{max}^{gr} = 134 MPa, σ_{min}^{gr} = 71 MPa are given in Table 7.13; the values of plates residual durability made of В95пч АТ1СВ л.5 (B=240 mm) with the center crack ($2l_0$=30 mm) at σ_{max}^{gr}=134 MPa, σ_{min}^{gr}=71 MPa, f = 10.2 Hz are given in Table 7.14.

Table 7.13

Residual durability of the plate made of Д16АТ л. 5 (B = 240 mm) with the center crack ($2l_0$= 30 mm)

N_i	Residual durability		
	5009А bolts with 1% radial interference and tightening M_{torq} = 8 N·m		
	σ_{stat}^{gr} = 0	σ_{stat}^{gr} = 60 MPa	σ_{stat}^{gr} = 180 MPa
N_1	303600	672400	2032400
N_2	352100	799800	2692700
N_3	375000	847500	3355600
N_{av}	343600	733200	2693600

Table 7.13 to be continued

N_i	«Joe»-bolts, ∅6 mm n dia., (18-OCT 1. 11200 -73) with 1% radial interference and tightening				
	σ_{stat}^{gr} = 0	σ_{stat}^{gr} = 40 MPa	σ_{stat}^{gr} = 60 MPa	σ_{stat}^{gr} = 120 MPa	σ_{stat}^{gr} =180 MPa
N_1	67000	73200	101300	795000	2907600
N_2	67100	83600	106200	921500	3465800
N_3	80000	112800	167600	939000	5729500
N_{av}	71400	89900	125000	885200	4034300

Table 7.14

Residual durability of plates of В95пч АТ1СВ л.5 (В=240 mm) with the center crack ($2l_0$= 30 mm)

N_i	Residual durability					
	5009A-6 bolts with 1% radial interference and tightening M_{torq} = 8 N·m					
	σ_{stat}^{gr} = 0	σ_{stat}^{gr} = 40 MPa	σ_{stat}^{gr} = 60 MPa	σ_{stat}^{gr} = 120 MPa	σ_{stat}^{gr} = 180 MPa	$\sigma_{cm}^{бр}$ =210 MPa
N_1	276000	491800	495400	537500	817900	978500
N_2	281800	532000	511 200	783100	1030000	1034000
N_3	290500	582 100	680300	783100	1146800	353200
N_4	308200					
N_5	339900					
N_{av}	299200	535500	562300	747400	998200	1121900
N_i	«Joe»-bolts, ∅6 mm in dia., (18-OCT 1. 11200-73) with1% radial interference and tightening					
	σ_{stat}^{gr} = 0	σ_{stat}^{gr} = 40 MPa	σ_{stat}^{gr} = 60 MPa	σ_{stat}^{gr} = 120 MPa	σ_{stat}^{gr} = 180 MPa	
N_1	46000	60300	92200	368900	1344500	
N_2	51400	63500	97500	406700	668600	
N_3	53800	83900	141800	535100	12246000	
N_4	65600	100000	153600		3076900	
N_5	82500	106700	169200			
N_{av}	60000	83300	130800	436900	2084000	

The dependence of plate durability with the center cracks on the tensile static loadings opening the crack and applying when the hole is made in crack apexes and with installation of fasteners with radial interference and tightening (It. 1 – for 5009A bolts; 2 – for OCT 1. 11200-73 bolts) is shown in Fig. 7.36.

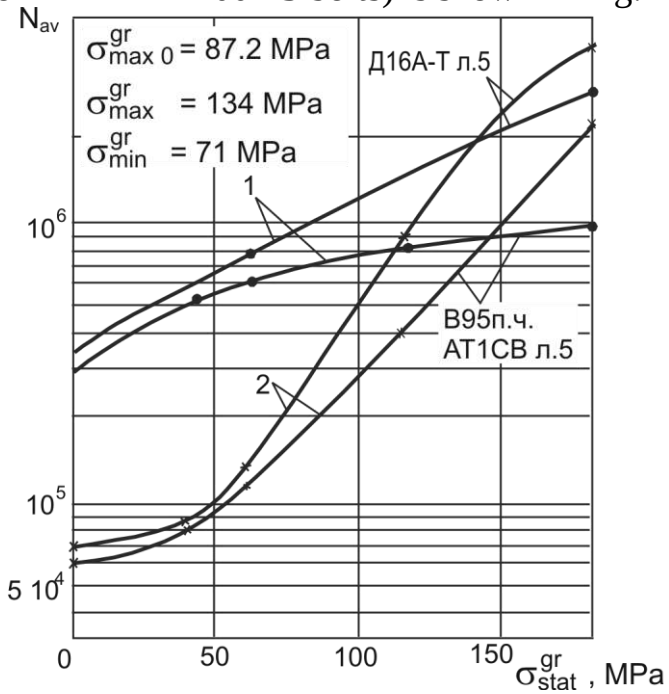

Fig. 7.36. Influence of tensile static loading opening the crack on durability of plates with center cracks

The experimental investigation of efficiency of the third of the developed ways is carried out on plates made of Д16АТ л.2 with working portion of 280 mm in width, at initial length of fatigue crack $2l_0$ = 30 mm, under loadings corresponding to σ^{gr}_{max}=141 MPa, σ^{gr}_{min} = 75 MPa and at frequency f = 10.2 Hz. The holes, ∅5.5 mm in dia., were drilled in crack apexes; two holes, $\varnothing 5.8_{-0.01}$ mm., were carried out on distances of 6 mm from the crack middle then the bolts in ∅6.08 mm with radial interference (without tightening) were pressed in these holes.

Holes in crack apexes were reamed to ∅5 mm and then bolts, ∅6.08 mm in dia., were pressed in these holes (without tightening).

The residual durability of plates at installation of fasteners along crack length is given in Table 7.15.

The analysis of test results shows the following.

Application of the industrial specification developed consisting of installation of fasteners, ∅6 mm in dia., with radial interference of 1 % of bolt diameter and tightening M_{torq} = 8 N·m in hole in crack apexes increases residual fatigue durability of plates made of Д1АТ л. 2,5 – in 22-25.3 times, Д16АТ л. 2 – in 47-71 times, Д16АТ л. 5 – in 12.6 times and В95пч АТ1СВ л. 5 – in 18.5

times in comparison with durability of plates with the center crack where the holes, ∅6 mm in dia., are made in its apexes.

Table 7.15

Residual durability of plates at fasteners installed along crack length

FCGDM method	N	N_{av}	$K_{res.d}$
Holes in ∅6 mm are made in crack apexes	12300 13400 16900	14200	1
Bolts with interference in 1% of bolt diameter are installed in holes of crack apexes	29300 39800 49000	39400	2.8
Bolts with interference in 1% of bolt diameter are installed in holes of crack apexes at σ_{stat}^{gr} = 140 MPa	271600 302700 342000	305400	21.5
Bolts in ∅6.08 mm with interference of 4% of bolt diameter are installed along crack length and bolts in ∅6.08 mm with interference in 2% of bolt diameter are installed in tips	183500 246900 213400 278100 308800	246 100	17.3

Application of FCGDM (Fatigue Cracks Growth Delay Method) consists of static tensile stress of plates, for example, to σ^{gr} = 180 MPa by efforts opening the crack while making the hole in crack apexes and installation of fasteners with radial interference and tightening in these holes increases residual durability of plates made of Д16АТ л. 5 and В95пч АТ1СВ л. 5 accordingly in 7.8 and 3.7 times while using the 5009A-C bolts and while using the «Joe»-bolts, ∅6 mm, increases in 56 and 34.7 times at the investigated levels of cyclic loadings in comparison with durability of plates in which crack growth is prevented only by installation of fasteners with radial interference and tightening without preliminary loading.

Application of the FCGDMs consisting in consecutive fasteners installation with radial interference in the holes made along crack length increased residual fatigue durability of plates of Д16АТ л. 2 in 17.3 times in comparison with durability of plates with drilled cracks apexes.

Application of the FCGDMs consisting in installation of fasteners with radial interference and axial interference in the holes made along crack length is preferable when two-sided access to structure area with the crack is available.

Application of the FCGDMs including the loading by static tensile efforts opening the crack with installation of fasteners with radial interference and

tightening in the holes made in crack apexes is expediently both at two-sided and one-sided access to structure area with a crack.

7.4.5. Influence of the fatigue cracks growth delay method on fatigue durability of plates with the with installing repair straps

Fatigue tests of plates of Д16АТ л. 2 are carried out (Fig. 7.37) to estimate the efficiency of applying the FCGDM developed during the installation of rectangular repair straps by means of rivets and the following variants of the cracks growth delay have been investigated:

– crack apexes are not drilled (Fig. 7.37, a);
– holes, ∅6 mm in dia., are made in crack apexes (Fig. 7.37, b);
– installation of bolts of the 5009A-6 type with 1% radial interference and tightening M_{torq} = 8 N·m in holes made in crack apexes (Fig. 7.37, c);
– installation of the strap bevelled across width and bolts with radial interference and tightening in the holes made in crack apexes (Fig. 7.37, d). Straps were made of Д16АТ л. 2 sheet.

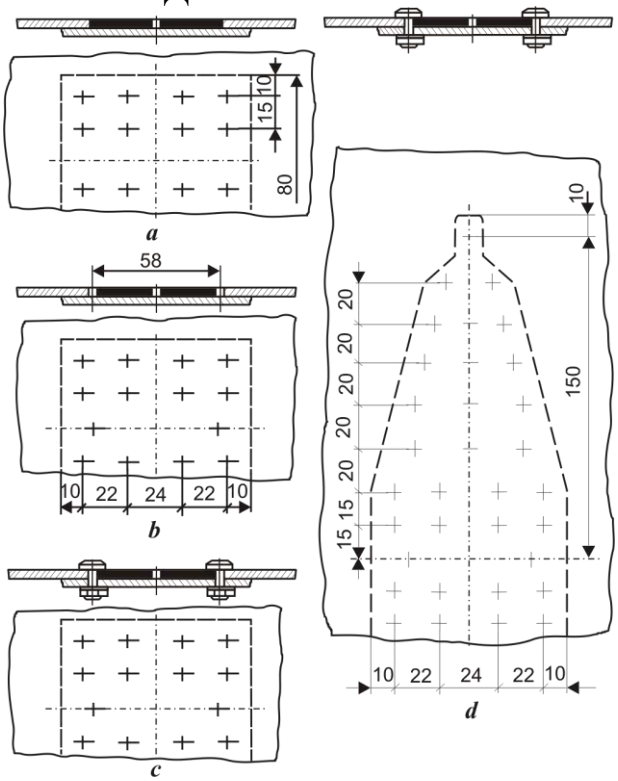

Fig. 7.37. Ways of fatigue cracks growth delay by installation of repair straps

Rectangular straps of 90×80×2 size were attached to the plate damaged by crack with rivets 5-10 (ОСТ 1. 34040-79) and the straps beveled across width of 310×90×2 size – with 4-9 (ОСТ 1. 34040-79) rivets. Riveting was carried out on the КП-204М press.

Fatigue tests results for residual durability (σ_{max}^{gr} = 134 MPa, σ_{min}^{gr} = 71 MPa) of plates of Д16АТ л. 2 (B = 280 mm) with the center crack ($2l_0$ = 58 mm) and straps are shown in Table 7.16.

The analysis of test results shows that installation of bolts with radial interference equal to 1% of bolt diameter and axial interference M_{torq} = 8 N·m in the holes made in crack apexes in the presence of the riveted repair straps has increased residual durability of plates with the center crack more than twice in comparison with durability of plates with straps and drilled tips. So it is expedient to install fasteners with radial interference and tightening in the holes made in crack apexes when installing repair straps in area of thin-walled structures with the crack.

Table 7.16

Residual durability of plates of Д16АТ л. 2 (B = 280 mm) with center crack ($2l_0$ = 58 mm) and straps

N_i	Residual durability of plates			
	Rectangular strap			Strap beveled across the width
	Crack without hole	Crack and hole ∅6 mm	Crack and holes filled with bolt with radial interference and tightening	Crack and hole filled with bolt with radial interference and tightening
N_1	46900	90900	179500	270300
N_2	47300	92200	188900	275300
N_3	49200	93000	205000	282 700
N_4	49300	94800	205900	343300
		96700	207600	393000
N_{av}	48200	93500	197400	313000

To attain further increase of fatigue durability of the damaged plate-to-repair straps joint expediently by unloading the fasteners of extreme rows on the strap by their installation with the clearance in the strap and with radial interference in the plate with crack [22, 102, 355, 356, 362, 375, 401].

To investigate the efficiency of installing the extreme row fasteners with clearances in the strap by fatigue durability increase criterion of joint with repair strap when applying of the industrial specification the specimens are designed and made (Fig. 7.38). In plates 4 with width of the working section of B = 280 mm in the МУП-50 hydraulic pulsator the fatigue crack 7 of 58 ±1 length mm was grown from the center concentrator (type B) by means of the uniaxial cyclic loadings $P_{\max}/P_{\min}$=75/40 [kN]. Then the 3501А-4-9 rivets were installed in the

holes, ∅$5.05^{+0.1}$ mm, made in crack apexes. The repair strap 2 was attached to the plate with the same rivets. The 3501A-4-9 (OCT 1. 34040-79) rivets were installed in extreme rows and the strap was installed with У-ЗОМЭС-5 sealant (It. 3, Fig. 7.38) and without it. The depth of snap heads of all rivets was carried out equal to half the nominal diameter of their shank d_{riv}. The exception was the rivets installed in crack apexes using the У-ЗОМЭС-5 sealant.

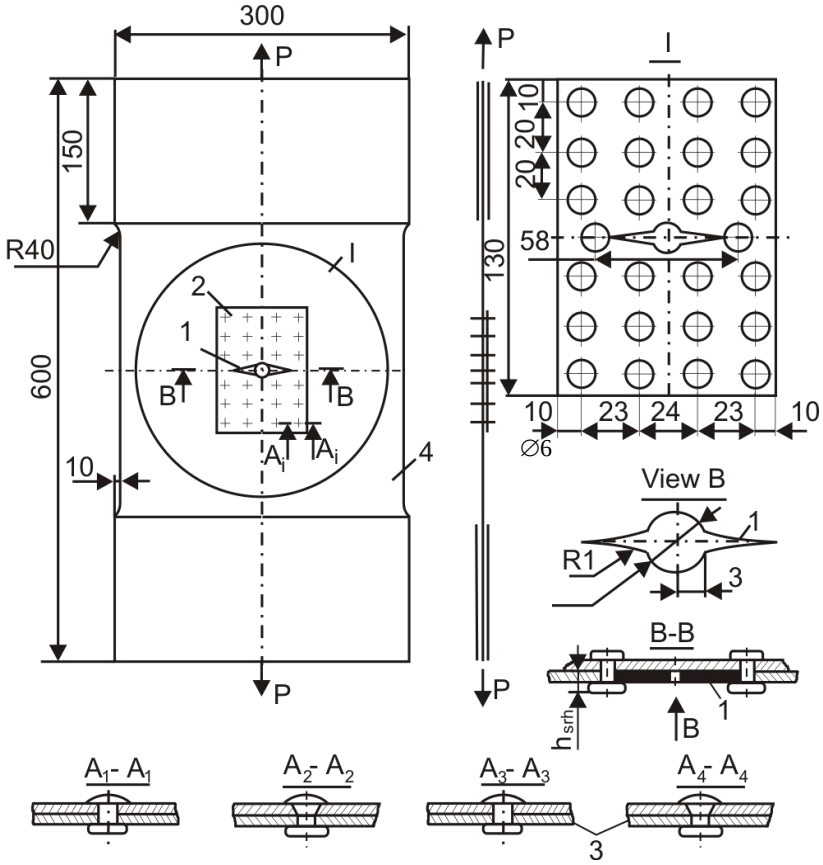

Fig. 7.38. Specimen of panel with center crack

The depth of snap heads of these rivets was equal to 0.5 and 0.3 the nominal diameter of the shank.

Rivets of the extreme row in section A-A of the second variant of performance (Fig. 7.39) of joint specimens were installed with the clearance in holes in the strap which provides drilling out the holes in the strap to ∅5 mm. The further fatigue tests of plates for residual durability under the same cyclic loadings were carried out when the repair straps and rivets in crack apexes were installed. Fatigue tests results for residual durability plate-to-repair strap joint and with repair strap with У-ЗОМЭС-5 sealant are given in Table 7.17 and 7.18.

Basically the plates have been damaged in area of extreme row rivets fastening the repair strap. The exception was the plates where the rivets in depth h_{srh} equal to 0.5 nominal diameter of the shank were installed in crack apexes and the rivets have been damaged in section of the plate along the axis of preliminary grown cracks.

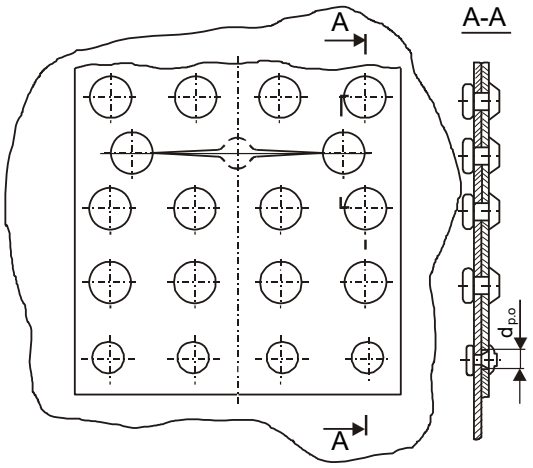

Fig. 7.39. Fragment of panel with the center crack in repair strap installation area

Table 7.17

Residual durability of plate-to-repair strap joint

N_i	Residual durability (extreme row rivets)	
	without clearances in strap	with clearances in strap
N_1	93700	456000
N_2	191400	458600
N_3	213800	560100
N_4	221200	609700
N_5	352800	706200
N_{av}	214600	558100

Table 7.18

Residual durability of plate-to-repair strap with У-ЗОМЭС-5 sealant

N_i	Residual durability (extreme row rivets)		
	without clearances in strap		with clearances in strap
	$h_{srh} = 0.5\ d_{riv}$	$h_{srh} = 0.3\ d_{riv}$	$h_{srh} = 0.3\ d_{riv}$
N_1	194100	212900	319700
N_2	194200	381 100	550900
N_3	202 100	399500	734500
N_4	208800	402300	814200
N_5	212200	411200	850100
N_{av}	202300	361400	653900

The result analysis of fatigue tests shows that at application of FCGDMs and installation of rivets of extreme row with the clearance in the strap the fatigue durability of connections with the repair strap which was determined by skin fatigue durability in area of this row increases in comparison with joint fatigue durability where the rivets are installed without the clearance on average in 1.8 times using the У-ЗОМЭС-5 sealant at performance of h_{srh}, equal to 0.3 of a shank diameter and in 2.6 times without sealant.

It is recommended to make $d_{dh} = 1.3 d_{riv}$ based on the experimental investigation of rivet shanks expansion according to pack height of the connected parts for rivets, ∅3-5 mm, unriveted by the press and manually and in the

presence of У-ЗОМЭС-5 sealant and without it unloading holes on mated surfaces and providing the clearance between extreme row rivet shanks and hole webs in straps.

7.4.6. Influence of fatigue cracks growth delay method on durability of riveted panel specimens

Efficiency of fatigue cracks growth delay methods were investigated on specimens of stringer panels (Fig. 7.40).

The panel consists of 1 skin and 2 strengthening strap of Д16АТ л.2, 4 two stringers and 3 gusset of the Д16Т Пр113-4 profile. Joint of skin with gusset, stringers and the strengthening strap was carried out by countersunk rivets, ∅4 mm in dia. (ОСТ 1. 34052-85).

Extreme rows of the strengthening strap-to-skin joint were carried out with rivets, ∅4 mm in dia. (ОСТ 1. 34052-85 or ОСТ 1.34040-79). Extreme row rivets were installed both with interference according to whole thickness of the pack and with interference in the skin and clearance in strengthening strap.

To provide the clearance between the shanks of unriveted rivets and hole webs the extreme row holes in straps were made ∅5.2 mm.

Riveting was carried out on the КП-204М press.

Fatigue tests were carried out on the МУП-5 hydraulic pulsator with maximum cyclic loading $P_{\max}$ = 9800 daN (σ^{gr}_{maxp} = 128 MPa in regular panel area) of frequency f = 10.5 Hz and coefficient of cycle asymmetry r = 0.53 until the visible fatigue cracks in length from 5 to 50 mm appear on the skin surface.

Cracks appeared in skin along the extreme row of its connection with the strengthening strap or in area of connection of skin with gusset and also in skin in regular area of its connection with stringer.

Repair of specimens were carried out to increase the panels durability, to obtain as many cracks as possible and to reveal the fatigue failure areas and also to investigate the efficiency of the industrial specification. Repair of skin-to-strengthening strap joint was made both by means of straps and without them but three rivets were installed in crack apex (Fig. 7.41, D-D section).

Snap rivet heads attaching the strengthening strap were cut flush with skin surface when the repair straps 1 were installed on the skin from the outside of stringer set. The repair rivets 2 in area of main rivets were installed with centre in points along perimeters of set rivet heads of installed during initial assembly and minimum removed from the lateral axis of the specimen.

Repair of skin-to-gusset and stringers joint was carried out by means of the repair straps installed on skin from the outside of the countersunk rivet heads. Repair rivets in area of the main rivets were installed with the centre on perimeters of set heads of the rivets installed in initial assembly in the points as much as possible remote from the cross-section axis of the specimen.

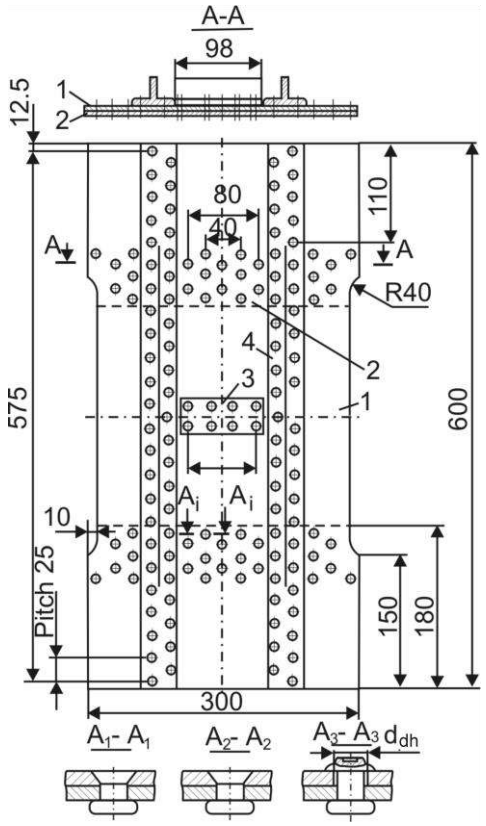

Fig. 7.40. Specimen of stringer panel

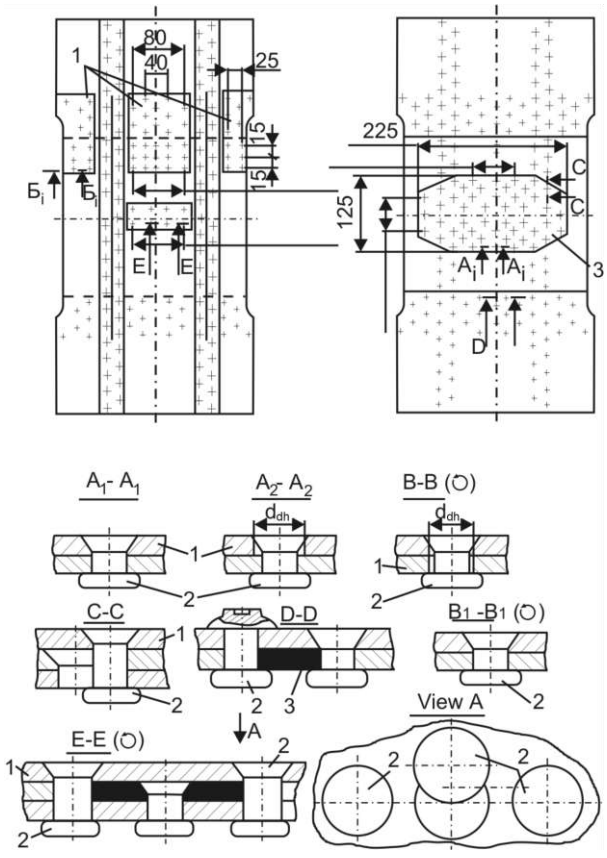

Fig. 7.41. Repair methods for stringer panels

Crack growth was delayed by installing rivets in crack apexes (OCT 1. 34052-85) d_{nom} = 4 mm and along its length on perimeters of set rivet heads from which fatigue cracks developed (Fig. 7.41, view A).

Extreme rows of rivets on repair straps was installed according to serial technology with interference along whole thickness of the pack of connected members (Fig. 7.41, A_1-A_1 section) or with interference in the skin and with the clearance in straps (Fig. 7.41, A_2-A_2, B_1-B_1 sections). The holes in repair straps, ∅5.2 mm, provided the clearance.

After repair, the tests were carried out by the same parameters of cyclic loading.

From two to seven fatigue cracks were obtained on one panel when fatigue cracks were delayed by developed ways resulted in the information increase of fatigue tests of panels.

Fatigue tests results of for durability before occurrence of cracks in the skin in extreme row area of its connection with strengthening straps in area of its connection with gusset and with stringer in the regular area, in extreme row area of its connection with repair straps, and also influence of the FCGDM on residual durability of repair variants of stringer panel are given in Table 7.19 – 7.22.

Table 7.19

Residual durability before occurrence cracks appear in the skin extreme row area of its connection with strengthening straps

N_i	Residual durability		
	Rivet (OCT 1. 34052-85) (Ref. Fig. 7.41)		Rivet (OCT 1. 34040-79) with unloading hole (A_3-A_3 section)
	without unloading hole (A_1-A_1 section)	with unloading hole (A_2-A_2 section)	
N_1	80000	106600	279600
N_2	87900	120 700	279600
N_3	89900	150600	337 100
N_4	89900	158800	337 100
N_5	91300	170200	
N_6	114000	209000	
N_7	118200	234800	
N_8	140600	248800	
N_9	150600	248900	
N_{10}	160000	266200	
N_{11}	160000	266200	
N_{12}	186700		
N_{13}	186700		
N_{av}	127 400	198300	308 100

Table 7.20

Residual durability before occurrence of cracks appear in the skin in area of its connection with gusset and stringer in regular area

N_i	Durability before crack occurrence	
	in gusset area	in stringer area
N_1	114000	127600
N_2	126200	241600
N_3	251000	300100
N_4	281400	
N_{av}	193200	223 100

Table 7.21

Residual durability before occurrence of cracks in the skin in extreme rows area of its connection with repair straps

N_i	Residual durability		
	4-11 rivet (OCT 1.34040-79)	Repair strap and rivet (OCT 1. 34052-85) in ∅4 mm	
	in crack apex	in crack apex	along the length and in crack apex
N_1	12300s	18300s	65300s*
N_2	12300s	18700g*	104900s*
N_3	39000s	65200s*	148800s*
N_4	39000s	65200s*	173600s*
		65200s*	200500s*
		110500g*	
		149500s	
		157100s	
N_{av}	30 100	81200	138600

Note. * – panel failure is not along the axis of the crack pointed by the FCGDM; cracks in the skin in area of its connection with the strengthening strap and gusset accordingly – «s», «g».

Table 7.22

Influence of industrial specifications on residual durability of repair variants of stringer panel

N_i	Residual durability			
	Strap in gusset area		Strap in strengthening straps area	
	without unloading hole	with unloading hole	without unloading hole	with unloading hole
N_1	100000	190400	65200	26700*
N_2	122000	190400*	65300	35000*
N_3	125600	-	104900	148800*
N_4	125600	-	155100	49500*
N_5	127600	-	171300	1193400*
N_6	129600	-	191300	232400*
N_7	129600	-	282600	
N_8	-	-	286500	
N_9	-	-	291800	
N_{av}	122900	190400	179300	131600*

Note. * – Specimens have been damaged on skin not in extreme row area on the repair strap.

The analysis of fatigue test results shows that skin repair of stringer panel with installation of repair straps promotes to durability increase of stringer panel in 1.7 – 2.1 times in comparison with its durability before occurrence of cracks.

Novelty of the developed fatigue cracks growth delay methods in thin-walled aircraft structures (Fig. 7.42) by installation of fasteners with radial interference and axial tightening in the holes made in tips, along length and in crack area including installation of repair strap is confirmed by inventors certificate. Technical efficiency of these ways is shown in Fig. 7.43.

Efficiency of fatigue cracks growth delay methods was estimated by value of coefficients of increase residual ($K_{res.d}$), relative ($K_{rel.d}$) and total (K_{fd}) fatigue durability.

The analysis testifies that the application of the developed methods of growth delay increases the residual fatigue durability aircraft structural members in 10 … 80 and more times and the total fatigue durability is approximately doubled.

Installation of bolts with radial interference and axial tightening in holes made in crack apexes

A.C. 725862

Loading of structure by static effort opening the crack. Effort is removed after installation of bolts with radial interference and axial tightening in holes made in crack apexes

A.C. 1054006

Opening and fastening of crack edges with the bolts installed in series with radial interference in holes made along crack length beginning from crack middle point

A.C. 1374670

Installation of wedge fastener in hole made in crack apex

A.C. 1165552

Making the holes in crack apexes and near crack edges and installation of fasteners in the holes with radial interference and axial tightening

A.C. 1191247

Attaching the repair strap with fasteners shifted from their centers according to "battle" filled holes along panel tension direction and with radial interference and axial tightening in the panel and strap but with clearance in strap along the hole in crack apex

A.C. 1516287

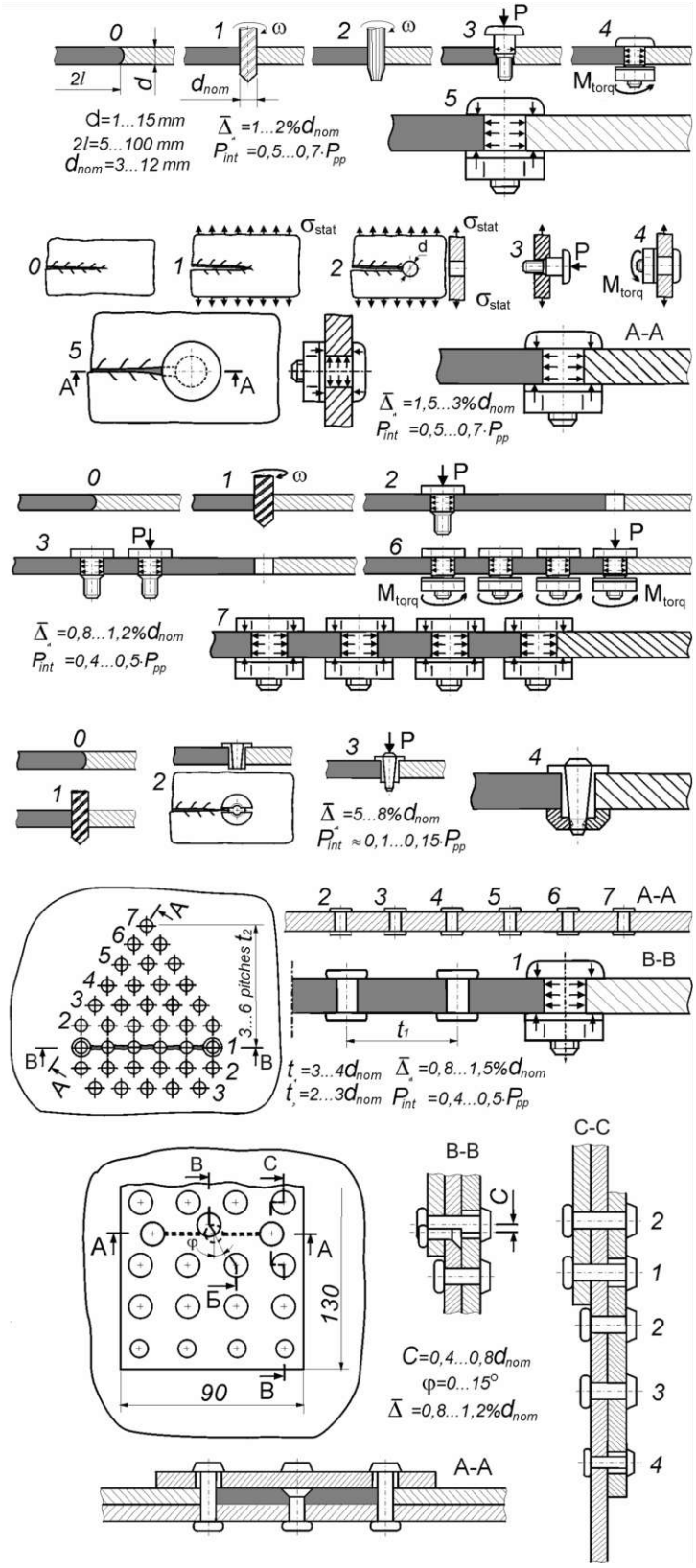

Fig. 7.42. Integrated ways of delay of growth of fatigue cracks in structures by installation of fasteners: 1, 2, 3, 4, 5, 6, 7 – number of the main technology steps of establishment of fasteners in area of fatigue crack

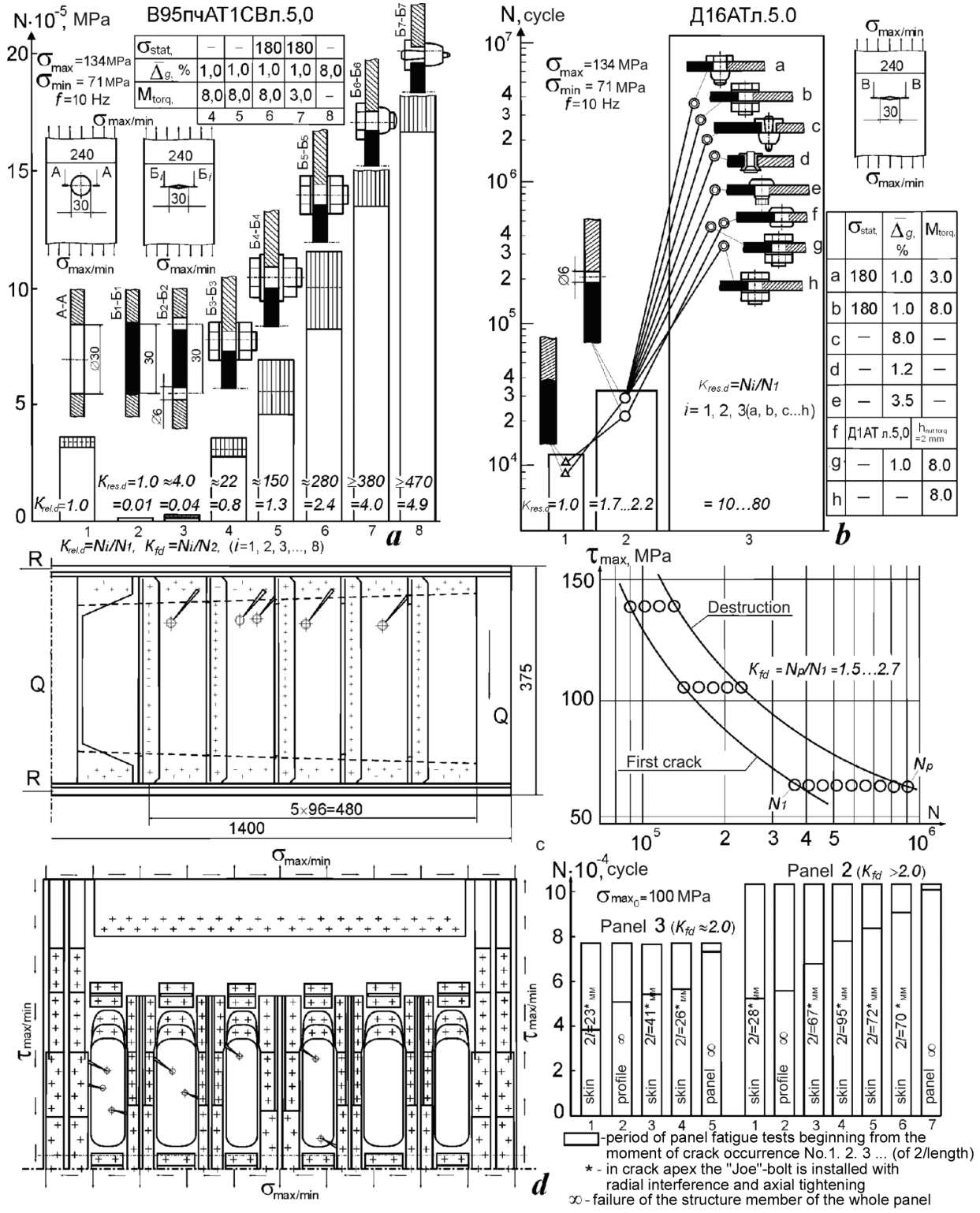

	σstat,	Δ̄g, %	Mtorq,
a	180	1.0	3.0
b	180	1.0	8.0
c	—	8.0	—
d	—	1.2	—
e	—	3.5	—
f	Д1АТ л.5,0	$h_{nut\ torq}$ =2 mm	
g	—	1.0	8.0
h	—	—	8.0

Fig. 7.43. Efficiency of fatigue cracks growth delay methods by installation of fasteners with radial interference and tightening:
a, b – under fatigue tests of the uniaxially loaded plate specimens and made of В95п.ч. АТ1СВ л5,0 and Д16АТ л5,0 aluminum alloys; c, d – under fatigue tests of specimens of full-scale spar sections and panels in wing box system correspondingly

7.5. CONSTRUCTIVE-TECHNOLOGICAL METHODS OF THE SERVICE LIFE PROLONGATION OF RIVETED JOINTS OF SPAR WEBS

The analysis of fatigue failures of aircraft structures in operation and under full-scale tests shows that fatigue cracks occur in web-to-cap joint of the assembled spar.

It is necessary to provide the static durability, rigidity, tightness and set fatigue durability of the damaged structure when the repair work is carried out. Repair straps are traditionally installed on the main frames of the structure damaged by the fatigue crack. The analysis of methods of strap parameter choice and technology of their installation [337] shows that questions of designing, manufacturing and joining of repair straps were basically considered according to providing conditions of the structure static durability.

It should be noted that modern aircraft spars have considerable extent and great number of the same concentrators. Fatigue crack occurrence in a spar web is possible long before exhaustion by the structure of its service life according to the hypothesis of "weak link" [376]. In this case it is necessary to repair local area, and so the actuality of repair procedures development and experimental ground increases efficiency.

Durability experimental researches of web repair area damaged by the fatigue crack were carried out on the specimens of spar sections modeling its separate sections, structure, manufacturing techniques and their loading conditions [178].

On the basis of the analysis of spar structures and proceeding from possibilities of the МУП-50 test machine the following initial parameters for designing the specimen are set: Д16АТВ material, σ_{ult} = 435 MPa; E = 70600 MPa; ν =0,3; lateral force in reference section is Q_{rs} = 120 kN; effective building height of web is H_{eff} = 320 mm; section length is L = 700 mm.

Designing the specimen was carried out according to techniques stated in works [7, 222, 434].

The general view of one console of the specimen is shown in Fig. 7.44.

Specimen caps are of variable cross-section area to obtain constant stress field along the section length of web-to-tensile cap joint. They are assembled and consist of the Д16Т Пр-315-9 Т-section profile and rhomboid straps of the Д16АТ л.5 sheet made by mechanical milling along the contour and joined by the ОСТ 1.31180-80 bolts.

The web is made by mechanical milling along the contour of the Д16АТВ л.2 sheet material. The longitudinal axis of a web coincides with direction of rolling fibers.

Stiffing racks of the constant section area on length are made by mechanical milling of the Д16Т-Пр111-3 profile.

The surface roughness corresponding to *Rz*40 is provided under mechanical treatment of all components. All components are anodized with «HX» according to the serial technology in compliance with OCT 1.90055-85.

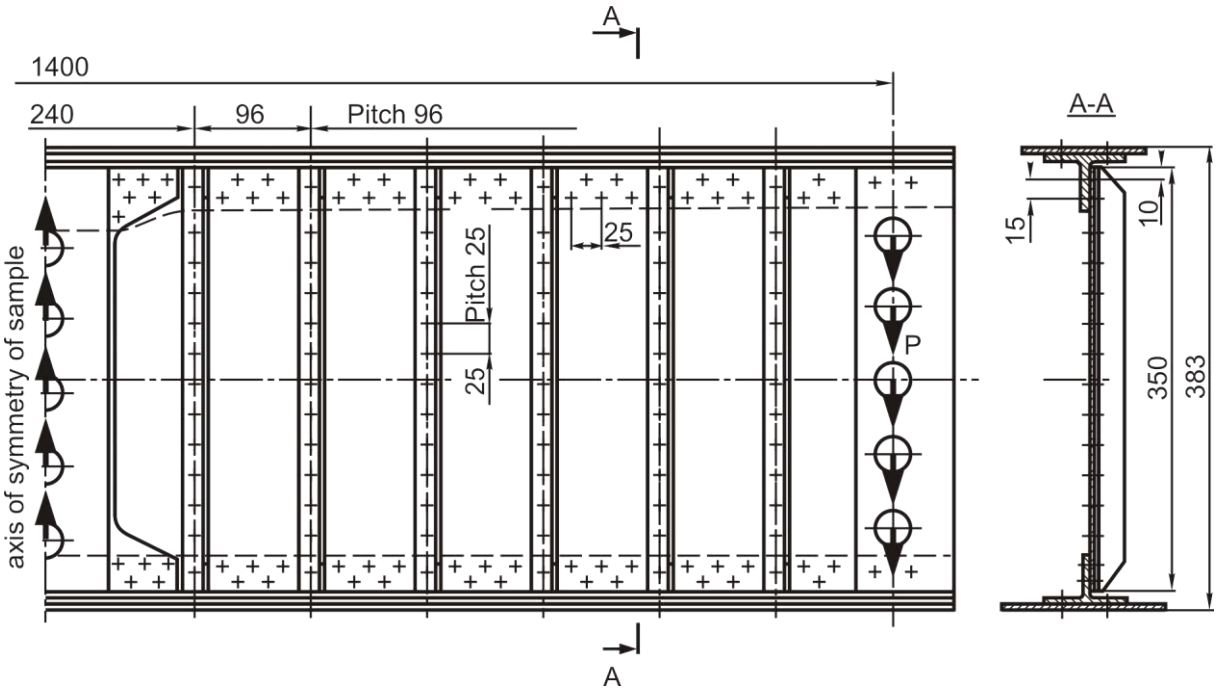

Fig. 7.44. One console of the specimen of the spar sections

The web-to-tensile cap joint is double-row with fasteners of chess board order location. The OCT 1.34040-79 rivets, 5 mm in dia., are applied, the rivets in 6 mm dia. are applied in area of connection of the web and stiffing rack with the tensile cap. All holes were drilled for fasteners in the web using the jig and further they were used as guides to drill the holes in caps, racks and straps. Holes were drilled out and reamed in common to reach the sizes of 5.1 H7 and 6.1 H7 for rivets both 5.0 H7 and 6.0 H7 for bolts of 5 and 6 mm in diameter according to the surface roughness of *Rz* 1.25. The hole edges were chamfered 0.3×45°.

Single riveting was carried out on the КП-204М pneumopress according to the ОПИ-412-74 instruction and the bolt installation and nut tightening were carried out according to OCT 1.00017-77.

Fatigue tests were carried out on the МУП-50 hydraulic pulsator at cyclic loadings with loading frequency f = 5.25 Hz, constant coefficient of cycle asymmetry R = 0,53 and maximum loading on two consoles P_{max} = 170 kN.

The fatigue cracks in the web appeared under cyclic loadings from holes of the first row of web-to-tensile cap edge connection. Cracks developed perpendicularly to a direction of the main tensile stress action in a web, i.e. at an angle of 45 – 60 ° to the longitudinal axis of the spar. Character of fatigue crack propagation is shown in Fig. 7.45. Propagation of consistently appearing fatigue cracks appearance in the web was stopped by installing fasteners with radial

interference and axial tightening in their apexes. The stop of fatigue crack growth by the specified way allowed to increase the test duration of specimens of spar sections in two and more times and in addition to reveal the areas of probable fatigue failure.

To prevent the crack growth it is necessary to install the fasteners with the guaranteed radial interference and axial tightening in the crack apex. However there is no compensation of decrease in static durability of the structure and tightness of structural spar portion with the crack in a web is not restored. It is necessary to note that at multiseat failure the occurrence of new cracks in other areas of longitudinal joint of the spar web occurs through 10 – 20 % of durability before the occurrence of the previous crack [435] that demands repeated performance of repair work.

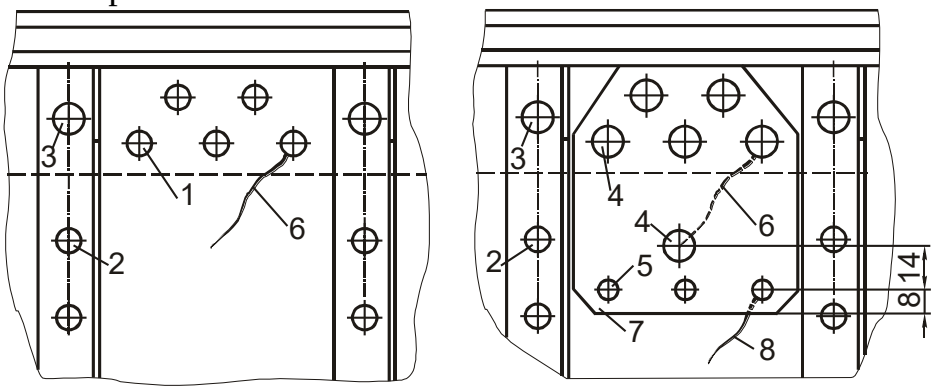

a b

Fig. 7.45. Character of the fatigue crack distribution in spar web before (a) and after (b) attaching the repair strap:
1 – 5-14-OCT 1.34040-79 rivet; 2 – 5-10-OCT 1.34040-79 rivet;
3 – 6-18-OCT 1.34040-79 rivet; 4 – 6-18-OCT 1.11857-76 bolt;
5 – 4-9-OCT 1.34040-79 rivet; 6 – initial fatigue crack;
7 – repair strap; 8 – secondary fatigue crack

To reinforce the web in the crack area the repair straps were installed. The strap was attached both using the holes available in a structure for rivets in which fasteners were replaced with repair ones, and installation of additional rivets. The fastener installed in crack apex, also connected strap with a web in the package.

The repair strap (versions are shown in Fig. 7.45 and 7.46) was made of Д16АТВл.2 sheet. Sizes of a strap were assigned using crack length, value of supporting upright pitch, width of the web-to-cap and web-to-strap joints.

During installing strap the rivets of 5 mm in dia. connecting a web with a cap were removed and replaced with bolts OCT 1.11857-76 of 6 mm in dia. In a crack apex the bolt OCT 1.11857-76 was also installed. An axial interference of a pack was carried out with 3302A nuts under which 3401A washers are installed. An opposite edge of a strap was attached to a web using rivets OCT 1.34040-79,

4 mm in dia. Holes were drilled and reamed in a pack according to series production technology, except for a hole for the fastener installed in a crack apex.

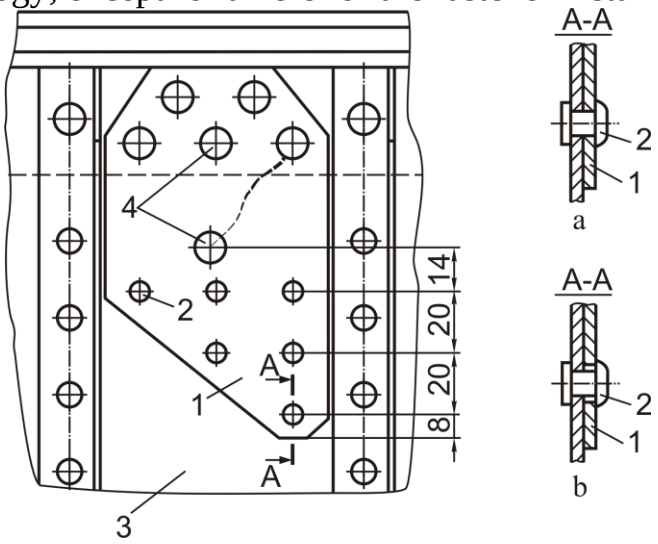

Fig. 7.46. Structure of a repair strap and versions of its attachment to to web according to conventional (a) and to offered production technology (b): 1 – repair strap; 2 – rivet 4-9 OCT 1.34040-79; 3 – spar web; 4 – bolt OCT 1.11857-76, 6 mm in dia

Efficiency of structurally-technological solutions of a web segment repair was evaluated by the following coefficient

$$k = N_{total} / N_{mp},$$

where N_{fric} and N_{full} – number of loading cycles before crack detection and up to specimen failure after repair accordingly.

Fatigue tests results of specimens of spar sections with a repair strap (Ref. Fig. 7.45, b) show that durability of a repair area was increased only in 1.27 times. Thus fatigue cracks in a web originated from holes for rivets of a single-shear joint of a strap with a web. Thus, attachment of a repair strap to a web using one row of the loaded fasteners installed by conventional production technology is ineffective.

In the following version of a web repair strap is of trapezoidal form. A large diagonal of a trapezium was disposed in the direction of main tensile stresses in a web. Rivets (4-9 OCT 1.34040-79) a strap-to-web joint were disposed in three rows (Ref. Fig. 7.46). In this case the rivet of the last (third) row of a web-to-strap joint was installed both according to the series production technology (Ref. Fig. 7.46, a), and with clearance in a strap and with interference in a web according to the work [369] (Ref. Fig. 7.46, b).

In so doing, the increase of fatigue life in a repair area in 1.45 times is achieved by using of standard production technology of riveting (Ref. Fig. 7.46, a) and in 1.62 times – during installation of rivets with clearance in a strap and with interference in a web (Ref. Fig. 7.46, b).

Fatigue cracks originated in the first case from the last row holes, and in the

second case – from holes of the first or second rows of fasteners (practically equiprobably). It should be noted that cases of growth renewal of the stopped crack or origination of fatigue cracks in other places in a repair area were not observed.

As in the case of installing the rivet with a clearance in a strap and interference in a web the greater effect was achieved, then the version of a strap under repair of the web-to-cap joint analogous to shown in Fig. 7.46 was investigated, in which all additional rivets attaching a spar web-to-repair strap joint are installed by such production technology. After combined preparation of all holes a strap was removed and its holes for rivets of 4 mm in dia. and the bolt installed in a crack apex (6 mm in dia.), were drilled out to diameters of 5 and 7 mm accordingly. While installing the bolts on a place of removed rivets in the web-to-cap joint a radial interference was ensured across all thickness of a pack.

It is necessary to note, that installation of fasteners with a clearance in a strap and with interference in a web does not reduce static strength of the web-to-strap joint as under loads close to breaking ones due to deformation of joint members the clearances are decreased and all fasteners are involved in taking up loads.

It has been found that efficiency of the proposed repair version is much higher. While testing of specimens new fatigue cracks origination in a repair area is not registered. Specimen failure of specimens occurred due to fatigue cracks originated in gripping parts of a specimen and growth of which was not delayed effectively. The effectiveness ratio calculated at the moment of a specimen failure reaches the value $k = 2$.

In Fig. 7.47 the diagram of effectiveness ratios for different structurally – technological repair versions is shown.

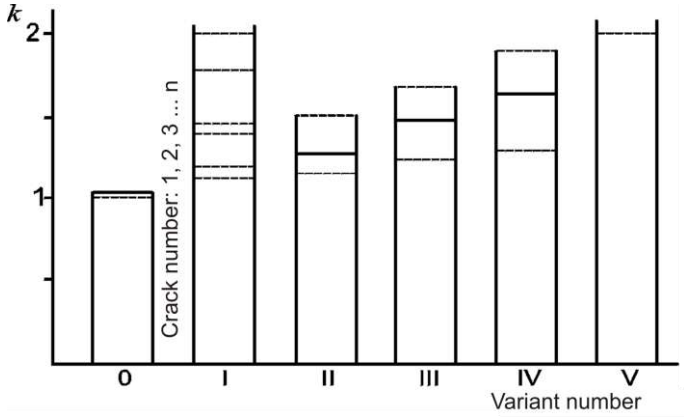

Fig. 7.47. Efficiency of repair versions in the first crack area:
0 – without repair; I – fasteners are installed in apexes of first and subsequent cracks with radial interference and axial tightening; II – fastener and rectangular strap are installed in a crack apex. Strap is attached to the web with rivets located in one row (Ref. Fig. 7.45, b); III – fastener and trapezoidal strap are installed in a crack apex (Ref. Fig. 7.46, a); IV – fastener and trapezoidal strap are installed in crack apex (Ref. Fig. 7.46, b); the rivet of the extreme row of joint is installed with interference in a web and clearance in a strap; V – fastener and trapezoidal

strap are installed in crack apex, a strap is analogous to one shown in Fig. 7.46, all rivets of the joint are installed with interference in a web and a clearance in a strap

Experimental investigations of structurally-technological repair versions of a spar segment structure with fatigue cracks in a web have shown, that with setting a fastener with radial and axial interference in a crack apex the spar web segment with a crack is effectively reinforced with a repair strap, the joint with web of which is made by the rivets installed with a clearance in a strap and with radial interference in a web. Application of the researched structurally-technological provisions allows to prolong service life of the segment of the longitudinal joint of spar webs damaged by a fatigue crack more than in 2 times.

7.6. CONCLUSIONS

1. New structurally-technological fatigue cracks growth delay methods and ways by installing fasteners in crack apexes and along crack length with an axial tightening and radial interference are considered. Their novelty is confirmed with inventor's certificates.

2. By means of ANSYS system the influence of a crack length and level of external load on the holes ovality and the local mode of deformation in structural members with a fatigue crack has been investigated.

The selection technique of the secured radial interference value has been offered in view of the holes ovality made in a crack fatigue tips.

3. The analysis of influence of an axial tightening and radial interference of the bolts installed in holes made in a fatigue crack apexes, on characteristics of the local mode of deformation of the plates has been carried out. It is shown that tightening reduces stress concentration in 1.3 … 2.8 times, and radial interference reduces a range of stress from zero cycle in a hole zone in a crack apexes in 1.9 … 3 times.

4. Efficiency of offered fatigue cracks growth delay methods is experimentally investigated. It is established that application of offered fatigue cracks growth delay methods ensures increase of durability of assembly aircraft structures not less than in 2 times. Offered ways and methods have been implemented in industry that has allowed to prolong service life of the airframe structural members during service life tests and in process.

Section 8

IMPLEMENTATION OF DEVELOPED METHODS OF INTEGRATED DESIGN AND STRUCTURALLY – TECHNOLOGICAL SOLUTIONS INTO THE THEORY AND PRACTICE OF CREATION OF ASSEMBLY AIRCRAFT STRUCTURES USING CAD/CAM/CAE INTEGRATED SYSTEMS

In KhAI the international training center on learning CAD/CAM/CAE systems is created with the direct participation of the author. The complex of hardware and software of the center is shown in Fig. 8.1 and includes laboratories of UNIGRAPHICS system, Compass, ADEM and AutoCAD CAD\CAM systems, the engineering analysis laboratory with the help of ANSYS system, laboratories of the engineering linguistics, open information production engineering, preparation of aeronautical publications, and also technical and software support. The author is a research supervisor during 30 years of studies in the department of applied-research laboratory of attachments of aircraft structures of the heightened service life equipped with the complex of test, assembly and measuring, and also machinery permitting to produce on factory production technology and carry static and fatigue tests of assembly members and aggregates of aircraft structures (Fig. 8.2). Thus, in KhAI the author has directly participated in creation and manages the complex ensuring experimental and theoretical researches on development and introduction the methods of the integrated design of assembly aircraft structures.

The scheme of implementation of results of activity is shown in Fig. 8.3.

Methods presented in this work of integrated design of assembly aircraft structures and new structurally-technological solutions offered on their basis were developed, confirmed by calculation and experiment in KhAI during carrying out combined researches with KSAMC, Antonov ASTC, TsAGI, Tupolev ASTC, UkrNIIAT, "Normal" association and other organizations of Ukraine and CIS for 30 years. In process of their development they were introduced into the theory and practice of creation of assembly aircraft structures at the aviation enterprises and for support of the educational process on training of aviation specialists in the Kharkov aviation institute.

Implementation of method of forming the geometry and analytical standard of assembly aircraft structures

The method of creation of geometry and analytical standard of assembly aircraft structures with the help of CAD/CAM/CAE/PLM systems on base of the unified computer measurement standard of the aircraft external surface, described in Section 2, is implemented while designing and creating AN-74TK-300, AN-140, AN-148 aircraft. The method ensures creation of the analytical standard of a surface which is initial for all further process of design and preproduction. This results in accuracy of aircraft geometry, high external surface quality and reduction of terms and the cost of preproduction. Specimens of executed analytical standards of aircraft are shown in Fig. 8.4.

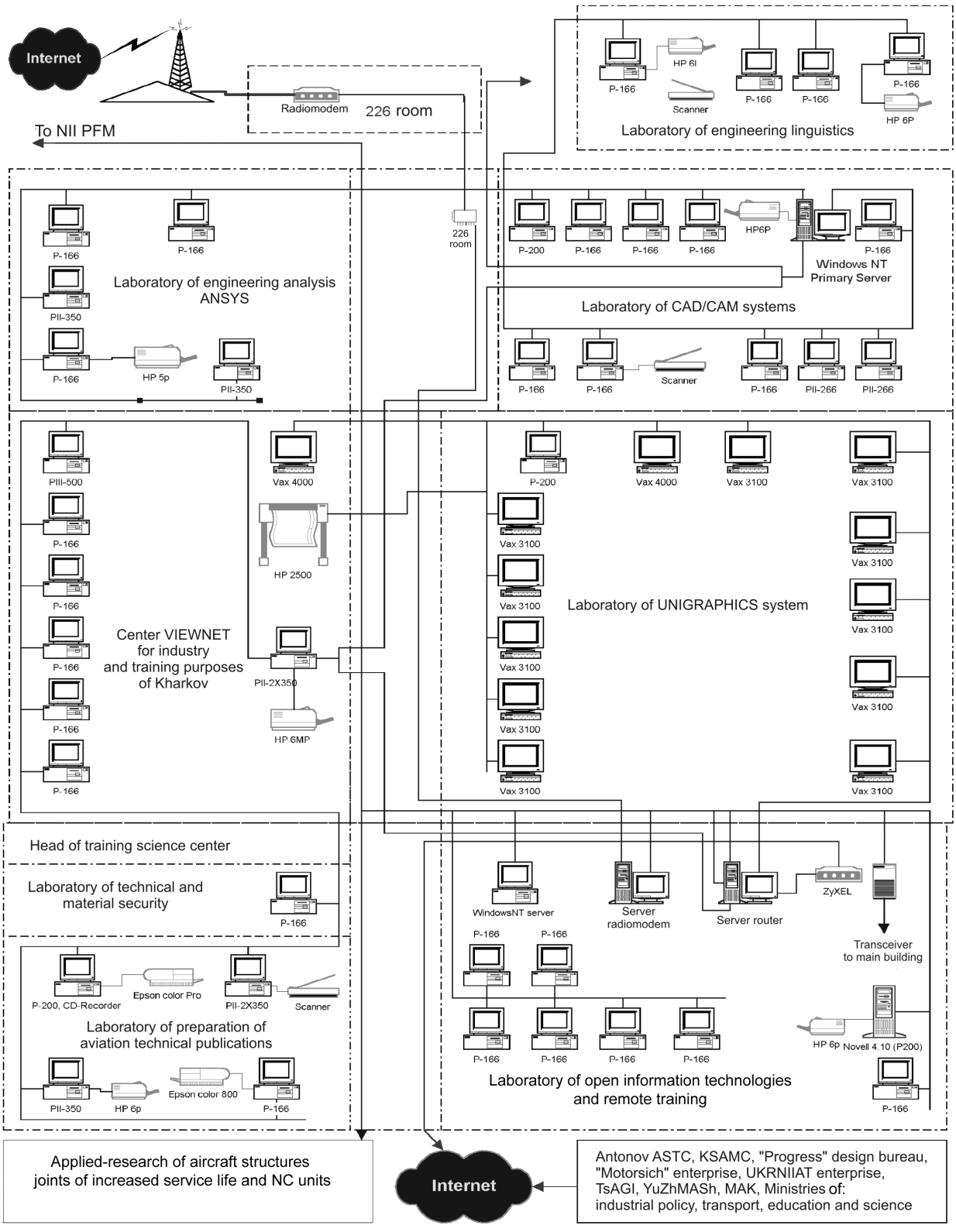

Fig. 8.1. Complex computer facilities and software of integrated design of assembly aircraft structures of regulated durability

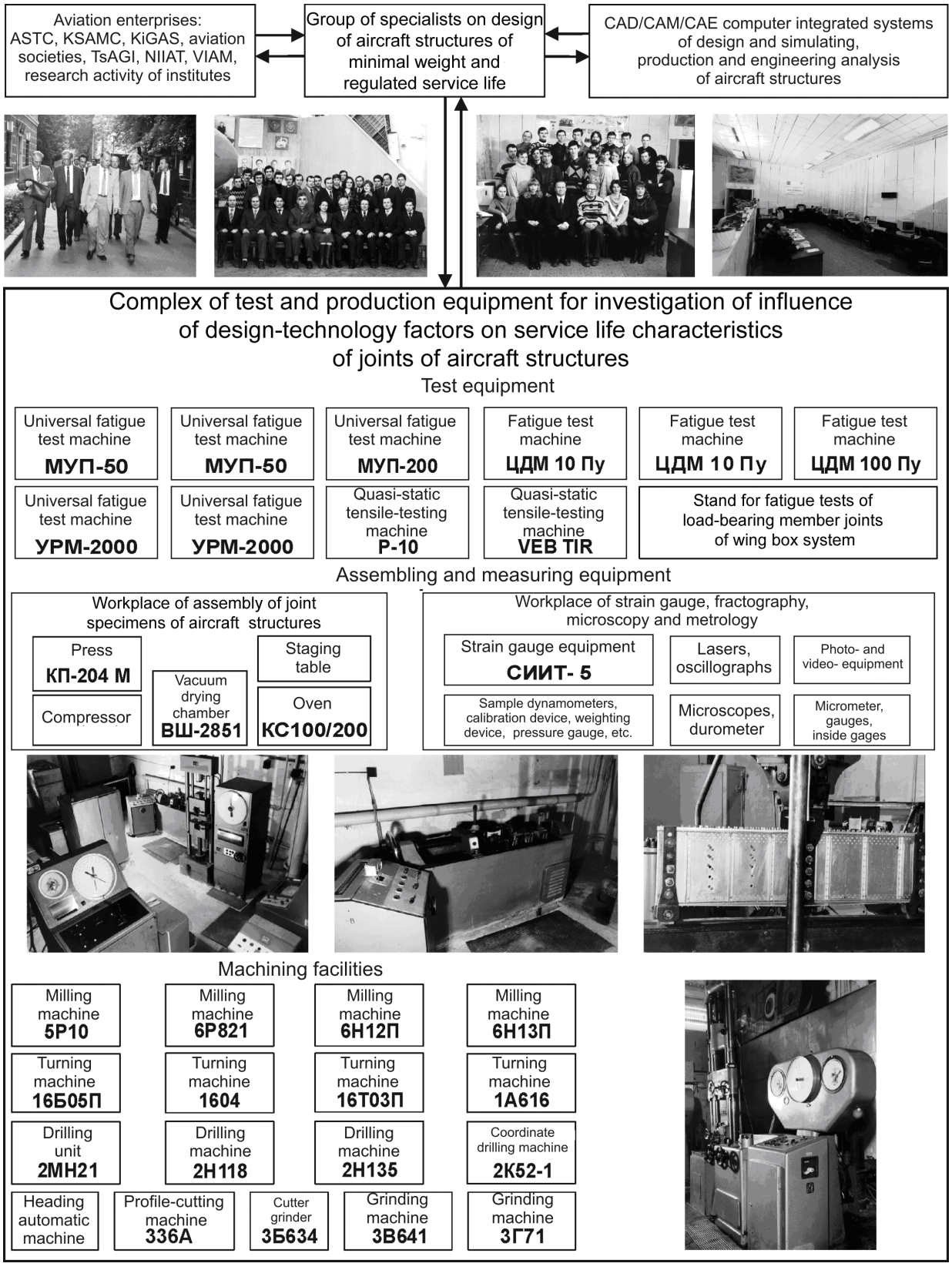

Fig. 8.2. Structure of resources for integrated design of aircraft structures of regulated durability

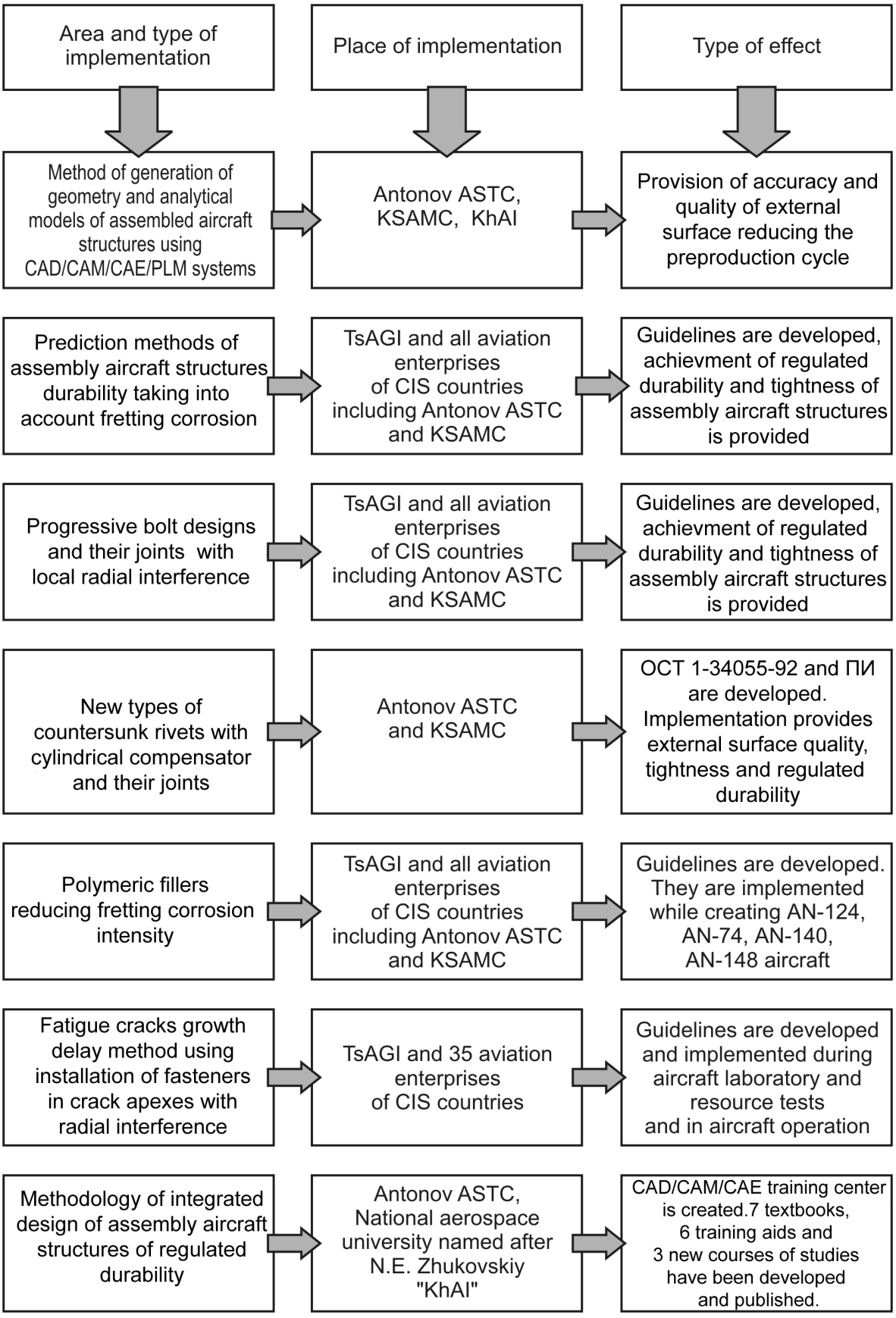

Fig. 8.3. Scheme of implementation of work results

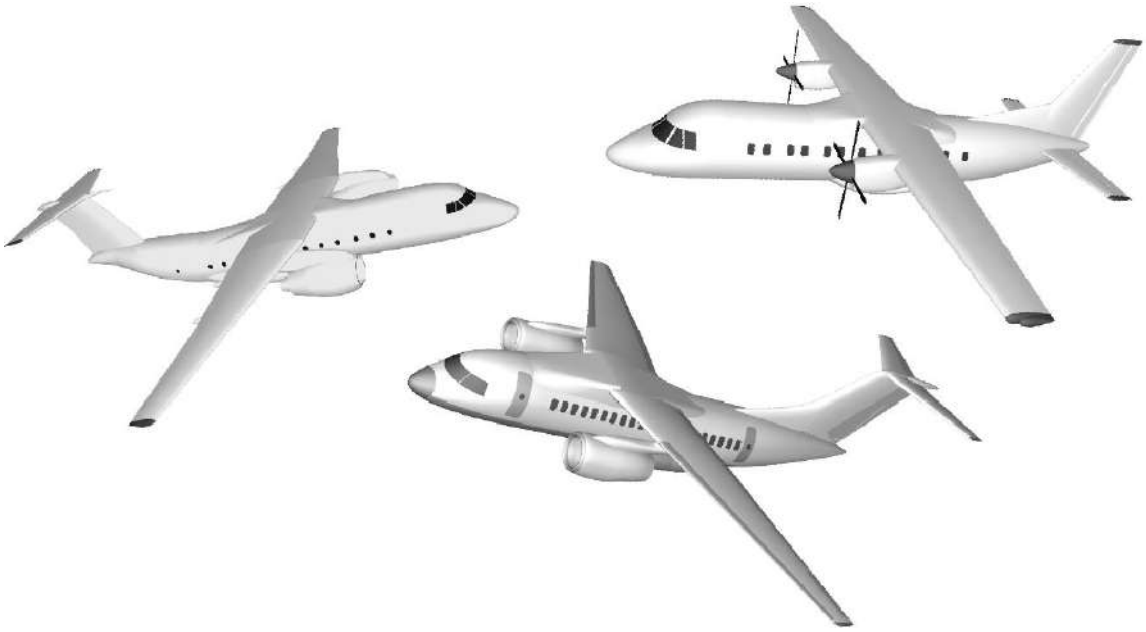

Fig. 8.4. Standards of AN-74TK-30, AN-140, AN-148 aircraft surfaces

The structurally – technological solutions ensuring regulated durability of bolt and riveted joints

To ensure regulated durability of joints of spars by calculation and experiment the efficiency of structurally – technological solutions permitting to control fasteners loading and, as consequence, joint service life characteristics in an assembly spar is proved (Fig. 8.5).

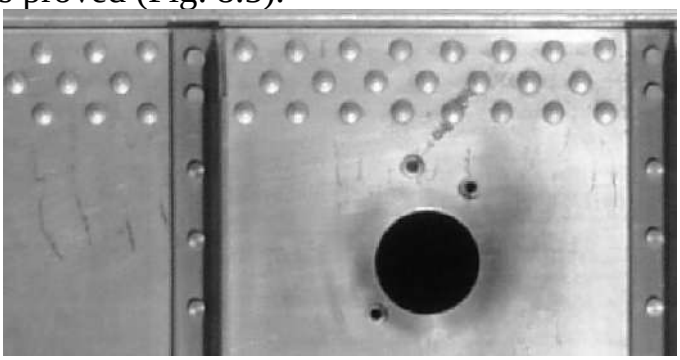

Fig. 8.5. Segment of assembled spar

It is shown that fasteners installation with radial interference, increase of flexural stiffness of supporting uprights, reduction of distance between supporting uprights, making the reinforcement of a web in a joint zone by sticking the straps or monolithic swelling, application of a discharging plate in a zone of web-to-cap joint and a longitudinal reinforcement of webs results in increase of fatigue life of web-to-cap joint in 2.0 – 7.5 times. Installation of additional rows of rivets along the web joint axis increases durability of web-to-strap joint in 1.4 – 1.5 times. Application of ways of preventing the fatigue cracks growth increases durability of segments twice.

Theoretical and experimental research of durability of longitudinal and transversal riveted joints with a load transfer eccentricity has shown that rational control of loading of joint rows, application of extreme rows unloading, control of bending stresses in straps of joints, manufacturing the special types of rivets can increase durability of attachments in 1.6 – 30 times without decreasing static strength.

Results of researches are approved by leading experts of TsAGI and Antonov ASTC, published as guidelines and technical publications «Structurally – technological ways of increasing of fatigue life of single-shear joints by means of extreme rows unloading » and used in practice of creation of aircraft structures by all enterprises of Ukraine and CIS countries.`

Development and implementation of progressive strucutres of bolts and joints on basis of investigations

On the basis of investigations of aircraft structures joints using computer (calculation, design) and physical (test) modelling (Fig. 8.6) the author obtained new structurally-technological solutions for joint structures described in Section 7. For all offered design solutions it is proved by calculation and tests that they are effective from the view point of durability and do not reduce static strength.

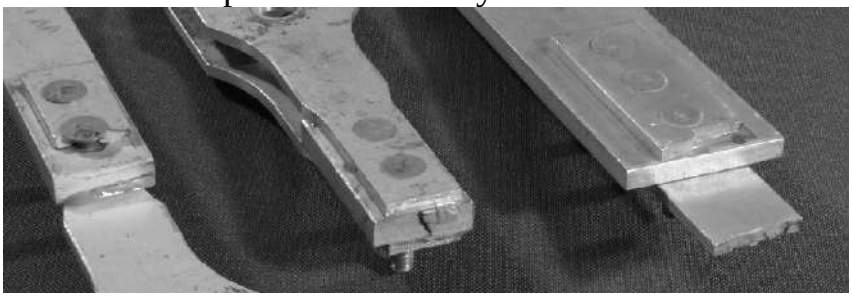

Fig. 8.6. Specimens of bolted joints with local interference

Efficiency of design solutions is ensured by application of radial interference along thickness of a package, including countersunk portion of a connected part; for this purpose the special geometry of fasteners is offered, rational control of joint rows unloading, application of doubler straps and glues, decrease of an eccentricity of transmitted load, reduction of flexural stresses in zones of a probable fatigue failure, application of polymeric fillers.

There are developed design procedure of durability of bolted both riveted joints of aircraft structures and the technique of joint parameters selection of regulated durability.

On the basis of listed structurally-technological solutions the technical guidelines «Structurally-technological ways of increase of fatigue life of transversal shear bolted joints of aircraft structures », guidelines and technical publications «Ways of increase of fatigue life of transversal shear bolted joints of aircraft airframe by unloading the zones of probable fatigue failure» have been published. Listed materials are approved by leading experts of Antonov ASTC

and TsAGI and published in TsAGI and implemented at all enterprises of the CIS countries.

Development and implementation of new types of countersunk rivets with a cylindrical compensator

For making countersunk joints of thin-walled structures with high service life the rivets with a cylindrical compensator (Ref. Section 6) are developed (Fig. 8.7). Application of new types of countersunk rivets allows to save assembly operations labor, and also external surface quality even if they are used for the joint of thin sheet parts, to provide required values of static strength, service life and tightness.

Calculation of a local stress state shows advantage of offered rivets by power criterion. The expediency of their application is experimentally proved as for service life, tightness and external surface quality.

New types of countersunk rivets with a cylindrical compensator and joints of thin-walled structures on their basis are implemented together with specialists Antonov ASTC and KSAMC during creation of AN-140, AN-148, TU-334 aircraft. OCT 1.34055-92 is developed, the technological instruction «Making of joints with rivets having cylindrical compensator» is approved and adopted for usage.

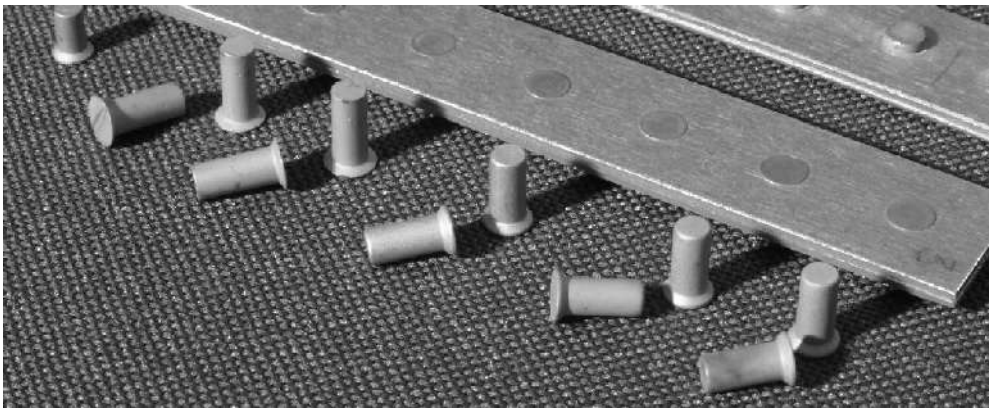

Fig. 8.7. New types of countersunk rivets

Implementation of the polymeric fillers lowering fretting corrosion intensity

To compensate technological deviations while assembling aircraft structural members to decrease fretting corrosion intensity on mating surfaces the complex of investigations which have revealed operational effectiveness of polymeric fillers of a different composition (Fig. 8.8) is carried out.

The received results allowed to develop guidelines and technical publications «Application of polymeric fillers in shear bolted joints of aircraft structures» which are approved by leading experts of TsAGI and Antonov ASTC, are implemented at the enterprises of CIS, in particular, in the process of manufacturing of AN-124, AN-74, AN-140, TU-334 aircraft.

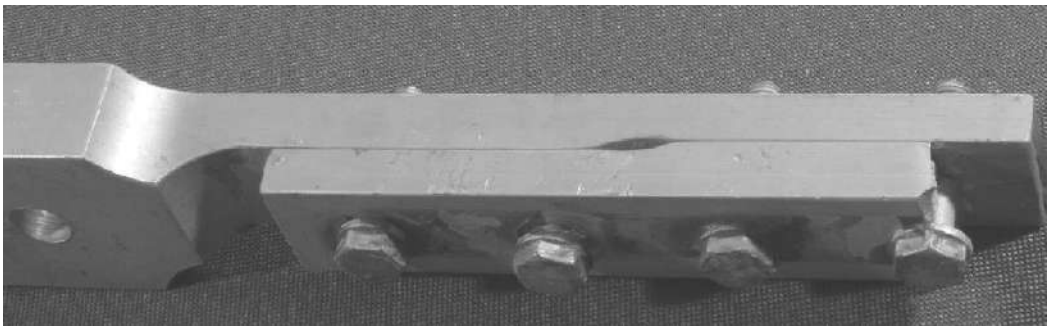

Fig. 8.8. Specimen of two-stage shear joint with polymeric filler between mating surfaces

Development and implementation of fatigue cracks growth delay ways methods in thin-walled structures

The carried out investigations have shown that the ways concluding in the installation of fasteners in holes made in crack apex with elastoplastic radial interference and tightening are most effective. In this case the hole made in crack apex reduces stress concentration, and radial interference and tightening create the local fields of residual stresses ensuring decrease of cyclical stresses amplitude in a zone of cracks propagation. By means of installation of fasteners with two-sided approach, it is possible to create residual stresses by means of both radial interference and tightening, and with single-sided approach residual stresses basically at the expense of radial interference (Fig. 8.9) and application of "Joe"-bolts.

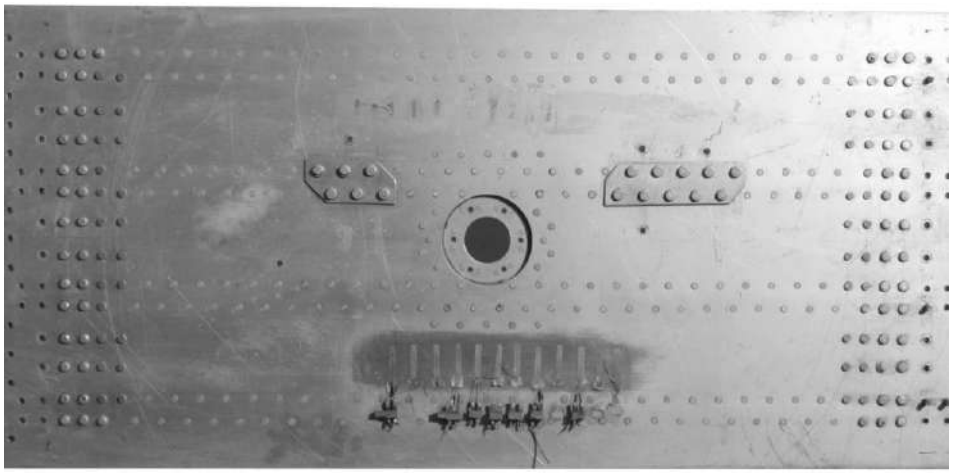

Fig. 8.9. Specimen of the stringer panel with cracks and applied ways of delay of their growth

Designed of fatigue cracks growth delay methods are described in Section 7, justified by calculations, approved in laboratory conditions by tests of plates and full-scale units.

By results of research of growth of fatigue cracks delay methods the technical guidelines «Fatigue cracks growth delay methods in aircraft structures

by setting fasteners with radial interference and tightening» are published in TsAGI and implemented during of service life testing of aircraft and their units in laboratories and at 35 aviation manufacturing and repair enterprises of Ukraine and the CIS.

Implementation of integrated design of assembly aircraft structures methodology in the training process

On the basis of developed methodology of the integrated design the author delivers «Aircraft and helicopters design in computer integrated systems» and «Computer design technology» courses.

The textbooks «Fundamentals of general design of turbine aircraft» in two parts, training manuals «Durability of airframe design irregularities» (the manual for laboratory practical work), «Aircraft design» (laboratory practical textbook), «Modelling the objects of aeronautical engineering with the help of computer systems» (laboratory practical work in two parts), «Modes of deformation analysis of aviation structures using ANSYS system» (training manual in two parts) are developed and published.

Results of activity are used for improvement of professional skill of aviation specialists and post-graduate students (Fig. 8.10).

Fig. 8.10. Seminar in CAD\CAM\CAE training center

The developed methodology of the integrated design of assembly aircraft structures of regulated durability will find wide application not only in an aircraft industry, but also in other industrial fields at implementation of CAD\CAM\CAE computer integrated systems and the computer integrated technologies of preproduction.

1. In the monography the scientific fundamentals of the integrated design methodology and achieving regulated durability of assembly aircraft structures using CAD/CAM/CAE computer systems for the solution of a great scientific-technological problem of providing resource and reliability passenger and transports aircraft are developed and implemented.

The new conceptual substantiation of the integrated design of assembly aircraft structures and their joint at all stages of aircraft life cycle in unified information space using computer integrated systems ensures improvement of the quality of creating the parametric analytical standards of assembly structures, improvement of the quality and an labour productivity of the designer, creation of bolted and riveted joints with minimum mass, regulated characteristics of durability, tightness and quality of their external surface.

2. To solve newly originating problems of creating the assembly aircraft structures and their joints of regulated durability the complex of new scientific principles, methods and techniques has been offered in the monograph:

– principle of creation of analytical standards of assembly aircraft structures;
– principle of creation of master-geometry of aircraft appearance;
– principle of design of regular zones of assembly aircraft structures;
– principle of design of non-regular zones of assembly aircraft structures;
– principle of maintenance and reaching the survivability of assembly aircraft structures;
– aircraft master-geometry creation method by means of computer integrated systems;
– integrated design techniques and computer modelling of wing, fuselage, tail unit using CAD/CAM/CAE systems;
– integrated design method of member joints of regular zone of assembly aircraft structures of regulated durability;
– durability forecasting technique of structural members of joints of assembly structures in view of fretting corrosion;
– integrated design method and computer modelling of shear bolted joints of assembly aircraft structures of regulated durability;
– integrated analysis technique of influence of structurally-technological parameters on characteristics of the local mode of deformation and contact interacting in units of shear bolted joints using ANSYS;
– determining technique of influence of structurally-technological parameters on compliance and allocation of force between rows of shear bolted joints using ANSYS system;
– forecasting technique of influence of structurally-technological parameters on durability of shear bolted joints in probable fatigue failure zones on the basis of power criterion and fatigue curves of standard specimens of joints;

– integrated design method and three-dimensional computer modelling of the standard riveted joints of assembly aircraft structures;
– analysis technique of the influence of design and technological parameters on the local mode of deformation characteristics of riveted joints;
– forecasting technique of influence of structurally-technological parameters of countersunk riveted joints on their durability;
– design procedure of distribution of force between rows of a shear riveted joint with account of production technology of the installation and structure of rivets;
– technique of design of riveted joints of skins of the given durability;
– methods of delay of growth of fatigue cracks in thin-walled constructions of airframe by installation of fasteners with interference in the holes made in crack apexes.

3. In the monograph the method of assembly aircraft structures geometry creation using CAD/CAM/CAE systems on the basis of the unified computer standard of an airplane external surface created by methods of an analytic geometry has been offered first.

4. For the first time process of providing regulated durability of assembly aircraft structures is firstly connected with life cycle phases of airplanes – design, production and operation.

5. For a design stage and designing calculations the new design-experimental models of forecasting the influence of structurally-technological parameters on bolted and riveted joints durability, taking into account change of a local specific energy of deformation and contact pressures in zones of a probable fatigue failure of joint members have been offered.

New ways of unloading the extreme rows of shear joints have been offered by application of additional straps and unloading holes, ensuring increase in 1.6 … 2 times.

On the basis of a new analysis method of performances of the local mode of deformation characteristics in bolted joints new constructions of sink bolts and production technology their installations ensuring raise of leak resistance and durability of attachments in 2 … of 7 time are developed.

New constructions increased resource countersunk rivets with cylindrical and cylinder-conical compensators and production technology of their installations ensuring given durability, leak resistance and quality of an external surface of riveted joints of airplanes without milling manufactured heads of rivets after riveting that reduces labour content of their fulfillment are developed.

6. For a production phase of assembly aircraft structures it is offered to design countersunk bolt and riveted joints with local elastoplastic radial and axial interference which efficiency is confirmed with significant volume of a signature analysis of the mode of deformation in attachments of details a finite element method implemented in ANSYS CAD/CAE system, and also an experimental

research of durability of standard attachments, assembled spars and panels.

The method of decrease of negative influence of a fretting corrosion on durability of the shear bolted joints made with technological deviations on mating surfaces by deposition on them of polymeric fillers, ensuring raise of durability of bolted joints in 1.8 … 3.6 times is offered, researched and implemented.

7. On the basis of a new method of the analysis of the mode of deformation of a plate with fatigue cracks with holes in their tips for an operation phase and service life tests create new structurally-technological ways of delay of fatigue cracks by the installation in the holes made in their tips, fasteners with axial and radial interference, ensuring extension of resources 1.5 … 2 times.

8. Reliability of scientific results and guidelines is confirmed with great volume of numerical experiment with the help of certificated ANSYS system, computer modeling of airplane units with the help of UNIGRAPHICS integrated system and an experimental research of durability of models of assembly aircraft structures in applied-research laboratory KhAI.

9. In the work it is introduced methodology of integrated design the projection of assembly aircraft structures of regulated durability is developed by the author in KhAI at fulfillment state budgetary and business contracts research works with Antonov ASTC, KSAMC, "UkrNIIAT" society, TsAGI, Tupolev ASTC, Ilyushin ASTC, Nizhniy Novgorod "Normal" society also is implemented at these enterprises. By results of activity for specialists of an aircraft industry five technical guidelines are developed, from them three are published in TsAGI.

All industry specifications have implemented at the enterprises of Ukraine and the CIS. A broad implementation in an aircraft industry the bolted joints with radial interference have received, countersunk rivets with a cylindrical compensator and a diminished altitude of manufactured head, ways of unloading of extreme rows of multirow attachments, polymeric fillers, designed the author at technical assistance of specialists of the industry and the Kharkov aviation institute.

10. For development and implementation of a methodology of the integrated projection of aircraft structures in the Kharkov aviation institute at direct involvement of the author the international science training centre on learning CAD/CAM/CAE UNIGRAPHICS, CADDS, ANSYS, Compass, ADEM systems on base of corporate information network with access in INTERNET is created. For experimental researches of new structurally-technological solutions in the Kharkov aviation institute the applied-research laboratory of attachments of aircraft structures of heightened resource is created.

11. The designed methodology of the integrated design of assembly aircraft structures of regulated durability is implemented at creation of AN-74TK-300, AN-140, TU-334, AN-148 aircraft, and as in the educational process on preparation of aviation specialists at National airspace university named by N.E. Zhoukovski «KhAI».

1. 35 лет на рынке высоких технологий / под ред. Г.А. Кривова. – К.: МИИВЦ, 1999. – 230 с.
2. 6-й Междунар. науч.-техн. симпозиум, авиационные технологии XXI века: новые рубежи авиационной науки: тез. докл. 14-19 августа в рамках международного авиасалона МАКС-2001. – Жуковский, Россия. – 427 с.
3. CALS (Continuous Acquisition and Life cycle Support – непрерывная информационная поддержка жизненного цикла изделия) в авиастроении / А.Г. Братухин, Ю.В. Давыдов, Ю.С. Елисеев и др.; под ред. А.Г. Братухина. – М.: Изд-во МАИ, 2000. – 304 с.
4. III Междунар. науч.-техн. конф. «Гиротехнологии, навигация, управление движением и конструирование подвижных объектов»: сб. докл. – К.: НТУУ «КПИ», 2001. – 358 с.
5. Гребеников А.Г. Методическое и программное обеспечение проектирования соединений стенок сборных лонжеронов в системе UNIGRAPHICS/ А.Г Гребеников, А.В. Баранов // Подготовка специалистов к работе в условиях открытых информационных и компьютерных технологий: тр. науч.-метод. конф. – Х.: ХАИ. –1996. – С. 94 – 96.
6. Основы изобретательской деятельности: учеб. пособие/ А.Г. Гребеников, П.Ф. Мороз, А.К. Мялица, В.Я. Фролов / Х.: Гос. аэрокосм. ун-т «ХАИ», 1999. – 434 с.
7. Абрамов В.Н. Проектировочный расчет на сдвиг тонкостенных балок / В.Н. Абрамов // Теория и практика проектирования пассажирских самолетов. – М.: Машиностроение, 1976. – С. 270 – 277.
8. Авиастроение: в 3 т. – М.: ВИНИТИ, 1976. – Т. 3: Машинное проектирование летательных аппаратов. – 215 с.
9. Авиастроение: летательные аппараты, двигатели, системы, технологии / Кол. авторов; под ред. А.Г. Братухина. – М.: Машиностроение, 2000. – 536 с.
10. Авиационно-космическая техника и технология: тр. Харьк. авиац. ин-та им. Н.Е. Жуковского за 1997 г. – Х.: ХАИ, 1998. – 498 с.
11. Авиационные материалы: справ. в 9 т. – Изд. 6-е, перераб. и доп. / под общ. ред. Р.Е. Шалина. – М.: ОНТИ, 1982. – Т. 4, ч. 1. – 627 с.
12. Авиационные материалы: справ. в 9 т. – Изд. 6-е, перераб. и доп. / под общ. ред. Р.Е. Шалина. – М.: ОНТИ, 1982. – Т. 4, ч. 2. – 520 с.
13. Автоматизированное конструирование в системе UNIGRAPHICS: учеб. пособие / А.Г.Гребеников, М.В.Синькевич, В.Н.Желдоченко и др. – Х.: Харьк. авиац. ин-т, 1994. – 98 с.
14. Автоматизированная система ресурсных испытаний конструкций

планера самолета с управлением от ЭВМ / С.И. Галкин, В.С. Дубинский, Е.А. Каляев и др. // II Всесоюз. съезд по теории машин и механизмов: тез. докл. – Одесса, 14-18 сент., 1982. – С. 98.
15. Автоматизированные системы расчета на прочность конструкций летательных аппаратов // По материалам иностр. печати. Обзоры. Переводы. Рефераты – М.: ЦАГИ, 1979. – № 564. – 79 с.
16. Автоматизированный авиационный комплекс пожарной охраны лесных массивов / В.Д. Белый, А.Г.Гребеников, В.О.Черановский и др. // Проектирование и производство самолетов и вертолетов: тр. Междунар. науч.-техн. конф. – Х.– Рыбачье: Нац. аэрокосм. ун-т «ХАИ». – 2003. – С. 8 – 10.
17. Автоматизированный расчет основных параметров свободнолетающих динамически подобных моделей самолетов: учеб. пособие / А.В. Бетин, А.И. Рыженко, В.И. Рябков, О.Р. Черановский. – Х.: ХАИ, 1992. – 50 с.
18. Аксентян О.К. Напряженно-деформированное состояние в окрестности вершин стыкового соединения / О.К. Аксентян, О.Е. Лущик // Прикладная механика. – 1982. – № 7. – С. 66 – 73.
19. Александров П.С. Лекции по аналитической геометрии, пополненные необходимыми сведениями из алгебры с приложением собрания задач. / П.С. Александров. – М.: Наука, 1968. – 912 с.
20. Анализ напряжений: анализ конечноэлементного подхода. Devolop. Adres. 2 London, Englewood, N. J., 1981, 45-81, место хранения ГПНТБ СССР.
21. Анализ напряженно-деформированного состояния авиационных конструкций с помощью системы ANSYS: учеб. пособие: в 2 ч. / А.Г. Гребеников, С.П. Светличный, В.Н. Король, В.Н. Анпилов. – Х.: Нац. аэрокосм. ун-т «ХАИ», CADFEM GmbH, АНТО «КНК», 2002. – Ч.1 – 310 с.
22. В.М. Андрющенко. Повышение усталостной долговечности односрезных заклепочных соединений / В.М. Андрющенко, Е.Т. Василевский, А.Г. Гребеников // Комплексное обеспечение ресурса авиаконструкций: тр. всесоюз. конф. – Жуковский: ЦАГИ. – 1984. – С. 689 – 697. ДСП.
23. Анурьев В.И. Справочник конструктора-машиностроителя: в 3 т.– Изд. 5-е, перераб. и доп. / В.И. Анурьев – М.: Машиностроение, 1978. – Т. 2. – 559 с.
24. Анцелиович Л.Л. Надежность, безопасность и живучесть самолета: учеб. для студентов вузов, обучающихся по специальности «Самолетостроение». – М.: Машиностроение, 1985. – 296 с.
25. Арсон Л.Д. Вопросы проектирования срезных болтовых соединений крыла с учетом выносливости: учеб. пособие. / Л.Д. Арсон,

А.Г.Гребеников. – Х.: ХАИ, 1981. – 112 с.
26. Арсон Л.Д. Исследование эффективности натяга в потайных болтовых соединениях самолетных конструкций/ Л.Д. Арсон, А.Г. Гребеников, В.Н. Желдоченко // Самолетостроение. Техника воздушного флота. – Х.: ХГУ. –1977. – Вып. 41. – С. 62 – 65.
27. Арсон Л.Д. Об оптимальных параметрах процесса постановки болтов с радиальным натягом / Л.Д. Арсон, А.Г. Гребеников, В.Н. Желдоченко // Вопросы оптимизации тонкостенных силовых конструкций. – Х.: ХАИ. –1976. –Вып. 2. – С. 108 – 112.
28. Арсон Л.Д. Методика расчета неравномерности контактных давлений в односрезных болтовых стыках / Л.Д. Арсон, А.Г. Гребеников, В.Н. Клименко // Автоматизация исследований несущей способности и длительной прочности летательных аппаратов: тр. всесоюз. конф. – Х.: ХГУ. – 1975. – С. 203.
29. Арсон Л.Д. Оценка напряженного состояния болтов в односрезных соединениях/ Л.Д. Арсон, А.Г. Гребеников, В.Н. Клименко // Усталостные характеристики летательных аппаратов. – Х.: ХАИ. – 1977. – Вып. 1. – С. 51 – 61.
30. Арсон Л.Д. Влияние касательных напряжений на выносливость поперечного болтового стыка тонкостенной конструкции/ Л.Д. Арсон, А.Г. Гребеников, Э.Н. Румянцев // Вопросы проектирования самолетных конструкций. – Х.: ХАИ. – 1978. – Вып. 1. – С. 102 – 106.
31. Арсон Л.Д. Исследование влияния сдвигающих напряжений на выносливость срезных поперечных болтовых соединений в условиях сложного напряженного состояния/ Л.Д. Арсон, А.Г. Гребеников, Э.Н. Румянцев // Проблемы оптимизации и автоматизации технологических процессов сборки и выполнения соединений в конструкциях самолетов и вертолетов: тр. всесоюз. семинара. – М.: МАИ. – 1978. – С. 78-87.
32. Арсон Л.Д. Исследование выносливости поперечных болтовых стыков тонкостенных конструкций в условиях сложного напряженного состояния/ Л.Д. Арсон, А.Г. Гребеников, Э.Н. Румянцев // Усталостные характеристики летательных аппаратов. – Х.: ХАИ. – 1977. – Вып. 1. – С. 11 – 14.
33. Арсон Л.Д. Вероятностный метод реализации принципа слабого звена в стыках самолетных конструкций / Л.Д. Арсон, А.Г. Гребеников, М.Н. Федотов // Вопросы оптимизации тонкостенных силовых конструкций. – Х.: ХАИ. – 1976. – Вып. 2. – С. 138 – 142.
34. Арсон Л.Д. Влияние локального упрочнения на выносливость односрезного усовидного стыка/ Л.Д. Арсон, А.Г. Гребеников, М.Н. Федотов // Вопросы проектирования самолетных конструкций. – Х.: ХАИ. – 1979. – Вып. 2. – С. 72 – 75.

35. Арсон Л.Д. Исследование влияния технологических отклонений на интенсивность фреттинг-коррозии в срезных болтовых стыках самолетных конструкций/ Л.Д. Арсон, А.Г. Гребеников, Б.А. Хохлов // Физико-химическая механика контактного взаимодействия и фреттинг-коррозии: тр. всесоюз. науч. конф. – К.: КИИГА. – 1973. – С. 218 – 229.
36. Арсон Л.Д. Рассеивание усталостных характеристик /Л.Д. Арсон, Л.А. Малашенко, А.Г. Гребеников // Самолетостроение. Техника воздушного флота. – Х.: ХГУ. –1970. – Вып.18. – С. 72 – 78.
37. Аэрокосмос. Еженедельный обзор российской и зарубежной прессы. – № 31 (239), 30 июля – 5 августа 2001 г. – М.: ТАСС, 2001. – 80 с.
38. Аэрокосмос. Еженедельный обзор российской и зарубежной прессы. – № 23 (179), 5 – 11 июня 2000 г. – М.: ТАСС, 2000. – 84 с.
39. Аэрокосмос. Еженедельный обзор российской и зарубежной прессы. – № 30 (134), 26 июля – 1 августа 1999 г. – М.: ТАСС, 1999. – 84 с.
40. Бадягин А.А. Проектирование легких самолетов/ А.А. Бадягин, Ф.А. Мухамедов. – М.: Машиностроение, 1978. – 208 с.
41. Балацкий Л.Т. Закономерности усталостного разрушения в контактных пятнах сопрягаемых деталей/ Л.Т. Балацкий // 2-й всесоюз. съезд по теории машин и механизмов: тез. докл. – Одесса, 14-18 сент.,1982. – К., 1982. – Ч.1.– С. 37.
42. Балацкий Л.Т. Прочность прессовых соединений/ Л.Т. Балацкий.– К.: Техніка, 1982. – 151 с.
43. Баринов С.М. Докритический рост трещины в хрупких материалах в условиях микрорастрескивания/ С.М. Баринов, Ю.Л. Красулин // Проблемы прочности. – 1982. – № 9. – С. 84 – 88.
44. Безпека життєдіяльності при проектуванні та виробництві аерокосмічних літальних апаратів: підруч. / О.Я. Азаревич, О.В. Гайдачук, В.М. Кобрін та ін. – Х.: ХАІ, 1997. – 366 с.
45. Беклемишев Д.В. Курс аналитической геометрии и линейной алгебры/ Д.В. Беклемишев. – М.: Наука, 1974. – 320 с.
46. Белый В.Д. Формирование мастер-геометрии планера патрульного летательного аппарата/ В.Д. Белый, А.Г. Гребеников, В.В. Парфенюк // Открытые информационные и компьютерные интегрированные технологии. – Х.: Нац. аэрокосм. ун-т «ХАИ». – 2003. – Вып. 20. – С. 44 – 49.
47. Биргер И.А. Резьбовые соединения. Библиотека конструктора/ И.А. Биргер, Г.Б. Иосилевич. – М.: Машиностроение, 1973. – 256 с.
48. Биргер И.А. Расчет на прочность деталей машин: справ. / И.А. Биргер, Б.Ф. Шорр, Г.Б. Иосилевич. – Изд. 3-е, перераб. и доп. – М.: Машиностроение, 1979. – 702 с.
49. Боборыкин Ю.А. Влияние технологических отклонений на

статическую прочность и усталостную долговечность соединений тонких обшивок планера самолета/ Ю.А. Боборыкин, А.Г. Гребеников, Н.М. Пархоменко // Самолетостроение. Техника воздушного флота. – Х.: ХГУ. – 1974. – Вып. 35. – С. 135 – 140.
50. Бойцов Б.В. Прогнозирование долговечности напряженных конструкций: Комплексное исследование шасси самолета/ Б.В. Бойцов. – М.: Машиностроение, 1985. – 232 с.
51. Большая энциклопедия транспорта: в 8 т. / Гл. ред. А.Г. Братухин, зам. гл. ред. А.Л. Гильберг. – М.: Машиностроение, 1995. – Т. 2: Авиационный транспорт. – 400 с.
52. Большой толковый словарь / под ред. С.А. Кузнецова. – Снб.: Норинт, 2000. – 1535 с.
53. Братухин А.Г. Наукоемкая авиационная продукция: организационные и экономические проблемы разработки / А.Г. Братухин, В.Д. Калачанов. – М.: Машиностроение, 1993. – 320 с.
54. Братухин А.Г. Конверсия авиакосмического комплекса России / А.Г. Братухин, Е.Н. Куличков, В.Д. Калачанов. – М.: Машиностроение, 1995. – 271с.
55. Броек Д. Основы механики разрушения/ Д. Броек. – М.: Высш. шк., 1980. – 368 с.
56. Бурмистров В.П. Обеспечение качества неразъемных соединений и полуфабрикатов/ В.П. Бурмистров – Л.: Машиностроение, 1985. – 223 с.
57. Бычков С.А. Концепция развития компьютерных интегрированных технологий в процессе создания авиационной техники/ С.А. Бычков, А.Г. Гребеников // Технологические системы: – К.: УкрНИИАТ. – 1999. – Вып. 1. – С. 60 – 67.
58. Бычков С.А. Технология создания моделей типовых заклепочных соединений самолетных конструкций в компьютерных интегрированных системах/ С.А. Бычков, А.Г. Гребеников, С.В. Воронов // Вопросы проектирования и производства конструкций летательных аппаратов. – Х.: Гос. аэрокосм. ун-т «ХАИ». – 1999. – Вып. 17(4). – С. 18 – 31.
59. Бюшгенс Г.С. ЦАГИ – центр авиационной науки/ Г.С. Бюшгенс, Е.Л. Бедржицкий. – М.: Наука, 1993. – 272 с.
60. Володин В.В. Автоматизация проектирования летательных аппаратов/ В.В. Володин. – М.: Машиностроение, 1991. – 256 с.
61. Варшавьяк Г.Б. Концепция создания системы информационного обеспечения проектирования самолета/ Г.Б. Варшавьяк, А.Г. Гребеников // Открытые информационные и компьютерные интегрированные технологии. – Х.: Гос. аэроком. ун-т «ХАИ». – 1998. – Вып. 2. – С. 301 – 307.
62. Василевский Е.Т. Конструктивно-технологические методы повышения

усталостной долговечности и живучести потайных соединений с радиальным натягом/ Е.Т. Василевский, А.Г. Гребеников, В.Н. Желдоченко // Вопросы проектирования самолетных конструкций. – Х.: ХАИ. – 1983. – Вып. 4. – С. 48 – 54.
63. Василевский Е.Т. Повышение усталостной долговечности потайных болтовых соединений с радиальным натягом/ Е.Т. Василевский, А.Г. Гребеников, В.Н. Желдоченко // Комплексное обеспечение ресурса авиаконструкций: тр. Всесоюз. конф. – Жуковский: ЦАГИ. – 1984. – С. 662 – 669. ДСП.
64. Василевский Е.Т. Методика назначений допускаемых напряжений для обеспечения заданного ресурса крыла / Е.Т. Василевский, В.А. Гребеников// Вопросы проектирования и производства конструкций летательных аппаратов – Х.: Гос. аэрокосм. ун-т «ХАИ». – 2000. – Вып. 25 (2). – С. 116 – 122.
65. Вигдорчик С.А. Исследование выносливости заклепочных соединений при циклических и случайных нагрузках / С.А. Вигдорчик, Л.Д. Арсон, А.Г. Гребеников // Методы обеспечения функциональной взаимозаменяемости и контроля качества в условиях серийного производства: тр. ВНИИНмаш. – М.: Изд-во Комитета стандартов. – 1970. – Вып. 3. ДСП.
66. Вигдорчик С.А. Моделирование технологических отклонений при исследовании выносливости болтовых стыков самолетных конструкций/ С.А. Вигдорчик, Л.Д. Арсон, А.Г. Гребеников // Выносливость и ресурс авиационных конструкций: матер. конф.– М.: ЦАГИ. – 1973. ДСП.
67. А.с. 1620711 СССР, МКИ F 16 C 11/00. Вильчатое соединение / Э.Н. Румянцев, А.Г. Гребеников, А.Г. Шаманов, В.Г. Бабичев (СССР). – № 4462816/27; заявл. 20.07.88; опубл. 15.01.91, Бюл. № 2. – 3 с.
68. Влияние контролируемой по углу закручивания и по возникающим пластическим деформациям затяжки болтовых соединений. Suzuri, Hideto, Kumo Tareshi «Dzaupe, J. Soc. Mater. Set. Jap», 1982, 31, № 346, 730-735// Реф. журнал «Механика», 1983, 3 Д81.
69. Влияние коррозионной среды на выносливость конструктивных элементов из титанового сплава / А.Г. Гребеников, В.Н. Клименко, В.И. Попович, В.Н. Стебенев // Вопросы проектирования самолетных конструкций. – Х.: ХАИ. – 1979. – Вып. 2. – С. 98 – 101.
70. Влияние способов разгрузки крайних рядов односрезных соединений на изгибные напряжения в соединяемых деталях / А.Г. Гребеников, В.М. Андрющенко, С.В. Трубаев и др. // Прочность конструкций летательных аппаратов. – Х.: ХАИ. – 1984. – Вып. 7. – С. 100 – 110.
71. Влияние среды на фреттинг-усталость. Fretting Fatique London, 1981,

143-158./Место хранения ГПНТБ СССР// Реф. журнал «Механика», 1983, 3 Д606.
72. Влияние технологических отклонений отверстий под заклепку АНУ 0347 на характер распределения радиального натяга по толщине пакета и качество внешней поверхности соединяемых элементов крыла ANSYS / С.А. Бычков, А.Г. Гребеников, Е.Т. Василевский, Ю.А. Мовчан // Вопросы проектирования и производства конструкций летательных аппаратов. – Х.: Нац. аэрокосм. ун-т «ХАИ». – 2003. – Вып. 35 (4). – С. 46 – 54.
73. Влияние фреттинг-коррозии на выносливость дюралюминовой пластины при кольцевой форме контакта / А.Г. Гребеников, Л.Д. Арсон, В.Н. Стебенев, В.Н. Желдоченко // Методы повышения ресурса соединений элементов конструкций. – М.: ЦАГИ. – 1974. – Вып. 1. – С. 63 – 75. ДСП.
74. Войт Е.С. Проектирование конструкций самолета: сб. задач / Е.С. Войт, З.А. Мелик-Саркисян, Ю.З. Ратмиров.– М.: МАИ, 1973. – 144 с.
75. Вопросы проектирования и производства конструкций летательных аппаратов: сб. науч. тр. – Х.: Гос. аэрокосм. ун-т «ХАИ». – 1999. – Вып. 17(4). – 142 с.
76. Вопросы проектирования и производства конструкций летательных аппаратов: сб. науч. тр. – Х.: Нац. аэрокосм. ун-т «ХАИ». – 2002. – Вып. 28(1). – 166 с.
77. Вопросы проектирования и производства конструкций летательных аппаратов: сб. науч. тр. Х.: Нац. аэрокосм. ун-т «ХАИ». – 2001. – Вып. 27 (4). – 145 с.
78. Вопросы проектирования и производства конструкций летательных аппаратов: сб. науч. тр.– Х.: Нац. аэрокосм. ун-т «ХАИ». – 2003. – Вып. 32 (1). – 149 с.
79. Вопросы проектирования и производства конструкций летательных аппаратов: сб. науч. тр. – Х.: Нац. аэрокосм. ун-т «ХАИ». – 2001. – Вып. 25 (2). – 136 с.
80. Вопросы проектирования и производства конструкций летательных аппаратов: сб. науч. тр. Нац. аэрокосм. ун-т «ХАИ». – 1999. – Вып. 15. – 152 с.
81. Выносливость авиационных конструкций при акустических нагрузках // По материалам иностранной печати за 1962 – 1965 гг. – № 218. Обзоры. Переводы. Рефераты – М.: ЦАГИ, 1967. – 146 с.
82. Выносливость сплава ВТ-6 в условиях фреттинг-коррозии / А.Г. Гребеников, В.Н. Клименко, В.И. Попович, В.Н. Стебенев // Вопросы проектирования самолетных конструкций. – Х.: ХАИ. – 1978. – Вып. 1. – С. 114 – 118.

83. Выполнение болтовых соединений в конструкциях из алюминиевых, магниевых, титановых сплавов и высокопрочных сталей: завод. производств. инструкция. – К.: КМЗ, 1982. – 45 с.
84. Галкин С.И. Применение метода сил к исследованию основного напряженного состояния элементов поперечного стыка панелей кессона с коробкой центроплана/ С.И. Галкин, В.С. Дубинский // Местная прочность конструктивных нерегулярностей планера самолета. – М.: ЦАГИ. – 1979. – Вып. 2018. – С. 21 – 51.
85. Галкина Н.С. Применение метода сил к решению задач о контактном взаимодействии узлов конструкций // Проблемы прочности/ Н.С. Галкина, В.И. Гришин, А.И. Сурков. – 1982. – № 6. – С. 74 – 77.
86. Гаража В.В. Конструкция самолетов: учеб. / В.В. Гаража.– К.: КМУГА, 1998. – 524 с.
87. Гвинтовкин И. Ф. Справочник по ремонту летательных аппаратов/ И. Ф. Гвинтовкин, О. М. Стояненко – М.: Транспорт, 1977. – 342 с.
88. Гетерогенная локальная информационно-вычислительная сеть учебного центра CAD/CAM/CAE Харьковского авиационного института / А.Г. Гребеников, А.В. Заозерский, А.Г. Анохин и др.// Подготовка специалистов к работе в условиях открытых информационных и компьютерных технологий: тр. Междунар. науч.-метод. конф. – Х.: ХАИ. – 1996. – С. 18 – 20.
89. Гиммельфарб А.Л. Основы конструирования в самолетостроении: учеб. пособие для высших авиац. учеб. заведений / А.Л. Гиммельфарб.– 2-е изд., перераб. и доп. – М.: Машиностроение, 1980. – 367 с.
90. Голего Н.Л. Фреттинг-коррозия металлов/ Н.Л. Голего, А.Я. Алябьев, В.В. Шевель. – К.: Наук. думка, – 1974. – 427 с.
91. Гонтаренко А.П. Методика расчета долговечности болтовых и заклепочных соединений по локальному напряженно-деформированному состоянию: автореф. дис. …канд. техн. наук.: 05.07.03/ Андрей Петрович Гонтаренко; Нац. аэрокосм. ун-т «ХАИ». – Х., – 2000. – 21 с.
92. Гребеников А.Г. Заклепки для высокоресурсных потайных клепаных соединений/ А.Г. Гребеников // Открытые информационные и компьютерные интегрированные технологии. – Х.: Гос. аэрокосм. ун-т «ХАИ». –1998. – Вып. 1. – С. 395 – 397.
93. Гребеников А.Г. Интегрированное проектирование самолетных конструкций / А.Г. Гребеников // Інтегровані комп’ютерні технології в машинобудуванні: тез. докл. Міжнар. наук.-техн. конф. Нац. аэрокосм. ун-ту «ХАІ». – Х., 2003. – С. 167 – 172.
94. Гребеников А.Г. Концепция интегрированного проектирования соединений самолетных конструкций/ А.Г. Гребеников // Открытые

информационные и компьютерные интегрированные технологии. – Х.: Нац. аэрокосм. ун-т «ХАИ». – 2003. – Вып. 18. – С. 5 – 18.
95. Гребеников А.Г. Методология обеспечения характеристик сопротивления усталости сборных конструкций планера самолета/ А.Г. Гребеников // Подготовка специалистов к работе в условиях открытых информационных и компьютерных технологий: тр. Междунар. науч.-метод. конф. – Х.: ХАИ. – 1996. – С. 86 – 87.
96. Гребеников А.Г. Обеспечение заданного ресурса крыла на стадии проектирования/ А.Г. Гребеников // Авиационно-космическая техника и технология: тр. Нац. аэрокосм. ун-та «ХАИ». – Х.: 2001. – Вып. 25. – С. 352 – 357.
97. Гребеников А.Г. Обеспечение качества соединений самолетных конструкций, выполненных потайными заклепками с цилиндрическим компенсатором/ А.Г. Гребеников // Технологические системы: – К.: УкрНИИАТ. – 2002. – Вып. 3(14). – С. 82 – 87.
98. Гребеников А.Г. Принципы и методы обеспечения усталостной долговечности соединений самолетных конструкций с учетом фреттинг-коррозии/ А.Г. Гребеников // Современные проблемы строительной механики и прочности летательных аппаратов: тр. IV всесоюз. конф. – Х.: ХАИ. – 1991. – С. 104.
99. Гребеников А.Г. Разработка технологии постановки самоконтрящихся гаек и сборки соединений съемных панелей, исключающей повреждение стенок отверстий/ А.Г. Гребеников // Открытые информационные и компьютерные интегрированные технологии. – Х.: Гос. аэрокосм. ун-т «ХАИ». – 1998. – Вып. 2. – С. 286 – 289.
100. Гребеников А.Г. Расчет выносливости срезного болтового стыка с учетом фреттинг-коррозии / А.Г. Гребеников // Вопросы оптимизации тонкостенных силовых конструкций. – Х.: ХАИ. – 1975. – Вып. 1. – С. 140 – 150.
101. Гребеников А.Г. Повышение усталостной долговечности тонкостенных конструктивных элементов с отверстием/ А.Г. Гребеников, В.М. Андрющенко // Вопросы механики деформируемого твердого тела. – Х.: ХАИ. – 1982. – Вып. 3. – С.135 – 138.
102. Гребеников А.Г. Влияние технологических отклонений на долговечность заклепочных соединений, крайние ряды которых установлены с зазорами в детали, образующей край нахлестки / А.Г. Гребеников, В.М. Андрющенко, Е.Т. Василевский // Вопросы проектирования и производства тонкостенных силовых конструкций. – Х.: ХАИ. – 1984. – С. 82 – 95.
103. Гребеников А.Г. Способ повышения усталостной долговечности тонкостенных конструктивных элементов с функциональным

отверстием малого диаметра с помощью заклепок/ А.Г. Гребеников, В.М. Андрющенко, Е.Т. Василевский // Самолетостроение. Техника воздушного флота. – Х.: ХГУ. – 1987. – Вып. 54. – С. 84 – 87.
104. Гребеников А.Г. Влияние предварительного растяжения на сопротивление усталости пластин со свободными цилиндроконическими отверстиями / А.Г. Гребеников, Ю.Н. Богдан, А.Е. Новожилов // Авиационно-космическая техника и технология: тр. Нац. аэрокосм. ун-та «ХАИ». – Х.: 2002. – Вып. 33. – С. 403 – 407.
105. Анализ характеристик общего и локального напряженно-деформированного состояния в элементах многорядного заклепочного соединения с помощью системы CAD/CAE ANSYS/ А.Г. Гребеников, С.А. Бычков, Ю.А. Мовчан // Технологические системы: – К.: УкрНИИАТ. – 2003. – Вып. 1(17). – С. 61 – 74.
106. Гребеников А.Г., Применение современных CASE-технологий в информационной системе проектирования самолета/ А.Г. Гребеников, Г.Б. Варшавьяк // Авиационно-космическая техника и технология: тр. Гос. аэрокосм. ун-та «ХАИ». – Х., 1999. – Вып. 11. – С. 157 – 161.
107. Гребеников А.Г. Применение CAD/CAM – систем для создания управляющих программ изготовления технологической оснастки на станках с ЧПУ/ А.Г. Гребеников, И.Г. Волокитин, С.А. Лихачев // Открытые информационные и компьютерные интегрированные технологии. – Х.: Гос. аэроком. ун-т «ХАИ». – 2000. – Вып. 8. – С. 148 – 162.
108. Гребеников А.Г. Влияние конструктивных параметров на концентрацию напряжений и долговечность панелей в зонах отверстий для перетекания топлива/ А.Г. Гребеников, Р.В. Воропаев // Вопросы проектирования и производства конструкций летательных аппаратов. – Х.: Гос. аэроком. ун-т «ХАИ». – 1999. – Вып. 15. – С. 72 – 87.
109. Гребеников А.Г. Особенности разработки чертежей форм для выклейки деталей интерьера салона пассажирского самолета из композиционных материалов с использованием графической системы КОМПАС-ГРАФИК 5.5/ А.Г. Гребеников, А.И. Глушкова, И.Г. Волокитин // Открытые информационные и компьютерные интегрированные технологии. – Х.: Гос. аэроком. ун-т «ХАИ». – 1998.– Вып. 2. – С. 275 – 280.
110. Гребеников А.Г. Технологические особенности выполнения соединений съемных панелей крыла с самоконтрящимися гайками/ А.Г. Гребеников, В.А. Гребеников, С.В. Трубаев // Открытые информационные и компьютерные интегрированные технологии. – Х.: Гос. аэрокосм. ун-т «ХАИ». – 1998. – Вып. 2. – С. 308 – 314.
111. Гребеников А.Г. Сопротивление усталости типовых моделей срезных болтовых соединений с шестигранной головкой болта/

А.Г. Гребеников, А.М. Гуменный, В.А. Гребеников // Вопросы проектирования и производства конструкций летательных аппаратов. – Х.: Нац. аэрокосм. ун-т «ХАИ». – 2002. – Вып. 29 (2). – С. 132 – 143.
112. Гребеников А.Г. Особенности создания аналитических эталонов сборных панелей крыла для экспериментальных исследований/ А.Г. Гребеников, А.М. Гуменный, А.Н. Назаренко // Открытые информационные и компьютерные интегрированные технологии. – Х.: Нац. аэрокосм. ун-т «ХАИ». – 2003. – Вып. 20. – С. 50 – 57.
113. Гребеников А.Г. Анализ влияния конструктивных параметров заклепочных соединений на податливость и характер распределения усилий между рядами с помощью системы инженерного анализа ANSYS/ А.Г. Гребеников, И.Н. Дубров // Вопросы проектирования и производства конструкций летательных аппаратов. – Х.: Нац. аэрокосм. ун-т «ХАИ». – 2003. – Вып. 33 (2). – С. 53 – 60.
114. Гребеников А.Г. Интегрированный анализ влияния типа установки болта и уровня нагружения на характеристики локального НДС в элементах двухсрезного однорядного потайного болтового соединения с помощью системы инженерного анализа ANSYS/ А.Г. Гребеников, И.Н. Дубров // Открытые информационные и компьютерные интегрированные технологии. – Х.: Нац. аэрокосм. ун-т «ХАИ». – 2002. – Вып. 15. – С. 59-93.
115. Гребеников А.Г. Метод прогнозирования влияния конструктивно-технологических параметров срезных потайных соединений на их долговечность/ А.Г. Гребеников, И.Н. Дубров // Проектирование и производство самолетов и вертолетов: тр. Междунар. науч.-техн. конф. – Рыбачье. – Х.: Нац. аэрокосм. ун-т «ХАИ». – 2003. – С. 16 – 23.
116. Гребеников А.Г. Метод прогнозирования долговечности срезных болтовых соединений, выполненных с осевым и радиальным натягом/ А.Г. Гребеников, И.Н. Дубров // Открытые информационные и компьютерные интегрированные технологии. – Х.: Нац. аэрокосм. ун-т «ХАИ». – 2004. – Вып. 22. – С. 16 – 29.
117. Гребеников А.Г. Методика расчета распределения усилий между рядами в срезных болтовых соединениях авиационных конструкций с помощью системы ANSYS / А.Г. Гребеников, И.Н. Дубров // Открытые информационные и компьютерные интегрированные технологии. – Х.: Нац. аэрокосм. ун-т «ХАИ». – 2003. – Вып. 17. – С. 31 – 41.
118. Гребеников А.Г. Прогнозирование долговечности типовых срезных болтовых соединений на основе расчета характеристик НДС в их элементах/ А.Г. Гребеников, И.Н. Дубров // Открытые информационные и компьютерные интегрированные технологии. – Х.:

Нац. аэрокосм. ун-т «ХАИ». – 2003. – Вып. 21. – С. 202 – 210.
119. Гребеников А.Г. Анализ локального НДС пластины с цилиндроконическим отверстием, заполненным болтом с потайной головкой/ А.Г. Гребеников, И.Н. Дубров, С.П. Светличный // Вопросы проектирования и производства конструкций летательных аппаратов. – Х.: Нац. аэрокосм. ун-т «ХАИ». – 2002. – Вып. 31 (4). – С. 38 – 63.
120. Гребеников А.Г. Исследование концентрации напряжений в пластине с цилиндроконическим отверстием методом конечных элементов в системе ANSYS 5.3/ А.Г. Гребеников, П.А. Дыбский, О.Д. Даниленко // Открытые информационные и компьютерные интегрированные технологии. – Х.: Гос. аэроком. ун-т «ХАИ». – 1998. – Вып. 1. – С 48 – 60.
121. Гребеников А.Г. Численное исследование в среде ANSYS 5.3 напряженного состояния проушины при посадке болта с натягом/ А.Г. Гребеников, П.А. Дыбский, И.П. Палади // Открытые информационные и компьютерные интегрированные технологии. – Х.: Гос. аэрокосм. ун-т «ХАИ». – 1998. – Вып.1. – С. 348 – 356.
122. Гребеников А.Г. Методика определения коэффициентов неравномерности контактных давлений между элементами односрезного болтового соединения с радиальным и осевым натягом/ А.Г. Гребеников, А.Ю. Ефремов, В.Н. Клименко // Вопросы проектирования и производства конструкций летательных аппаратов. – Х.: ХАИ. – 1998. – Вып. 13. – С. 134 – 159.
123. Гребеников А.Г. Особенности определения коэффициентов неравномерности контактных давлений между элементами одно-срезного потайного болтового соединения с радиальным и осевым натягом/ А.Г. Гребеников, А.Ю. Ефремов, В.Н. Клименко // Вопросы проектирования и производства конструкций летательных аппаратов. – Х.: Нац. аэрокосм. ун-т «ХАИ». – 2002. – Вып. 28 (1). – С. 111 – 130.
124. Гребеников А.Г. Влияние покрытий на выносливость потайного односрезного болтового соединения/ А.Г. Гребеников, В.Н. Желдоченко, В.Н. Стебенев // Вопросы оптимизации тонкостенных силовых конструкций. – Х.: ХАИ. – 1976. – Вып. 2. – С. 142 – 145.
125. Гребеников А.Г. Влияние формы головки болта на выносливость потайных срезных соединений/ А.Г. Гребеников, В.Н. Желдоченко, В.Н. Стебенев // Усталостные характеристики летательных аппаратов. – Х.: ХАИ. – 1977. – Вып. 1. – С. 83 – 88.
126. Гребеников А.Г. Оценка влияния фреттинг-коррозии на выносливость алюминиевых сплавов/ А.Г. Гребеников, В.Н. Желдоченко, В.Н. Стебенев // Автоматизация исследований несущей способности и длительной прочности летательных аппаратов: тр. Всесоюз. конф. –

Х.: ХГУ. – 1975. – С. 102 – 103.
127. Гребеников А.Г. Создание поверхностной модели пассажирского самолета в компьютерной интегрированной системе UNIGRAPHCS/ А.Г. Гребеников, Ю.В. Железняков, А.М. Гуменный // Авиационно-космическая техника и технология: тр. Харьк. авиац. ин-та за 1997 г. – Х., 1998. – С. 42 – 48.
128. Гребеников А.Г. Концепция дистанционного инженерного образования/ А.Г. Гребеников, А.В. Заозерский, А.Н. Петров // Авиационно-космическая техника и технология: тр. Гос. аэрокосм. ун-та «ХАИ». – Х., 1999. – Вып. 10. – С. 187 – 195.
129. Гребеников А.Г. Влияние глубины зенкования на концентрацию напряжений и долговечность пластины с отверстием при нагружении ее сдвигом/ А.Г. Гребеников, В.В. Звягинцев, Э.Н. Румянцев // Открытые информационные и компьютерные интегрированные технологии. – Х.: Гос. аэрокосм. ун-т «ХАИ». – 1998. – Вып. 2. – С. 48 – 63.
130. Гребеников А.Г. Исследование влияния зазоров и их заполнения полимерным заполнителем на выносливость стыковых элементов конструкций/ А.Г. Гребеников, Г.Г. Кантер // Матер. III всесоюз. совещания по проблемам усталости и долговечности авиационных конструкций. – М.: ЦАГИ. – 1970. ДСП.
131. Гребеников А.Г. Эффективность методов повышения усталостной долговечности срезных соединений из сплава ВТ-6 в условиях фреттинг-коррозии / А.Г. Гребеников, В.Н. Клименко // Комплексное обеспечение ресурса авиаконструкций: тр. всесоюз. науч. конф. – Жуковский: ЦАГИ. – 1984. – С. 649 – 654. ДСП.
132. Гребеников А.Г. Разработка программного обеспечения для расчета неравномерности распределения усилий между рядами в срезном болтовом соединении с осевым и радиальным натягом/ А.Г. Гребеников, А.Ю. Ефремов, В.Н. Клименко // Подготовка специалистов к работе в условиях открытых информационных и компьютерных технологий: тр. Междунар. науч.-метод. конф. – Х.: ХАИ. – 1996. – С. 90 – 93.
133. Гребеников А.Г. Оценка усталостной долговечности конструктивных элементов без геометрических концентраторов напряжений из титанового сплава ВТ-6 в условиях фреттинг-коррозии/ А.Г. Гребеников, В.Н.Клименко, И.С. Кошелев // Вопросы проектирования и повышения ресурса самолетных конструкций. – Х.: ХАИ. – 1989. – С. 13 – 20.
134. Гребеников А.Г. Исследование влияния затяжки и радиального натяга болтов, поверхностного упрочнения на выносливость срезных соединений из сплава ВТ-6 / А.Г. Гребеников, В.Н. Клименко, В.Н. Стебенев // Вопросы проектирования самолетных конструкций. –

Х.: ХАИ. – 1979. – Вып. 2. – С. 76 – 79.
135. Гребеников А.Г. Исследование технологических особенностей выполнения высокоресурсных соединений из сплава ВТ-6 / А.Г. Гребеников, В.Н.Клименко, В.Н. Стебенев // Проблемы оптимизации и автоматизации технологических процессов сборки и выполнения соединений в конструкциях самолетов и вертолетов: тр. всесоюз. семинара – М.: МАИ. – 1978. – С. 28 – 55.
136. Гребеников А.Г. Оценка изгибных напряжений в накладках односрезного соединения. / А.Г. Гребеников, В.Н. Клименко, С.В. Трубаев // Вопросы механики деформируемого твердого тела. – Х.: ХАИ. – 1982. – Вып. 3. – С. 78 – 85.
137. Гребеников А.Г. Интегрированные технологии проектирования самолётных конструкций/ А.Г. Гребеников, В.С. Кривцов // Информационные технологии в наукоёмком машиностроении: Компьютерное обеспечение индустриального бизнеса / под общ. ред. А.Г. Братухина. – К.: Техніка. – 2001. – С. 154 – 177.
138. Гребеников А.Г. Интегрированные технологии проектирования самолётных конструкций / А.Г. Гребеников, В.С. Кривцов // Технологические системы: – К.: УкрНИИАТ. – 2001. – Вып. 1(7). – С. 66 – 83.
139. Гребеников А.Г. Методика создания управляющих программ для станков с ЧПУ с применением CAD/CAM систем/ А.Г. Гребеников, С.А Лихачев // Авиационно-космическая техника и технология: тр. Гос. аэрокосм. ун-та «ХАИ». – Х., 2000. – Вып. 18. – С. 72 – 87.
140. Гребеников А.Г. Анализ характеристик общего и локального напряженно-деформированного состояния в элементах срезных соединений, выполненных с помощью заклепок по ОСТ1 3455-92 (АНУ 0309) / А.Г. Гребеников, Ю.А. Мовчан // Открытые информационные и компьютерные интегрированные технологии. – Х.: Нац. аэрокосм. ун-т «ХАИ». – 2003. – Вып. 19. – С. 87 – 112.
141. Гребеников А.Г. Метод прогнозирования усталостной долговечности пластин с отверстием/ А.Г. Гребеников, Ю.А. Мовчан // Авиационно-космическая техника и технология: тр. Нац. аэрокосм. ун-та «ХАИ». – Х., – 2003. – Вып. 38/4. – С. 89 – 93.
142. Гребеников А.Г. Анализ характеристик локального НДС с помощью системы ANSYS в пластине с отверстиями, подверженной упрочнению дорнированием или глубоким пластическим деформированием и растяжению/ А.Г. Гребеников, Ю.А. Мовчан, В.А. Гребеников // Вопросы проектирования и производства конструкций летательных аппаратов. – Х.: Нац. аэрокосм. ун-т «ХАИ». – 2003. – Вып. 32 (1). – С. 124 – 138.
143. Гребеников А.Г. Анализ характеристик локального НДС в элементах

типовых срезных соединений самолетных конструкций/ А.Г. Гребеников, Ю.А. Мовчан, И.Н. Дубров // Открытые информационные и компьютерные интегрированные технологии. – Х.: Нац. аэрокосм. ун-т «ХАИ». – 2003. – Вып. 16. – С. 59 – 105.
144. Повышение циклической долговечности соединений с радиальным натягом путем их предварительного растяжения /А.Г. Гребеников, А.Е. Новожилов, А.Г. Шаманов // Современные проблемы обеспечения ресурса авиаконструкций: тр. VIII всесоюз. конф. – М.: ЦАГИ. – 1986. – С. 42. ДСП.
145. Гребеников А.Г. Влияние предварительного растяжения и радиального натяга на долговечность конструктивных элементов с отверстиями/ А.Г. Гребеников, А.Е. Новожилов, А.Г. Шаманов // Проектирование самолетных конструкций и их соединений. – Х.: ХАИ. – 1987. – С. 9 – 14.
146. Гребеников А.Г. Исследование влияния контактных давлений на напряженно-деформированное состояние плоской пластины при ее растяжении / А.Г. Гребеников, И.П. Палади // Открытые информационные и компьютерные интегрированные технологии. – Х.: Гос. аэрокосм. ун-т «ХАИ». – 1998. – Вып. 2. – С. 36 – 47.
147. Гребеников А.Г. Исследование влияния осевого и радиального натяга на напряженное состояние пластины с цилиндрическим отверстием, заполненным болтом, при растяжении/ А.Г. Гребеников, И.П. Палади // Открытые информационные и компьютерные интегрированные технологии. – Х.: Гос. аэрокосм. ун-т «ХАИ». – 1998. – Вып. 2. – С. 63 – 78.
148. Гребеников А.Г. Моделирование в системе ANSYS™ контактного взаимодействия элементов двусрезного соединения с болтом, края которого свободны от закрепления/ А.Г. Гребеников, И.П. Палади // Открытые информационные и компьютерные интегрированные технологии. – Х.: Гос. аэрокосм. ун-т «ХАИ». –1998. – Вып. 2. – С. 290 – 300.
149. Гребеников А.Г. Моделирование влияния осевого натяга на напряженно-деформированное состояние элементов односрезного соединения/ А.Г. Гребеников, И.П. Палади // Авиационно-космическая техника и технология: тр. Гос. аэрокосм. ун-та «ХАИ». – Х., 2000. – Вып. 17. – С. 244 – 258.
150. Гребеников А.Г. Создание каркасных, поверхностных и твердотельных геометрических моделей деталей и узлов горизонтального оперения самолета в компьютерной интегрированной системе CAD\CAM\CAE UNIGRAPHICS/ А.Г. Гребеников, В.В. Парфенюк // Открытые информационные и компьютерные интегрированные технологии. – Х.: Гос. аэрокосм. ун-т «ХАИ». – 1999. – Вып. 3. – С. 18

– 27.
151. Гребеников А.Г. Технология создания твердотельных моделей типовых болтовых соединений самолетных конструкций в системе CAD\CAM\CAE UNIGRAPHICS / А.Г. Гребеников, В.В. Парфенюк // Открытые информационные и компьютерные интегрированные технологии. – Х.: Гос. аэрокосм. ун-т «ХАИ».– 1999. – Вып. 4. – С. 245 – 252.
152. Гребеников А.Г. Алгоритм проектирования горизонтального оперения пассажирского самолета с ТВД/ А.Г. Гребеников, В.В. Парфенюк, А.А. Кобылянский // Вопросы проектирования и производства конструкций летательных аппаратов. – Х.: Гос. аэрокосм. ун-т «ХАИ». – 2000. – Вып. 20(3). – С. 13 – 32.
153. Гребеников А.Г. Применение мультимедийных технологий дистанционного обучения для проведения учебных занятий / А.Г. Гребеников, А.Н. Петров // Открытые информационные и компьютерные интегрированные технологии. – Х.: Нац. аэрокосм. ун-т «ХАИ». – 2003. – Вып. 18. – С. 211 – 225.
154. Гребеников А.Г. Особенности расчета долговечности срезных болтовых соединений в условиях действия фреттинг-коррозии и сложного напряженного состояния/ А.Г. Гребеников, Э.Н. Румянцев, В.Н. Стебенев // Современные проблемы обеспечения ресурса авиаконструкций: тр. VIII всесоюз. конф.– М.: ЦАГИ. – 1986. – С. 43. ДСП.
155. Гребеников А.Г. Способы повышения циклической долговечности многорядных срезных болтовых соединений путем разгрузки крайних рядов/ А.Г. Гребеников, Э.Н. Румянцев, В.Н. Стебенев // Современные проблемы обеспечения ресурса авиаконструкций: тр. VIII всесоюз. конф.– М.: ЦАГИ. – 1986. – С. 138. ДСП.
156. Гребеников А.Г. Усталостная долговечность срезных болтовых соединений самолетных конструкций в условиях действия растягивающих и сдвигающих усилий/ А.Г. Гребеников, Э.Н. Румянцев, В.Н. Стебенев // Вопросы проектирования самолетных конструкций. – Х.: ХАИ. – 1982. – Вып. 3. – С. 79 – 87.
157. Гребеников А.Г. Экспериментальное исследование усталостной долговечности срезных болтовых соединений в условиях совместного действия растяжения и сдвига/ А.Г. Гребеников, Э.Н. Румянцев, В.Н. Стебенев // Комплексное обеспечение ресурса авиаконструкций: тр. всесоюз. конф.– Жуковский: ЦАГИ. – 1984. – С. 346 – 351. ДСП.
158. Гребеников А.Г. Технологические способы повышения усталостной долговечности многорядных соединений путем разгрузки крайних рядов/ А.Г. Гребеников, Э.Н. Румянцев, А.Г. Шаманов // Опыт механизации выполнения соединений повышенного ресурса,

надежности, герметичности и перспективы повышения уровня механизации: тр. III всесоюз. семинара – К.: УкрНИИАТ. – 1988. – С. 69 – 70. ДСП.
159. Гребеников А.Г. Анализ напряженно-деформированного состояния в элементах односрезного болтового соединения с радиальным и осевым натягами с помощью системы ANSYS / А.Г. Гребеников, С.П. Светличный // Открытые информационные и компьютерные интегрированные технологии. – Х.: Гос. аэрокосм. ун-т «ХАИ». – 2000. – Вып. 8. – С. 35 – 51.
160. Гребеников А.Г. Анализ напряжённо-деформированного состояния при растяжении пластины с отверстием, заполненным болтом, установленным с радиальным и осевым натягами/ А.Г. Гребеников, С.П. Светличный // Авиационно-космическая техника и технология: тр. Нац. аэрокосм. ун-та «ХАИ». – Х., 2001. – Вып. 24. – С. 392 – 405.
161. Гребеников А.Г. Влияние затяжки болтов, установленных в вершинах усталостной трещины, на локальное напряженно-деформированное состояние пластины/ А.Г. Гребеников, С.П. Светличный // Вопросы проектирования и производства конструкций летательных аппаратов. – Х.: Гос. аэрокосм. ун-т «ХАИ». – 1999. – Вып. 16(3). – С. 134 – 155.
162. Гребеников А.Г. Влияние осевого и радиального натягов на податливость болтовых соединений/ А.Г. Гребеников, С.П. Светличный // Авиационно-космическая техника и технология: тр. Нац. аэрокосм. ун-та «ХАИ». – Х., 2002. – Вып. 33. – С. 164 – 172.
163. Гребеников А.Г. Влияние радиального натяга болтов на напряженно-деформированное состояние пластины с усталостной трещиной и отверстиями, выполненными по ее длине/ А.Г. Гребеников, С.П. Светличный // Открытые информационные и компьютерные интегрированные технологии. – Х.: Гос. аэрокосм. ун-т «ХАИ». – 1999. – Вып. 3. – С. 39 – 67.
164. Гребеников А.Г. Влияние уровня нагружения на изменение напряженно-деформированного состояния пластины с цилиндрическим отверстием, заполненным болтом/ А.Г. Гребеников, С.П. Светличный // Открытые информационные и компьютерные интегрированные технологии. – Х.: Гос. аэрокосм. ун-т «ХАИ». – 2001. – Вып. 10. – С. 199 – 211.
165. Гребеников А.Г. Интегрированное проектирование и анализ локального напряженно-деформированног о состояния в элементах односрезного болтового соединения/ А.Г. Гребеников, С.П. Светличный // Открытые информационные и компьютерные интегрированные технологии. – Х.: Нац. аэрокосм. ун-т «ХАИ». – 2002. – Вып. 11. – С. 159 – 186.
166. Гребеников А.Г. Интегрированный анализ локального НДС в

элементах двусрезного болтового соединения/ А.Г. Гребеников, С.П. Светличный // Открытые информационные и компьютерные интегрированные технологии. – Х.: Нац. аэрокосм. ун-т «ХАИ». – 2002. – Вып. 12. – С. 22 – 47.
167. Гребеников А.Г. Исследование овализации отверстий и напряженно-деформированного состояния в пластине с усталостной трещиной в системе ANSYS 5.3/ А.Г. Гребеников, С.П. Светличный // Открытые информационные и компьютерные интегрированные технологии. – Х.: Гос. аэрокосм. ун-т «ХАИ» . – 1998. –Вып. 2. – С. 79 – 95.
168. Гребеников А.Г. Исследование с помощью системы ANSYS влияния натяга на характеристики локального напряжённо-деформированного состояния элементов болтового соединения/ А.Г. Гребеников, С.П. Светличный // Технологические системы: – К.: УкрНИИАТ. – 2002. – Вып. 1(12). – С. 15 – 25.
169. Гребеников А.Г. Анализ локального НДС в элементах срезных болтовых соединений самолетных конструкций/ А.Г. Гребеников, С.П. Светличный, Ю.А. Мовчан // Открытые информационные и компьютерные интегрированные технологии. – Х.: Нац. аэрокосм. ун-т «ХАИ». – 2002. – Вып. 13. – С. 63 – 91.
170. Гребеников А.Г. Методология создания поверхностной модели пассажирского самолета с ТВД в системе параметрического моделирования CADDS-5/ А.Г. Гребеников, С.П. Светличный, А.Н. Петров // Открытые информационные и компьютерные интегрированные технологии. – Х.: Гос. аэрокосм. ун-т «ХАИ». – 1998. – Вып. 2. – С. 256 – 265.
171. Гребеников А.Г. Интегрированные способы задержки роста усталостных трещин в тонкостенных конструкциях/ А.Г. Гребеников, С.П. Светличный, А.М. Тимченко // Технологические системы. – К.: УкрНИИАТ. – 2002. – Вып. 4(15). – С. 11 – 21.
172. Гребеников А.Г. Моделирование конструктивных элементов вертикального оперения пассажирского самолета в компьютерной интегрированной системе CAD/CAM/CAE UNIGRAPHICS/ А.Г. Гребеников, А.А. Сердюков // Вопросы проектирования и производства конструкций летательных аппаратов. – Х.: Гос. аэрокосм. ун-т «ХАИ». – 1999. – Вып. 14. – С. 122 – 132.
173. Гребеников А.Г. Конструктивно-технологические методы повышения усталостной долговечности и живучести многоточечных срезных соединений элементов самолетных конструкций/ А.Г. Гребеников, В.Н. Стебенев // Комплексное обеспечение ресурса авиаконструкций: тр. всесоюз. науч. конф. – Жуковский: ЦАГИ. – 1984. – С. 609 – 615.
174. Гребеников А.Г. Исследование эффективности технологических способов задержки роста усталостных трещин в соединениях

тонкостенных конструкций/ А.Г. Гребеников, В.Н. Стебенев, А.М. Тимченко // Авиационная промышленность. – М.: Машиностроение. – 1980. – С. 1 – 3. ДСП.
175. Гребеников А.Г. Проектирование продольных соединений стенок лонжеронов на заданную долговечность / А.Г. Гребеников, В.Н. Стебенев, С.В. Трубаев // Проектирование самолетных конструкций и их соединений. – Х.: ХАИ. – 1987. – С. 74 – 86.
176. Гребеников А.Г. Методы повышения усталостной долговечности соединений в регулярной части лонжеронов / А.Г. Гребеников, А.М. Тимченко, В.Н. Стебенев // Комплексное обеспечение ресурса авиаконструкций: тр. всесоюз. конф. – Жуковский: ЦАГИ. – 1984. – С. 676 – 681. ДСП.
177. Гребеников А.Г. Конструктивно-технологические методы продления ресурса заклепочных соединений стенок лонжерона/ А.Г. Гребеников, А.М. Тимченко, С.В. Трубаев // Вопросы проектирования и производства конструкций летательных аппаратов. – Х.: Гос. аэрокосм. ун-т «ХАИ». – 1999. – Вып. 15. – С. 133 – 139.
178. Гребеников А.Г. Технология исследования усталостной долговечности сборных отсеков лонжеронов с вырезами в стенке/ А.Г. Гребеников, А.М. Тимченко, С.В. Трубаев // Открытые информационные и компьютерные интегрированные технологии. – Х.: Нац. аэрокосм. ун-т «ХАИ». – 1999. – Вып. 4. – С. 27 -36.
179. Гребеников А.Г. Исследование технологических способов задержки роста усталостных трещин в соединениях тонкостенных конструкций/ А.Г. Гребеников, А.М. Тимченко, В.Н. Стебенев // Проблемы оптимизации и автоматизации технологических процессов сборки и выполнения соединений в конструкциях самолетов и вертолетов: тр. всесоюз. семинара. – М.: МАИ. – 1978. – С. 67-76.
180. Гребеников А.Г. Распределение усилий между болтами односрезного усовидного соединения/ А.Г. Гребеников, М.Н. Клименко, М.Н. Федотов // Вопросы проектирования самолетных конструкций. – Х.: ХАИ. – 1978. – Вып. 1. – С. 97 – 101.
181. Гребеников А.Г. Исследование влияния технологических отклонений по плоскости стыка на долговечность односрезных болтовых соединений самолетных конструкций/ А.Г. Гребеников, А.Н. Чайка // Труды XI НТК МС и НТО п/я А3395. – К., 1973. ДСП.
182. Гребеников А.Г. Исследование влияния характера контакта по плоскостям двусрезного болтового соединения на его выносливость/ А.Г. Гребеников, А.Н. Чайка // Труды XI НТК МС и НТО п/я А3395. – К., 1973. ДСП.
183. Гребеников А.Г. Интегрированные технологии проектирования высокоресурсных самолетных конструкций/ А.Г. Гребеников //

Открытые информационные и компьютерные интегрированные технологии. – Х.: Гос. аэрокосм. ун-т «ХАИ». – 2000. – Вып. 7. – С. 15 – 37.
184. Гречищев Е.С. Соединение с натягом: расчеты, проектирование, изготовление/ Е.С. Гречищев, А.А. Ильяшенко. – М.: Машиностроение, 1981. – 247 с.
185. Грилицкий Д.В. Периодическая контактная упруго-пластическая задача для полуплоскости/ Д.В. Грилицкий, В.В. Матус, А.М. Ригин // Прикладная механика. – 1981. – № 5. – С. 89 – 94.
186. Гришин В.И. Прочность элементов авиационных конструкций с концентраторами напряжений/ В.И. Гришин, В.Ю. Донченко, Г.Л. Кожевников. – М.: ЦАГИ. – 1983. – № 620 (По материалам иностранной печати за 1970-1982 гг.). – С. 76.
187. Гребеников В.А. Экспериментальное исследование влияния способов обработки полосы в зоне цилиндроконического отверстия на характеристики ее усталостной долговечности / В.А. Гребеников // Открытые информационные и компьютерные интегрированные технологии: сб. науч. тр. Нац. аэрокосм. ун-та им. Н.Е. Жуковского «ХАИ». – Вып. 47. – Х., 2010. – С. 62 – 68.
188. Гузь А.Н. Теория трещин в упругих телах с начальными напряжениями (жесткие материалы)/ А.Н. Гузь // Прикладная механика. – 1981. – № 4. – С. 3 – 9.
189. Давыдов Ю.В. Геометрия крыла: Методы и алгоритмы проектирования несущих поверхностей/ Ю.В. Давыдов, В.А. Злыгарев. – М.: Машиностроение, 1987. – 136 с.
190. Джур Е.А. Технология создания термокатодов на основе гексаборида лантана / Е.А. Джур. – Днепропетровск: ДДУ, 1994. – 52 с.
191. Дитрих Я. Проектирование и конструирование: системный подход/ пер. с польск. / Я. Дитрих. – М.: Мир, 1981. – 456 с.
192. Долговечность конструктивных нерегулярностей планера самолета: учеб. пособие по лаб. практикуму, курс. и дипл. проектированию / А.Г. Гребеников, В.И. Рябков, С.В.Трубаев и др. – Х.: Нац. аэрокосм. ун-т «ХАИ», 2001. – 117 с.
193. Дорошенко Ю.О. Політканинні перетворення у деформативному конструюванні геометричних об’єктів/ Ю.О. Дорошенко. – К.: Педагогічна думка, 2001. – 390 с.
194. Егер С.М. Основы автоматизированного проектирования самолетов: учеб. пособие для студентов авиационных специальностей вузов / С.М. Егер, Н.К. Лисейцев, О.С. Самойлович. – М.: Машиностроение, 1986. – 232 с.
195. Егер С.М. Основы авиационной техники: учебник; под ред. И.А. Шаталова. – Изд. 3-е, исправл. и доп. / С.М. Егер,

А.М. Матвиенко, И.А. Шаталов. – М.: Машиностроение, 2003. – 720 с.
196. Единые нормы летной годности гражданских самолетов. – М.: Машиностроение, 1985. – 470 с.
197. Ефремов А.Ю. Влияние конструктивных параметров односрезного болтового соединения на коэффициенты концентрации контактных давлений/ А.Ю. Ефремов, А.Г. Гребеников, В. Н. Клименко // Открытые информационные и компьютерные интегрированные технологии. – Х.: Гос. аэрокосм. ун-т «ХАИ». – 1999. – Вып. 5. – С. 139 – 148.
198. Жоголев Е.А. Курс программирования/ Е.А. Жоголев, Н.П. Трифонов. – М.: Наука, 1971. – 400 с.
199. Задачи контактного взаимодействия элементов конструкций / А.Н. Подгорный, П.П. Гонтаровский, Б.Н. Киркач и др.; отв. ред. В.Л. Рвачев; АН УССР. Ин-т проблем машиностроения. – К.: Наук. думка, 1989. – 232 с.
200. Зайцев Н.А. Применение «численного микроскопа» в методе конечных элементов к исследованию полей напряжений в окрестности трещин/ Н.А. Зайцев, К.М. Гумеров // Сб. науч. тр. Челяб. политехн. ин-та. – 1981. – С. 10-18.
201. А.с. 1439307 СССР, МКИ F 16 B 5/02. Заклепка / Э.Н. Румянцев, А.Г. Гребеников, В.Н. Стебенев, В.Г. Бабичев (СССР). – № 4262397/31-27; заявл. 29.04.87; опубл. 23.11.88, Бюл. № 43. – 3 с.
202. А.с. 1447023 СССР, МКИ F 16 B 5/02. Заклепка / А.Г. Гребеников, Э.Н. Румянцев, В.Н. Стебенев, Е.Т. Василевский, А.Г. Шаманов (СССР). – № 4230399/31-27; заявл. 04.03.87. ДСП
203. А.с. 1581883 СССР, МКИ. F 16 B 19/08. Заклепка / Э.Н. Румянцев, А.Г. Гребеников, В.Н. Стебенев, В.Г. Бабичев (СССР). – № 4334438/31-27; заявл. 13.10.87; опубл. 30.07.90, Бюл. № 28.– 3 с.
204. А.с. 1541436 СССР, МКИ. F 16 B 5/04, 19/06. Заклепочное соединение деталей/ Э.Н. Румянцев, А.Г. Гребеников, В.Н. Стебенев, Е.А. Большаков, В.Г. Бабичев (СССР). – № 4364210/31-27; заявл. 11.01.88; опубл. 07.02.90, Бюл. № 5. – 3 с.
205. Закономерности развития трещин усталости в пластинах из сплава АК41-Т1 при двухосном напряженном состоянии в условиях нормальных и повышенных температур / С. В. Бутушин, Я.Я. Погребняк, В.Г. Смыков, А.Ф. Тимофеев // Динамика, выносливость и надежность авиационных конструкций и систем. – М., 1979. – С. 67 – 76.
206. Заявка на винахід № 93080819 Україна, МКІ 5 G 01 B13/08. Спосіб визначення локальної посадки у потайному механічному з′єднанні / В.І. Рябков, О.Г. Гребеніков, В.В. Губарев, В.М. Андрющенко, Е.М. Румянцев, С.Г. Шиян (Україна). – № 4634527/31-27;заявл.

04.02.93; опубл. 28.12.94, Бюл. № 7. – 4 с.
207. Заявка на изобретение СССР, B 21 J 15/36. Обжимка для клепки / А.Г. Гребеников, Н.М. Панченко, И.О. Паньковский, Э.Н. Румянцев, Е.Т. Василевский, И.А. Уличкин (СССР). – № 4942027/27/046310. заявл. 03.06.91; решение о выдаче патента 25.03.92.
208. Заявка на изобретение Российская Федерация, МКИ F 16 B 5/02 Болтовое соединение деталей / А.Г. Гребеников (UA), Э.Н. Румянцев (UA), В.А. Винник (RU), В.Н. Стебенев (RU) (СССР). – № 5026331/27/079703, заявл. 27.12.91; решение о выдаче патента 23.09.93.
209. Зенкевич О. Метод конечных элементов в теории сооружений и в механике сплошных сред/ пер. с англ. А.П. Троицкого и С.В. Соловьева; под ред. Ю. К. Зарецкого/ О. Зенкевич, И. Чанг. – М.: Недра, 1974. – 240 с.
210. Интегрированная система создания оригинал-макетов технической, научной и учебной документации на английском языке / А.Г. Гребеников, Ю.Н. Богдан, В.В. Звягинцев, М.В. Кириленко // Открытые информационные и компьютерные интегрированные технологии. – Х.: Гос. аэрокосм. ун-т «ХАИ». – 1998. – Вып. 1. – С. 102 – 108.
211. Информационные технологии в наукоемком машиностроении: Компьютерное обеспечение индустриального бизнеса / под общ. ред. А.Г. Братухина– К.: Техніка, 2001. – 728 с.
212. Иосилевич Г.Б. Концентрация напряжений и деформаций в деталях машин/ Г.Б. Иосилевич. – М.: Машиностроение, 1981. – 224 с.
213. Исследование влияния величины контактных давлений на выносливость конструктивных элементов из титанового сплава ВТ-6 / А.Г. Гребеников, В.Н. Клименко, В.Н. Попович, В.Н. Стебенев // Усталостные характеристики летательных аппаратов. – Х.: ХАИ. – 1977. – Вып. 1. – С. 20 – 25.
214. Исследование влияния осевого и радиального натягов на выносливость полосы с отверстием / Л.Д. Арсон, А.Г. Гребеников, В.Н. Клименко и др. // Вопросы оптимизации тонкостенных силовых конструкций. – Х.: ХАИ. – 1976. – Вып. 2. – С. 84 – 92.
215. Исследование влияния характера контакта и полимерного заполнителя ЗП-2 на выносливость срезных болтовых стыков самолетных конструкций / С.А. Вигдорчик, Л.Д. Арсон, А.Г. Гребеников, В.Ф. Воронов // Методы повышения ресурса соединений элементов конструкций. – М.: ЦАГИ. – 1974. – Вып. 1. – С. 57 – 62. ДСП.
216. Исследование выносливости моделей усовидных стыков самолетных конструкций / Л.Д. Арсон, А.Г. Гребеников, А.М. Тимченко, М.Н. Федотов // Вопросы оптимизации тонкостенных силовых

конструкций. – Х.: ХАИ. – 1976. – Вып. 2. – С. 76 – 84.
217. Исследование выносливости потайных болтовых стыков с натягом / Л.Д. Арсон, А.Г. Гребеников, В.Н. Желдоченко, В.Н. Стебенев // Методы повышения ресурса соединений элементов конструкций. – М.: ЦАГИ. – 1974. – Вып. 1. – С. 44 – 46. ДСП.
218. Исследование долговечности срезных болтовых стыков при использовании полимерного заполнителя ЗП-2 / С.А. Вигдорчик, Л.Д. Арсон, А.Г. Гребеников, В.Ф. Воронов // Вопросы оптимизации тонкостенных силовых конструкций. – Х.: ХАИ. – 1975. – Вып. 1. – С. 113 – 119.
219. Исследование кинетики разрушения пластичных материалов на заключительной стадии деформирования / А.А. Лебедев, О.И. Марусий, Н.Г. Зайцев, Н.Г. Чаусов // Проблемы прочности. – 1982. – № 1. – С. 12 – 18.
220. Исследование концентрации контактных давлений в односрезном болтовом соединении / А.Г. Гребеников, В.Н. Желдоченко, В.Н. Клименко, В.Н. Стебенев // Вопросы оптимизации тонкостенных силовых конструкций. – Х.: ХАИ. – 1975. – Вып. 1. – С. 150 – 159.
221. Исследование усталостных характеристик полосы с заполненным отверстием в условиях фреттинг-коррозии / Л.Д. Арсон, А.Г. Гребеников , В.Н. Клименко и др. // Усталостные характеристики летательных аппаратов. – Х.: ХАИ. – 1977. – Вып. 1. – С. 35 – 39.
222. К исследованию выносливости соединений стенки с поясами и стойками в лонжеронах / Л.Д. Арсон, А.Г. Гребеников, А.М. Тимченко, В.Н. Стебенев // Вопросы проектирования самолетных конструкций. – Х.: ХАИ. – 1978. – Вып. 1. – С. 85 – 89.
223. Казанцев В.Г. Конечноэлементный анализ поля напряжений в окрестности трещин энергетическими и прямыми методами/ В.Г. Казанцев, А.И. Мишичев // Прикладная механика. – 1982. – № 3. – С. 77 – 81.
224. Карпов Г. Н. Задачи конструкционного торможения трещин: автореф. дис. …канд. техн. наук: 05.07.03/ Григорий Николаевич Карпов; Моск. ин-т хим. машиностроения. – М., 1982. – 34 с.
225. Качество и сертификация промышленной продукции: учеб. пособие / А.Г. Гребеников, А.К. Мялица, В.М. Рябченко и др. – Х.: Гос. аэрокосм. ун-т «ХАИ», 1998. – 396 с.
226. Кинетика роста несквозных усталостных трещин в элементах самолетных конструкций / А.А. Шанявский, А.В. Карасев, С.Д. Попов, К.А. Вонцович // Наука и техника гражд. авиации. Сер. ЛА и двигатели: сб. науч. труд. ГосНИИГ.– 1982. – Вып. 2. – С. 19 – 22.
227. Кирдюк А.М. Об учете условий эксплуатации при прогнозировании роста усталостных трещин/ А.М. Кирдюк, В.П. Павелко // Динамика,

выносливость и надежность авиационных конструкций и систем. – М., 1979. – С. 59 – 62.
228. Кириленко А.Б. Некоторые закономерности роста ранних усталостных трещин в образцах из Д16 АТВ / А.Б. Кириленко // Сб. науч. тр. КИИ ГА. Эксплуатационная надежность планера и систем воздушных судов. – К, 1981. – С. 34 – 36.
229. Кишкина С. И. Сопротивление разрушению алюминиевых сплавов/ С.И. Кишкина. – М.: Металлургия, 1981. – 280 с.
230. Клюев П.А. Система создания двуязычного каталога деталей и сборочных единиц самолета/ П.А. Клюев, А.Г. Гребеников, С.В. Воронов // Открытые информационные и компьютерные интегрированные технологии. – Х.: Гос. аэрокосм. ун-т «ХАИ». – 1998. – Вып. 1. – С. 111 – 114.
231. Кобелев Е.А. Численный метод исследования напряженно-деформированного состояния около подкрепленного отверстия для пластин конечных размеров/ Е.А. Кобелев // Строительная механика сооружений. – Л., 1982. – С. 46 – 52.
232. Кобылянский А.А. Характеристики газотурбинных двигателей: учеб. пособие/ А.А. Кобылянский, А.Г. Гребеников. – Х.: ХАИ, 1985. – 82 с.
233. Когаев В. П. Расчеты деталей машин и конструкций на прочность и долговечность / В. П. Когаев, Н. А. Махутов, А. П. Гусенков. – М.: Машиностроение, 1985. – 347 с.
234. Когаев В.П. Сопротивление усталости в зонах концентрации напряжений с малыми радиусами/ В.П. Когаев // Машиноведение. – 1983. – № 1. –С. 61 – 66.
235. Комплекс технических, системных и программных средств для проектирования и анализа авиационных конструкций / Г.Б. Варшавьяк, А.Г. Гребеников, А.М. Гуменный, А.В. Заозерский // Открытые информационные и компьютерные интегрированные технологии. – Х.: Гос. аэрокосм. ун-т «ХАИ». – 1998. – Вып. 1. – С. 42 – 46.
236. Комплексное обеспечение ресурса авиаконструкций: докл. науч.-техн. конф. по ресурсу авиаконструкций: в 6 кн. – М.: ЦАГИ, 1984. – Кн 4. – 856 с.
237. Компьютерное моделирование летательного аппарата многофункционального беспилотного авиационного комплекса гражданского назначения / В.Д. Белый, А.К. Мялица, А.Г. Гребеников, и др. // Авиационно-космическая техника и технология: тр. Нац. аэрокосм. ун-та «ХАИ». – Х., 2001. – Вып. 25. – С. 88 – 100.
238. Компьютерно-физическое моделирование в авиации / Я.И. Скалько, Г.Ю. Дукин, В.И. Лахно и др. / под ред. В.И. Лахно. – Х.: Септима ЛТД, 2001. – 224 с.

239. Компьютерные интегрированные и открытые информационные технологии в учебном процессе / А.Г. Гребеников, А.В. Заозерский, Ю.В. Шипилов и др.// Подготовка специалистов к работе в условиях открытых информационных и компьютерных технологий: тр. Междунар. науч.-метод. конф. – Х.: ХАИ. – 1996. – С. 20 – 24.
240. Компьютерные технологии проектирования: консп. лекций / А.Г. Гребеников, А.М. Гуменный, В.В. Парфенюк и др. – Х.: Нац. аэрокосм. ун-т «ХАИ», 2001. – Ч. 1. – 449 с.
241. Компьютерные технологии проектирования: консп. лекций / А.Г. Гребеников, Ю.В. Железняков, А.М. Гуменный и др. – Х.: Нац. аэрокосм. ун-т «ХАИ», 2000. – Ч.2. – 226 с.
242. Компьютерные технологии проектирования: консп. лекций в 2 ч. // А.Г. Гребеников, А.А. Кобылянский, Ю.В. Железняков и др. – Х.: Нац. аэрокосм. ун-т «ХАИ», 2000. – Ч.1. – 172 с.
243. Компьютерные технологии проектирования: лаб. практикум в 2 ч. // А.Г. Гребеников, А.А. Кобылянский, В.Н. Желдоченко и др. – Х.: Нац. аэрокосм. ун-т «ХАИ», 2001. – Ч.1.– 103 с.
244. Конструирование крыла пассажирского самолета в компьютерной интегрированной системе CAD/CAM/CAE UNIGRAPHICS / Ю.В. Железняков, А.Г. Гребеников, А.М. Гуменный и др. // Подготовка специалистов к работе в условиях открытых информационных и компьютерных технологий: тр. Междунар. науч.-метод. конф.– Х.: ХАИ. – 1996. – С. 52 – 56.
245. Конструктивно-технологические методы повышения усталостной долговечности односрезных заклепочных соединений / А.Г. Гребеников, В.М. Андрющенко, Е.Т. Василевский, В.Н. Стебенев // Вопросы проектирования самолетных конструкций. – Х.: ХАИ. – 1983. – Вып. 4. – С. 59 – 67.
246. Конструктивно-технологические способы повышения усталостной долговечности поперечных срезных болтовых соединений самолетных конструкций: руковод. техн. материалы / В.Н. Стебенев, А.Г. Гребеников, В.Н. Желдоченко, Э.Н. Румянцев // Сопротивление усталости и трещиностойкость сплавов, элементов и агрегатов авиационных конструкций. – М.: ЦАГИ. – 1990. – Вып. 6. – 80 с. ДСП.
247. Конструктивно-технологические способы повышения усталостной долговечности соединений стенок с поясами и перестыковочными накладками в сборных лонжеронах: руковод. техн. материалы / В.Н. Стебенев, А.Г. Гребеников, А.М. Тимченко и др.// Сопротивление усталости и трещиностойкость сплавов, элементов и агрегатов авиационных конструкций. –М.: ЦАГИ. – 1987. – Вып. 2. – 40 с. ДСП.
248. Конструктивные способы задержки роста усталостных трещин в стенках лонжеронов / А.Г. Гребеников, С.В. Трубаев, А.М. Тимченко,

В.Н. Стебенев // Проектирование самолетных конструкций и их соединений. – Х.: ХАИ. –1986. – С. 32 – 39.
249. Концепция подготовки специалистов для работы в условиях компьютерно-интегрированных производств / В.И. Рябков, В.Н. Фурашев, В.С. Кривцов и др. // Подготовка специалистов к работе в условиях открытых информационных и компьютерных технологий: тр. Междунар. науч.-метод. конф.– Х.: ХАИ. – 1996. – С. 9 – 12.
250. Концепция создания автоматизированного беспилотного авиационного диагностического комплекса для контроля технического состояния трубопроводного транспорта / В.Д. Белый, А.К. Мялица, А.Г. Гребеников и др.// Технологические системы: – К.: УкрНИИАТ. – 2001. – Вып. 5(11). – С. 37 – 44.
251. Концепция создания корпоративной информационно-вычислительной сети Харьковского авиационного института / Н.Т. Березюк, В.И. Рябков, В.С. Кривцов и др. // Подготовка специалистов к работе в условиях открытых информационных и компьютерных технологий: тр. Междунар. науч.-метод. конф.– Х.: ХАИ. -1996. – С. 13 – 16.
252. Концепция создания корпоративной информационно-вычислительной сети предприятий авиационно-промышленного комплекса / А.К Мялица, А.Г. Гребеников, А.В. Заозерский и др.// Открытые информационные и компьютерные интегрированные технологии. – Х.: Гос. аэрокосм. ун-т «ХАИ». – 1998. – Вып. 2. – С. 13 – 29.
253. Крагельский И.В. Основы расчетов на трение и износ/ И.В. Крагельский, М.Н. Добычин, В.С. Комбалов. – М.: Машиностроение, 1977. – 526 с.
254. Крепежные изделия односторонней клепки и безударной постановки по отраслевым стандартам и чертежам собственной разработки: каталог в 5 ч. – Нижний Новгород: АО «Нормаль», 1996. – Ч. 3. – 82 с.
255. Крепежные изделия по национальным стандартам Германии и США: каталог в 5 ч.– Нижний Новгород: АО «Нормаль», 1995. – Ч. 4. – 100 с.
256. А.с. 781422 СССР, МКИ F 16 B 19/06/ Крепежный элемент/ Л.Д. Арсон, А.Г. Гребеников, В.Н. Желдоченко, А.М. Тимченко, Е.Т. Василевский, В.П. Рычик, В.Н. Стебенев (СССР). – № 2692339/25-27; заявл. 06.12.78; опубл. 23.11.80, Бюл. № 43 – 3 с.
257. Кривов Г.А. Технология самолетостроительного производства/ Г.А Кривов. – К.: УкрНИИАТ, 1997. – 459 с.
258. Кривов Г.А. Мировая авиация на рубеже XX-XXI столетий. Промышленность, рынки/ Г.А. Кривов, В.А. Матвиенко, Л.Ф. Афанасьева. – К.: УкрНИИАТ, 2003. – 296 с.
259. Кривцов В.С. Проектирование вертолетов: учеб./ В.С. Кривцов, Я.С. Карпов, Л.И. Лосев. – Х.: Нац. аэрокосм. ун-т «ХАИ», 2003. – 344 с.

260. Критический анализ некоторых вероятностных моделей развития усталостных трещин // Экспресс-информация «Воздушный транспорт» ГосНИИ ГА. Сер. Надежность, вечность, ресурс, техническое обслуживание и ремонт. – 1981. – Вып. 2. – С. 9 – 12.
261. Крысин В.Н. Технологическая подготовка авиационного производства/ В.Н. Крысин. – М.: Машиностроение, 1984. – 200 с.
262. Кукишев В.Л. О разновидности метода конечных элементов /В.Л. Кукишев, Ю.Н. Санкин // Прикладная механика. – 1982. – № 7. – С. 29 – 33.
263. Лагутин В.Г. Растяжение пластины с трещиной вблизи упрочненного отверстия, заполненного упругим диском/ В.Г. Лагутин // Учен. записки ЦАГИ. – 1982. – Вып. 13. – № 5. – С. 148 – 154.
264. Лебедев А.А. К оценке трещиностойкости пластичных матереалов/ А.А. Лебедев, Н.Г. Чаусов // Проблемы прочности. – 1982. – № 2. – С. 11 – 13.
265. Леонтьев В.П. Новейшая энциклопедия Интернет/ В.П. Леонтьев. – М.: ОЛМА-ПРЕСС, 2002. – 607 с.
266. Летные испытания самолетов: учебник для студентов высш. техн. учеб. заведений / К.К. Васильченко, В.А. Леонов, И.М. Пашковский, Б.К. Поплавский. – М.: Машиностроение, 1996. – 720 с.
267. Лизин В.Т. Проектирование тонкостенных конструкций/ В.Т. Лизин, В.А. Пяткин. – М.: Машиностроение, 1976. – 408 с.
268. Лисейцев Н.К. Вопросы машинного проектирования и конструирования самолетов/ Н.К. Лисейцев, О.С. Самойлович. – М.: МАИ, 1977. – 82 с.
269. Локальная информационно-вычислительная сеть самолетостроительного факультета Харьковского авиационного института / Л.А. Малашенко, А.Г. Гребеников, А.В. Заозерский и др.// Подготовка специалистов к работе в условиях открытых информационных и компьютерных технологий: тр. Междунар. науч.-метод. конф.– Х.: ХАИ. – 1996. – С. 43 – 45.
270. Мазепа А.Г. Методика определения длины трещины по раскрытию берегов нагрева/ А.Г. Мазепа, Е.А. Гринь, Т.Н. Мерозова // Проблемы прочности. – 1982. – № 6. – С. 21 – 24.
271. Матвиенко В.А. Производство пассажирских и транспортных самолетов / В.А. Матвиенко, А.А. Щурбак // Техн. информ. УкрНИИАТ 1 (9). – К.: УкрНИИАТ, 1999. – С. 136.
272. Матусевич В.И. Концепция и планы комплексного решения задач автоматизированного проектирования, технологической подготовки и управления самолетостроительным производством/ В.И. Матусевич, Ю.Р. Бойко // Технологические системы. – К.: УкрНИИАТ. – 1999. – Вып. 1. – С. 77 – 82.

273. Машиностроение: самолеты и вертолеты: энцикл. – Кн. 1/ Ред. совет: К.В. Фролов и др. – М.: Машиностроение. Т. IV-21. Аэродинамика, динамика полета и прочность / Г.С. Бюшгенс, Ю.А. Азаров, Г.А. Амирьянц и др.; под общ. ред. Г.С. Бюшгенса. – 2002. – 800 с.
274. Методика оценки влияния конструктивных параметров на долговечность соединений стенок лонжерона / А.Г. Гребеников, В.Н. Стебенев, А.М. Тимченко, С.В. Трубаев // Самолетостроение. Техника воздушного флота. – Х.: ХГУ. – 1988. – Вып. 55. – С. 71 – 77.
275. Методика оценки влияния конструктивных параметров на долговечность соединений стенок лонжеронов / А.Г. Гребеников, В.Н. Стебенев, А.М. Тимченко, С.В. Трубаев // Современные проблемы обеспечения ресурса авиаконструкций: тр. VIII всесоюз. конф – М.: ЦАГИ. – 1986. – С. 142. ДСП.
276. Методика создания управляющих программ на станки с ЧПУ для изготовления формовочных приспособлений с использованием системы CAD/CAM/CAE UNIGRAPHICS / А.К. Мялица, С.А. Филиппов, А.Г. Гребеников, С.А. Лихачев // Открытые информационные и компьютерные интегрированные технологии. – Х.: Гос. аэрокосм. ун-т «ХАИ». – 1998. – Вып 2. – С. 96 – 101.
277. Методические указания к дипломному проектированию для студентов специальности 1301 (специализация – самолетостроение) Сост.: А.Г. Гребеников, А.А. Кобылянский, В.И. Рябков. – Х.: ХАИ, 1990. – 39 с.
278. Методология создания твердотельной модели носка нервюры руля направления самолета с применением компьютерных интегрированных систем CADDS5 и UNIGRAPHICS / А.Г. Гребеников, А.Н. Петров, С.П. Светличный и др. // Открытые информационные и компьютерные интегрированные технологии. – Х.: Гос. аэроком. ун-т «ХАИ». – 1998. – Вып. 2. – С. 266 – 274.
279. Методы обеспечения заданной долговечности и герметичности неподвижных потайных болтовых соединений / А.Г. Гребеников, В.Н. Желдоченко, В.А. Гребеников, А.М. Гуменный // Открытые информационные и компьютерные интегрированные технологии. – Х.: Нац. аэрокосм. ун-т «ХАИ». – 2002. – Вып. 15. – С. 131 – 153.
280. Методы определения влияния конструктивно-технологических параметров на выносливость элементов планера самолёта / А.Г. Гребеников, С.В. Трубаев, В.А. Гребеникови др.// Открытые информационные и компьютерные интегрированные технологии. – Х.: Нац. аэрокосм. ун-т «ХАИ». – 2001. – Вып. 10. – С. 19 – 54.
281. Методы оптимизации авиационных конструкций/ Н.В. Баничук, В.И. Бирюк, А.П. Сейранян и др. – М.: Машиностроение, 1989. – 296 с.
282. Механика разрушения. Разрушение конструкций: пер. с англ. / под

ред. Р.В. Гольдштейна. – М.: Мир, 1980. – 255 с.
283. Младенцев И.П. Исследование прочности заклепочных соединений/ И.П. Младенцев // Тр. ЦАГИ. – Вып. №1471. – М.: ЦАГИ. – 1972. – С. 88.
284. А.с. 1751461 СССР, МКИ F 16 B 5/02. Многорядное соединение деталей / Э.Н. Румянцев, В.М. Андрющенко, А.Г. Гребеников, В.Г. Бабичев (СССР). – № 4858982/27; заявл. 13.08.90; опубл. 30.07.92, Бюл. № 28.– 3 с.
285. Моделирование авиационных конструкций с помощью системы КОМПАС-ГРАФИК5.Х: учеб. пособие / И.Г. Волокитин, А.Г.Гребеников, А.К. Мялица, О.Н. Лысенко. — Х.: Нац. аэрокосм. ун-т «ХАИ», – 2002. – 285 с.
286. Моделирование объектов авиационной техники с помощью компьютерных систем: лаб. практикум в 2 ч. / А.Г. Гребеников, В.Н. Король, Ю.В. Железняков и др.– Х.: Нац. аэрокосм. ун-т «ХАИ», 2002. – Ч. 1. – 181 с.
287. Науменко В.П. Метод определения раскрытия трещин в условиях плоской деформации/ В.П. Науменко // Проблемы прочности. – 1981. – Т. 9. – С. 28 – 34
288. Науменко П.О. Исследование с помощью системы CAD\CAE ANSYS влияния технологических отклонений, образующихся при изготовлении заклепок по ОСТ1 34040-79 и выполнении отверстий под их установку, на характер распределения радиального натяга и НДС по толщине пакета после процесса клепки/ П.О. Науменко, А.Г. Гребеников, Ю.А. Мовчан // Технологические системы. – К.: УкрНИИАТ. – 2003. – Вып. 2(18). – С. 15 – 24.
289. Науменко П.О. Метод определения усилий запрессовки, втягивания и выпрессовки болтов при их установке в алюминиевые пакеты с радиальным натягом отверстиями / П.О. Науменко, А.Г. Гребеников, Ю.А. Мовчан // Авиационно-космическая техника и технология: тр. Нац. аэрокосм. ун-та «ХАИ». – Х., 2003. – Вып. 38/3. – С. 14 – 23.
290. Нормы летной годности самолетов транспортной категории (АП-25). М.: МАК, 1994. – 322 с.
291. О базисе системы качества промышленной продукции в современных социально-экономических условиях / В.И. Рябков, В.Н. Фурашев, А.Г. Гребеников, А.В. Юрченко // Методологические проблемы качества обучения и обучение качеству: тр. науч.-метод. конф.– Х.: ХАИ. – 1996. – С. 70-79.
292. Обзор современных методов расчета и корреляции при оценке усталости. Fatique offs kore Struct Dteels Implicit. Dep. Engergy's Res. Programme Proc. Cont., London, 24-25 Febr, 1984, London.1981, 113-121. //Реф. журнал «Механика», 1983, 3 Д625.

293. Оборудование самолетов: учеб. пособие / А.Г. Гребеников, А.А. Кобылянский, В.В. Буланов, С.А. Бычков – Х.: ХАИ, 1988. – 103 с.
294. Общее проектирование вертолетов / В.А. Богуслаев, В.С. Кривцов, Л.И. Лосев, В.И. Рябков. – Запорожье: ОАО Мотор Сич, 2001. – 324 с.
295. Определение усталостной долговечности элементов конструкций, выполненных из сталей: учеб. пособие / М.Н. Федотов, В.И. Рябков, А.Г. Гребеников и др. – Х.: ХАИ, 1989. – 33 с.
296. Опыт внедрения в учебный процесс самолетостроительного факультета ХАИ системы CAD/CAM КОМПАС / В.И. Рябков, А.Г. Гребеников, А.А. Сердюков, И.Г. Волокитин // Открытые информационные и компьютерные интегрированные технологии. – Х.: Гос. аэрокосм. ун-т «ХАИ». – 1998. – Вып. 1. – С. 39 – 42.
297. Опыт создания учебного процесса по курсу «Информационные ресурсы и услуги INTERNET» / А.Г. Гребеников, А.В. Заозерский, А.Г. Анохин, С.Н. Емельянцев // Подготовка специалистов к работе в условиях открытых информационных и компьютерных технологий: тр. Междунар. науч.-метод. конф. – Х.: ХАИ. – 1996. – С. 27 – 30.
298. Организация учебного процесса по курсу «Информационные ресурсы и услуги сети INTERNET» / В.И. Рябков, А.Г. Гребеников, А.В. Заозерский, С.Н. Емельянцев // Открытые информационные и компьютерные интегрированные технологии. – Х.: Гос. аэрокосм. ун-т «ХАИ». – 1998. – Вып. 1. – С. 7 – 9.
299. Орлов К.Я. Ремонт самолетов и вертолетов/ К.Я. Орлов, В.А. Пархимович. – М.: Транспорт, 1986. – 295 с.
300. Основы общего проектирования самолетов с газотурбинными двигателями: учеб. пособие в 2 ч. / П.В. Балабуев, С.А. Бычков, А.Г. Гребеников и др. – Х.: Нац. аэрокосм. ун-т «ХАИ», 2003. – Ч. 1. – 454 с.
301. Основы общего проектирования самолетов с газотурбинными двигателями: учеб. пособие в 2 ч. / П.В. Балабуев, С.А. Бычков, А.Г. Гребеников. – Х.: Нац. аэрокосм. ун-т «ХАИ», 2003. – Ч. 2. – 390 с.
302. Особенности интегрированного проектирования заклепочных соединений самолетных конструкций / А.Г. Гребеников, С.А. Бычков, С.В. Трубаев и др.// Открытые информационные и компьютерные интегрированные технологии. – Х.: Нац. аэрокосм. ун-т «ХАИ». – 2002. – Вып. 14. – С. 99 – 154.
303. Особенности перевода авиационной технической документации на английский язык: учеб. / Ю.Г. Андриенко, Ю.Н. Богдан, А.Г. Гребеников. – Х.: Нац. аэрокосм. ун-т «ХАИ», 2003. – 441 с.
304. Особенности создания высокоресурсных потайных заклепочных соединений тонких обшивок / А.Г. Гребеников, В.В. Губарев,

С.В. Воронов, С.А. Третьяков // Открытые информационные и компьютерные интегрированные технологии. – Х.: Гос. аэрокосм. ун-т «ХАИ». – 2000. – Вып. 6. – С. 87 – 106.
305. Парамонов Ю.М. Надежность, живучесть и ресурс конструкций летательных аппаратов/ Ю.М. Парамонов. – Рига: РКИИ ГА, 1980. – 79 с.
306. Пат. 2066003 Российская Федерация, МКИ F 16 B 19/06. Заклепка. / А.Г. Гребеников (UA), В.В. Губарев (UA), В.М. Андрющенко (UA), С.Г. Васильченко (UA), С.Г. Шиян (UA), Е.А. Большаков (UA), В.М. Пупышев (UA), Е.Т. Василевский (UA), В.Н. Стебенев (RU), В.Ф. Воронов (RU). – № 5023844/08; заявл. 27.01.92; опубл. 27.08.96, Бюл. № 24. – 3 с.
307. Пат. 51545 Україна, МКІ B64C39/02, B64C31/036, B64C37/00, B64F1/02, G05D1/00, G08G5/02, G08G9/00. Авіаційний комплекс дистанційної діагностики. / В.Д. Бєлий, О.Г. Гребеніков, А.К. М′ялиця, В.О. Черановський, І.І. Капцов, В.І. Холодов, О.М. Тимченко, В.В. Парфенюк (Україна). – № 2002054162; заявл. 21.05.02, опубл. 15.11.02, Бюл. № 11.
308. Пат. № 3469305, США, Кл. 29-527, 4, 1969.
309. Петриков В.Г., Власов А.П. Прогрессивные крепежные изделия/ В.Г. Петриков, А.П. Власов. – М.: Машиностроение, 1991. – 256 с.
310. Петухов А.Н. Сопротивление усталости деталей ГТД/ А.Н. Петухов. – М.: Машиностроение, 1993. – 240 с.
311. Писаренко Г. С. Исследование явления остановки трещины в пластине зонами поперечного сжатия/ Г. С. Писаренко // Проблемы прочности. – 1978. – № 1. – С. 8 – 12.
312. Писаренко Г.С. Деформирование и прочность материалов при сложном напряженном состоянии/ Г.С. Писаренко, А.А. Лебедев. – К.: Наук. думка, 1976. – 415 с.
313. Писаренко Г.С. Методика исследования разрушения листовых материалов при двухосном нагружении/ Г.С. Писаренко, В.П. Науменко, Е.Е. Онищенко // Проблемы прочности. – 1982. – № 3. – С. 3 – 9.
314. Повышение долговечности болтовых стыков с помощью полимерных заполнителей / Л.Д. Арсон, А.Г. Гребеников, В.Ф. Воронов, С.А. Вигдорчик // Авиационная промышленность. – М.: Машиностроение. – 1976. – Вып. 1. – С. 13 – 14. ДСП.
315. Повышение долговечности и живучести тонкостенных конструкций с усталостными трещинами / Е.Т. Василевский, А.Г. Гребеников, В.Н. Стебенев, А.М. Тимченко // Комплексное обеспечение ресурса авиаконструкций: тр. Всесоюз. конф.– Жуковский: ЦАГИ. – 1984. – С. 682 – 688. ДСП.

316. Повышение усталостной долговечности соединений обшивок с накладками путем разгрузки крайних рядов / А.Г. Гребеников, В.М. Андрющенко, А.М. Тимченко и др. // Проектирование самолетных конструкций и их соединений. – Х.: ХАИ. – 1986. – С. 50 – 58.
317. Предельные нагрузки болтовых соединений с накладкой при растяжении или изгибе. Constr. Met, 1982, 19, № 2, 35-59 // Реф. журнал «Механика», 1983, 1 Д64.
318. Перевод № 1630. Смазывающая способность дисульфида молибдена. Источник: Industrial Lubrication and Tribology. – 1969. – P. 241-247.
319. Приложение механики разрушения к прогнозированию фреттинг-усталости. Fretting Fatique London, 1981, 67-97/Место хранения ГПНТБ СССР // Реф. журнал «Механика», 1983, 3 Д569.
320. Применение вероятностно-статистических методов к вопросам прочности летательных аппаратов // По материалам иностранной печати. – № 502. Обзоры. Переводы. Рефераты. – М.: ЦАГИ, 1976. – 81 с.
321. Применение полимерных заполнителей при ремонте неподвижных срезных соединений элементов планера самолета / М.Н. Федотов, А.Г. Гребеников, В.М. Андрющенко и др. // Инженерно-авиационное обеспечение безопасности полетов: тр. всесоюз. науч. конф. – М.: МИИГА. – 1985. – С. 54. ДСП.
322. Проектирование гражданских самолетов: теории и методы / И.Я. Катырев, М.С. Неймарк, В.М. Шейнин и др.; под ред. Г.В. Новожилова. – М.: Машиностроение, 1991. – 672 с.
323. Проектирование конструкций самолетов: учеб. для студентов вузов, обучающихся по специальности «Самолетостроение» / Е.С. Войт, А.И. Ендогур, З.А. Мелик-Саркисян, И.М. Алявдин. – М.: Машиностроение, 1987. – 416 с.
324. Проектирование оптимальных конструкций летательных аппаратов // По материалам иностранной печати за 1957-1967 гг. № 308. Обзоры. Переводы. Рефераты. – М.: ЦАГИ, 1970. – 144 с.
325. Проектирование самолетных конструкций и их соединений: тем. сб. науч. тр. – Х.: ХАИ. – 1986. – 220 с.
326. Проектирование самолётов: лаб. практикум // А.Г. Гребеников, А.А. Кобылянский, В.Н. Король и др. – Х.: Нац. аэрокосм. ун-т «ХАИ», 2002. – 176 с.
327. Проектирование самолетов: учеб. для вузов / С.М. Егер, В.Ф. Мишин, Н.К. Лисейцев и др.; под. ред. С.М. Егера. – Изд. 3-е, перераб. и доп. – М.: Машиностроение, 1983. – 616 с.
328. Проектирование соединений стенок в сборных лонжеронах с учетом усталостной долговечности: учеб. пособие / А.Г. Гребеников,

А.М. Тимченко, С.В. Трубаев и др. – Х.: ХАИ, 1988. – 90 с.
329. Проектирование элементов самолетных конструкций с учетом усталости: учеб. пособие по лаб. практикуму / А.Г. Гребеников, В.И. Рябков, В.М. Андрющенко и др. – Х.: ХАИ, 1993. – 112 с.
330. Прочность самолета (методы нормирования расчетных условий прочности самолета)/ под. ред. А.И. Макаревского. – М.: Машиностроение, 1975. – 280 с.
331. Радиопрозрачные обтекатели летательных аппаратов. Проектирование, конструкционные материалы, технология производства, испытания: учеб. пособие / А.Г. Ромашин, В.Е. Гайдачук, Я.С. Карпов, М.Ю. Русин. – Х.: Нац. аэрокосм. ун-т «ХАИ», 2003. – 239 с.
332. Радченко С.Г. Математическое моделирование технологических процессов в машиностроении/ С.Г. Радченко. – К.: ЗАО «Укрспецмонтажпроект», 1998. – 274 с.
333. Разработка геометрической модели общего вида пассажирского самолета в компьютерной интегрированной системе CAD/CAM/CAE UNIGRAPHICS / А.Г. Гребеников, Ю.В. Железняков, С.В. Федченко и др. // Подготовка специалистов к работе в условиях открытых информационных и компьютерных технологий: тр. Междунар. науч.-метод. конф. – Х.: ХАИ. – 1996. – С. 25 – 26.
334. Разработка конструкций потайных заклепок с компенсатором в виде двойного усеченного конуса для соединения элементов крыла самолета / С.А. Бычков, А.Г. Гребеников, Е.Т. Василевский, Ю.А. Мовчан // Проектирование и производство самолетов и вертолетов: тр. Междунар. науч-техн. конф. – Х., Рыбачье: Нац. аэрокосм. ун-т «ХАИ». – 2003. – С. 11 – 15.
335. Разработка математического и программного обеспечения выбора параметров пассажирского самолета в компьютерной интегрированной системе / А.Г. Гребеников, В.Н. Желдоченко, А.А. Кобылянский и др.// Подготовка специалистов к работе в условиях открытых информационных и компьютерных технологий: тр. Междунар. науч.-метод. конф. – Х.: ХАИ. – 1996. – С. 49 – 51.
336. Расчет распределения усилий между крепежными элементами в соединениях листовых деталей методом подконструкций / А.Г. Гребеников, А.М. Тимченко, Э.Д. Голод, С.А. Востроknутов // Вопросы проектирования и повышения ресурса самолетных конструкций. – Х.: ХАИ. – 1989. – С. 31 – 42.
337. Ремонт летательных аппаратов: учеб. для вузов гражданской авиации; / под ред. Н.Л. Голего: – М.: Транспорт, 1977. – 424 с.
338. Рудаков А.Г. Эффективность местного глубокого пластического деформирования как способа повышения ресурса деталей самолета:

автореф. дис. …канд. техн. наук: 05.07.04/ Рудаков Александр Григорьевич / Всесоюз. ин-т авиац. материалов. – М., 1983. – 28 с.
339. Румянцев Э.Н. Выносливость поперечных болтовых соединений в условиях растяжения со сдвигом / Э.Н. Румянцев, А.Г. Гребеников, Л.Д. Арсон // Авиационная промышленность. – М.: Машиностроение. –1980. – С. 3 – 5. ДСП.
340. Румянцев Э.Н. Исследование выносливости поперечных болтовых панелей в условиях растяжения со сдвигом / Э.Н. Румянцев, А.Г. Гребеников, Л.Д. Арсон // Вопросы проектирования самолетных конструкций. – Х.: ХАИ. – 1979. – Вып. 2. – С. 76 – 79.
341. Рябков В.И. Открытые информационные и компьютерные интегрированные технологии в учебном процессе Государственного аэрокосмического университета «ХАИ»/ В.И. Рябков, А.Г. Гребеников, А.В. Заозерский // Открытые информационные и компьютерные интегрированные технологии. – Х.: Гос. аэрокосм. ун-т «ХАИ». – 1998. – Вып. 2. – С. 9 – 12.
342. Рябков В.И. Концепция современного инженерного образования/ В.И. Рябков, А.Г. Гребеников, В.Н. Фурашев // Методологические проблемы качества обучения и обучение качеству: тр. науч.-метод. конф.– Х.: ХАИ. – 1996. – С. 7 – 9.
343. Савинаев И. А. Исследование способов задержки роста усталостных трещин в тонкостенных конструкциях: автореф. дис. …канд. техн. наук: 05.07.05 / Савинаев Иван Александрович/ Рижск. авиац. ин-т. – Рига, 1973. – 26 с.
344. Савченко Н.И. Прогнозирование процесса развития усталостных трещин / Н.И. Савченко // Эксплуатационная надежность планера и систем воздушных судов. – К.: КИИ ГА, 1980. – С. 47 – 52.
345. Сб. докл. науч.-техн. конф. – М.: ЦАГИ, 1984. – Кн. 1. – 211 с.
346. Сб. докл. науч.-техн. конф. – М.: ЦАГИ, 1984. – Кн. 2. – 428 с.
347. Сб. докл. науч.-техн. конф. – М.: ЦАГИ, 1984. – Кн. 3. – 641 с.
348. Сб. докл. науч.-техн. конф. – М.: ЦАГИ, 1984. – Кн. 5. – 1025 с.
349. Сеник В.Я. Анализ характеристик развития усталостных трещин в элементах авиационных конструкций по данным эксплуатации/ В.Я. Сеник // Тр. ЦАГИ. – М., 1975. – С. 17 – 18.
350. Системное обеспечение корпоративной информационно-вычислительной сети ХАИ / В.С. Кривцов, В.И. Рябков, А.Г. Гребеников и др. // Открытые информационные и компьютерные интегрированные технологии. – Х.: Гос. аэрокосм. ун-т «ХАИ». – 1998. – Вып. 1. – С. 3 – 7.
351. Системы машинного проектирования конструкций и машинного конструирования // По материалам зарубежной печати за 1967-1975 гг. – № 493. Обзоры. Переводы. Рефераты. – М.: ЦАГИ, 1976. – 75 с.

352. Смирнов Н.Н. Обслуживание и ремонт авиационной техники по состоянию/ Н.Н. Смирнов, А.А. Ицкович. – 2-е изд., перераб. и доп. – М.: Транспорт, 1987. – 272 с.
353. Современные технологии авиастроения / под ред. А.Г. Братухина, Ю.Л. Иванова. – М.: Машиностроение, 1999. – 832 с.
354. Современные технологические процессы сборки планера самолета / под ред. Ю.Л. Иванова. – М.: Машиностроение, 1999. – 304 с.
355. А.с. 1186844 СССР, МКИ F 16 B 5/04. Соединение деталей внахлестку / А.Г. Гребеников, В.М. Андрющенко, А.М. Тимченко, С.В. Трубаев, А.Е. Литвиненко, Е.Т. Василевский, В.Н. Стебенев (СССР). – №3735962/25-27; заявл. 04.05.84; опубл. 23.10.85, Бюл. № 39. – 2 с.
356. А.с. 978649 СССР, МКИ F 16 B 5/04, F 16 B 19/04. Соединение деталей внахлестку / А.Г. Гребеников, В.М. Андрющенко, А.М. Тимченко, В.Н. Стебенев, А.Е. Литвиненко, Е.Т. Василевский (СССР). – № 3231978/25-27; заявл. 05.01.81; ДСП.
357. А.с. 1208335 СССР, МКИ F 16 B 5/02. Соединение деталей и способ сборки деталей/ А.Г. Гребеников, Э.Н. Румянцев, В.Н. Стебенев, А.М. Тимченко, Е.Т. Василевский, А.Е. Литвиненко (СССР). – № 3789860/25-27; заявл. 09.07.84; опубл. 30.01.86, Бюл. № 4. – 3 с.
358. А.с. 1444566 СССР, МКИ F 16 B 5/02. Соединение деталей и способ сборки деталей / А.Г. Гребеников, Э.Н. Румянцев, В.Н. Стебенев, Е.Т. Василевский, А.Г. Шаманов (СССР). – № 4136037/31-27; заявл. 15.10.86; опубл. 15.12.88, Бюл. № 46. – 4 с.
359. А.с. 1203252 СССР, МКИ F 16 B 5/02. Соединение деталей / А.Г. Гребеников, Э.Н. Румянцев, В.Н. Стебенев, А.М. Тимченко, Е.Т. Василевский (СССР). – № 3788939/25-27; заявл. 03.07.84; опубл. 07.01.86, Бюл. № 1. – 3 с.
360. А.с. 1303747 СССР, МКИ F 16 B 5/02. Соединение деталей / А.Г. Гребеников, Э.Н. Румянцев, В.Н. Стебенев, А.М. Тимченко, Е.Т. Василевский (СССР). – № 3995735/31-27; заявл. 25.12.85; опубл. 15.04.87, Бюл. №14. – 3 с.
361. А.с. 1355780 СССР, МКИ F 16 B 5/02. Соединение деталей / Э.Н. Румянцев, А.Г. Гребеников, В.Н. Стебенев, А.Г. Шаманов (СССР). – № 4005759/40-27; заявл. 10.01.86; опубл. 30.11.87, Бюл. № 44. – 3 с.
362. А.с. 1418524 СССР, МКИ F 16 B 5/02. Соединение деталей / А.Г. Гребеников, В.М. Андрющенко, А.М. Тимченко, В.Н. Стебенев, Е.Т. Василевский (СССР). – № 4182974/31-27; заявл. 15.01.87; опубл. 23.08.88, Бюл. № 31. – 2 с.
363. А.с. 1428844 СССР, МКИ F 16 B 5/02. Соединение деталей / Э.Н. Румянцев, А.Г. Гребеников, В.Н. Стебенев, А.Г. Шаманов (СССР). – № 4138664/31-27; заявл. 20.10.86; опубл. 07.10.88, Бюл. №

37. – 3 с.
364. А.с. 1477011 СССР, МКИ F 16 B 5/02. Соединение деталей / Э.Н. Румянцев, А.Г. Гребеников, В.Н. Стебенев, В.Г. Бабичев (СССР). – № 4241184/31-27; заявл. 11.05.87. ДСП.
365. А.с. 1493804 СССР, МКИ F 16 B 5/02. Соединение деталей / Э.Н. Румянцев, А.Г. Гребеников, А.Г. Шаманов, В.Г. Бабичев (СССР). – № 4317956/31-27; заявл. 20.10.87; опубл. 15.07.89, Бюл. № 26. – 3 с.
366. А.с. 1735624 СССР, МКИ F 16 B 5/02. Соединение деталей / Э.Н. Румянцев, А.Г. Гребеников, А.Г. Шаманов, В.Г. Бабичев (СССР). – № 4837914/27; заявл. 12.06.90; опубл. 23.05.92, Бюл. № 19. – 3 с.
367. А.с. 1754923 СССР, МКИ F 16 B 5/02. Соединение деталей / Э.Н. Румянцев, А.Г. Гребеников, В.Н. Стебенев, Е.Т. Василевский, Е.А. Большаков (СССР). – № 4251829/63; заявл. 29.05.87; опубл. 15.08.92, Бюл. № 30. – 3 с.
368. А.с. 627252 СССР, МКИ F 16 B 5/02. Соединение деталей / Л.Д. Арсон, Е.А. Большаков, А.Г. Гребеников, А.М. Тимченко (СССР). – № 2462838/25-27; заявл. 09.03.77; опубл. 05.10.78, Бюл. № 37. – 2 с.
369. А. с. 1010325 СССР. Соединение листовых деталей внахлестку / А. Г. Гребеников, В.М. Андрющенко, А.М. Тимченко, В.Н. Стебенев, С.А. Бычков, Е.Т. Василевский. – № 3231827/25-27; опубл. 15.07.93, Бюл. № 13. – 2 с.
370. А.с. 649894 СССР, МКИ F 16 B 35/04. Соединительное устройство / Л.Д. Арсон, Е.Т. Василевский, А.Г. Гребеников, В.Н. Желдоченко, В.Н. Стебенев, А.М. Тимченко (СССР). – № 2444630/25-27; заявл. 19.01.77; опубл. 28.02.79, Бюл. № 8. – 3 с.
371. Сопротивление усталости металлов при многоосном напряженном состоянии. Curr Adv. Mech. Des and Prod Proc. Ist Int Conf., Cairo, 27-29, Dec, 1979, Oxford e-a, 1981. 329-340 // Реф. журнал «Механика», 1983, 1 Д428.
372. Сопротивление усталости моделей типовых потайных болтовых соединений / А.Г. Гребеников, С.В. Трубаев, В.А. Гребеников, А.М. Гуменный // Авиационно-космическая техника и технология. – Х.: Гос. аэрокосм. ун-т «ХАИ». – 2002. – Вып. 32. – С. 390 – 401.
373. Сопротивление усталости пластин с заполненными болтами или втулками отверстиями, выполненными при действии на пластину растягивающей нагрузки / А.Г. Гребеников, Е.Т. Василевский, Ю.Н. Богдан, А.Е. Новожилов // Вопросы проектирования и производства конструкций летательных аппаратов. – Х.: Нац. аэрокосм. ун-т «ХАИ». – 2002. – Вып. 29 (2). – С. 144 – 151.
374. Сопротивление усталости пластин с отверстиями и типовых заклепочных соединений / А.Г. Гребеников, В.М. Андрющенко,

В.А. Гребеников и др. // Авиационно-космическая техника и технология: тр. Нац. аэрокосм. ун-та «ХАИ» – Х., 2002. – Вып. 32. – С. 73 – 86.
375. Сопротивление усталости ремонтных вариантов заклепочных соединений / В.М. Андрющенко, Е.Т. Василевский, А.Г. Гребеников, В.Н. Стебенев // Современные проблемы обеспечения ресурса авиаконструкций: тр. VIII Всесоюз. конф – М.: ЦАГИ. – 1986. – С. 44. ДСП.
376. Сопротивление усталости элементов конструкций / А.З. Воробьев, Б.И. Олькин, В.Н. Стебенев и др. – М.: Машиностроение, 1990. – 240 с.
377. А.с. 1165552 СССР, МКИ В 23 Р 6/00. Способ задержки роста усталостных трещин в конструкциях / А.Г. Гребеников, А.М. Тимченко, Е.Т. Василевский, В.Н. Стебенев, В.В. Шипилов (СССР). – №3707286/25-27; заявл. 23.11.83; опубл. 07.07.85, Бюл. № 25. – 3 с.
378. А.с. 1191247 СССР, МКИ В 23 Р 6/04. Способ задержки роста усталостных трещин/ А.Г. Гребеников, А.М. Тимченко, Э.Д. Голод, С.В. Трубаев, В.Н. Стебенев, Е.Т. Василевский (СССР). – № 3746532/25-27; заявл. 30.05.84; опубл. 15.11.85, Бюл. № 42. – 4 с.
379. А.с. 1374670 СССР. Способ задержки роста усталостных трещин МКИ В 64 F 5/00, В 23 Р 6/04. / А.Г. Гребеников, А.М. Тимченко, Э.Д. Голод, В.Н. Стебенев, Е.Т. Василевский, В.М. Андрющенко (СССР). – № 3739654/31-27/063398; заявл. 16.05.84; ДСП.
380. А.с. 1697369 СССР, МКИ В 64 F 5/00. Способ изготовления лонжерона крыла самолета / Э.Н. Румянцев, А.Г. Гребеников, А.Г. Шаманов, В.Г. Бабичев (СССР). – № 4800811/27; заявл. 11.03.90; ДСП.
381. А.с. 1766571 СССР, МКИ В 21 J 15/02. Способ клепки / А.Г. Гребеников, В.В. Губарев, В.М. Андрющенко, С.Г. Васильченко, И.В. Павлов, Е.А. Большаков, В.М. Пупышев (СССР). – № 4858182/27; заявл. 08.08.90; опубл. 07.10.92, Бюл. № 37. – 4 с.
382. А.с. 1738460 СССР, МКИ В 21 J 15/02. Способ образования заклепочного соединения / Э.Н. Румянцев, А.Г. Гребеников, А.Г. Шаманов, В.Г. Бабичев (СССР). № 4827099/27; заявл. 18.05.90; опубл. 07.06.92, Бюл. № 21. – 3 с.
383. А.с. 1796336 СССР, МКИ В 21 J 15/02, F 16 B 19/06. Способ образования заклепочного соединения / Э.Н. Румянцев, А.Г. Гребеников, Е.Т. Василевский, В.И. Мишин (СССР). – № 4911193/27; заявл. 15.02.91; опубл. 23.02.93, Бюл. № 7. – 3 с.
384. А.с. 1805278 СССР, МКИ G 01 B 5/30. Способ определения деформации крепежного элемента / Э.Н. Румянцев, А.Г. Гребеников, В.Н. Стебенев, В.Г. Бабичев, И.О. Паньковский (СССР). –

№4914562/28; заявл. 25.02.91; опубл. 30.03.93, Бюл. № 12. – 3 с.
385. А.с. 1809355 СССР, МКИ G 01 N 3/08. Способ определения податливости срезных крепежных элементов / Э.Н. Румянцев, А.Г. Гребеников, А.Г. Шаманов, В.Г. Бабичев, (СССР). № 4902956/28; заявл. 18.01.91; опубл. 15.04.93, Бюл. № 14. – 3 с.
386. А.с. 1796780 СССР, МКИ F 16 B 37/04. Способ получения анкерного соединения деталей / В.М. Андрющенко, Э.Н. Румянцев, В.В. Губарев, А.Г. Гребеников, В.Г. Бабичев (СССР). – № 4881474/27; заявл. 11.11.90; опубл. 23.02.93, Бюл. № 7. – 4 с.
387. А.с. 1751463 СССР, МКИ F 16 B 5/02, B 23 P 11/02. Способ получения болтового соединения деталей / Э.Н. Румянцев, А.Г. Гребеников, А.Г. Шаманов, В.Г. Бабичев (СССР). – № 4911192/27; заявл. 15.02.91; опубл. 30.07.92, Бюл. № 28.– 3 с.
388. А.с. 1735627 СССР, МКИ F 16 B 5/04. Способ получения заклепочного соединения деталей / Э.Н. Румянцев, В.М. Андрющенко, А.Г. Гребеников, В.Г. Бабичев (СССР). – № 4860945/27; заявл. 20.08.90; опубл. 23.05.92, Бюл. № 19. – 4 с.
389. А.с. 1794582 СССР, МКИ B 21 J 15/02, F 16 B 19/06. Способ получения заклепочного соединения деталей / А.Г. Гребеников, Э.Н. Румянцев, Е.Т. Василевский, В.И. Мишин (СССР). – № 4945183/27; заявл. 13.06.91; опубл. 15.02.93, Бюл. № 6. – 4 с.
390. А.с. 1735625 СССР, МКИ F 16 B 5/02. Способ получения многорядного срезного соединения деталей / Э.Н. Румянцев, А.Г. Гребеников, А.Г. Шаманов, В.Г. Бабичев (СССР). – № 4837924/27; заявл. 12.06.90; опубл. 23.05.92, Бюл. № 19. – 3 с.
391. А.с. 1742535 СССР, МКИ F 16 B 5/02. Способ получения соединения деталей / Э.Н. Румянцев, А.Г. Гребеников, А.Г. Шаманов, В.Г. Бабичев (СССР). – № 4785502/27; заявл. 23.01.90; опубл. 23.06.92, Бюл. № 23. – 3 с.
392. А.с. 1054006 СССР, МКИ B 23 P 6/04, B 23 P 6/00. Способ предотвращения роста усталостных трещин в тонкостенных конструкциях / А.Г. Гребеников, А.М. Тимченко, Е.Т. Василевский, А.Е. Литвиненко, Г.Ю. Бенгус, В.Н. Стебенев (СССР). – № 3474616/25-27; заявл. 22.07.82; опубл. 15.11.83, Бюл. № 42. – 3 с.
393. А.с. 725862 СССР, МКИ B 23 P 7/04. Способ предотвращения роста усталостных трещин / Л.Д. Арсон, А.Г. Гребеников, В.Н. Стебенев, А.М. Тимченко (СССР). – № 2657996/25-27; заявл. 01.09.78; опубл. 05.04.80, Бюл. № 13. – 2 с.
394. А.с. 1516287 СССР, МКИ B 23 P 6/04. Способ ремонта сборной панели/ А.Г. Гребеников, В.М. Андрющенко, А.М. Тимченко, В.Н. Стебенев, Е.Т. Василевский (СССР). – № 4340661/31-27; заявл. 07.12.87; опубл. 23.10.89, Бюл. № 39. – 3 с.

395. А.с. 1631917 СССР, МКИ В 64 F 5/00. Способ сборки крыла самолета Э.Н. Румянцев, А.Г. Гребеников, В.Н. Стебенев, В.Г. Бабичев. (СССР). – № 4371155/00-23; заявл. 01.02.88; ДСП.
396. А.с. 1707899 СССР, МКИ В 64 F 5/00. Способ сборки крыла самолета / Э.Н. Румянцев, А.Г. Гребеников, А.Г. Шаманов, В.Г. Бабичев (СССР). – № 4815048/23; заявл. 16.04.90. ДСП.
397. А.с. 1492847 СССР, МКИ F 16 B 5/02. Способ сборки пакета листовых деталей / Э.Н. Румянцев, А.Г. Гребеников, В.Н. Стебенев, В.Г. Бабичев (СССР). – № 4255570/31-27; заявл. 02.06.87; ДСП.
398. А.с. 1559810 СССР, МКИ. F 16 B 5/02. Способ сборки соединения деталей / Э.Н. Румянцев, А.Г. Гребеников, В.Н. Стебенев, В.Г. Бабичев (СССР). – № 4424975/31-27; заявл. 13.04.88; ДСП.
399. А.с. 1388176 СССР, МКИ В 21 J 15/02, F 16 B 5/02. Способ соединения деталей/ А.Г. Гребеников, А.М. Тимченко, А.Е. Новожилов, А.Г. Шаманов, А.Е. Большаков, Е.Т. Василевский, В.Ф. Воронов, В.Н. Стебенев (СССР). – № 4138540/31-27; заявл. 20.10.86; опубл. 15.04.88, Бюл. № 14. – 3 с.
400. Способы задержки роста усталостных трещин в самолетных конструкциях постановкой крепежных элементов с радиальным натягом и затяжкой: руковод. техн. материалы / В.Н. Стебенев, А.Г. Гребеников, А.М. Тимченко и др. // Сопротивление усталости и трещиностойкость сплавов, элементов и агрегатов авиационных конструкций. – М.: ЦАГИ. – 1989. – Вып. 4. – 51 с. ДСП.
401. Способы повышения усталостной долговечности односрезных соединений путем разгрузки крайних рядов: руковод. техн. материалы / В.Н. Стебенев, А.Г. Гребеников, В.З. Брагилевский и др. // – М.: ЦАГИ. – 1983. – 165 с.
402. Справочная книга по расчету самолета на прочность / М.Ф. Астахов, А.В. Караваев, С.Я. Макаров, Я.Я. Суздальцев. – М.: Гос. изд-во оборонной промышленности, 1954. – 377 с.
403. Справочник машиностроителя: в 3 т. – М.: Машгиз, 1951. – Т. 3. – 1098 с.
404. Справочник по текущему и среднему ремонту авиационной техники / под ред. В. Г. Александрова. – М.: Воениздат, 1975. – 296 с.
405. Справочные материалы и методики по расчету статической прочности. Расчет заклепочных соединений. – Х.: ХАПО, 1974. – 42 с.
406. А.с. 1479733 СССР, МКИ F 16 B 5/02. Срезное многорядное соединение деталей / Э.Н. Румянцев, А.Г. Гребеников, В.Н. Стебенев, Е.Т. Василевский (СССР). – № 4306096/31-27; заявл. 14.09.87; опубл. 15.05.89, Бюл. № 18. – 3 с.
407. Стандартная спецификация на тип самолета (вертолета): учеб. / А.Г. Гребеников, П.А. Клюев, В.Н. Король и др.– Х.: Нац. аэрокосм.

ун-т «ХАИ», 2004. – 336 с.
408. Статистическая оценка экономически обоснованного ресурса авиационных конструкций // Экспресс-информация «Воздушный транспорт» ГосНИИ ГА. – Сер. Надежность, долговечность, ресурс, техническое обслуживание и ремонт. – 1980. – Вып. 6. – С. 5 – 12.
409. Стебенев В.Н. Методика оценки сопротивления усталости соединений / В.Н. Стебенев // Сопротивление усталости элементов авиаконструкций. – М.: ЦАГИ. – 1981. – Вып. 2117. – С. 42 – 54.
410. Степанов М.Н. Усталость легких конструкционных сплавов/ М.Н. Степанов, Е.В. Гиацинтов. – М.: Машиностроение, 1973. – 320 с.
411. Степин П.А. К расчету на срез соединений с прерывными связями/ П.А. Степин // Вестник инженеров и техников. – 1951. – № 4. – С. 175 – 179.
412. Столбов В. В. Ремонт самолетов/ В. В. Столбов, Н. В. Музыкин. – Рига: РКВИАВУ, 1954. – 312 с.
413. Сухарев И.П. Прочность шарнирных узлов машин: справ. пособие/ И.П. Сухарев. – М.: Машиностроение, 1977. – 168 с.
414. Тез. докл. VIII науч.-техн. конф. по ресурсу авиаконструкций. – Жуковский: ЦАГИ. – 1986. – 228 с.
415. Тез. докл. Междунар. науч.-техн. конф. «Экспериментальное оборудование и сертификация авиационной техники», 22-27 августа 1995 г. – Жуковский: ЦАГИ, 1995. – 136 с.
416. Тейлор Д. Нагрузки, действующие на самолет/ Д. Тейлор. – М.: Машиностроение, 1971. – 372 с.
417. Теория и практика проектирования пассажирских самолетов. – М.: Наука, 1976. – 439 с.
418. Теплый М.И. Контактные задачи для областей с круговыми границами/ М.И. Теплый – Л.: Вища шк., 1983. – 176 с.
419. Технический прогресс в самолетостроении / под ред. В.А. Степанченко. – М.: Машиностроение, 1975. – 360 с.
420. Технологические особенности выполнения титановых соединений с радиальным натягом болтов / Л.Д. Арсон, А.Г. Гребеников, В.Н. Клименко, В.И. Попович // Вопросы проектирования самолетных конструкций. – Х.: ХАИ. – 1978. – Вып. 1. – С. 106 – 112.
421. Технологические процессы и оборудование для выполнения соединений в конструкциях самолетов/ под ред. В.П. Григорьева. – Ташкент: Фан, 1971. – 96 с.
422. Технологическое обеспечение авиационного производства / Г.Б. Строганов, Ю.Г. Роик, В.И. Климентьев и др.; под общ. ред. Г.Б. Строганова. – 2-е изд., доп. – М.: Машиностроение, 1991. – 368 с.
423. Технология выполнения высокоресурсных заклепочных и болтовых соединений в конструкциях самолетов / А.И. Ярковец, О.С. Сироткин,

В.А. Фирсов, Н.М. Киселев. – М.: Машиностроение, 1987. – 192 с.
424. Технология выполнения высокоресурсных соединений / под ред. В.Ф. Пширкова. Сер. № 8. Технология. – М.: Отраслевая библиотека «Технический прогресс и повышение квалификации», 1980. – 170 с.
425. Теоретические и экспериментальные основы норм прочности самолетов / под общ. ред. А.И. Макаревского. – М.: ЦАГИ, 1969.
426. Технология производства космических ракет: учеб. / Е.А. Джур, С.И. Вдовин, Л.Д. Кучма и др. – Днепропетровск: Изд-во ДГУ,1992. – 184 с.
427. Технология производства летательных аппаратов (курсовое проектирование) / под общ. ред. В.Г. Кононенко. – К.: Вища шк., 1974. – 224 с.
428. Технология самолетостроения: учеб. для авиационных вузов / А.Л. Абибов, Н.М. Бирюков, В.В. Бойцов и др.; под ред. А.Л. Абибова. – 2-е изд., перераб. и доп. – М.: Машиностроение, 1982. – 551 с.
429. Технология создания твердотельной модели монолитной панели крыла с использованием компьютерной интегрированной системы UNIGRAPHICS / А.Г. Гребеников, В.В. Парфенюк, О.И. Парфенюк, А.М. Гуменный // Открытые информационные и компьютерные интегрированные технологии. – Х.: Гос. аэрокосм. ун-т «ХАИ». – 1999. – Вып. 4. – С. 3 – 14.
430. Циганков О.С. Технологічна діяльність космонавта: підруч. для студентів авіац. вищих навч. закладів / О.С. Циганков, В.М. Кобрін. – Х.: ХАІ, 1995. – 288 с.
431. Технологія виробництва літальних апаратів із композиційних матеріалів/ С.А. Бичков, О.В. Гайдачук, В.Є. Гайдачук та ін. – К.: ІСДО, 1995. – 376 с.
432. Тимченко А.М. Выбор параметров отверстий, выполняемых в вершинах усталостных трещин, в тонкостенных конструкциях/ А.М. Тимченко // Вопросы проектирования и производства тонкостенных силовых конструкций. – Х.: ХАИ. – 1984. – С. 96 – 101.
433. Тимченко А.М. Повышение живучести тонкостенных конструкций/ А.М. Тимченко, А.Г. Гребеников // Вопросы проектирования самолетных конструкций. – Х.: ХАИ. – 1979. – Вып. 2. – С. 105 – 109.
434. Тимченко А.М. Исследование влияния конструктивно-технологических факторов на НДС и усталостную долговечность сборных тонкостенных балок типа лонжеронов/ А.М. Тимченко, А.Г. Гребеников, В.Н. Стебенев // Совершенствование технологии упрочнения и ее влияние на повышение надежности и ресурса изделий машиностроения: тр. IV республ. конф. – Казань: КАИ. – 1983. – С. 53 – 54.
435. Тимченко А.М. Исследование методов повышения усталостной долговечности соединений в сборных лонжеронах / А.М. Тимченко,

А.Г. Гребеников, В.Н. Стебенев // Вопросы проектирования самолетных конструкций. – Х.: ХАИ. – 1982. – Вып. 3. – С. 87 – 91.
436. Торенбик Э. Проектирование дозвуковых самолетов/ Э. Торенбик. – М.: Машиностроение, 1983. – 618 с.
437. Трощенко В.Т. Деформирование и разрушение металлов при многоцикловом нагружении/ В.Т. Трощенко. – К.: Наук. думка, 1981. – 344 с.
438. Трощенко В.Т. Деформирование и разрушение металлов при многоцикловом нагружении в условиях неоднороднего напряженного состояния. Сообщение 1/ В.Т. Трощенко, Н.И. Жабко // Проблемы прочности. – 1981. – № 9. – С. 3 – 11.
439. Трощенко В.Т. Деформирование и разрушение металлов при многоцикловом нагружении в условиях неоднородного напряженного состояния. Сообщение 2 / В.Т. Трощенко, Н.И. Жабко // Проблемы прочности. – 1981. – № 11. – С. 3 – 10.
440. Трощенко В.Т. Сопротивление усталости металлов и сплавов: справ./ В.Т. Трощенко, Л.А. Сосновский. – К.: Наук. думка, 1987. – Ч. 1. – 602 с.
441. Трощенко В.Т. Сопротивление усталости металлов и сплавов: справ./В.Т. Трощенко, Л.А. Сосновский – К.: Наук. думка. 1987. – Ч. 2. – 1303 с.
442. Трощенко В.Т. Расчет на прочность и долговечность конструктивных элементов с трещинами при циклическом нагружении / В.Т. Трощенко, П.В. Ясний, В.В. Покровский // Проблемы прочности. – 1982. – № 11. – С. 12 – 16.
443. Уотерхауз Р.Б. Фреттинг-коррозия: пер. с англ; под ред. Г.Н. Филимонова / Р.Б. Уотерхауз – Л.: Машиностроение, 1976. – 272 с.
444. А.с. 1616297 СССР, МКИ G 01 M 5/00. Устройство для нагружения кессона крыла летательного аппарата изгибом с кручением / Э.Н. Румянцев, А.Г. Гребеников, В.Н. Стебенев, А.Г. Шаманов, В.Г. Бабичев (СССР). – № 4409144/40-23; заявл. 13.04.88; ДСП.
445. А.с. 1319446 СССР, МКИ. F 16 B 5/02. Устройство для соединения стенок лонжеронов/ А.Г. Гребеников, С.В. Трубаев, А.М. Тимченко, В.Н. Стебенев, Е.Т. Василевский (СССР). – № 3910406/40-23; заявл. 18.06.85; ДСП.
446. Фаерберг И.И. Распределение усилий между болтами стыкового соединения за пределом пропорциональности/ И.И. Фаерберг, А.А. Рубина // Тр. ЦАГИ. – М., 1950. – С. 1 – 18.
447. Федосенко И.Г. О постановке болтов с натягом импульсным методом/ И.Г. Федосенко, А.Г. Гребеников, В.Н. Лепетюха // Методы повышения ресурса соединений элементов конструкций – М.: ЦАГИ. – 1974. – Вып. 1. – С. 32 – 34. ДСП.

448. Федотов М.Н. Определение коэффициентов воздействий при исследовании усталостных характеристик стыковых соединений самолетных конструкций/ М.Н. Федотов, А.Г. Гребеников // Самолетостроение. Техника воздушного флота. – Х.: ХГУ. – 1975. – Вып. 38. – С. 66 – 70.
449. Федотов М.Н. Влияние компенсации технологических отклонений в срезном усовидном стыке на его выносливость / М.Н. Федотов, А.Г. Гребеников, Е.Т. Василевский // Вопросы проектирования самолетных конструкций. – Х.: ХАИ. – 1978. – Вып.1. – С. 123 – 127.
450. Фомичев П.А. Энергетический метод расчета долговечности элементов авиаконструкций / П.А Фомичев. // Авиационно-космическая техника и технология. – Х.: Гос. аэрокосм. ун-т «ХАИ». – 1999. – Вып. 15. – С. 168 – 171.
451. Формирование облика многофункционального беспилотного авиационного комплекса гражданского назначения / В.Д. Белый, А.К. Мялица, А.Г. Гребеников и др. // Открытые информационные и компьютерные интегрированные технологии. – Х.: Нац. аэрокосм. ун-т «ХАИ». – 2001. – Вып. 9. – С. 3 – 17.
452. Фрактографические методы определения роста усталостных трещин в элементах самолетных конструкций // Экспресс-информация «Воздушный транспорт» ГосНИИ ГА. Сер. Надежность, долговечность, ресурс, техн. обслуживание и ремонт. – 1982. – № 1. – С. 2 – 3.
453. Фреттинг и фреттинг-усталость титановых сплавов в условиях высоконормальных нагрузок Titanium 80. Sci and Techovol Proc. 4 Int Cont. Kyoto May 19-22, 1980, Vol 3. New York, 1980, 1837-1847// Реф. журнал «Механика», 1983, 1 Д470.
454. Фреттинг-усталость Appl. Sci Publ. LTD,1981б Х., 244 pp./англ./Место хранения ГПНТБ СССР // Реф. журнал «Механика», 1983. – 3 Д613К.
455. Фурашев В.Н. Система подготовки специалистов промышленности по обеспечению качества выпускаемой продукции / В.Н. Фурашев, А.Г. Гребеников, В.В. Юрченко // Методологические проблемы качества обучения и обучение качеству: тр. науч.-метод. конф. – Х.: ХАИ. – 1996. – С. 66 – 70.
456. Хейвуд Р.Б. Проектирование с учетом усталости/ Р.Б Хейвуд. – М.: Машиностроение, 1969. – 504 с.
457. Хилл П. Наука и искусство проектирования/ П. Хилл / пер. с англ. Е.Г. Коваленко; под ред. к.т.н. В.Ф. Венды. – М.: Мир, 1973. – 264 с.
458. Циклические деформации и усталость металлов / В.Т. Трощенко, Л.А. Хамалза, В.В. Покровский и др. – К.: Наук. думка, 1985. – Т. 2: Долговечность металлов с учетом эксплуатационных и технологических факторов. – 224 с.

459. Шанявский А.А. Корреляция величины скорости распространения усталостной трещины с шагом усталостных бороздок при двухосном нагружении элементов самолетных конструкций/ А.А. Шанявский, В.Г. Смыков // Тр. ГосНИИГА. – 1981. – Вып. 202. – С. 101 – 107.
460. Шейнин В.М. Весовое проектирование и эффективность пассажирских самолетов: в 2 т. / В.М. Шейнин, В.И. Козловский. – М.: Машиностроение, 1977. – Т. 1: Весовой расчет самолета и весовое планирование. – 344 с.
461. Шейнин В.М. Роль модификаций в развитии авиационной техники/ В.М. Шейнин, В.М. Макаров. – М.: Наука, 1982. – 247 с.
462. Шишков В.В. Особенности создания математической модели поверхности легкого многоцелевого самолета / В.В. Шишков, А.Г. Гребеников, А.М. Гуменный // Открытые информационные и компьютерные интегрированные технологии. – Х.: Гос. аэрокосм. ун-т «ХАИ». – 1998. – Вып. 1. – С. 10 – 14.
463. Школьник Л.М. Методика усталостных испытаний: справ./ Л.М. Школьник. – М.: Металлургия, 1978. – 303 с.
464. А.с. 1765966 СССР, МКИ В 21 J 15/36. Штамп для одиночной прессовой клепки / В.В. Губарев, С.Г. Васильченко, В.М. Андрющенко, А.Г. Гребеников, Е.А. Большаков, В.М. Пупышев (СССР). – № 4896386/27; заявл. 25.12.90, ДСП.
465. Шульженко М.Н. Курс конструкций самолетов: учеб. – Изд. 2-е, испр. и доп. /М.Н. Шульженко, А.И. Мостовой. – М.: Машиностроение, 1965. – 564 с.
466. Щетинин Г.М. Механизация образования соединений при сборке авиационных конструкций / Г.М. Щетинин, М.И. Лысов, В.М. Буров. – М.: Машиностроение, 1987. – 256 с.
467. Экспериментальное исследование выносливости клепаной панели с вырезом / А.Г. Гребеников, В.М. Андрющенко, В.А. Гребеников, А.М. Гуменный// Открытые информационные и компьютерные интегрированные технологии. – Х.: Нац. аэрокосм. ун-т «ХАИ». – 2002. – Вып. 13. – С. 169 – 183.
468. Экспериментальное исследование выносливости усовидного болтового соединения при симметричных циклических нагрузках / Л.Д. Арсон, А.Г. Гребеников, М.Н. Федотов, В.Н. Рычик // Выносливость и ресурс авиационных конструкций. – Жуковский: ЦАГИ. – 1978. ДСП.
469. Экспериментальное исследование общего напряженно-деформированного состояния и сопротивления усталости образцов сборных панелей крыла без вырезов / А.Г. Гребеников, С.А. Бычков, С.В. Воронов, В.А. Гребеников // Вопросы проектирования и производства конструкций летательных аппаратов. – Х.: Нац.

аэрокосм. ун-т «ХАИ». – 2002. – Вып. 30 (3). – С. 144 – 166.
470. Энгельке У.Д. Как интегрировать САПР и АСТПП: Управление и технология/ У.Д. Энгельке; пер. с англ. В.В. Мартынюка, Д.Е. Веденеева; под ред. Д.А. Корягина. – М.: Машиностроение, 1990. – 320 с.
471. Ярковец А.И. Основы механизации и автоматизации технологических процессов в самолетостроении: учеб. пособие для вузов/ А.И. Ярковец. – М.: Машиностроение, 1981. – 192 с.
472. ANSYS workbook Release 5.3, 1994. – P. 7 – 40.
473. An-74T-200A Aircraft. Standard Specification / A.G. Grebenikov, P.A. Kluyev, V.N. Korol, P.O. Naumenko, S.A. Pavlenko, Y.I. Povaliy. – Textbook. – Kharkov: National Aerospace University «Kharkov Aviation Institute», 2004. – 320 p.
474. ANSYS Analysis Guide. Structural Analysis Guide. Chapter 8. Nonlinear structural analysis. 001087. 4th Edition. SAS IP©.
475. Hertel. H. Ermudungsfestigkeit der konstructionen. Springer Verlag. Berlin, Hebelberg, New-York, 1969.
476. Structural integritity for the next millennium. Volume 1. Lecture papers. Editors J.L. Rudd, R.M. Bader. Proceedings of the 20th symposium of the international committee on aeronautical fatigue 14-16 july 1999, Bellevue, Washington, USA. – 664 p.
477. Structural integritity for the next millennium. Volume 2. Lecture papers. Editors J.L. Rudd, R.M. Bader. Proceedings of the 20th symposium of the international committee on aeronautical fatigue 14-16 july 1999, Bellevue, Washington, USA. – 1232 p.

Навчальне видання

ГРЕБЕНІКОВ ОЛЕКСАНДР ГРИГОРОВИЧ

МЕТОДОЛОГІЯ ІНТЕГРОВАНОГО ПРОЕКТУВАННЯ ТА МОДЕЛЮВАННЯ ЗБІРНИХ ЛІТАКОВИХ КОНСТРУКЦІЙ

Редактор Н.С. Малашенко

Технічний редактор Л.О. Кузьменко

Комп'ютерне верстання: Н.В. Єфремова

Перекладачі: С.М. Шаповалов, М.В. Кириленко, О.М. Чмовж, Н.В. Шевель

Зв. план, 2010.
Підписано до друку 28.12.2010.
Формат 60x84$^{1}/_{8}$. Папір офс. № 2. Офс. друк
Ум. друк. арк 23,7. Обл.-вид. арк. 26,56. Наклад 100 прим. Замовлення 439.
Ціна вільна

Національний аерокосмічний університет ім. М.Є. Жуковського

«Харківський авіаційний інститут»

61070, Харків-70, вул. Чкалова, 17

http://www.khai.edu

Видавничий центр ХАІ

61070, Харків-70, вул. Чкалова, 17

izdat@khai. edu